DOE/MC/24022-3654
(DE94004074)
Distribution Category UC-114

Long-Term Durability Testing of Ceramic Cross-Flow Filter

Final Report
September 29, 1987 - December 31, 1992

T. E. Lippert
E. E. Smeltzer
M. A. Alvin
D. M. Bachovchin

Work Performed Under Contract No.: DE-AC21-87MC24022

For
U.S. Department of Energy
Office of Fossil Energy
Morgantown Energy Technology Center
P.O. Box 880
Morgantown, West Virginia 26507-0880

By
Westinghouse Electric Corporation
Science and Technology Center
1310 Beulah Road
Pittsburgh, Pennsylvania 15235

August 1993

CONTENTS

CONTENTS (cont'd)

LIST OF FIGURES

LIST OF FIGURES

LIST OF TABLES

ABSTRACT

Long term durability testing of the cross flow filter is described. Two high temperature, high pressure test facilities were built and operated. The facilities were designed to simulate dirty gas environments typical of Pressurized Fluidized Bed Combustion (PFBC) and coal gasification. Details of the design and operation of the test facilities and filter testing results are described.

EXECUTIVE SUMMARY

INTRODUCTION

The Department of Energy, Morgantown Energy Technology Center (DOE/METC) and Westinghouse are developing and evaluating a cross flow hot gas particulate filter for application in coal based, advanced power generation systems.

The cross flow filter concept and system design are described herein. Filter and system development have evolved through the stages of initial exploratory studies to proof-of-concept bench-scale tests, and, more recently, to pilot scale tests on the New York University (NYU) Pressurized Fluid Bed Combustor (PFBC) and on the Texaco gasifier at Montebell , California.[1,2,3]

The objective of the current program entitled "Long Term Durability Testing of Ceramic Cross Flow Filters" is to evaluate the materials and mechanical design aspects of the filter system and the operational requirements for integration with a prototypical gasifier or combustor. This work was accomplished through extended testing using flow facilities that could simulate the high temperature filtration process typical in advanced fossil process conditions such as PFBC and Integrated Gasification Combined Cycle (IGCC). Such long term filter testing could not be economically accomplished using existing pilot plant PFBC or gasifier facilities.

PROJECT DESCRIPTION

Two dedicated high temperature, high pressure (HTHP) filter test facilities were constructed and operated. These test facilities provide HTHP gas environments for evaluating the filter using ash materials from

PFBC and coal gasification facilities. Both facilities have HTHP flow capabilities to test up to four commercial scale (12 x 12 x 4 inch/ 30.5 x 30.5 x 10.2 cm) cross flow filter elements.

The PFBC simulator facility is designed for a maximum gas flow of 1500 lb/hr (650 kg/hr) and pressures of 150 psig (11 bar). Natural gas is combusted to provide the thermal input to raise the filter temperature as high as 1600°F (870°C). A gravimetric dust feeder with a pneumatic transport line is used to reentrain ash into the hot combustion gas. The facility is capable of simulating various plant operations including steady state and transient conditions (e.g., startup/shutdown, turbine trip and pulse cleaning). This is important when evaluating the effects of mechanical and thermal stresses on the filter module.

The gasification simulator system is a closed flow loop that is electrically heated and designed to provide a HTHP reducing gas environment, while permitting the feeding of gasifier char/ash material. In this facility, a maximum of 1500 lb/hr (650 kg/hr) of gas flow is recirculated using a specially designed high temperature, high pressure eductor. Approximately 10 percent of the gas is used as the motive flow, and system pressures of 150 psig (11 bar), and temperatures of 1200°F (650°C) are possible. A gravimetric dust feeder with a pneumatic transport line are used to feed the chosen char/ash.

Both test loops have the following characteristics:

1. Isokinetic sampling on the outlet of the filter to determine the particulate removal efficiency,
2. An adjustable high pressure gas supply for reverse pulse cleaning of the filters,
3. On-line ash collection and removal capability that permit round-the-clock operation over extended test periods (e.g., 100 hours or more), and
4. Instrumented to provide filter operating and system performance data, including a computer based data acquisition system.

PROJECT RESULTS

The program provides for 3000 hours of testing under PFBC conditions and 2000 hours under simulated gasification conditions. The goal was to achieve this testing utilizing a single set of filter elements, respectively. For the simulated gasifier testing utilizing a char feed, this goal was achieved. In the simulated PFBC testing a total of 3080 test hours was accomplished, but events precluded the use of a single filter set.

Table S-1 provides a summary of results from the filter testing programs. Average outlet dust loadings were below 1 ppmw, demonstrating particle collection efficiencies significantly better than the 99% program criteria.

Figure S-1 compares the outlet dust measurement data from this testing with the emission and turbine tolerance requirements projected for advanced, coal based systems. Data is also included from earlier cross flow filter testing on an actual PFBC pilot plant.[1] These results demonstrate the high performance potential of the cross flow filter in meeting both turbine tolerance and environmental emission requirements.

Results from the current simulator testing of the cross flow filter have been compared to filter testing in pilot plant facilities. This comparison for the PFBC case shows filters operated in HTHP simulator facilities behave very similar to filters tested in coal fired pilot plants. In both cases stable filter permeance is achieved in relatively few (<500) cleaning cycles. These results confirm that filter system operating characteristics (pressure drop, cleaning cycle, etc.) for PFBC application can be reasonably predicted based on HTHP simulator testing.

Table S-1 - Summary of Cross Flow Filter Performance in Long Term Durability Simulator Testing

	PFBC Ash Test Loop		Gasifier Char Test Loop
	Test Module #1	Test Module #2	Test Module #1
No. of Filters	2	4	2
Operating Conditions			
Temperature, °F	1550	1550	350-1200
Pressure, psia	85	85	85
Inlet Dust Loading, ppm	1000	1000	1000-1500
Face Velocity, ft/min	6 to 10	3 to 5	2-5
Cumulative Hrs.	1300	1100 2400	2000
Performance			
Avg. Outlet Loading, ppm	<1	<1	<1
Baseline Δp, in wg	8-20	4-10	1-4
Comments	Flange Failure	New Mount	No Failures

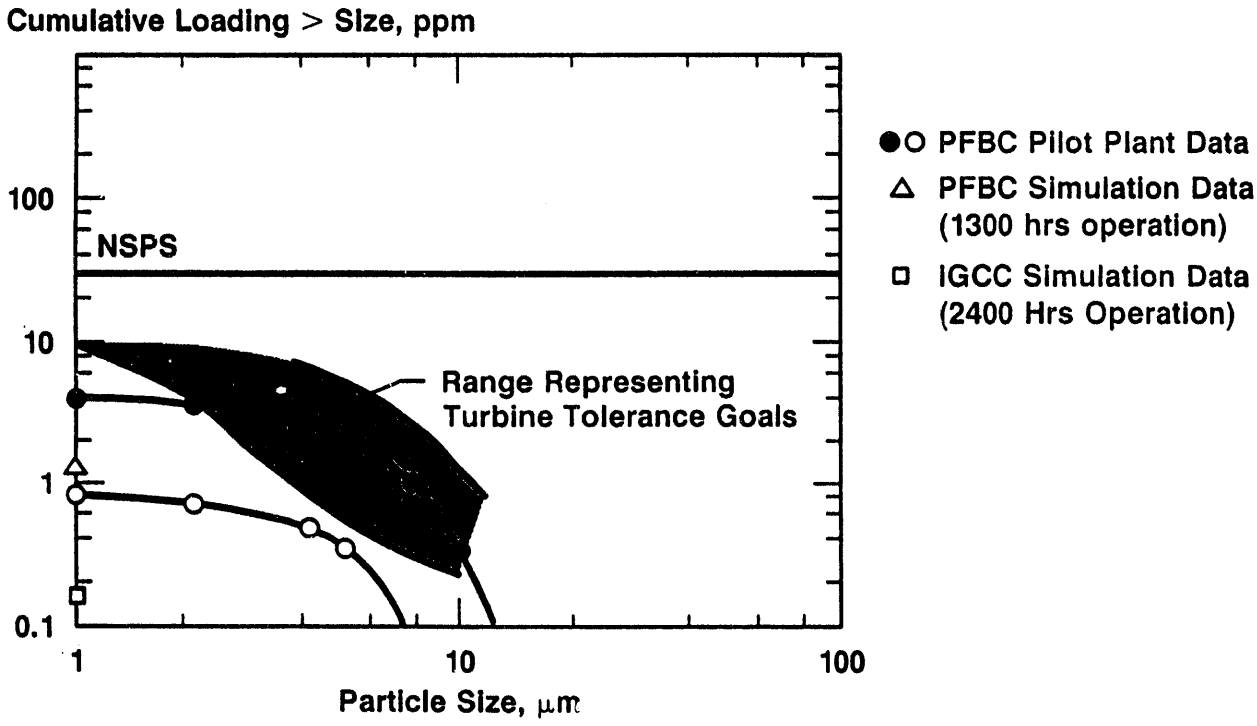

Figure S-1 - Comparison of Measured Cross Flow Filter Performance with Gas Turbine Tolerance

The cross flow filter testing in the gasifier simulator facility also shows stable filter permeance after a short initial conditioning period. The simulator testing however did not directly reproduce pilot plant results since filter permeance appears to be different for different gasifier types. This difference is attributed to the significantly different design and process conditions of gasifiers and the physical properties of the generated ash/char fines. The low particle density of gasifier fines suggests high reentrainment potential that may lead to apparent low filter permeance.

An important focus of the extended testing of the current program has been the evaluation of filter system component durability. In the PFBC simulator testing both filter element and gasket failures occurred that compromised filter performance. Although no gasket or filter failures were experienced in the gasifier simulator testing, ongoing cross flow filter testing in gasifier pilot plant systems have experienced such failures.[8] In the early phases of the PFBC simulator testing an improved design of the ceramic mat gasket was developed by Westinghouse and backfitted to both the PFBC simulator testing and ongoing gasifier pilot plant filter tests. This improved gasket design was also implemented into the gasifier simulator testing. In all subsequent testing, gasket failures have been eliminated utilizing this modified gasket design. The improved gasket utilized NEXTEL(R) fibers wrapped in a NEXTEL(R) ceramic cloth. The cloth encapsulates the fiber and prevents bulk material loss during process operation.

Cross flow filter element failures under service condition can be characterized as one or more of the following types: debonding of plate seams, delaminations (hairline cracks that follow plate seams), by cracks that propagate across the plate seams and cracks that occur along the mounting flange.

Uncontrolled plant thermal transients represent the major concern regarding delamination and filter plate cracking. Simulator testing has demonstrated that the cross flow filter can endure controlled plant transients typical of PFBC plant startup and turbine trip. A deficiency in the filter mount design that was not apparent from earlier short term tests, caused flange cracking terminating the 1300 hour run in the PFBC simulator testing. A redesign of the filter mount was made to eliminate the root cause of the observed failure; nonuniform loading of the flange and the buildup of dust fines in crevices between the mount and filter flange. This design was implemented in subsequent PFBC simulator and pilot plant testing. Although testing has been limited (1000 to 2000 hours), no further failures in the filter flange were experienced.

An important consideration in the long term durability of the cross flow filter is the stability of the ceramic matrix. This aspect of the filter development is being addressed in detail in a separate program, "Thermal/Chemical Stability of Ceramic Cross Flow Filter Materials," DE-AC21-88MC25034. This program is investigating for a variety of materials the combined and separate effects on long term material properties of the base matrix structure in the presence of alkali and possible generation of microcracking due to effects of pulse cleaning thermal fatigue. This work has demonstrated the relative inertness of the cross flow filter alumina/mullite matrix in both high temperature oxidizing and reducing gas environments of PFBC and gasifier systems, respectively. The cross flow filters exposed in the simulator testing reporting herein have confirmed the potential benefits of the alumina/mullite matrix.

PROJECT CONCLUSIONS

- Improvements in the long term durability of the cross flow filter has been achieved through improved filter manufacture and design of the filter mounting and gasket system. Further improvements in manufacturing quality assurance and

development of nondestructive testing techniques are needed to ensure filter manufacturing specifications are met.

- Extended testing (>1000 hrs) has confirmed the high performance potential of the cross flow filter that was previously demonstrated in short term tests.

- The alumina/mullite matrix currently used for the cross flow filter appears as a preferred material choice for the wide range of process gas conditions represented by the different Advance Fossil Power Generation Systems that would use hot gas cleaning. Further improvements in material thermal fatigue toughness are needed to protect the filter system from unplanned plant process upsets.

- High temperature, high pressure PFBC simulator facilities are effective in reproducing filtration conditions representative of actual plant operations.

- Gasifier simulation testing using hot inert gas and char produced only similar plant trends regarding filter operating characteristics. Both simulator facilities should reproduce thermal and mechanical stressing typical of plant operations.

REFERENCES

1. Lippert, T. E., et al., 1989, "Performance Evaluation of a Ceramic Cross Flow Filter at New York University PFBC," Proceedings of the Sixth Annual Coal-Fueled Heat Engines and Gas Stream Cleanup Systems Contractors Meeting, p. 304. DOE/METC-89/6101.

2. Haldipur, G. B., et al., 1989, "Sub-Pilot Scale Gasifier Evaluation of Ceramic Cross Flow Filters," Proceedings of the Ninth Annual Gasification and Gas Stream Cleanup Systems Contractors Meeting, p. 119-128. DOE/METC-89/6107.

3. Haldipur, G. B., et al., 1990, "Sub-Pilot Scale Gasifier Evaluation of Ceramic Cross Flow Filters," Proceedings of the Tenth Annual GAsification and Gas Streams Cleanup Systems Contractors Meeting, p. 73-82. DOE/METC-90/6115.

1. INTRODUCTION

High temperature and pressure (HTHP) particulate control is an essential component of advanced coal-fired power generation systems that are under development by the DOE Morgantown Energy Technology Center for clean coal programs and future commercialization. These systems include gasification combined cycles (IGCC), pressurized fluidized-bed combustion (PFBC), and direct coal fueled turbines (DCFT) and each of these systems rely on a gas turbine to generate all or a portion of the electrical power. Ceramic barrier filters have been identified as a viable particulate control option for use in these coal-based power systems. The ceramic filter elements are near absolute filters (removing >99.9% of the entrained fines) have high throughput capability, are relatively inert to gas phase contaminants, and maintain stability and material strength at high temperatures. These characteristics provide for a filter system that protects the gas turbine from particle erosion and deposition and cleans the gas to meet environmental emission standards without additional expensive stack gas cleanup devices. The cross flow filter concept has been identified as one of the most cost effective technologies for advanced particle filtration.[1]

1.1 CROSS FLOW FILTER CONCEPT

The ceramic cross flow filter is illustrated in Figure 1.1. The filter element is comprised of thin porous ceramic plates that contain channels formed by ribbed sections. The plates are stacked and fired to form a monolithic porous structure. The two filter faces of the short side channels are exposed to the dirty gas. The gas flows into the short side channels, through the porous plates that form the "roof" and "floor" of the channels and into the longer channels that form the clean

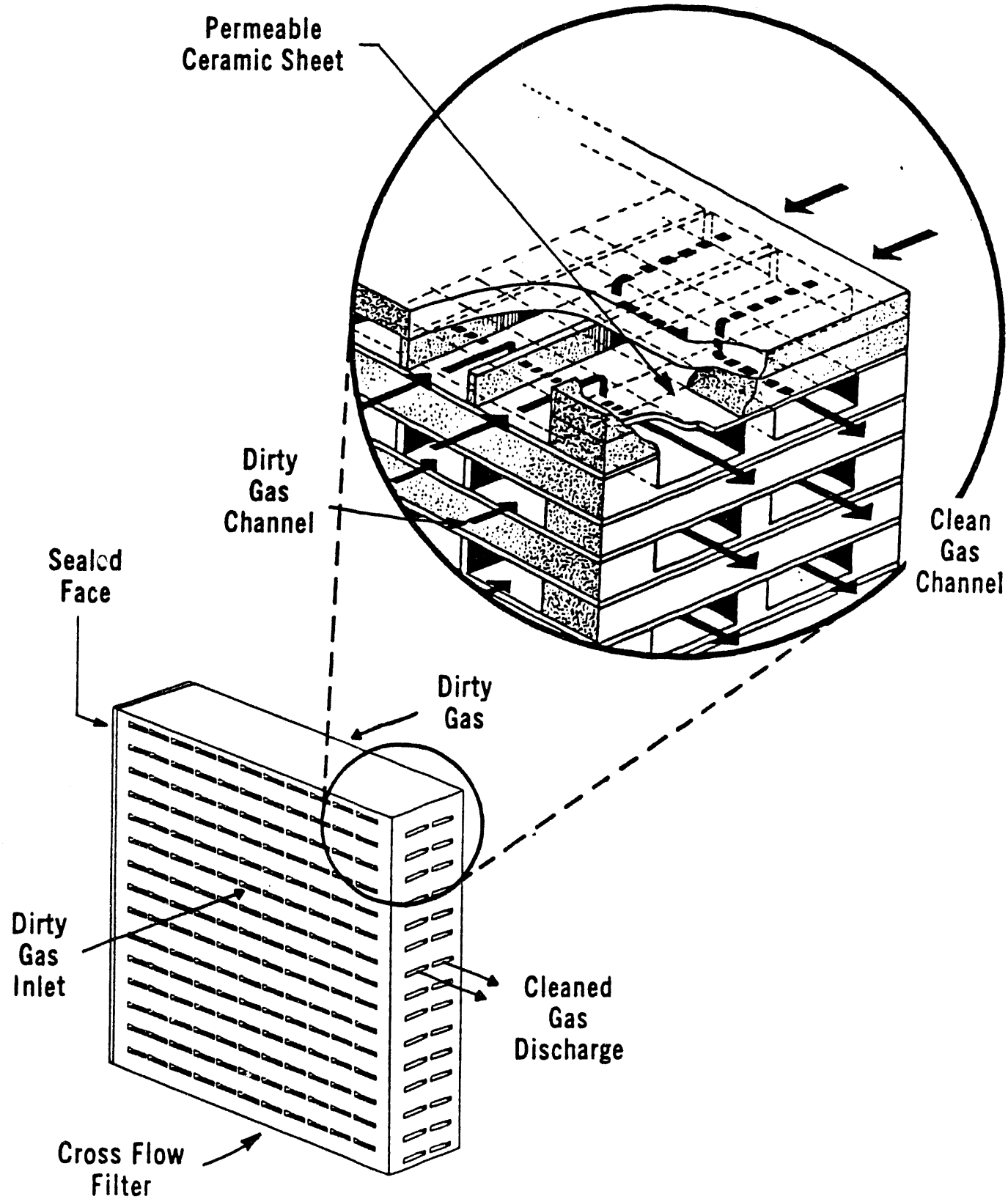

Figure 1.1 - Schematic Representation of Cross Flow Filter

gas side. One end of the clean side channels is sealed to force the filtered gas to flow to a central collection plenum to which the filter is mounted.

The Westinghouse cross flow filter system design is schematically shown in Figures 1.2 and 1.3. The system consists of a refractory lined, coded pressure vessel that contains arrays of the cross flow filter element assemblies, Figure 1.2. The arrays are formed by attaching individual cross flow elements (Item 1, Figure 1.3) to a common plenum (Item 2, Figure 1.3) and discharge pipe. The arrays are cleaned from a single pulse nozzle source. For efficient packaging, several of the individual plenum assemblies are arranged vertically from a common support structure, forming a filter cluster (Item 3, Figure 1.3). The filter cluster represents the basic module needed for constructing a large filter system. The individual clusters are supported from a common, high alloy tubesheet and expansion assembly that spans the pressure vessel and divides it into the "clean" and "dirty" gas sides. The cluster concept provides a modular approach to scaleup and permits maintenance and replacement of individual filter elements.

Hot, dirty gas enters the filter housing, and passes through the filter elements into the central plenum pipes, collected on the clean side of the tubesheet and passes through the vessel outlet nozzle. The ash collected on the short side channels of the filter elements is removed by reverse pulse jet cleaning and falls into the ash collection system attached to the bottom of the pressure vessel housing.

The major attributes of this filter concept are its absolute filtration characteristics on ash material and capability to be operated at relatively high flow capacity (high face velocity) with low pressure drop. Since each of the filter plates represent a filter surface, the cross flow configuration provides very high filter surface area to volume characteristic and the potential to be compact and economic.

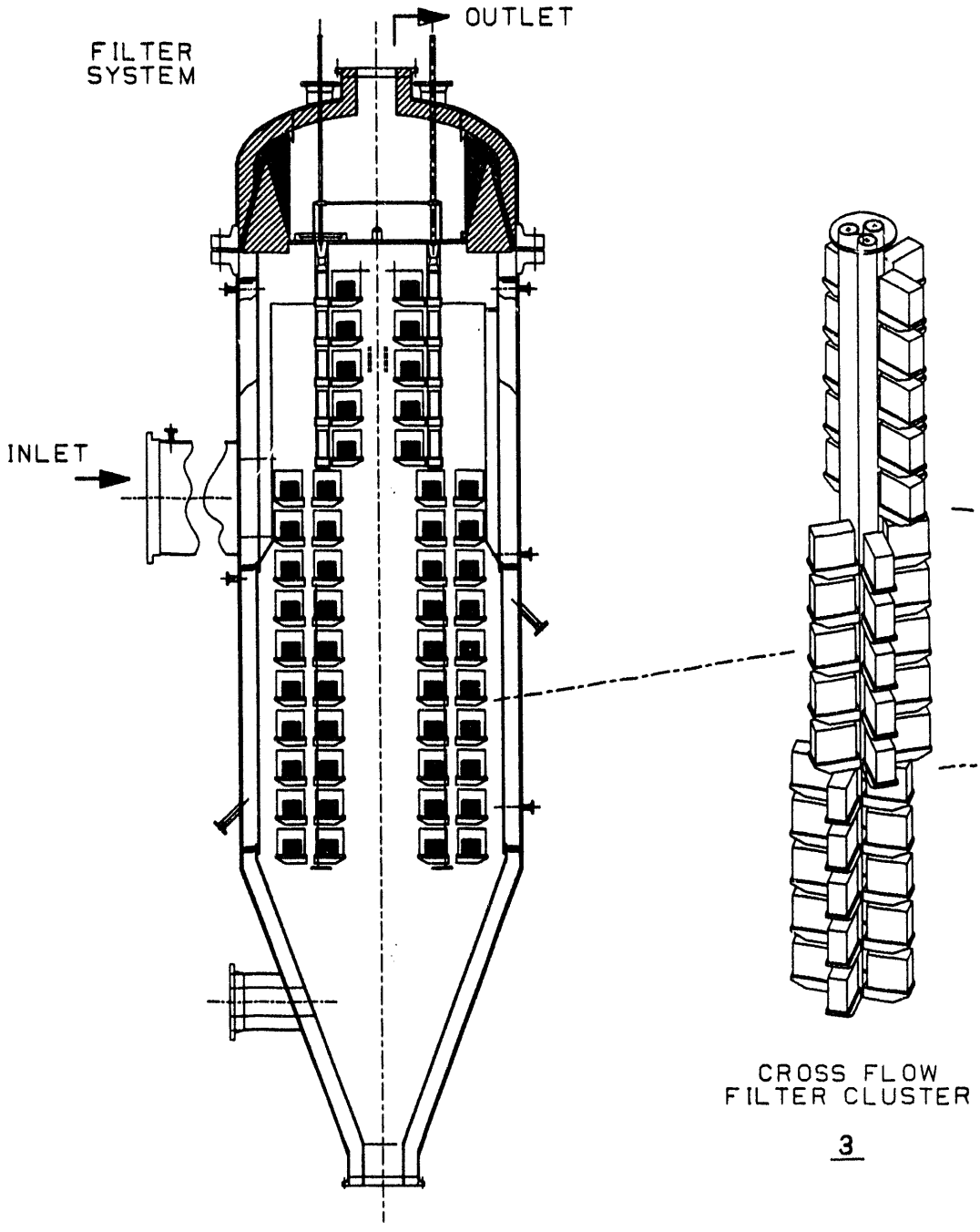

Figure 1.2 - Westinghouse Cross Flow Filter System Concept

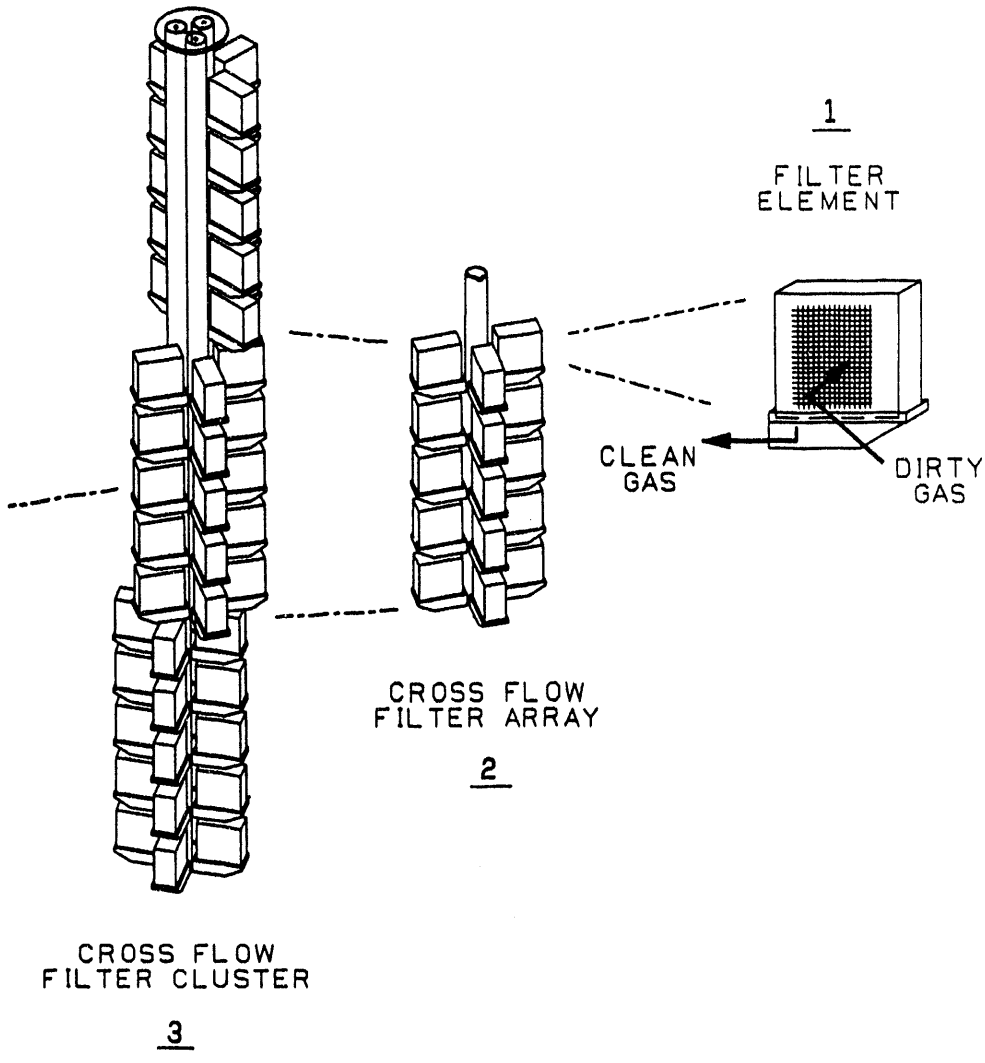

Figure 1.3 - Westinghouse Concept for Contstructing Filter System from Single Cross Flow Filter Elements

1.2 CROSS FLOW FILTER DEVELOPMENT

Westinghouse has focused on cross flow filters that have been fabricated from an alumina/mullite ($Al_2O_3/3Al_2O_3 \cdot 2SiO_2$)-based material. The development of the cross flow filter has evolved through the stages of initial exploratory studies to proof-of-concept test at various bench-scale gasification and combustion facilities.

Initial exploratory studies were focused on subscale filter elements (15.2 x 15.2 x 5.1 cm - 6 x 6 x 2 inch) tested in a bench-scale PFBC simulator and small fluid bed PFBC and gasifier facility.[2,3] These studies focused on evaluating the basic filtration properties of the cross flow geometry and methods to seal and mount the filter in high temperature gas streams. These studies also demonstrated the technical and economic potential of the unique cross flow geometry.

Bench-scale test results showed that the conditioned filter resistance was low compared to other types of filter and inertial devices; that simple pulse-jet methods could be used to clean the filters; and that essentially absolute filtration on coal ash and char materials could be achieved. Delamination of the filter at the rib to plate bonded joints was identified as a manufacturing development issue.

Modifications were made in the fabrication and manufacturing of the cross flow filter elements to improve retention of the base material strength and porosity properties while maintaining a crack-free, dimensionally stable, plate assembly with improved bond strength.[4] Additional features which were incorporated into the cross flow filter design included: 1) a radiused flange section which eliminates stress risers, and provides a more delamination-resistant filter body and 2) incorporation of a mid-ribbed bond (MRB) configuration. The MRB provides a symmetric plate design that has improved manufacturing characteristics, and eliminates high stress sharp channel corners by moving the bond to a low stress region.[5]

Initial scaleup of the filter element to commercial size (30.5 x 30.5 x 10.2 cm - 12 x 12 x 4 inch) and its testing was also accomplished. This testing included a very successful, 160 hour operation of an eight (8) element, four (4) module system under simulated PFBC conditions of the mid-rib bond cross flow filter design. The filters were flange mounted and compressively braced, an approach implemented to mitigate filter delamination. Post test inspection revealed that six (6) of the commercial scale filter elements had no structural damage but two (2) of the elements had suffered hairline delaminations that had apparently initiated from the mounting flange. Even with the delaminations, excellent filter system performance was achieved with outlet dust loadings ranging between 2 to 6 ppm.[3]

Following the subscale and initial full scale element testing summarized above, program emphasis was focused on integrated testing on pilot scale PFBC and gasification facilities. At the New York University PFBC facility located at the Antonio Ferri Laboratory in Westbury, New York, a Westinghouse cross flow filter system was integrated into the test facility and operated in two separate 50 hour test programs.[8] The filter unit consisted of five filter modules, each containing three filter elements,or fifteen total elements (30.5 x 30.5 x 10 cm - 12 x 12 x 4 inch). During the initial 50 hour test segment, operating at temperatures between 1300 and 1500°F (705 and 815°C), system pressure of 120 psia (8.3 bar), and filter face velocity of 5.2 ft/min (2.6 cm/sec) stable baseline operating pressure drop of 35 in wg (8.68 kPa) was achieved with simple pulse jet cleaning. Inlet PFBC dust loadings of 350 to 1056 ppm were reduced to outlet dust loadings of 2.9 to 8.9 ppm. Outlet cascade impactor dust sampling was also obtained that showed both loading and size distribution fall within published gas turbine tolerance requirements, Figure 1.4. In the second 50 hour test run, the filter was operated at a 10 ft/min (5.1 cm/s). Higher outlet dust loadings (up to 103 ppm) were encountered due to dust seal leaks that occurred after three of the five pulse valves malfunctioned and other facility operating problems were encountered.

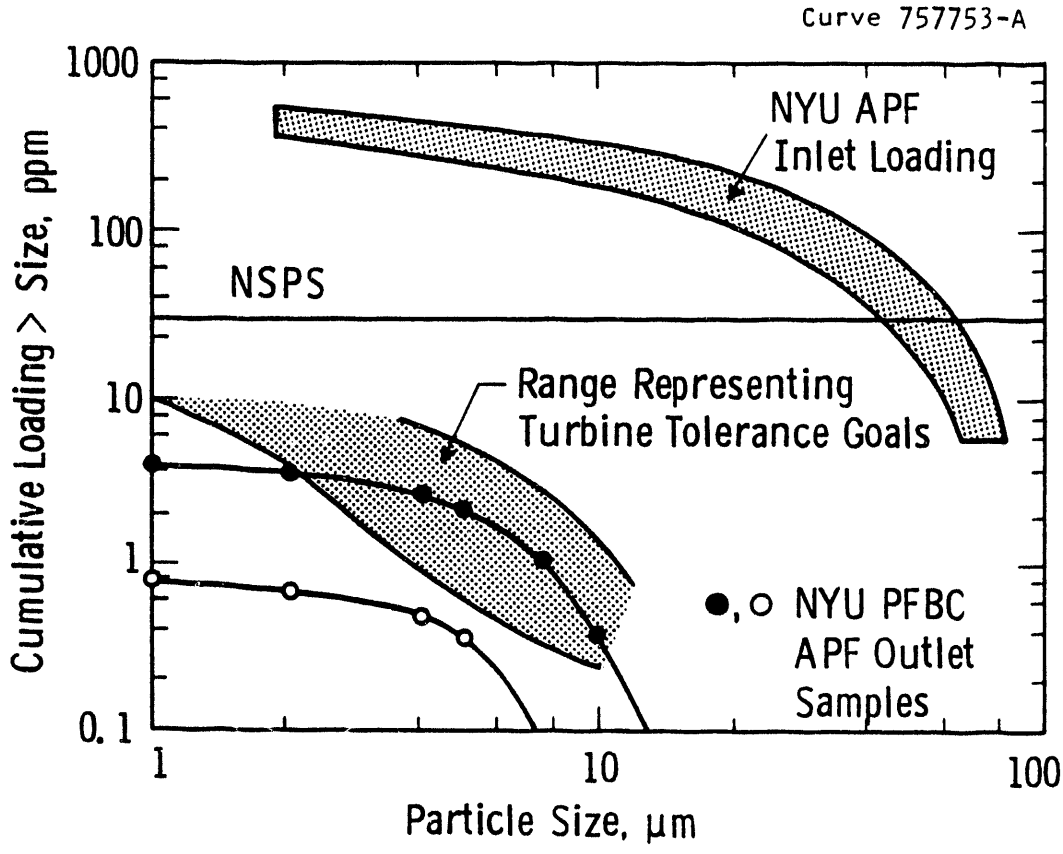

Figure 1.4 - Data Comparing Outlet Particle Size Distribution with Turbine Tolerance Goals

Inspection of the test unit showed that five of the fifteen filters had experienced hairline delamination cracks although none appeared to present a significant dust leak path. This testing also demonstrated that the 3M INTERAM® brand mat material used for gasketing was not sufficiently tolerant to temperature transients and was susceptible to eventual eroding from between the filter and its mount.

Concurrently with the PFBC testing, Westinghouse, under DOE/METC sponsorship (DE-AC21-88MC24021), initiated a program to test the ceramic cross flow filter on the Texaco entrained gasifier pilot unit located in Montebello, California.[7] In this test program, a four (4) element (and later eight (8) element) cross flow filter system was integrated with a 15 tpd Texaco entrained gasifier, wherein a number of hot gas desulfurization technologies were investigated. Except for the initial 48 hour long commissioning test, the filter unit operated in support of the Texaco base gasification/desulfurization program. Approximately 400 total hours of operation were attained that cover seven (7) different test runs and a range of flow conditions. Because of the high resistance to flow of gasifier ash and its low bulk density (high reentrainment potential), operating filter face velocity was maintained relatively low, 1 to 3 ft/min resulting in acceptable and generally stable baseline pressure drop.

Isokinetic sampling in the Texaco tests showed outlet dust loadings as low as 2 to 6 ppm, demonstrating the high collection efficiency potential of the filter in gasification applications. Filter flange and gasket failures were also encountered, but were corrected with the design and implementation of an improved high temperature filter mount and reinforced alumina fiber gasket. This same mount and gasket design were also implemented into the Long Term Durability test program described herein.

1.3 LONG TERM DURABILITY TESTING

Although cross flow filter field test programs provide opportunity for integrated operation in gas environments typical of large scale or commercial systems, they generally do not afford long operating periods. Also, filter test time is often compromised because of operational issues associated with the gasifier, combustor other ancillary equipment or because of other test priorities.

The Long Term Durability Testing of Ceramic Cross Flow Filter program reported herein was designed to provide dedicated filter test operations for test periods significantly longer than current pilot plant test programs. The program utilizes facilities that simulate coal based combustion and gasification process operating conditions to expose the filter to the mechanical and thermal stressing imposed in actual applications. By reentraining actual ashes obtained from operating plants, the basic filtration properties, such as collection efficiency, cleaning and filter permeance are evaluated.

1.4 REFERENCES

1. "Technical and Economic Evaluation of Ten High Temperature, High Pressure Particulate Cleanup Systems for Pressurized Fluidized Bed Combustion," DOE/MC19196-1654, July 1984.

2. Ciliberti, D. F., "Hot Gas Cleanup Using Ceramic Cross Flow Membrane Filters," Final Report DOE Contract DE-AC21-79ET15491, DOE/ET/15491-1565, December 1983.

3. Lippert, T. E. et al., "Performance Evaluation of a Ceramic Cross Flow Filter on a Bench-Scale Coal Gasifier," Final Report DOE/MC/21338-2749, September 1989.

4. Lippert, T. E. and D. M. Bachovchin, "Mechanical Analysis of a Ceramic Cross Flow Filter," Proceedings of Advanced Research and Technology Development (AR&TD), Direct Utilization and Instrumentation and Diagnostics Contractors' Review Meeting, Sponsored by PETC and METC, U.S. DOE, Pittsburgh, PA, pp. 164-171, 1988.

5. Ciliberti, D. F., T. E. Lippert, and R. N. Kleiner, "A Mechanical Analysis of a Cross Flow Filter," Proceedings of the Seventh Annual Gasification and Gas Stream Cleanup Systems Contractors' Review Meeting, Vol. 1, DOE/METC 87/6079, pp. 308-320, 1987.

6. Lippert, T. E., G. B. Haldipur, E. E. Smeltzer, and J. H. Meyer, "Performance Evaluation of a Cross Flow Filter on a Subpilot-Scale Pressurized Fluid Bed Coal Combustor," Final Report, Westinghouse Electric Corporation, DOE METC Contract No. DE-AC21-85MC22136, 1989.

7. Haldipur, G. B., T. E. Lippert, J. H. Meyer, W. C. Yang, M. A. Alvin, and N. D'Amico, "Subpilot Scale Gasifier Evaluation of Cross Flow Filters," Proceedings of the Tenth Annual Gasification and Gas Stream Cleanup Systems Contractors' Review Meeting, DOE/METC Contract No. DE-AC21-88MC24021, 1990.

2. EXPERIMENTAL TEST PLAN

This section describes the overall test plan used in the long term durability testing program. The plan includes overall test objectives, a description of the test facilities, a description of test procedures and criteria utilized in evaluating filter performance. At the beginning of the contract period, a formal experimental test plan document was developed and submitted to DOE. During the course of the program, this initial plan was modified as required to accommodate actual test events and learning experience. However, the program in general proceeded as originally planned. The test plan provides for efficient and cost effective long term testing of cross flow filters under simulated pressurized fluidized bed combustion (PFBC) and integrated gasification combined cycle (IGCC) filter process conditions.

2.1 OBJECTIVE

The objective of this work is to evaluate the long term mechanical and material stability of components used in the design and construction of ceramic cross flow filter systems, and to evaluate the stability of their filtration properties over time while operating at high temperature, high pressure (HTHP) conditions. The testing is accomplished using HTHP flow facilities that are capable of feeding combustor and gasifier ashes under simulated process conditions. The program provides for 3000 hours of testing under PFBC conditions and 2000 hours under IGCC conditions. The goal was to achieve this testing utilizing a single set of filter elements. For the IGCC conditions, this goal was achieved. In the PFBC testing, a total of 3080 test hours was accomplished, but events precluded the use of a single filter set. Two filters achieved over 1300 hours, three other filters 1000 hours and

one filter that was also utilized in the IGCC simulator testing had an accumulated exposure of over 2500 hours.

2.2 DESCRIPTION OF TEST FACILITIES

In this program, two high temperature, high pressure (HTHP) test loops were designed, constructed and operated. A photograph of the two test loops is shown as Figure 2.1. One test loop is a natural gas fired combustion facility that utilizes reentrained fly ash to simulate Pressurized Fluidized Bed Combustion (PFBC) process conditions. The second test loop uses recirculated gas that is electrically heated, and reentrained gasifier char and ash to simulate gasifier process conditions. A detailed description of these test loops is provided below. Both loops are installed in the same laboratory (building), sharing common service facilities and control room and could be operated in parallel. The laboratory has approximately 2042 ft^2 of floor area, 20 ft overhead height with a 5 ton X-Y hoist that provides full coverage for assembly and disassembly of the test systems.

2.2.1 PFBC Simulator Test Loop

The PFBC simulator test loop, shown schematically in Figure 2.2, is designed for a gas flow up to 1500 lb/hr and pressures up to 150 psig. This unit is an upgraded and larger version of an existing Westinghouse facility and utilizes many of the features of this earlier design.[1] In the upgraded design, the filter test unit is housed in a 3 ft (0.91 m) diameter, 10 ft (3.05 m) high refractory lined pressure vessel that is designed to contain hot gas up to 1650°F (900°C).

Thermal input is provided by the combustion of natural gas. A gravimetric dust feeder and pneumatic transport line are used to reentrain fly ash and produce a hot dirty gas at the filter test unit. The cleaned gas is exhausted through a water cooled exhaust line and through a water cooled back pressure control valve. Collected ash is

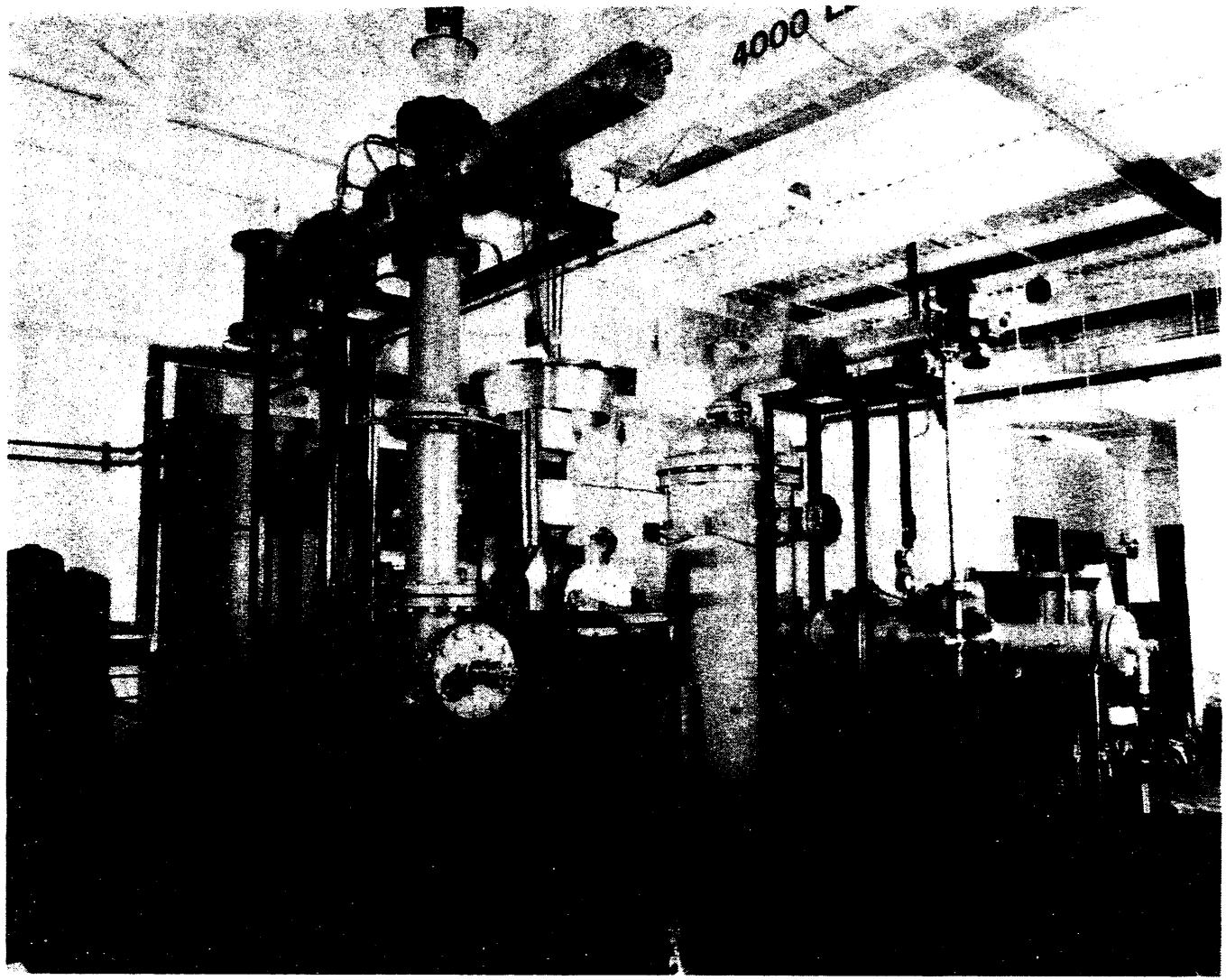

Figure 2.1 - Photograph of Westinghouse High Temperature, High Pressure IGCC and PFBC Simulator Test Loops

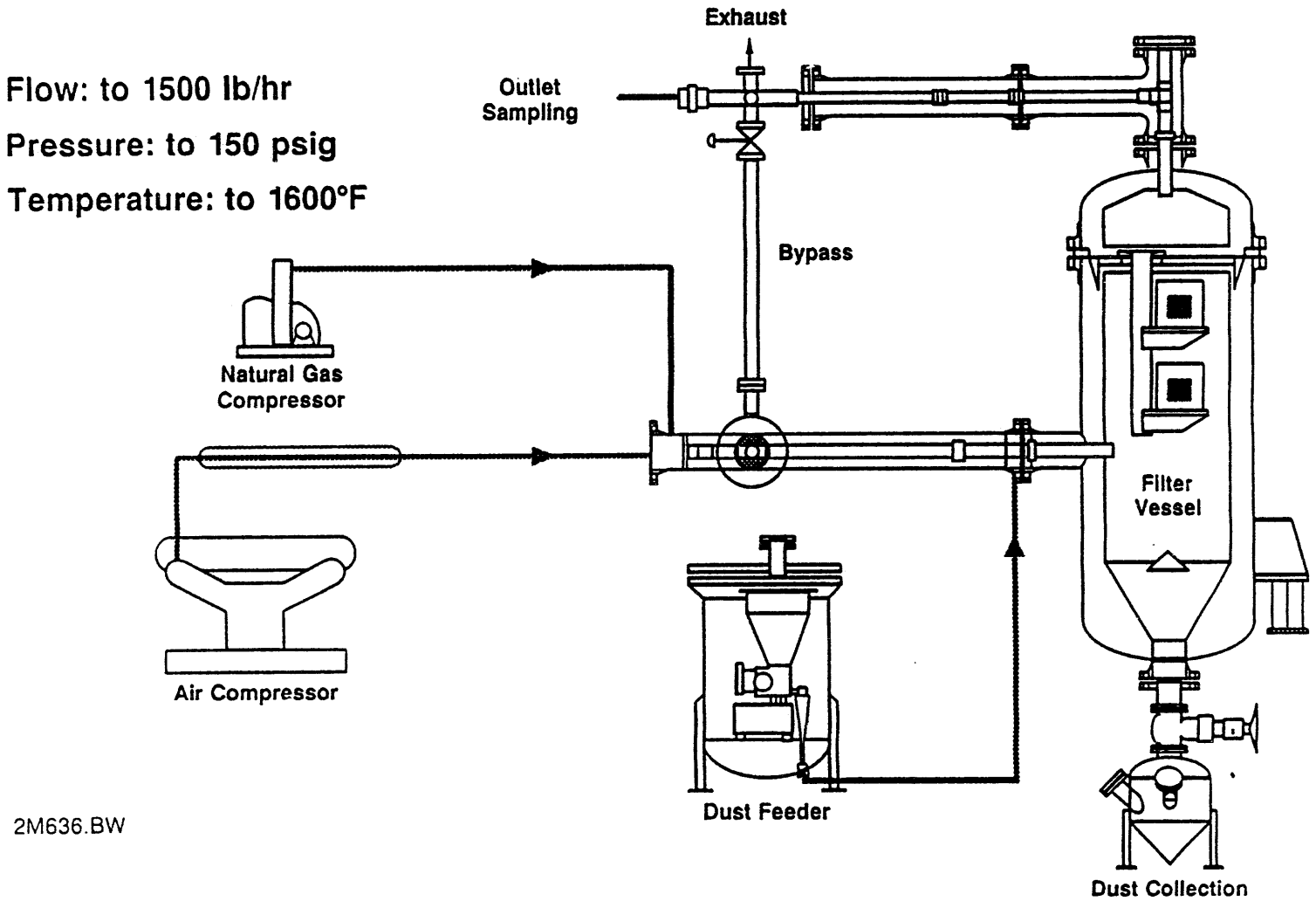

Figure 2.2 - Schematic of Westinghouse PFBC Simulator Test Loop

discharged from the filter by pulse-jet cleaning provided by a separate high pressure nitrogen source and controlled with fast acting solenoid valves. The discharged ash is collected in a hopper below the main filter vessel. This hopper is designed to be pressure cycled in order to remove the collected ash while filter operation is continued (or only minimally disrupted).

The test loop is fully instrumented and automatically controlled to set point conditions. A computer based control and data acquisition system is provided. The detailed Process and Instrumentation Diagram (P&ID's) and mechanical drawings of the major piping and vessel components are provided in Appendix A. A brief description of the subsystems comprising the PFBC simulator loop is provided below.

Gas Supply

The high-pressure air supply is a 75 hp two-stage reciprocating compressor that is capable of continuously providing up to 285 scfm (8.1 m^3/min) of air to 200 psig (14.8 bar). A second, 250 psig (18.2 bar), 130 scfm (3.7 m^3/min) unit is currently connected in parallel to the air supply and can be operated to extend the range of flow conditions to those required for this test passage, i.e., 100 actual cubic feet per minute, at a nominal pressure up to 150 psig (11.4 bar).

A natural gas fired combustor system is used to raise the temperature of the supplied air to a temperature between 1550°F (844°C) and 1700°F (927°C) at the filter and to give a gas composition that is representative of the combustion products from a PFBC facility. The approximate gas composition is:

Nitrogen	73%
Water Vapor	14%
Carbon Dioxide	7%
Oxygen	6%

assuming that the natural gas is all methane and that it all oxidizes to carbon dioxide. These are reasonable assumptions for the combustion conditions used for this test passage.

The combustor is fired on natural gas from a new, larger, oil-free compressor, that is used to boost house-supplied natural gas from 15 to 200 psig (2 to 14.8 bar) for use in the passage. The high-pressure natural gas is piped through the flow control valve directly to the combustor section of the passage. In this refractory-lined spool piece, a small aerodynamically shaped flame holder stabilizes the flame as the bulk of the passage flow is mixed and heated. It has been our experience that direct fired systems such as this prove to be very reliable systems operating at high temperatures.

Dust Feed/Metering System

The ash feed system consists of a K-Tron loss in weight powder feeder with a twin screw feed barrel, Model LWF20 with a capacity of 22.0 lb/hr (100 kg/hr). The feeder is enclosed in a pressure vessel sized to house both the feeder and storage hopper. A small quantity of pressurized air is used to entrain the metered ash and carry the ash into the main gas flow. PFBC fly ash obtained from various operating facilities is used.

Process Instrumentation and Control Devices

The passage flow, temperature, and pressure control system ensures accurate and constant passage test conditions. The flow control systems consist of conventional orifice plates with pressure, differential pressure, and temperature transmitters reporting to a standard utility type of recording mass flow controller. Temperature control is effected by sensing passage temperature and subsequent automatic adjustment of the fuel (natural gas) flow control valve. Passage pressure is maintained by a system back pressure control valve

and controller. All passage operating parameters are controlled, displayed digitally, and strip chart recorded at the main passage control panel, and transmitted to a computer for later data reduction and graphing.

The Piping and Vessel Design

The piping and device pressure housings are refractory lined, carbon steel pipe sections so that the pressure boundaries run at relatively low temperature. The inlet 8 inch diameter pipe section is provided in a length that minimizes heat loss while enabling a proper particulate/gas sample to be taken from the gas entering the filter housing proper. The system is configured for cross flow filter PFBC testing at high temperature and pressure.

2.2.2 Gasifier Char, HTHP Recirculating Gas Test Loop

The gasifier simulator test loop is shown schematically in Figure 2.3. The filter unit is housed on a 3 ft diameter (0.91 m), 10 ft (3.05 m) high refractory lined pressure vessel that is designed to contain the recirculating hot gases. This facility is a closed loop system that is electrically heated and designed to provide a HTHP reducing or inert gas environment, and permitting the feeding of gasifier char/ash materials. The system is first charged with a mixed (or inert) gas, pressurized and the gas circulated at a rate up to 1500 lb/hr (680 kg/hr) using a specially designed high temperature, high pressure eductor unit. Approximately 10 percent of the gas is extracted, cooled, recompressed, heated and then reintroduced as the motive gas flow to drive the eductor. The gas is capable of being heated to about 1200°F (650°C).

A gravimetric dust feeder and pneumatic transport line are used to reentrain the char ash and produce a hot dirty gas at the filter unit simulating gasifier filter operation. Collected char ash is discharged

RECIRCULATING GAS TEST LOOP

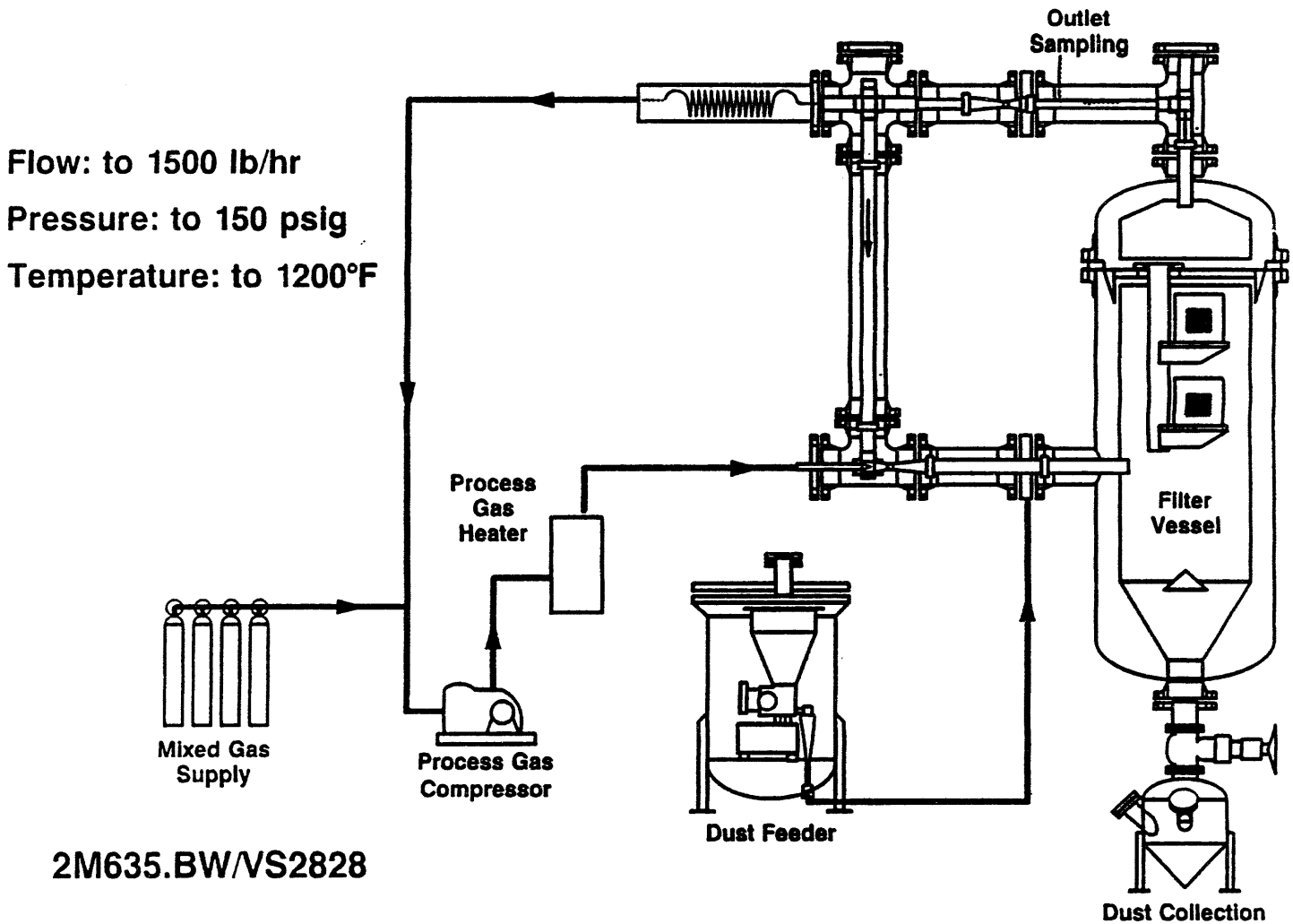

Figure 2.3 - Schematic of the Westinghouse Gasifier Simulator Test Loop

from the filter by pulse jet cleaning provided by the high pressure mixed gas (inert gas) source and controlled with fast acting solenoid valves. The discharged char ash is collected in a hopper below the main pressure vessel. This hopper is designed to be pressure cycled in order to remove the collected ash while filter operation is continued (or only minimally disrupted).

The test loop is fully instrumented and automatically controlled to set point conditions. A computer based control and data acquisition system is provided. The detailed process and instrumentation diagrams (P&ID's) and mechanical drawings of the major piping and vessel components are provided and described in Appendix B. A brief description of the subsystems is provided below.

Gas Supply

The gas supply for this system is provided by pre-mixing the desired gases. The gas flow rate is maintained at a minimum of 50 acfm (1.4 m^3/min). The temperature is controlled to between 900° and 1200°F (482 and 650°C) with a nominal value of 1000°F (538°C) during steady-state operation. Heating of the gas is achieved with electrical heaters. An electrical process gas heater is used to heat the high pressure motive gas mixture as it enters the closed system. A unit with a capacity of approximately 24 KW is used for this duty. Armstrong Engineering Associates, Inc. supplied a radiant furnace with an Incoloy 800 H helically wound coil to contain the gas for this service.

Throughout the rest of the gas flow path, electrical heaters are imbedded in the refractory lining to offset the heat loss from the system. Since this duty was estimated to be 0.2 KW/ft of piping, low heat flux, rugged service, heaters were utilized for this application.

The pressure can be maintained between 160 and 290 psia (11 to 20 bar) with a nominal value of 160 psia (11 bar) by pressure regulation

of the mixed gas reservoir. This high pressure gas supply is maintained with a small gas compressor that recompresses approximately 10% of the system flow that is used as the motive gas for the jet eductor, the dust feed system and the blow-back system. Since the system is of a closed loop, recycle design, once the simulated gas is introduced into the system and the test conditions are established, the gas composition remains constant.

Jet Eductor System

The jet eductor serves to recirculate the hot pressurized gas that must overcome filter and piping flow losses. The analysis, design and qualification of this key component is provided in Appendix C. The jet eductor pump operates by accelerating the heated motive gas flow through a convergent nozzle that is positioned at the inlet of a converging/diverging venturi. The venturi section connects the gas piping in the recirculation loop.

Dust Feed/Metering System

Dust feed to the system consists of redispersed and sized char, metered into the system by the powder feed system described for the PFBC loop. In this case a small amount of the pressurized motive gas is used to entrain the metered char into the test loop. The particle dust loading is between 1000 and 4000 parts per million by weight. Two sources of char were utilized: the filter catch from the KRW fluidized bed gasifier and a filter catch from the Texaco entrained bed gasifier.

Pulse Jet Cleaning System

Pulse jet cleaning of the cross-flow filters is accomplished using high pressure system gas from the motive gas compressor. System gas is used in order to maintain the gas composition. The gas is held in a pressure regulated reservoir at 300 to 500 psig (22 to 35.5 bar).

Fast acting, 1/2 inch pipe size solenoid valves are actuated with an electronic timer, with a typical "ON" time of 0.1 second. The solenoid valves have a block valve on either side so they can be changed during operation in case of a failure. The gas is released through a 3/4 inch tube nozzle into the filter plenum. This reverse flow of gas removes the collected dust from the filter. The blowback sequence can be initiated manually or automatically based on time or pressure drop.

Process Instrumentation and Control Devices

The passage flow, temperature, and pressure control systems ensure accurate and constant passage test conditions. A jet eductor pump is used to recirculate the hot, pressurized gas. Flow is increased or decreased by controlling the quantity of motive gas used to drive the eductor (see Appendix C). Temperature control is accomplished by sensing passage temperature and adjusting the process gas and the electrical heaters to compensate for heat losses. Passage pressure is maintained by a pressure relief control valve and controller. All passage operating parameters are controlled, displayed digitally, and recorded on a strip chart at the main passage control panel. The data is also stored on a computer for data reduction and graphing.

Piping and Vessel Design

The piping and device pressure housing are refractory lined carbon steel pipe sections so that the pressure boundaries remain at relatively low temperature. A 2 inch (5.1 cm) diameter stainless steel liner is used to separate the process gas stream from the refractory material (e.g., Fiberfrax or castable ceramic). The inlet pipe section is provided in a length that minimizes heat loss while enabling a proper particulate/gas sample to be taken from the gas entering the filter housing proper, if required. The pressure boundary is 8 inch (20.3 cm) diameter carbon steel pipe and the filter vessel is a 40 inch (1.02 m) diameter coded pressure vessel with a 30 inch (0.76 m) diameter liner.

The filter vessel has an internal straight section, from the tube sheet used to support the filters to the start of a discharge cone section, of approximately 6 feet (1.8 m). This provides adequate volume for positioning the filters to be tested and enough flexibility to test a wide variety of configurations. Electrical heaters in the pipe and vessel maintain the desired operating temperature by compensating for the system heat losses.

2.3 OPERATING PROCEDURES AND TEST CRITERIA

This section describes the overall operation of the test facilities and summarizes the criteria used to evaluate filter system operation.

Facility Operation

In general, both test loops were operated in parallel, which provided scheduling, manning and cost benefits. Two different test approaches were utilized. One approach was to operate the facility over a 12-hour test day period (7:30 am to 7:30 pm) followed by a shutdown and restart the following morning, continuing Monday through Friday. The overnight shutdown resulted in only a partial cooldown of the facility, thus allowing a hot restart of the test unit. The second approach was to operate the facility 24-hours per day over a 5 day period followed by a weekend shutdown. In both scenarios, the weekend shutdown would result in a cold restart the following Monday. It was concluded that both hot and cold restarts were important operating modes and would be included in the test program. Specific PFBC plant transients corresponding to plant startup and turbine trip were also identified and repeatedly simulated in one segment of the test program. A second segment in the PFBC simulator testing included accelerated pulse cleaning. Table 2.1 outlines the range of operating parameters incorporated in the test program. System pressures were below maximum values to maintain a high volumetric flow and keep filter face velocity as high as possible when utilizing more than one filter element.

Table 2.1
Summary of Test Facility Operating Parameters
Utilized in the Test Program

Test Parameters	PFBC Simulator	Gasifier Char/Ash Recirculating Gas Loop
Operating Pressure, psig	85 to 165	85
Operating Temperature, °F	1500 - 1600	350 - 1200
Dust Loading, ppm	1000 - 2000	1000 - 2000
Ash Type	PFBC	Gasifier Char
Filter Face Velocity, ft/min	3 - 10	2 - 5
No. of Filters Tested at One Time	2 - 4	2

In the gasifier char/ash recirculating gas loop, system temperature and pressure were varied to increase gas density. This provided test flexibility to reproduce potential reentrainment effects of low particle to gas density ratios representative of actual entrained gasifier environments.

Test Criteria

Filter evaluations were based on the following performance criteria:

- Outlet dust loading
- Collection efficiency (>99%)
- Baseline pressure drop (<100 in H_2O)
- Stability of baseline pressure drop, i.e., constant filter permeance
- Materials characterization

1. Outlet Dust Loading

In advanced coal based power generation application, the purpose of the hot gas filter is to remove sufficient particulate to meet regulatory stack gas emission requirements and protect downstream components (such as the gas turbine and heat exchange components) from particle erosion and deposition. Requirements for the latter depend on manufacturing specification and overall process integration of this equipment into the plant. It is generally accepted that both particle loading and particle size distribution are important in the erosion and deposition mechanism. Thus, criteria for turbine protection is likely to include both loading and particle size distribution.

In the long term durability test program, outlet dust loading is determined from simple isokinetic extractive grab samples that are suitable for gravimetric analysis and subsequent particle size analysis if desired. The particle size distribution is determined using coulter-counter or x-ray sedimentation methods. It is noted, however, that

under normal filter operating conditions, the quantity of dust collected on the outlet sample is small (even with relatively long sampling times) and not generally amenable to size distribution analysis. When sufficient dust quantity is collected, it is generally indicative of a dirty side breach or failure in the filter. In these cases, the outlet size distribution is expected to be the same as the inlet. In the test program, outlet sampling was conducted nearly continuously. This is accomplished because the outlet sampling system is designed with an isolation valve that permit removal and quick replacement of the collected sample. Thus, a continuous outlet loading history of the testing is obtained. This is extremely beneficial since the sampling can also be used to pinpoint dust leaks indicative of filter or system failures and correlate these events in time with various operating events.

2. Collection Efficiency

Filter collection efficiency (1- outlet loading/inlet loading) x 100 is a parameter measuring the fraction of the inlet dust removed and is of general value in comparing the relative performance of different filter devices. It depends on knowledge of both inlet and outlet loading. In the long term durability testing, the inlet loading is not sampled but calculated from the dust feed rate based on the loss-in-weight gravimetric dust feeder and material gas flow. Experience has shown that inlet dust loadings based on these measurements is as reliable and accurate as extractive sampling techniques.

3. Baseline Pressure Drop

Equation 2-1 relates the gas pressure drop through the filter media and ash cake to the filter and cake physical properties and process parameters of the operating system.

$$\Delta p = \frac{\mu V}{K_f} + \frac{\mu C V^2 \theta}{\rho_c K_c} \qquad (2\text{-}1)$$

where

μ = gas viscosity
V = filter face velocity (actual gas volumetric flow/filter area)
C = dust concentration
θ = time
ρ_c = bulk density of the dust cake
K_f = filter permeance
K_c = cake permeance

Baseline pressure drop in this test program is defined as the gas pressure drop through the filter immediately following the cleaning event and is represented by the first term of Equation 2.1, i.e.,

$$\Delta p_{bl} = \frac{\mu V}{K_f} \qquad (2\text{-}2)$$

The filter permeance, K_f, establishes the baseline pressure drop and may be considered a property of the conditioned filter media. It is generally accepted that in barrier filter devices, that some quantity of ash will become trapped in the surface pore structure of the filter media and become a permanent layer that contributes significantly to filter permeance.

Low filter permeance leads to high baseline pressure drop with corresponding parasitic loss in cycle energy efficiency. Also, high baseline pressure drop can adversely impact the design and integrity of the metal structures used to support the filter system. Increasing filter surface area to reduce face velocity and therefore pressure drop can adversely impact system economics.

In the long term durability testing, baseline pressure drop is directly measured by differential pressure measurements made across the filter unit. This data is recorded and displayed on strip charts.

4. Stability of Baseline Pressure Drop (Constant Filter Permeance)

Following an initial filter conditioning period, it is required that the filter display "stable" baseline pressure drop characteristics to maintain operability. Thus, effective cleaning of the filter (dust cake removal) must occur. Effective cleaning depends on a variety of physical and operating parameters such as ash cake properties, and the design and operation of the pulse gas system. Detailed analytical models have been developed to help guide the design and operation of the filter cleaning system. The reverse cleaning pulse intensity generated on the filter clean side represents one of the most significant parameters in the cake removal process.

In the long term durability testing, periodic measurements were made of pulse gas intensity. This was accomplished by placing a small diameter pressure tube on the clean side of the filter plenum and connecting the tube to a fast response differential pressure transducer. The transducer output was recorded on a high-speed oscillographic recorder.

Ash cake properties such as cohesivity, adhesivity and flow resistance are also important in establishing pulse gas cleaning requirements. These parameters may vary widely with ash type and as yet have not been well defined or characterized for hot gas systems.

5. Material Characterization

A wide range of analytical and microscopic methods are available for examining and evaluating both dust and filter materials. The porous ceramic material used in manufacturing barrier filters generally contain

an amorphous (glass) phase and possibly clay binders that can react to gas phase alkali and/or steam. Crystallization of the amorphous phase can occur at process temperatures which may cause a mismatch in the thermal/physical properties of the ceramic matrix. Subsequent thermal cycling may result in microcracking and loss of material strength, or perhaps failure. In the long term durability program various analytical techniques were applied to evaluate material response of the filter exposed to testing.

2.4 REFERENCES

1. Ciliberti, D. F., "Hot Gas Cleanup Using Ceramic Cross Flow Membrane Filters," Final Report, DOE Contract No. DE-AC21-79ET15491, DOE/ET/15491-1565, December 1983.

3. SUMMARY OF TEST RESULTS

This section describes the sequence of testing, events that occurred during testing, and summarizes results from both the PFBC and gasifier simulator testing. Section 4 provides an evaluation of these test results, compares this simulator data to actual plant filter data and, generally assesses cross flow filter development.

3.1 OVERVIEW

PFBC Simulator Testing

Approximately 3080 hours of cross flow filter testing was accomplished in the PFBC simulator facility, but events precluded the use of a single set of filter elements. In this testing, fifteen (15) different cross flow filters were utilized in sets of either two (2) or four (4) and exposed to steady state and/or thermal transient testing. Six (6) of the fifteen (15) filters failed as a result of inadvertent exposure to severe thermal transients.

Four (4) cross flow filters were exposed to programmed thermal transients simulating repeated PFBC plant startup, turbine trip and accelerated pulse cleaning. Two of these filters experienced partial delamination cracks but no significant dust penetration was experienced. Delaminations are hairline cracks that occur along the plate seams that are formed during the current cross flow filter manufacturing process. Flawed, or incomplete, bonding can occur along the seams during filter manufacturing that provides active sites for initiating delamination.

Two (2) filters achieved over 1300 hours of testing but then experienced cracks in their mounting flange. This resulted in

measurable outlet dust exceeding New Source Performance Standards (NSPS) and the testing of these elements was therefore terminated. A redesign of the filter mounting system was made and implemented. In subsequent testing, no further flange failures were experienced.

Three (3) filters experienced over 1000 hours of testing and a fourth filter, that was initially utilized in the gasifier testing rig, had an accumulated exposure of over 2500 hours.

In the early portions of the PFBC filter durability testing, failure in the filter mount gasketing system was experienced. This earlier gasket design utilized the 3M INTERAM® gasket media originally developed for automobile catalytic support insulation. This material performs well in short term tests but will vitrify under PFBC temperature conditions and eventually erode. A modified gasket was developed by Westinghouse that uses a contained ceramic fiber mat. This gasket has performed without failure or leakage in all subsequent filter testing.

In the PFBC simulator testing, filter performance in general was excellent, with low outlet dust loadings (<1 ppm on average) and stable and acceptable baseline pressure drop.

Gasifier Simulator Testing

Over 1900 hours of cross flow filter testing was accomplished in the gasifier char, gas recirculating test loop utilizing a single set of filter elements. No filter failures were experienced in this testing.

The filter used in this testing was from the same manufacturing lot as the filters in the PFBC testing. Stable pressure drop characteristics and excellent particle collection efficiencies were achieved. Outlet particle loadings were in general less than 1 ppm on

average. Testing utilized chars obtained from both the KRW fluid bed and Texaco entrained bed gasifiers.

Most testing in this loop was conducted at relatively low temperature <500°F (<260°C) in an attempt to reproduce entrained gasifier gas density conditions. The low bulk density of gasifier char/ash and relatively high fuel gas density (high gasifier pressure), provides high potential for fines reentrainment due to drag effects. The operating pressure of the Westinghouse gasifier simulator facility was limited to less than 100 psia (6.9 bar). Therefore, to reproduce the reentrainment potential of actual gasifiers, required operating in the simulator at reduced gas temperatures.

3.2 PFBC SIMULATOR FILTER TESTING

Table 3.1 shows a summary of test filters and cumulative operating experience. A summary of test experience of each filter set is given below.

Filters WRTX-11 and WRTX-1

These filters were separately tested in the existing, smaller PFBC simulator rig to achieve initial filter conditioning and qualify other filters from this same manufacturing lot for use in a DOE field test program (DE-AC21-88MC24021). The intent was to then mount these filters into the new long term durability test loop whose construction was in the process of being completed. This initial testing showed acceptable filter permeance and qualified the balance of the filters for field test implementation.

PFBC simulator testing on these filters was conducted on a 2 shift, 24 hour/day basis. After 127 hours of testing on filter WRTX-11, a facility operational problem caused combustor flame-out that

Table 3.1 -- Summary of Cross Flow Filter Testing
in PFBC Simulator Facility

Test Filter	Cumulative Test Hrs	No. of Pulse Cleaning Cycles	No. of Startup/ Shutdowns Standby	Cold
WRTX-11	127	123	15	6
WRTX-1	366	508	20	7
WRTX-9	1304	2068	43	6
WRTX-10	1304	2068	43	6
WRTX-48	335	472	12	12
WRTX-53	335	472	12	12
WRTX-66	38	3	2	4
WRTX-70	38	3	2	4
WRTX-76	1096	390	48	20
WRTX-77	1096	390	48	20
WRTX-78	1096	390	48	20
WRTX-81	320	141	5	5
WRTX-80	191	31	0	2
WRTX-84	104	32	8	2
WRTX-21*	2400	747	35	(73) 11

* Approximately 1900 hours accumulated in gasifier rig testing (see Table 3.6).

went undetected. This allowed full compressor flow of cold air to impinge on the hot filter subjecting it to severe thermal shock. Severe cracking occurred across the filter plates, but the filter remained intact on the mount with no evidence of delamination along plate seams.

Filter WRTX-1 was also conditioned in the existing and smaller PFBC simulator rig. Testing on this filter was initially interrupted after 278 hours when outlet loadings suggested some dust leakage. Subsequent examination showed the filter to be intact but a corner of the INTERAM® gasket had blown out. The gasket was replaced and testing continued.

After approximately 366 hours of exposure, a similar (to WRTX-11) thermal transient and subsequent filter cracking pattern was experienced. Testing was terminated and a modification made to the facility to incorporate an audible alarm to detect combustion flame-out and alert the operator to take appropriate actions to initiate opening of the filter bypass leg. Although combustor flame-out has occurred in subsequent testing, appropriate actions were taken and there has been no evidence of filter failures caused by inadvertent thermal transients in this test rig.

At this time, Westinghouse also undertook the development of a contained gasket seal that utilizes a silica-boria-alumina fiber mat and Nextel fabric. This gasket design was implemented in subsequent testing.

Figures 3.1 and 3.2 show the measured performance of cross flow filter WRTX-1. Filter permeance and measured outlet dust concentration are shown. Fitler permeance is defined and discussed in Section 4. The data points given in Figure 3.1 represent the filter system pressure drop (normallized for flow conditions) following each cleaning cycle. Figure 3.2 gives the filter outlet dust loading measured at regular intervals using isokinetic sampling techniques.

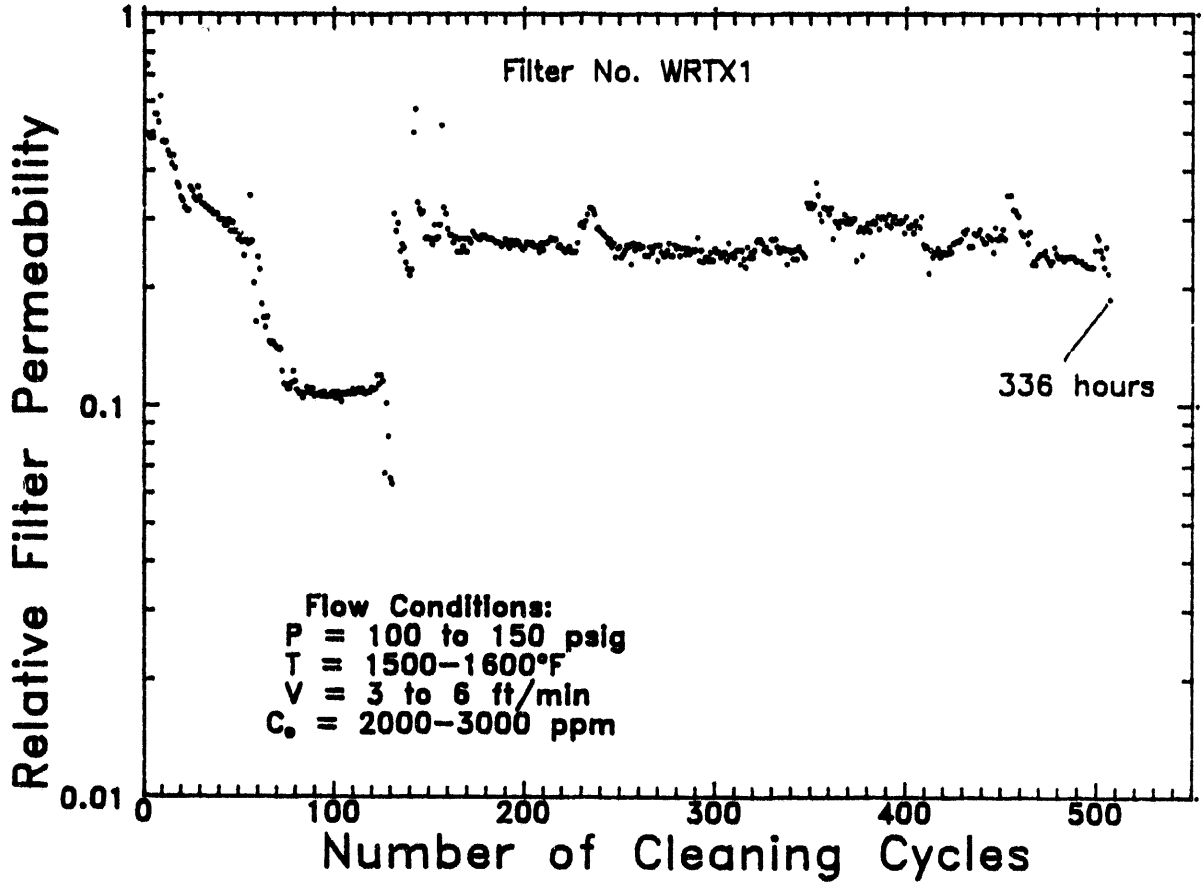

Figure 3.1 - Cross Flow Filter Permeance Trend in Long Term Durability Tests

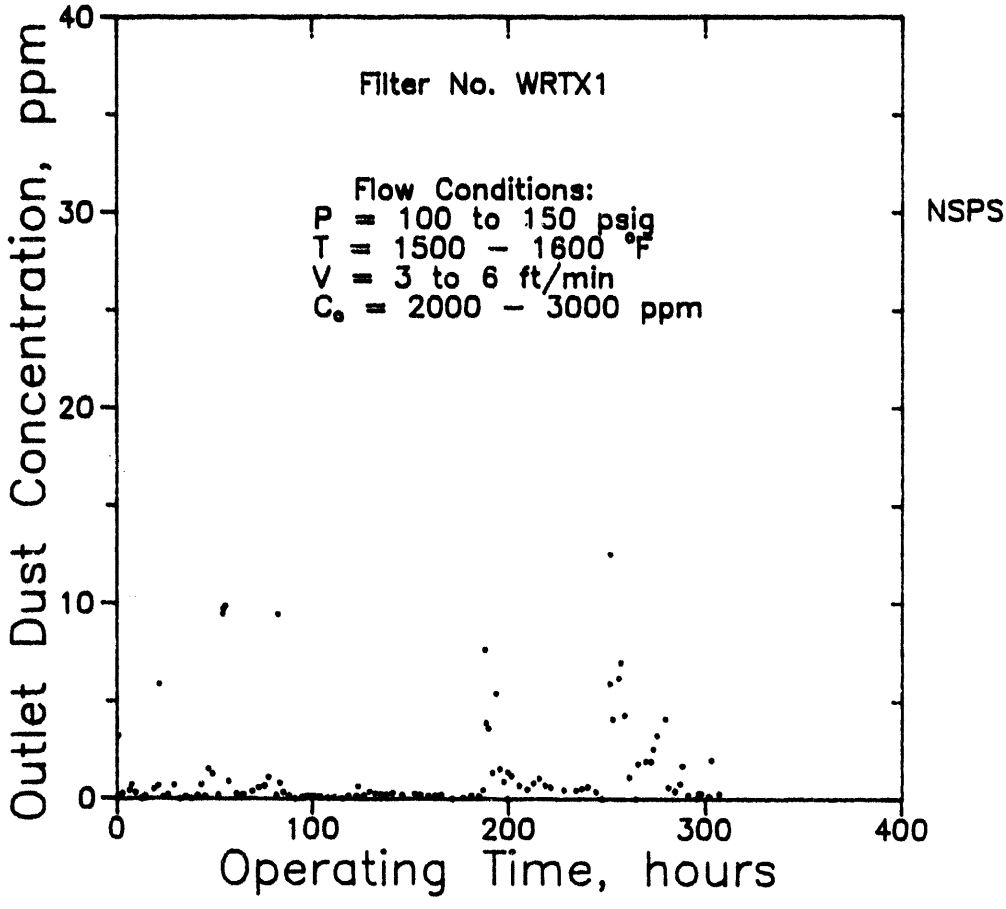

Figure 3.2 - Cross Flow Filter Outlet Dust Loading in Long Term Durability Tests

Steady state filter permeance ranged around 0.25 to 0.30, Figure 3.1, with the conditioned baseline pressure drop between about 7 to 10 in wg (2 to 2.5 kPa). In the early part of testing, filter permeance decreased to 0.10 but subsequent inspection showed the pulse nozzle to be misaligned. Figure 3.2 shows outlet dust loading measured over the course of testing. In general, excellent performance is indicated.

Filter WRTX-9 and WRTX-10

Filters WRTX-9 and -10 were installed in the new PFBC simulator rig. Each filter was mounted on its own plenum and cleaned with separate pulse nozzles. The Westinghouse upgraded, contained fiber mat gasket was utilized with the standard, horizontal flange mount. Approximately 1304 hours of operation were achieved with 2068 cleaning cycles, 6 cold starts and 43 startups from hot (~800°F, 430°C) standby. Table 3.2 provides additional operating history of this filter set. The filter was operated at face velocities of 6 and 10 ft/min utilizing two different PFBC ash materials. The specific pressure drop characteristics for this test run are provided by the computer developed traces given in Appendix D. Typically, the baseline pressure drop ranged around 12-14 inches wg at 6 ft/min (3 to 3.5 kPa at 3 cm/sec) and increased correspondingly at the 10 ft/min (5 cm/sec) condition.

Filter permeance (expressed as a ratio of actual to initial) for this testing is shown in Figure 3.3. Initial filter conditioning was achieved within the first 50 to 100 cleaning cycles with stable baseline operation achieved over the test period. Conditioned filter permeance appeared to range around 20 to 25%, completely acceptable for cross flow filters as evidenced by the low actual pressure drop characteristics (see Appendix D). Excellent filter performance was also achieved over the testing period as indicated by the outlet dust sampling, Figure 3.4.

At the 1304 hour mark, a sharp peak (100 ppm) in outlet dust loading was evidenced suggesting some breach between dirty and clean gas

Table 3.2 - Testing Summary - PFBC Simulator Filter Elements WRTX-9 and WRTX-10

	Operating Period, Hours			
	0-672	672-1188	1189-1258	1259-1304
Test Conditions:				
Gas Temperature, °F	1500-1600	1550-1600	1550-1600	1550-1600
System Pressure, psig	70	70	70	70
Inlet Loading, ppm	1000	1000	1000	1000
Ash Type	PFBC Exxon-Ground	PFBC Exxon-Ground	PFBC Grimethorpe	PFBC Grimethorpe
d_{50}, μ	6.1	6.1	5	5
Face Velocity, ft/min	6	10	10	6
Baseline ΔP, in. w.g.	8-13	15-19	16-20	12-14

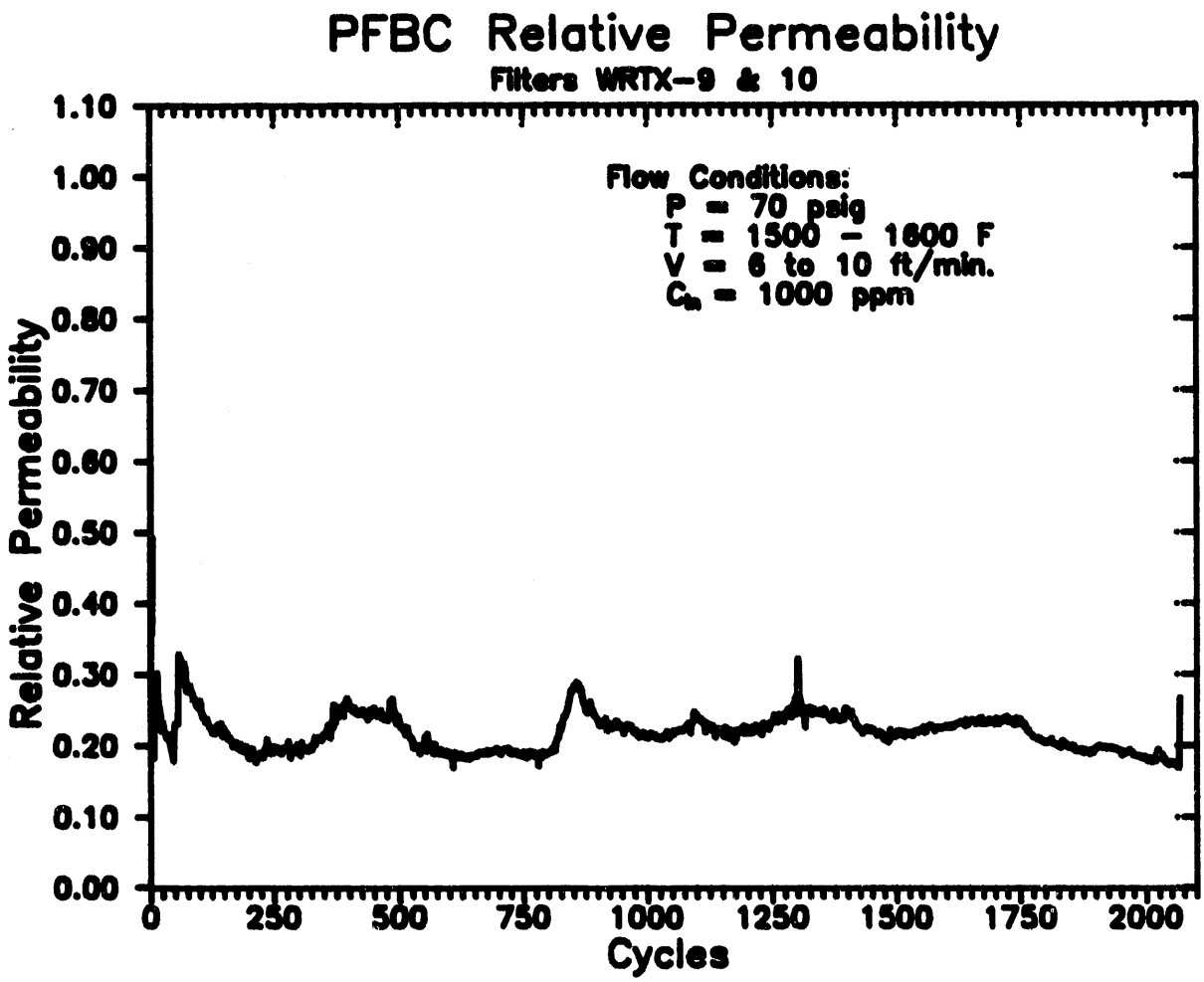

Figure 3.3 - Filter Permeance Trend in 1300 Hour PFBC Simulator Testing (WRTX-9 and WRTX-10)

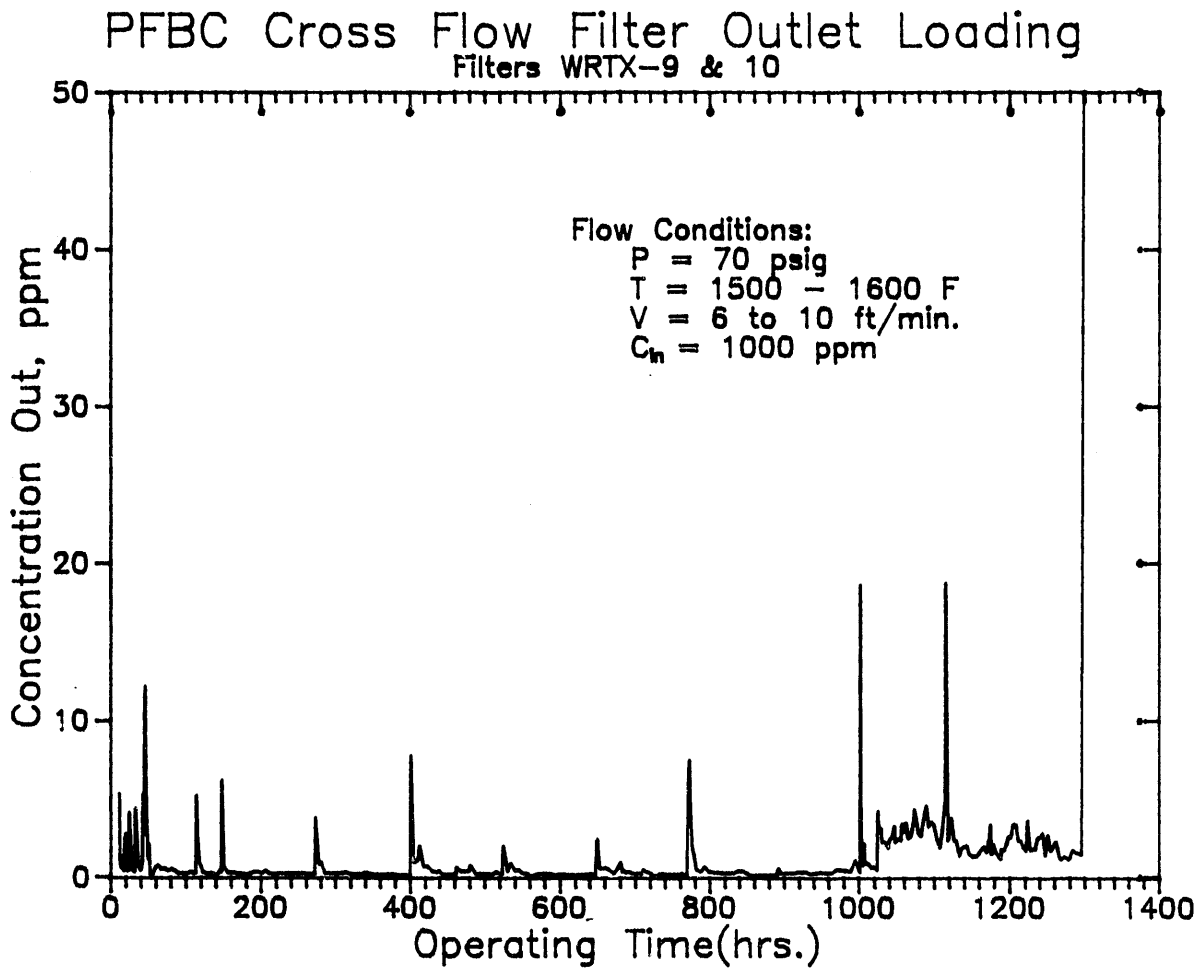

Figure 3.4 - Cross Flow Filter Outlet Dust Loadings Measured in 1300 Hour PFBC Simulator Testing (WRTX-9 and WRTX-10)

side had occurred. Testing was terminated and the filter unit inspected. A substantial crack along the flange of WRTX-10 had occurred which accounted for dust penetration, Figure 3.5. Filter WRTX-9 also exhibited a similar flange crack, but further inspection indicated there was no significant leakage of dust. Based on this test run it was concluded that the design of the filter mount was not optimum and led to the cracking of the filter flanges under the applied thermal and mechanical stresses. A comprehensive analysis of the failure and mount deficiencies was undertaken, and a revised mount design developed. This effort is described in detail in Appendix E. It is also noted that similar flange failures were being experienced in the field test program (DE-AC21-88MC24021). The revised mount design was implemented in subsequent in-house long term durability and field tests. No further flange failures were experienced in the PFBC simulator testing utilizing the revised mount design.

Filters WRTX-48 and WRTX-53

Following the testing of WRTX-9 and 10 described above, filters WRTX-48 and 53 were installed utilizing the revised mount design. Tables 3.1 and 3.3 summarize the initial 297 hours of operation of these filters under steady state conditions. In this time period, both filters experienced 469 cleaning cycles coupled with 8 cold facility starts and 10 hot restarts. At the 6 ft/min (3 cm/sec) face velocity, pressure drop was similar to the WRTX-9 and WRTX-10 testing. Outlet dust loadings were again low, averaging below 2 ppm.

Following this initial 297 hours, testing was halted and the filters were visually inspected and found to be in excellent condition. It was also decided at this point to implement thermal transient testing that would simulate PFBC startup and plant turbine trip conditions. Accelerated pulse cleaning transients were included. This work was in conjunction with Proof-of-Concept testing that was part of the DOE/AEP (American Electric Power) hot gas filter program (DE-FC21-89MC26042).

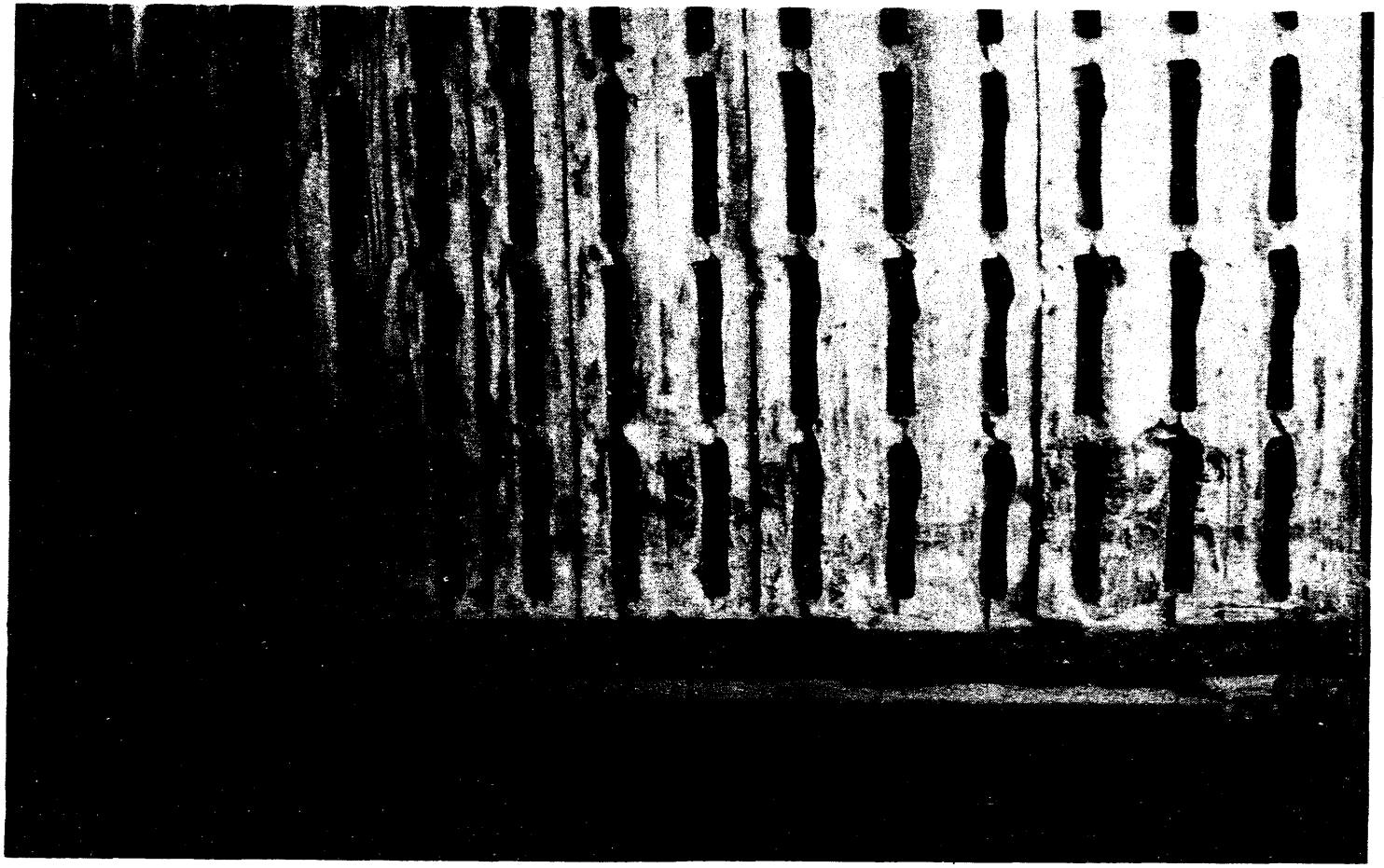

Figure 3.5 - Photograph Showing Flange Failure Experience in Cross Flow Filter WRTX-10

Table 3.3 -- Summary of Steady State PFBC Simulator Testing, Cross Flow Filter WRTX-48 and WRTX-53

	Operating Period, Hours
	0 - 297
Test Conditions:	
Gas Temperature, °F	1500 - 1600
System Pressure, psig	70
Inlet Loading, ppm	1000
Ash Type	PFBC Grimethorpe
d_{50}, μ	5
Face Velocity, ft/min	6
Baseline ΔP, in. wg.	2.5 - 10

For this purpose, two additional cross flow filters were added, filter WRTX-66 and WRTX-70.

Filter WRTX-48, WRTX-53, WRTX-66 and WRTX-70 (Thermal Transient Testing)

For this testing the filter system configuration was modified by placing two filters each on two separate plenum pipes. One pulse nozzle cleaned two filters, Figure 3.6. Initial transient testing was to simulate PFBC turbine trip conditions.

The simulated turbine trip transient, shown in Figure 3.7, produces a cooling of the gas passing through the filters. The transient is produced by shutting-off fuel flow an quickly increasing air flow and decreasing system pressure. The imposed thermal transient simulates the steepest gradient predicted to occur in an actual PFBC turbine trip scenario. In pursuit of simulating the turbine trip thermal transient, a significantly more severe transient (estimated to be about twice the thermal gradient) resulted and all four filters experienced partial or full delamination cracking. Testing was halted, and a more complete analysis undertaken to understand the projected thermal transients and how to better control them in the simulation testing.

Filter WRTX-76, WRTX-77, WRTX-78 and WRTX-81 (and WRTX-80 and WRTX-84) (Thermal Transient Testing)

Four new filters were installed, and thermal transient testing restarted. However, facility conditions were modified to better simulate actual PFBC transients (shown in Figure 3.7) and avoid the severe transients incurred in earlier testing. Table 3.4 provides a summary of the nominal test conditions corresponding to steady state conditions. Pressure drop and gas temperature during the transient testing are given in Appendix F. A total of 615 hours of testing was accumulated in this test period.

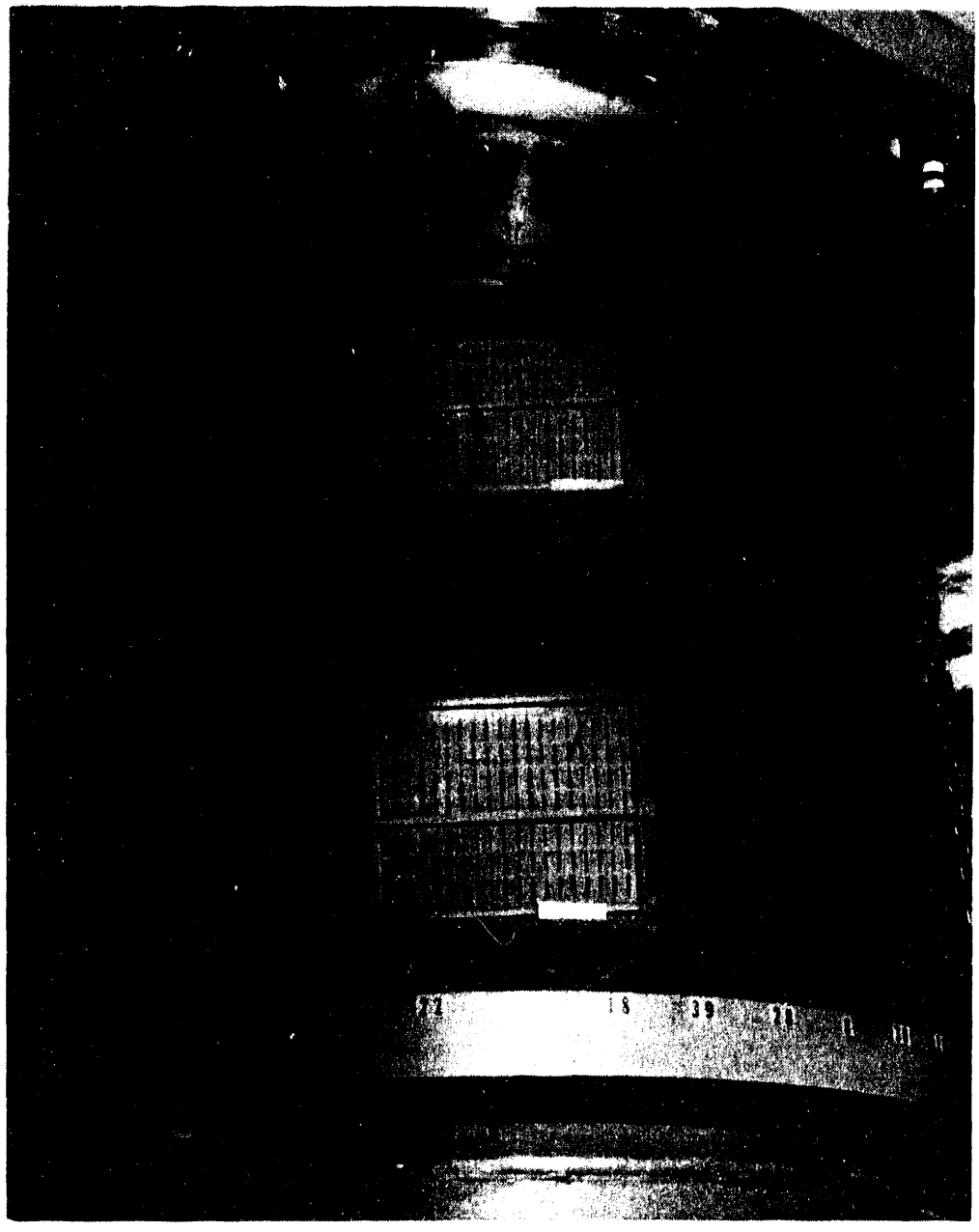

Figure 3.6 - Photograph showing two cross flow filter elements arranged on a single plenum pipe and cleaned with a single pulse nozzle. A second plenum pipe (not visible) is also present with two additional filter elements.

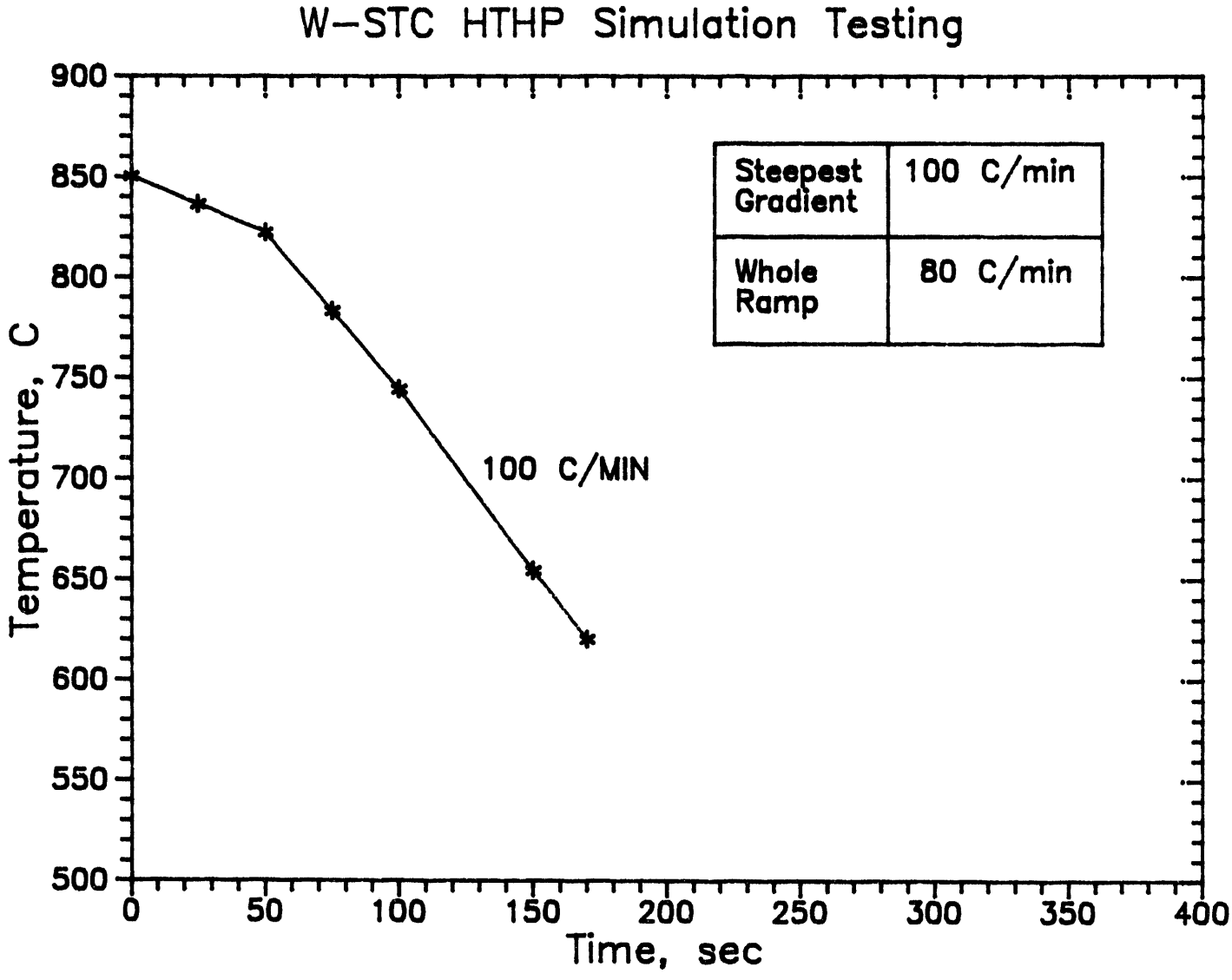

Figure 3.7 - Rapid Cooling Transient Testing PFBC Turbine Trip

Table 3.4 -- Summary of PFBC Simulator Testing Conditions (Nominal) Cross Flow Filter Elements WRTX-76, 77, 78 and (81, 80 and 84) (Including 10 Turbine Trip Transients, 90 Startup Transients, and 1000 Pulses)

	Operating Period, Hours
	0 - 615 (320, 101, and 104)
Test Conditions:	
Gas Temperature, °F	1500 - 1600
System Pressure, psig	75
Inlet Loading, ppm	1000
Ash Type	PFBC Grimethorpe
d_{50}, μ	5
Face Velocity, ft/min	4
Baseline ΔP, in. wg.	1 - 10

The first 300 hours were conducted at steady state to condition the filters and establish baseline performance. Following the steady operation, ten (10) turbine trip transients were conducted followed by a brief period of steady state operation. During this period (at about 320 hours) a small, but discernible, dust leak (about 10 ppm) was observed from outlet dust sampling. Inspection showed that filter WRTX-81 had experienced a small delamination, this filter was replaced with WRTX-80, and testing continued.

Again, about 70 hours (390 hours cumulative) of steady state testing was completed prior to initiating the second set of thermal transient tests. These tests simulated PFBC plant startup. Ninety (90) startup thermal cycles were conducted in groups of ten (10) followed by a period of dust feeding and outlet sampling. The outlet sampling was used as a means of detecting if any failure in the filters occurred during the particular thermal cycle sequence. The startup thermal transient testing covered about 124 hours (524 hours cumulative).

Following the last thermal transient tests a brief steady state test period was conducted. A small dust leak (~14 ppm) was again observed and the testing stopped and filter system inspected. Filter WRTX-80 (which had replaced WRTX-81) showed a delamination and was replaced with WRTX-84.

Thermal transient testing was continued. Accelerated pulse cleaning cycles were conducted under HTHP conditions. One thousand (1000) cycles were completed over a 50 hour period (574 cumulative hours) followed by a short 41 hour steady state test period (615 cumulative hours). Outlet dust loadings were very low suggesting no failed filters.

Testing was halted, however, and the system inspected. All filters appeared in excellent condition. Filter WRTX-84 was replaced with WRTX-21, taken from the gasifier char, recirculating test loop

(where it had achieved over 1900 hours of exposure). Testing in the gasifier char loop had been completed.

Filter WRTX-76, WRTX-77, WRTX-78, WRTX-21 (Steady State)

Following thermal transient testing and filter system inspection as described above, the system was reassembled and filter testing continued. Table 3.5 summarizes the normal operating conditions for this test period. A total of 480 additional test hours were achieved operating with a single shift, 12 hour per day schedule. Filter system pressure drop characteristics for this period are given in Appendix G. Typically, the baseline pressure drop ranged around 4 to 5 inch of wg indicative of the low face velocities. Maintaining the 4-element test configuration was chosen over higher face velocity (fewer filters) since all 4 filter elements had significant test history. Filter permeability and outlet dust concentration for this final test segment is shown in Figures 3.8 and 3.9, respectively.

Prior to system shutdown, it was decided to pulse clean only the filters on plenum pipe number 1. This would provide a visible contrast between a "dirty" and "pulse cleaned" cross flow filter after long term exposure to dust, Figures 3.10 and 3.11, respectively. These photographs suggest that during filtration bridging across channels will occur with considerable dust buildup over the filter face. Closure of some channels occurred. The cleaned filter shows substantial removal of the ash and appearance of opened channels. Following disassembly, the filters were inspected and found in excellent conditions.

3.3 GASIFIER CHAR, RECIRCULATING GAS TESTING

In this testing, two (2) cross flow filters (WRTX-20 and WRTX-21) were exposed to 1919 hours of testing that used two different types of reentrained gasifier char in a hot, pressurized inert gas flow. Over the test period, Table 3.1, the filters were pulse cleaned 561

Table 3.5 -- Summary of PFBC Simulator Test Conditions,
Cross Flow Filter Elements WRTX-76, 77, 78 and 21

	Operating Period, Hours
	616 - 1096 (1919 - 2400)
Test Conditions:	
Gas Temperature, °F	1500 - 1600
System Pressure, psig	80 - 100
Inlet Loading, ppm	1000
Ash Type	PFBC Grimethorpe
d_{50}, μ	5
Face Velocity, ft/min	2.5 - 2.9
Baseline ΔP, in. wg.	4 - 6

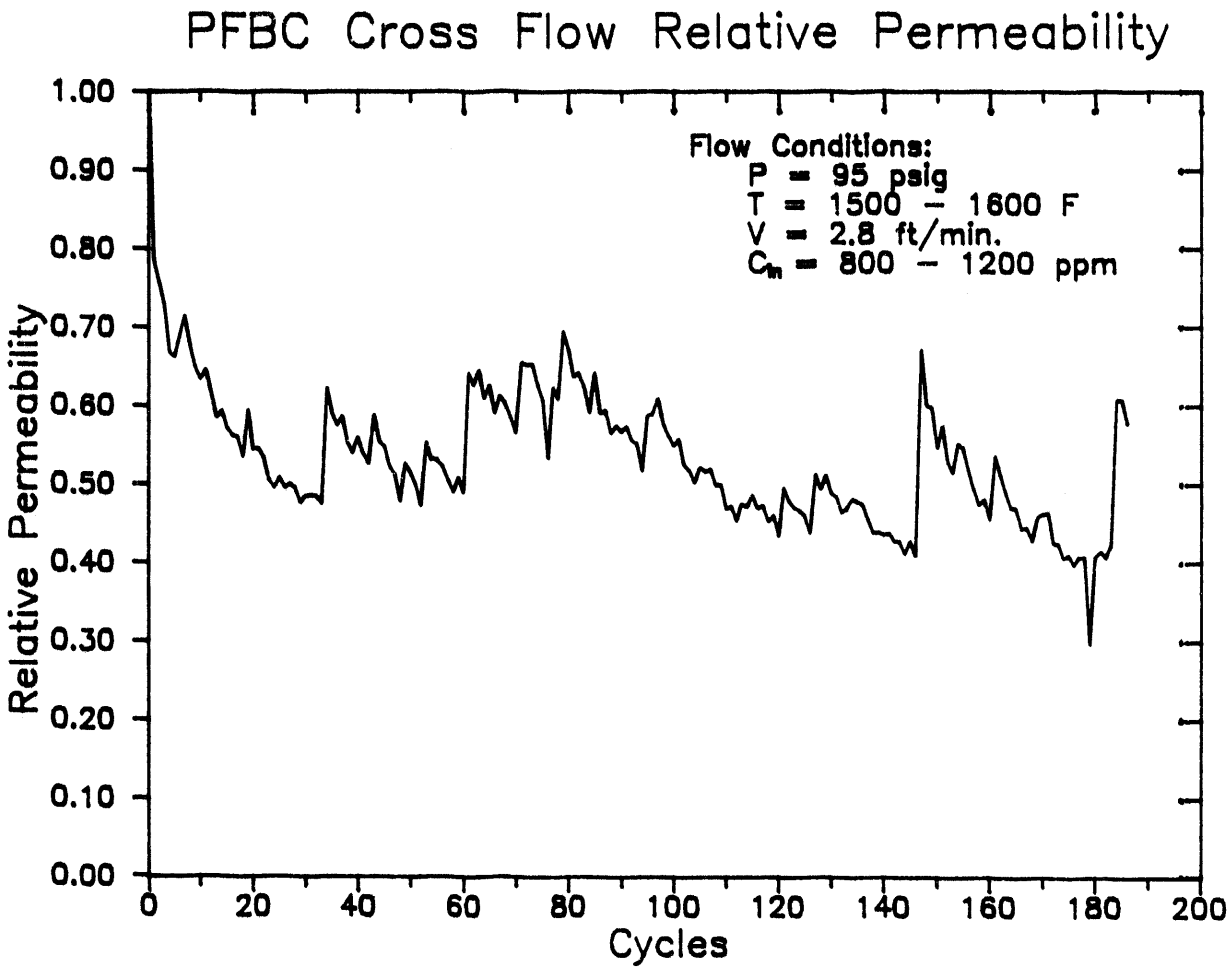

Figure 3.8 - Filter Permeance Trend During Final Steady State Test Segment, WRTX-76, WRTX-77, WRTX-78 and WRTX-21

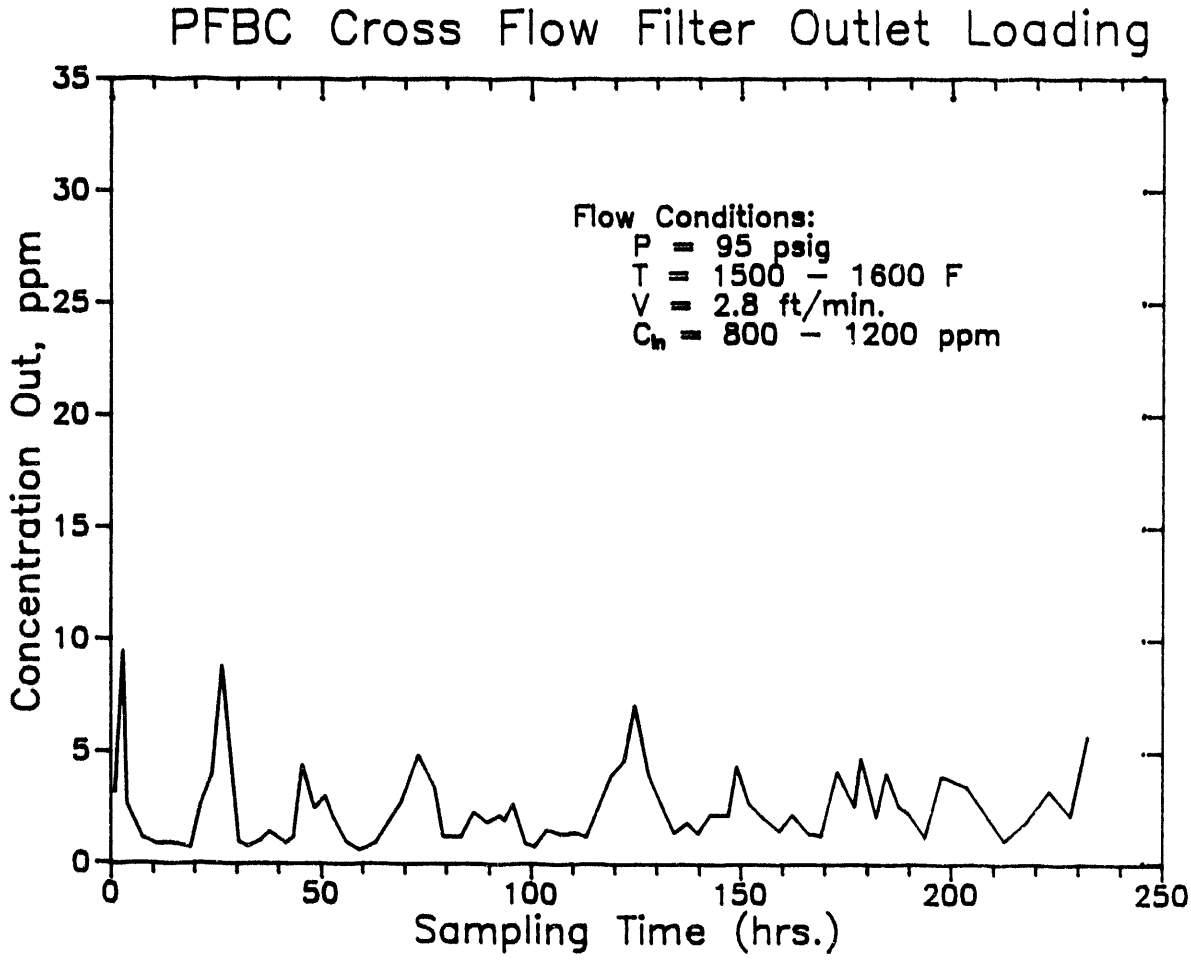

Figure 3.9 - Filter Permeance Trend During Final Steady State Test Segment, WRTX-76, WRTX-77, WRTX-78 and WRTX-21

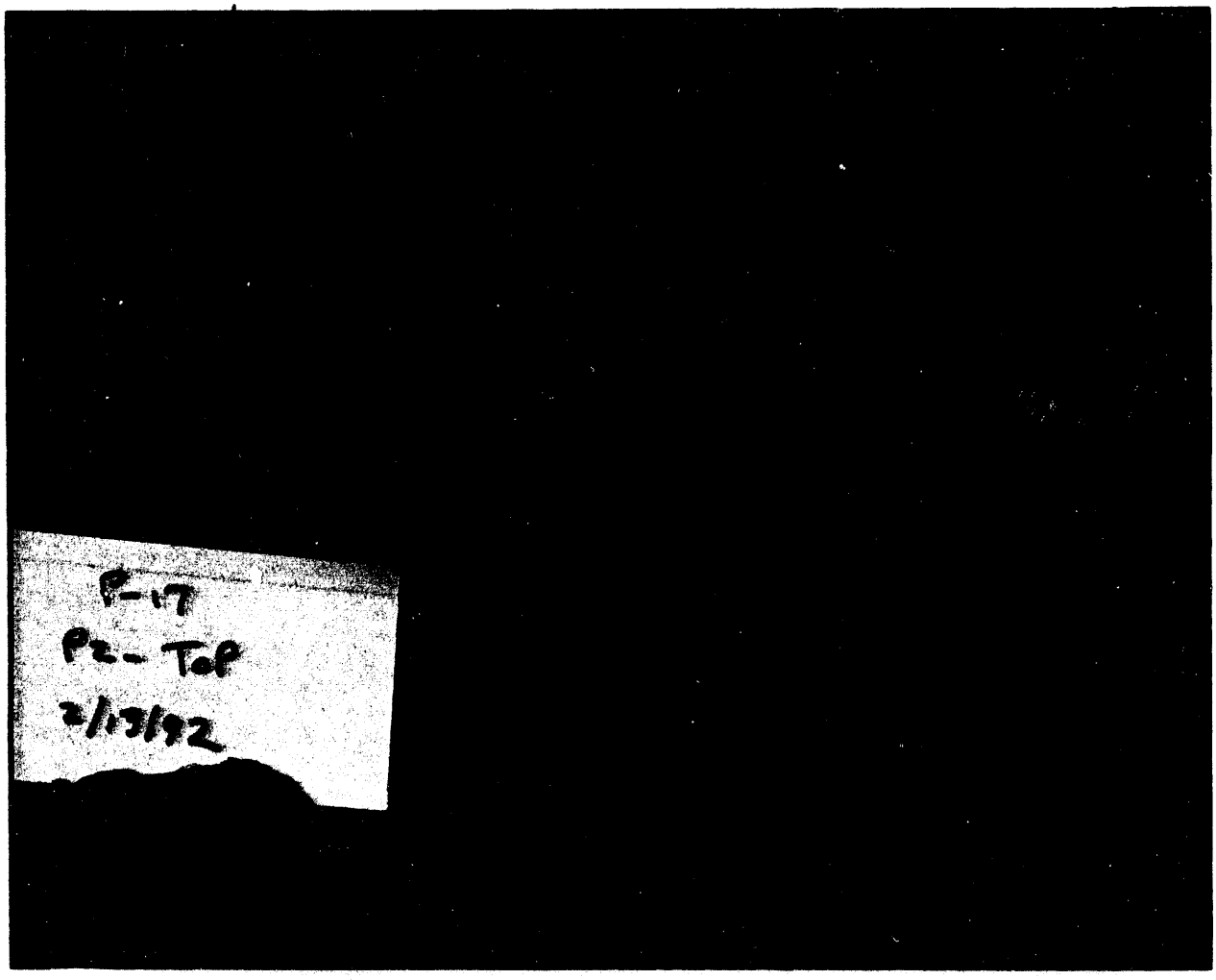

Figure 3.10 - Photograph Showing Condition of Cross Flow Filter Prior to Pulse Cleaning

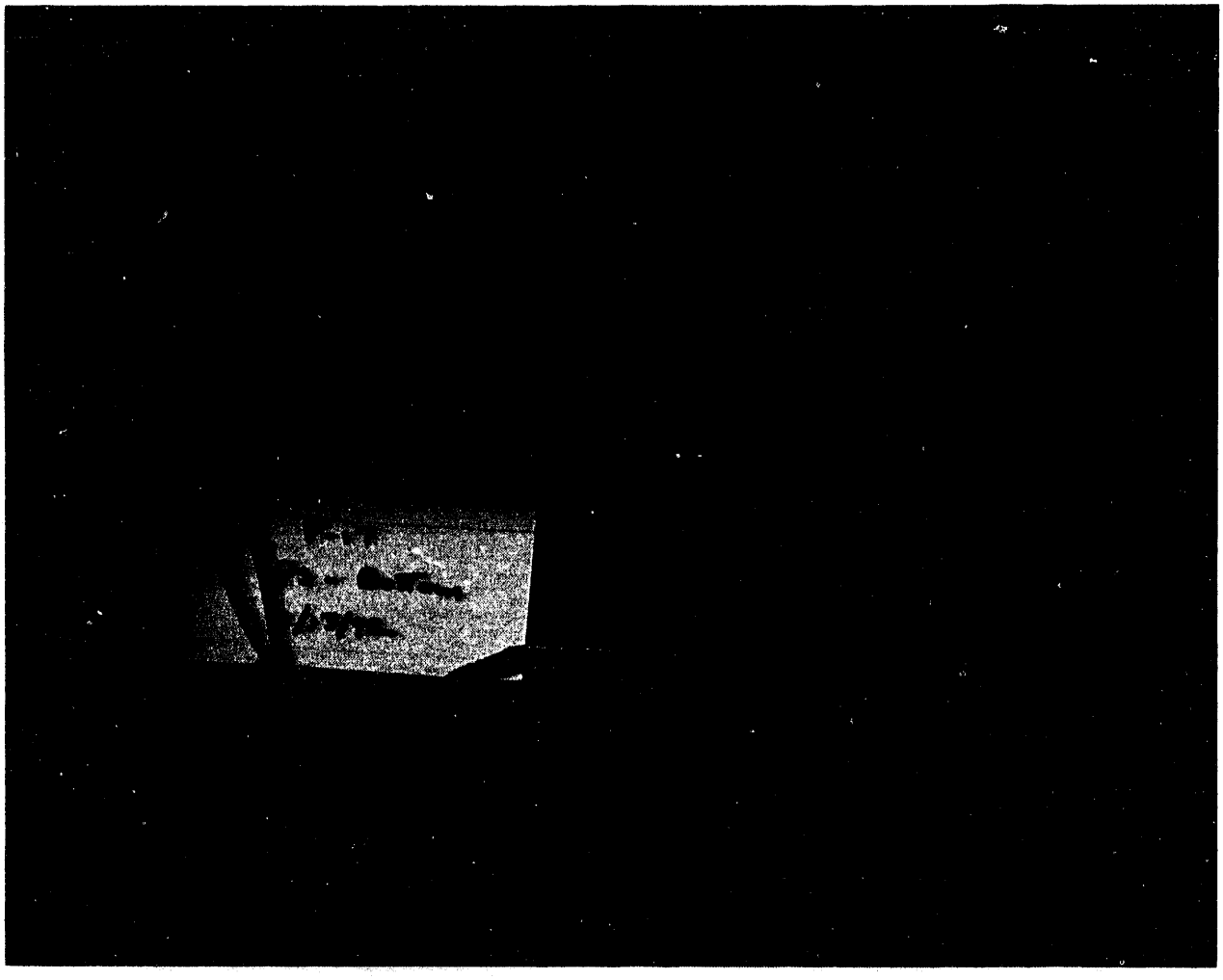

Figure 3.11 - Photograph Showing Cross Flow Filter After Pulse Cleaning

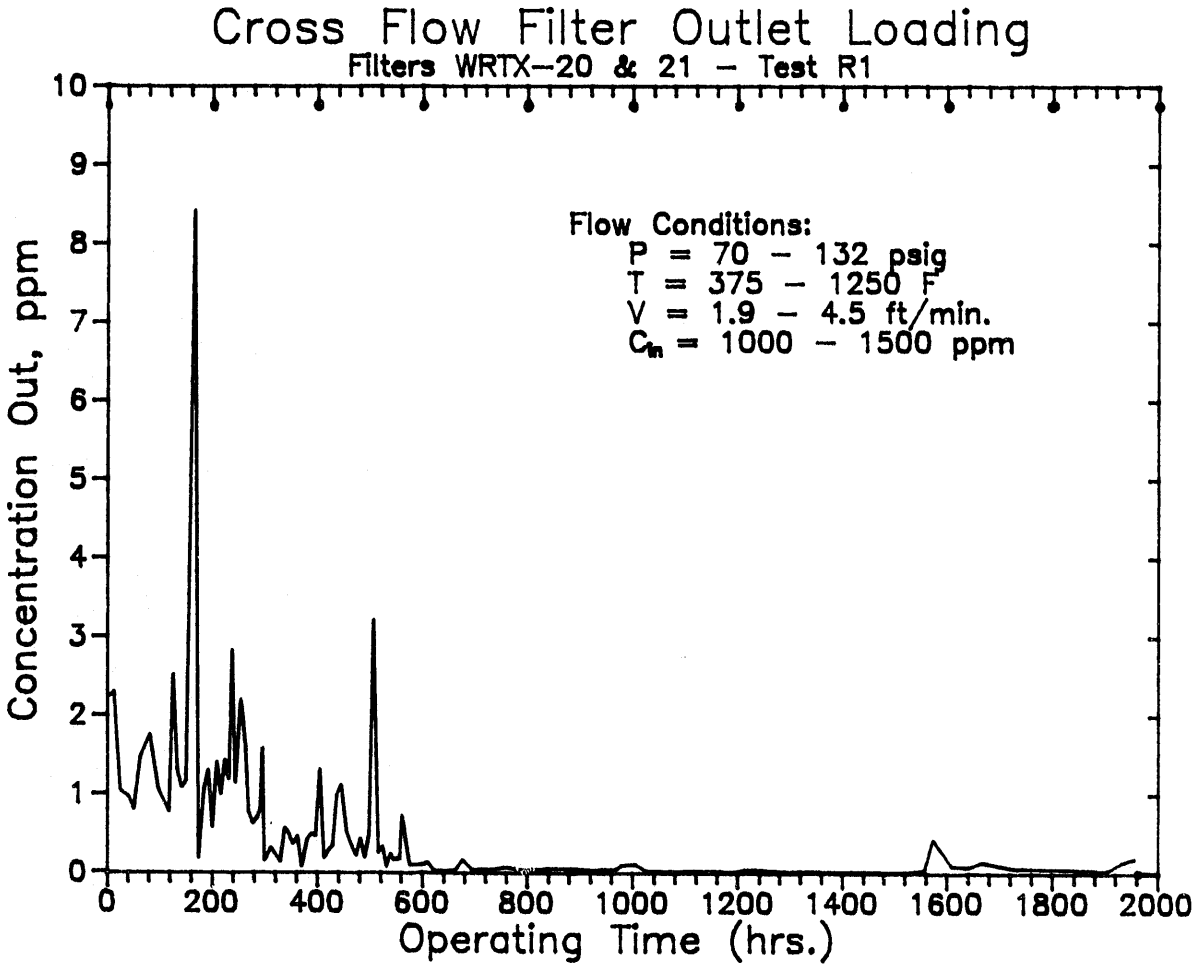

Operation Notes for Test R1
561 Cycles
1919 Hours Flow Exposure time

Figure 3.12 - Measured Outlet Dust Loadings During Cross Flow Filter Gasifier Simulator Testing - Filters WRTX-20 and WRTX-21

times, and experienced 73 startup/shutdown cycles. Testing was conducted over range of operating conditions (see Table 3.6). Filter face velocity was maintained at relatively low values corresponding to gasifier field test programs. Throughout the test program, filter performance was excellent with outlet dust loading averaging below 1 ppm. Figure 3.12 shows the measured outlet dust loading as recorded from isokinetic grab samples taken over the test period. In general, baseline filter pressure drop was low, ranging from 2 to 5 in wg, varying with face velocity and depending on operating temperature. Pressure drop traces from selected portions of the test program are given in Appendix H. Stable filter permeance appeared to be achieved after about 150 cleaning cycles, Figure 3.13.

Following test segment 6, the filter system was disassembled and inspected. Figure 3.14 shows a photograph of one pulse cleaned filter as it appeared on disassembly. Both filters were found to be in excellent condition. Filter WRTX-21 was placed into the PFBC simulator rig and was exposed to an additional 600 hours of testing under combustion conditions at 1550°F (nominal).

Table 3.6 - Summary of Cross Flow Filter Test Condition Exposed to Gasifier Char (WRTX-20 and WRTX-21)

Test Conditions:	Operating Period, Hours				
	(1) 0 - 458	(2) 459 - 766 and (3) 903 - 1311	(4) 767 - 902	(5) 1312 - 1493	(6) 1494 - 1919
Gas Temperature, °F	850 - 1200	334	334	334	334
System Pressure, psig	70	132	132	132	70
Inlet Loading, ppm	1000	1500	1500	1500	1500
Ash Type, Gasifier Char	Texaco	Texaco	KRW	Texaco	Texaco
d_{50}, μ	5.4	5.3	4	5.3	5.3
Face Velocity, ft/min	3	1.9	1.9	3.3	4.5
Baseline ΔP, in w.g.	1 - 2	1.1	1.1	2-3	3-4

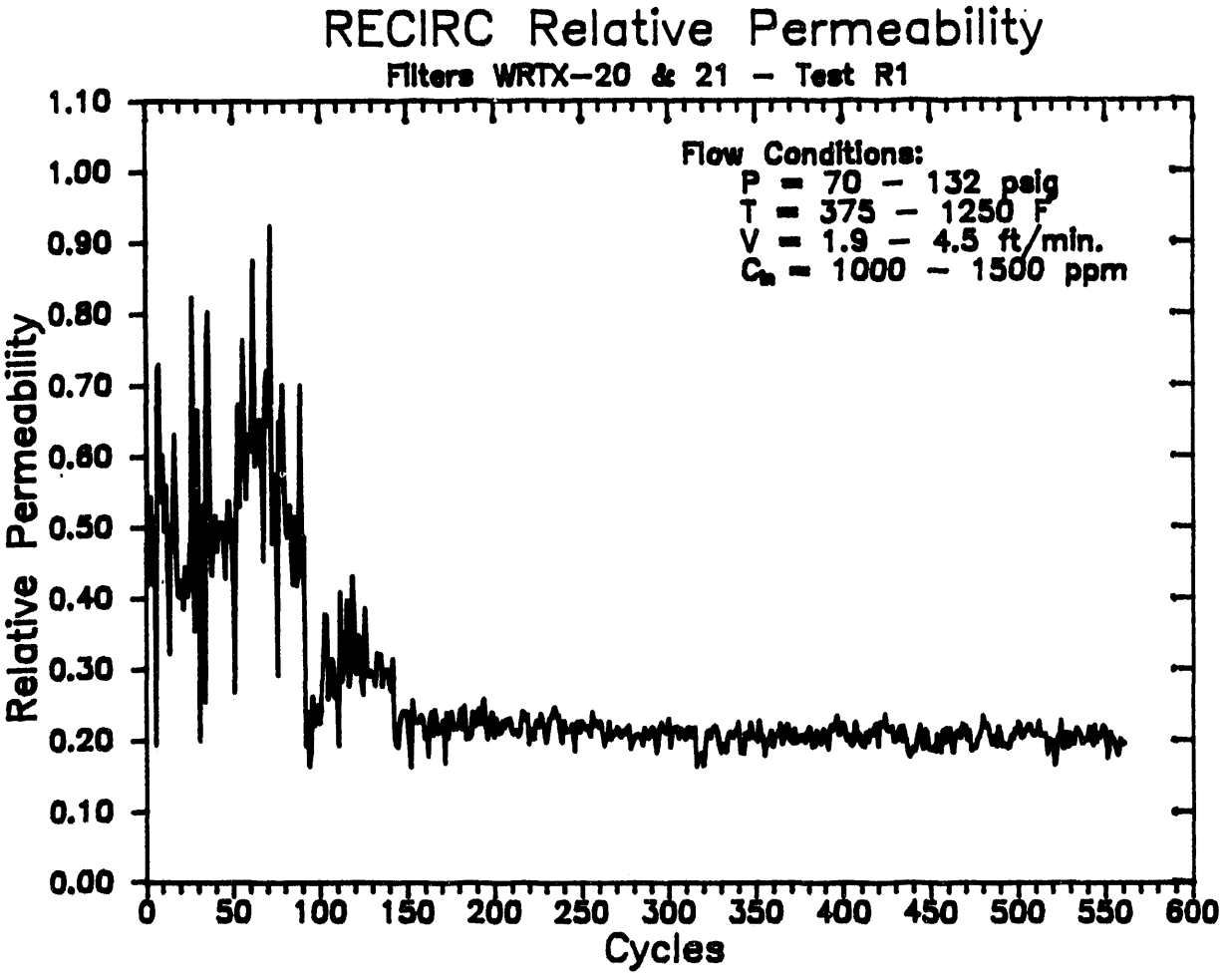

Operation Notes for Test R1
561 Cycles
1919 Hours Flow Exposure time

Figure 3.13 - Measured Cross Flow Filter Permeance in Simulated Gasifier Testing - WRTX-20 and WRTX-21

Figure 3.14 - Photograph Showing General Appearance of Pulse Cleaned Cross Flow Filter After About 1900 Hours of Testing with Gasifier Char

4. DISCUSSION OF RESULTS

The purpose of this section is to report the evaluation of the cross flow filter long term durability simulator testing data, compare this filter data to actual plant filter data, and assess results on cross flow filter development.

4.1 COMPARISON OF PFBC SIMULATOR AND PLANT FILTER TESTING

Table 4.1 compares the pertinent operating parameters of PFBC (nominal) with the PFBC simulator facility used in this test program. Although the Westinghouse simulator facility is methane fired, the major gas phase constituents (CO_2, H_2O) are reasonably similar. Operating at the same system temperature and pressure in the simulator facility (with reentrained PFBC ash) reproduces the relevant filtration properties of gas to particle density ratio and gas viscosity.

Equation 4.1 shows that if the filter unit in the simulator facility is operated at the same face velocity, V, and solids loading, C, the filter pressure drop characteristics should be reproduced if filter and cake permeance, K_f, K_c are reproduced.

$$\Delta p = \frac{\mu V}{K_f} + \frac{\mu C V^2 \theta}{\rho_c K_c} \qquad (4\text{-}1)$$

where

μ = gas viscosity
V = filter face velocity
C = dust (ash) concentration
θ = time
ρ_c = bulk density of the dust cake
K_f = filter permeance
K_c = cake permeance

Table 4.1 - Comparison of PFBC and Simulator Operating Conditions

	Actual PFBC	Simulator
Pressure, psia	164	80-164
Temperature, °F	1550	1550
Gas Composition (Mole %)		
CO_2	13.5	17
H_2O	10.4	14
SO_2	233 ppm	-
O_2	3.7	6
N_2	72.3	73
Alkali	<2 ppm	(1)
Molecular Wt.	29.3	~29
Gas/Solid Properties		
Gas Viscosity (lbm/ft-sec)	3.1×10^{-5}	3.1×10^{-5}
Solids Bulk Density (lb/ft^3)	40-60	40-60
Solids/Gas Density Ratio	250	250
Mass Mean Particle Size	~2 μ	(2)

(1) Alkali condensed on ash particles may be released during reentrainment.

(2) Agglomerated fines may not be redispersed during reentrainment.

Filter permeance, K_f, establishes the filter baseline pressure drop after cleaning. Fine particulate entrained in the gas may reach the filter surface and become trapped in the pore structure of the filter resulting in a decrease in K_f with time.

Figure 4.1 compares the relative permeance (K_f/K_c) of both candle and cross flow barrier filters in PFBC simulator data with actual PFBC tested filters. By comparing the relative permeance of the filters over time (or number of cleaning cycles), the effect of initial filter permeability is normalized. Figure 4.1 shows that barrier filters operated in the PFBC simulator facility show permeance trends similar to actual PFBC tested filters. Thus, on this basis, the baseline pressure drop characteristics experienced in long term durability simulator testing of the cross flow filter should be representative of actual plant data.

Reproducing the particle size distribution using redispersed ash is highly problematic in simulator facilities. It is generally accepted that the fraction of very fine reentrained ash will not be dispersed in simulator facilities. This is qualitatively substantiated by comparing the cascade impactor sampling conducted during the PFBC plant tests at the New York University facility during cross flow filter testing[1] with coulter counter data of the PFBC ash feed used in the simulator testing, Table 4.2. Assuming the coulter counter data represents what can be achieved in dispersing ash in the simulator facility, this data suggests particles smaller than 1μ are not present as discreet fines in simulator testing. Some loss in the 2μ particle range may also occur.

Scanning electron micrographs (SEM) taken from filter samples operated in the PFBC simulator facilities, given in Appendix I, show particle morphology characteristics and provide evidence of particle penetration into the pore structure at the surface of the cross flow filter. Particle fines are found only in the first few pore layers of the filter. Penetration of fines into the interior of

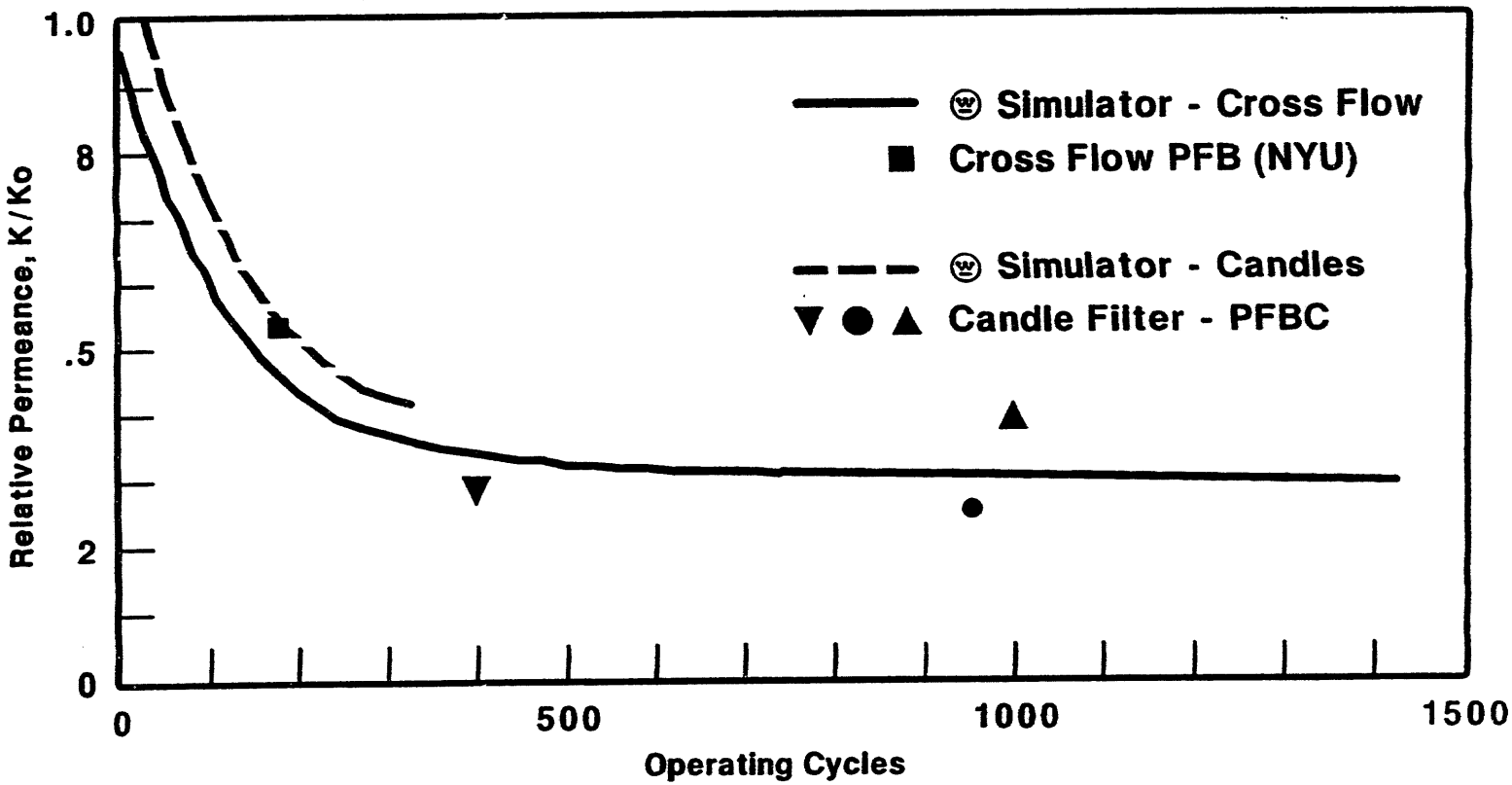

2T786.BW/VS2828

Figure 4.1 - Comparison of Westinghouse Simulator PFBC and Plant Experience

Table 4.2 - Comparison of Coulter Counter and Cascade Impactor Data From Simulator and Plant Tests

Fraction Less Than	Coulter Counter Data - PFBC Ash Samples	Cascade Impactor Data (1) at Filter Inlet
1 μ	0	2%
2 μ	7 to 12%	7 to 20%

the filter matrix is negligible. Typically fines that are retained within the filter matrix are seen principally to adhere to the amorphous (glass) phase. Similar particle behavior has been experienced in field tested cross flow filters.

The cross flow filter is characterized by an average pore structure that may range from 40 to 60 microns. Thus, in the simulator testing the fine particle fraction ($<2\mu$) that are not redispersed are likely carried to the filter surface and into the surface pore structure on the surface of the larger 10 to 20 μ particles. This behavior is thought to reproduce the "surface blinding" that accounts for the very similar behavior in filter permeance experienced in actual plant and simulator testing. The presence of fines, as seen in the SEM's, do not present any substantial pore blockage, even in the filters exposed for 1300 hours of operation.

Ash cake permeance, K_c, establishes filter cake pressure drop properties and may be important in establishing requirements for filter cleaning. Factors that are thought to effect cake permeance include particle size distribution, porosity, compressibility, presence of alkali and particle chemistry. These parameters obviously depend on coal type, sorbent and actual process conditions. Differentiating Equation 4.1 with respect to time, θ, and solving for K_c gives the following expression that is dependent on known or experimentally measured parameters,

$$K_c = \frac{CV^2\mu}{\rho_c(\Delta p/\Delta\theta)} \qquad (4\text{-}2)$$

where $\Delta p/\Delta\theta$ is the slope of the pressure drop (saw-tooth) curve generated during filter testing. Table 4.3 compares values of K_c determined from various filter testing, including the long term durability program. The data include simulation testing using reentrained ash from PFBC and data from pilot scale PFBC operations. These results appear to show a correlation with particle size, i.e.,

Table 4.3 - Comparison of Ash Cake Permeability for Different Ashes and Test Conditions

Test System	Dust Type	Average Particle Diameter d_{50}	Cake Permeability ft^2 (10^{-12})
W HTHP long term durability rig - cross flow filter	• Reentrained PFBC ash 2nd stage catch-ground	6.5 μ	2.1 to 4.0
	• Grimethorpe filter catch	5.0 μ	.7 to 1.9
W HTHP facility, candles (Ref. 1)	• Reentrained PFBC ash 2nd stage catch-ground	5.5 μ	4.8 to 10.7
W HTHP facility candles (Ref. 1)	• Reentrained PFBC Ash 2nd stage catch	25 μ	43
METC Atm fluid bed - candle (Ref. 2)	• Coal combustor, with cyclone	6.8 11.4 8.2 4.2	1.5 6.7 1.2 0.33
New York University PFBC cross flow	• Coal combustor, with primary cyclone	3.5 to 5 μ	1.6

increased permeability with larger mass mean size. The actual plant data also compares well with the K_c values indicative of the reentrained (simulator) ash cases. The favorable comparison between the K_c values measured in actual and simulator testing may again be the result of the non-dispersed fines fraction remaining as agglomerates to larger particles, but depositing on the filter surface in a manner that is representative of the original cake structure.

The relationship of filter cleanability to cake permeance (flow resistance) has also been demonstrated in simulator testing. Table 4.4 compares qualitative results of cleaning tests using different PFBC ash materials. These ashes were obtained from different operating facilities that utilized different coal and sorbent types. With increasing cake flow resistance (decreasing permeance) cleaning pulse intensity had to be increased to achieve filter cleaning.

The effect of cake permeance on cleaning can also be demonstrated by comparing filter pressure drop traces taken from the long term durability test program where different PFBC ashes were used, Figures 4.2 and 4.3. Figure 4.2 shows a test sequence using a "high" permeance ash (ash sample 3) where very repeatable and stable filter pressure drop characteristics are experienced (good cleaning). Changing to the "low" permeance ash (ash sample 4) and initiating filter cleaning operation at the same pulse conditions gave dramatically unstable pressure conditions, Figure 4.3. The poor cleaning with the number 4 PFBC ash sample was also experienced at the Grimethorpe PFBC hot gas filter test facility.

4.2 COMPARISON BETWEEN SIMULATOR AND GASIFICATION PLANT EXPERIENCE

Figure 4.4 shows a comparison of the gasifier simulator filter testing with plant experience. The cross flow filter relative permeance (K_f/K_{f_o}) is shown as a function of filter cleaning cycles. The

Table 4.4 - Comparison of PFBC Ash Properties and Filter Cleaning

PFBC Ash Sample	Cake Bulk Density* gm/cc	Flow Resistance (Relative)	Mass Mean Particle Size* (μm)	Cleaning Pulse Intensity Required (Relative)
1	0.4	1	7.8	Lowest
2	0.6	1.8	5.3	Medium
3	0.3	2.7	3.5	High
4	0.2	6.8	4.0	Highest

*Cake Sample

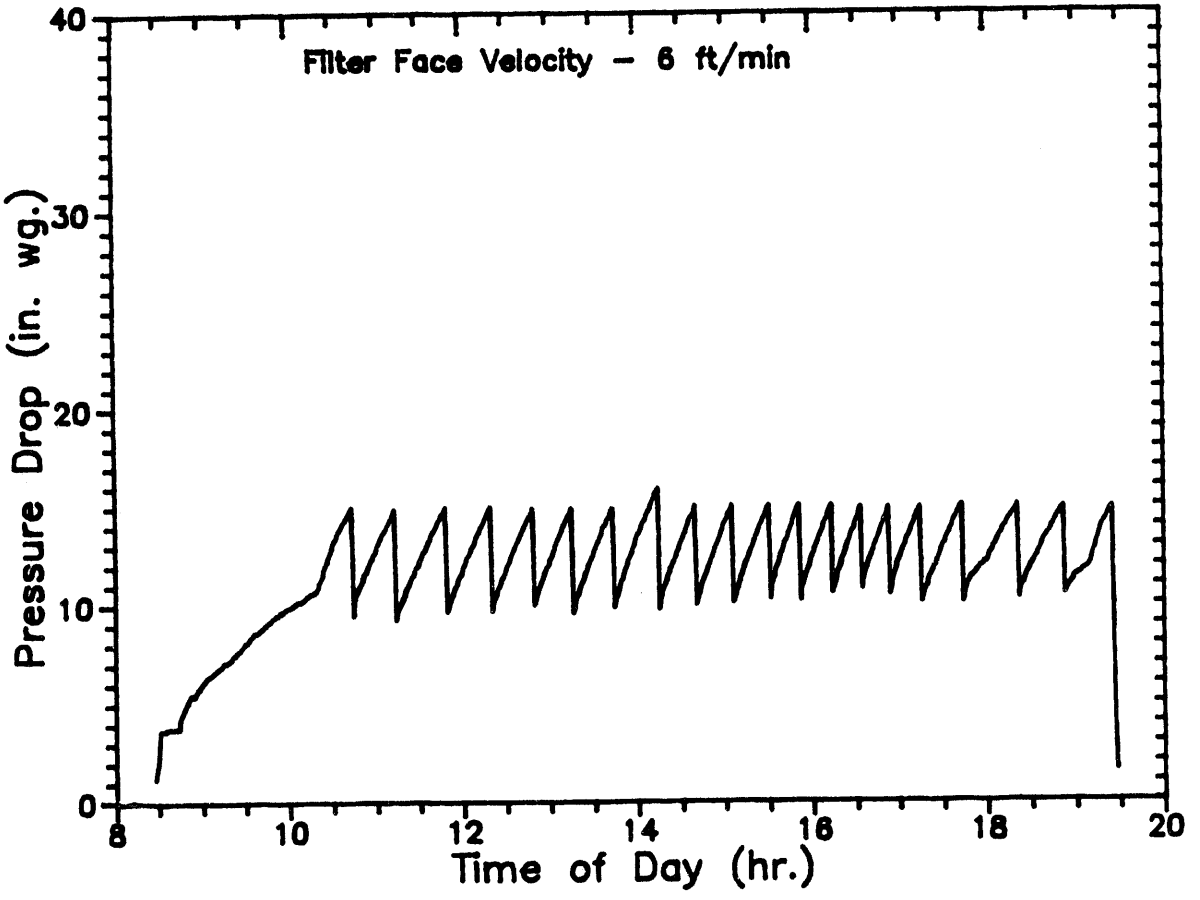

Figure 4.2 - Cross Flow Filter Pressure Drop Characteristics Using "High" Cake Permeance PFBC Ash

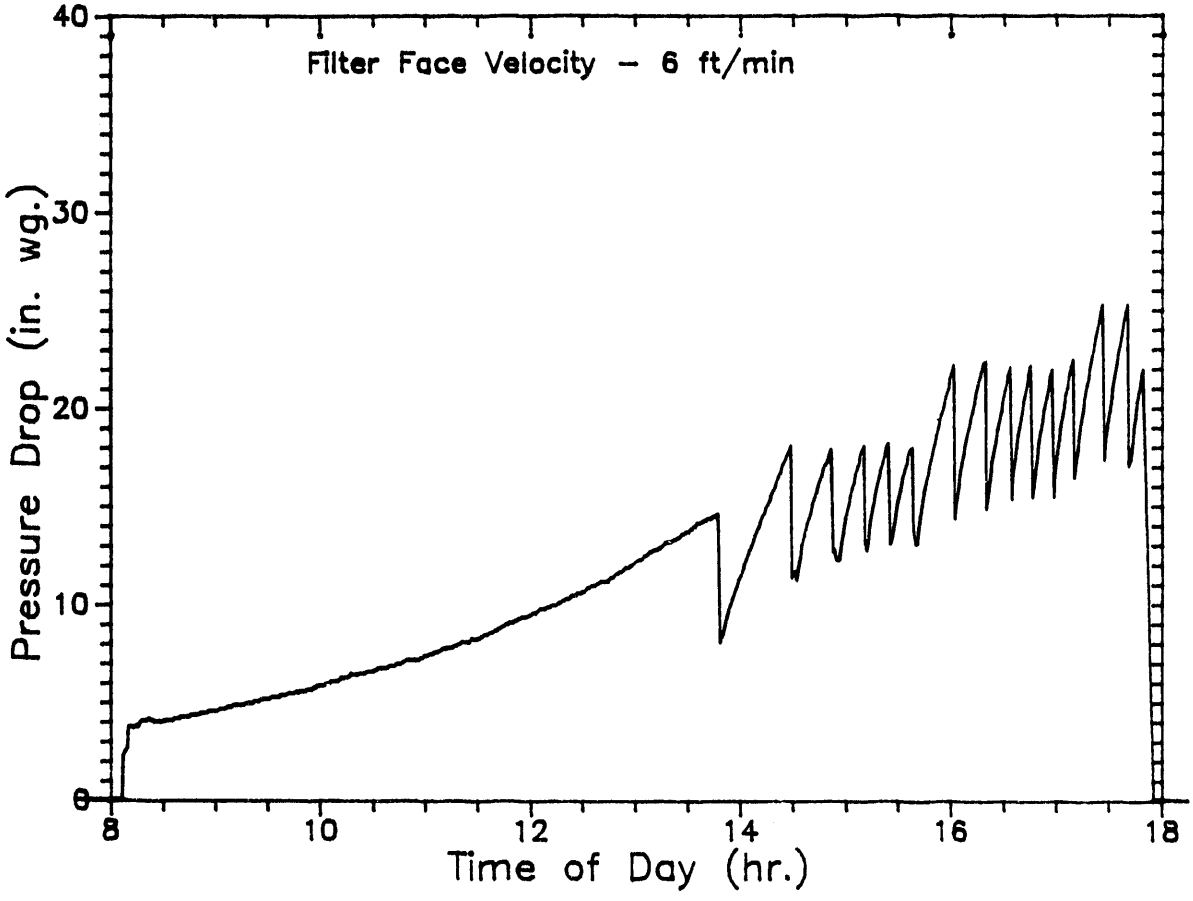

Figure 4.3 - Cross Flow Filter Pressure Drop Characteristics Using "Low" Cake Permeance PFBC Ash (Grimethorpe Red)

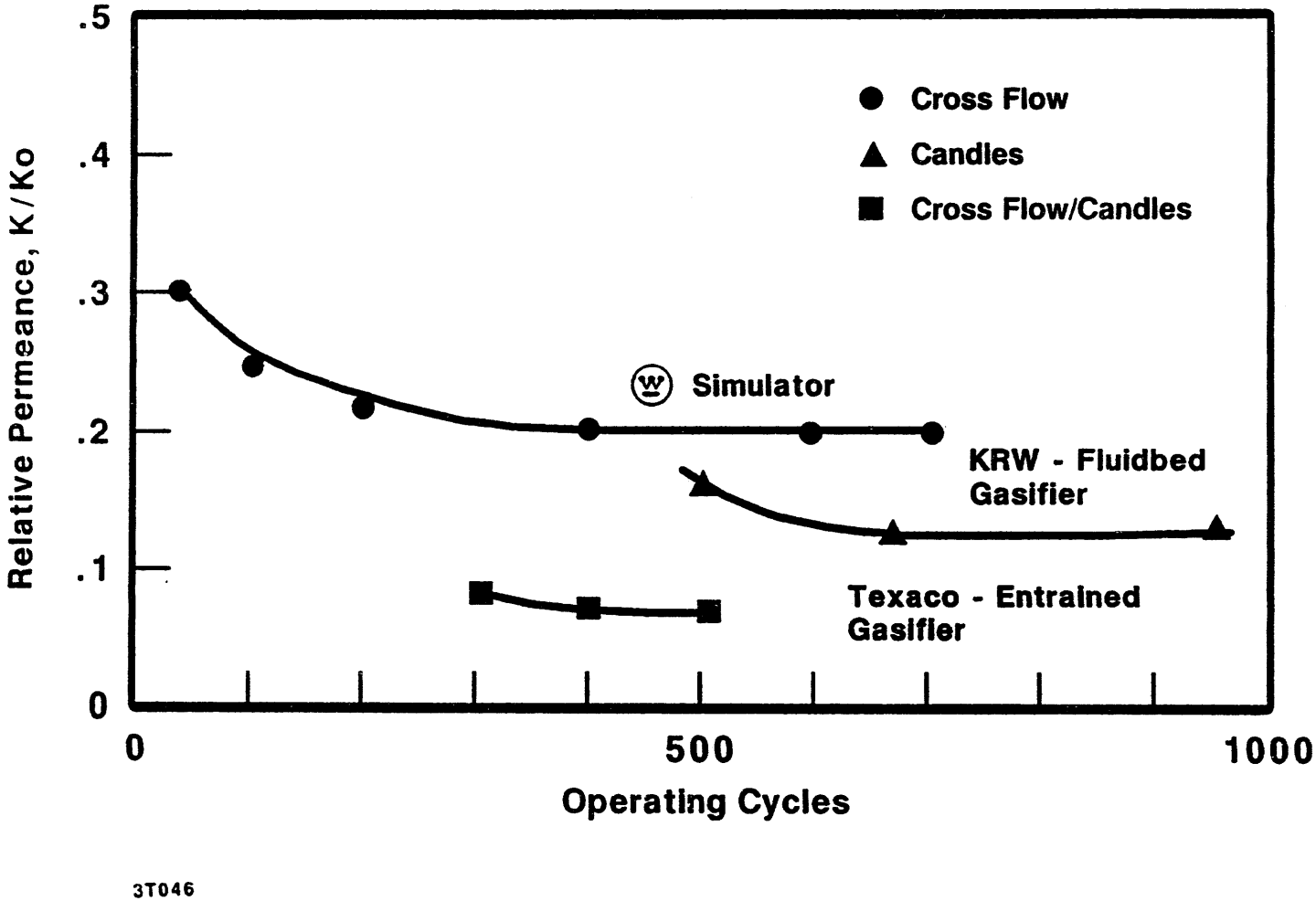

Figure 4.4 - Comparison of W Gasifier Simulator and Plant Experience

simulator data is compared with cross flow and candle filter data from previous gasifier pilot plant test programs. Plant data is shown for the KRW fluid bed gasification PDU that utilized the silicon carbide candle filters[2] and for the Texaco entrained gasifier pilot plant that has now utilized both cross flow and candles.[3]

As with the PFBC filter data, filter permeance decreases with operation. However, in the gasification case, the simulator and plant data show similar trends but do not correspond as well as the PFBC data. Significant differences in filter permeance is also evident between the two different gasifier types. This difference is likely indicative of the significant difference in the two gasification processes and resulting generation of ash and char.

The KRW char is generated in a sulfur sorbent containing fluid bed that operates at relatively low temperatures (1600°F, 870°C). Thus the fuel gas contains both char, ash and attrited sorbent particles.

The entrained gasification pilot plant process occurs at over 2500°F (1370°C), generally above the ash softening point. Sulfur sorbents were not utilized upstream of the filter. Thus, in this case, the fuel gas contains primarily char and ash particles, see Appendix I. Particle morphology, size distribution and fraction of fines present in the fuel gas are therefore significantly different in the two cases. These differences may substantially influence the filter surface conditions.

Additional factors in gasification systems may influence filter operating conditions. Both the fluid bed and entrained gasifier ashes are very noncohesive, contain a bimodal size distribution with a substantial weight fraction of particulate in the less than 2.3 μm range and exhibit very low cake bulk density.[3] These ash cake characteristics suggest high reentrainment potential in the pilot plant testing. Possible reentrainment effects in the gasifier simulator testing was

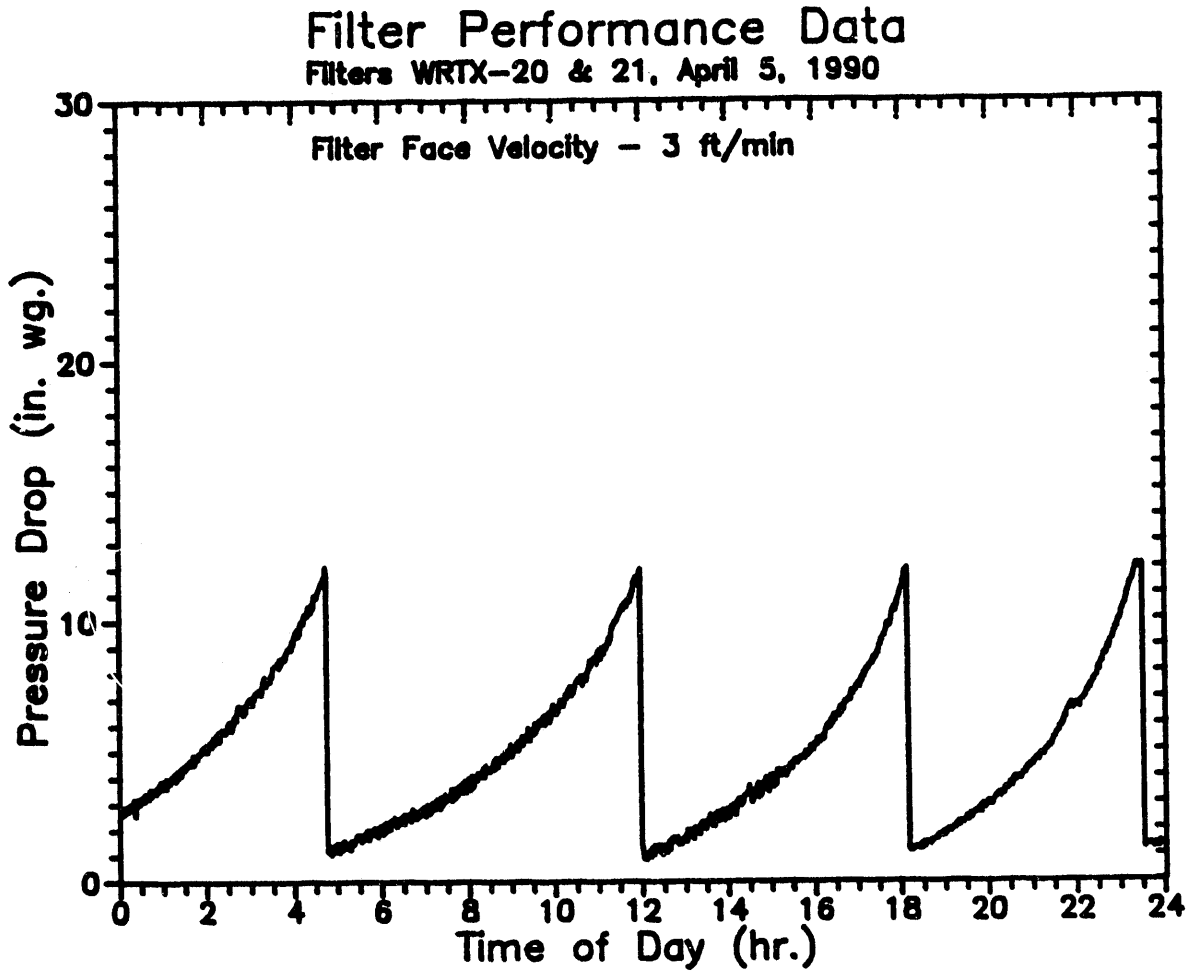

Operation Notes for April 5, 1990

2153 Changed Process Gas make-up to N_2

ΔP Trigger = 12" wc

Pulse Cleaning - 200 psig/0.1 sec

Figure 4.5 - Cross Flow Filter Pressure Drop Characteristics from Gasifier Simulator Test Series 1

investigated. Test Series 1 (Table 3.6) was operated at relatively high temperature and low pressure corresponding to relatively low gas density. Typical filter pressure drop characteristics from this test segment are shown in Figure 4.5.

In Test Series 2 (and subsequent gasifier simulator testing) it was decided to operate at low temperature and higher system pressure to increase gas density (comparable to entrained gasification), and therefore, provide a better simulation of potential particle reentrainment effects. In addition, operating conditions (inlet loading, face velocity and trigger Δp) in Test Series 2 were adjusted (see Table 3.6). The intent of changing the operating conditions was to approximate the cleaning frequency experienced in Test Series 1, assuming no significant char reentrainment effects, i.e.,

Cleaning frequency (2) = Cleaning frequency (1) if:

$$\frac{\Delta p_1}{\Delta p_2} = \frac{C_2}{C_1} \times \left[\frac{V_2}{V_1} \right]^2 = 1$$

Substituting actual test conditions, Table 3.6, would predict that the Test Series 2 cleaning should be approximately:

$$\theta_2 = \frac{6}{12} \times \frac{1000}{1500} \times \left[\frac{3}{1.9} \right]^2 \times 7 = 6.3 \text{ hours}$$

Figure 4.6 shows a segment of the pressure drop trace for the Test Series 2 sequence. As apparent, cleaning frequency ranged around 1 hour or approximately 6 times more frequent than would be anticipated based on the Series 1 testing. This comparison strongly suggests potential reentrainment effects have been promoted in the simulator facility by increasing gas density.

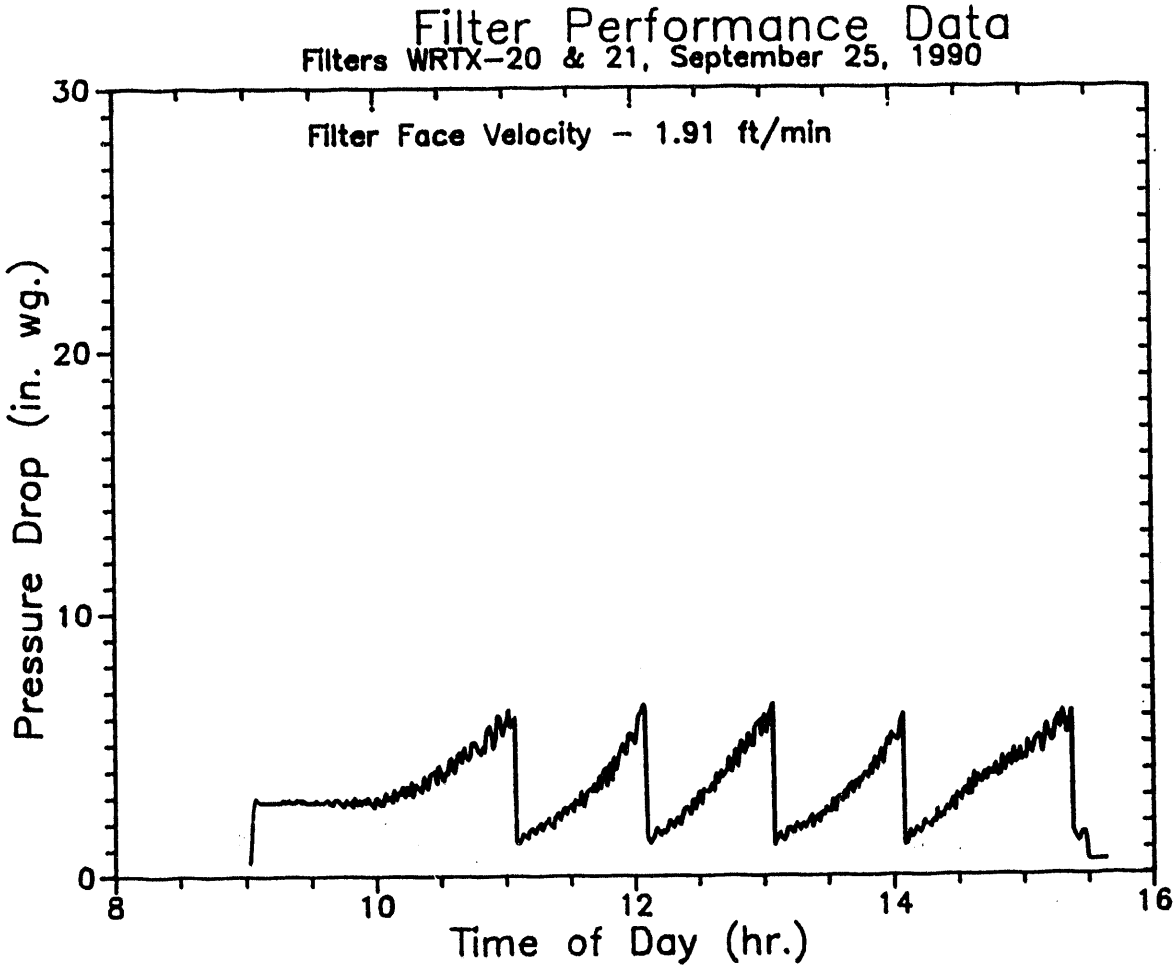

Operation Notes for September 24, 1990:

8 hour test

ΔP Trigger = 6" wc

Pulse Cleaning - 300 psig/0.1 sec

Figure 4.6 - Cross Flow Filter Pressure Drop Characteristics from Gasifier Simulator Test Series 2

Comparison of this simulator testing with field data suggests that the filter operating characteristics in the actual gasifier environment are significantly underestimated from the simulator testing.[3] Reentrainment effects in the simulator testing may be mitigated because the fine fraction may not be effectively redispersed, but remain attached to the larger particle fraction. PFBC ashes appear to be very cohesive with low reentrainment potential.

A second major difference between gasifier and PFBC ash characteristics is filter cake permeability (or flow resistance). Data taken from plant tests suggest that the gasifier char may be 4 to 7 times more resistive than PFBC ash that exhibit similar mass mean particle diameter. Similar data has also been reported by others.[4] Simulator cake permeance data, Table 4.5 , also show higher flow resistances (lower cake permeability) for the gasifier char over PFBC cakes exhibiting similar mass mean particle size.

The above data and analysis suggest that the operating and performance characteristics of barrier filter devices for PFBC application can be reasonably predicted based on simulator testing. Gasifier simulator testing showed similar trends experienced in plant testing but did not effectively reproduce the reentrainment conditions that are thought to be significant in pilot plant facilities. Gasifier gas composition was not reproduced in the simulator facility which may also be a contributing factor. Both the PFBC and gasifier simulator facilities utilize full scale filter components and operate at temperature and pressure conditions that expose the filter to thermal, hydrothermal and mechanical stressing of actual plant conditions. Thus, the major materials durability factors are reproduced. Cross flow filters examined after simulator and plant testing have also shown very similar changes in materials morphology. These and other aspects of the cross flow filter long term durability testing are discussed below.

Table 4.5 - Comparison of Filter Cake Permeance in Gasifier and PFBC Simulator Testing

Test System	Dust Type	Average Particle Diameter	Cake Permeability ft^2 (10^{-12})
• Long Term Durability PFBC Simulator, Cross Flow Filter	PFBC - Exxon Ash	6.5 μ	2.1 to 4.0
• Long Term Durability Gasification Simulator, Cross Flow Filter	Char from Entrained Gasifier	5.3 μ	0.9 - 1.2

4.8 CROSS FLOW FILTER PERFORMANCE POTENTIAL

Table 4.6 shows a summary of cross flow filter performance from both PFBC and gasification simulator testing. Only the longest two segments of PFBC testing are included. The data show the range of filter face velocities and baseline pressure drop over which the filter test units were operated. As described in Section 3, nearly continuous isokinetic particle sampling was conducted on the outlet side of the filters in both the gasification and PFBC simulator testing. As given in Table 4.6, these data when averaged over the respective test periods show the average outlet particle loading to be less than 1 ppm, demonstrating the high performance potential of the cross flow filter. These results are also pictorially illustrated in Figure 4.7 which compares a photograph of one outlet sample (right) with a sample representing the filter inlet concentration (1000 ppm).

The high performance potential of the cross flow filter is significant because of the stringent requirement for gas cleanup in advanced fossil power generation cycles. In these applications, hot gas filter particle removal requirements include meeting emission limits (New Source Performance Standards, NSPS) and protecting the gas turbine from particle erosion and deposition. Figure 4.8 illustrates these requirements for PFBC and compares cross flow filter performance data from recent pilot plant and the current PFBC simulator testing.[1] The cross flow filter pilot plant data includes cascade impactor sampling that provides estimates of the outlet particle size distribution. The simulator data is total outlet mass and therefore is represented as a single data point.

NSPS, shown as a horizontal solid line in Figure 4.8, when expressed as a mass loading depends on coal type and PFBC cycle efficiency but in general will range between 20 to 30 ppm. Both the pilot plant and simulator data show outlet measurements that fall well below NSPS emission requirements. It should also be noted that even

Table 4.6 - Summary of Cross Flow Filter Performance in Long Term Durability Simulator Testing

	PFBC Ash Test Loop		Gasifier Char Test Loop
	Test Module #1	Test Module #2	Test Module #1
No. of Filters	2	4	2
Operating Conditions			
Temperature, °F	1550	1550	350-1200
Pressure, psia	85	85	85
Inlet Dust Loading, ppm	1000	1000	1000-1500
Face Velocity, ft/min	6 to 10	3 to 5	2-5
Cumulative Hrs.	1300	1100 2400	2000
Performance			
Avg. Outlet Loading, ppm	<1	<1	<1
Baseline Δp, in wg	8-20	4-10	1-4
Comments	Flange Failure	New Mount	No Failures

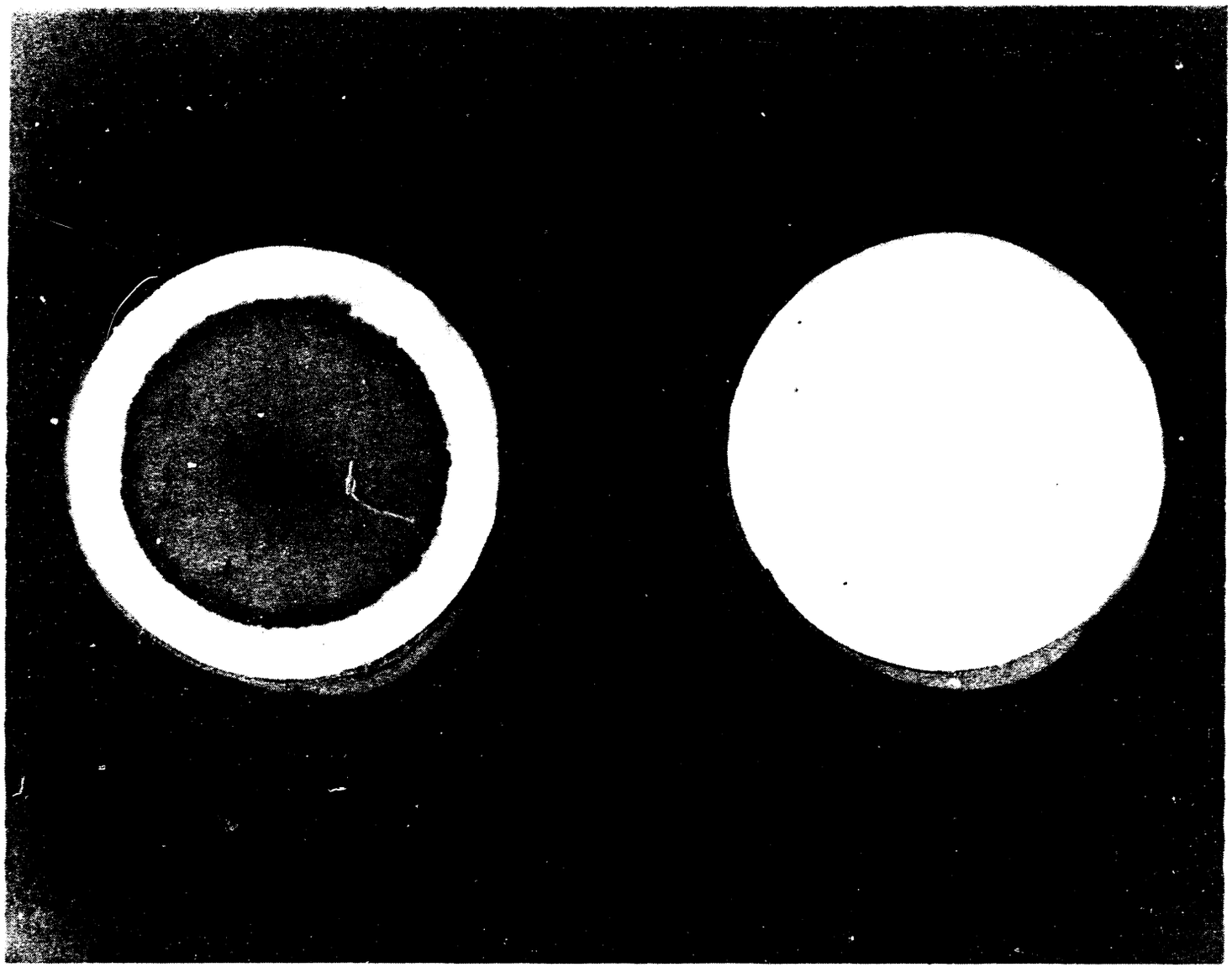

Figure 4.7 - Photograph Comparing Outlet Loading Sample Taken from PFBC Simulator Testing with 1000 ppm Inlet Loading

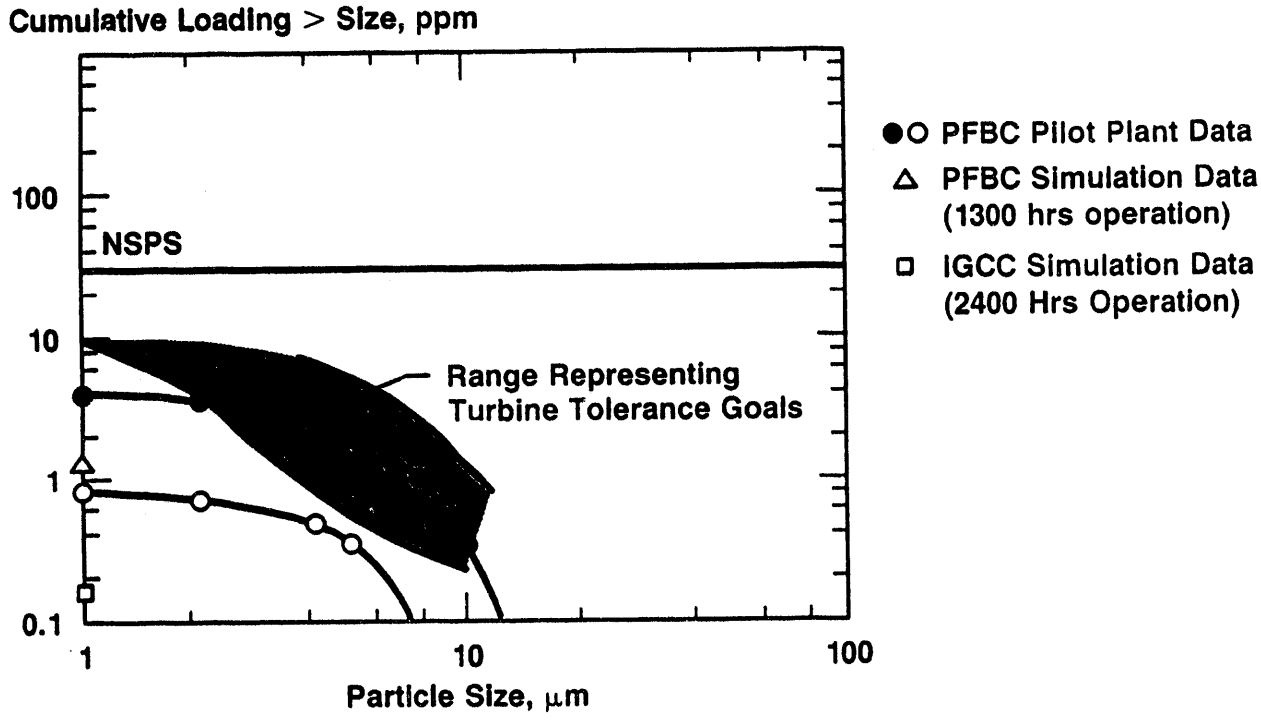

3T087 / VS8429

Figure 4.8 - Comparison of Cross Flow Filter Performance with Cleanup Requirements

larger performance margins exist with the gasifier systems since the fuel gas following hot gas filtration is subsequently diluted with combustion air. Thus, results from the long term durability testing confirm shorter term pilot plant test results and show the cross flow filter when operating over extended test periods can meet and significantly improve upon NSPS requirements.

Gas turbine tolerance to particulates, as nominally represented by the shaded region in Figure 4.8, will depend on the specifics of the turbine design. Turbine tolerance depends on both total loading and size distribution. Although actual size distributions were not measured in the simulator testing, the <1 ppm average total loading would clearly suggest a performance level consistent with the most stringent turbine tolerance requirement.

4.4 CROSS FLOW FILTER DURABILITY

As suggested above, the cross flow filter is basically an absolute filter when component integrity is maintained, i.e., no failed filter elements or gaskets. In the PFBC simulator testing, and in ongoing pilot plant gasification filter testing,[3] both filter element and gasket failures have occurred. In these instances, depending on the type of failure, the performance of the cross flow filter can be substantially compromised.

Filter Gasket Durability

In high temperature applications, some type of a ceramic dust seal (gasket) must be used between the filter element and its mount. In general, these seals have typically utilized some type of unconstrained ceramic fiber blanket or mat gasket. Failure of these seals can result in substantial compromise in the filter system performance, even though no damage has occurred with the filter element. Gasket failures result in a one (1) to two (2) order of magnitude increase in the outlet

particle loading, i.e., 10 to 100 ppm. As discussed in Section 3, gasket failures were encountered when utilizing the unconstrained fiber blanket and mat type gasket. A modified gasket design described in Appendix E was developed that utilizes a reenforced ceramic fiber mat. This design has substantially eliminated gasket failure.

Filter Element Durability

Cross flow filter element failures under service conditions can be characterized as debonding, as delaminations (hairline cracks that follow plate seams), by cracks that propagate across the plate seams or as cracks that occur along the mounting flange. Although no filter failures of any type were experienced in the gasifier simulator testing, parallel testing in an actual entrained gasifier system did show filter flange cracking (prior to mount redesign), delamination, and cracking across filter plate seams. However, significant plant transients and upsets have been experienced in the gasifier plant tests, as opposed to the very controlled and nearly steady state conditions of the gasifier simulator testing. The PFBC simulator testing included both steady state and thermal transient testing. Under these conditions filter element failures were experienced.

Although debonding, delamination and filter plate cracking have all been identified in earlier filter development program testing, the occurrence of the filter flange cracks represent a relatively new and potentially serious deficiency in the filter system design. Cracking of the flange had occurred in earlier versions of the cross flow filter, but was apparently corrected by increasing flange thickness. In the current long term durability test program, however, the deficiency of the filter mounting system was identified. This aspect of the program is described and evaluated in detail in Appendix E. A modified mount design, illustrated in Figure 4.9, was developed and implemented into

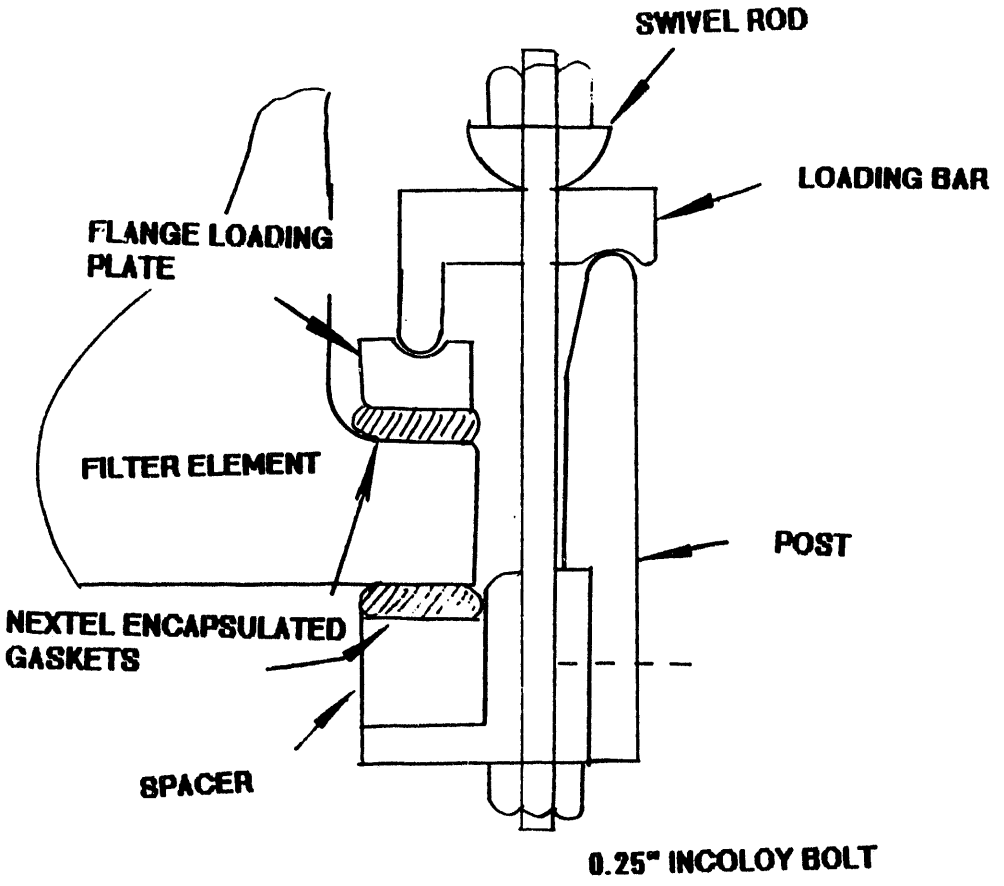

Figure 4.9 - End View of Modified Element Mount Fixture

the subsequent simulator testing as well as the ongoing entrained gasifier pilot plant filter testing. The salient features of the design include:

1. The Nextel reinforced gaskets are used on the upper and lower surfaces of the ceramic flange. Note that the upper gasket after compression now provides a compliant layer to smooth out the seating forces imposed by the flange loading plate and also ensures a resilient shock-absorbing layer to cushion the vibrational forces generated during pulse cleaning.

2. The single clamp plate is now substituted by a flange loading plate and a separate loading bar with a swivel action. This type of clamping arrangement ensures that, regardless of the ceramic flange geometric variations, the loading plate will remain parallel and horizontal whereas the loading bar can rotate as necessary without actually interfering with the edge of the ceramic flange.

3. A metal post is attached to the outside of the existing fixture such that the loading bar is simply supported on either side of the bolting axis. Thus the bolting forces are directly transferred into an equivalent seating force on the filter, without the use of shims.

4. The eight 316 stainless steel bolts are substituted by fourteen bolts made of creep resistant Incoloy 800 alloy. During the assembly procedure a weight is placed on the element to precompress the bottom gasket. The clamping device is now mounted and the 14 bolts are sequentially torqued up to 10 in-lbs. After removal of the weight, the two gaskets will be loaded in series to approximately 2700 lbs of seating force.

5. The filter seating area is elevated by the use of a spacer such that no dust can accumulate between the flange and the metal fixture. Notwithstanding the rugged gasket seating properties of the modified design, this feature ensures that no residual transverse stresses can act on the flange during shutdown conditions.

Although testing has been limited, with the implementation of this modified mount design in both simulator and pilot plant facilities, no further failures in the filter flange have been experienced.

In the PFBC simulator testing that included plant thermal transient testing as outlined in Section 3 and detailed in Appendix J, debonding, delamination and filter plate cracking were experienced. Photographs showing the different failure modes are provided in Appendix J. Nine different cross flow filter elements in groups of four were subjected to thermal transients testing. The first filter grouping of four elements all failed during a very severe thermal transient that occurred initially when trying to produce a much less severe, but PFBC indicative turbine trip transient. These filters were replaced. Although not considered as representative of controlled PFBC transient conditions, the data and discussion of these four filters are included in Appendix J for completeness. These filters failed by debonding (WRTX-53) partial delamination (WRTX-53, 48, 70) and horizontal plate cracking (WRTX-66). It is interesting to note that even with these different type "failures," there was substantial evidence that very little dust actually penetrated to the clean gas side of filters. Longer operation in the failed mode, however, may have produced a substantial compromise in filter performance; this testing was not conducted. It is also noteworthy that in the failed mode, no section or piece of the filter actually dropped off the mount, i.e., each filter appeared to be intact until it was physically removed from its mount (the photographs given in Appendix J are after mount disassembly).

Following the initial severe thermal transient testing, better control of the PFBC simulator facility was achieved. Five different filters were then tested under PFBC transient conditions. Three of these filters survived with no visible damage. Two of the filters suffered in-service failure; one filter showed a debonding while the second a partial delamination crack. Debonding failures (complete separation at a plate seam) is viewed as a manufacturing deficiency that as yet cannot be detected by current nondestructive inspection techniques. Again, evidence suggests that only a very small amount of dust penetration occurs as a result of a simple delamination crack. In general, cross flow filter performance appears significantly more tolerant to in-service cracking of the ceramic elements than candle or tube geometries. However, efforts continue to develop the cross flow filter manufacturing process to improve bulk material properties and uniformity.

Cross Flow Filter Materials Characterization

Cross flow filter material stability is being investigated in a companion DOE program (DE-AC21-88MC25034). This work has demonstrated the relative inertness of alumina/mullite in both high temperature oxidizing and reducing gas conditions representative of PFBC and gasifier systems, respectively. At high temperature (1300-1600°F, 700-870°C) alumina/mullite undergoes conversion of its amorphous or glass containing phase(s) to a crystalline anorthite structure which appear to impart high temperature strength to the filter matrix. Conversion or crystallization is enhanced by the presence of steam and gas phase sodium. Continued conversion of the anorthite to the long-term production of tridymite appears to level material strength gain. Testing in this program has also shown exposure of the alumina/mullite material to simulated pulse cleaning thermal transients reduces material bulk strength. Thus, initially, competing effects appear to occur; an increase in strength due to anorthite formation and formation of microcracks due to pulse cleaning thermal transient effects that decrease strength. Quantitative XRD

analysis of the cross flow filter tested for 1300 hours in the long term durability program under simulated PFBC conditions has confirmed the conversion of the amorphous to anorthite, paralleling actual plant experience and the bench scale testing reported in the DE-AC21-88MC25034 contract work.[5]

Detailed material property characterizations have been conducted on the cross flow filters exposed to 1300 hours of PFBC simulator testing. These data include room temperature bulk material strength data and Weibull statistics determined from 4-point bend bar data and material property data (4-point bend) under process temperature conditions, Appendix K and Appendix L.

In summary, findings from these material strength studies suggest the following:

- The initial (unused filter) hot strength is lower than initial cold strength. Apparently, the higher amorphous content of the unused filter is reflected as a higher cold strength bulk property.

- Although room temperature material strength decreases with operating time, actual hot strength increases (because of the above described phase conversion). Once conversion of the amorphous phase is complete, the hot and cold bulk strength should be comparable (this had not yet occurred in the 1300 hour test sequence reported herein).

- Cold strength data suggests after 1300 hours of long term durability testing, the web (filter core) and flange sections of the cross flow filter to exhibit lower strength than the top closed end of the filter element. This is not unexpected because of the thermal cycling duty experienced by both the web and flange sections compared to the filter top end.

Actual stressing conditions in cross flow filters have been predicted.[6] These models indicate the possibility of stressing conditions during pulse cleaning that would begin to approach the room temperature bulk strength measured in the filter. Although the model calculations are based on somewhat incomplete process and material property input data, they do suggest that the loss of material cold strength shown in the 1300 hour test could be sufficient to cause concern regarding possible failure (as had occurred). To date there is insufficient confidence in the models to draw firm conclusions regarding actual filter stressing. However, it appears prudent to evaluate means to increase filter strength even if lower flow permeability must be accepted.

4.5 REFERENCES

1. Lippert, T. E., G. B. Haldipur, E. E. Smeltzer, and J. H. Meyer, "Performance Evaluation of a Cross Flow Filter on a Subpilot-Scale Pressurized Fluid Bed Coal Combustor," Final Report, Westinghouse Electric Corporation, DOE/METC Contract No. DE-AC21-85MC22136, 1989.

2. Ciliberti, D. F., "Hot Gas Cleanup Using Ceramic Cross Flow Membrane Filters," Final Report DOE Contract DE-AC21-79ET15491, DOE/ET/15491-1565, December 1983.

3. Lippert, T. E., et al., "Subpilot Scale Gasifier Evaluation of Cross Flow Filters," Proceedings of the Eleventh Annual Gasification and Gas Stream Cleanup Systems Contractors' Review Meeting, DOE/METC Contract No. DE-AC21-88MC24021, 1991.

4. Pontius, D.H., "Characterization of Particles Emitted in Gasification and Combustion Processes," Paper presented at the Second EPRI Workshop on Filtration of Dust From Coal-Derived Reducing and Combustion Gases at High Temperature, San Francisco, March 1992.

5. Alvin, M. A., et al., "Thermal/Chemical Stability of Ceramic Cross Flow Filter Materials," Proceedings of the Eleventh Annual Gasification and Gas Stream Cleanup Systems Contractors' Review Meeting, DOE/METC, Contract No. DE-AC21-88MC25034, 1991.

6. Singh, J. P., et al., "Materials Qualification Technology for Ceramic Cross Flow Filters," ANL/FE-91/1.

5. CONCLUSIONS AND RECOMMENDATIONS

Based on the long term (>1000 hr) cross flow filter testing and evaluations conducted in this program, the following conclusions and recommendations are offered:

- The extended testing (>1000 hr) accomplished in this program using simulator facilities has confirmed the cross flow filter high collection efficiency on ash type material meeting both current emission and turbine tolerance requirements. Prior to this testing, long term filter performance was extrapolated based on short term test results. Integral to achieving this high performance level was the development of an improved, long term, high temperature, ceramic dust seal for seating and fixing the cross flow filter element.

- Improved cross flow filter durability to steady state filtrations and pulse cleaning was demonstrated. The increase in base material strength of the filter matrix and the improvements made in the filter mount and dust seal system were primary factors in achieving this improvement. However, improvements to filter fracture toughness may yet be needed to achieve filter durability to thermal process transients that can occur during plant upsets. Detecting and eliminating weak plate bonding and/or critical flaws developed during filter manufacturing will be essential to achieve this goal. Alternate filter manufacturing techniques that produce truly monolithic structures should be pursued.

- The alumina/mullite oxide matrix currently used for the cross flow filter appears suitable for a wide range of process gas conditions typical of Advanced Fossil Power Generation Systems. The gas

environment of the simulator facilities used in the current testing program does not however reproduce all process gas conditions representative of actual coal fired plants. Field based material studies are being utilized for this purpose.

- Comparison of results show that the high temperature high pressure PFBC simulator facilities used in this program was effective in reproducing filtration conditions representative of actual plant operation. In addition, the simulator facilities are effective tools to reproduce filter thermal and mechanical stressing that is typical of actual plant operations. Such testing is an important dimension to evaluating long term filter durability issues. Thermal transient testing should be an integral part of any and all future hot gas filter development programs.

- Gasifier simulation testing using hot inert gas and injected char produced only similar plant trends regarding filter operating characteristics. Better simulation may be achieved if reducing gas conditions could be utilized and operated at actual temperature and pressure conditions of the gasifier applications. It appears important that both a temperature and gas density effect be included in the gasifier simulation testing.

Appendices

CONTENTS

APPENDIX A

PFBC SIMULATOR PROCESS AND MECHANICAL DRAWINGS

Figure 1 (Dwg 2D27878)	Schematic of HTHP PFBC Simulator
Figure 2 (Dwg 1301J68)	PFBC Simulator Process and Instrumentation Diagram - sheet 1
Figure 3 (Dwg 1301J67)	PFBC Simulator Process and Instrumentation Diagram - sheet 2
Figure 4 (Sketch)	PFBC Simulator General Assembly
Figure 5 (Dwg 1503E74)	Dust Collection Vessel
Figure 6 (Sketch)	Layout of Tubesheet for Two Filter Holders
Figure 7 (Dwg 2235D75)	Modified PFBC Simulator Filter Stack Weldment
Figure 8 (Dwg 2235D83)	Modified PFBC Simulator Top Half Liner Weld
Figure 9 (Dwg 2235D84)	Modified PFBC Simulator Liner Collar Weld
Figure 10 (Dwg 2235D74)	Modified PFBC Simulator Spool Transition Detail
Figure 11 (Dwg 2235D85)	Modified PFBC Simulator Piping Weldments
Figure 12 (Dwg 2235D89)	Modified PFBC Simulator Liner Pipe Weldments

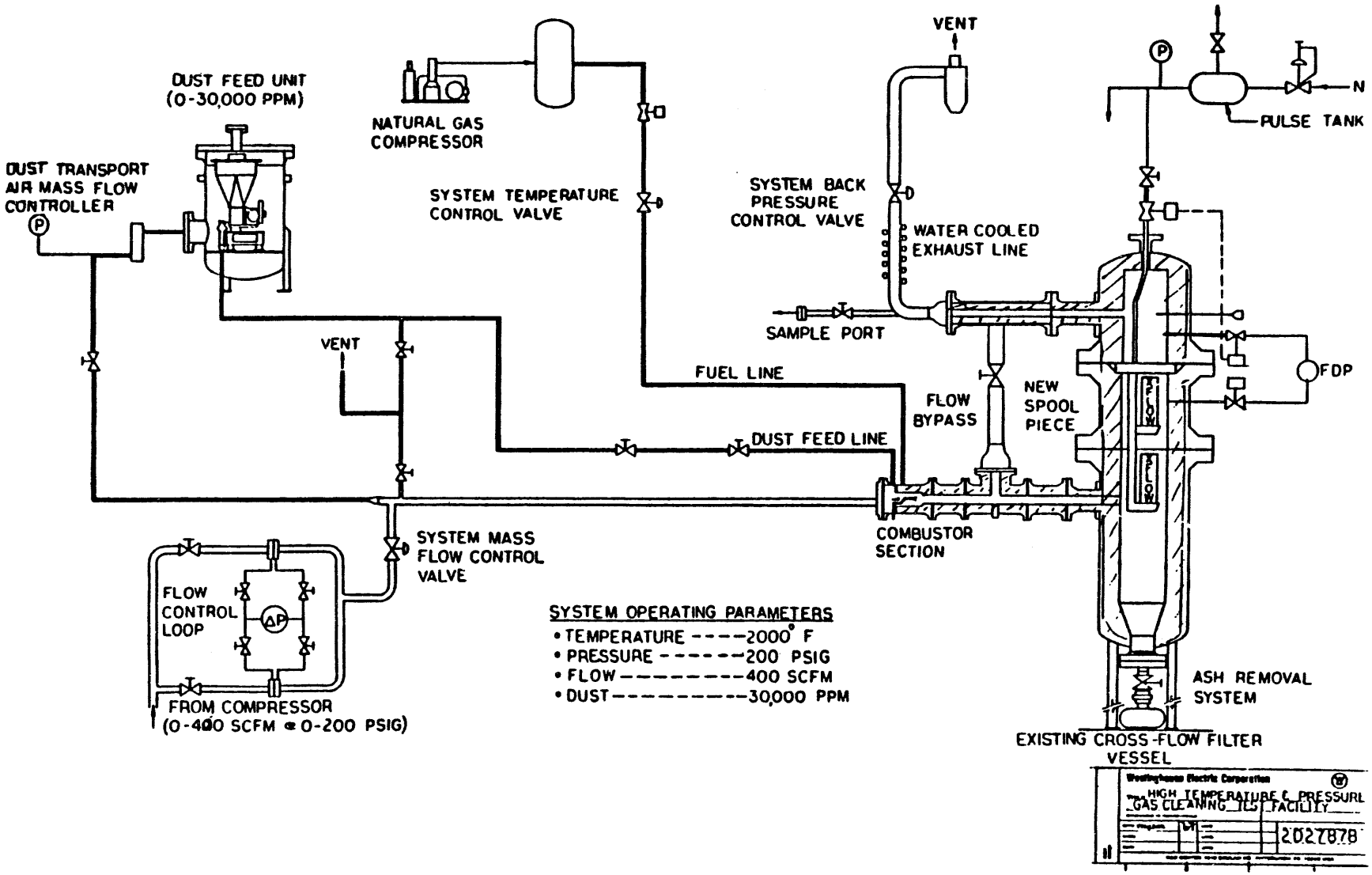

Figure A.1 - Westinghouse HTHP Simulator for PFBC Filter Testing - Schematic

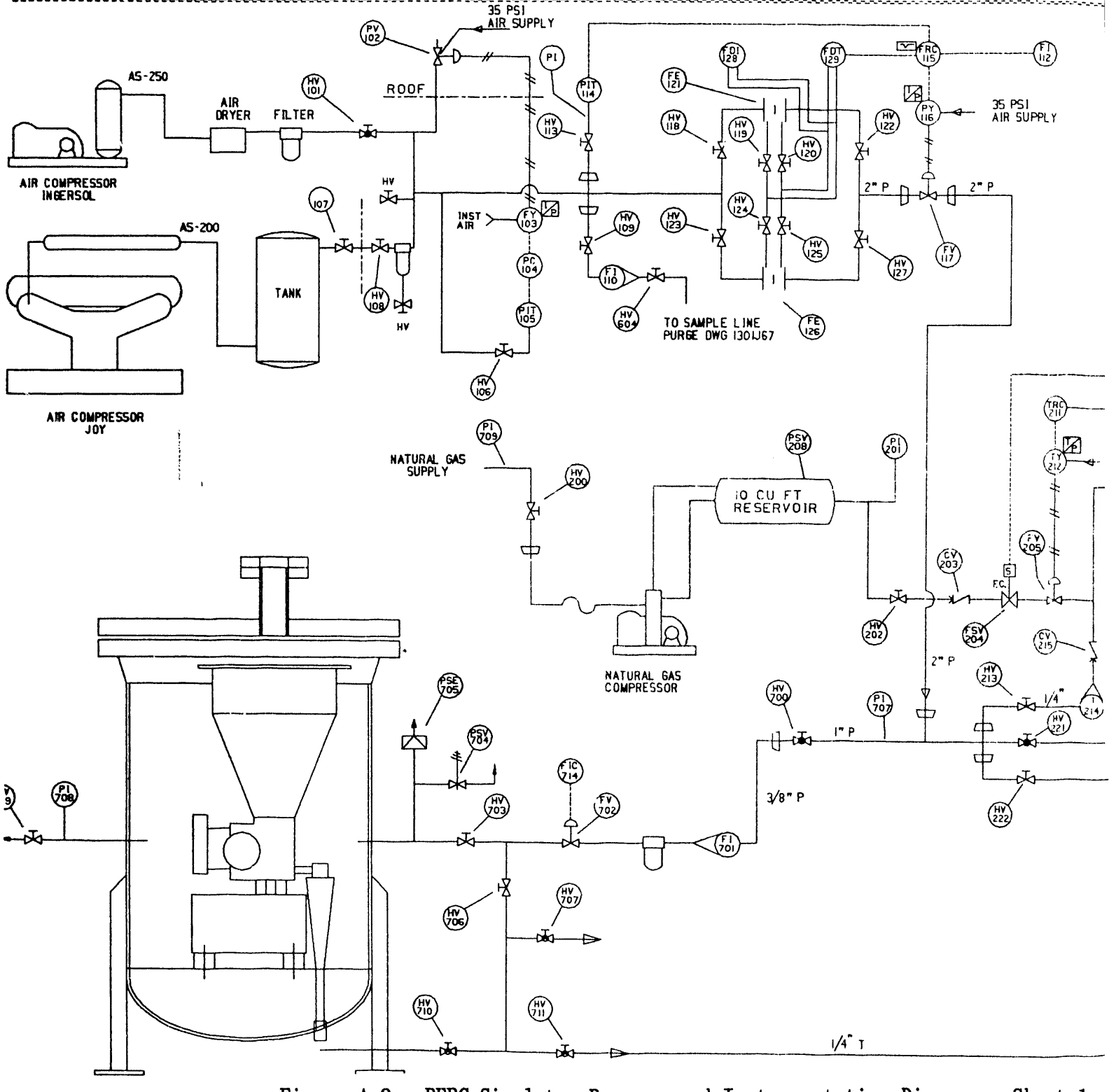

Figure A.2 - PFBC Simulator Process and Instrumentation Diagram - Sheet 1

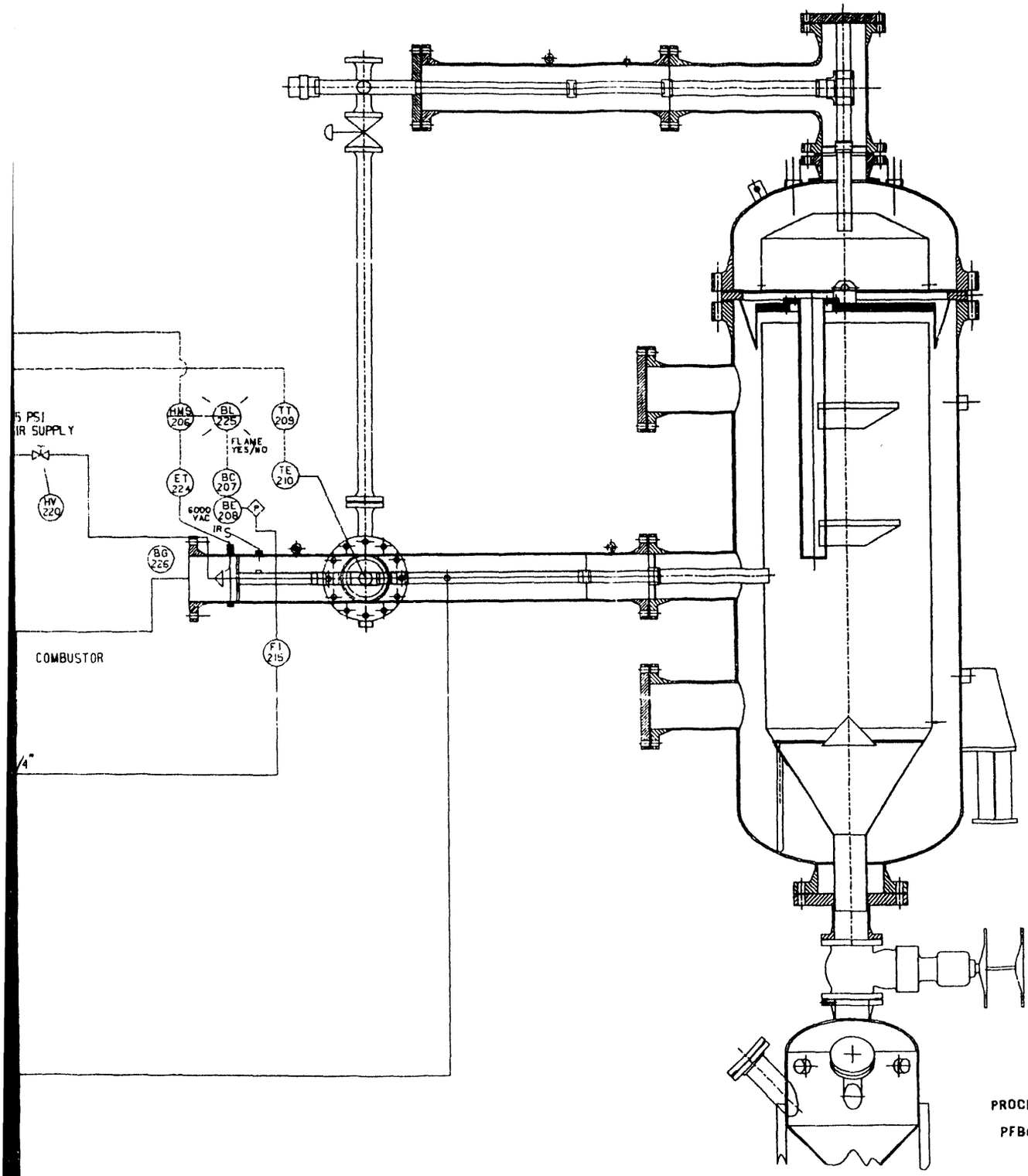

PROCESS AND INSTRUMENTATION

PFBC SIMULATOR

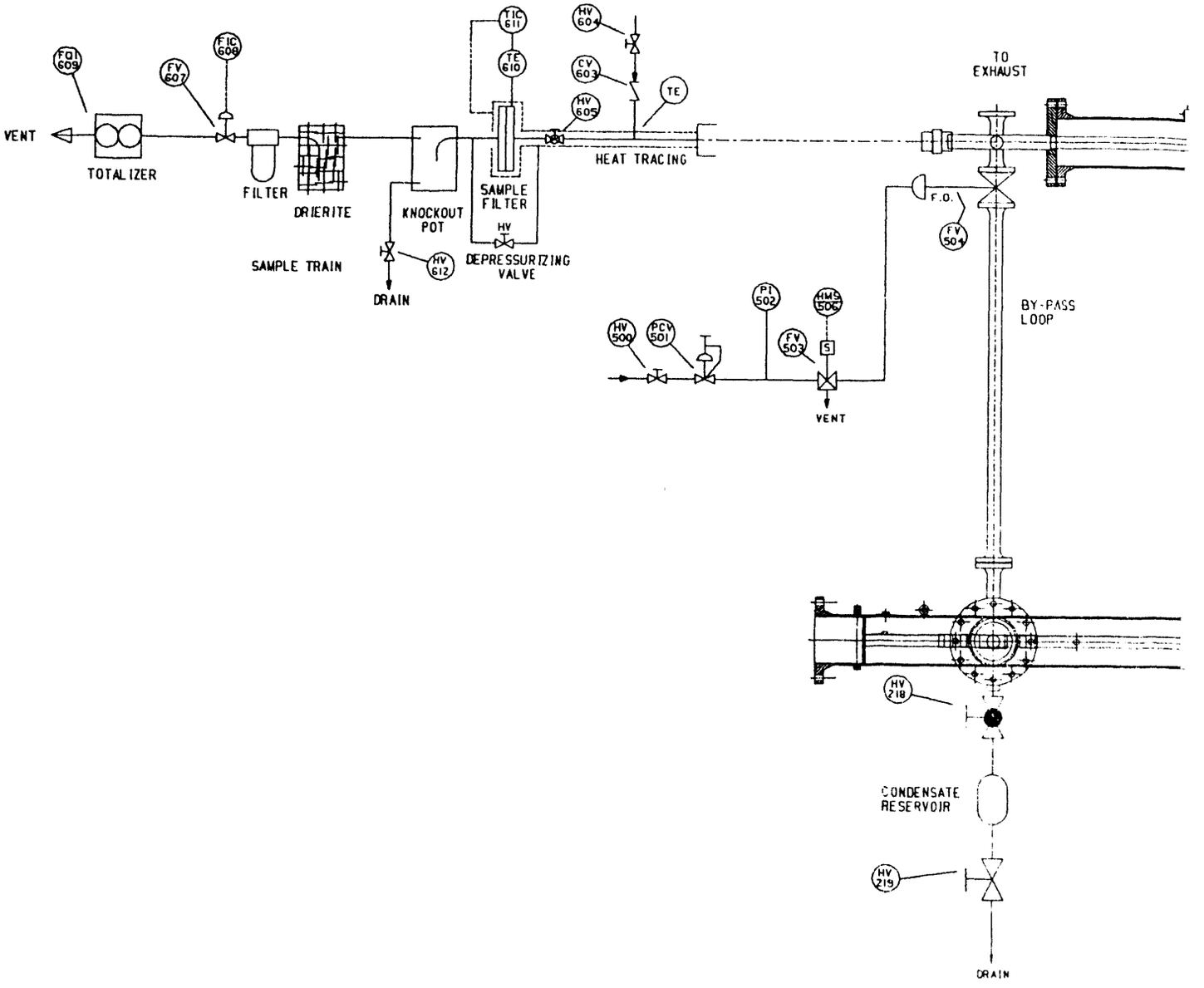

Figure A.3 - PFBC Simulator Process and Instrumentation Diagram - Sheet 2

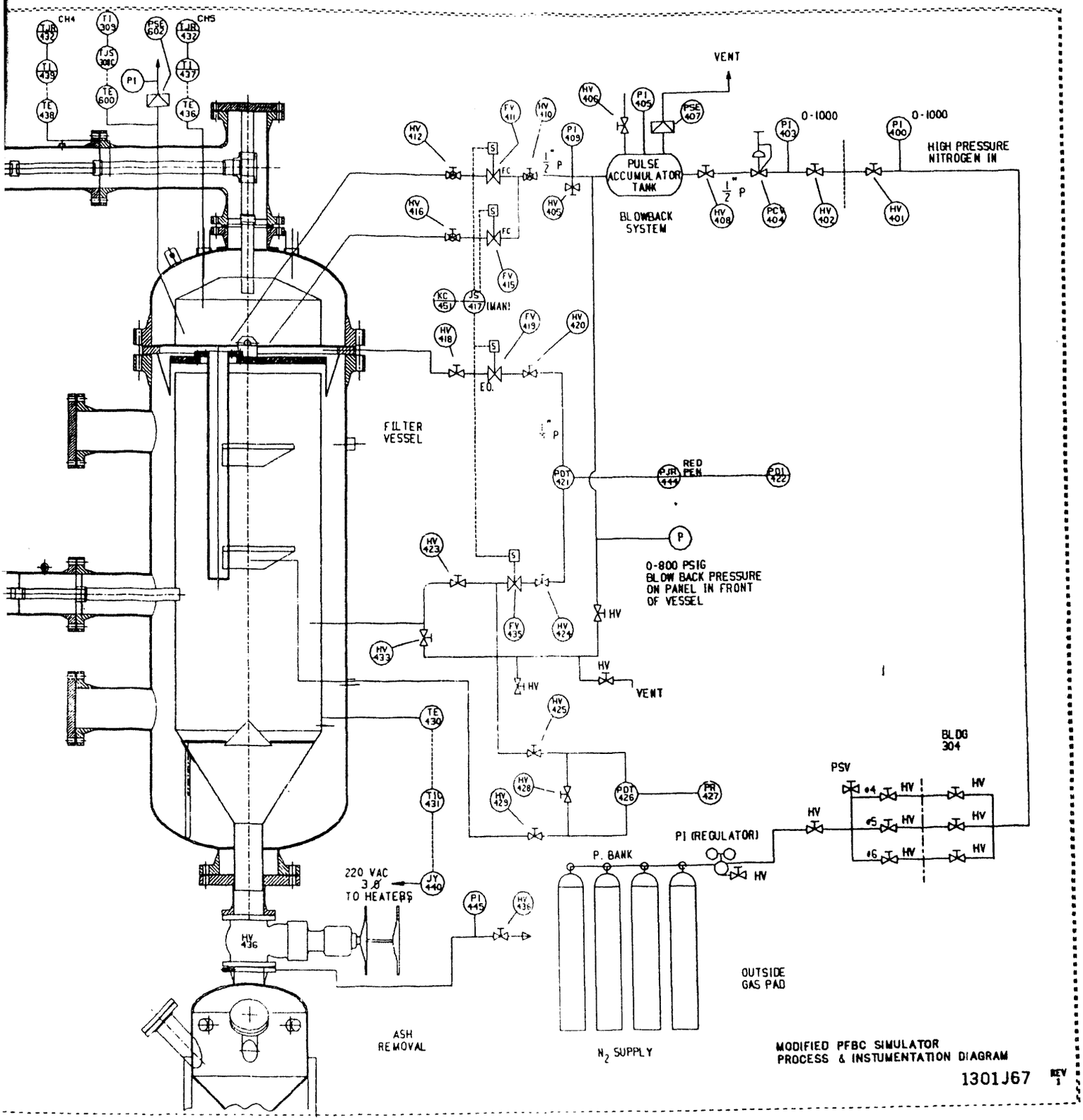
CH4
CH5
VENT
PULSE ACCUMULATOR TANK
BLOWBACK SYSTEM
0-1000
0-1000
HIGH PRESSURE NITROGEN IN
FILTER VESSEL
RED PEN
0-800 PSIG BLOW BACK PRESSURE ON PANEL IN FRONT OF VESSEL
VENT
BLDG 304
PSV
PI (REGULATOR)
P. BANK
220 VAC 3 Ø TO HEATERS
OUTSIDE GAS PAD
ASH REMOVAL
N2 SUPPLY
MODIFIED PFBC SIMULATOR
PROCESS & INSTUMENTATION DIAGRAM
1301J67
REV 1

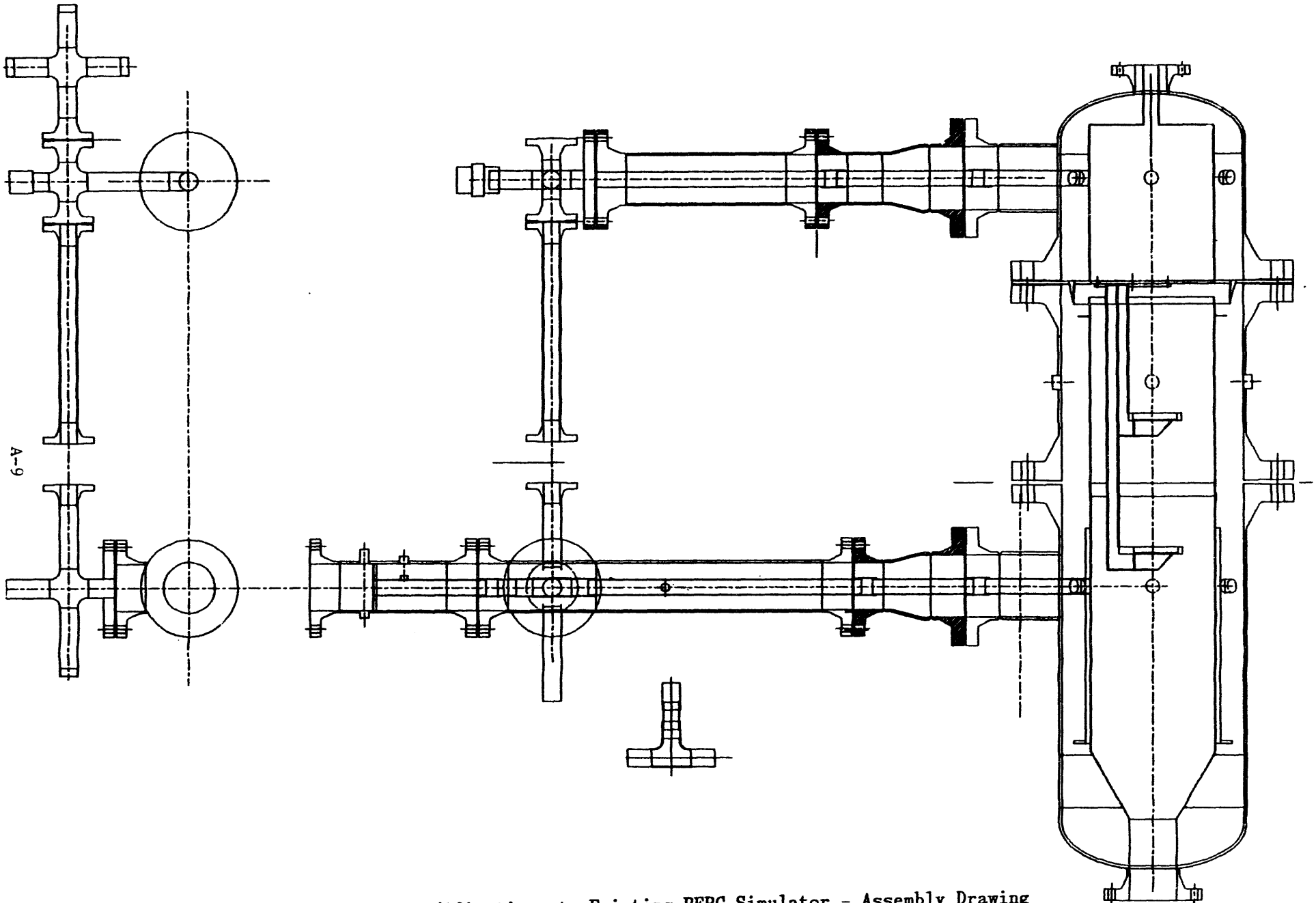

Figure A.4 - Modifications to Existing PFBC Simulator - Assembly Drawing

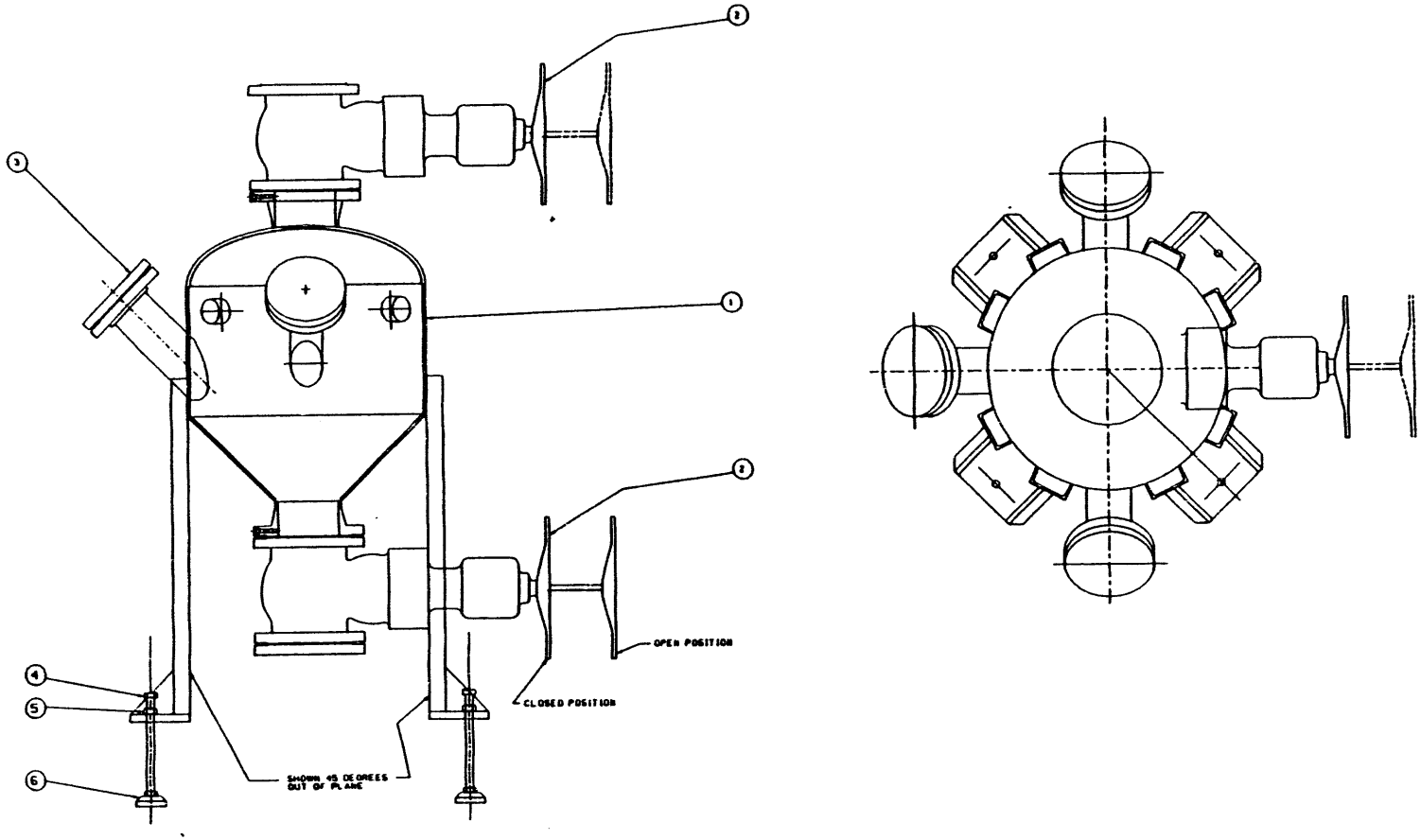

Figure A.5 - Dust Collection Vessel for New PFBC Simulator

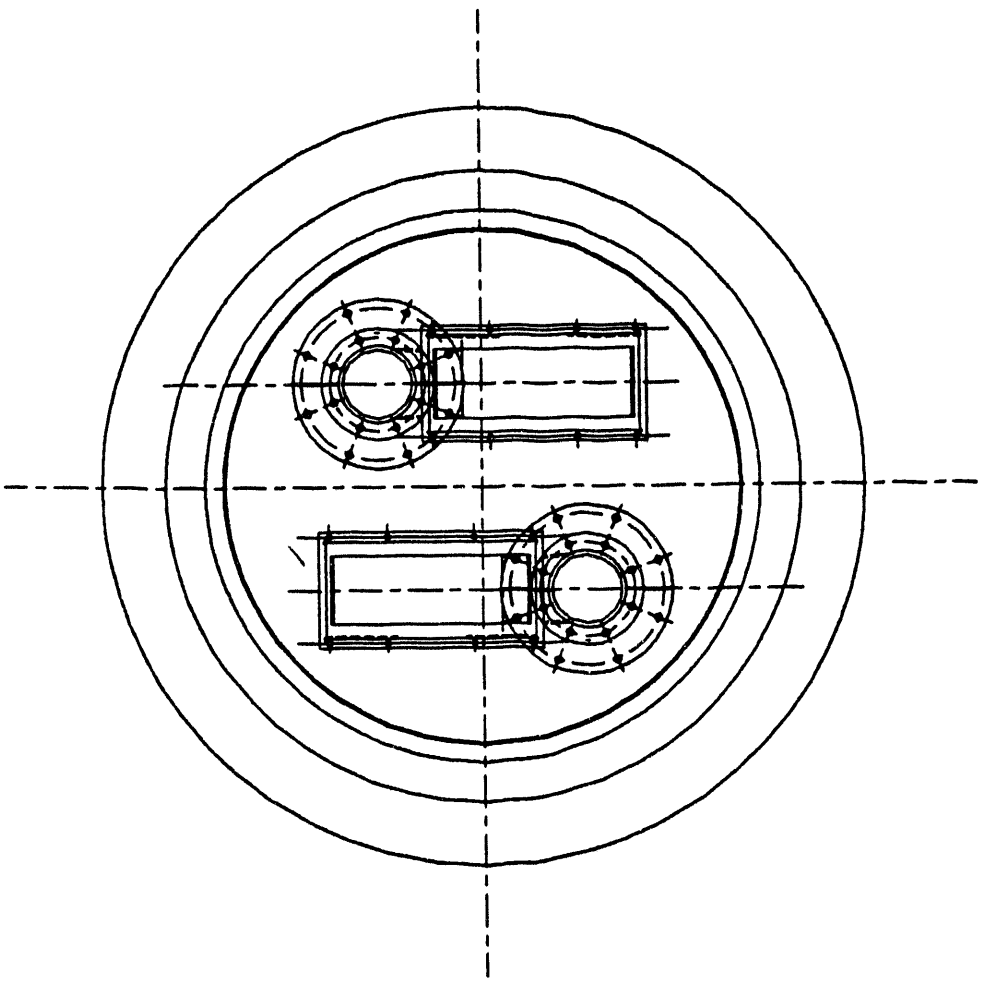

Figure A.6 - Layout of Tubesheet to Accommodate Two Filter Holders

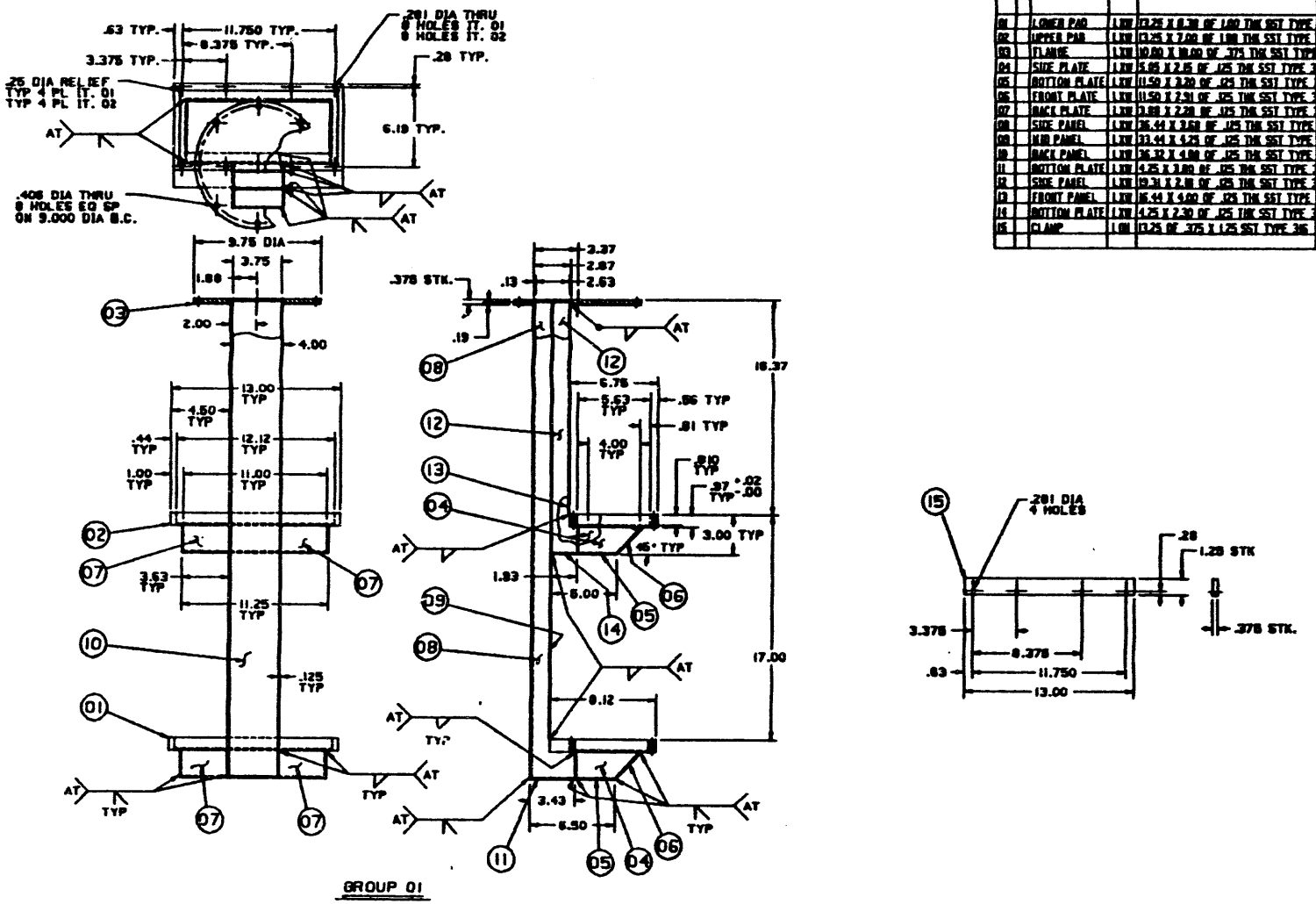

ITEM	QTY	PART NAME	MAT'L	DESCRIPTION
01	1	LOWER PAD	1.0W	13.25 X 8.38 OF 1.00 THK SST TYPE 316
02	1	UPPER PAD	1.0W	13.25 X 7.00 OF 1.00 THK SST TYPE 316
03	1	FLANGE	1.0W	10.50 X 10.00 OF .375 THK SST TYPE 316
04	4	SIDE PLATE	1.0W	5.88 X 2.15 OF .125 THK SST TYPE 316
05	2	BOTTOM PLATE	1.0W	11.50 X 3.20 OF .125 THK SST TYPE 316
06	2	FRONT PLATE	1.0W	11.50 X 2.31 OF .125 THK SST TYPE 316
07	4	BACK PLATE	1.0W	3.88 X 2.28 OF .125 THK SST TYPE 316
08	2	SIDE PANEL	1.0W	16.44 X 3.68 OF .125 THK SST TYPE 316
09	1	HUB PANEL	1.0W	13.44 X 4.25 OF .125 THK SST TYPE 316
10	1	BACK PANEL	1.0W	16.32 X 4.88 OF .125 THK SST TYPE 316
11	1	BOTTOM PLATE	1.0W	4.25 X 3.80 OF .125 THK SST TYPE 316
12	2	SIDE PANEL	1.0W	19.31 X 2.18 OF .125 THK SST TYPE 316
13	1	FRONT PANEL	1.0W	16.44 X 4.00 OF .125 THK SST TYPE 316
14	1	BOTTOM PLATE	1.0W	4.25 X 2.30 OF .125 THK SST TYPE 316
15	1	CLAMP	1.0W	13.25 OF .375 X 1.25 SST TYPE 316

TITLE MODIFIED PFBC SIMULATOR
FILTER STACK WELDMENT
2235D75 REV 1

Figure A.7 - Modified PFBC Simulator Filter Stack Weldment

T.B. 11-6-87

Westinghouse Electric Corporation

MODIFIED PFBC SIMULATOR
FILTER STACK WELDMENT

D 01269 2235D75 1 OF 1

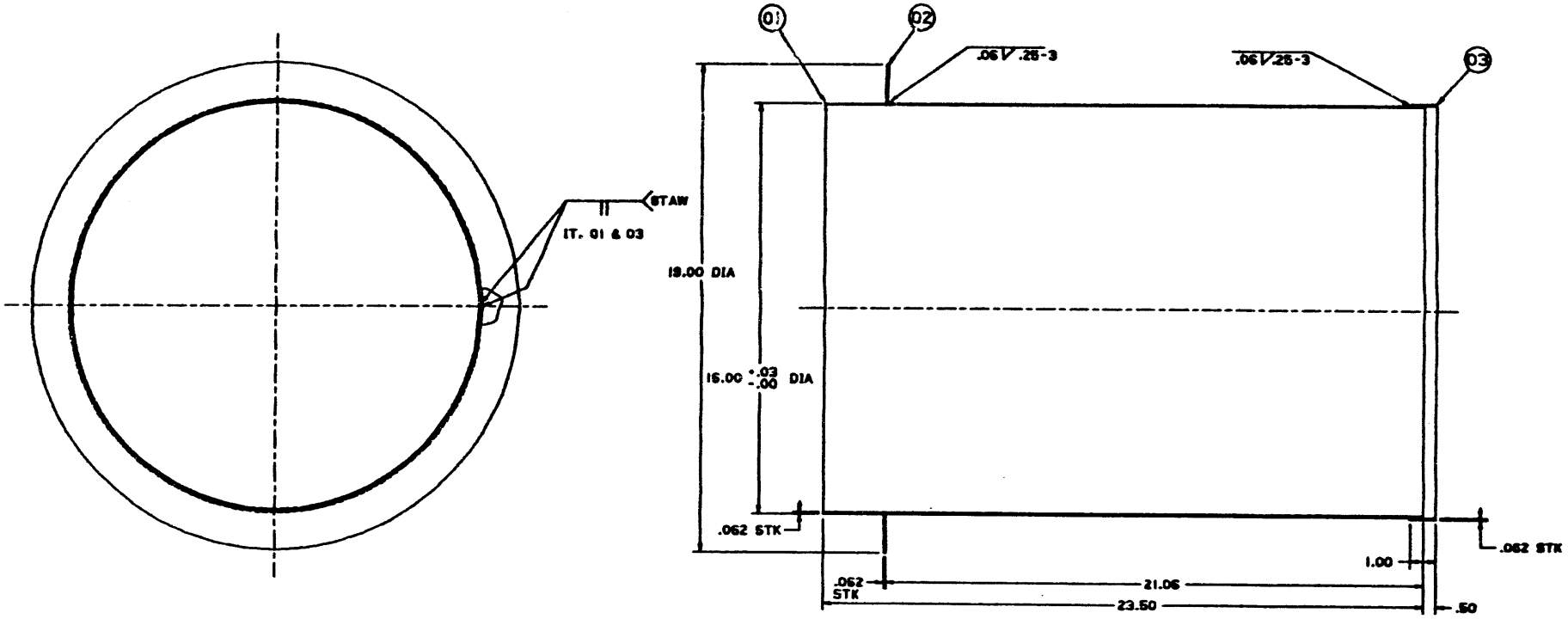

A-13

Figure A.8 - Modified PFBC Simulator Top Half Liner Weld

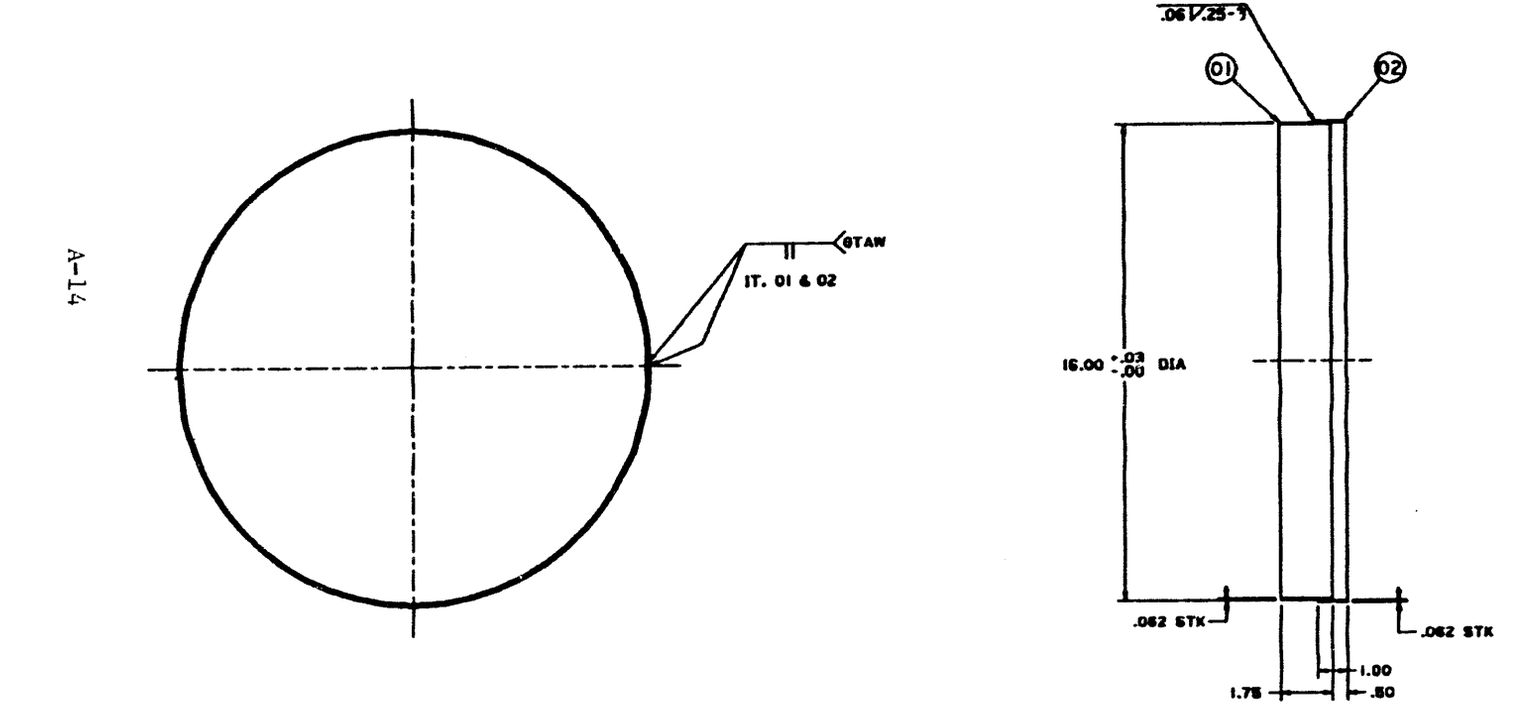

Figure A.9 - Modified PFBC Simulator Liner Collar Weld

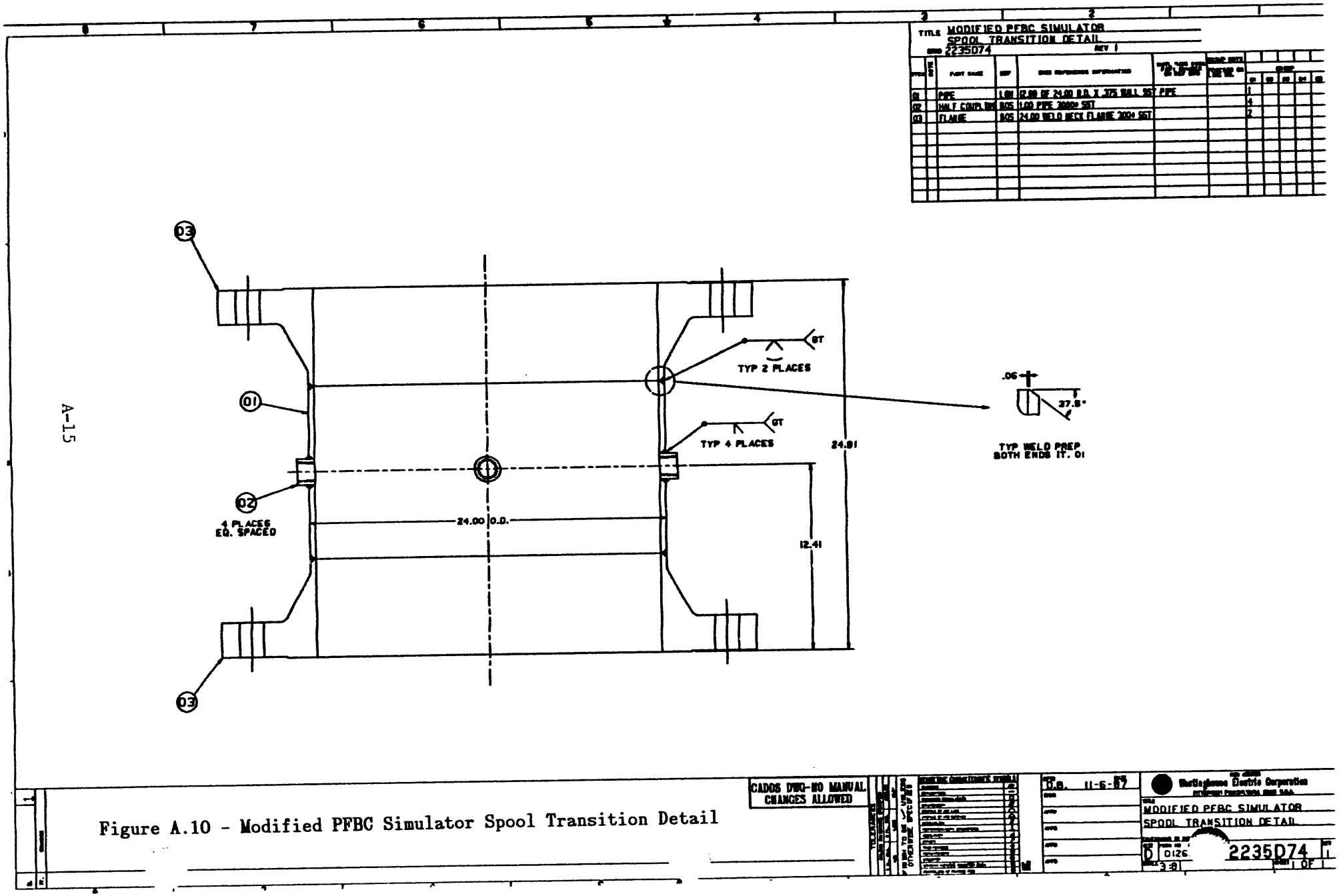

Figure A.10 - Modified PFBC Simulator Spool Transition Detail

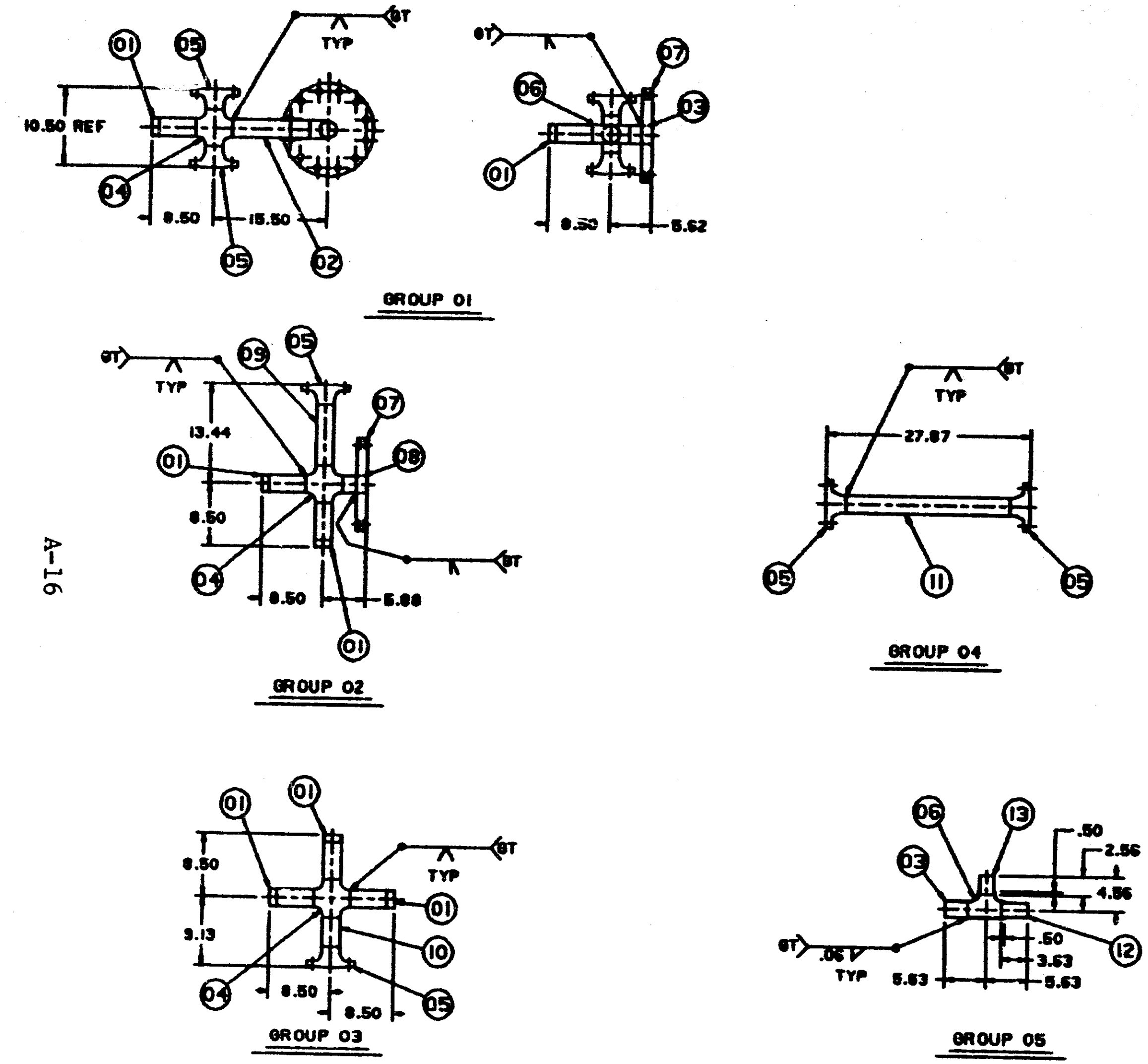

TITLE MODIFIED PFBC SIMULATOR PIPING WELDMENTS

DWG 2235D85 REV 1

		PART NAME					GROUP 01	GROUP 02	GROUP 03	GROUP 04	GROUP 05
01	A	HALF NIPPLE	B06	6.00 OF 2.375 OD X .154 WALL SST PIPE TYPE 316			2	2	1		
02		PIPE	B06	10.75 OF 2.375 OD X .154 WALL SST PIPE TYPE 316			1				
03		PIPE	B06	3.38 OF 2.375 OD X .154 WALL SST PIPE TYPE 316			1				1
04		CROSS	B05	2 IN X .154 WALL SST CROSS TYPE 316			1	1	1		
05		FLANGE	B05	2 IN 300# WEL NECK FLANGE SST TYPE 316			2	1	1	2	
06		TEE	B05	2 IN X .154 WALL SST TEE TYPE 316			1				1
07		FLANGE	B05	6 IN 300# BLIND FLANGE SST TYPE 316			1	1			
08		PIPE	B06	3.62 OF 2.375 OD X .154 WALL SST PIPE TYPE 316				1			
09		PIPE	B05	8.44 OF 2.375 OD X .154 WALL SST PIPE TYPE 316				1			
10		PIPE	B05	4.12 OF 2.375 OD X .154 WALL SST PIPE TYPE 316					1		
11		PIPE	B05	22.62 OF 2.375 OD X .154 WALL SST PIPE TYPE 316						1	
12		TUBE	B05	3.88 OF 2.00 OD X .035 WALL SST TUBE TYPE 304							1
13		TUBE	B05	2.81 OF 2.00 OD X .035 WALL SST TUBE TYPE 304							1

A- ONE 12.00 NIPPLE MAKES TWO HALF NIPPLES

Figure A.11 - Modified PFBC Simulator Piping Weldments

CADDS DWG-NO MANUAL CHANGES ALLOWED

D.B. 11-10-87

Westinghouse Electric Corporation

MODIFIED PFBC SIMULATOR PIPING WELDMENTS

D 2235D85 1

1:8 1 OF 1

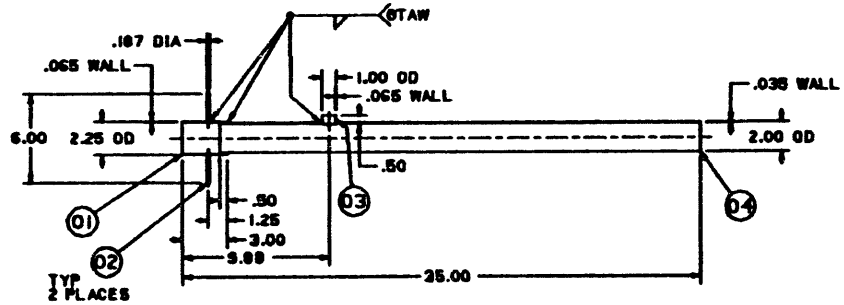

GROUP 01

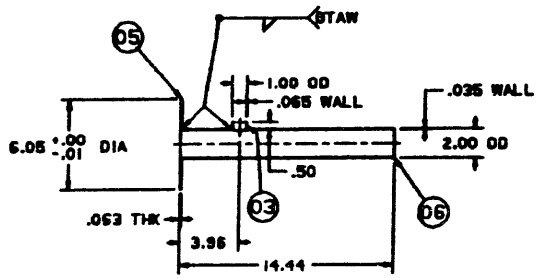

GROUP 02

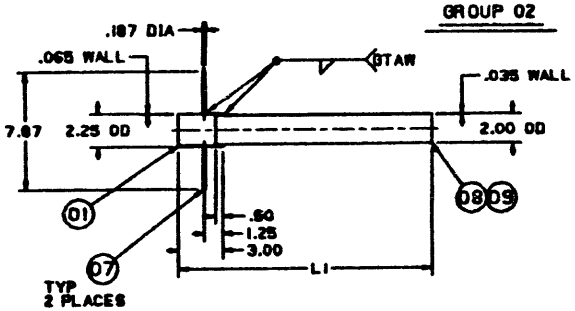

ITEM NO.	L1	GROUP NO.
06	17.00	03
05	19.88	04

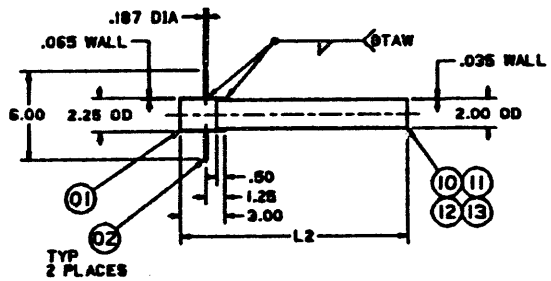

ITEM NO.	L2	GROUP NO.
10	4.88	05
11	6.94	06
12	15.38	07
13	33.00	08

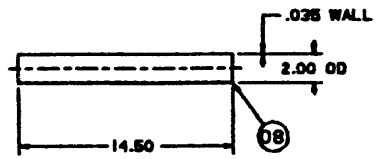

ITEM NO.	PART NAME	QTY	DESCRIPTION OR IDENTIFYING NUMBER	MATERIAL SPEC.	GROUP NO.
01	SLIP JOINT	1 EA	3.25 OF 2.250 OD X .065 WALL SST	TUBE TYPE 304	1 1 1 1 1 1 1 1
02	LEG	1 EA	2.12 OF .187 DIA SST ROD TYPE 304		2 2 2 2 2 2
03	PORT	1 EA	1.00 OF 1.000 OD X .065 WALL TUBE	SST TYPE 304	1 1
04	LINER	1 EA	32.25 OF 2.000 OD X .035 WALL SST	TUBE TYPE 304	1
05	FLANGE PLATE	1 EA	6.38 X 6.38 OF .063 THK SST TYPE	304	1
06	LINER	1 EA	14.69 OF 2.000 OD X .035 WALL SST	TUBE TYPE 304	1
07	LEG	1 EA	3.86 OF .187 DIA SST ROD TYPE 304		2 2
08	LINER	1 EA	14.75 OF 2.000 OD X .035 WALL SST	TUBE TYPE 304	1
09	LINER	1 EA	17.63 OF 2.000 OD X .035 WALL SST	TUBE TYPE 304	1
10	LINER	1 EA	2.63 OF 2.000 OD X .035 WALL SST	TUBE TYPE 304	1
11	LINER	1 EA	4.63 OF 2.000 OD X .035 WALL SST	TUBE TYPE 304	1
12	LINER	1 EA	13.13 OF 2.000 OD X .035 WALL SST	TUBE TYPE 304	1 1
13	LINER	1 EA	30.75 OF 2.000 OD X .035 WALL SST	TUBE TYPE 304	1 1

TITLE MODIFIED PFBC SIMULATOR
LINER PIPE WELDMENTS
DWG 2235D89 REV 1

Figure A.12 - Modified PFBC Simulator Liner Pipe Weldments

CADDS DWG-NO MANUAL CHANGES ALLOWED

D.B. 11-12-87

Westinghouse Electric Corporation

MODIFIED PFBC SIMULATOR
LINER PIPE WELDMENTS

6 01269 2235D89 1

SCALE 1:4 SHEET 1 OF 1

APPENDIX B

HIGH TEMPERATURE, HIGH PRESSURE (HTHP) CERAMIC FILTER TEST FACILITY PROCESS AND DESIGN DESCRIPTION

HTHP Ceramic Filter Test Facility and Process Description

1. Introduction

This document describes the test facility and process to be used for investigating the long-term durability of the ceramic cross flow filter, per DOE Contract No. DE-AC21-87MC24022. The test plan that will be conducted in this facility provides for efficient and economic long-term durability tests under simulated reducing gas (similar to coal gasifier product gas) and simulated pressurized fluidized bed combustion (PFBC) conditions.

The objective of this work is to assess the long-term mechanical integrity and stability of components and materials used in the construction of the ceramic cross flow filter as well as the stability of filtration properties over time. This objective will be met by conduct of the test plan, which provides for 2000 hours of testing under both simulated reducing gas and PFBC conditions. The reducing gas and PFBC tests will be carried out in parallel with four test segments of at least 500 continuous hours each at steady-state conditions.

The experimental test facilities consist of a new gasifier simulator test loop plus an existing PFBC simulator test loop that will be upgraded. This document will describe both systems in terms of gas supply, particulate injection, ceramic cross flow filter, process instrumentation and control devices, and piping and vessel design.

These systems will be installed in a new hot gas cleaning laboratory that Westinghouse is currently constructing. The preliminary equipment lay-out and floor plan for the new laboratory is shown in Figure B.1. This facility will have a floor area of approximately 2045 ft^2 and will enable both systems to be operated simultaneously. The filter loops will be in an area with usable head space to approximately 20 feet. An isometric drawing of the area is shown in Figure B.2. An overhead X-Y, 2 ton hoist will provide full coverage for assembly and disassembly of the test systems. This laboratory provides a large, flexible site for the conduct of hot gas cleaning programs.

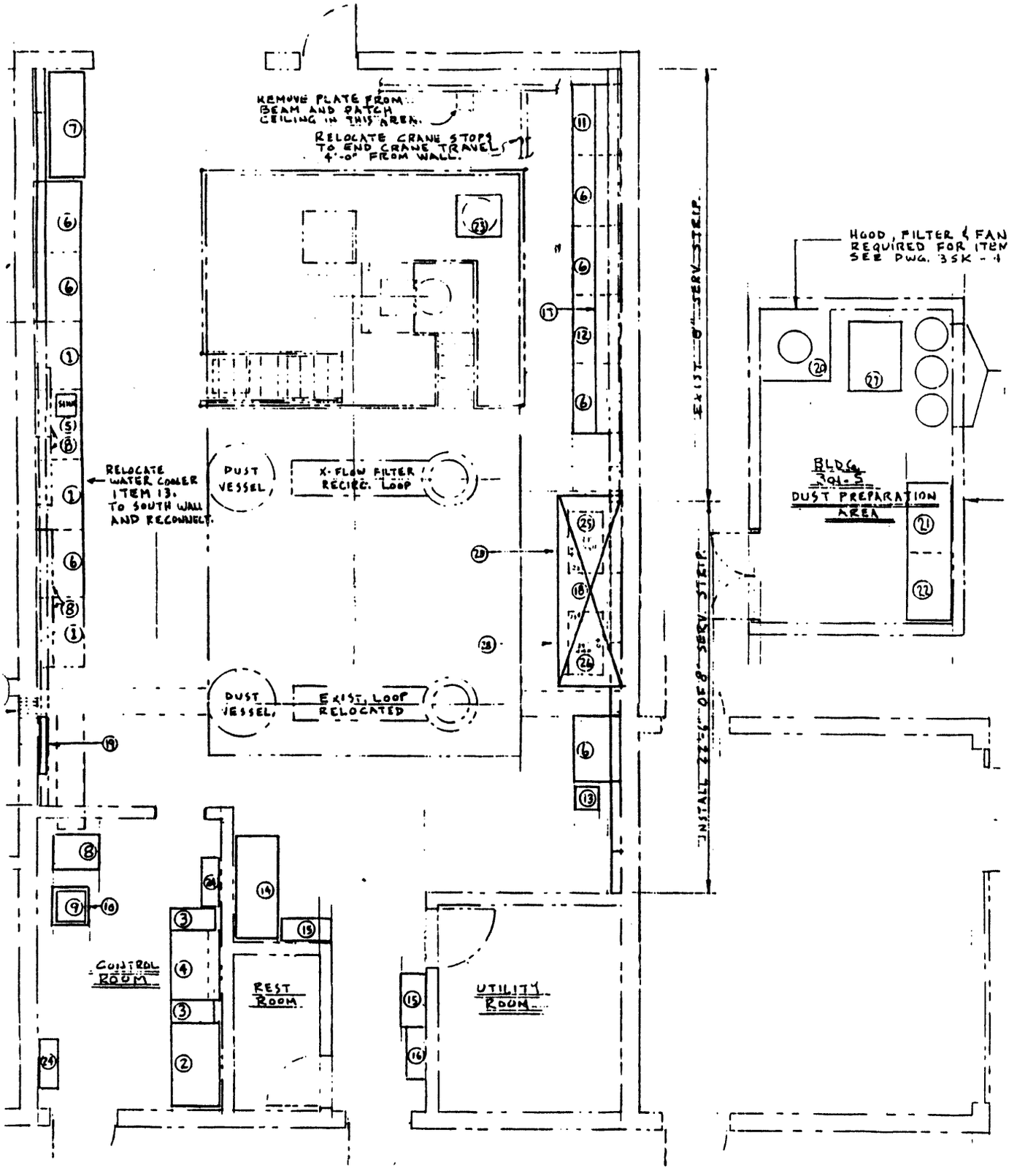

Figure B.1 – Facility Floor Plan

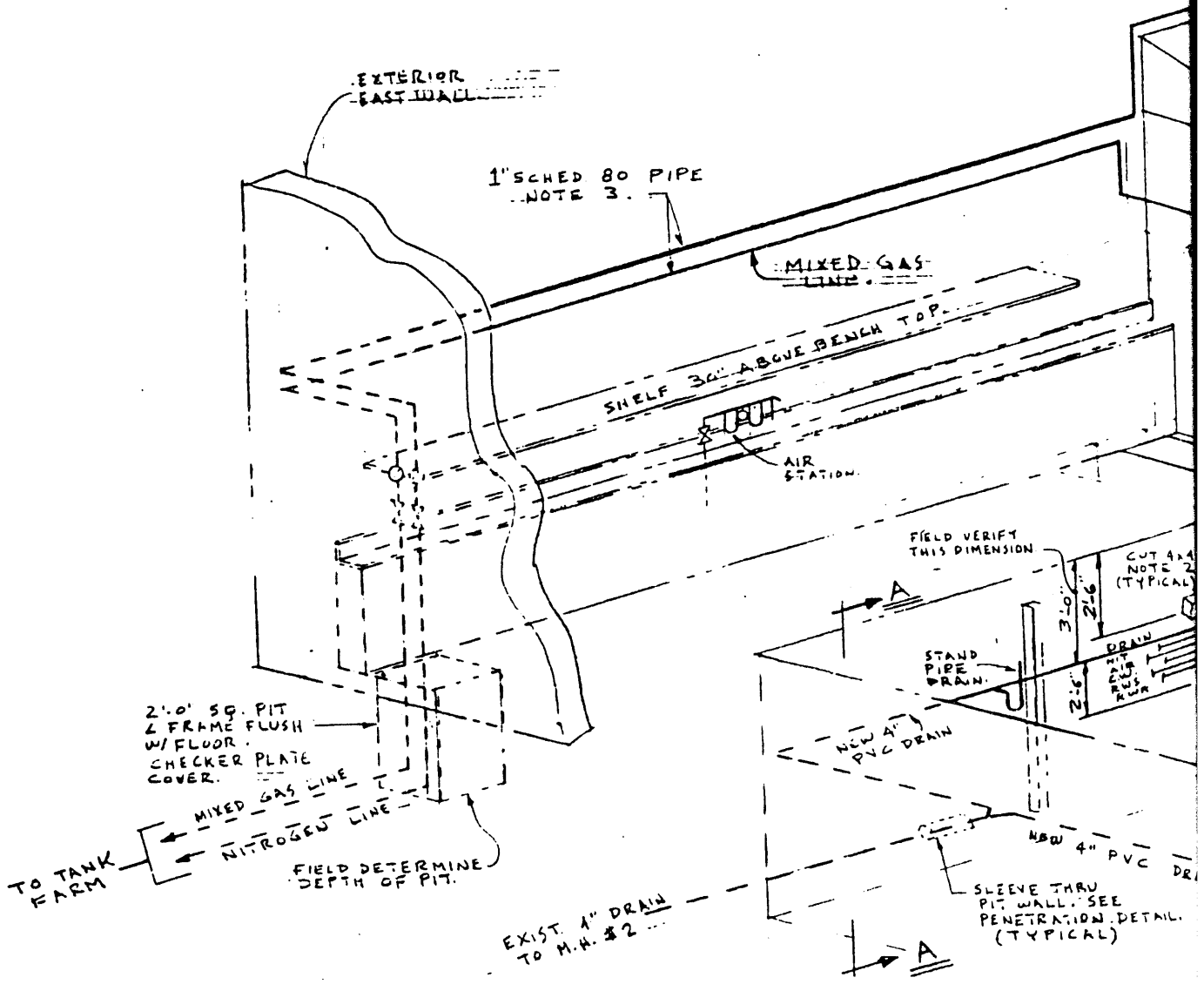
EXTERIOR EAST WALL
1" SCHED 80 PIPE NOTE 3.
MIXED GAS LINE
SHELF 36" ABOVE BENCH TOP
AIR STATION
FIELD VERIFY THIS DIMENSION
A
3'-0"
2'-6"
2'-6"
STAND PIPE DRAIN
NEW 4" PVC DRAIN
2'-0" SQ. PIT W/ FLOOR. CHECKER PLATE COVER.
MIXED GAS LINE
NITROGEN LINE
TO TANK FARM
FIELD DETERMINE DEPTH OF PIT.
EXIST. 1" DRAIN TO M.H. #2
SLEEVE THRU PIT WALL. SEE PENETRATION DETAIL. (TYPICAL)
A

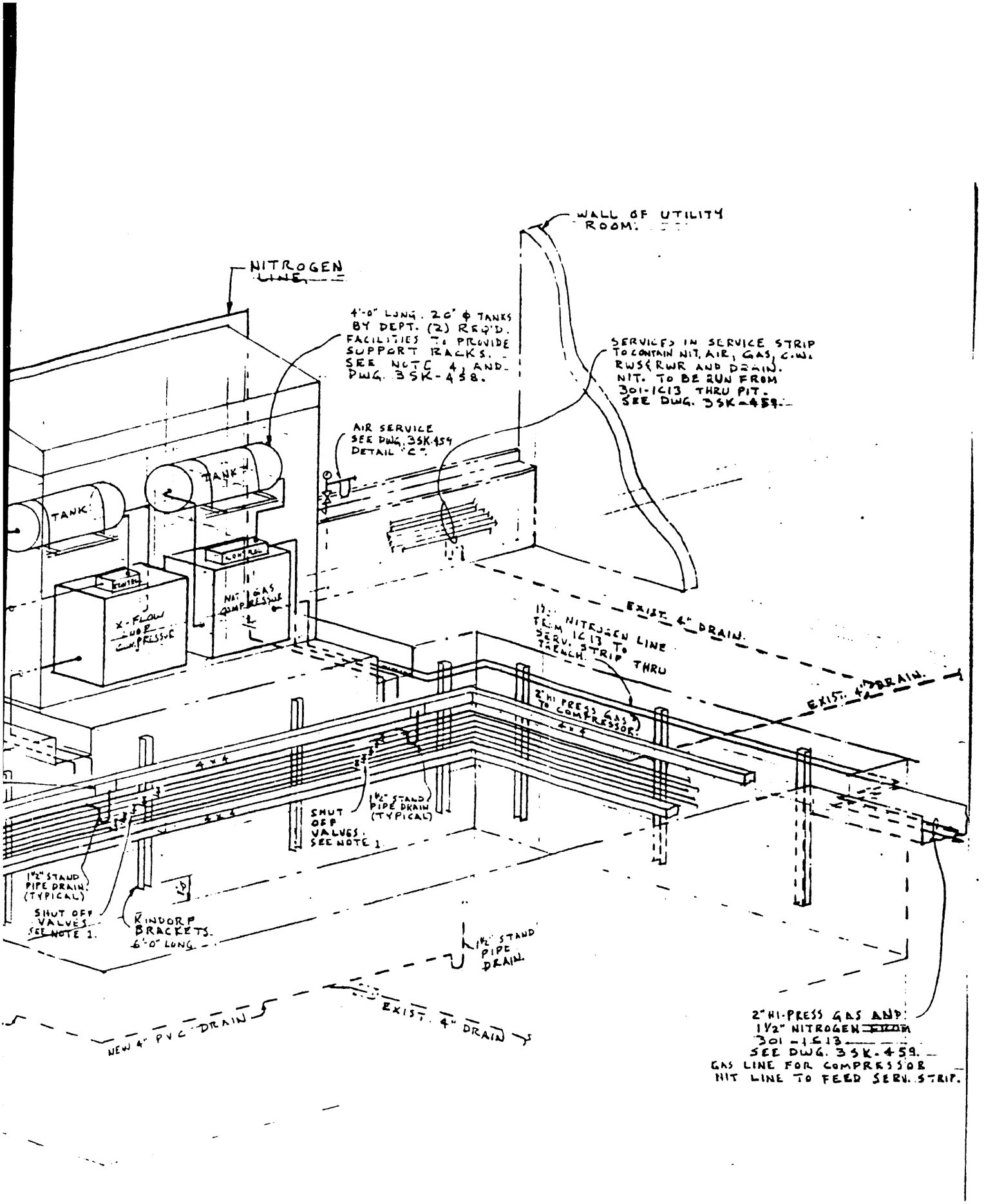

Figure B.2 – Isometric of Facility

2. Gasifier Simulator Test Loop

2.1 General Description and Operating Basis

The gasifier simulator test loop will be designed and built following the general arrangement shown in Figure B.3 to provide the necessary gas flow at the desired pressure and temperature. This system will consist of a closed recirculating loop so that a fixed gas composition can be maintained. The gas supply for this system will be provided by pre-mixing a simulated reducing gas with the following composition:

Nitrogen	64%
Carbon Monoxide	23%
Carbon Dioxide	13%

The test loop will be operated to provide approximately 100 actual cubic feet per minute (acfm) at 150 psig and 1500°F, through the cross flow filters installed in the filter vessel. With two filter elements installed, this flow will provide a filter face velocity of approximately 7 feet per minute. After the gas stream passes through the filters, the total flow is determined by measuring the pressure drop through a venturi which along with the system pressure and temperature, are used to calculate the total mass flow in a mass flow controller.

Approximately 10 percent of the gas flow will be used as high pressure motive gas for an eductor that will recirculate the system gas to maintain flow through the filter. The design basis for the eductor is given in Appendix C. The eductor flow is removed from the system after the mass flow venturi, cooled, and then recompressed to 500 psig. This high pressure gas is then heated to above 1500°F in a process gas heater before being reinjected into the eductor nozzle, causing the balance of the gas flow to recombine with the motive gas. A metered dust flow will be added to this stream before it enters the filter vessel. The dust (char) laden gas enters the test vessel at a point below the filter mounts. A dust removal system will allow on-line removal of the collected dust from the filter vessel so that long-term test can be conducted without interruption.

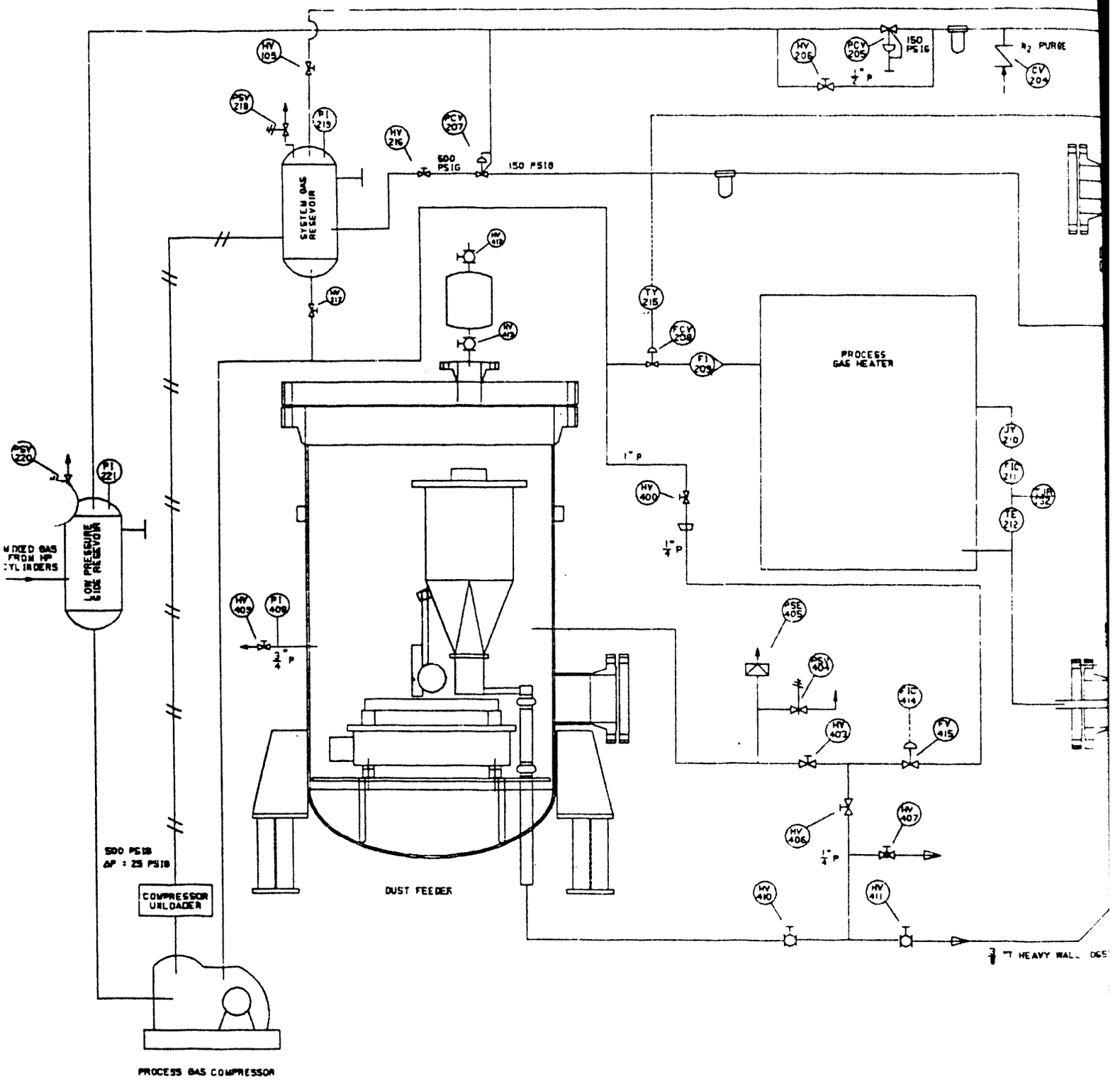
HV 105
PSV 218
PI 219
HV 216
PCV 207
600 PSIG
150 PSIG
SYSTEM GAS RESEVOIR
HV 118
HV 117
HV 206
PCV 205
150 PSIG
1" P
N2 PURGE
CV 204
TY 215
PCV 208
FI 209
PROCESS GAS HEATER
JY 210
TIC 211
TE 212
PSV 220
PI 221
MIXED GAS FROM HP CYLINDERS
LOW PRESSURE SIDE RESEVOIR
HV 400
1" P
HV 409
PI 408
3/4" P
PSE 405
PCV 404
TIC 414
HV 403
FV 415
HV 406
HV 407
1/4" P
HV 410
HV 411
500 PSIG
ΔP = 25 PSIG
COMPRESSOR UNLOADER
DUST FEEDER
PROCESS GAS COMPRESSOR

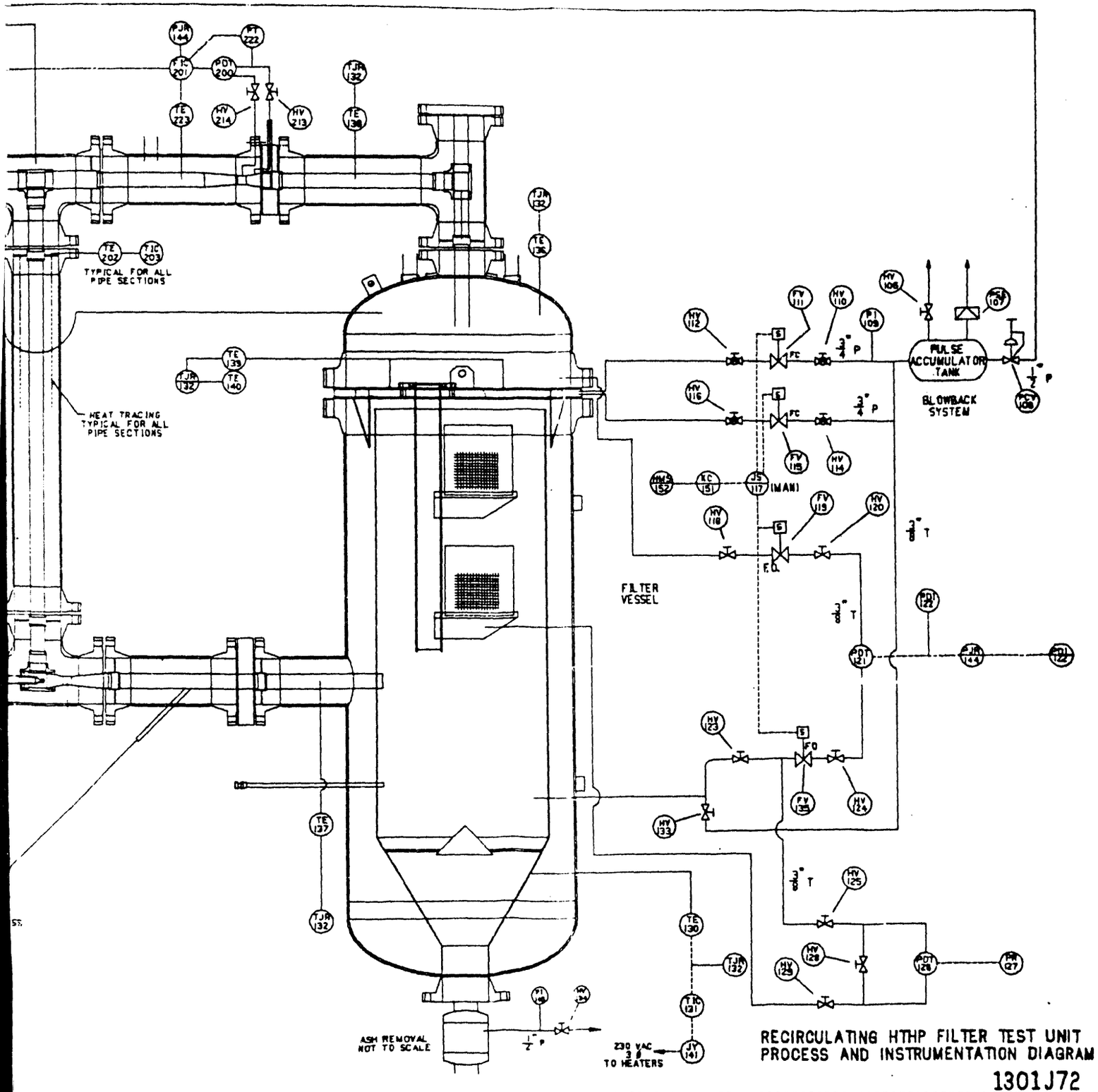

Figure B.3 – Recirculating HTHP Filter Test Unit

Electrical heaters will provide internal heat tracing of all the insulated piping and the filter vessel to maintain the desired operating temperature.

A blow-back system using the simulated reducing gas from the high pressure compressor will be used to clean the filters on-line. The use of that gas as the blow-back medium will maintain the gas composition in the closed loop system.

A full complement of instrumentation will be available to automatically control the operation of the system and to collect data.

A detailed description of the subsystems and process is provided in the following sections.

2.2 Piping and Vessel Design

2.2.1 Piping and Vessel Specification

The piping and device pressure housings will be refractory lined carbon steel pipe sections so that the pressure boundaries remain at relatively low temperature. Figure B.3 shows the general arrangement of the vessel, piping and filter internals. Figures B.4 through B.7 show the design drawings for vessel and piping components.

A 2-1/2 inch diameter stainless steel liner is used to separate the process gas stream from the refractory material (e.g., Fiberfrax or castable ceramic). The pressure boundary will be 8 inch diameter carbon steel schedule 40 pipe with 300 series flanges. The filter vessel will be a 40 inch diameter ASME coded pressure vessel designed for 350 psig maximum working pressure. The filter vessel will have an internal straight section formed by a 30 inch diameter, 316 stainless steel liner, from the tube sheet used to support the filters to the start of a discharge cone section, of approximately 6 feet. This provides adequate volume for positioning the filters to be tested and enough flexibility to test a wide variety of configurations.

2.2.2 Heat Tracing

The heat tracing for the system will be provided by two different styles of Watlow Electric heaters. All of the pipe liners

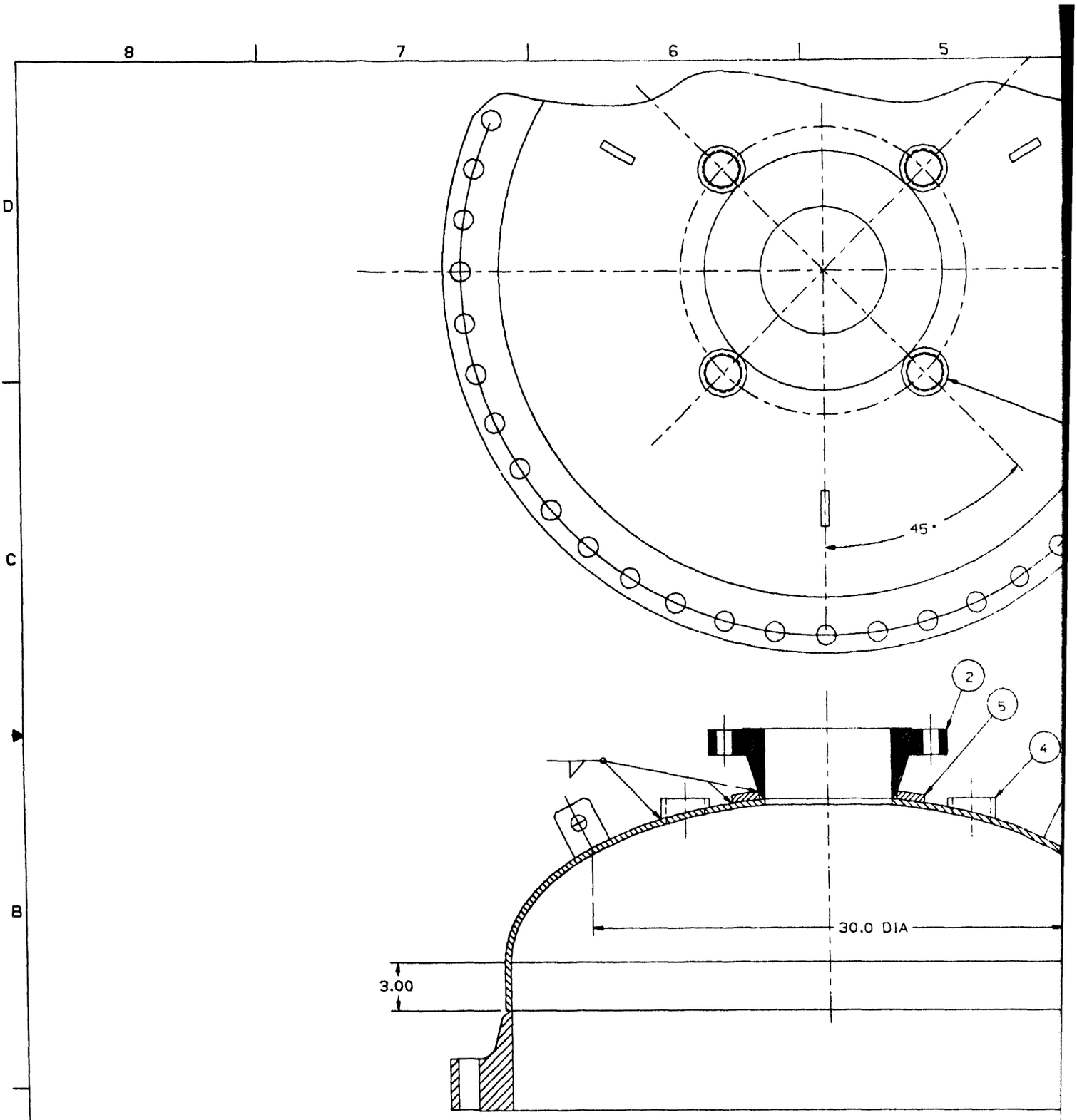

Figure B.4 – Recirculating HTHP Filter Test Unit Main Vessel Cap

TITLE RECIRCULATING HTHP FILTER TEST UNIT
MAIN VESSEL CAP
DWG 2236D44 REV 2

ITEM	NOTE	PART NAME	DEF	SIZE REFERENCE INFORMATION	MATL SIZE CODE PART NUMBER OR REF DWG	GROUP NOTE PROCESS OR LINE NO.	GROUP 01	02	03	04	05
1		CAP		40.00 I.D. .375 THK 2:1 ELLIPTICAL HEAD		STL	1				
2		WELD NECK		8.00 300 LB WELD NECK FLANGE		STL	1				
3		FLANGE		350#WELD NECK PRESSURE VESSEL FLANGE		STL	1				
4		HALF CPLG		2.00 NPT 3000# HALF CPLG		STL	4				
5		REINF PAD		12.00 DIA OF .50 THK		STL	1				
6		LIFT LUG		FROM .500 THK BAR		STL	3				

NOTE: REINFORCING PAD IT. 5 TO BE ROLLED TO FIT IT. 1 BEFORE WELDING.

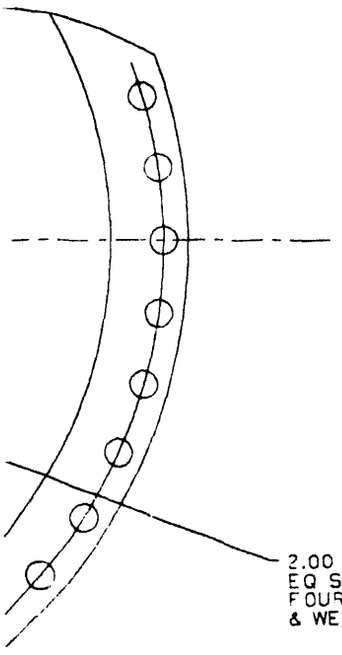

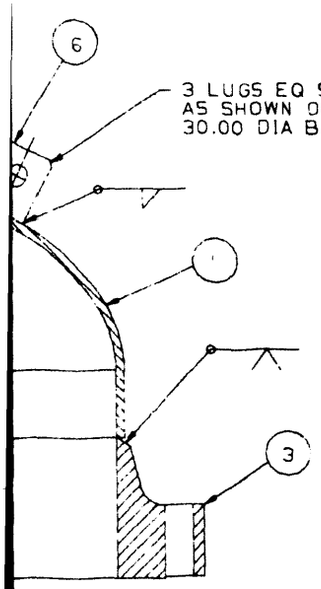

DESIGN SPECS:

1. DESIGN CONDITIONS 350 PSIG - 650° F
2. CONSTRUCTION - FUSION WELDED - DYE PENETRANT TEST ROOT PASS AND FINAL PASS.
3. CODE REQUIREMENTS - ASME SECT VIII
4. WELDERS QUALIFIED PER ASME CODE SECT IX
5. TESTING - 500 PSI HYDROSTATIC COMPLETE ASSY.
6. STAMPING - PER CODE.

CADDS DWG-NO MANUAL CHANGES ALLOWED

TOLERANCES UNLESS OTHERWISE SPECIFIED: 2 PL. DEC. ±.005, ANGLES ±0.5°, 3 PL. DEC. ±.001

FINISH TO BE √ UNLESS OTHERWISE SPECIFIED

GEOMETRIC CHARACTERISTIC SYMBOLS

DFTR W.DILMORE DATE
CHKR
APPD
APPD
APPD
APPD

R&D CENTER
Westinghouse Electric Corporation
PITTSBURGH PENNSYLVANIA 15235 U.S.A.

TITLE
RECIRCULATING HTHP FILTER TEST UNIT
MAIN VESSEL CAP

DIMENSIONS IN INCHES
SIZE D | FSCM NO 01269 | DWG NO 2236D44 | REV 2
SCALE 1:2 | D.301 | SHEET 1 OF 1

DESIGN SPECS:

1. DESIGN CONDITIONS 350 PSIG - 650° F
2. CONSTRUCTION - FUSION WELDED - DYE PENETRANT TEST ROOT PASS AND FINAL PASS.
3. CODE REQUIREMENTS - ASME SECT VIII
4. WELDERS QUALIFIED PER ASME CODE SECT IX
5. TESTING - 500 PSI HYDROSTATIC COMPLETE ASSY.
6. STAMPING - PER CODE.

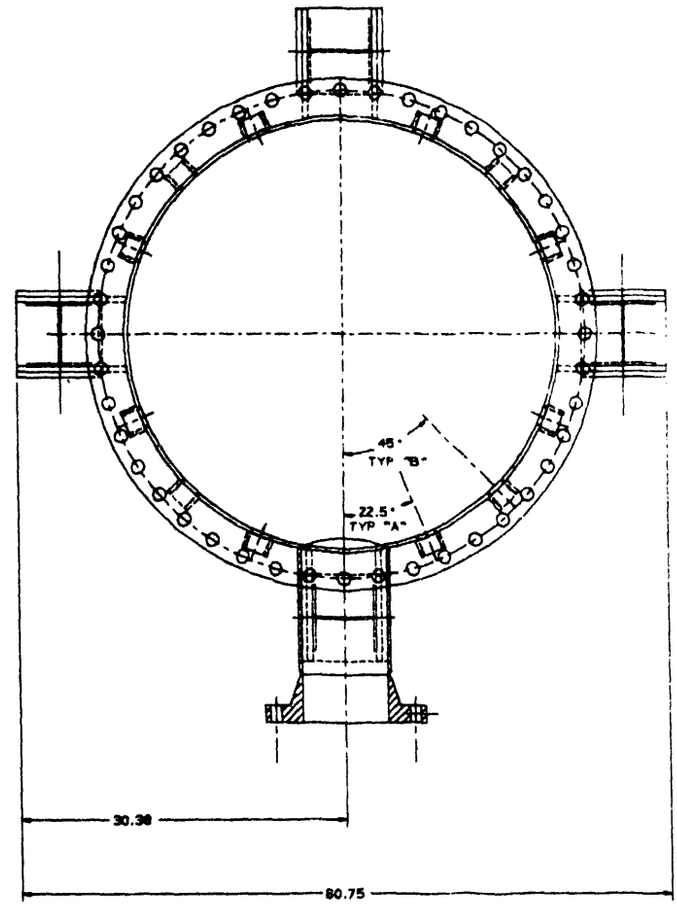

40.00

Figure B.5 – Recirculating HTHP Filter Test Uni

TITLE RECIRCULATING HTHP FILTER TEST UNIT
MAIN VESSEL
DWG 1503E22 REV 1

ITEM	NOTE	PART NAME	REF	SIZE REFERENCE INFORMATION	[illegible]	[illegible]	01	02	03	04	05
1		PIPE		81.00 OF 40.00 I.D. .375 WALL PIPE		STL	1				
2		WELD NECK		40.00 DIA 350 LB. PRES. VESSEL FLANGE		STL	1				
3		WELD NECK		8.00 DIA 300 LB. WELD NECK FLANGE		STL	2				
4		ELL HEAD		40.00 I.D. .375 WALL 2:1 ELL HEAD		STL	1				
5		PIPE		MAKE FROM 8.00 STD WALL PIPE		STL	1				
6		REINF PAD		MAKE FROM .50 THK		STL	1				
7		REINF PAD		MAKE FROM .50 THK		STL	1				
8		COUPLING		1.50 NPT 3000# HALF COUPLING		STL	12				
9		LEG ASSY			1503E24802		4				

NOTE:

1. REINFORCING PADS ITS 6 AND 7 ARE TO BE ROLLED TO FIT BEFORE WELDING.

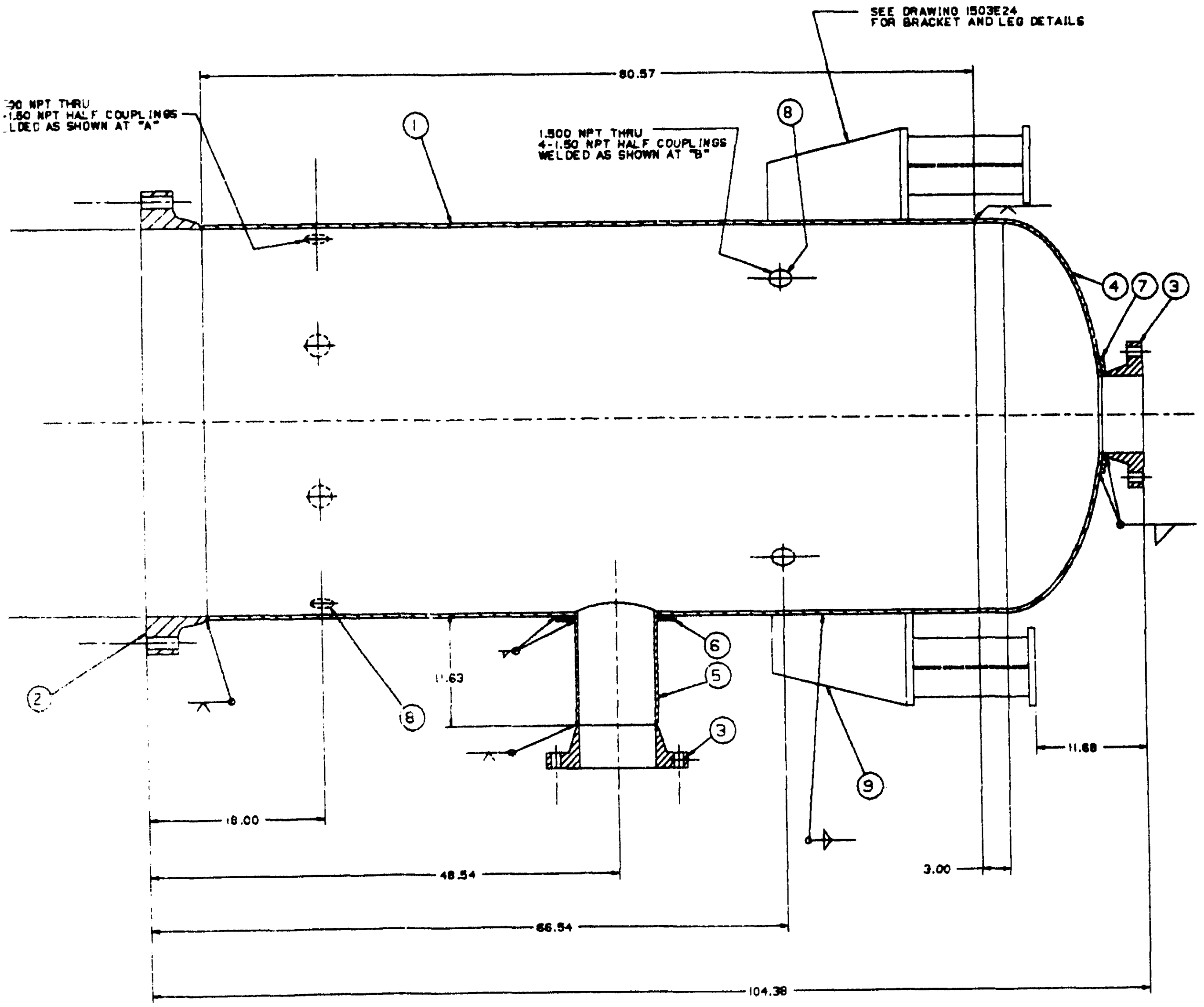

Main Vessel

CADDS DWG-NO MANUAL CHANGES ALLOWED

Westinghouse Electric Corporation

RECIRCULATING HTHP FILTER TEST UNIT
MAIN VESSEL

E 01269 1503E22 1

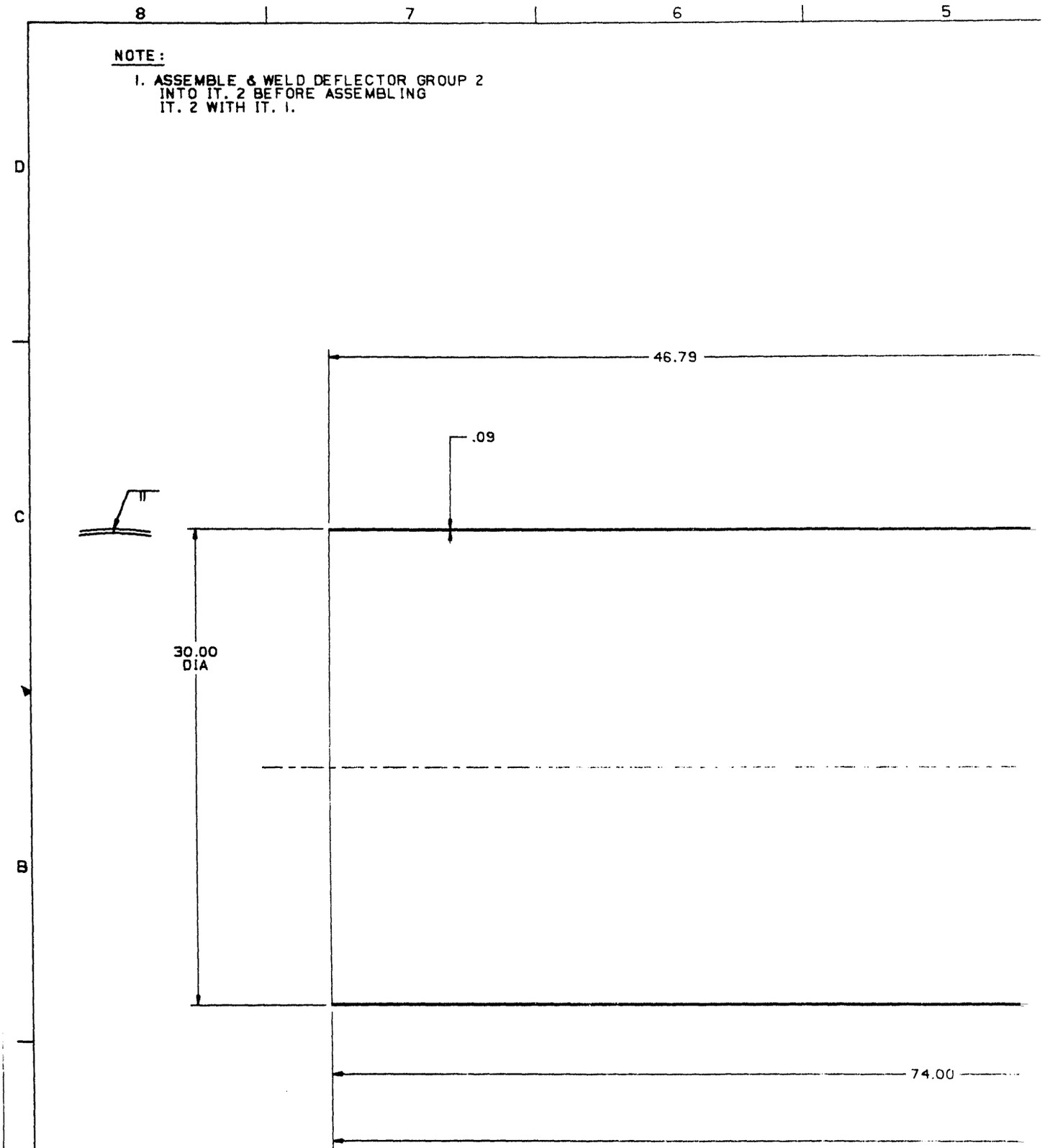

Figure B.6 – Recirculating HTHP Filter Test Unit Liner Assembly

TITLE RECIRCULATING HTHP FILTER TEST UNIT
LINER ASSY
DWG 2236D47 REV 2

ITEM	NOTE	PART NAME	DEF	SIZE REFERENCE INFORMATION	MATL SIZE CODE PART NUMBER OR REF DWG	GROUP NOTE PROCESS OR LINE NO.	GROUP 01	02	03	04	05
1		LINER		ROLL FROM .093 THK	SST 310		1	1			
2		CONE		ROLL FROM .093 THK	SST 310		1	1			
3		LINER		ROLL FROM .093 THK	SST 310		1	1			
4		DEFLECTOR		ROLL FROM .093 THK	SST 310			1			
5		SUPPORT		.375 DIA SST ROD	SST 310			4			

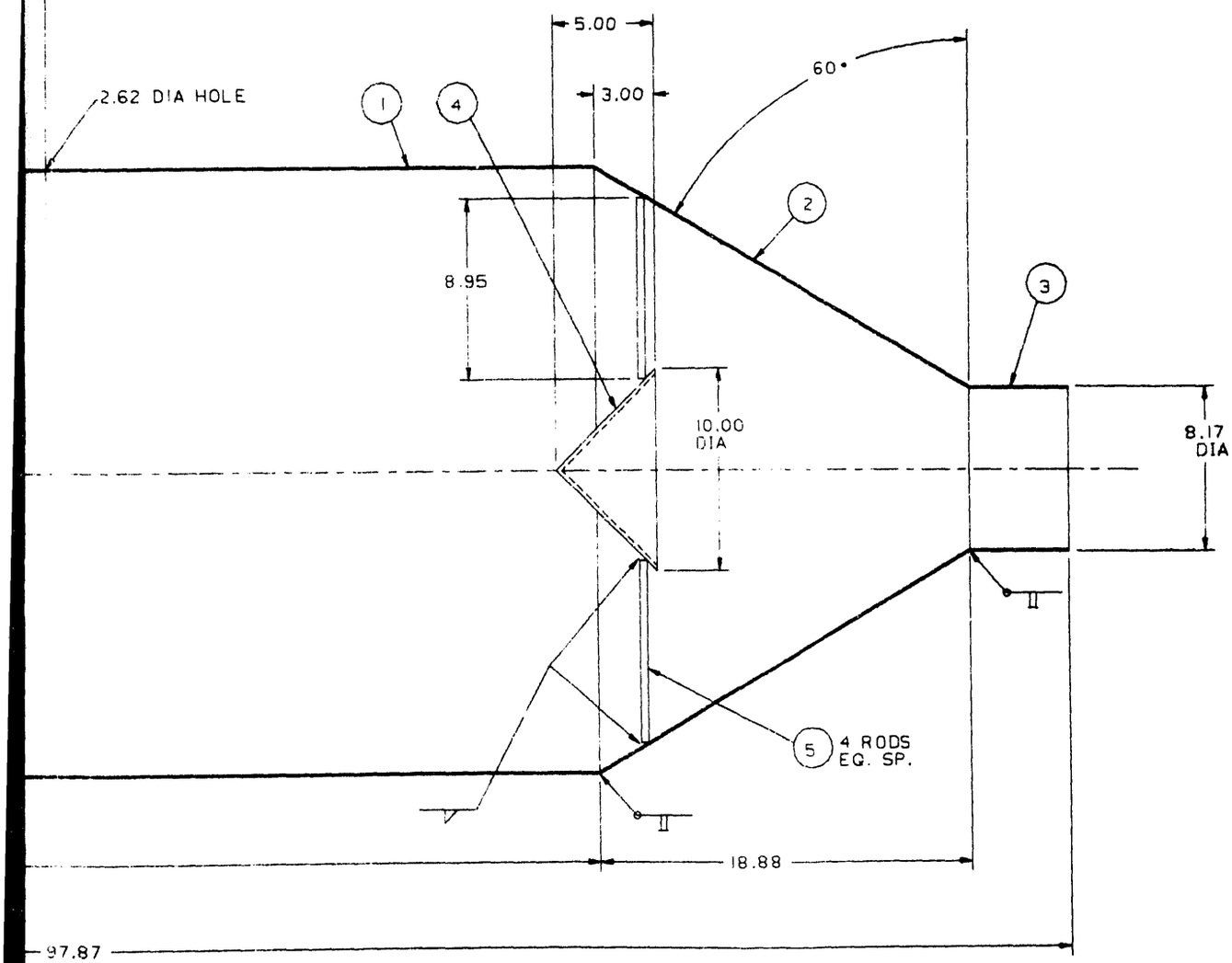

CADDS DWG-NO MANUAL CHANGES ALLOWED

TOLERANCES UNLESS OTHERWISE SPECIFIED
FINISH TO BE √ UNLESS OTHERWISE SPECIFIED

GEOMETRIC CHARACTERISTIC SYMBOLS

DFTR W.DILMORE DATE
CHKR
APPD
APPD
APPD
APPD

R&D CENTER
Westinghouse Electric Corporation
PITTSBURGH PENNSYLVANIA 15235 U.S.A.

TITLE RECIRCULATING HTHP FILTER TEST UNIT
LINER ASSY
DIMENSIONS IN INCHES
SIZE D FSCM NO 01269 DWG NO 2236D47 REV 2
SCALE 1:4 0.301 SHEET 1 OF 1

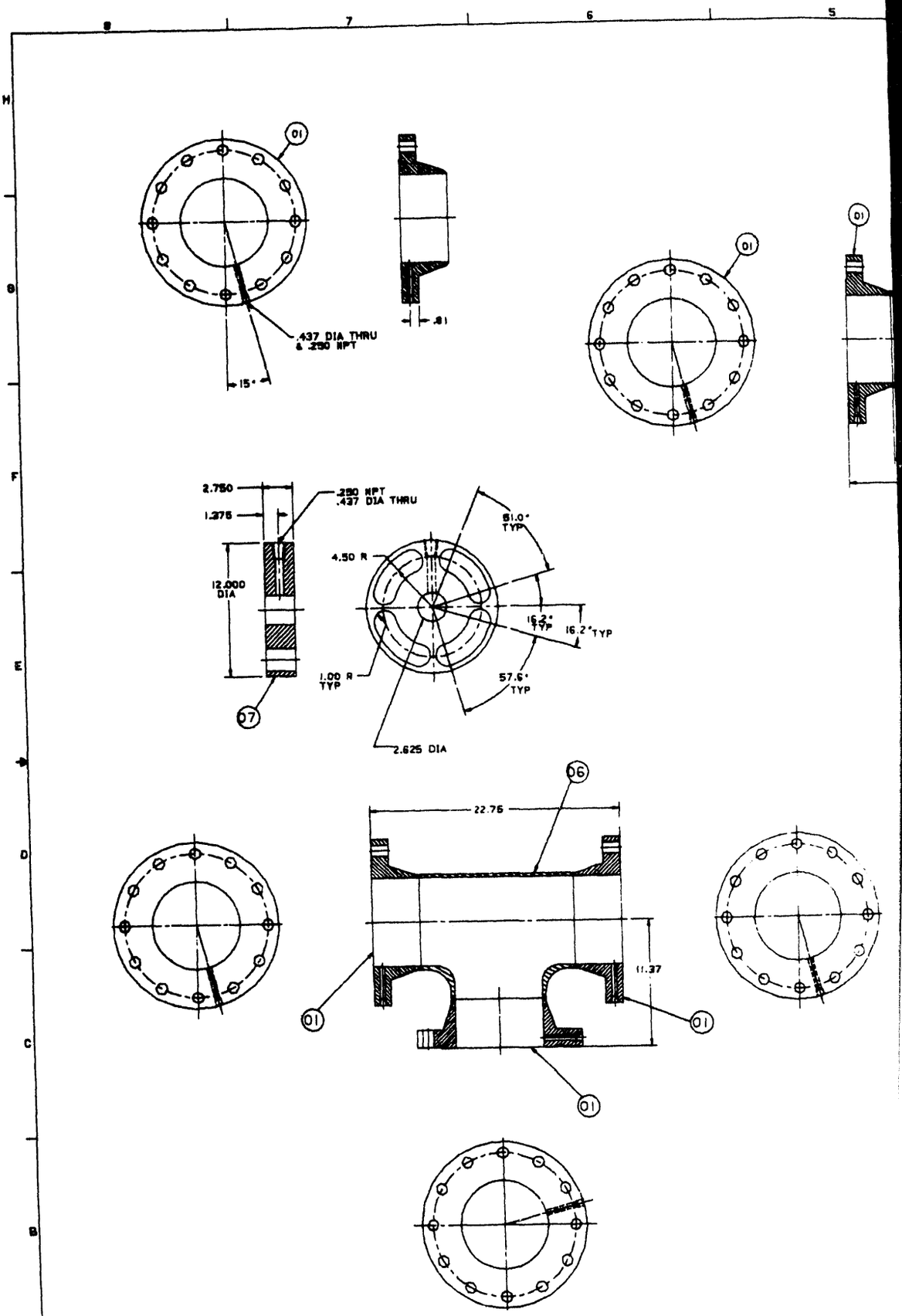

Figure B.7 – Recirculating HTHP Filter Test Unit Recirculating Pi

TITLE RECIRCULATING HTHP FILTER TEST UNIT
RECIRCULATING PIPE
DWG 1503E28 REV 2

ITEM	[illegible]	PART NAME	[illegible]	[illegible] REFERENCE INFORMATION	MATL [illegible]	[illegible]	01	02	03	04	05
1		WELD FLANGE		8.00 300# WELD NECK FLANGE	STL		2	2	2	3	3
2		PIPE		MAKE FROM 8.00 STD STL PIPE	STL		1				
3		PIPE		MAKE FROM 8.00 STD STL PIPE	STL			1			
4		PIPE		MAKE FROM 8.00 STD STL PIPE	STL				1		
5		PIPE		MAKE FROM 8.00 STD STL PIPE	STL					1	
6		WELD TEE		8.00 300# WELD TEE	STL					1	1
7		INS FLANGE		12.00 DIA OF 3.00 THK SST	SST 310						
8		INS FLANGE		12.00 DIA OF 3.00 THK SST	SST 310						

	A	B
1	18.50	27.25
2	54.12	62.88
3	13.88	22.62

DESIGN SPECS:

1. DESIGN CONDITIONS 350 PSIG - 650° F
2. CONSTRUCTION - FUSION WELDED - DYE PENETRANT TEST ROOT PASS AND FINAL PASS.
3. CODE REQUIREMENTS - ASME SECT VIII
4. WELDERS QUALIFIED PER ASME CODE SECT IX
5. TESTING - 500 PSI HYDROSTATIC COMPLETE ASSY.
6. STAMPING - PER CODE.

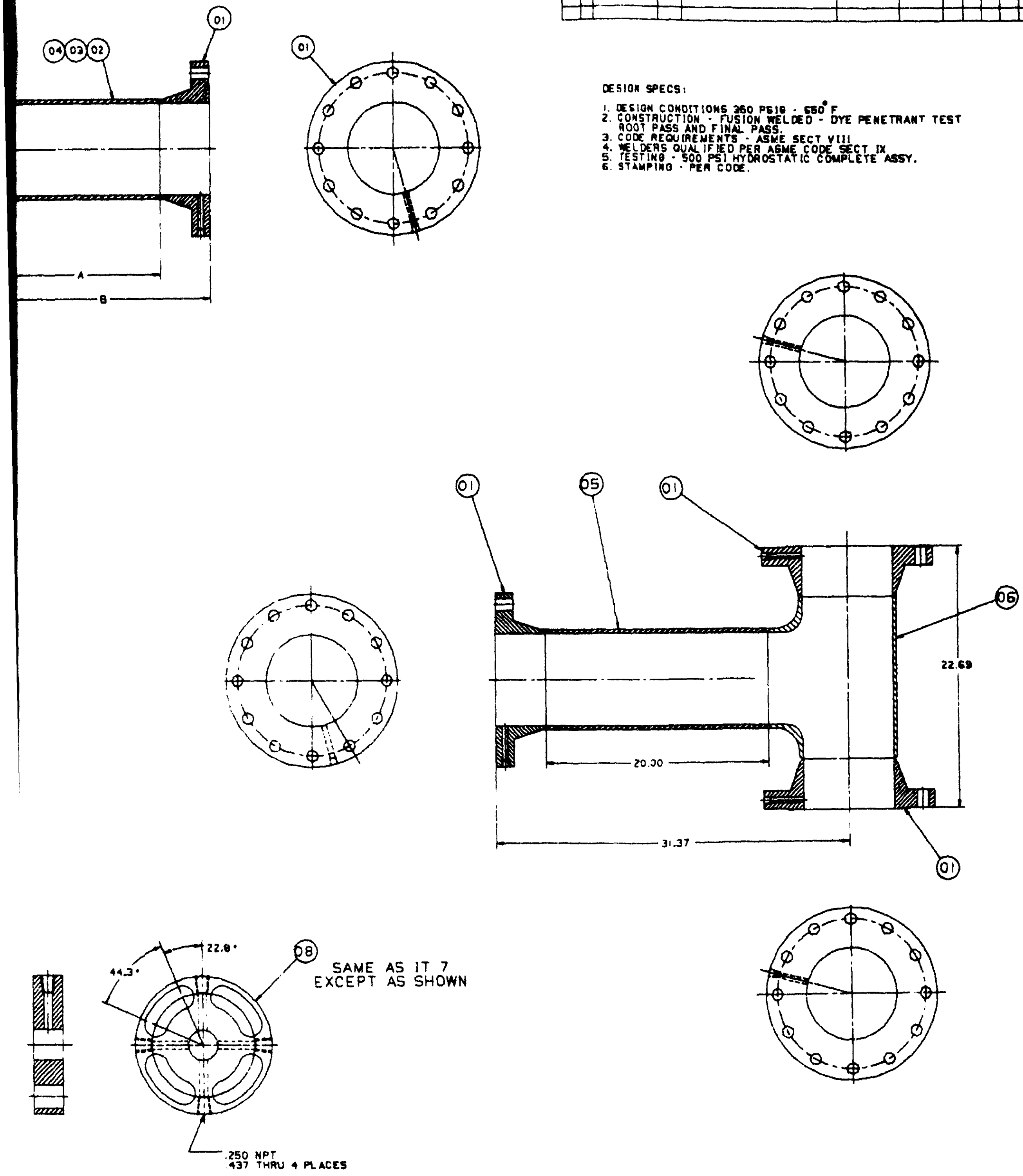

CADDS DWG-NO MANUAL CHANGES ALLOWED

B. DR.MORE 1-15-88

Westinghouse Electric Corporation

RECIRCULATING HTHP FILTER TEST UNIT
RECIRCULATING PIPE

E 01269 1503E28 REV 2

SCALE 0.301

will use 1/8 inch diameter cable heaters and the filter vessel will use single ended Firebars. Both types have an Inconel 600 sheath and use internal type K thermocouples to control the element temperature and provide for a more reliable operation.

The cable heaters will have a 60 inch heated length and a 5 inch unheated length. Each heated section will be able to supply approximately 600 watts. They will be wrapped around the internal liners to provide approximately 600 watts/foot. Each heater will be controlled independently with digital temperature controllers, Omron Model E5CS-R1KJX-F. This will provide the most reliable level of control for these heaters, since each heater could see different duty cycles to maintain the operating temperature.

The Firebars will have a 60 inch heated length and a 6 inch unheated length. Each heater will be able to supply approximately 1200 watts. Ten heaters will be banded to the filter vessel liner to supply a total of approximately 12 kw. They will all be connected in parallel and use one digital temperature controller, a Watlow Series 910. The thermocouple from one of the heaters will be used for the control temperature, and the other thermocouples will be connected to a switch and a digital readout, a Watlow Model 873, so each heater temperature can be monitored.

2.3 Process Gas Circuit and Equipment

2.3.1 Process Gas Compressor

The process gas will be compressed from below 150 psig to 475/500 psig with a 15 HP single stage, oil free, vertical, air cooled, Corken Model D491AM9FBA-103 gas compressor. It will be capable of providing approximately 84 SCFM when operating continuously at 400 RPM. The system requirements at this time indicate that only approximately one half of this flow would be needed. Therefore, the compressor will be provided with a pneumatic valve unloader that will allow constant speed regulation. The unloader will be adjusted for a maximum of 500 psig, at which point the unloader opens the discharge valves. Using

a 25 psig differential, when the system gas reservoir pressure drops to 475 psig the unloader closes the discharge valves and allows the compressor to operate until the 500 psig pressure is recovered.

A 10 cubic foot gas receiver (Figure B.8), the low pressure side reservoir at below 150 psig, will be used on the inlet (suction) side of the compressor (see Figure B.3 for the process and instrumentation diagram, P&ID, for the interconnections and instrumentation designations). This reservoir is where the mixed gas from high pressure tanks will be introduced for the initial charging of the system, and also where the side stream from the test loop will be returned. (See Section 2.3.2 for the description of the flow and pressure control strategy.) The required system gas flows will be drawn from the 500 psig system gas reservoir, a 10 cubic gas receiver vessel, on the discharge side of the compressor. Both of these receivers will be ASME coded vessels with the appropriate pressure safety relief valves and pressure gages.

The system flows include the gas going to the process gas heater through the flow control valve, FCV 208; to the dust feed system, through flow valve FV 415; to the pressure control regulator, PCV 207; and to the filter blow back system, via the pressure control regulator, PCV 108, to the pulse accumulator tank. (See Section 2.2.2, 2.3, and 2.6 for additional details on these subsystems.)

2.3.2 Flow and Pressure Control

The total mass flow through the filters will be calculated in a mass flow controller, FIC 201, using the pressure drop, PDT 200, through the venturi located in the clean gas outlet pipe, the system pressure from PT 222, and the system temperature from TE 223. This flow is compared against the set point (approximately 1500 pounds/hour for 100 acfm) and the controller output adjusts the flow control valve FCV 208 accordingly. The flow of high pressure (500 psig) gas through FCV 208 is indicated on flow indicator FI 209, approximately 150 pounds/hour, before it enters the process gas heater (described in Section 2.2.3) where it will be heated to approximately 1550°F. When

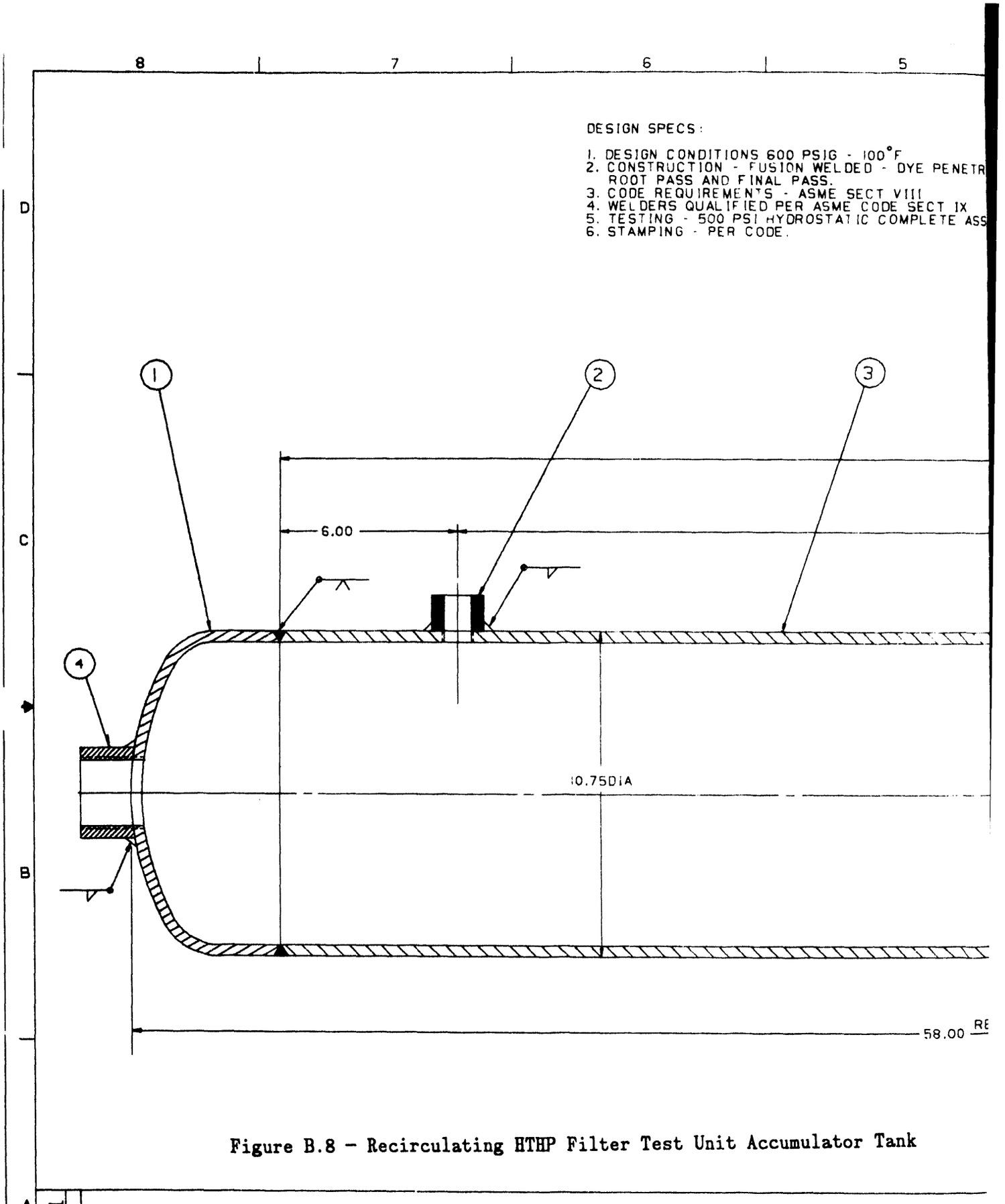

Figure B.8 – Recirculating HTHP Filter Test Unit Accumulator Tank

NT TEST

TITLE RECIRCULATING HTHP FILTER TEST UNIT
ACCUMULATOR TANK
DWG 2236D46 REV 1

ITEM	NOTE	PART NAME	DEF	SIZE REFERENCE INFORMATION	MATL SIZE CODE PART NUMBER OR REF DWG	GROUP NOTE PROCESS OR LINE NO.	GROUP 01	02	03	04	05
1		CAP		10.00 STD WT WELD CAP	STL	ASTM A234	2				
2		HALF COUP		1.00 NPT HALF COUPLING	STL		2				
3		PIPE		48.00 OF 10.00 STD PIPE	STL	ANSI B36.10	1				
4		HALF CPLG		2.00 N.P.T. HALF CPLG	STL		2				

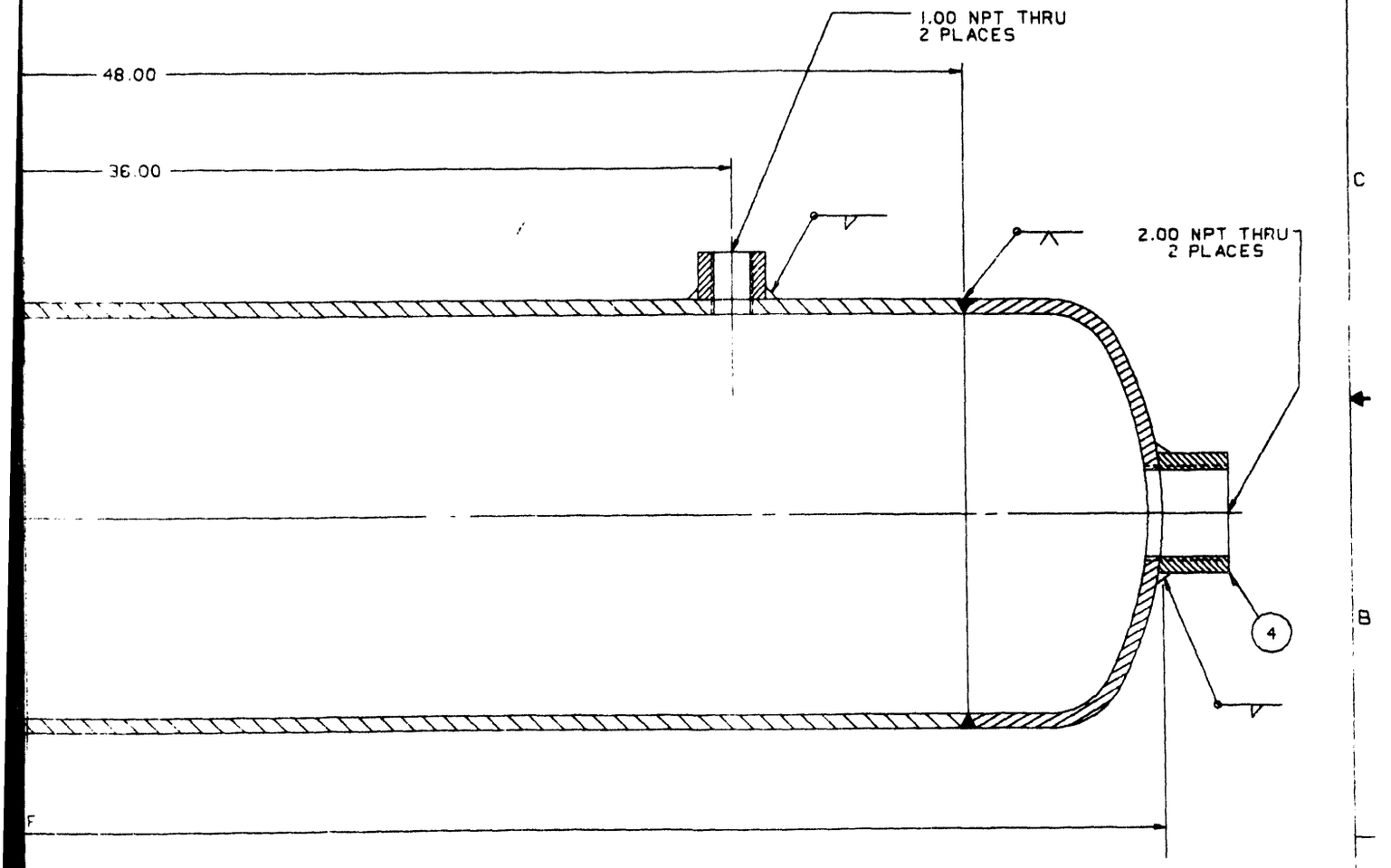

CADDS DWG-NO MANUAL CHANGES ALLOWED

TOLERANCES UNLESS OTHERWISE SPECIFIED
FINISH TO BE √ UNLESS OTHERWISE SPECIFIED

GEOMETRIC CHARACTERISTIC SYMBOLS

DFTR	DATE
DMGR	
APPD	
APPD	
APPD	
APPD	

R&D CENTER
Westinghouse Electric Corporation
PITTSBURGH PENNSYLVANIA 15235 U.S.A.

TITLE
RECIRCULATING HTHP FILTER TEST UNIT
ACCUMULATOR TANK

DIMENSIONS IN INCHES

SIZE	FROM NO	DWG NO	REV
D	01269	2236D46	1

SCALE 1:2 D.301 SHEET 1 OF 1

the heated gas leaves the heater it will pass through a heat traced and insulated pipe to the test loop where it enters through a small diameter nozzle to act as the motive gas for the recirculating eductor. This causes approximately 90% of the total flow to be recirculated through the test loop. The remaining 10% will be taken out after the flow measuring venturi and cooled before it passes through the back pressure regulator, PCV 205 or the hand valve, HV 206. These help to maintain the system pressure at 150 psig. The gas then goes to the low pressure side reservoir before it is recompressed to 500 psig.

The system pressure is also maintained by pressure control valve PCV 207. This will be set at 150 psig and be supplied from the system gas reservoir that is at 500 psig. PCV 207 will be equipped with a vent set at 160 psig that will allow any system over pressure to be directed to the low pressure side reservoir. The filter vessel will also have a pressure relief valve to insure that the maximum working pressure (350 psig) is not exceeded.

2.3.3 Process Gas Heater

The process gas heater will be a vertical, cylindrical, electrically heated radiant tube furnace, approximately 52 inches diameter by 80 inches high, supplied by Armstrong Engineering Associates. Heat input to the furnace will be 24 kw, supplied by 80/20 Ni/Cr rod heaters. The gas will be contained and heated in a 1 inch double extra heavy Incoloy 800H helically wound pipe coil, 68 feet long inside the furnace. The coil will be designed for 550 psig at 1600°F. The pressure drop through the coil will be less than 10 psi. Figure B.9 shows the initial drawing of the heater.

A thermocouple on the exit side of the heater, TE 212, provides the actual temperature of the gas stream to the temperature controller, TIC 211, that compares this to the set point temperature (e.g., 1550°F) and adjusts the electrical power to the heating elements in the heater accordingly.

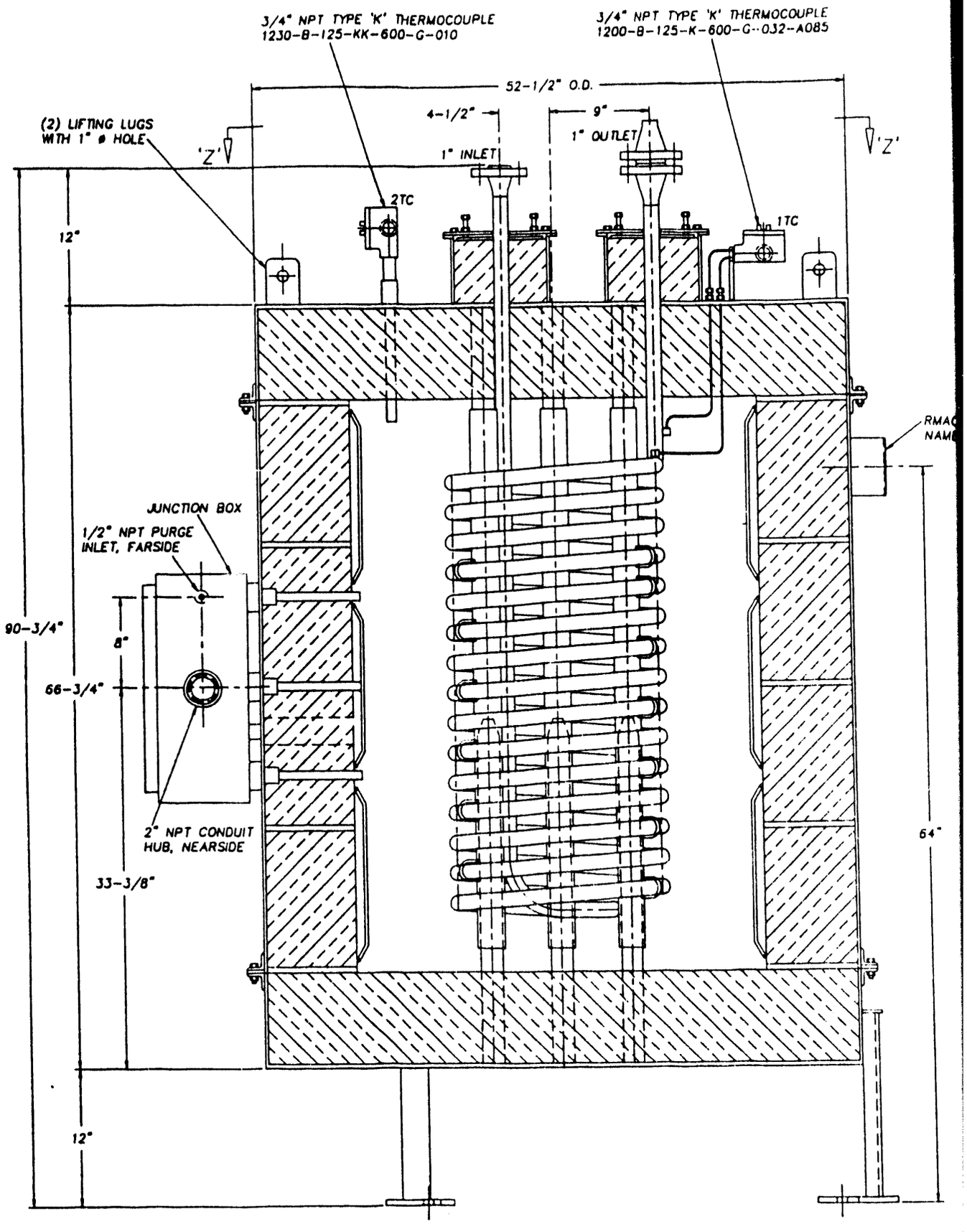

Figure B.9 – Process Gas Heater Drawing

NOTES.

1. ELECTRICAL CLASSIFICATION: CL I, GRP. B, DIV. 2 FURNACE TO BE MANUALLY PURGED TO NFPA 496, TYPE 'Z' TO MAKE IT SUITABLE FOR USE IN CL 1, GRP. B, DIV. 2 AREA.
2. ELECTRIC POWER: 215 V., 3 PH., 60 HZ.
3. DESIGN DATA:
   DESIGN PRESS. COIL: 550 PSIG
   TEST PRESS. COIL: 11138 PSIG
   TEST PRESS. COIL OUTLET FLG: 9157 PSIG
   TEST PRESS. COIL INLET FLG: 2160 PSIG
   DESIGN TEMP. COIL: 1600°F. (EXCEPT INLET FLANGE 600°F)
4. UNIT WEIGHT: EMPTY 2550 LBS.
5. FURNACE TO BE SHIPPED ASSEMBLED AS SHOWN PURGE ITEMS/PIPING WILL BE PACKED SEPARATELY FOR SHIPMENT.
6. MATERIALS OF CONSTRUCTION:
   COIL PIPE-1" IPS SCH. XXH SMLSS. SB-407 ALLOY 800H
   COIL INLET FLG.-1" ANSI 600# WNRTJ SB-564 ALLOY 800
   COIL OUTLET FLG.-1" PC-4S XXS WN MALE W/ FEMALE COMPANION FLANGE SB-564 ALLOY 800H
   COIL SUPPORTS-INCONEL 600
   FURNACE SHELL & SUPTS.-CARBON STEEL
   INSULATION-8" TK. X 10 LB. CERAMIC FIBER
7. COIL DESIGNED TO ASME CODE SECTION VIII, DIV. 1 WHERE POSSIBLE, NO STAMP REQUIRED.
8. PAINTING: WIREBRUSH & PAINT (1) COAT OF 180° SHOP PRIMER.
9. FOR PURGE SCHEMATIC PLEASE REFER TO DWG. 1843-B.

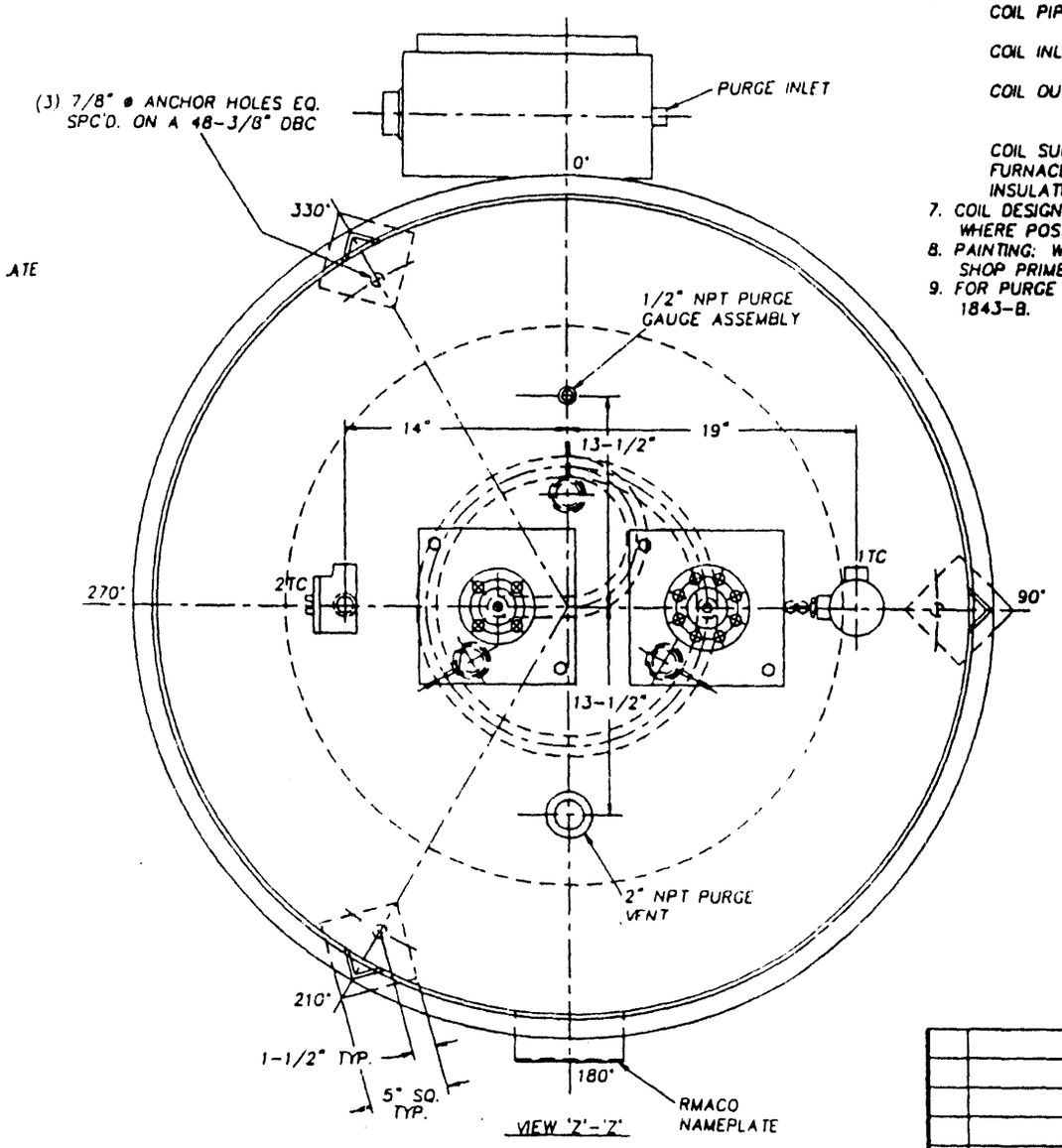

VIEW 'Z'-'Z'

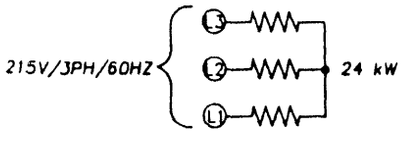

ELECTRICAL SCHEMATIC

Cust. P.O. No: 34-82692-EY

Tag No: C9816

No. Required: ONE

REVISIONS	DATE

52" DIA. ELECTRIC RADIANT GAS HEATER			REFERENCE DRAWINGS 1843-B 10477-D
WESTINGHOUSE ELECTRIC CORP. PITTSBURGH, PA.			
RICHARD M. ARMSTRONG CO. WEST CHESTER, PA.			TEMPLATE MADE
DRAWN BY	BROOKS	ORDER NO.	DRAWING NO.
DATE	25JAN88	A8733345	CAD 10476-D
CHECKED	MV		
DATE	2 FEB 88		

2.4 Dust Feed/Metering

Dust feed to the system will consist of redispersed and sized char, metered into the system by a Westinghouse developed powder feeder system. The dust metering and injection system currently used at the test facility also represents the product of an evolutionary process, as the problem of metering small amounts of fine powders into high-pressure systems has proven to be a formidable one. Westinghouse recently invested a significant amount of capital in the design, fabrication, installation and proof-testing of a system that delivers a wide range of powder feed rates accurately and smoothly to the high-pressure system. The dust feed system is currently capable of providing an on-line read-out of the powder and transport gas mass flow rates. This is of great value in the analysis of the performance of a test device. This highly accurate powder feed system consists of a K-TRON "loss in weight" powder feeder with a twin screw feed barrel for uniform powder feeding, Model LWF 20 with a capacity of 10,000 grams/hour. The device is enclosed in a pressure vessel sized to house the feeder and its hopper, Figure B.10. This vessel is an ASME coded vessel with a pressure relief valve to insure that the maximum working pressure (350 psig) is not exceeded. A small amount of pressurized motive gas, controlled by flow valve FV 415 and flow controller FIC 414, will be used to entrain the metered char into the test loop, as shown in Figure B.3. The particle dust loading will be between 2000 and 4000 parts per million by weight and have a mean mass particle diameter between 5 and 10 microns. It will be injected into the main gas stream downstream of the eductor or into the filter vessel directly.

Two sources of char are currently being considered: the cyclone catch from the KRW fluidized bed gasifier and from an appropriate location downstream of the Texaco entrained bed gasifier. The decision on which one to be used will be made prior to testing, based on the program directions at that time.

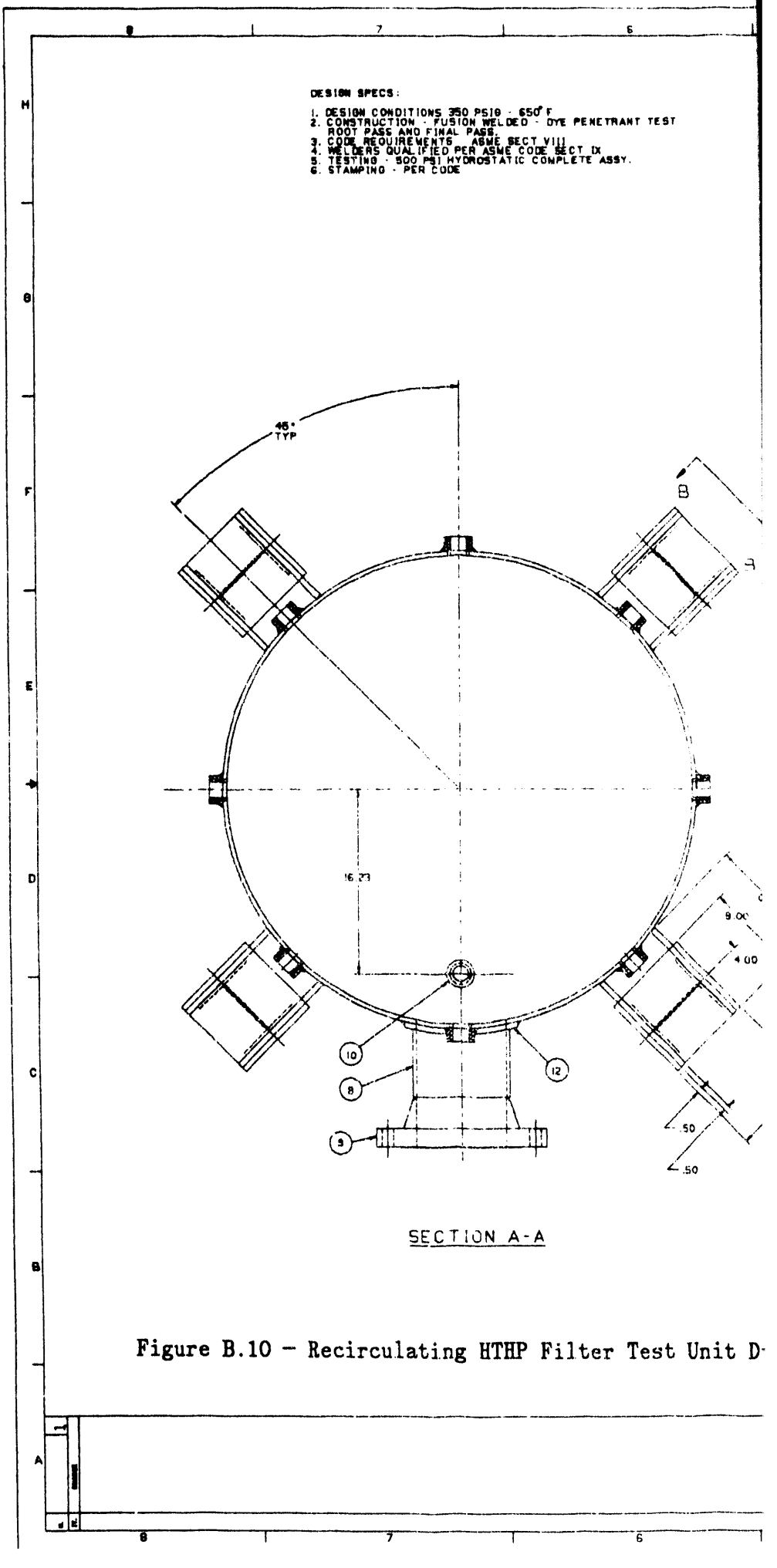

Figure B.10 – Recirculating HTHP Filter Test Unit D

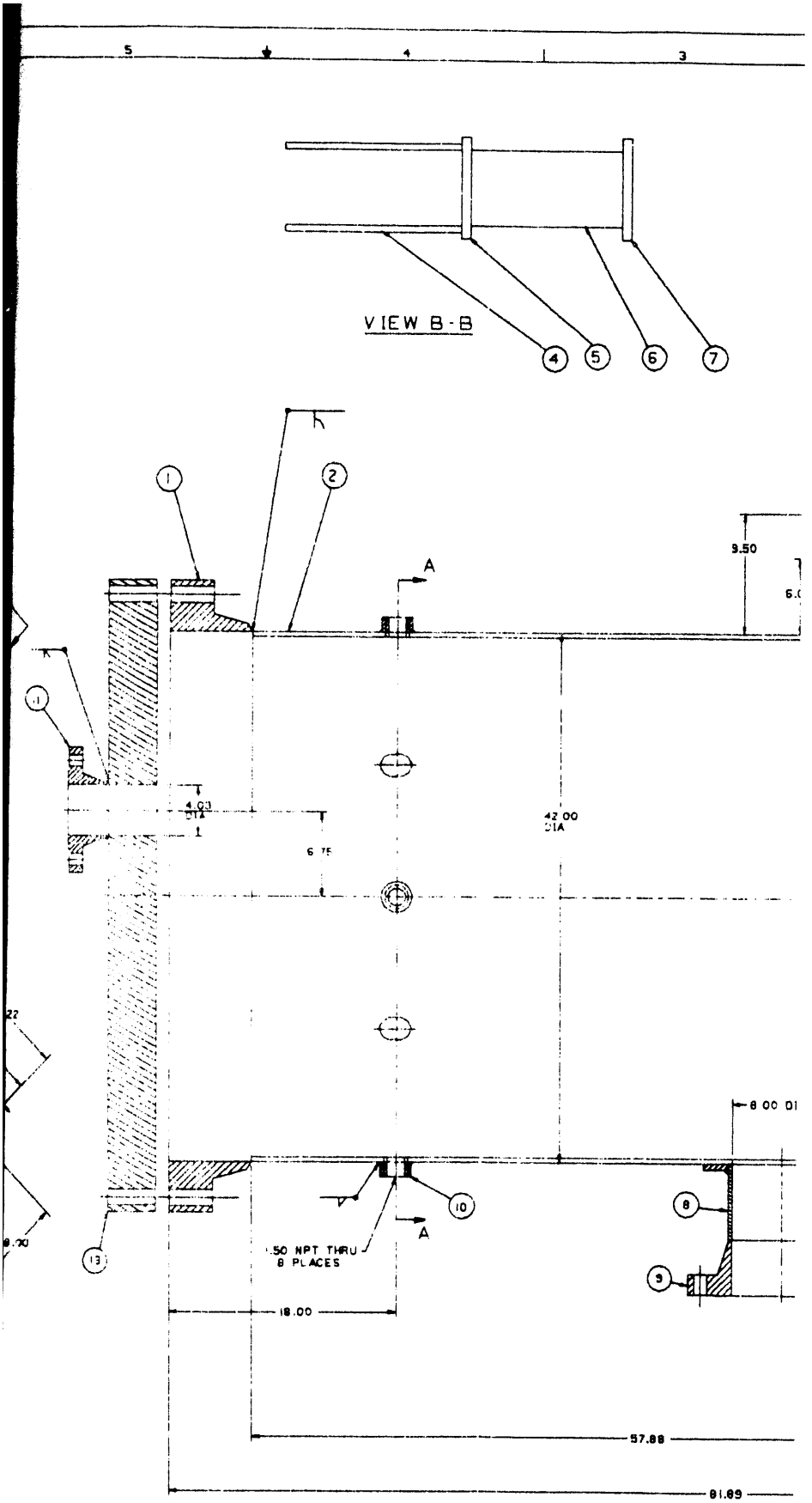

st Feeder Vessel

CADDS D'WO-NO MANUAL CHANGES ALLOWED

2.5 Dust Removal (TBD)

Two options were evaluated for removing the dust collected in the filter vessel. Figure B.11 shows these options. On the right side of the figure, a large collection vessel is attached directly to the filter vessel. The vessel would hold the char injected for one 500 hour test. At the end of the test, the char would be recycled for the next test.

The other option is shown on the left side of the figure. This option uses a small (e.g., 3 ft^3) collection hopper that would hold approximately 1 day's worth of operation. A large valve would then be closed to isolate the hopper and the hopper would be depressurized. The hopper would be disconnected and another one would be connected. The filled hopper would be moved to the dust feeder vessel location and used to refill the dust feeder hopper.

The small vessel option would add less volume to the system, but requires a high temperature valve to isolate the system during hopper changes. Additional design of this part of the system is in progress.

2.6 Filter System

The following deals with the actual filter elements, support structure and cleaning system.

2.6.1 Filter Elements

The ceramic cross flow filters that will be tested in this program will be of the "commercial" scale filter designs manufactured by Coors. Each filter will be nominally 12 x 12 x 4 in. and have approximately 7 ft^2 of active filter area. Currently the most favorable design parameters for the cross flow filter include the following:

Pore Size	70-100μ
Porosity	45-50%
Back Wall Thickness	65 mils
Mid Rib Design	
• corner radius	110 mils
• rib height	150 mils
• slip coated ribs	

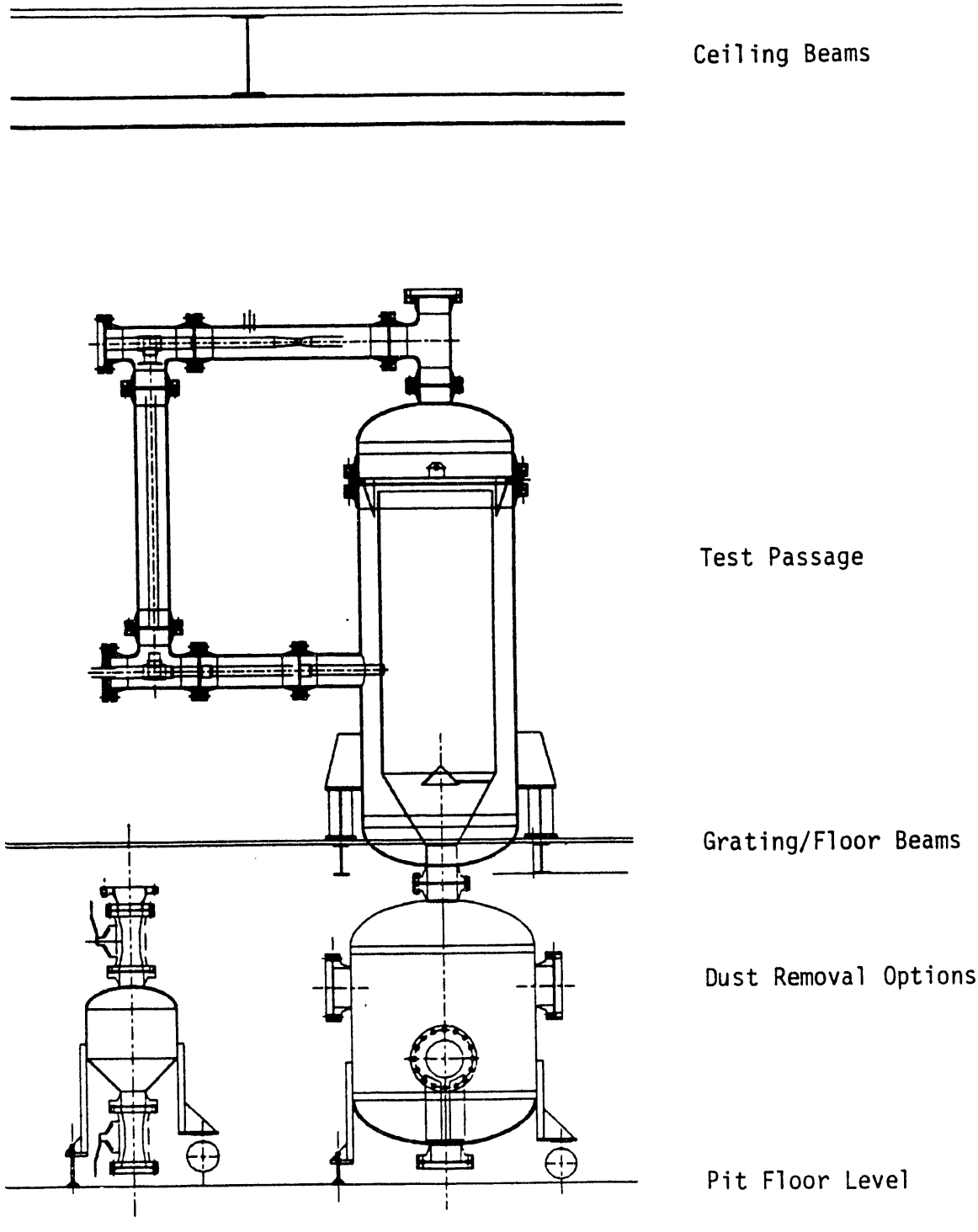

Figure B.11 – Dust Removal Options

Optimization of the firing cycle is currently under way and it appears that the full manufacturing process will require a bisque fire, a primary fire and a final high fire. In related cross flow filter development programs, progress is being made in the evolution of more rugged filter elements, so the exact filter specification is not certain at this point; however, the best filter design available at the time of testing will be used.

2.6.2 Filter Mount and Support Structure

The filter elements will be mounted in a filter holder that is designed to hold two filters, as shown in Figure B.12. The filter mounting assembly consists of a clean gas plenum chamber, made from 4 inch, schedule 40, type 316 stainless steel pipe, and the two horizontal flange mounts for the filter elements. The flange mounts are welded to the clean gas plenum to insure a dust tight seal. The filter elements are gasketed with a high temperature ceramic gasketing material called Interam made by 3M Company. The filter elements have a flange designed into the base and the mount has a corresponding recess for the filter flange. Metal bars are bolted to the mount to clamp the filter flange in place, with the Interam gasketing providing the seal.

Two filter plenums can be mounted on the tube sheet, as shown in Figure B.13. This allows up to four filter elements to be tested at one time. A split-ring flange design is used to fasten the filter holders to the tube sheet. This design prevents the bolts from being in tension at the operating temperature.

The overall arrangement of the tube sheet assembly is shown in Figure B.14. The tube sheet plate, Figure B.15, supports the filter plenum mount and serves as the dirty gas to clean gas barrier across the pressure vessel. The cylindrical and cone section form a bellow type expansion section that is used to support the assembly and accommodate vertical and radial thermal growth. The assembly is supported from a ring section that clamps between the main vessel flange. The ring section is sealed by two (top-bottom) flexitallic gaskets that also permits slight rotational motion of the ring section. The cylinder and

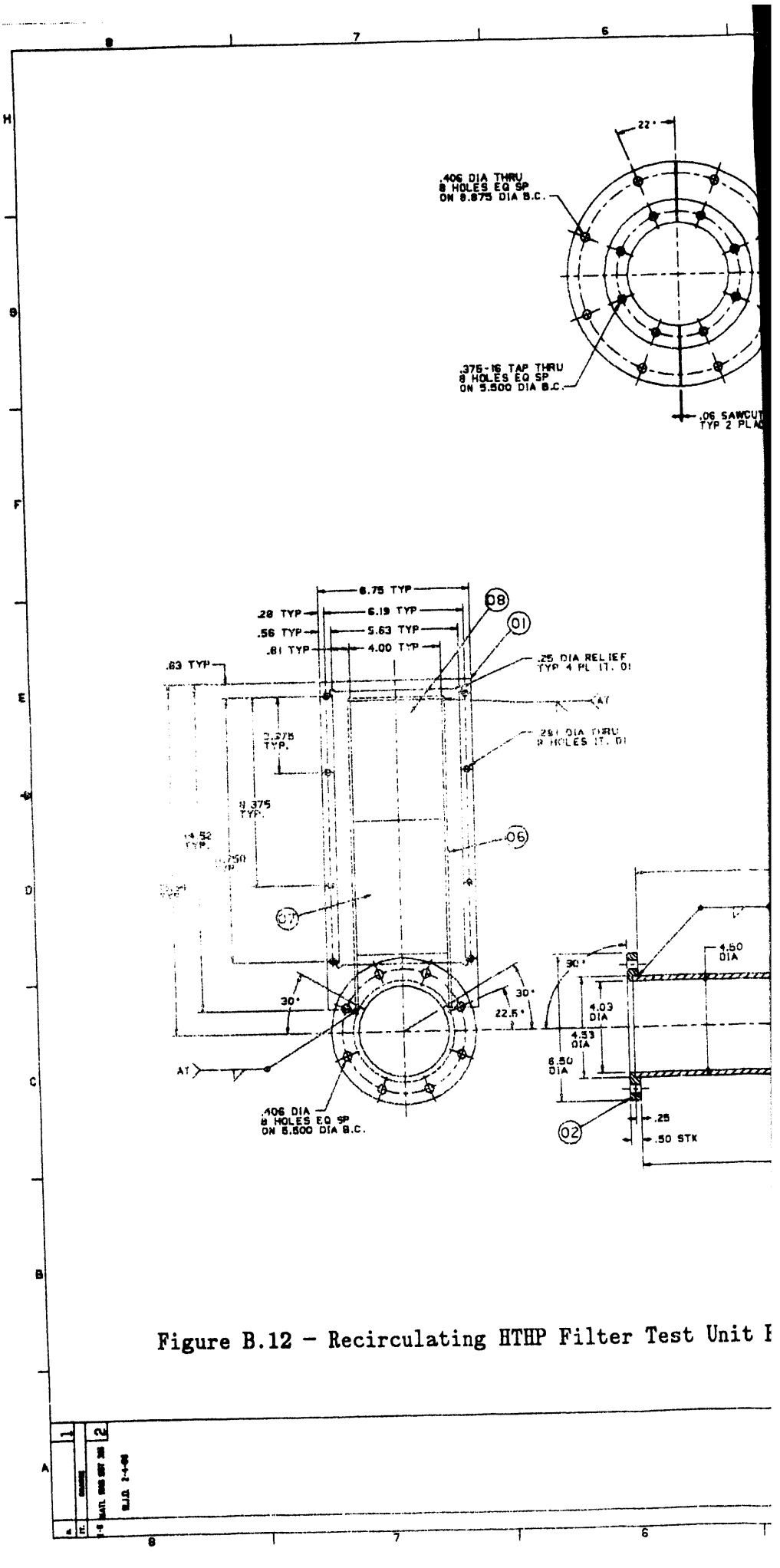

Figure B.12 – Recirculating HTHP Filter Test Unit H

ITEM	NOTE	PART NAME	REF	[illegible]	[illegible]	[illegible]	01	02	03	04	05
01		FILTER PAD	LXIII	14.75 X 7.00 OF 1.00 THK SST TYPE 310			2				
02		FLANGE	LXIII	6.75 X 6.75 OF .50 THK SST TYPE 310			1				
03		SPLIT FLANGE	LXIII	10.12 X 10.12 OF 1.00 THK SST TYPE 310			—				
04		PIPE	LXIII	46.50 OF 4.00 SCH 40 SST PIPE TYPE 310			1				
05		PLUG	LXIII	4.25 X 4.25 OF .312 THK SST TYPE 310			1				
06		SIDE PLATE	LXIII	13.88 X 3.62 OF .125 THK SST TYPE 310			4				
07		BOTTOM PLATE	LXIII	8.62 X 4.50 OF .125 THK SST TYPE 310			2				
08		FRONT PLATE	LXIII	6.62 X 4.50 OF .125 THK SST TYPE 310			2				

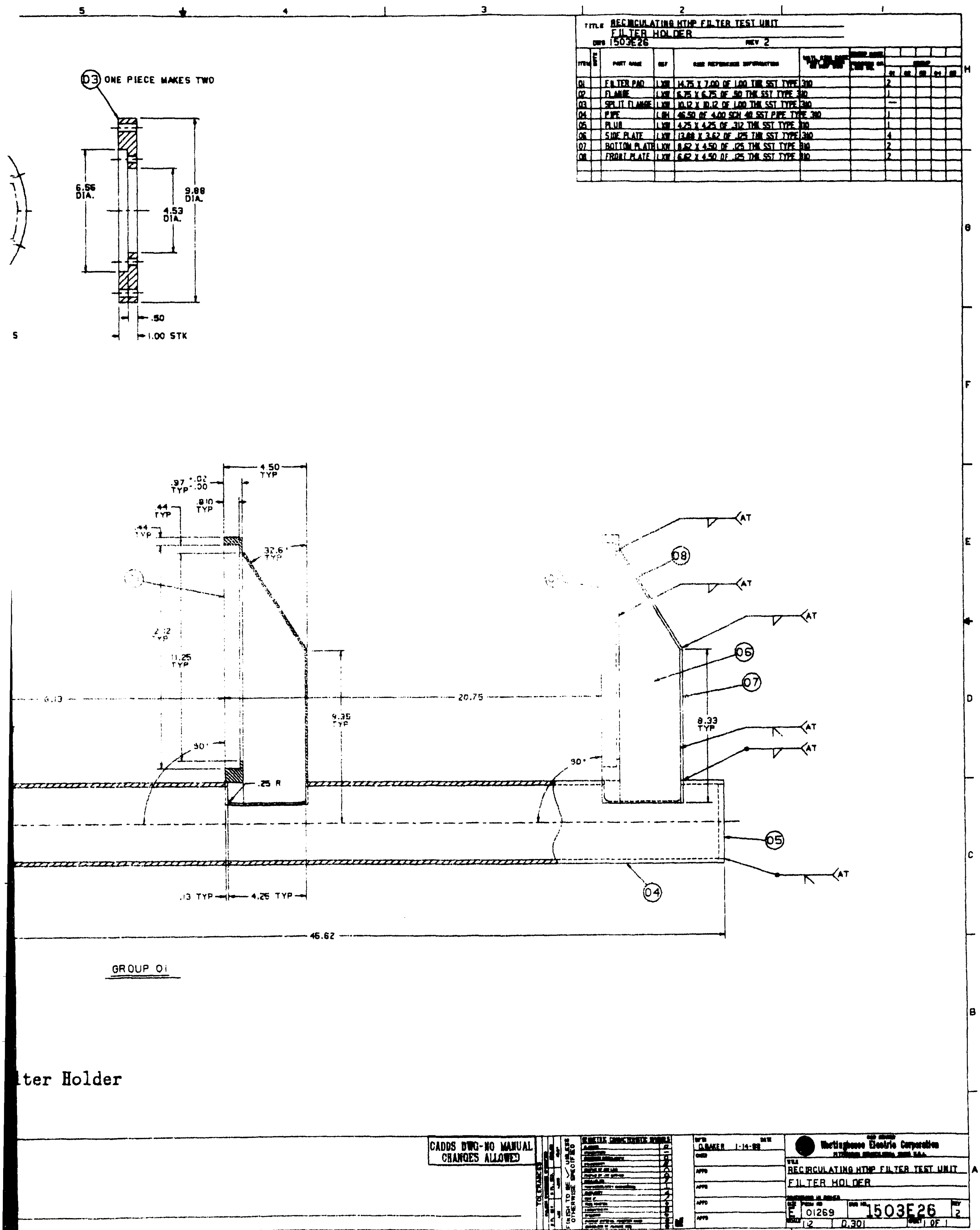

ter Holder

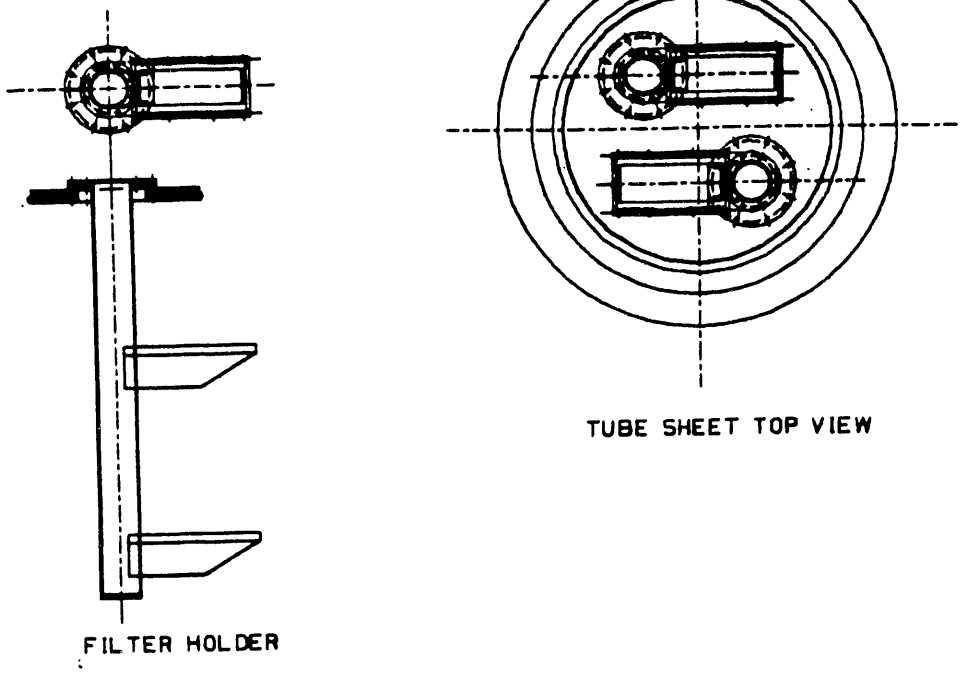

Figure B.13 – Filter Holder and Tube Sheet Layout

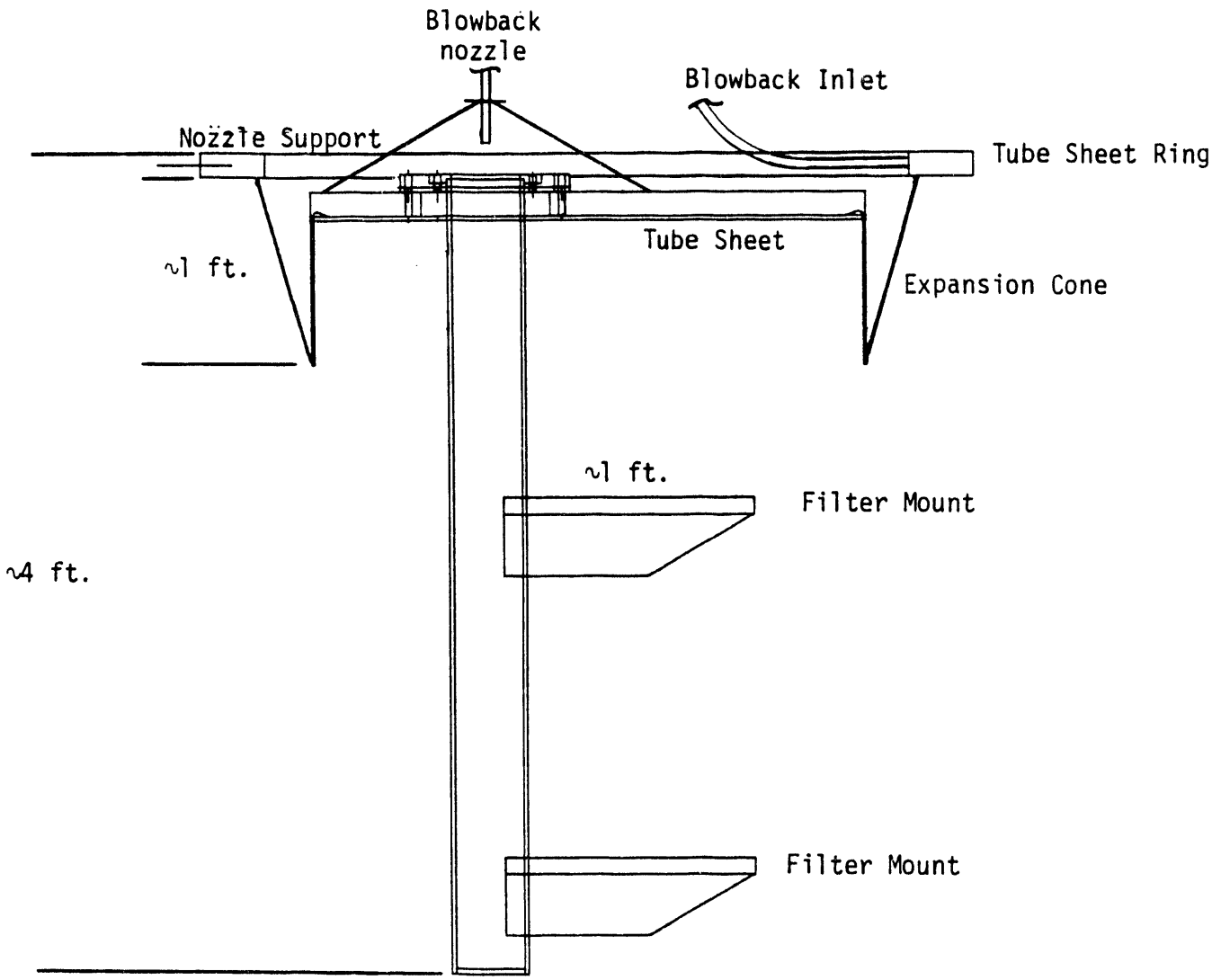

Figure B.14 – Tube Sheet and Filter Holder Assembly

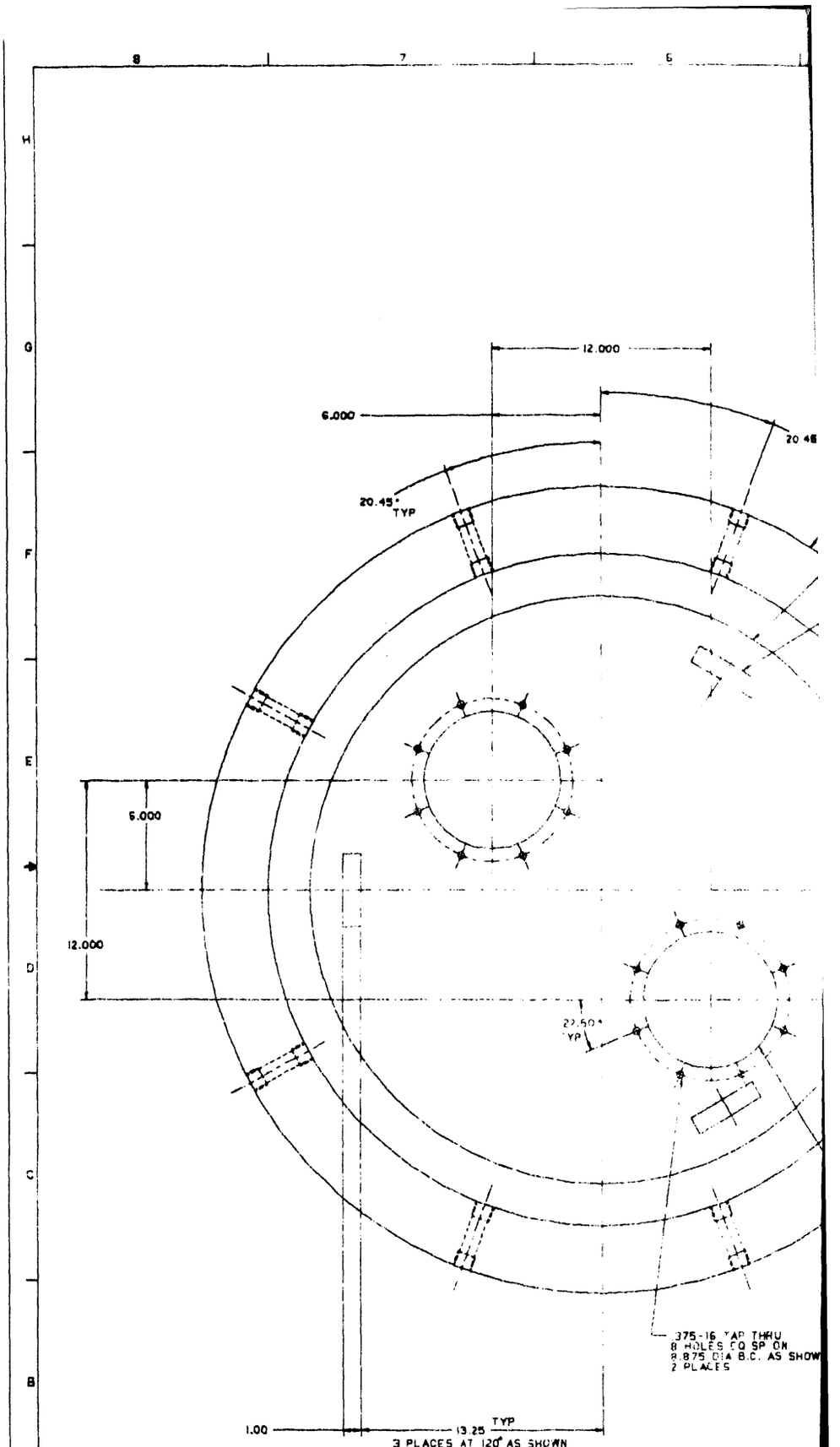

Figure B.15 – Recirculating HTHP Filter Test Unit Tu

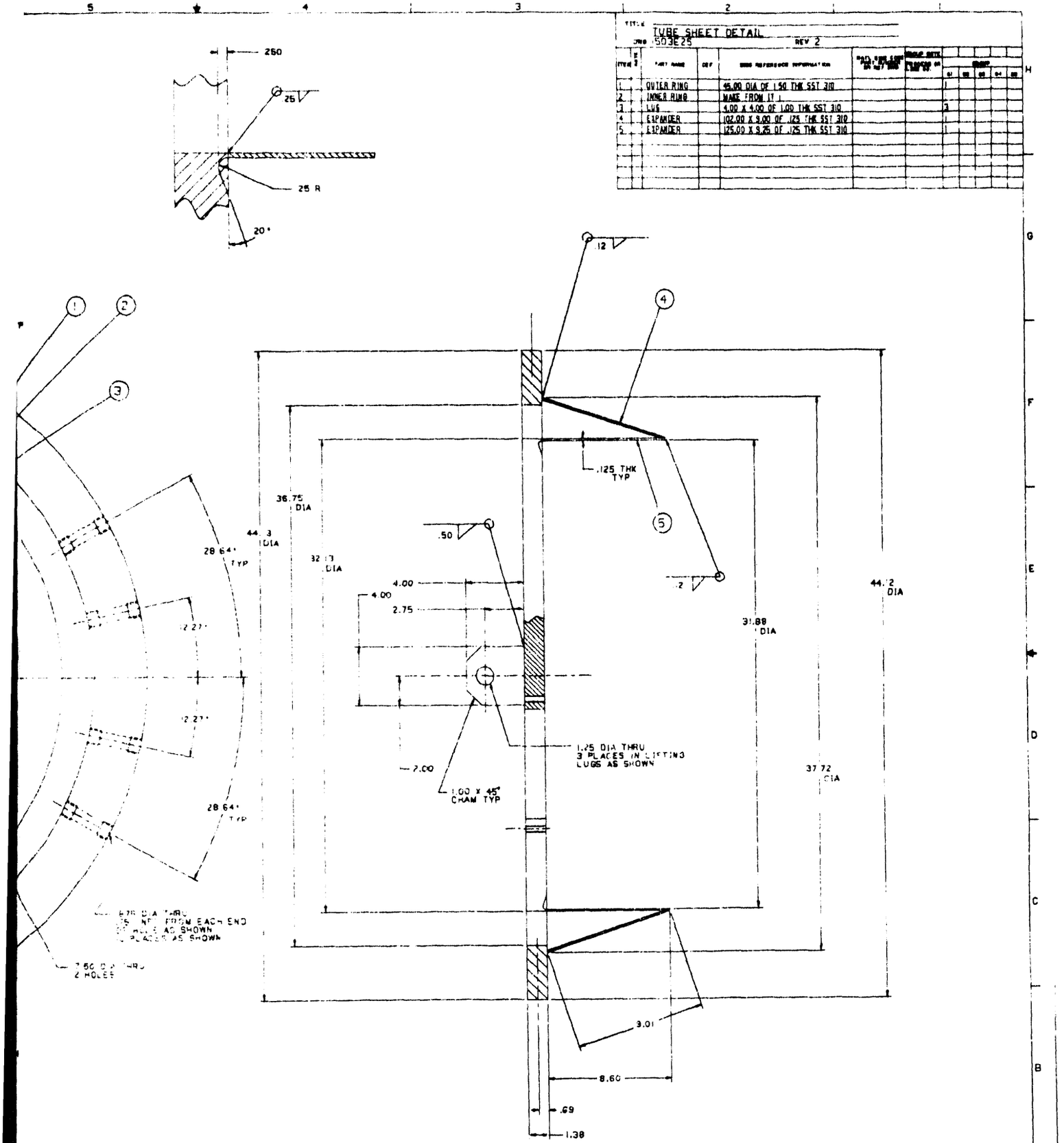

be Sheet Details

cone sections are insulated with a blanket refractory to reduce temperature and temperature gradients through critical sections of the assembly. The tube sheet design is premised on a similar system that has been used successfully at larger scale and at higher operating temperatures.

The tube sheet outer ring section is also fitted with 3/4 inch pipe penetrations to bring the pulse jet cleaning pipes into the filter plenum, as described in the next section. These penetrations can also be used for other instrumentation access points, such as temperature and pressure.

2.6.3 Pulse Jet Cleaning

Pulse jet cleaning of the cross flow filters will be accomplished using high pressure (500 psig) system gas from the system gas reservoir. System gas will be used in order to maintain the gas composition. The gas will be held in a pressure regulated pulse accumulator tank at 300 to 500 psig. Fast acting, 1/2 inch pipe size solenoid valves (FV 111 and FV 115) will be actuated with an electronic timer (KC 151), with a typical "ON" time of 0.1 second. The solenoid valves will have a block valve (HV 110 and HV 112, and HV 114 and HV 116) on either side so they can be changed during operation in case of a failure. The gas is delivered through a 3/8 to 1/2 inch tube nozzle into the filter plenum, as shown in Figure 2.5. This reverse flow of gas removes the collected dust from the filter. The blow back sequence can be initiated manually (with HMS 152) or automatically when the filter pressure drop reaches a predetermined level or on a timed basis.

The blow back sequence also closes two solenoid valves (FV 119 and FV 135) to isolate the filter pressure drop transmitter, PDT 121. This transmitter gives the pressure drop versus time reading used to determine when the filter should be cleaned and the effectiveness of the blow back pulse.

During a blow back pulse, the pressure rise in the filter plenum can be measured with a fast response differential pressure transducer, PDT 126, and it can be recorded on a high speed strip chart recorder,

PR 127. This can be used to determine the long term effectiveness of the blow back pulse in relation to the degree of cleaning seen on the filter at the end of a test segment.

2.7 Material Specifications

The gasifier simulator test loop will be constructed of the following materials:

Item	Material
Filter test vessel	Carbon steel (coded for 350 psig @ 650°F)
Pressure piping	Carbon steel (coded for 350 psig @ 650°F)
Filter test vessel liner	316 stainless steel
Filter holders	316 stainless steel
Tube sheet and expansion cone	TBD
Pipe liners	316 stainless steel
Vessel insulation	Fiberfrax blanket
Piping insulation	Fiberfrax blanket
Dust feed vessel	Carbon steel (coded for 350 psig @ 650°F)
Dust removal vessel	Carbon steel (coded for 350 psig @ 650°F)
Process gas heater piping	Incoloy 800H (designed for 550 psig @ 1600°F)

The selection of 316 stainless steel was made as a result of discussions with material specialists at the R&D Center on stress, strain, and creep, given the operating conditions and test duration and gas composition expected in the test system.

2.8 Data Acquisition

The data acquisition for the test passage will be primarily accomplished with a Molytek Model 3702 data logger. This unit has 32 input channels and 12 alarm output relays. It has chart paper to print out data at set intervals and a RS-232 output that can be connected to a computer directly or transmitted via telephone wires. This allows immediate access to the data as it is generated and also permits storing data for later analysis.

The system pressure and temperature and filter pressure drop will be recorded continuously on a three pen strip chart recorder, Capp model P100M. The filter pressure drop is used to determine when to clean the filters with a reverse pressure pulse, and how well the filter was cleaned. Since the system pressure and temperature affect this value, all three are recorded simultaneously so they can be compared easily.

APPENDIX C

ANALYSIS, DESIGN AND QUALIFICATION OF THE EDUCTOR JET PUMP SYSTEM FOR THE RECIRCULATION GAS TEST LOOP

1. INTRODUCTION

The objective of the work under DOE Contract No. DE-AC21-87MC24022 (Long-Term Durability Testing of Ceramic Cross Flow Filters) is to assess the mechanical integrity and stability of components and materials of the filter, as well as the stability of filtration properties over long time spans of use. This assessment will be done by testing the filters under both pressurized air-blown gasification and pressurized fluidized bed combustion (PFBC) conditions.

The gasification tests will be performed in a new gasifier simulator, the general arrangement of which is shown in Figure C.1.1, being designed by Westinghouse. The system is to consist of a closed recirculation loop so that a fixed gas composition can be maintained. The plan is for approximately 10% of the total gas flow to be used as high pressure motive gas for an eductor that recirculates the system gas and provides the pumping needed to maintain flow through the filter. Since only a small amount of gas is to be mechanically pumped, this design greatly reduces requirements for mechanical gas compression, as well as for the necessary cooling and reheating before and after compression.

This concept relies heavily on the presumed ability of an eductor system to operate with a high entrained-to-motive gas flow ratio. Verification of this capability was needed early in the facility design exercise. Consequently, we performed several studies which are discussed in this report. First, the existing analytical model of the recirculation loop fluid dynamics was improved to include more rigorous treatments of the reversible and irreversible pressure losses in the flow loop and of the compressible flow mechanics of the eductor nozzle gas. Second, the existing hot gas filtration test facility was used to

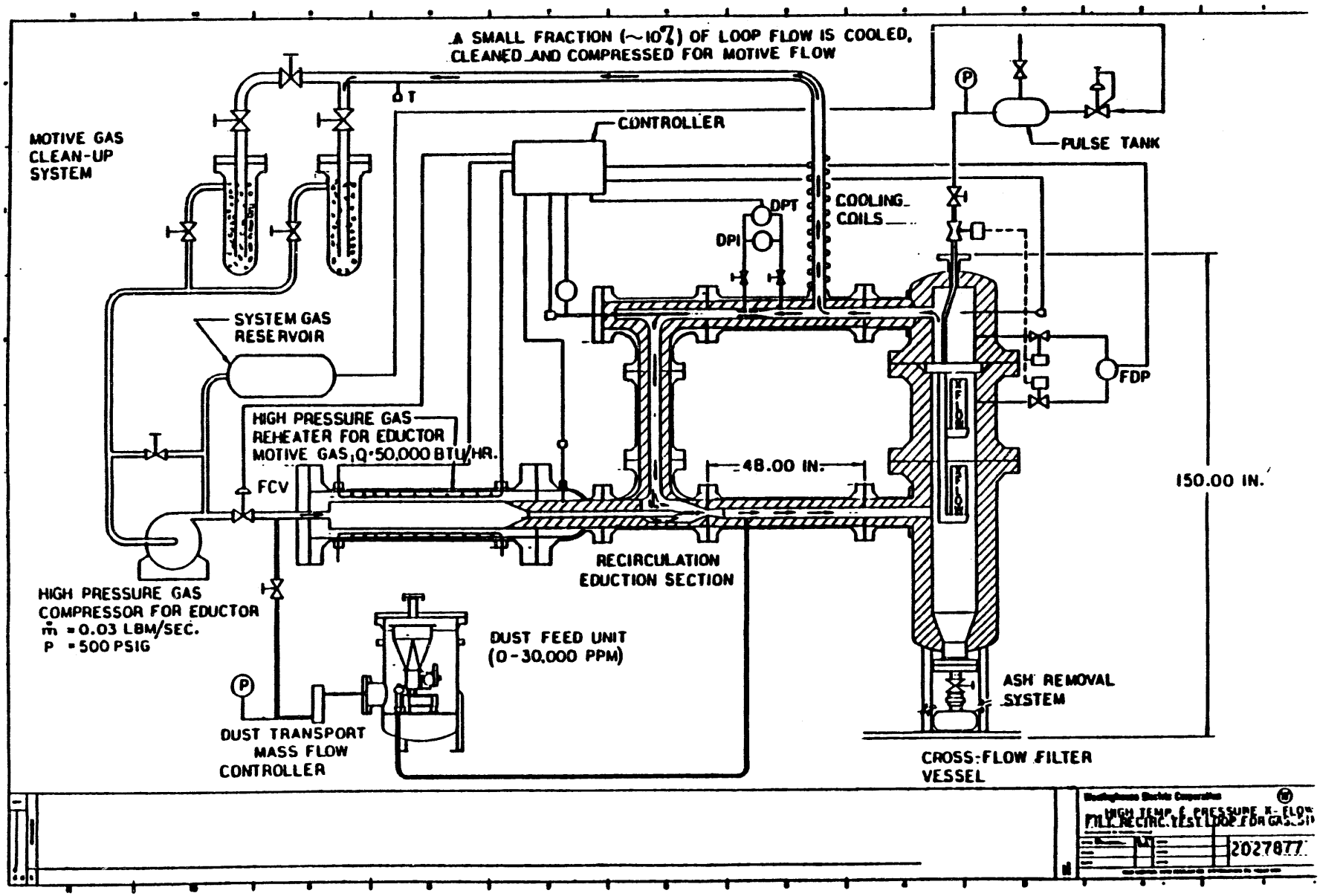

Figure C.1.1 - HTHP Gasifier Simulator for Cross Flow Filter Testing

perform cold flow eductor-driven recirculation tests to validate the analytical model. Third, the model was used to project performance of the gasifier simulator recirculation system, and to evaluate eductor system design details.

2. CONCLUSIONS

1. The eductor-driven recirculation model has been demonstrated to be an effective tool for predicting recirculation rates.

2. The hot gas eductor recirculation concept is practical, and should work with reasonable motive to total gas flow rate ratios.

3. Eductor design details have been chosen based on the model results.

3. EDUCTOR RECIRCULATION MODEL

3.1 DETAILED MODEL DESCRIPTION

The gas recirculation analytical model was developed prior to this program and used as the basis of a rigorous BASIC computer program for examination of recirculation system design parameters. At the heart of the model were mass, momentum, and energy balances for the eductor, based on filter blowback modelling that had been performed earlier[1]. Given a set of design parameters, the model calculates steady-state entrained and total recirculation flows. Different sets of parameters may be tested to see what combination meets system design requirements. Table C.3.1 summarizes input design parameters. The model treats a constant diameter nozzle as a special case of a converging/diverging nozzle (exit diameter equals throat diameter).

For a given set of input parameters, the model performs the following steps:

1. Determine flow rate, pressure, and temperature of gas exiting eductor nozzle. The desired flow may or may not be possible given available pressure from the motive-gas supply compressor and nozzle dimensions. Also, flow through the nozzle may fall into any of several flow regimes, depending on throat velocity and system pressure at the discharge. To sort out these possibilities, the following possible states are investigated with the use of compressible flow relations[2], in the order given, until one is found to be possible for the given target motive gas flow rate and the maximum available motive pressure:

TABLE C.3.1 - DESIGN PARAMETERS AND UNITS

	ENTRAINED GAS
P1	Pressure, atm
T1	Temperature, °F
	MOTIVE GAS
P2M*	Maximum stagnation pressure (maximum compressor discharge pressure), atm
T2S*	Stagnation temperature (temperature in nozzle feed tube), °F
W2T*	Desired flow (lb/sec)
MW	Molecular weight
CP	Heat Capacity, Btu/lb °F
K	Ratio of specific heats
	EDUCTOR SYSTEM GEOMETRY
D1	Inside diameter of eductor entrained gas inlet, in.
D2*	Nozzle exit inside diameter, in.
DT*	Nozzle throat inside diameter, in.
D2O	Nozzle outside diameter, in.
D3*	Eductor diffuser inside diameter, in.
	SYSTEM GEOMETRY
DP**	Inside diameter of main recirculating gas piping, in. Lengths of various main gas recirculation flow path component, in.
	FILTER
RW	Resistance coefficient, /ft
AF	Filtration area, ft^2
	TOTAL FLOW MEASUREMENT (VENTURI OR ORIFICE)
DOR	Throat or orifice diameter, in.
CD	Discharge coefficient
F	Ratio of permanent to measured pressure loss

*Prompted input, others must be changed within program.

**Various symbols particular to the specific design.

1a. Assume motive gas flow equals target value and subsonic flow through nozzle throat. This is not possible if the resulting throat Mach number is greater than one, or if the resulting stagnation pressure at the throat is greater than the available pressure.

1b. Assume motive gas flow equals target value, sonic flow through the nozzle throat, and supersonic flow throughout the diverging section. This is not possible if the system pressure (into which the nozzle discharges) is greater than the resulting maximum allowable pressure outside the nozzle required to avoid shock in the converging nozzle[3], or if the resulting stagnation pressure at the throat is greater than the available pressure.

1c. Assume motive gas flow equals target value, sonic flow through the nozzle throat, and that a normal shock occurs in the diverging section. This is not possible if the resulting stagnation pressure at the throat is greater than the available pressure.

1d. Assume stagnation pressure at the throat equals the maximum available pressure, and subsonic flow through nozzle throat. This is not possible if the resulting throat Mach number is greater than one.

1e. Assume stagnation pressure at the throat equals the maximum available pressure, sonic flow through the nozzle throat, and supersonic flow throughout the nozzle diverging section. This is not possible if the system pressure (into which the nozzle discharges) is greater than the resulting maximum allowable pressure outside the nozzle required to avoid shock in the converging nozzle.

1f. Assume stagnation pressure at the throat equals the maximum available pressure, sonic flow through nozzle throat and a normal shock in the diverging section.

Note that states 1a through 1c represent the situation where a valve is used between the motive gas compressor and the nozzle, to let

down the pressure and control the flow rate. States 1d through 1f represent the situation where this valve is wide open, and maximum flow is occurring. States 1b, 1c, 1e, and 1f represent "choked" flow through the nozzle. The result of step 1 is that the flow rate, pressure, and temperature of gas issuing from the nozzle are known.

2. Guess total (entrained plus motive) flow to equal motive flow.

3. Guess mixture temperature.

4. Guess mixture pressure equal to entrained pressure.

5. Determine pressure drop around filter test loop. The loop pressure drop includes the following irreversible pressure loss components:

- friction loss in eductor
- expansion from eductor diffuser to main piping
- friction loss in piping into filter test vessel
- expansion into test vessel
- loss across filter
- contraction out of filter vessel
- outlet piping friction loss
- irreversible component of venturi or orifice pressure drop
- contraction of entrained gas into eductor suction end

and the following two reversible components (accounting for velocity changes due to area changes):

- total gas flow between eductor diffuser and main piping into splitter tee (where gas is drawn off for compression to become motive gas)
- entrained gas flow between splitter tee and eductor suction area

6. Estimate mixture pressure as entrained pressure plus loop pressure drop.

7. Estimate mixture velocity from a momentum balance on the entrainment zone, accounting for pressures and velocities in each of the three streams: motive gas, entrained gas, and mixed gas. Then determine

the mixed gas density from the velocity and flow rate, and the mixed gas temperature from the density and pressure.

8. Estimate the mixed gas temperature from an energy balance on the entrainment zone, accounting for temperatures and velocities in each of the three streams.

9. Compare estimated mixture temperatures from previous two steps. If they are close, go to step 10. Otherwise, a numerical procedure is used to re-estimate a total mixture flow rate that will reduce the difference between these two estimated temperatures. The mixture temperature and mixture pressure are assumed to be those given by steps 8 and 6, respectively, and calculations resume with step 5. (It has been found that when convergence on mixture temperature is achieved, convergence on mixture pressure will also have occurred.)

10. Print recirculation loop performance parameters.

3.2 APPROXIMATE MOMENTUM BALANCE

In an eductor with a straight (i.e., not converging/diverging) sleeve, the momentum balance is

$$(W_3^2/S_3\ \rho_3) + P_3S_3g_c = (W_1^2/S_1\ \rho_1) + P_1S_1g_c + (W_2^2/S_2\rho_2) + P_2S_2g_c + P_1(S_3-S_1-S_2)g_c \qquad (3\text{-}1)$$

where the variables are:

W = Gas flow rate, lb_m/sec

S = Flow area, ft^2

P = Pressure, lb_f/ft^2

ρ = Gas density, lb_m/ft^3

g_c = Conversion constant, 32.174 lb_m-ft/(lb_f-sec^2)

and the subscripts are:

1 = Entrained gas

2 = Motive gas

3 = Combined (entrained plus motive) gas

Note that S_1, S_2, and S_3 are areas referring to the eductor inside diameter minus the nozzle outside diameter, the nozzle exit inside diameter, and the eductor inside diameter, respectively.

If the momentum contributions of the entrained and combined gas streams are assumed to be small, then Equation 3.1 simplifies to:

$$(P_3-P_1)S_3g_c = (W_2^2/S_2\rho_2) + (P_2-P_1)S_2g_c \qquad (3\text{-}2)$$

At steady state, the eductor pressure gain (P_3-P_1), will equal the pressure drop around the loop. This pressure difference will therefore increase with increasing total gas flow rate around the loop, and will decrease with increasing sleeve i.d., since that would offer less resistance to flow. If the sleeve inside diameter is less than the balance-of-loop pipe i.d., then these proportionalities are roughly approximated by:

$$(P_3-P_1) = K\rho_3 W_3^2 / \sqrt{S_3 - S_n} \qquad (3\text{-}3)$$

where K = a proportionality constant

S_n = area based on outside diameter of nozzle, ft^2

Combining Equations 3.2 and 3.3 gives an indication of how the loop pressure drop will depend on major eductor parameters, as indicated in Equation 3.4:

$$W_3 = \left[\frac{\sqrt{S_3 - S_n}}{K\rho_3 S_3 g_c} \left[\frac{W_2^2}{S_2\rho_2} + (P_2 - P_1) S_2 g_c \right] \right]^{1/2} \qquad (3\text{-}4)$$

Note that when the sleeve i.d. is considerably larger than the nozzle o.d., the total flow rate through the loop varies inversely with approximately the square root of the sleeve i.d. (or with approximately the fourth root of the area S_3). This explains the predictions and experimental data concerning the effect of sleeve diameter in the following sections. Note also that when the sleeve i.d. is smaller and approaches the nozzle o.d., Equation 3.4 predicts that the flow rate will fall with decreasing sleeve i.d. -flow is being choked off by the narrowing annulus around the nozzle.

This simplified model is presented for help in understanding qualitative effects. In subsequent calculations the detailed eductor recirculation model was used. The detailed model differs from the simplified version in that the pressure drop relationship corresponding to Equation 3.3 is replaced by a much more rigorous treatment of all actual sources of pressure losses and gains in the loop, and in that the momentum balance of Equation 3.1 is not simplified to the form of Equation 3.2.

4. COLD-FLOW RECIRCULATION TESTS

4.1 SYSTEM DESCRIPTION

The existing high-temperature, high-pressure test facility was modified to accommodate a sequence of recirculation verification tests. Figure 4.1 shows the modified system configuration. The combustor, inlet gas, exhaust gas, and bypass piping were replaced with standard 2 inch pipe. An eductor was designed and fabricated for causing recirculation. As shown in Figures C.4.1 and C.4.2, the eductor nozzle was fabricated from a piece of 0.5 inch tubing, with one end plugged to give an opening of 0.15 inches. An eductor sleeve with an inside diameter of about 1 inch was fabricated and installed. The purpose of this sleeve was to maximize conversion of motive gas kinetic energy into pressure energy so as to drive the combined gas through the flow resistances around the loop. This is explained by derivation of an approximate momentum balance as described in Section 3.2. Design dimensions were selected based upon preliminary parametric studies using the existing rigorous eductor recirculation model described above.

The system was operated at room temperature because there was no provision for pre-heating the eductor gas. Nevertheless, the resulting experiments, as described in the next section, were a valid test of the rigorous recirculation loop model, since that model's critical assumptions are not related to temperature. The system was run pressurized, however, since exhaust flow was still controlled by the back-pressure regulator.

The effectiveness of recirculation, as determined by the ratio of total flow to motive flow, is very sensitive to the flow resistance around the loop. This particular cold-flow test configuration has relatively high flow resistance, the major components of which are:

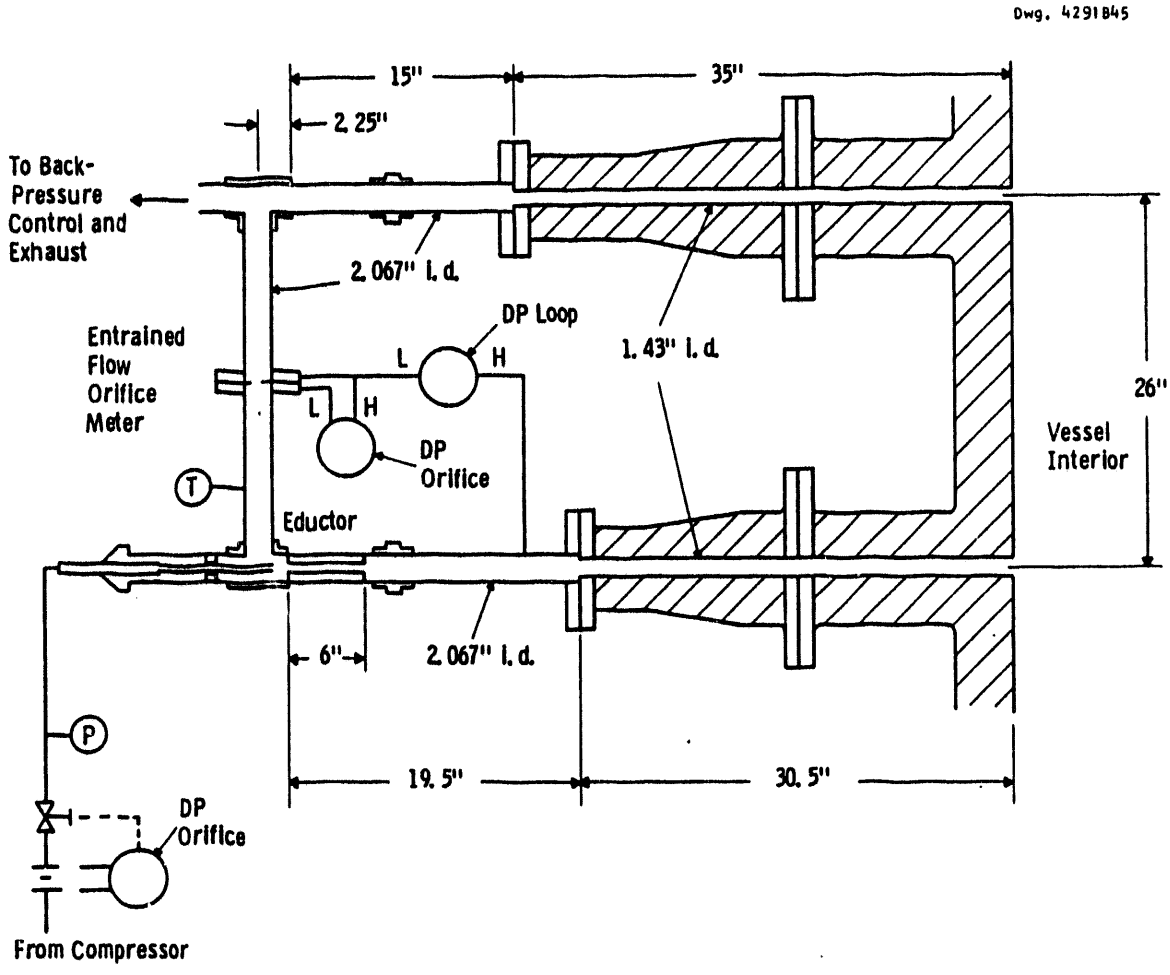

Figure C.4.1 - Test Facility Modification for Cold Flow Recirculation

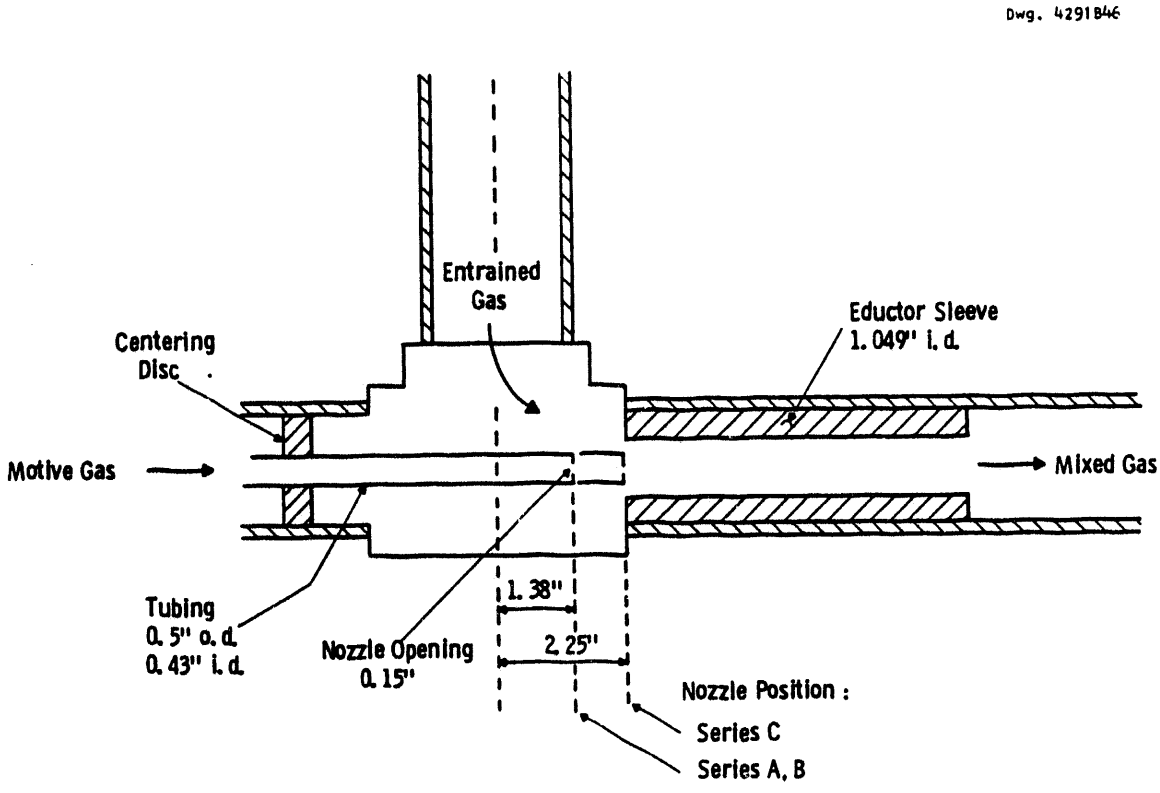

Figure C.4.2 - Eductor Detail

1. expansion from eductor sleeve to main pipe
2. contraction from main pipe into vessel inlet nozzle
3. expansion into vessel
4. contraction into vessel outlet nozzle
5. expansion into main pipe
6. flow through orifice flow meter (permanent loss component)
7. contraction into eductor sleeve

The cold flow test loop was set up by a quick and inexpensive modification to an existing facility not intended for eductor-driven recirculation operation. Consequently, the magnitudes of the flow resistances in this loop are relatively large. The high-temperature loop, on the other hand, was designed to minimize these resistances: resistances 2 and 5 from the preceding list were eliminated, by making the vessel nozzle i.d.'s the same as the rest of the piping; resistances 1 and 7 were greatly reduced, by using a venturi-shaped eductor sleeve; and resistance 6 was reduced by using venturi flow meter rather than an orifice meter. Because already high total resistance in the cold flow tests, it was decid to further increase resistance by the use of a filter in the test vessel. However, a filter is assumed to be in place for the application of the model to the hot system.

4.2 TEST RESULTS

Three series of tests were run to verify model performance. In Series A, summarized in Table C.4.1, a 1.0 inch orifice was used to measure entrained gas flow rate in the position shown in Figure C.4.1, and the motive gas nozzle was inserted as shown in Figure C.4.2. The eductor sleeve shown in both Figures was not used, i.e., the eductor throat had the same i.d. as the general piping, 2.067 inches. "Actual" entrained flow rates were measured with the orifice meter and "predicted" entrained flow rates are from the detailed eductor recirculation model given the system dimensions, pressure, and motive gas flow rate as shown. In general, the actual and predicted values

TABLE C.4.1 - RECIRCULATION TEST RESULTS - SERIES A

Orifice Diameter, in.	1.0							
Sleeve	Not used							
Test No.	1	2	3	4	5	6	7	8
Motive Gas Flow, lb/hr	60	100	150	200	250	280	280	200
System Pressure, atm (abs)	1.68	2.02	2.63	3.31	4.06	4.54	6.71	6.85
ΔP Orifice, in Water								
Actual	4.4	6.0	8.2	11.0	13.5	15.5	13.5	8.0
Predicted	2.2	4.9	8.1	11.1	14.0	15.7	13.4	7.3
ΔP Loop, in Water								
Actual	4.0	5.0	6.0	9.0	10.0	11.0	10.0	7.0
Predicted	2.0	4.1	6.6	8.9	11.2	12.6	10.0	5.4
Entrained Flow, lb/hr								
Actual	181	234	311	405	497	563	638	497
Predicted	128	212	309	407	506	567	636	475
Ratio (Actual/ Predicted)	1.41	1.11	1.01	1.00	0.98	0.99	1.00	1.05
Flow Ratio (Total/ Motive)								
Actual	4.0	3.3	3.1	3.0	3.0	3.0	3.3	3.5
Predicted	3.1	3.1	3.1	3.0	3.0	3.0	3.3	3.4

agreed well, except at the lowest flow rate, where orifice pressure drops could have easily been in error enough to explain the difference. At the bottom of Table C.5.1, the actual and predicted ratios of total gas flow (motive to entrained) to motive gas flow are shown, and it is seen that a typical such ratio is about 3.0. The important point is that the model was able to accurately predict eductor performance. An essential element in this model capability is that the flow resistance characteristics of the recirculation loop are rigorously and accurately modeled, as shown by the close agreement between measured and predicted loop pressure drop values in the cases where actual and predicted flow rates agreed well.

Series B tests differed from those in Series A only in that the sleeve was inserted into the eductor, thus reducing the throat i.d. to 1.049 inches. This change was expected to increase eductor performance, for the reasons discussed in Section 3.2, and it did, as shown in Table C.4.2. The achieved ratios of total to motive gas flow rates were increased to about 4.0 (from 3.0 without the sleeve). This represents a 50 percent increase in entrained flow rate over the no-sleeve case. As is also shown in Table C.4.2, the model predicted performance reasonably well, usually under-predicting entrained flow by a few percent.

The series C tests were also performed with the sleeve in place, but with a 1.4 inch orifice in use instead of the 1.0 inch orifice in prior tests. The motive gas nozzle was also inserted so as to be flush with the start of the sleeve. The results are shown in Table C.4.3. The achieved ratios of total to motive gas flow rates increased further, to about 5.0, representing about a 25 % additional increase in entrained flow relative to Series B. The reason for this is the important but small decrease in resistance to flow recirculation caused by the small decrease in permanent pressure drop across the orifice. A permanent pressure loss in the case of the 1 inch orifice is about 77 % of the actual measured value listed in Table C.4.2 or C.4.3, and for the 1.4 inch orifice, it is about 54 % of the value in Table C.4.3. It can readily be seen that the permanent pressure drops for the smaller orifice were similar in magnitude to the overall loop pressure drops.

TABLE C.4.2 - RECIRCULATION TEST RESULTS - SERIES B

Orifice Diameter, in.	1.0							
Sleeve	Used							
Test No.	1	2	3	4	5	6	7	8
Motive Gas Flow, lb/hr	60	100	150	200	250	280	280	200
System Pressure, atm (abs)	1.68	2.02	2.56	3.04	3.72	4.54	6.71	6.92
ΔP Orifice, in Water								
Actual	11.0	14.0	20.0	25.0	32.0	35.0	32.0	19.0
Predicted	6.6	13.8	22.1	30.6	38.6	42.3	35.5	19.3
ΔP Loop, in Water								
Actual	6.6	8.9	12.0	15.0	18.5	20.5	16.0	8.9
Predicted	4.0	8.2	13.3	18.5	23.2	25.1	20.3	10.9
Entrained Flow, lb/hr								
Actual	289	356	481	586	732	846	984	769
Predicted	224	354	506	648	804	930	1036	775
Ratio (Actual/ Predicted)	1.29	1.01	0.95	0.90	0.91	0.91	0.95	0.99
Flow Ratio (Total/ Motive)								
Actual	5.8	4.6	4.2	3.9	3.9	4.0	4.5	4.8
Predicted	4.7	4.5	4.4	4.2	4.2	4.3	4.7	4.9

TABLE C.4.3 - RECIRCULATION TEST RESULTS - SERIES C

Orifice Diameter, in.	1.4							
Sleeve	Used							
Test No.	1	2	3	4	5	6	7	8
Motive Gas Flow, lb/hr	60	100	150	200	250	280	280	200
System Pressure, atm (abs)	1.75	2.02	2.70	3.38	4.2	4.67	6.85	6.78
ΔP Orifice, in Water								
Actual	3.1	4.5	6.5	8.2	10.8	12.0	10.0	6.5
Predicted	2.1	4.5	7.1	9.7	12.2	13.7	11.4	6.4
ΔP Loop, in Water								
Actual	8.0	11.0	15.0	20.0	24.0	26.0	21.0	15.0
Predicted	5.3	11.3	17.7	24.2	30.3	34.0	27.7	15.4
Entrained Flow, lb/hr								
Actual	334	433	603	758	968	1076	1194	955
Predicted	275	433	630	824	1029	1150	1275	948
Ratio (Actual/ Predicted)	1.21	1.00	0.96	0.92	0.94	0.94	0.94	1.01
Flow Ratio (Total/ Motive)								
Actual	6.6	5.3	5.0	4.8	4.9	4.8	5.3	5.8
Predicted	5.6	5.3	5.2	5.1	5.1	5.1	5.6	5.7

From these test sequences we learned that:

- the analytical model is able to predict eductor-induced recirculation rates quite accurately and can therefore be used for parametric design studies
- the dimensional design envisioned for the eductor, including its throat, is appropriate
- it is very important to minimize flow resistance to get high recirculation ratios.

5. DURABILITY TEST SYSTEM PERFORMANCE PROJECTIONS

The eductor recirculation model was used to project performance in the planned gasification simulator loop. The results have been used to fine-tune design details for optimizing recirculation performance.

5.1 SYSTEM DESCRIPTION

Figure C.5.1 shows the configuration of the planned recirculation loop, with dimensions applicable to the pressure drop calculations in the eductor recirculation model. Figure C.5.2 shows a possible set of dimensional details for the eductor nozzle and sleeve. The dimensions in Figure C.5.2 may be considered adjustable parameters, since they can be easily changed via replacement of the component.

Not shown in Figure C.5.1, but important with regard to recirculation performance, is the feed of dust and transport gas to the system. Transport gas is supplied by the same compressor as is the eductor motive gas. Whereas the motive gas from the compressor is reheated to near system temperature prior to injection, the transport gas is not heated, but is passed through the dust feed system and thence to the system. The entry point will be somewhere in the horizontal line between the eductor and the vessel inlet, and is assumed to be a piece of 3/8 inch tubing inserted into the center of the main gas flow path, and bent to point downstream.

The recirculation flow loop and model have the following pressure drop and flow resistance components:

1. wall friction in eductor sleeve, corrected to account for variable diameter
2. irreversible expansion loss from eductor sleeve
3. reversible gain due to velocity gain from eductor sleeve to main pipe

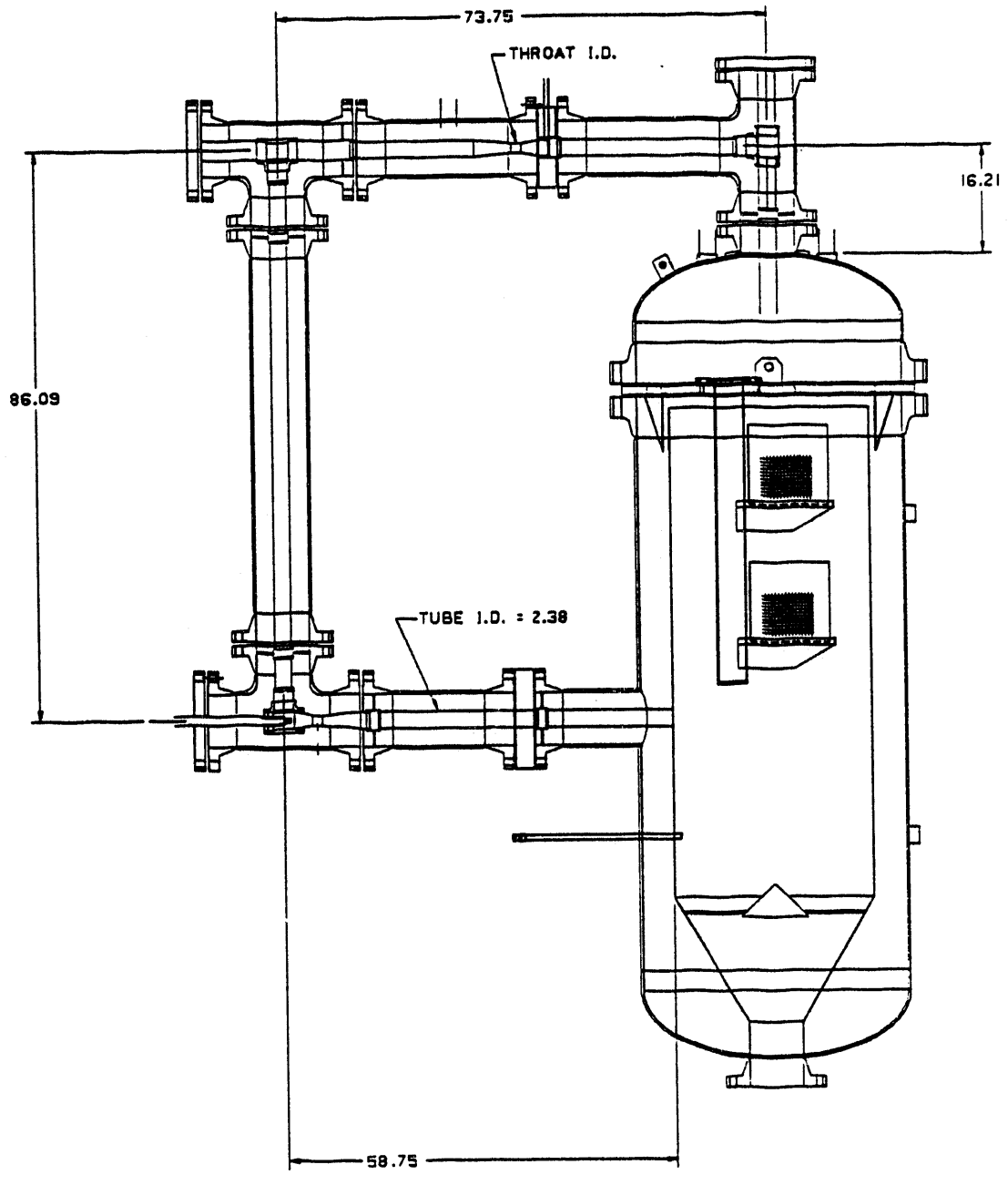

Figure C.5.1 - High Temperature Recirculation Loop

EDUCTOR VENTURI

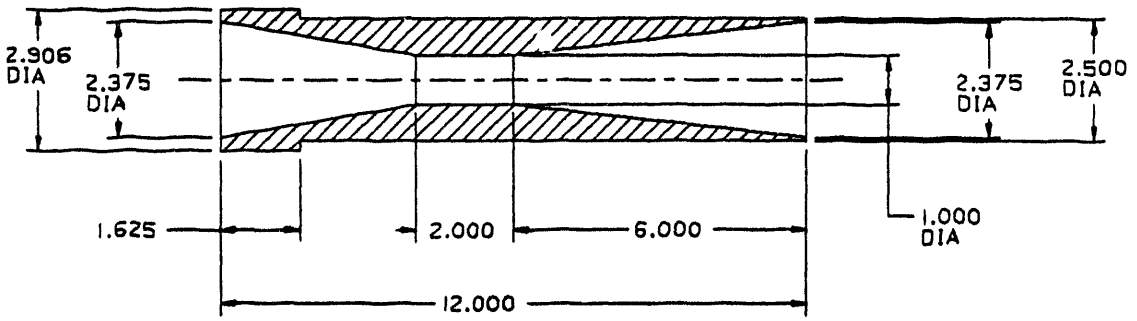

MOTIVE GAS NOZZLE

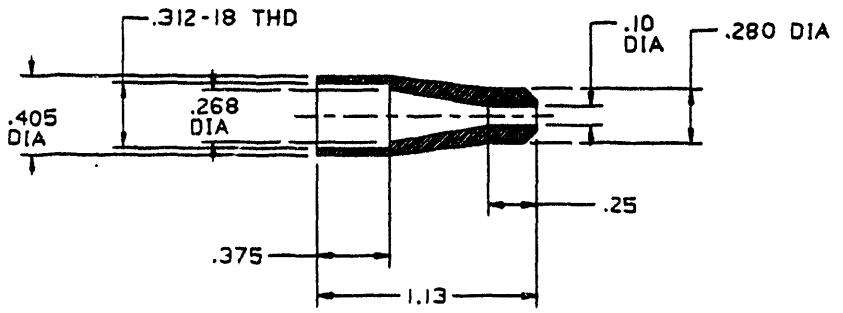

Figure C.5.2 - Eductor Component Details.

4. flow through horizontal pipe after eductor
5. friction loss passing dust injection nozzle
6. loss or gain due to mixing with dust transport gas
7. flow through horizontal pipe entering vessel
8. expansion into vessel
9. loss across filter
10. contraction out of vessel
11. flow through vertical pipe upward out of vessel
12. flow through tee used as elbow
13. flow through upper horizontal run
14. irreversible component of loss across venturi flow meter
15. flow though tee dividing total flow into recirculating flow heading back to eductor and flow to compressor
16. reversible gain due to velocity change from inlet pipe to vessel to after flow branching at tee in item 15
17. flow through vertical run downward toward eductor
18. flow through eductor tee used as elbow
19. contraction to get around motive gas nozzle
20. flow through the short horizontal run between the tee and eductor sleeve
21. contraction into sleeve
22. reversible loss of recirculating gas due to velocity change from downward vertical pipe to inside throat of eductor sleeve

5.2 PROJECTED PERFORMANCE

The target flow rate of gas through the filter is 0.35 lb/sec (1260 lb/hr). It is desired to keep the motive gas flow rate at not much more than a tenth of this. The system operating pressure and temperature are 10 atm and 1550°F, respectively. The dimensions (other than nozzle orifice diameter) shown in Figures C.5.1 and C.5.2 are assumed, as are the following additional parameters:

motive gas temperature	1400°F
maximum available motive gas pressure	30 atm (abs)
flow rate of dust transport gas	0.01 lb/s
temperature of transport gas	100°F
venturi throat diameter	1.25 inch

Based upon previous filter testing, the filter pressure drop immediately after a successful blow back pulse is assumed to be

$$\Delta P = R_W \mu v \qquad (5\text{-}1)$$

where ΔP = pressure drop, $lb_m/(ft\text{-}sec^2)$
R_W = resistance coefficient, ft^{-1}
μ = gas viscosity, $lb_m/(ft\text{-}sec)$
v = superficial gas velocity (face velocity) through filter, ft/sec

The actual filter pressure drop is assumed to be given by a multiple of the clean pressure drop from Equation 5.1. In the worst case, this filter pressure drop multiple is assumed to be 2.0.

Table C.5.1 summarizes the effects of motive gas flow rate and nozzle orifice size (nozzle not converging/diverging) on total gas flow through the filter given the above assumptions, including the pressure drop multiplier of 2.0. The "nozzle" pressure shown in the table is that in the nozzle prior to the nozzle orifice. Essentially, the motive gas flow rate is controlled by a valve after the compressor and before

TABLE C.5.1 - EFFECT OF NOZZLE ORIFICE SIZE ON EDUCTOR PERFORMANCE

Nozzle Diameter, In.	Motive Flow, lb/s	Total Flow, lb/s	Nozzle Pressure, atm	Exit Pressure, atm	Motive Gas Mach No.	Pressure Gain, psi
0.215	0.035	0.107	10.6	10.0	0.31	0.70
	0.070	0.296	12.6	10.0	0.61	2.47
	0.080	0.353	13.5	10.0	0.69	3.15
0.15	0.035	0.185	12.8	10.0	0.62	1.46
	0.040	0.223	13.7	10.0	0.71	1.87
	0.050	0.301	15.9	10.0	0.87	2.82
	0.057	0.356	17.9	10.0	0.98	3.57
0.12	0.035	0.248	17.2	10.0	0.94	2.24
	0.040	0.294	19.6	10.7	1.0	2.84
	0.045	0.337	22.0	12.0	1.0	3.45
	0.047	0.353	23.0	12.5	1.0	3.70
0.10	0.035	0.296	24.7	13.4	1.0	2.94
	0.040	0.339	28.2	15.4	1.0	3.57
	0.042	0.355	29.6	16.1	1.0	3.82
0.095	0.035	0.306	27.4	14.9	1.0	3.11
	0.0383*	0.335	30.0	16.3	1.0	3.53
0.090	0.0344*	0.310	30.0	16.3	1.0	3.19

Filter pressure drop multiplier = 2.0.

*Maximum possible flow, given 30 atm pressure limit.

the heater, and the nozzle pressure increases as the valve is opened. In the case of sonic flow through the orifice, the velocity is a constant at a given temperature, while the total flow will be proportional to this nozzle pressure. The actual pressure of the gas exiting the system ("exit" pressure in Table C.5.1) will be the system pressure (10 atm) for sub-sonic flow, and a constant fraction, given by the critical pressure ratio, of the nozzle pressure for sonic flow. As shown in this table, larger nozzle orifice sizes (.215 and .15 inches) require higher than desirable motive gas flow rates to achieve the needed total gas flow rate at this degree of filter resistance. The 0.10 inch nozzle requires a motive flow of 12% of the total gas flow. Smaller nozzles cannot achieve the total flow, because the flow rate of motive gas through the nozzle orifice is limited to critical flow at the maximum available motive gas pressure. Based on Table C.5.1, a nozzle orifice diameter of 0.10 inches has been selected.

The question arose as to whether using a converging/diverging nozzle could result in improved eductor performance, as measured by the ratio of entrained to motive gas flow rates. Such a nozzle could allow supersonic flow at the nozzle exit, at the expense of pressure of the exiting gas. Since both velocity and pressure are important in the momentum balance that determines entrained flow rate, there must be a tradeoff with using converging/diverging nozzles. Table C.5.2 looks at the effect of such nozzles relative to straight nozzles, in the vicinity of the selected 0.10 inch straight nozzle. It can be seen that very slight divergences have very slight beneficial effects. Divergences that increase the exit diameter to 10% more than the nozzle throat diameter have a deleterious effect, i.e., the resulting fall in pressure of the exiting gas is much more important than the increased diameter. We conclude that the straight nozzle is appropriate for this system.

Another important design parameter is the diameter of the sleeve of the eductor. A sleeve diameter of 1.0 inches, as shown in Figure 5.2, was assumed for the Table C.5.1 calculations. Table C.5.3 shows

TABLE C.5.2 - BEHAVIOR OF CONVERGING/DIVERGING NOZZLES

Throat Diameter, In.	Exit Diameter, In.	Motive Flow, lb/s	Total Flow, lb/s	Nozzle Pressure, atm	Exit Pressure, atm	Exit Mach No.	Exit Velocity ft/s
0.10	0.10	0.035	0.330	24.7	13.4	1.0	1867
	0.101	0.035	0.331	24.7	11.1	1.16	2114
	0.105	0.035	0.330	24.7	8.4	1.37	2414
	0.11	0.035	0.327	24.7	6.9	1.53	2628
	0.12	0.035	0.316	24.7	4.7	1.77	2910
	0.15	0.035	0.248	24.7	2.1	2.25	3380
	0.20	0.035	0.141	24.7	10.0	0.36*	710
0.12	0.12	0.045	0.373	22.0	12.0	1.0	1867
	0.121	0.045	0.373	22.0	10.1	1.14	2092
	0.125		0.372	22.0	7.9	1.33	2367
	0.13	0.045	0.368	22.0	6.4	1.48	2566
0.08	0.08	0.0272	0.296	30.0	16.3	1.0	1867
	0.084	0.0272	0.298	30.0	10.3	1.37	2414
	0.088	0.0272	0.297	30.0	8.1	1.53	2629

Filter pressure drop multiplier = 1.5.

*Normal shock in diverging section.

TABLE C.5.3 - EFFECT OF SLEEVE DIAMETER

Nozzle Diameter, In.	Motive Flow, lb/s	Sleeve Diameter, in.	Total Flow, lb/s	Pressure Gain, psi
0.10	0.035	2.38	0.109	0.54
		2.0	0.147	0.76
		1.5	0.233	1.30
		1.2	0.300	2.00
		1.1	0.319	2.40
		1.0	0.330	3.01
		0.9	0.329	3.97
		0.8	0.311	5.56
		0.7	0.271	8.18
		0.6	0.208	12.1
		0.5	0.125	16.2

Filter pressure drop multiplier = 1.5.

how this sleeve diameter is expected to affect total flow rate, based upon the detailed eductor recirculation model. There is an optimum sleeve diameter of 1.0 inch at which total recirculation flow rate is highest. This effect can be understood in terms of the conversion of motive gas momentum into the product of pressure and flow area, as demonstrated in the cold flow study, and as explained in Section 3.2.

Table C.5.4 shows how total flow rate varies with motive gas flow rate in this case, as well as how motive gas flow rates would have to be varied as filter flow resistance varies, in order to keep a constant total gas flow rate. If the filter pressure drop multiplier were to vary between 1 and 2 during a test (i.e., blowback would be triggered at a multiple of 2.0) then the motive gas would vary from 0.033 to 0.042 lb/sec during each period between blowback events, assuming a single filter module. Motive gas flow will be controlled by automatically reading the pressure drop across the venturi flow meter and automatically adjusting the motive gas flow control valve (and hence the nozzle pressure) to keep that pressure drop constant.

If the motive gas preheater does not deliver gas at the vendor-promised temperature, there will be an effect on eductor performance as shown in Table C.5.5. Slightly higher motive gas flow rates will be required if the motive gas temperature is only 1200°F. This is because sonic velocity varies directly with the square root of the absolute temperature.

The magnitudes of the pressure drop terms listed in Section 5.1 are listed in Table C.5.6, for the case of a straight 0.10 inch nozzle orifice, a 1.0 inch sleeve, an average filter pressure drop multiplier of 1.5, and a motive gas flow rate of 0.38 lb/sec at 1400°F.

TABLE C.5.4 - EFFECT OF FHLTER RESISTANCE AND MOTIVE GAS FLOW RATE ON TOTAL GAS FLOW RATE

Filter ΔP Multiplier	Motive Flow, lb/s	Total Flow, lb/s	Pressure Gain, psi	Filter ΔP, in. H_2O	Flow Meter ΔP, in. H_2O	Nozzle Pressure, atm
* 2.0	0.042	0.355	3.82	60.4	23.9	29.6
1.5	0.042	0.392	3.91	50.1	29.2	29.6
1.0	0.042	0.436	4.03	37.1	36.0	29.6
0.5	0.042	0.485	4.22	20.7	44.7	29.6
2.0	0.038	0.322	3.32	54.9	19.7	26.8
* 1.5	0.038	0.358	3.39	45.8	24.3	26.8
1.0	0.038	0.400	3.50	34.1	30.4	26.8
0.5	0.038	0.449	3.67	19.1	38.3	26.8
2.0	0.033	0.277	2.69	47.4	14.7	23.3
1.5	0.033	0.311	2.75	39.9	18.5	23.3
* 1.0	0.033	0.352	2.84	30.1	23.6	23.3
0.5	0.033	0.399	2.98	17.1	30.4	23.3
2.0	0.029	0.239	2.19	40.9	10.9	20.5
1.5	0.029	0.271	2.23	34.8	14.0	20.5
1.0	0.029	0.309	2.30	26.5	18.3	20.5
* 0.5	0.029	0.356	2.42	15.2	24.1	20.5

*Locus of operating points.

TABLE C.5.5 - EFFECT OF MOTIVE GAS TEMPERATURE

Filter ΔP Multiplier	Temperature, °F	Motive Flow, lb/s	Total Flow, lb/s	Nozzle Pressure, atm	Exit Velocity, ft/s	Exit Mach No.
2.0	1400	0.042	0.355	29.6	1867	1
	1200	0.042	0.338	28.0	1764	1
	1200	0.044	0.354	29.3	1764	1
1.0	1400	0.033	0.352	23.3	1867	1
	1200	0.033	0.335	22.0	1764	1
	1200	0.035	0.354	23.3	1764	1

TABLE C.5.6 - MAGNITUDES OF FLOW RESISTANCES AT NOMINAL CONDITIONS

	Loss Component	Pressure Loss, in. H_2O
1.	Eductor Sleeve	4.9
2.	Irreversible Expansion From Eductor Sleeve	11.6
3.	Reversible, From Eductor Sleeve to Main Pipe	-55.6
4.	Horizontal Pipe After Eductor	0.3
5.	Passing Dust Injection Nozzle	0.6
6.	Mixing With Dust Transport Gas	-0.1
7.	Horizontal Pipe Entering Vessel	0.4
8.	Expansion Into Vessel	1.9
9.	Across Filter	45.8
10.	Contraction Out of Vessel	1.0
11.	Vertical Pipe From Vessel	0.4
12.	Tee	0.7
13.	Upper Horizontal Run	1.4
14.	Irreversible Component Across Flow Meter	3.7
15.	Tee Dividing Flow	0.7
16.	Reversible, From Vessel Inlet Pipe to After Branching in Tee in Item 15	-0.5
17.	Vertical Run Downward to Eductor	1.2
18.	Eductor Tee	0.5
19.	Contraction Around Nozzle	0.5
20.	Short Horizontal Run Before Eductor Sleeve	0.1
21.	Contraction Into Sleeve	8.5
22.	Reversible, From Downward Vertical Pipe to Inside Throat of Eductor Sleeve	65.8
Total Pressure Loss (= Pressure Rise Due to Eductor)		93.8

6. REFERENCES

1. D. F. Ciliberti, E. E. Smeltzer, M. A. Alvin, D. L. Keairns, and D.M. Bachovchin, Hot Gas Cleanup Using Ceramic Cross Flow Membrane Filters. Westinghouse R&D final report to DOE (Contract No. DE-AC21-79ET15491), 1983.

2. A. G. Hansen, Fluid Mechanics. New York: John Wiley & Sons, 1967, Chapter 7.

3. Ibid, pp. 252-256.

APPENDIX D

PRESSURE DROP TRACES FROM PFBC SIMULATOR FILTER TEST WRTX-9 AND WRTX-11

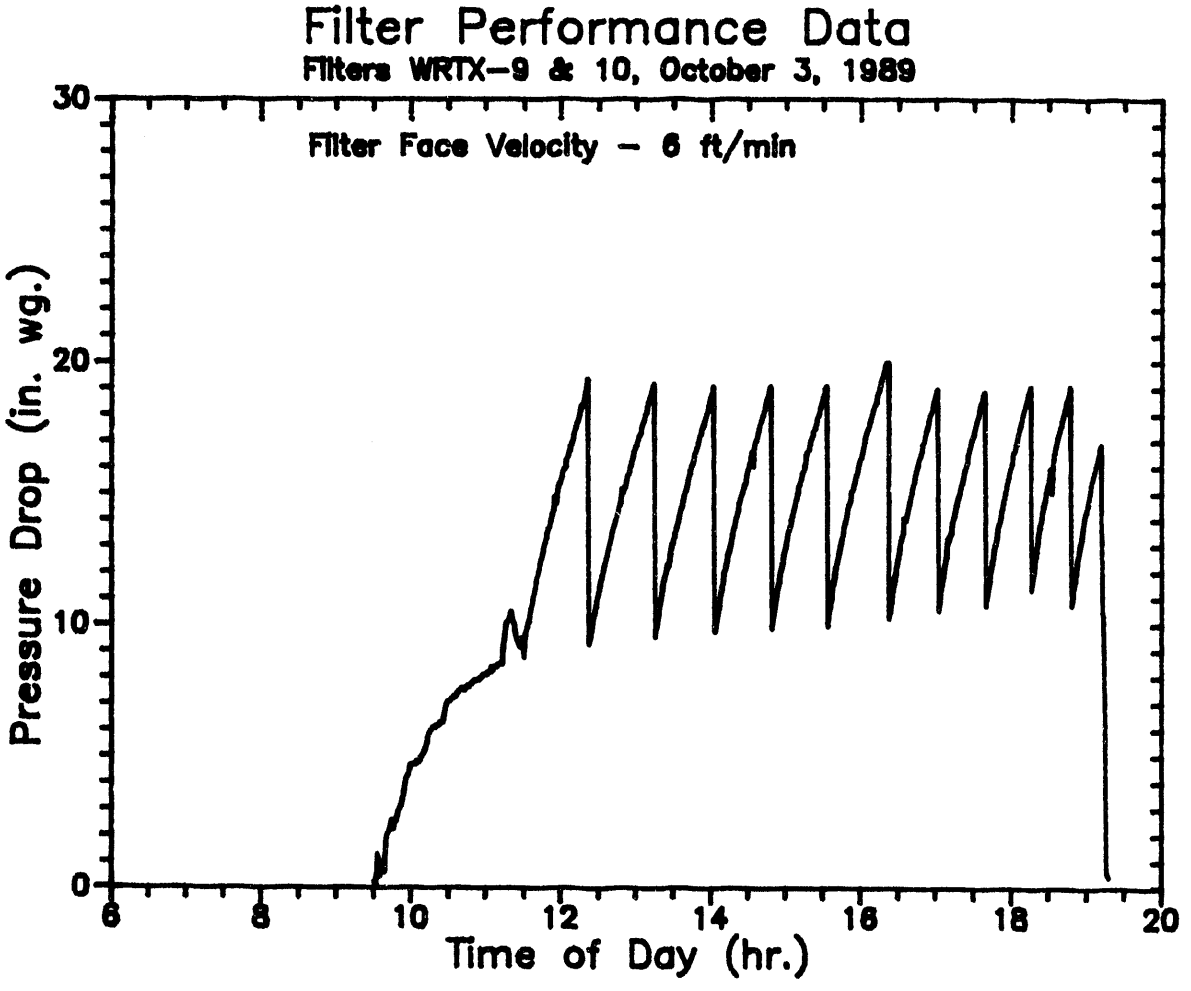

Operation Notes for October 3, 1989:

12 hour test, includes startup and shutdown
ΔP Trigger = 19.0" WC
Pulse Cleaning - 250 psig/0.1 sec

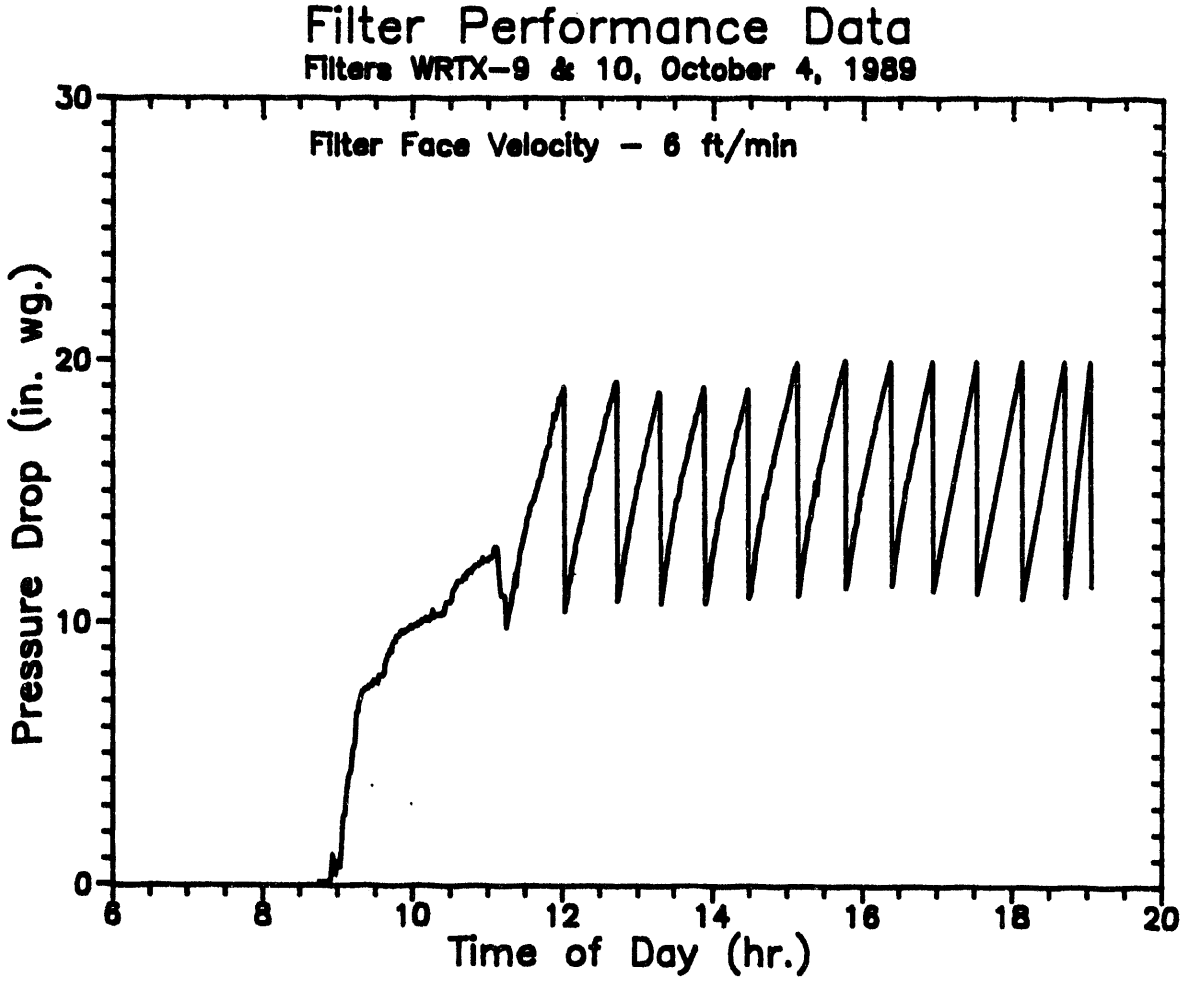

Operation Notes for October 4, 1989:
12 hour test, includes startup and shutdown
ΔP Trigger = 19.0" WC then increased to 20.0" WC
Pulse Cleaning - 250 psig/0.1 sec

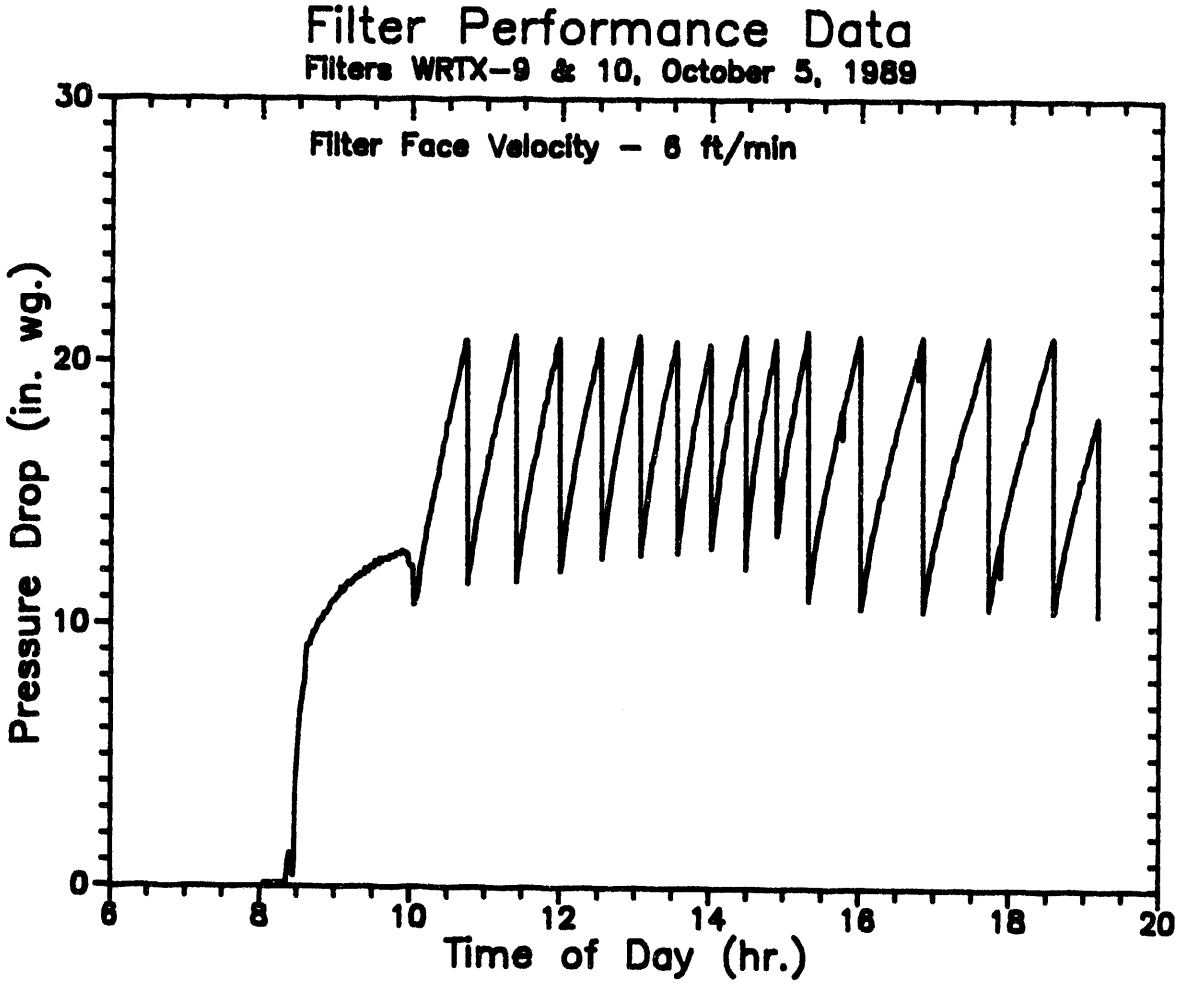

Operation Notes for October 5, 1989:

12 hour test, includes startup and shutdown
ΔP Trigger = 21.0" WC
Pulse Cleaning - 1045 - 250 psig/0.1 sec
1455 - 280 psig/0.1 sec

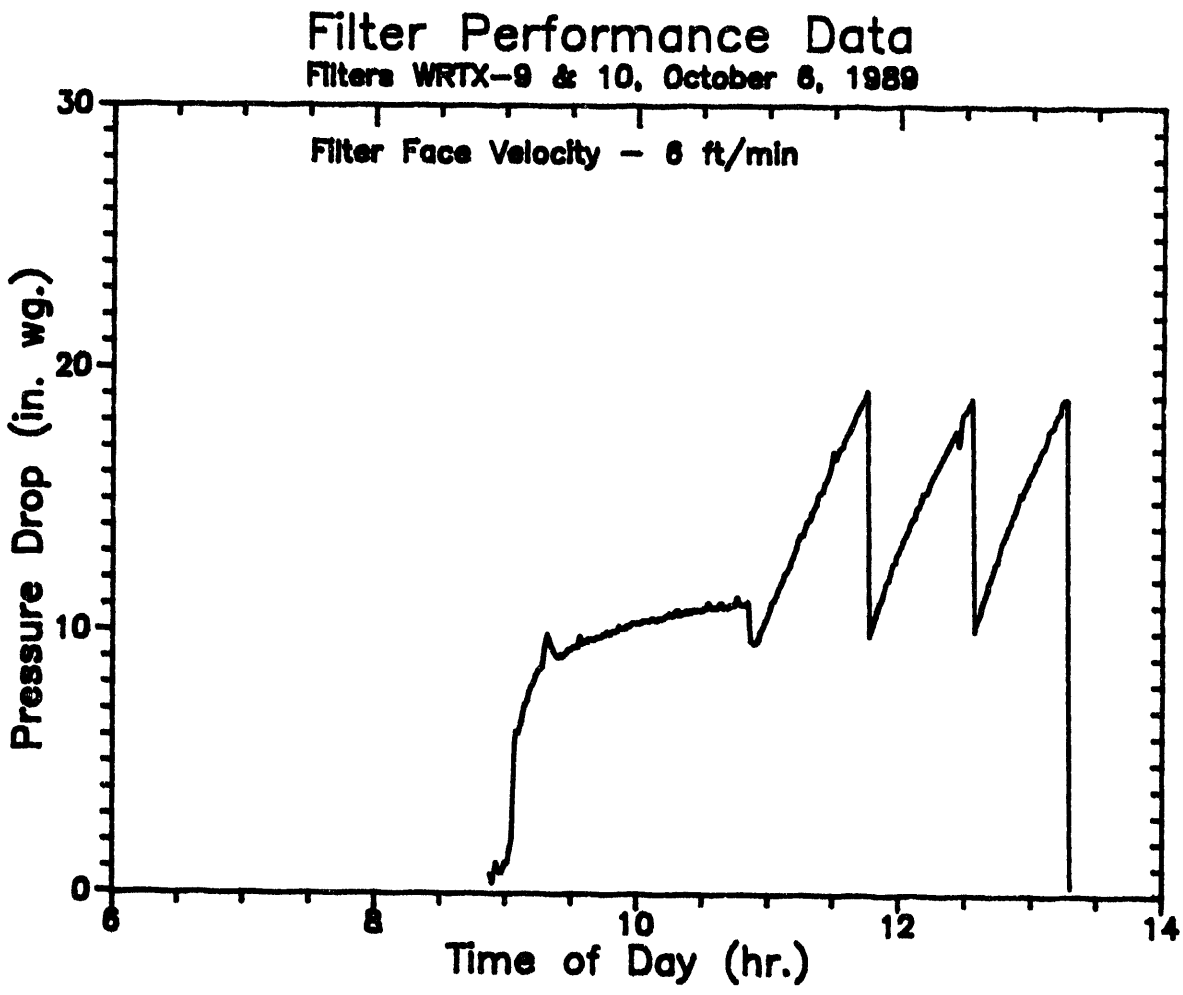

Operation Notes for October 6, 1989:

8 hour test, includes startup and shutdown
ΔP Trigger = 19.0" WC
Pulse Cleaning - 280 psig/0.1 sec

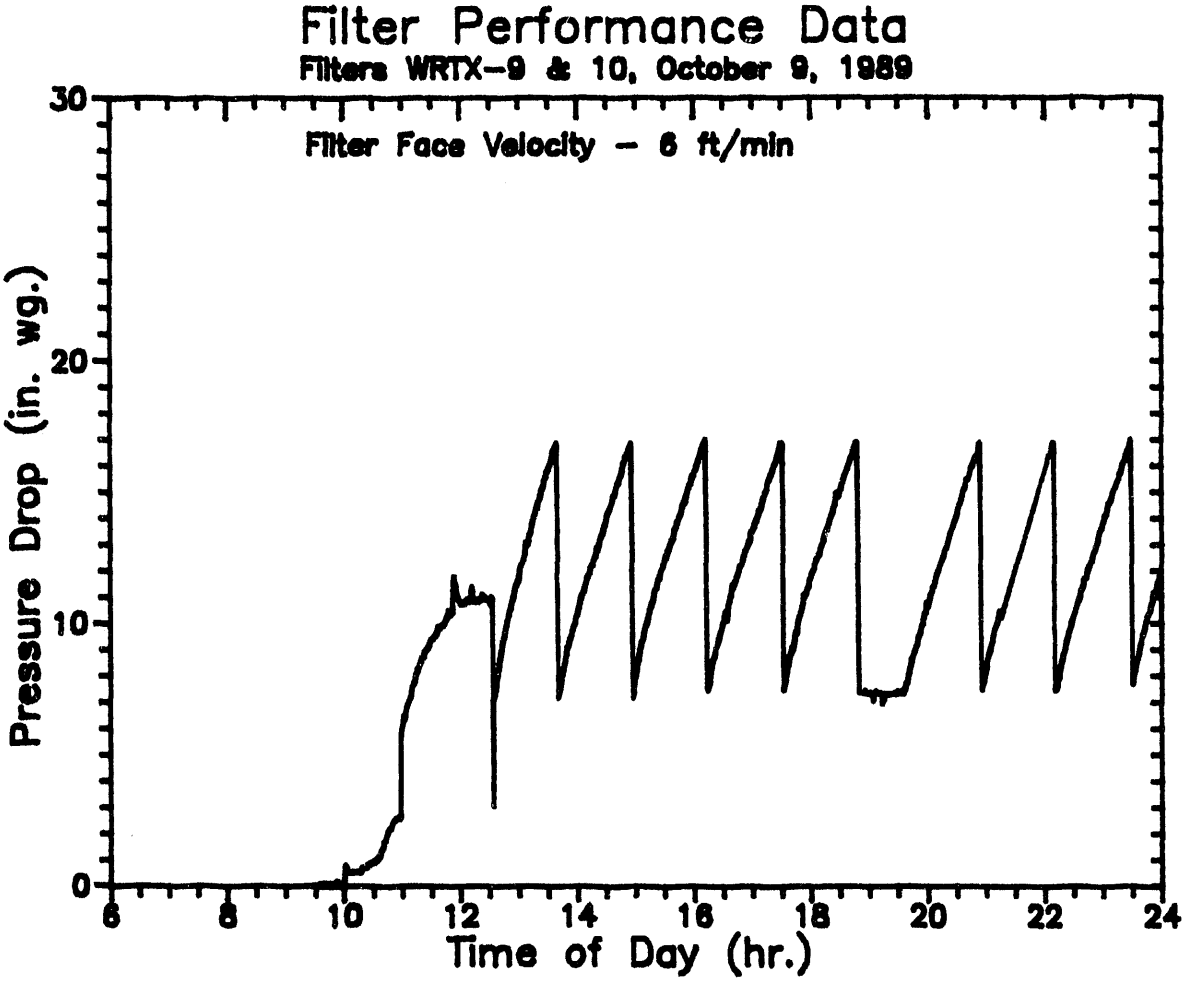

Operation Notes for October 9, 1989:

Begin week long test
Startup
ΔP Trigger = 17.0" WC
Pulse Cleaning - 280 psig/0.1 sec

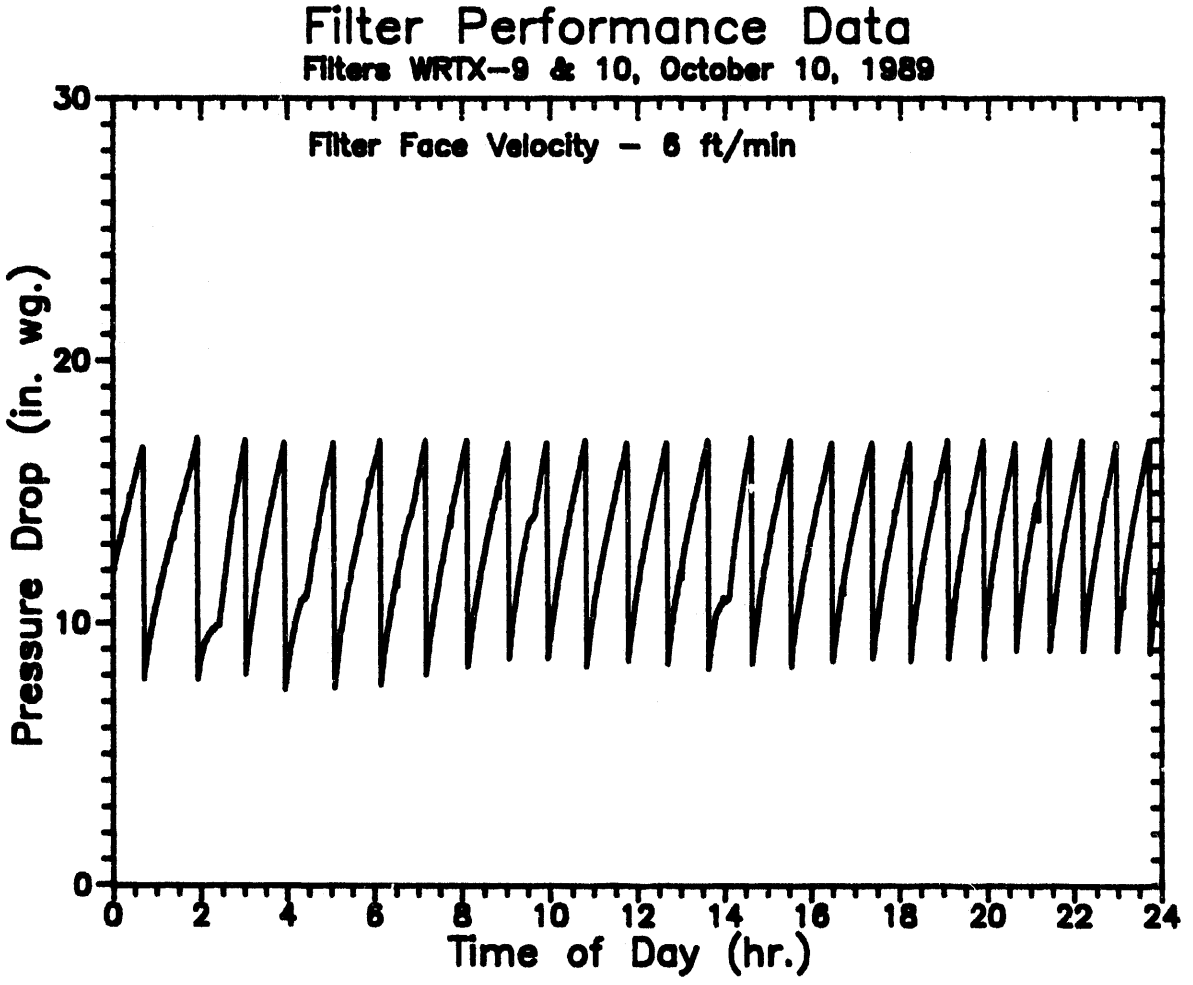

Operation Notes for October 10, 1989:
ΔP Trigger = 17.0" WC
Pulse Cleaning - 280 psig/0.1 sec

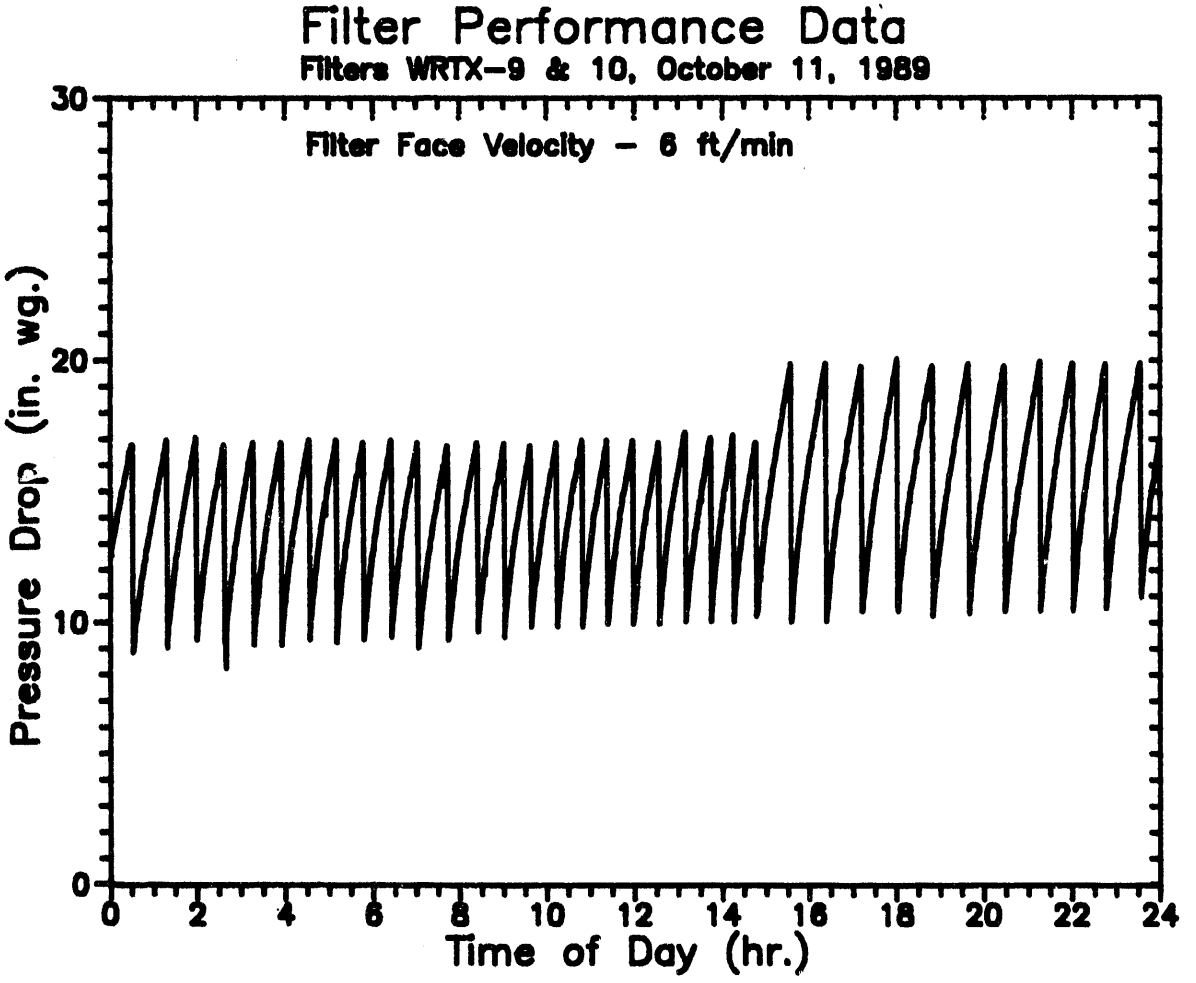

Operation Notes for October 11, 1989:
ΔP Trigger initially 17.0" WC increased to 20" WC
Pulse Cleaning - 280 psig/0.1 sec

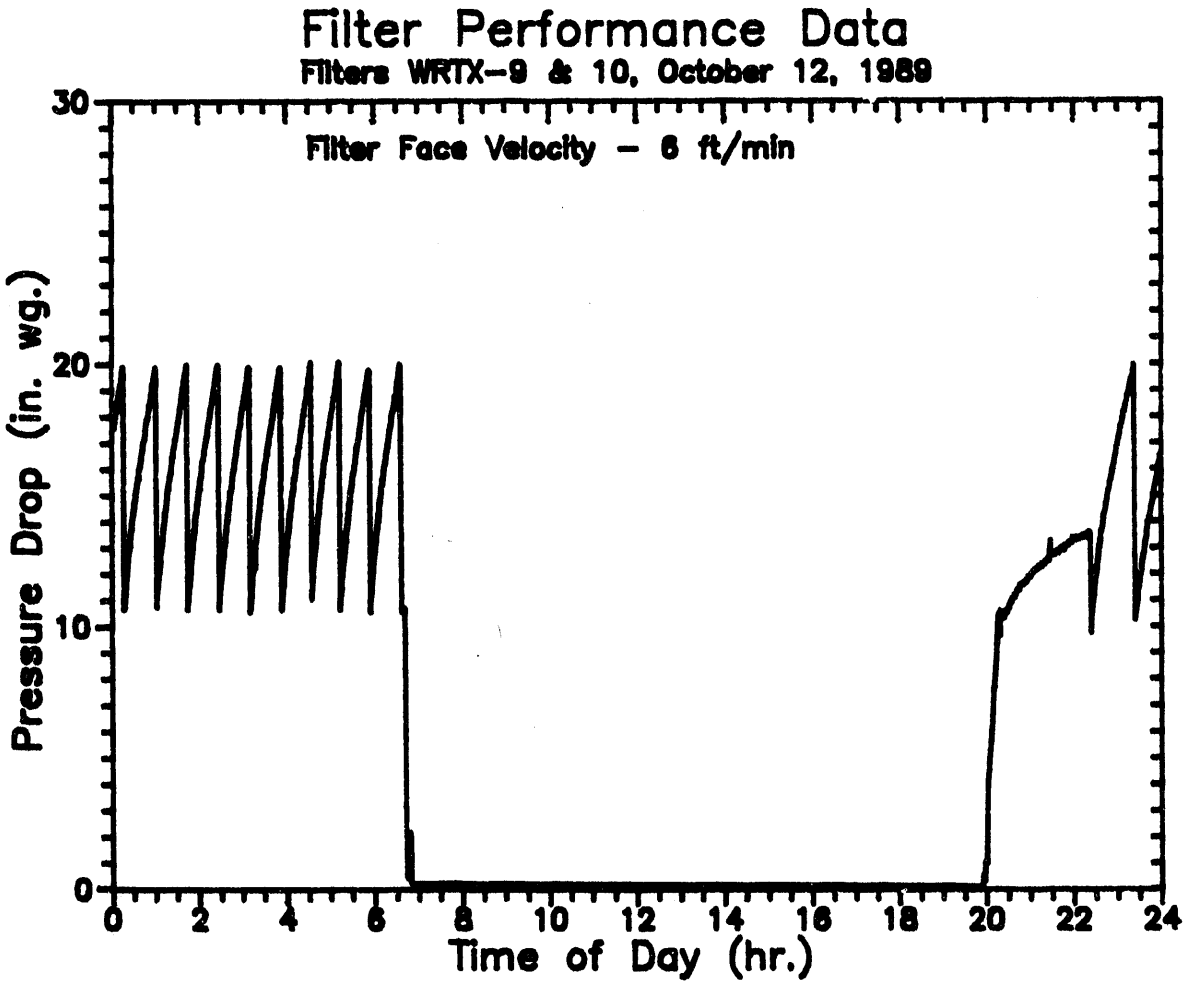

Operation Notes for October 12, 1989:

Scheduled shutdown
Dust added to vessel
Restart @ 20:00 hr
ΔP Trigger = 20.0" WC
Pulse Cleaning - 280 psig/0.1 sec

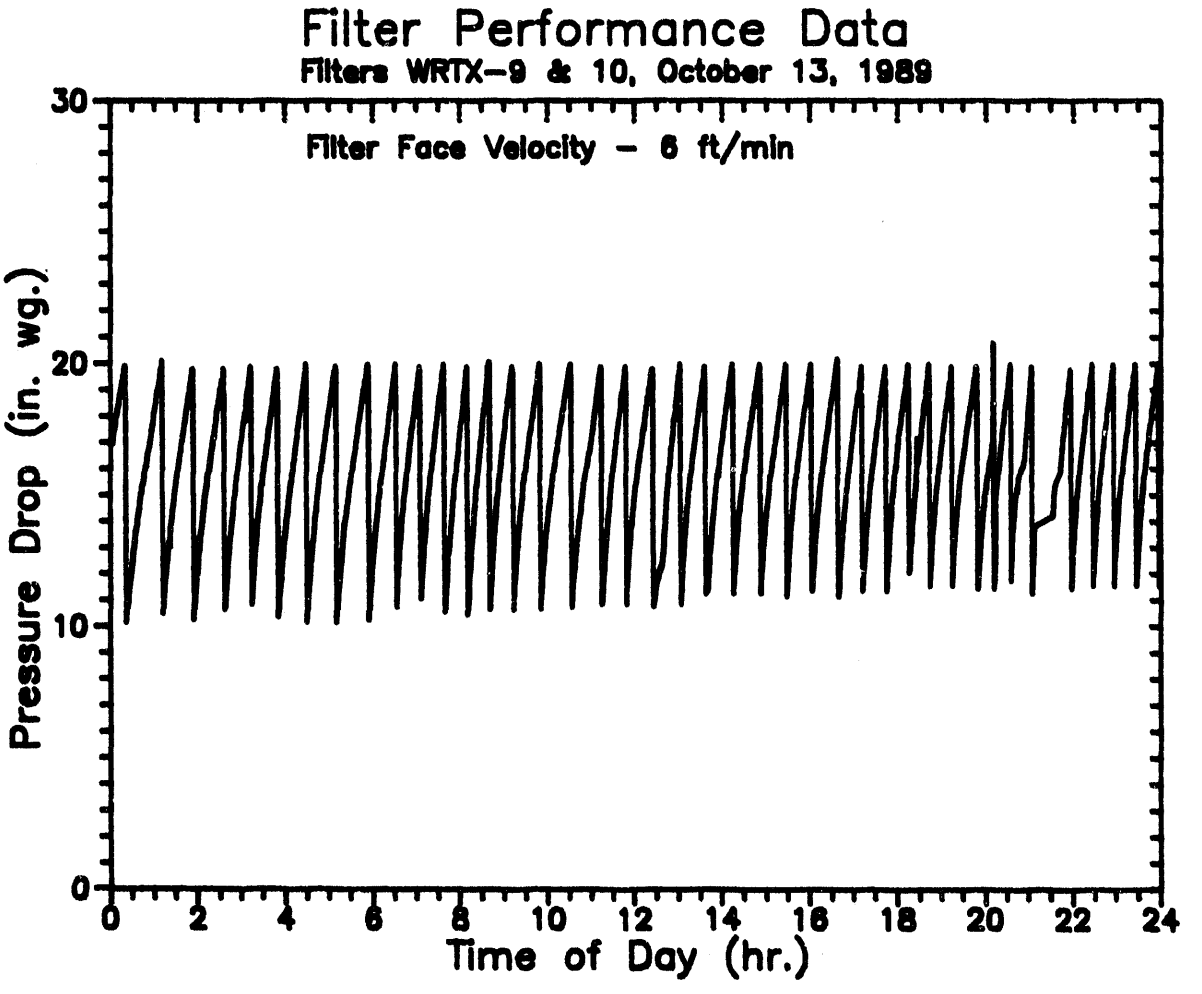

Operation Notes for October 13, 1989:
ΔP Trigger = 20.0" WC
Pulse Cleaning - 280 psig/0.1 sec

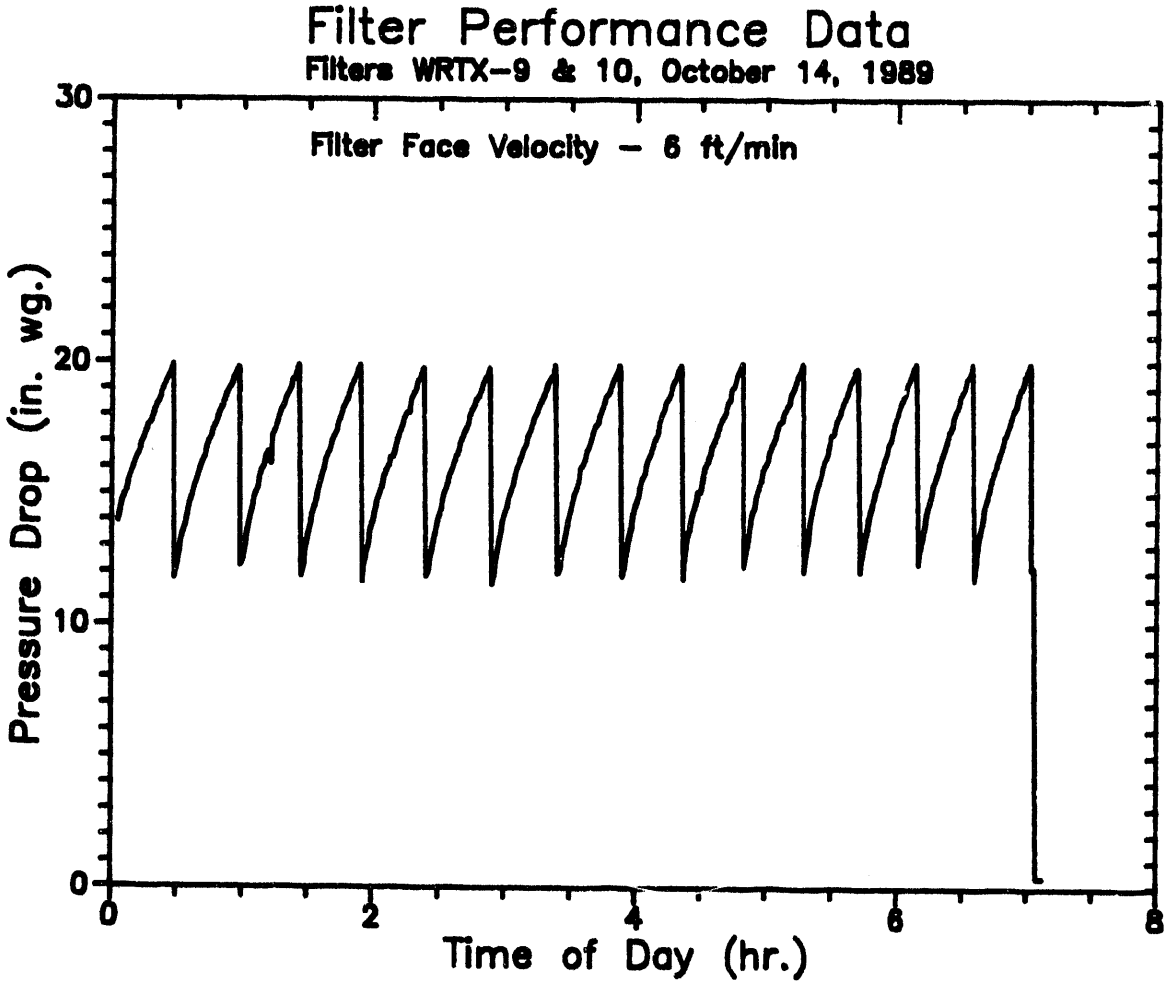

Operation Notes for October 14, 1989:
Week long test completion.
Scheduled shutdown
ΔP Trigger = 20.0" WC
Pulse Cleaning - 280 psig/0.1 sec

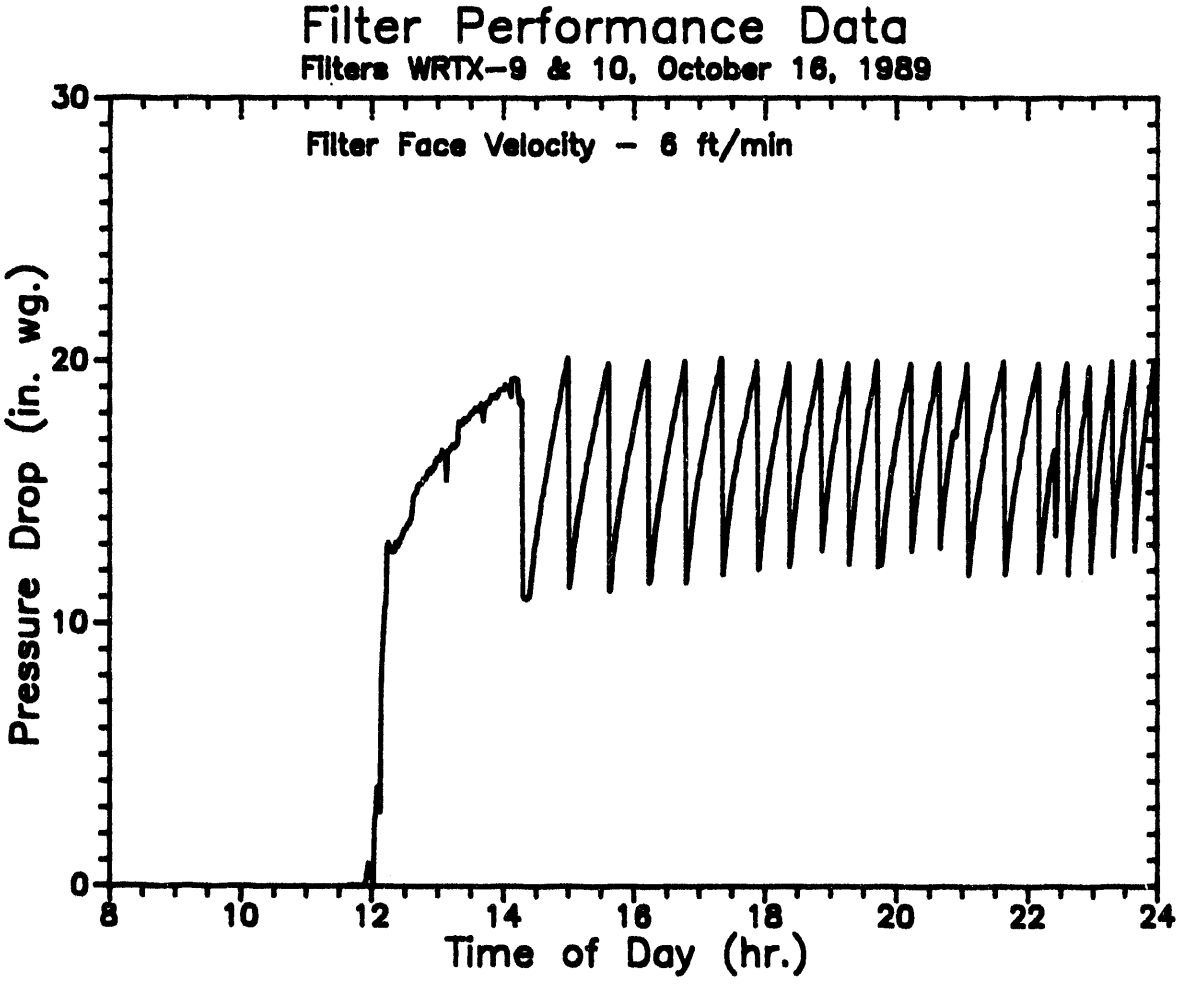

Operation Notes for October 16, 1989:

Week long test startup
ΔP Trigger = 20.0" WC
Pulse Cleaning - 280 psig/0.1 sec
Spike in cycle @ 2227 is system pressure drop caused by compressor shutdown, corrected, no flame out.

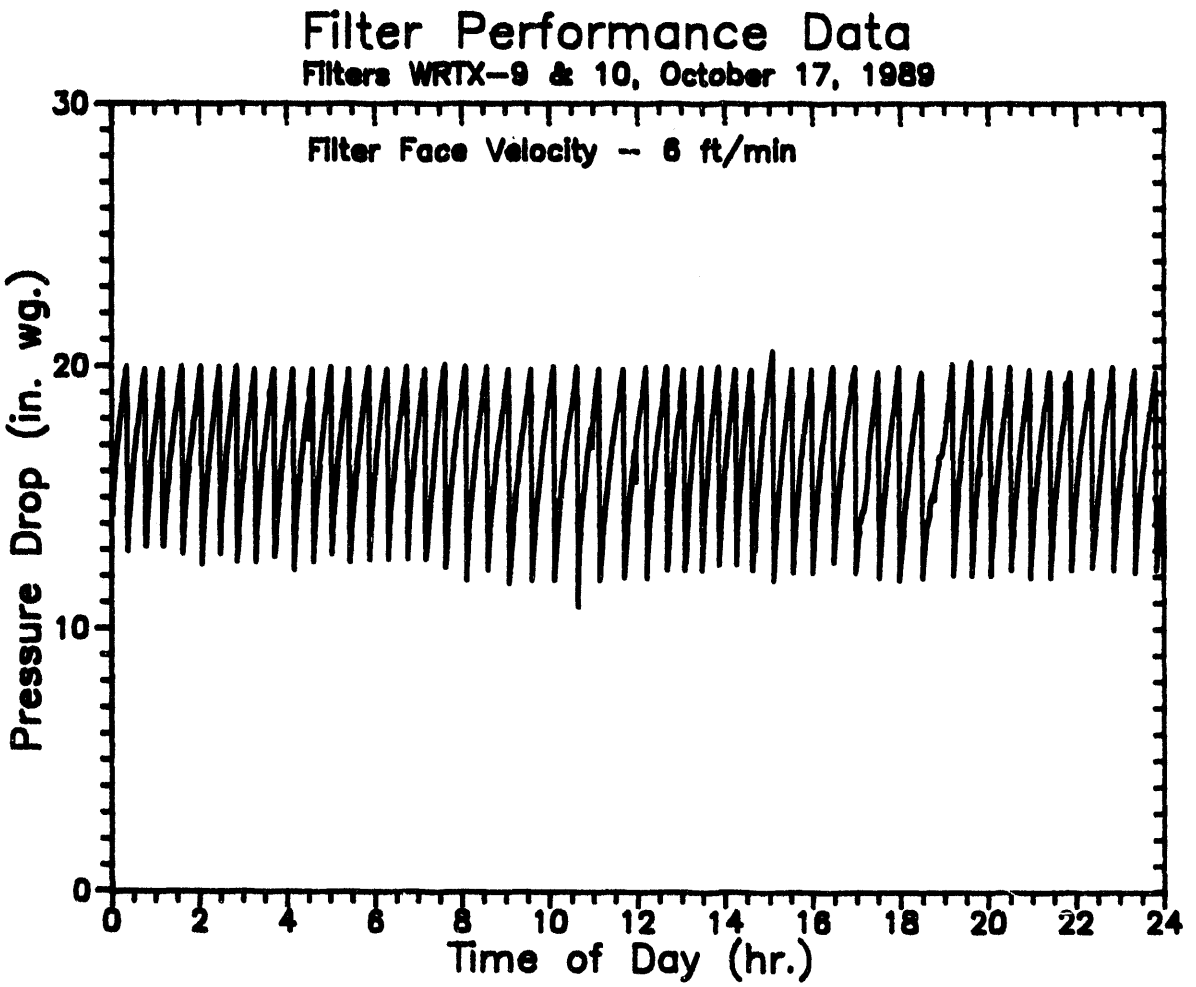

Operation Notes for October 17, 1989:

ΔP Trigger = 20.0" WC
Pulse Cleaning -
0000 - 280 psig/0.1 sec
0738 - 290 psig/0.1 sec
2253 - 285 psig/0.1 sec

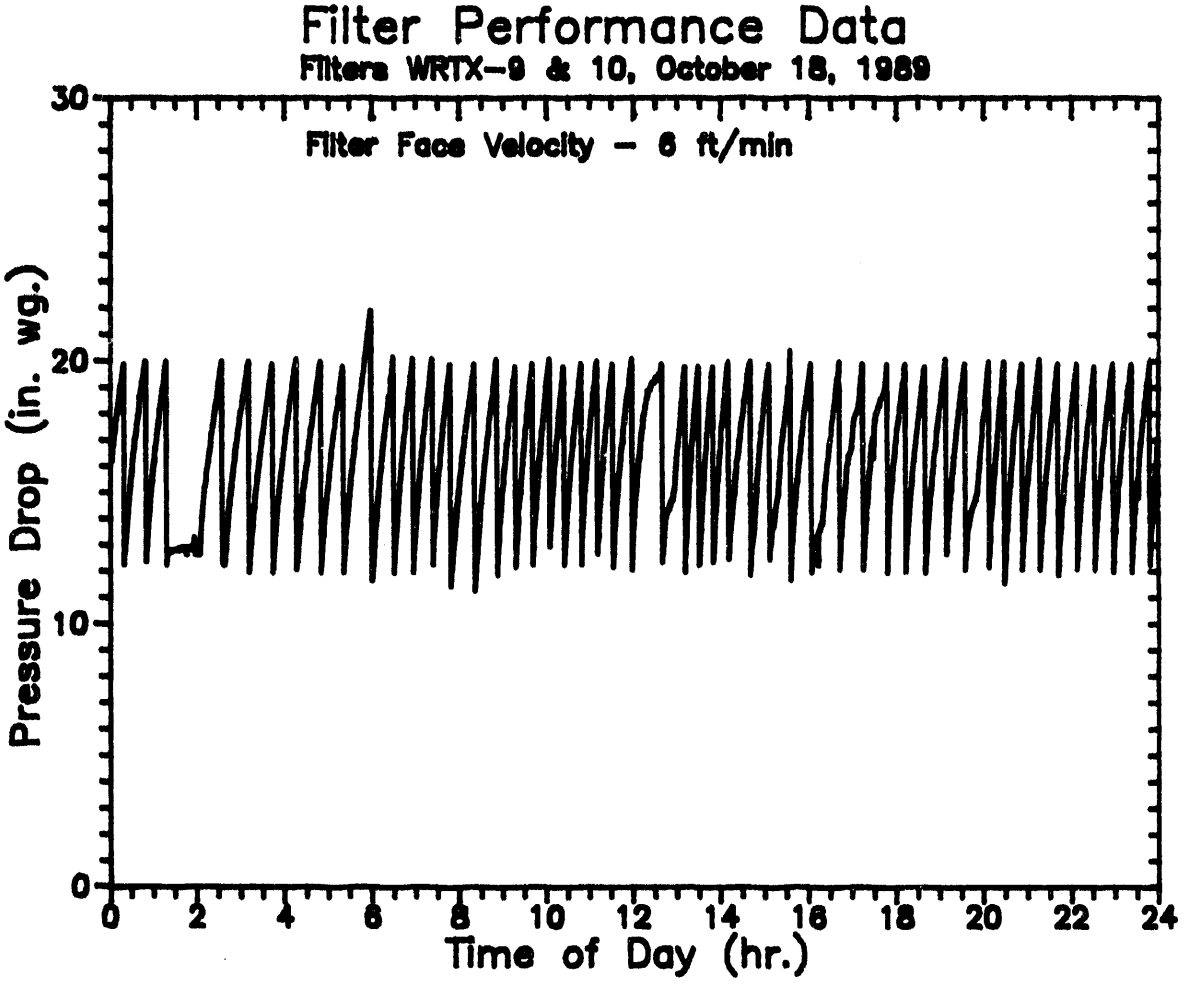

Operation Notes for October 18, 1989:

ΔP Trigger = 20.0" WC
Pulse Cleaning - 280 psig/0.1 sec until 0749
290 psig/0.1 sec
Then dust off, dust added to the vessel @ 0119.
Dust on - 0207
1242 erratic dust feed

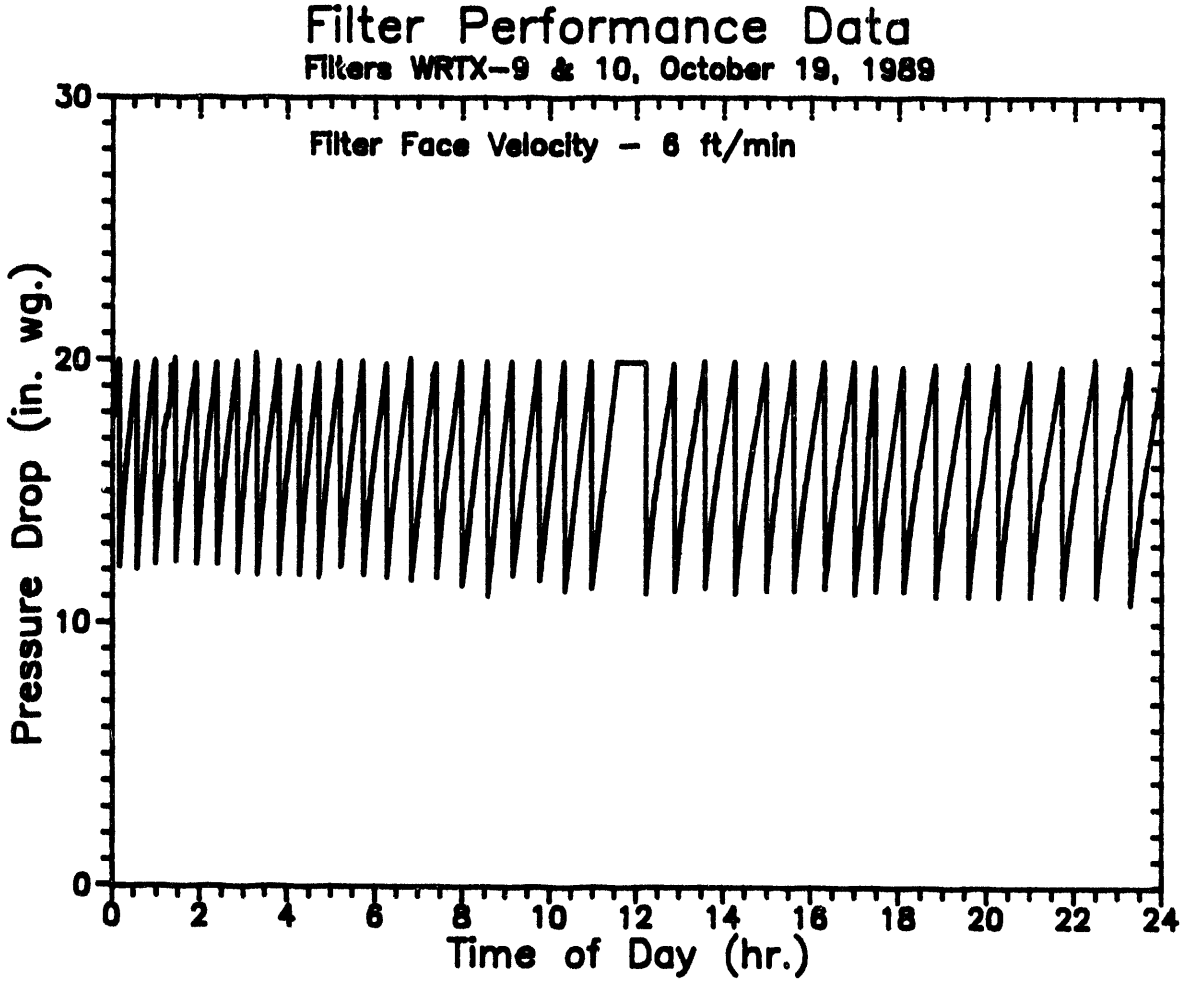

Operation Notes for October 19, 1989:
ΔP Trigger = 20.0" WC
Pulse Cleaning - 290 psig/0.1 sec

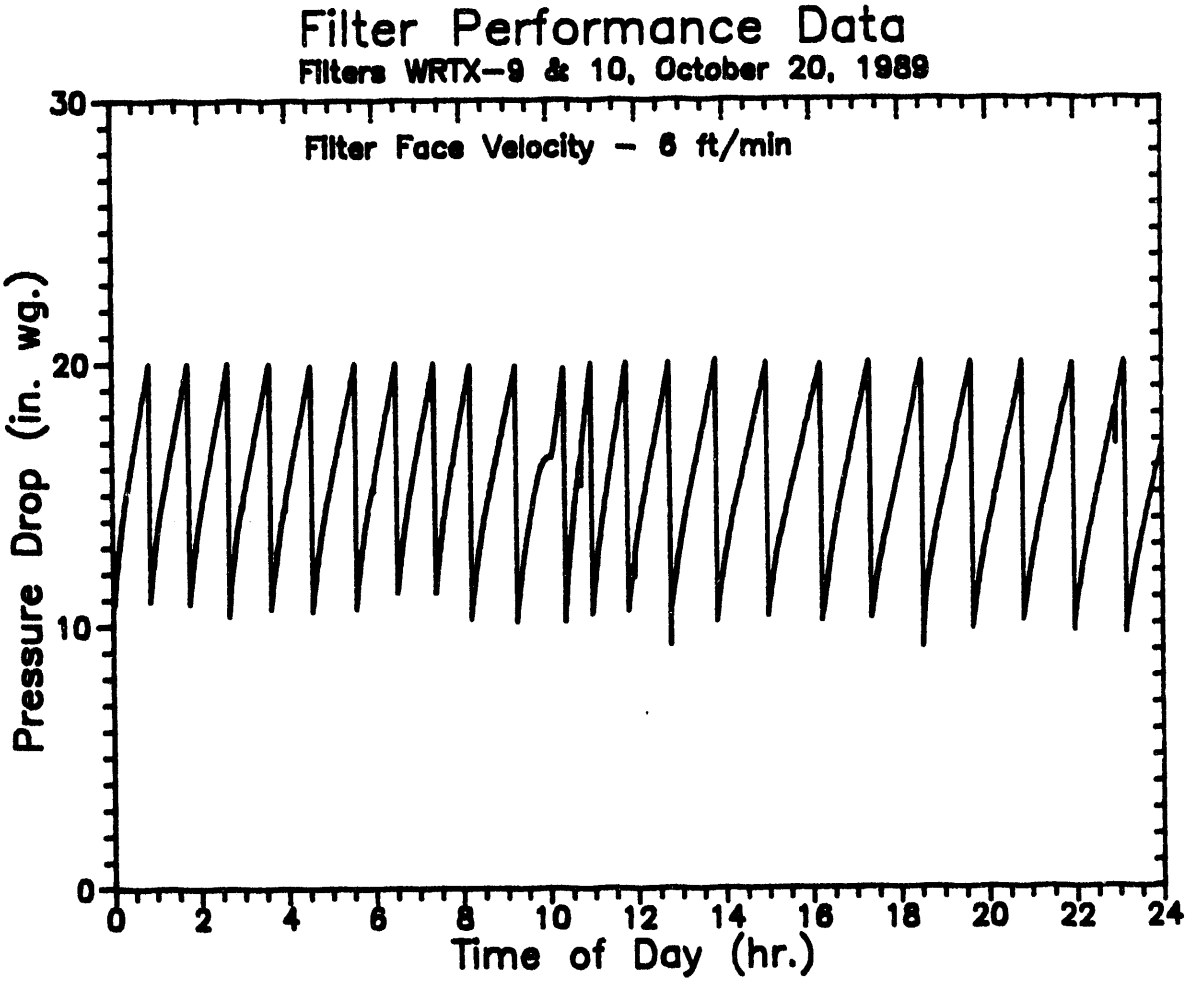

Operation Notes for October 20, 1989:
ΔP Trigger = 20.0" WC
Pulse Cleaning - 290 psig/0.1 sec

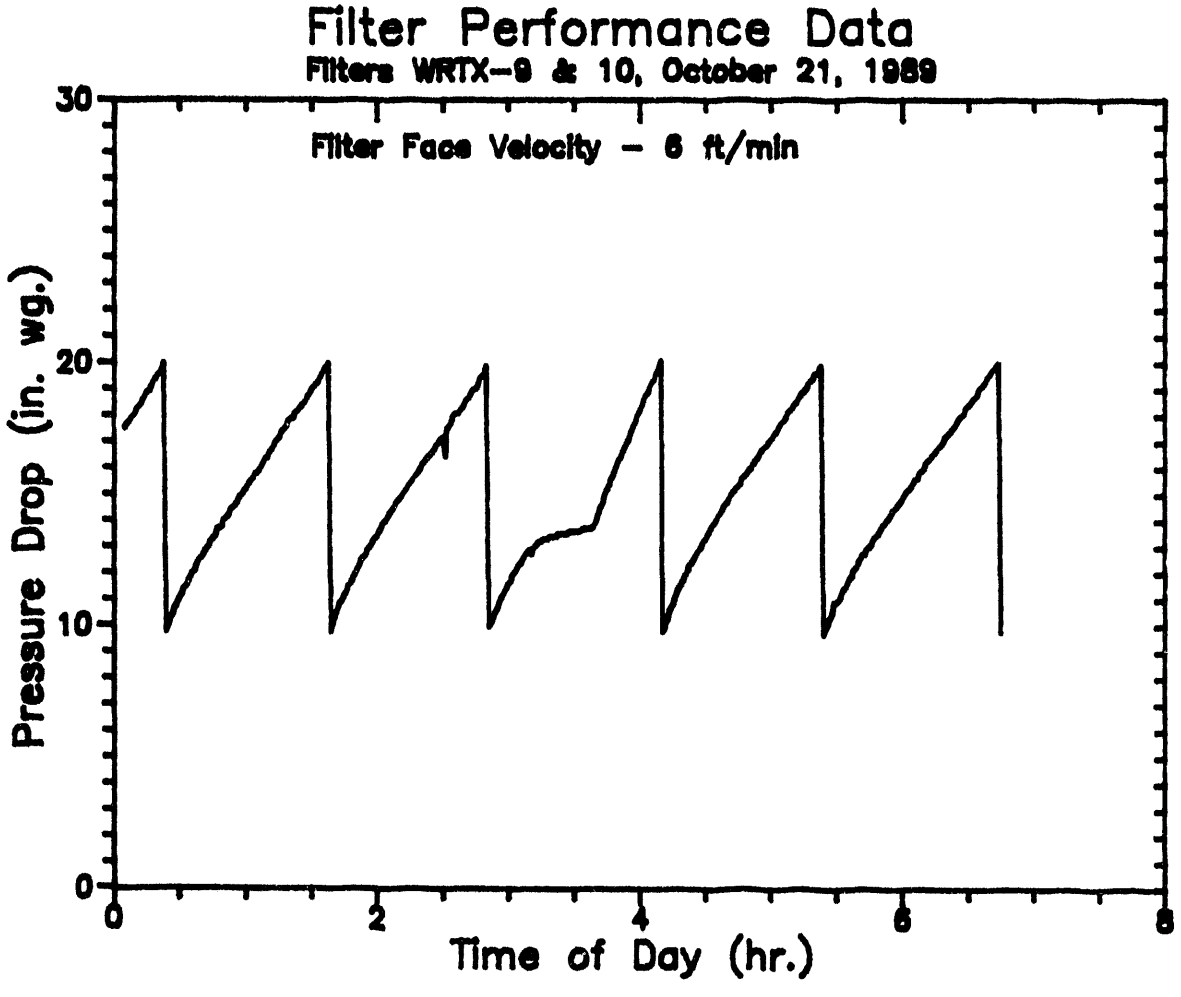

Operation Notes for October 21, 1989:
End week long test
Scheduled shutdown
ΔP Trigger = 20.0" WC
Pulse Cleaning - 290 psig/0.1 sec

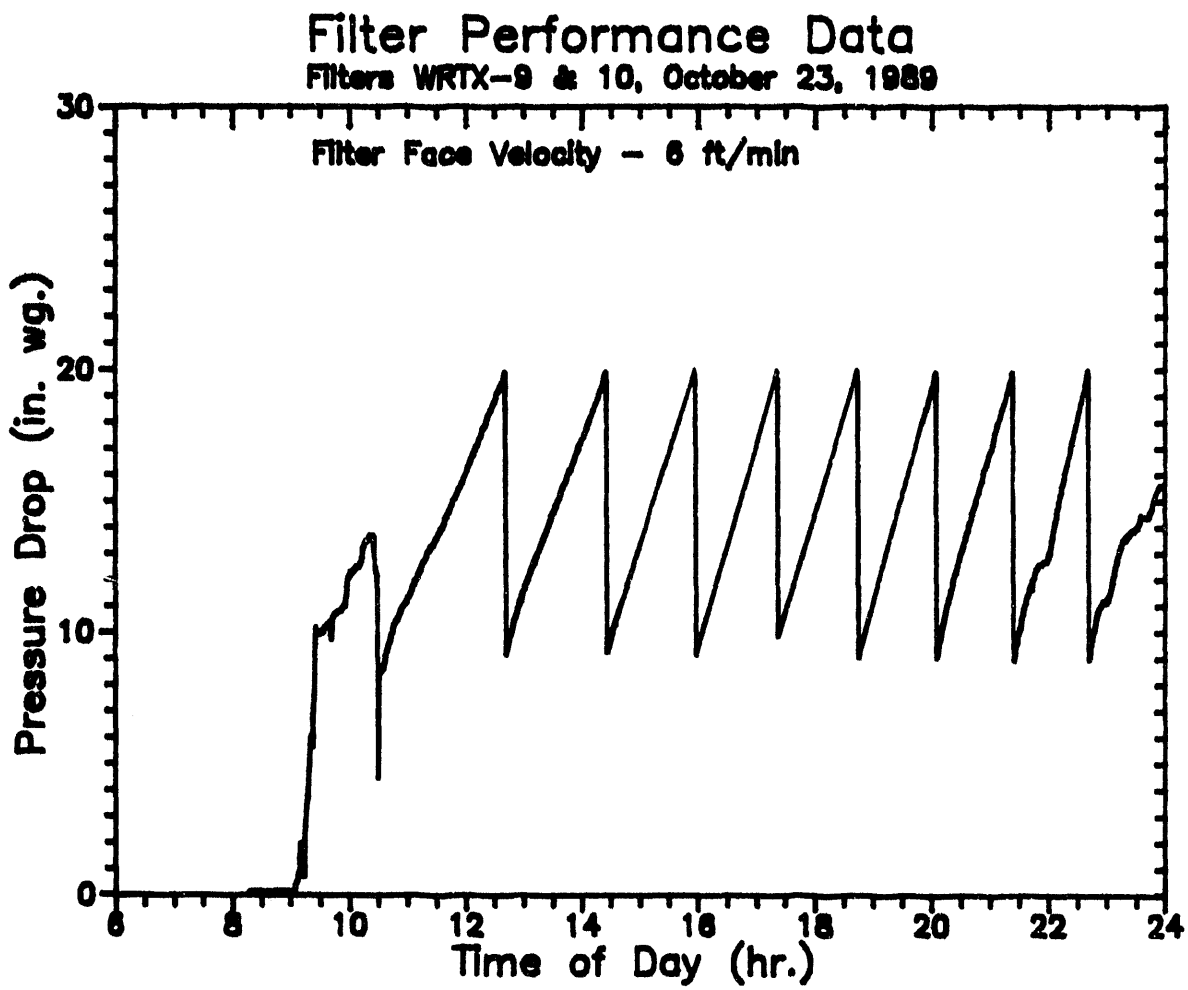

Operation Notes for October 23, 1989:

Begin week long test
Startup
ΔP Trigger = 20.0" WC
Pulse Cleaning - 290 psig/0.1 sec

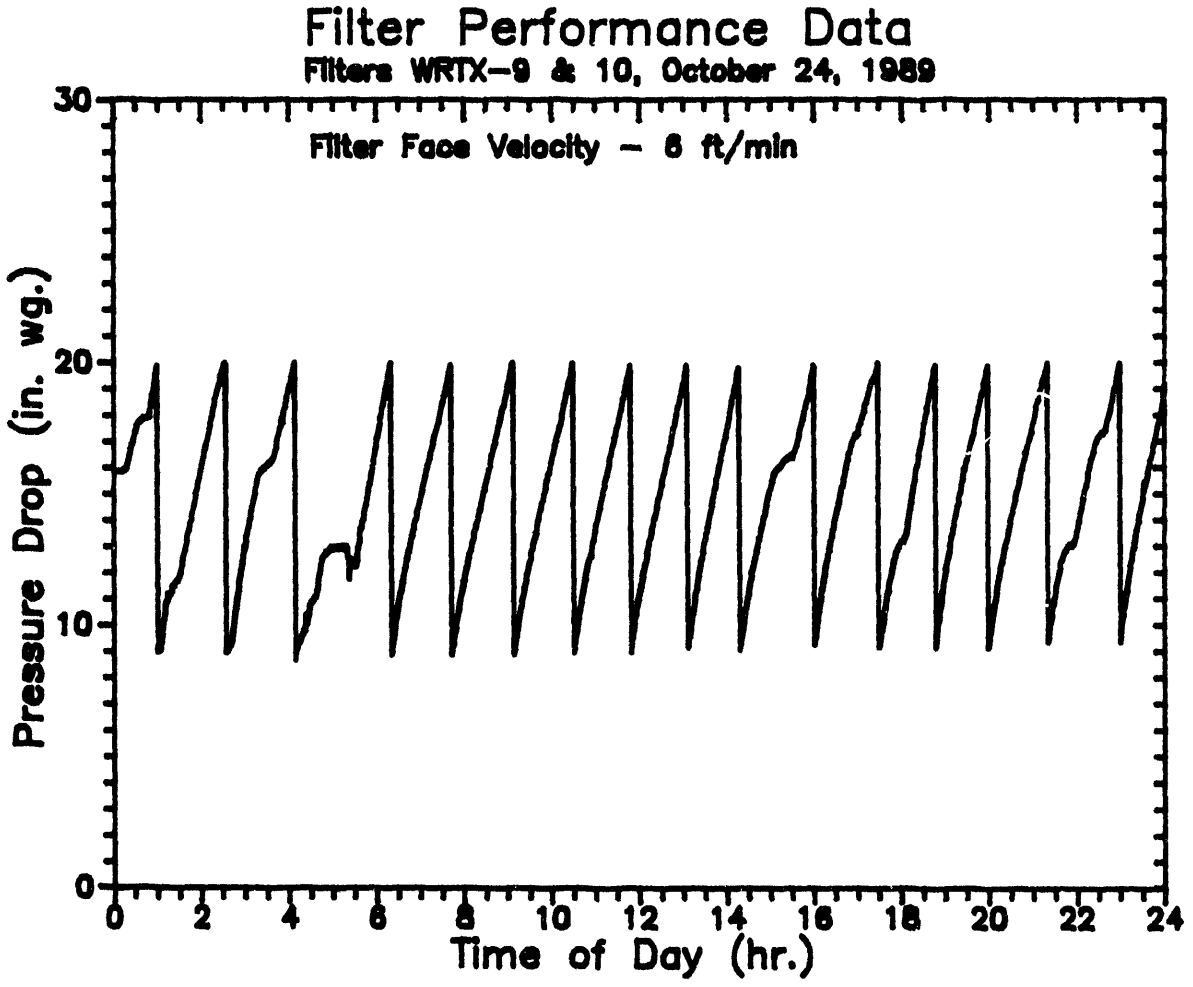

Operation Notes for October 24, 1989:

ΔP Trigger = 20.0" WC
Pulse Cleaning - 280 psig/0.1 sec
Erratic dust feed:
0001→0059
0400→0530
2140→2230

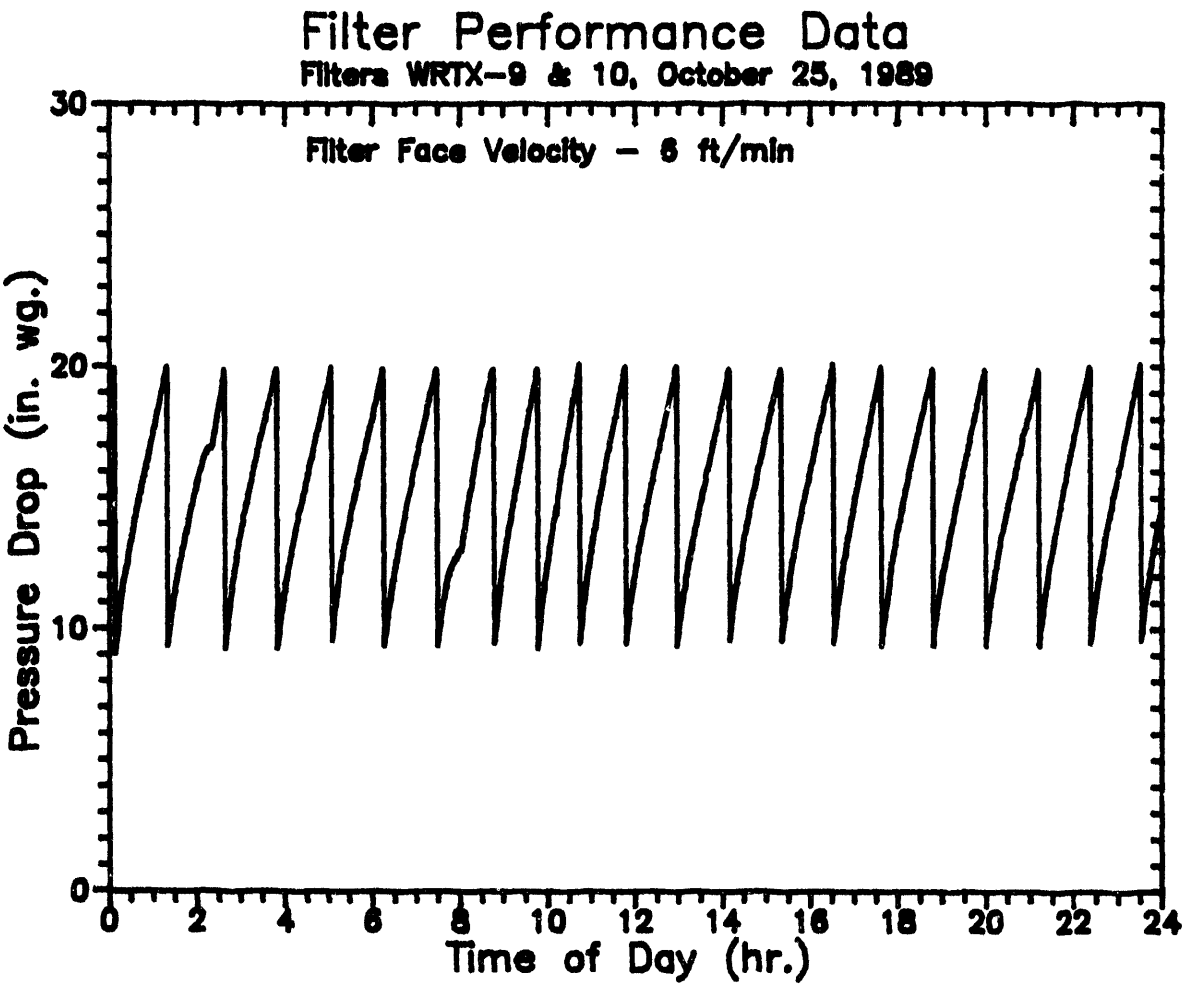

Operation Notes for October 25, 1989:
ΔP Trigger = 20.0" WC
Pulse Cleaning - 290 psig/0.1 sec

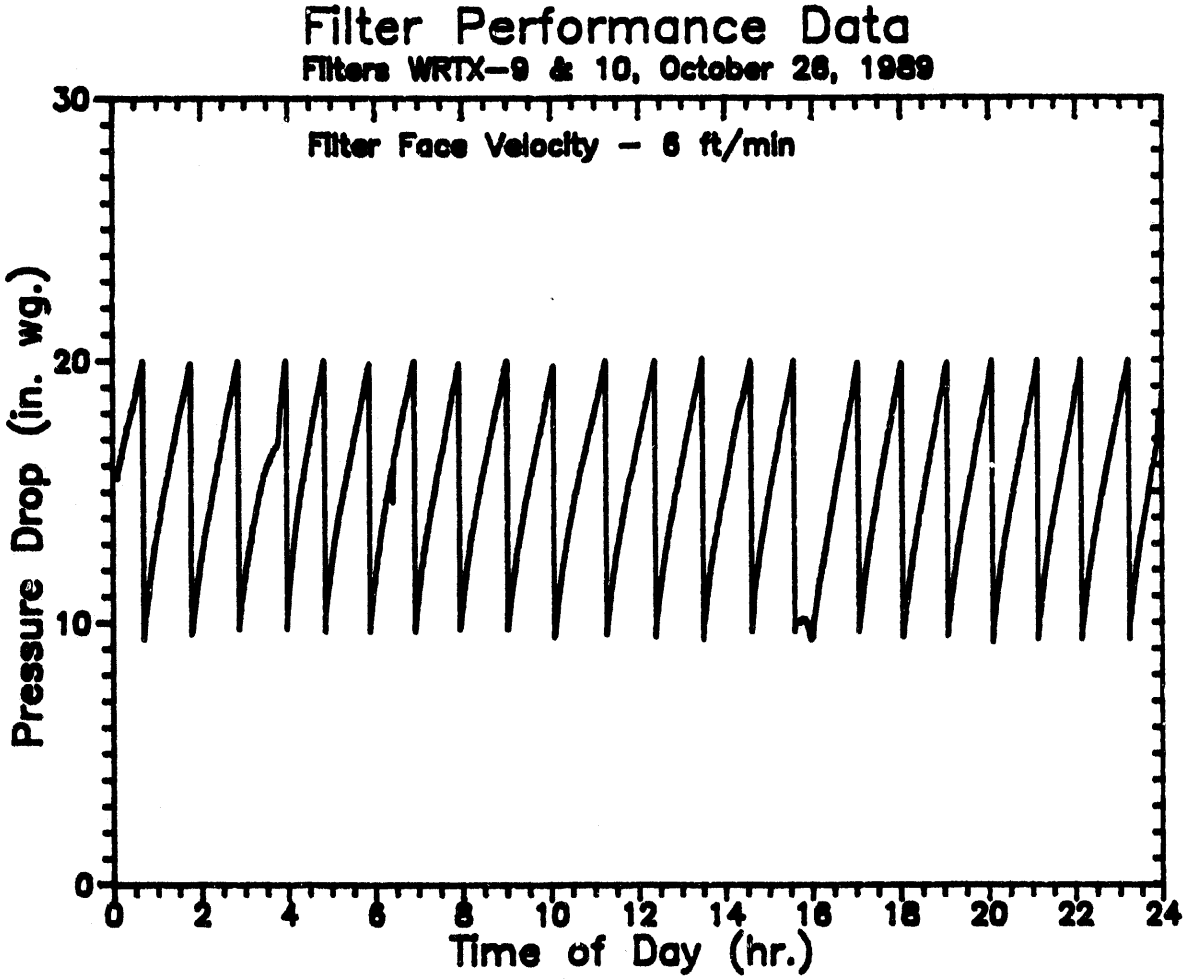

Operation Notes for October 26, 1989:

ΔP Trigger = 20.0" WC
Pulse Cleaning - 290 psig/0.1 sec
1536 - dust feed off
Dust added to dust vessel
1605 - dust feed on

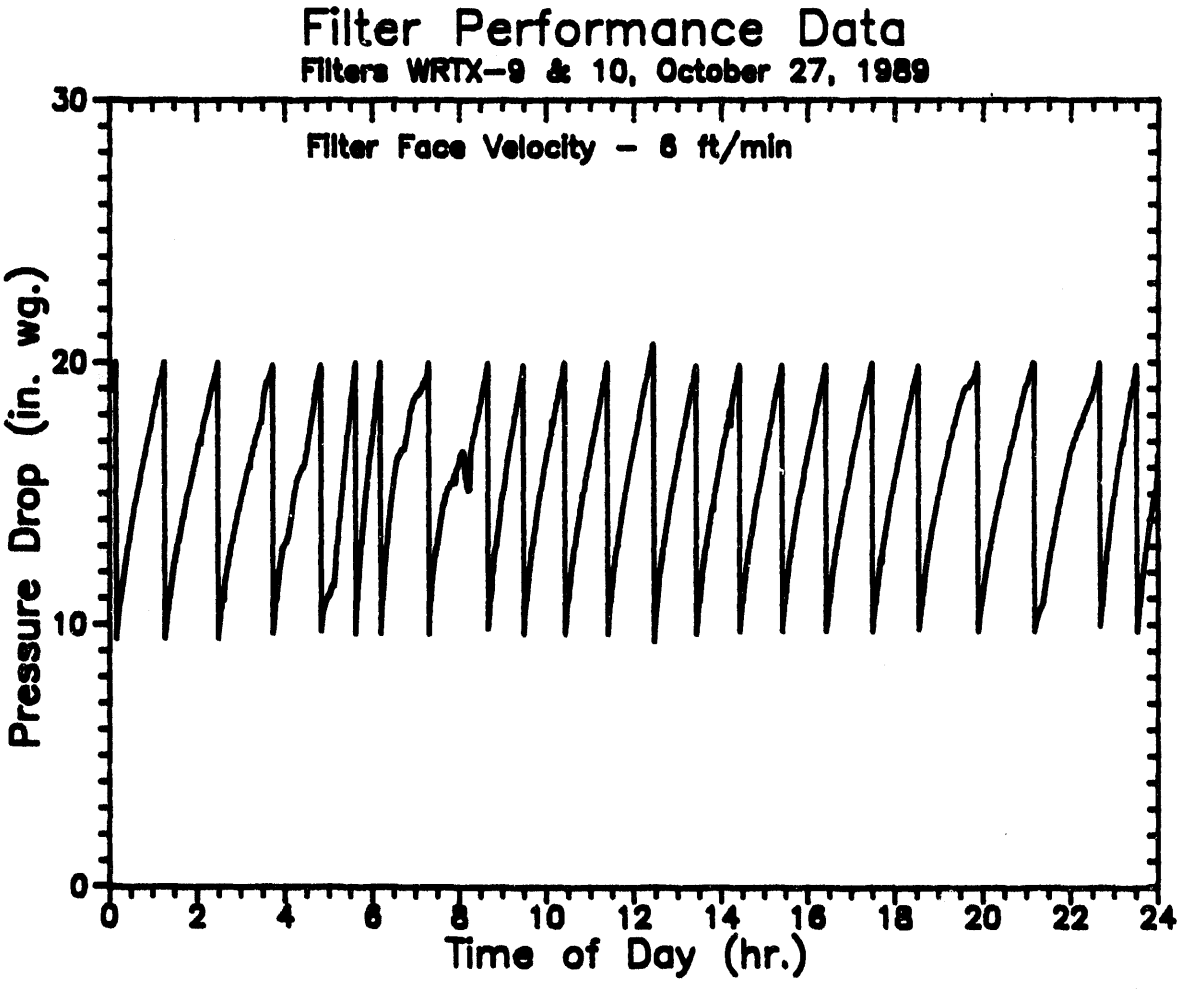

Operation Notes for October 27, 1989:

ΔP Trigger = 20.0" WC
Pulse Cleaning - 290 psig/0.1 sec
0537→0800
Erratic dust feed, unable to correct online
Dust off. Dust vessel depressurized, dust stirred.
Repressurized. Dust on @ 0816

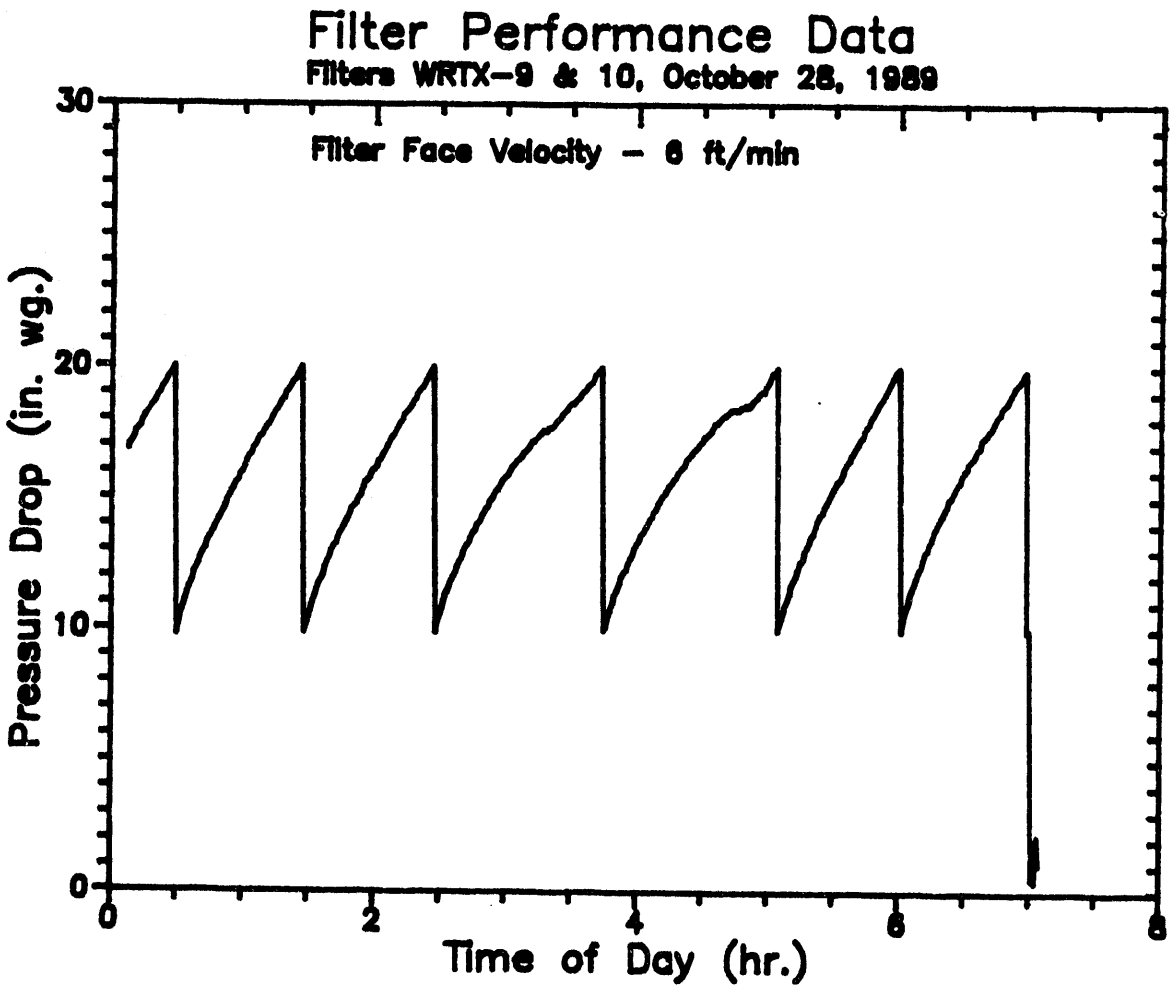

Operation Notes for October 28, 1989:

End week long test
Scheduled shutdown
ΔP Trigger = 20.0" WC
Pulse Cleaning - 290 psig/0.1 sec

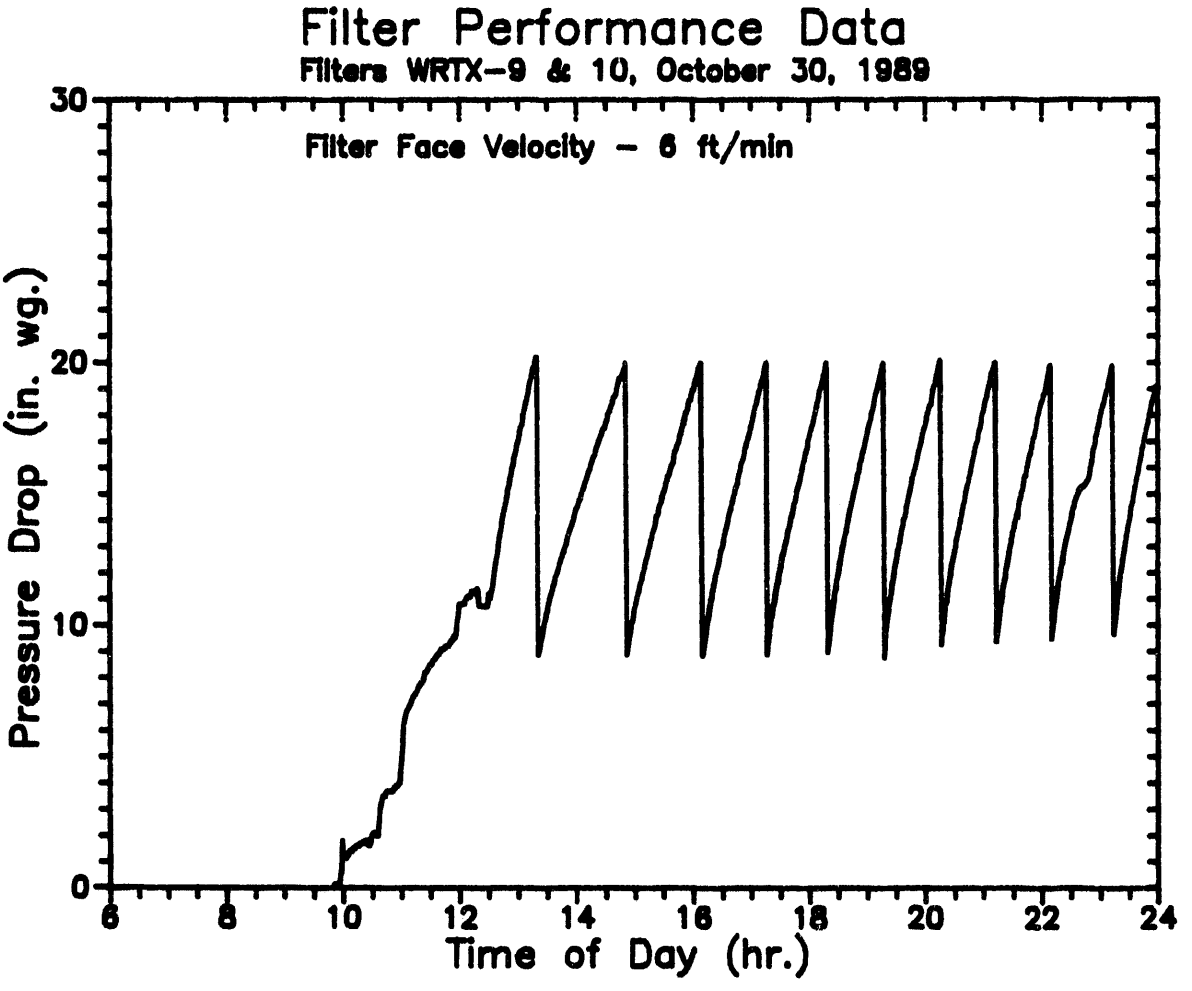

Operation Notes for October 30, 1989:

Start week long test
Startup
ΔP Trigger = 20.0" WC
Pulse Cleaning - 290 psig/0.1 sec

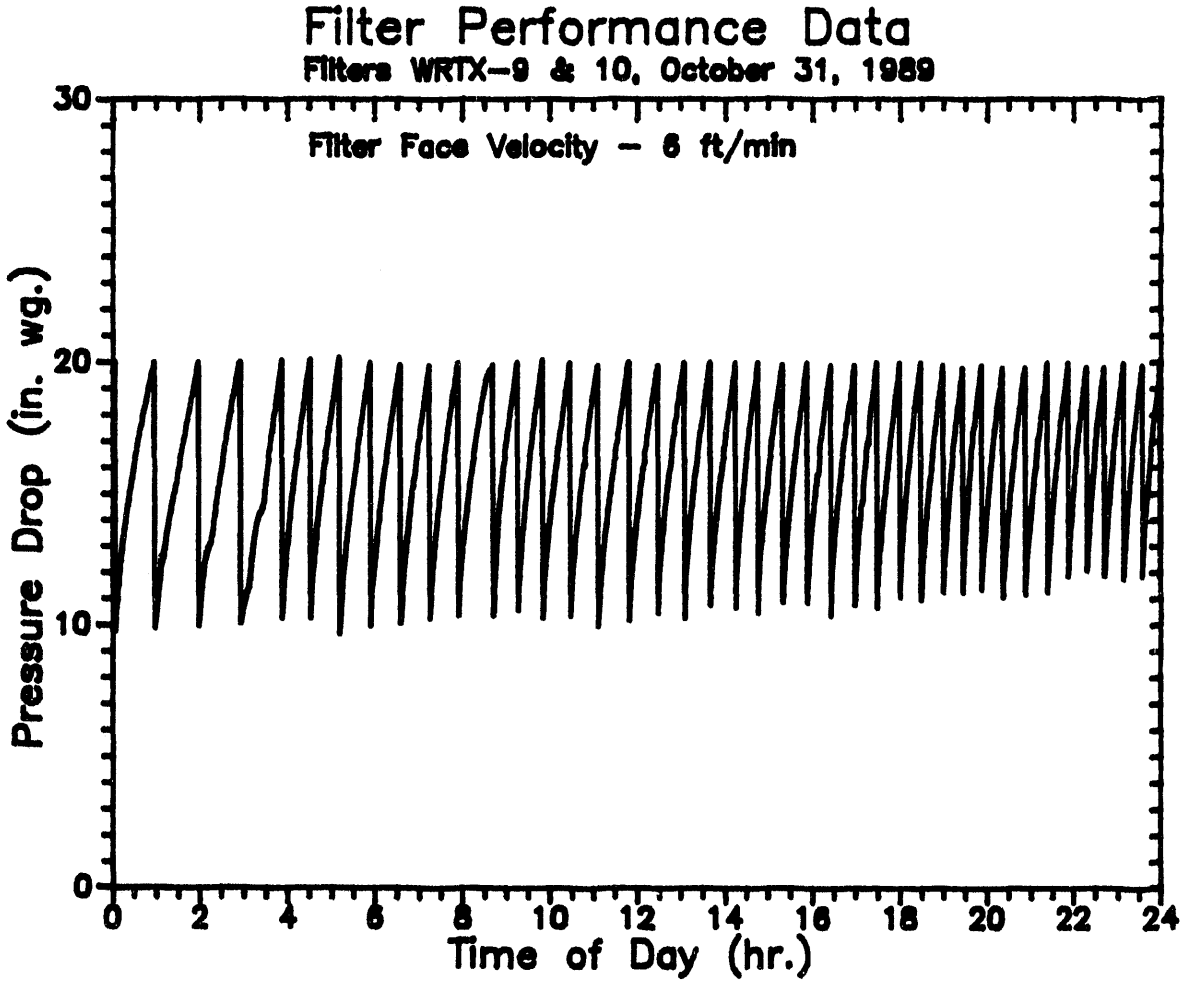

Operation Notes for October 31, 1989:
ΔP Trigger = 20.0" WC
Pulse Cleaning - 290 psig/0.1 sec

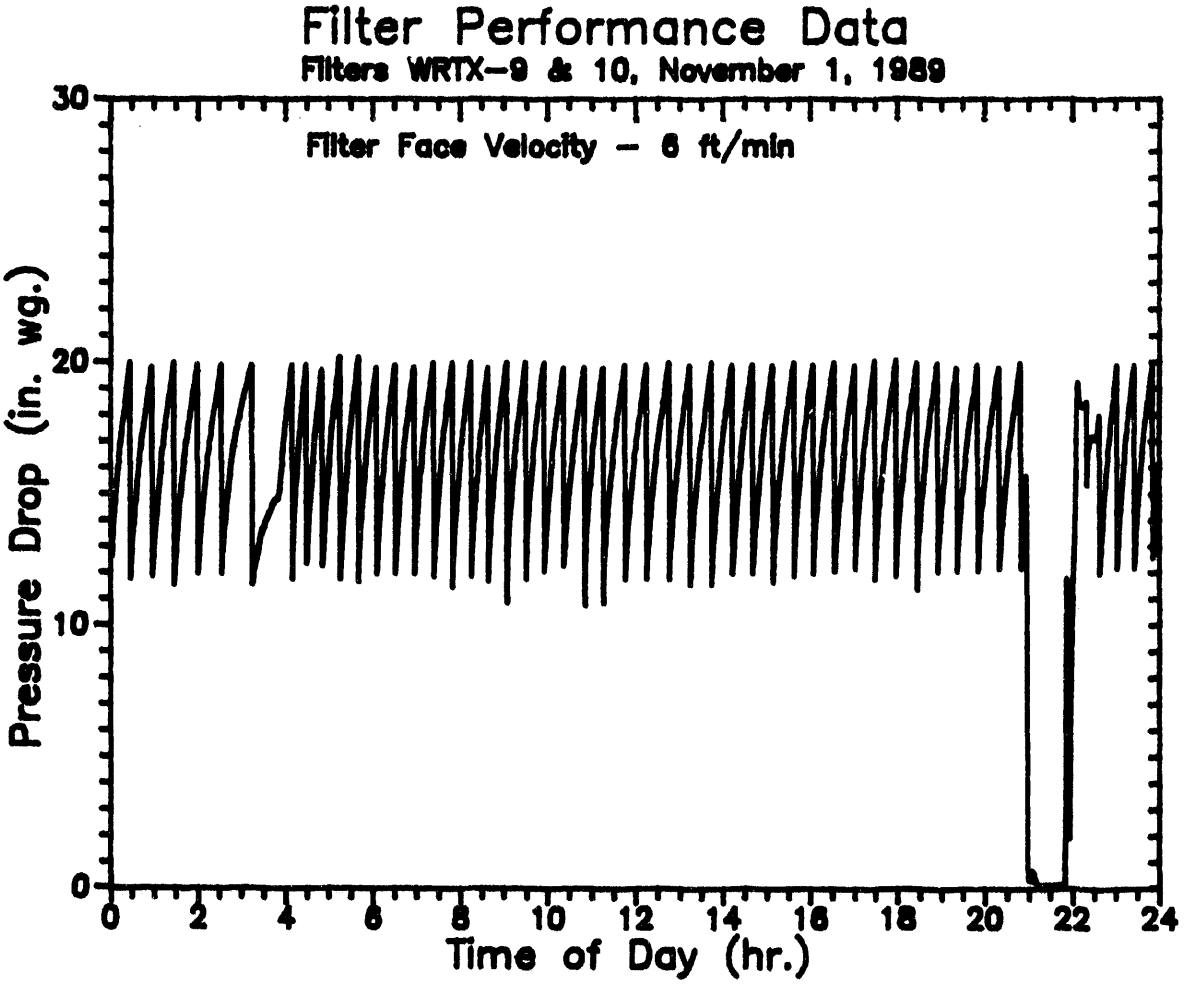

Operation Notes for November 1, 1989:

ΔP Trigger = 20.0" WC
Pulse Cleaning - 290 psig/0.1 sec
Unscheduled shutdown 2057
Compressor shutdown due to low recirculating water pressure.
Problem corrected.
Restart - 2153

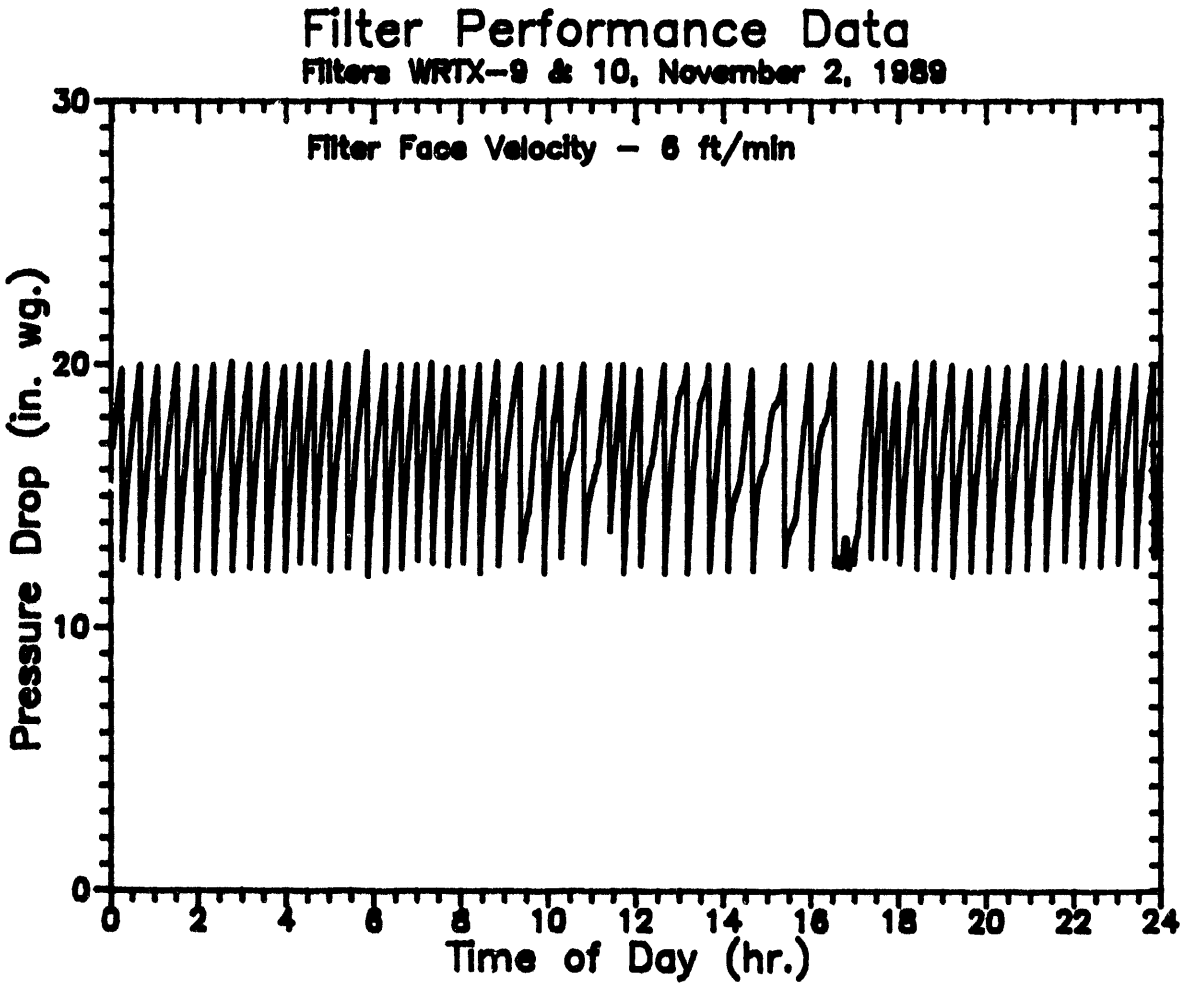

Operation Notes for November 2, 1989:

ΔP Trigger = 20.0" WC
Pulse Cleaning - 290 psig/0.1 sec
Erratic dust feed
1634 - dust off, vessel depressurized, dust stirred for even feeding
1705 dust on

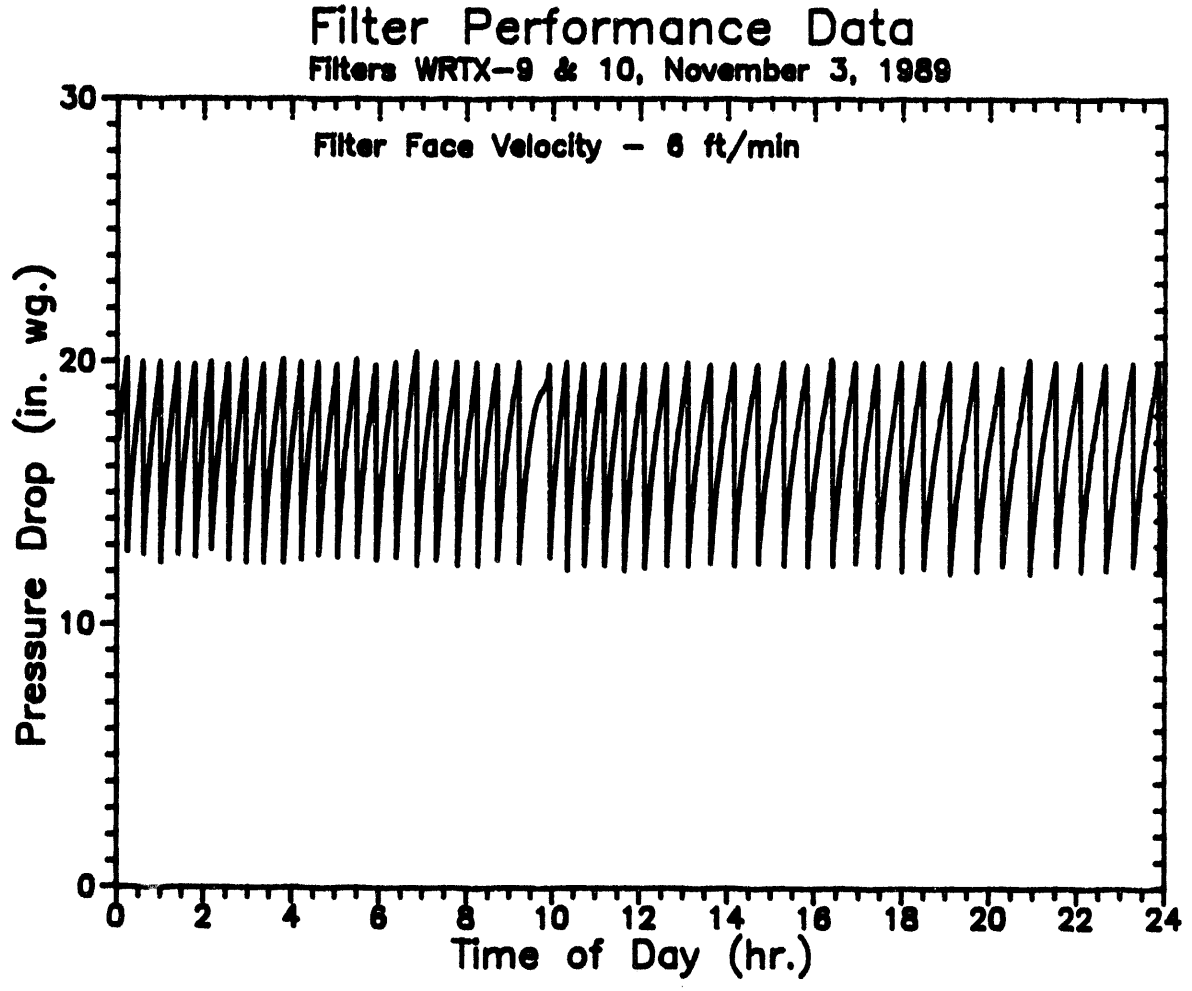

Operation Notes for November 3, 1989:
ΔP Trigger = 20.0" WC
Pulse Cleaning - 290 psig/0.1 sec

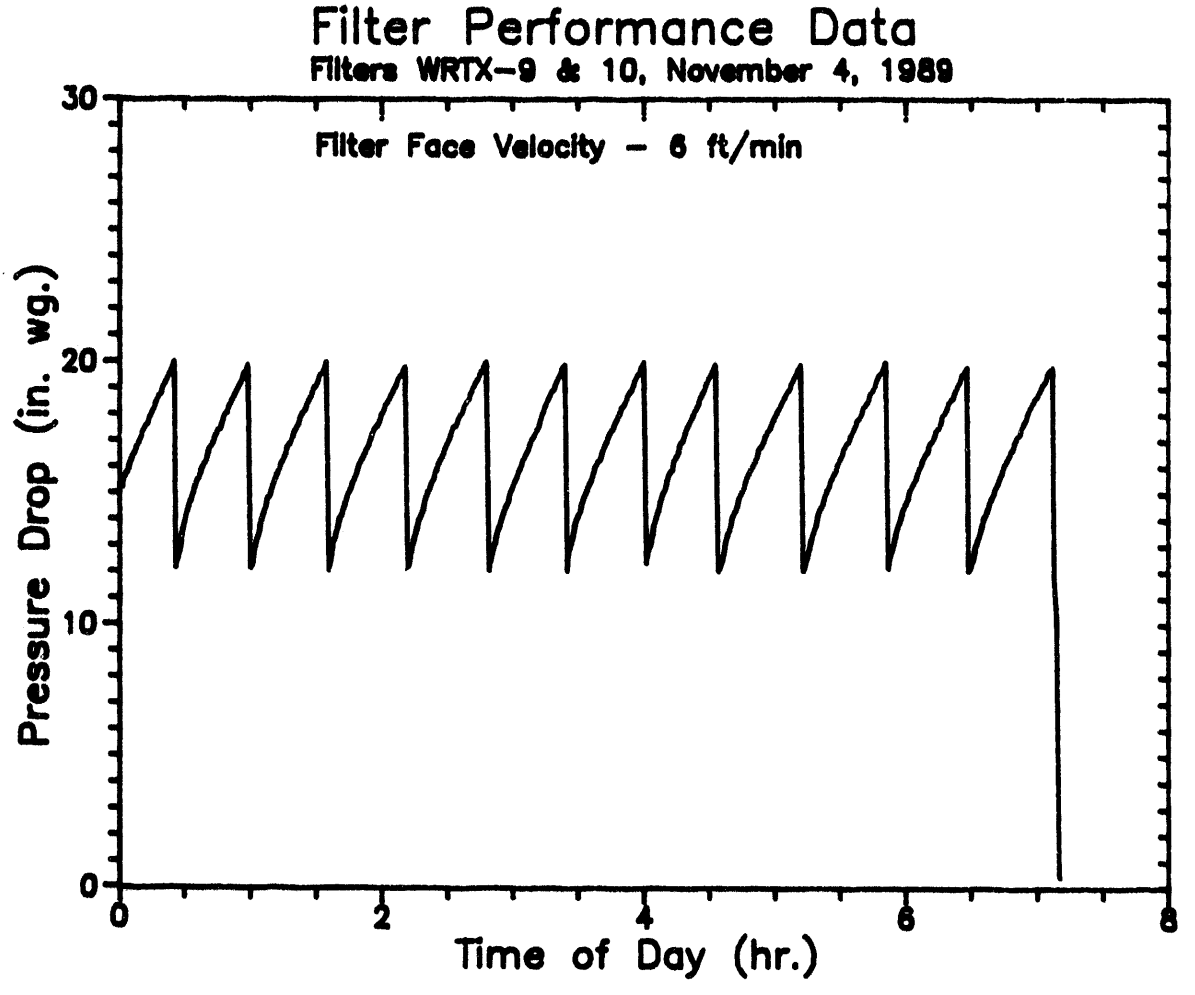

Operation Notes for November 4, 1989:
End of week long test
Scheduled shutdown
ΔP Trigger = 20.0" WC
Pulse Cleaning - 290 psig/0.1 sec

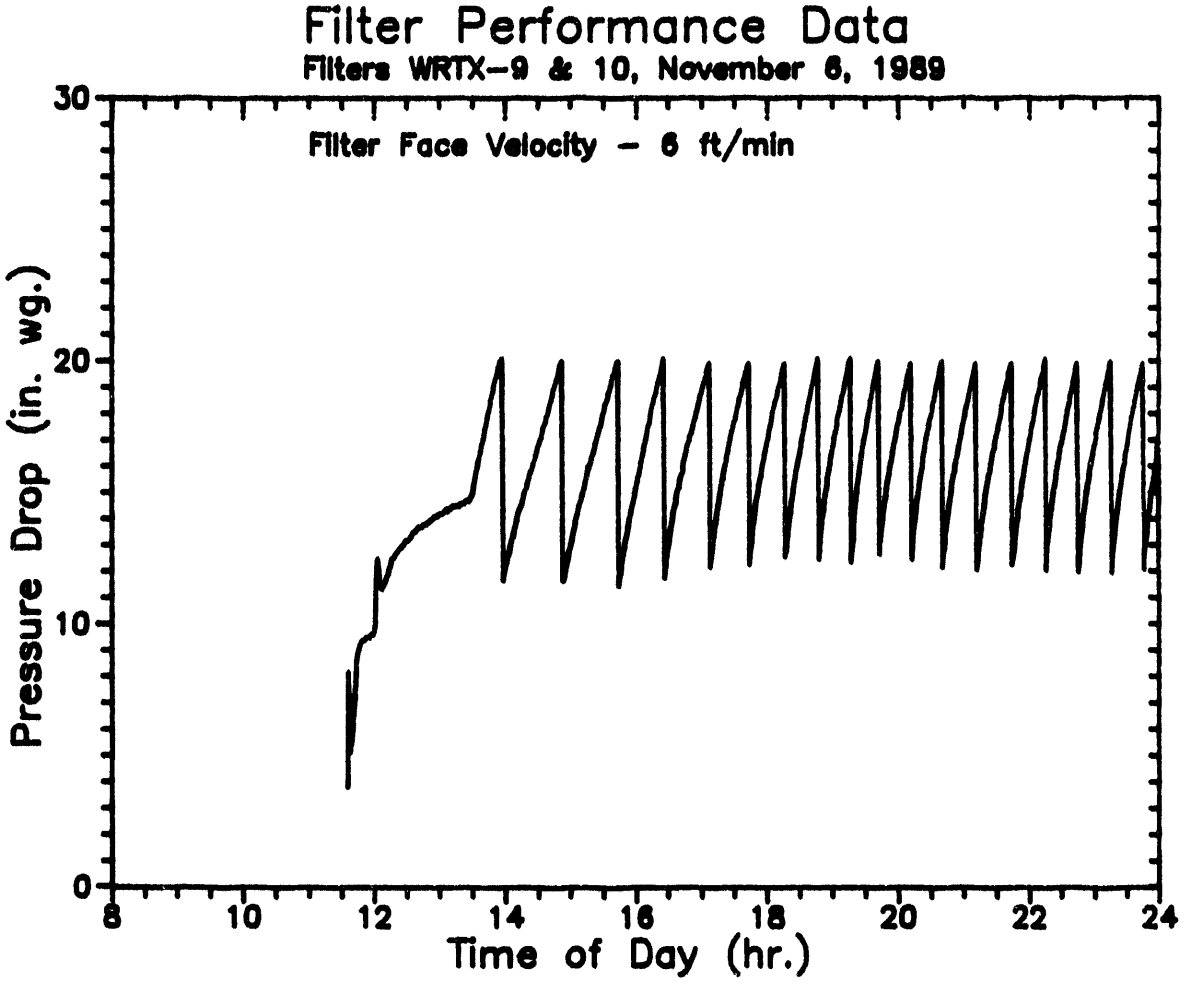

Operation Notes for November 6, 1989:

Start week long test
Startup
ΔP Trigger = 20.0" WC
Pulse Cleaning - 290 psig/0.1 sec

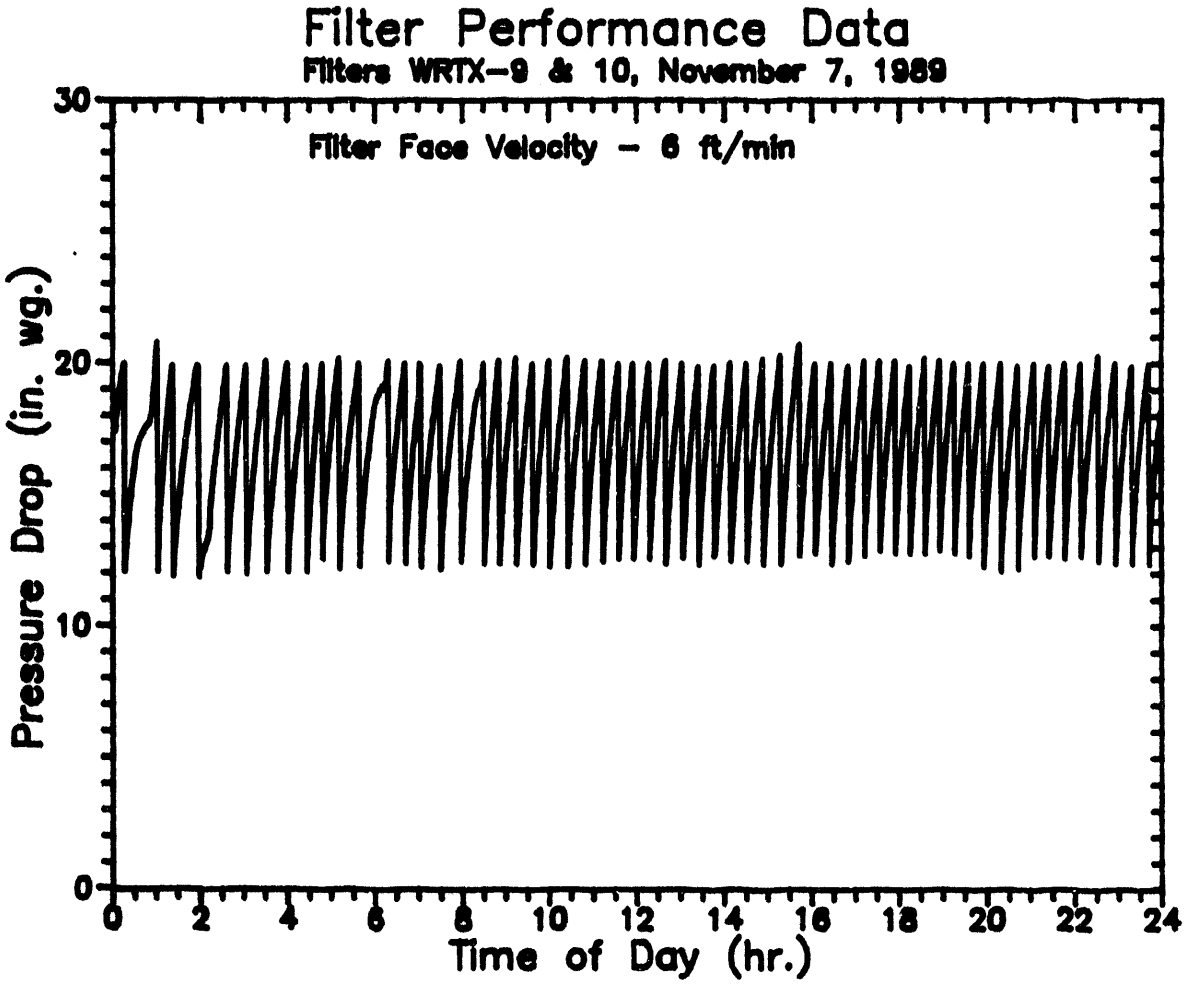

Operation Notes for November 7, 1989:
ΔP Trigger = 20.0" WC
Pulse Cleaning - 290 psig/0.1 sec

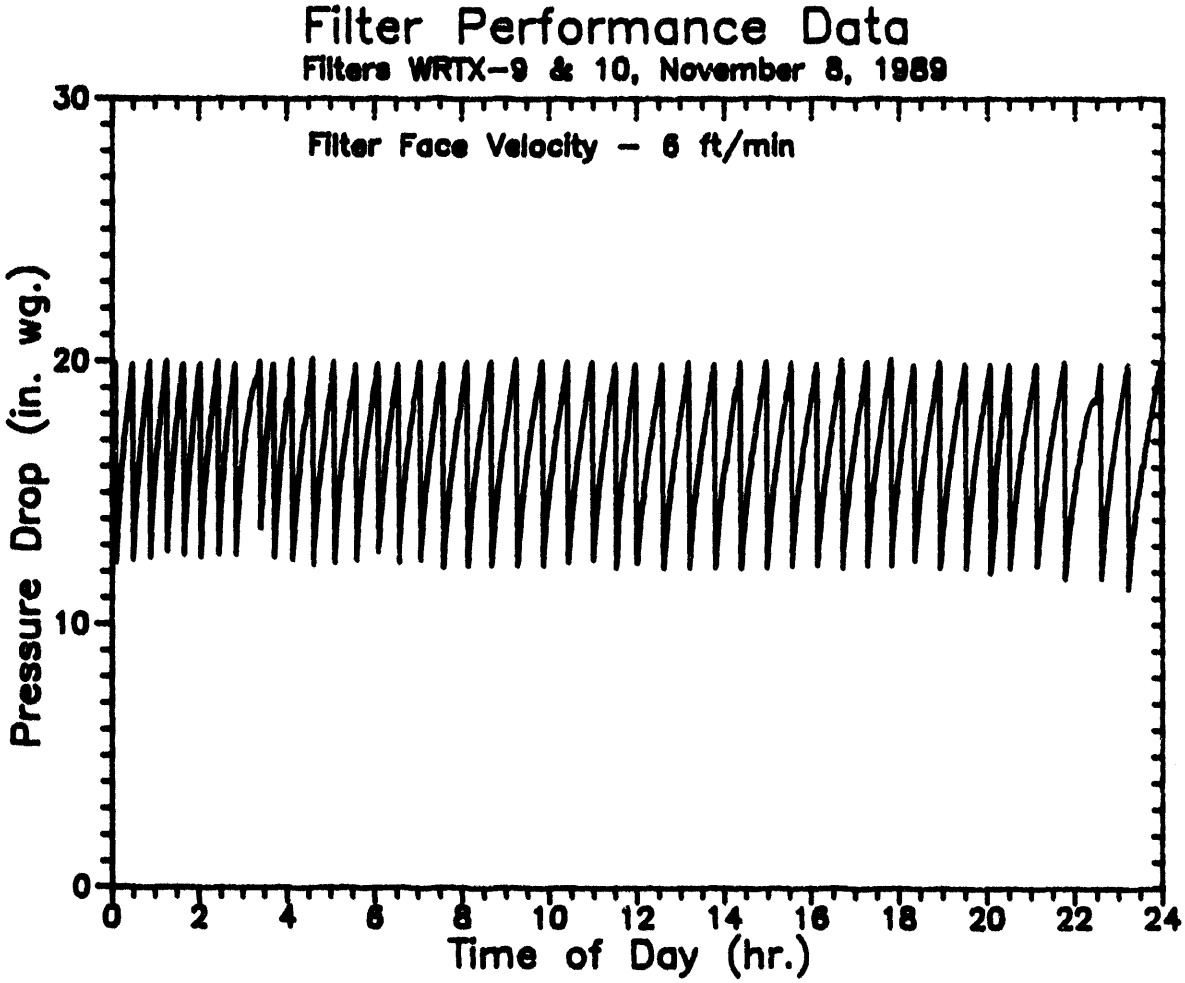

Operation Notes for November 8, 1989:
ΔP Trigger = 20.0" WC
Pulse Cleaning - 290 psig/0.1 sec

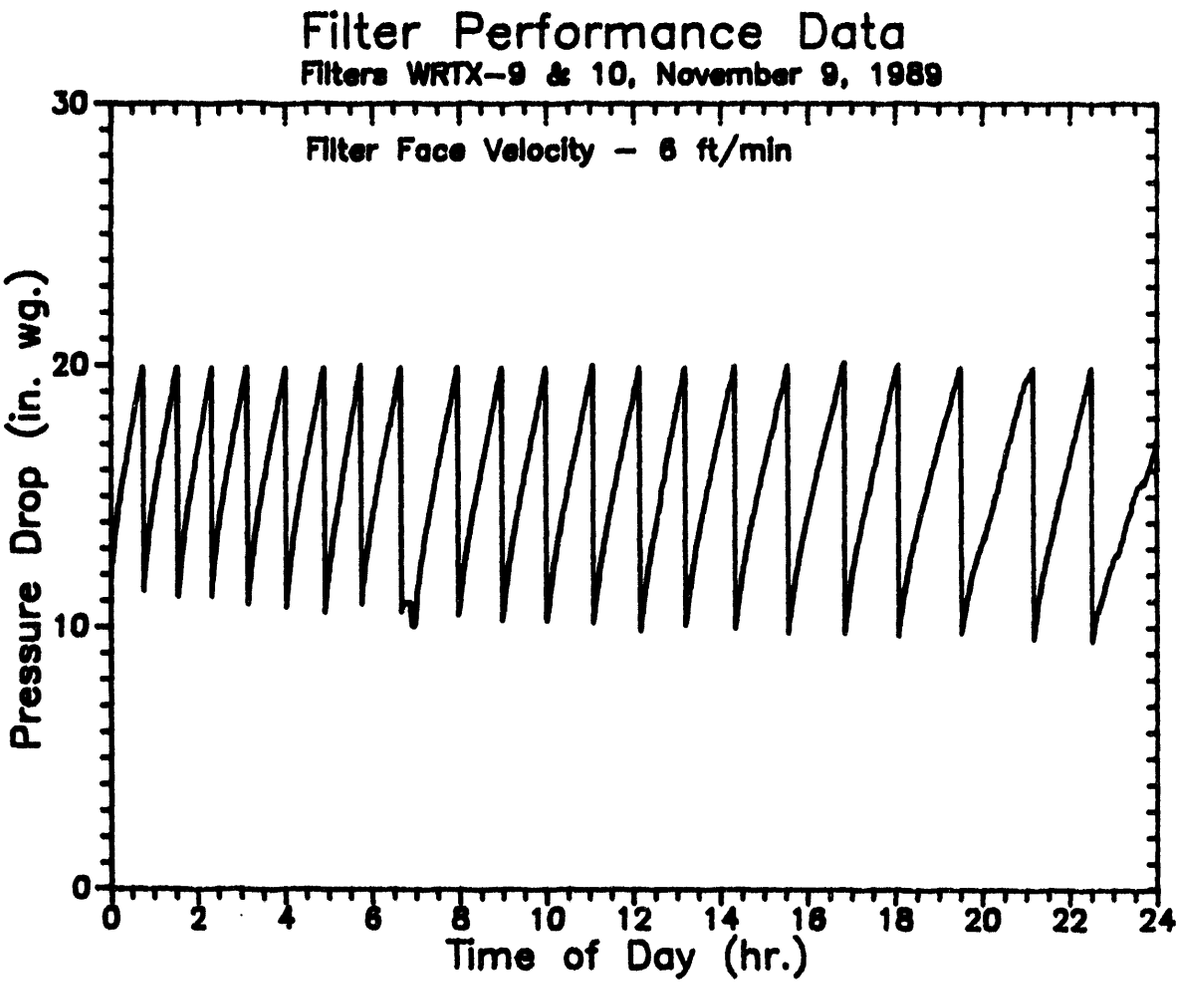

Operation Notes for November 9, 1989:

ΔP Trigger = 20.0" WC
Pulse Cleaning - 290 psig/0.1 sec
0639 dust off
Vessel depressurized; dust added to vessel
Repressurized
0702 dust on

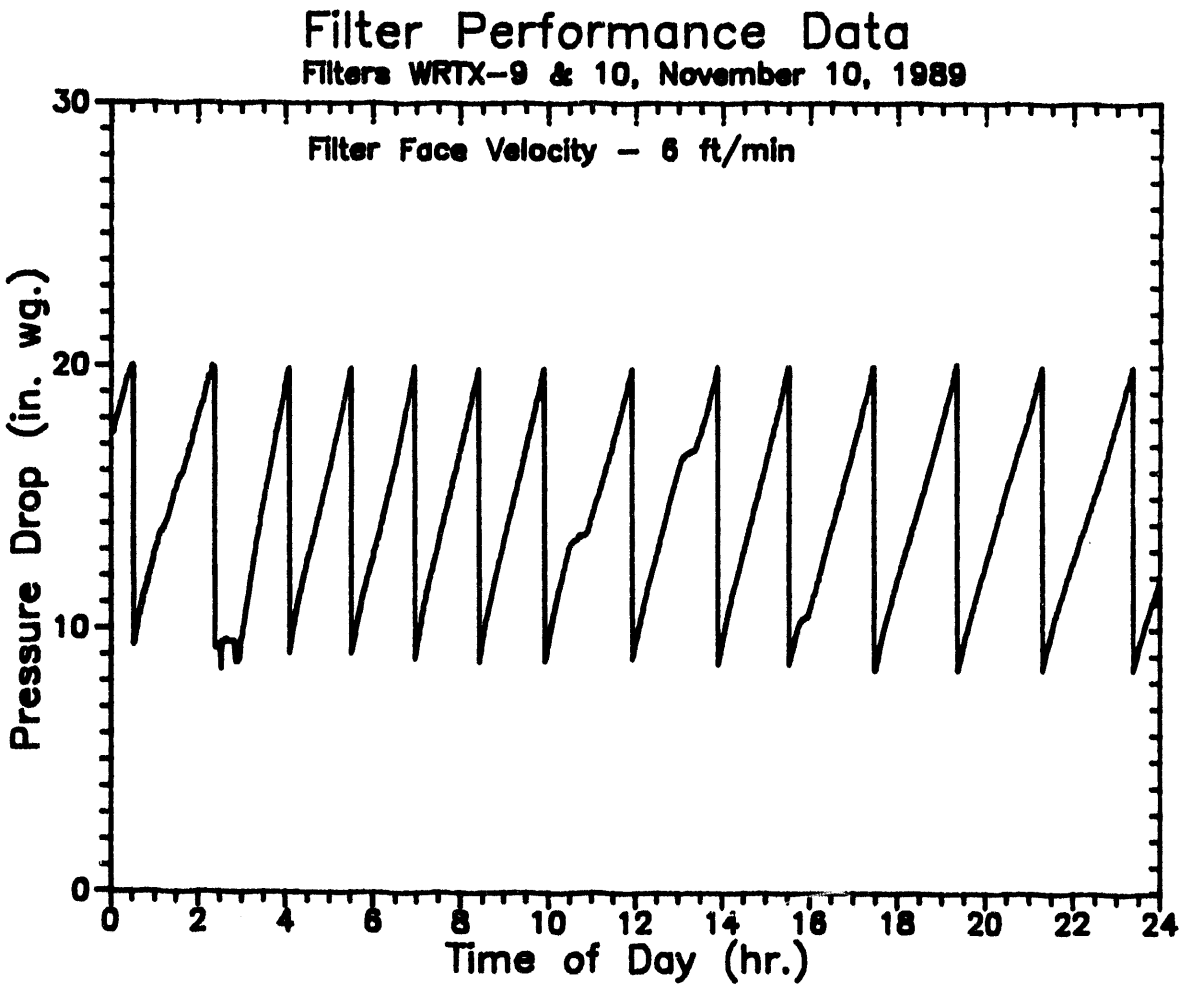

Operation Notes for November 10, 1989:

ΔP Trigger = 20.0" WC
Pulse Cleaning - 290 psig/0.1 sec
0227 - dust off
Depressurized vessel, dust stirred & added
0300 - dust on
1055 - erratic dust feed - corrected

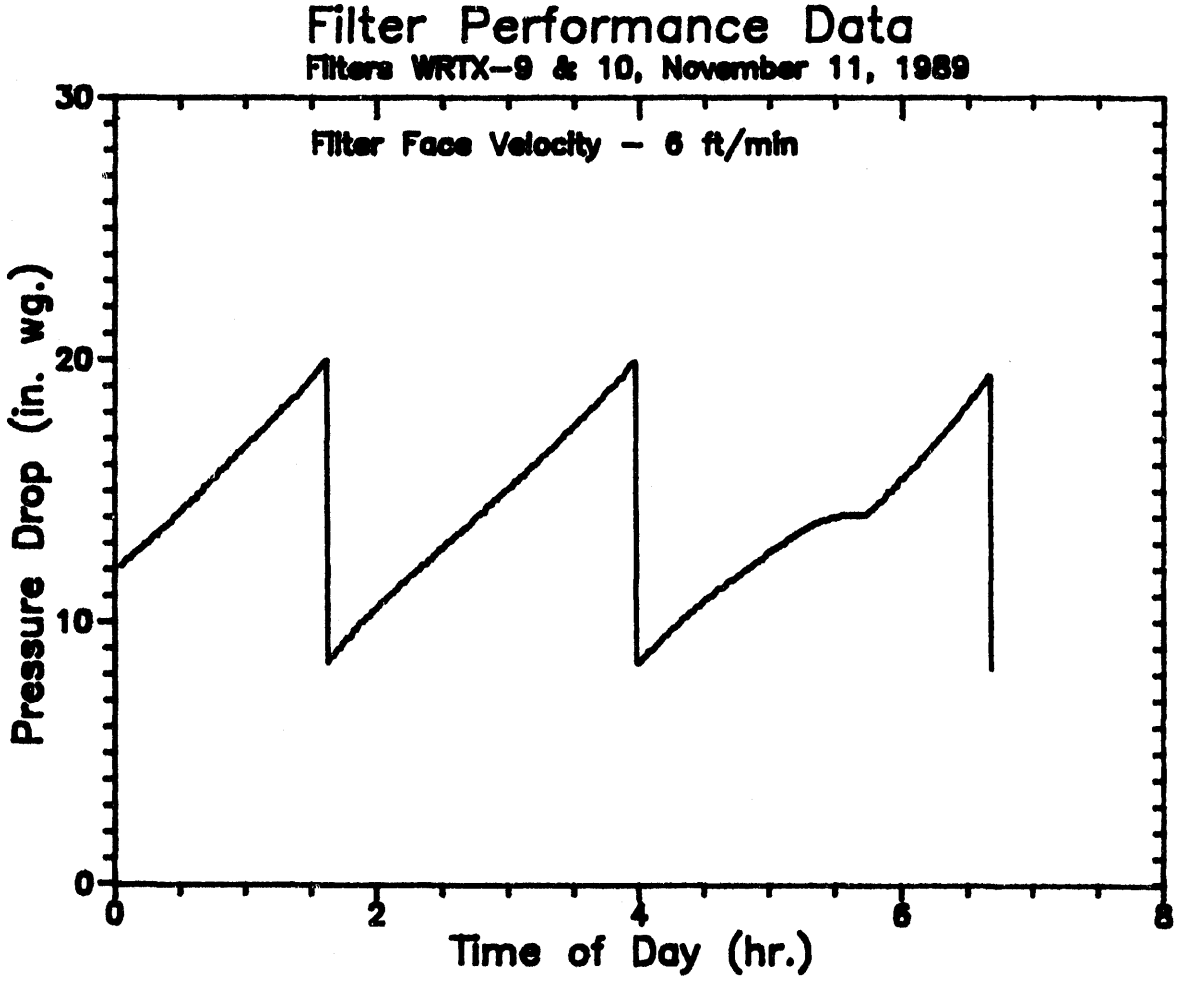

Operation Notes for November 11, 1989:

End week long test
Scheduled shutdown
ΔP Trigger = 20.0" WC
Pulse Cleaning - 290 psig/0.1 sec

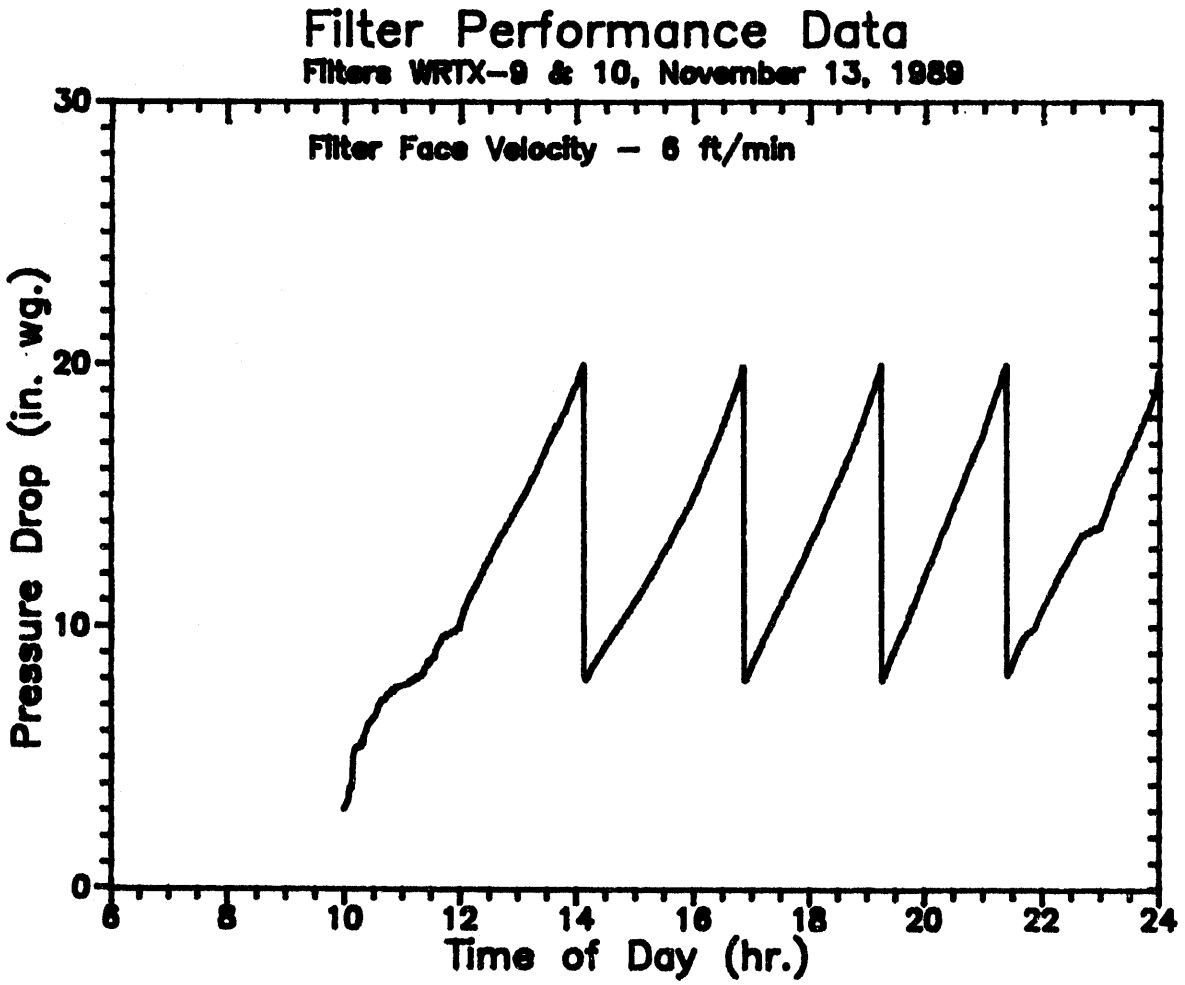

Operation Notes for November 13, 1989:

Begin week long test
Startup
ΔP Trigger = 20.0" WC
Pulse Cleaning - 290 psig/0.1 sec

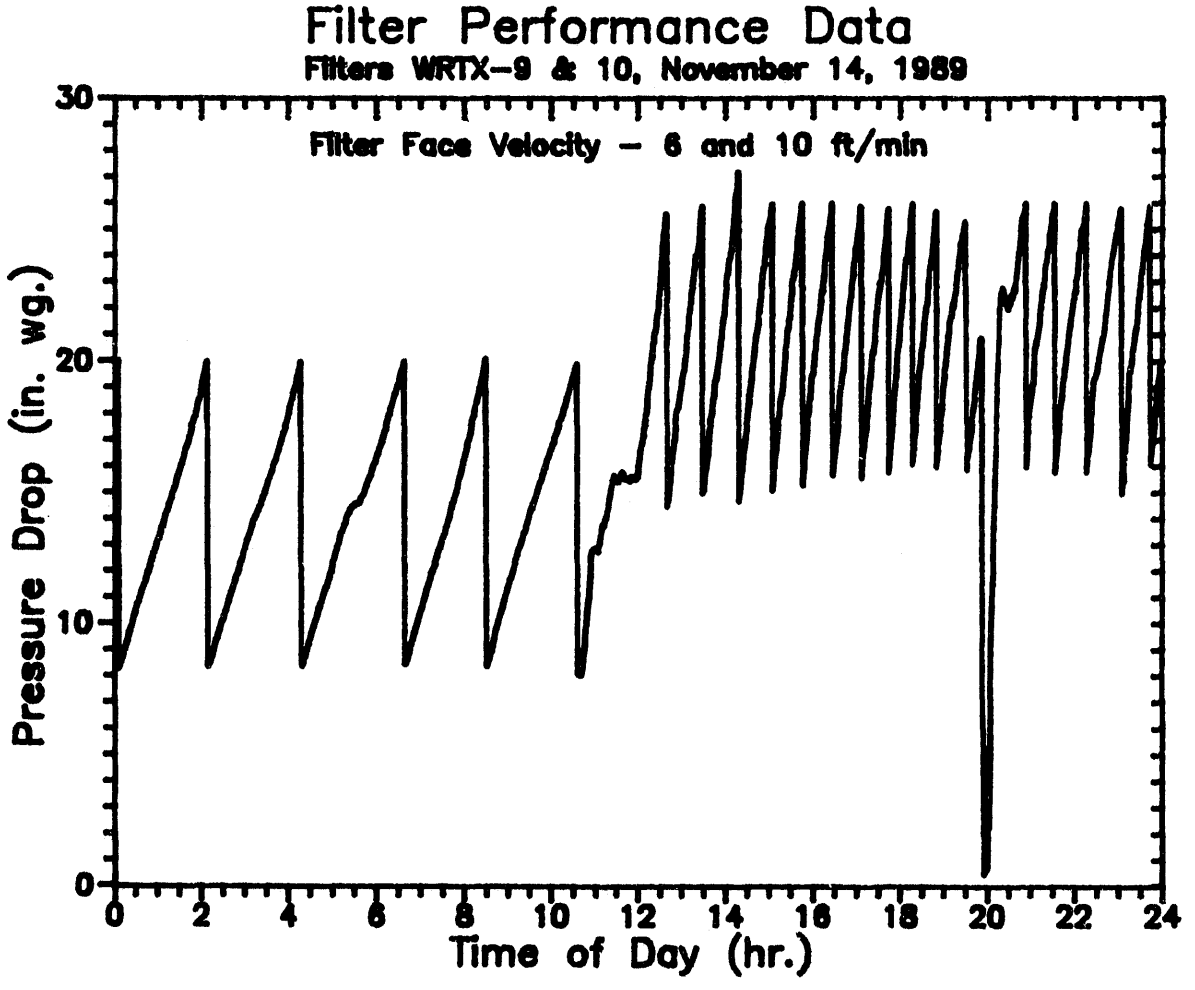

Operation Notes for November 14, 1989:

ΔP Trigger = 20.0" WC
Pulse Cleaning - 290 psig/0.1 sec
1040 - conditions changed to 10 ft/min; dust feed rate increased
ΔP Trigger = 26.0" WC
Pulse Cleaning - 290 psig/0.1 sec
1954 - Unscheduled shutdown power loss; heat tape short
Blown fuse, corrected
Restart: 2000

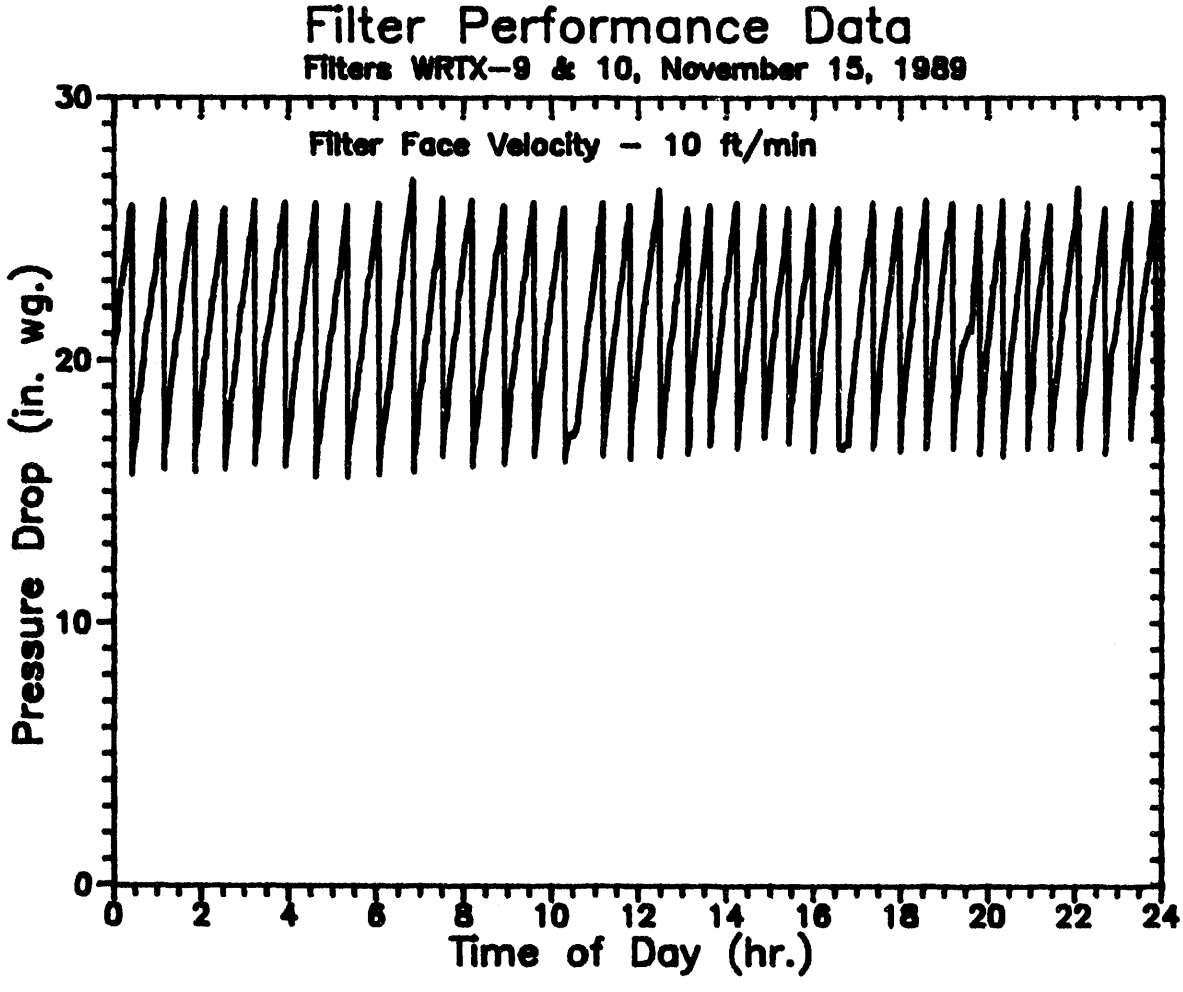

Operation Notes for November 15, 1989:
ΔP Trigger = 26.0" WC
Pulse Cleaning - 290 psig/0.1 sec

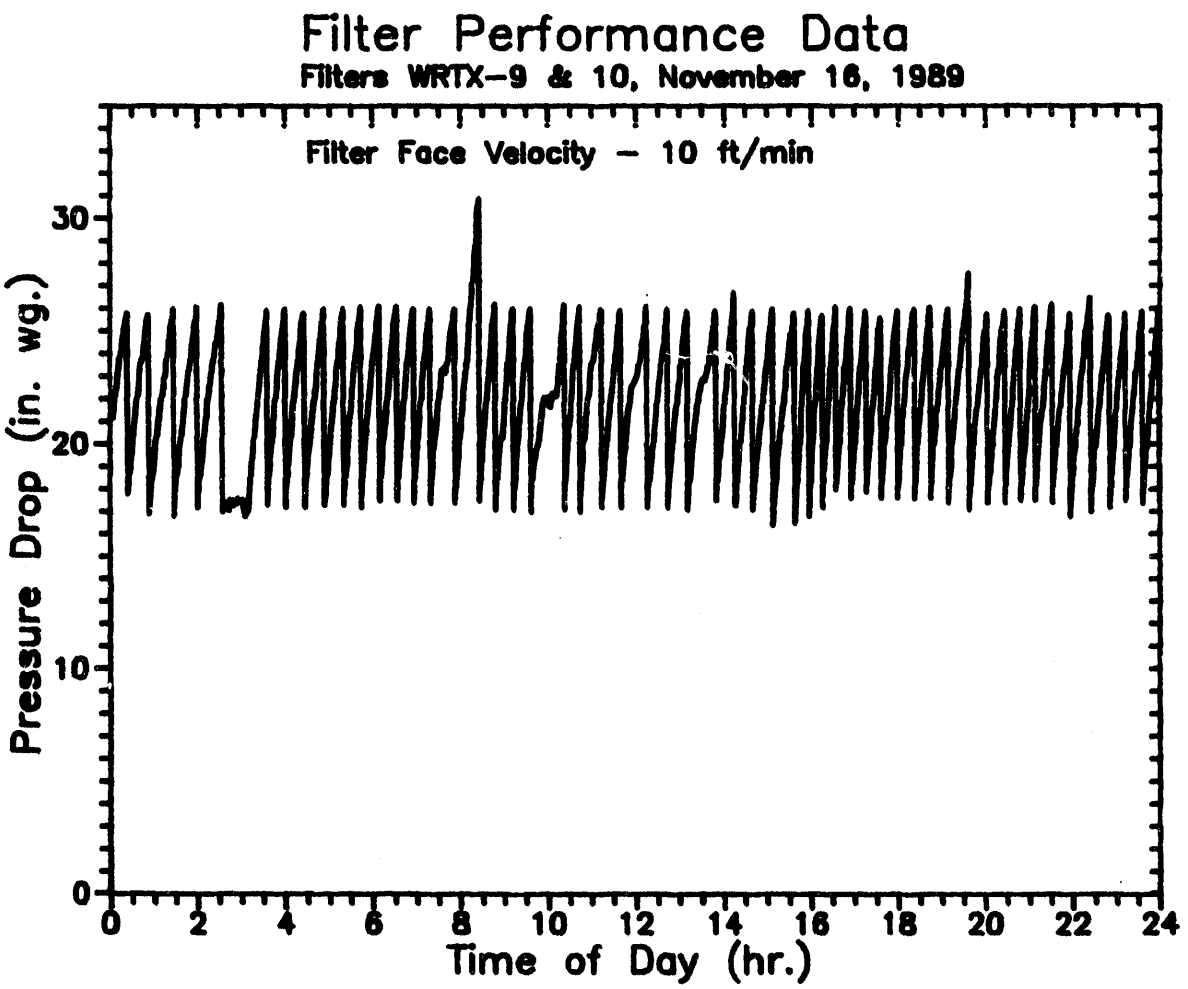

Operation Notes for November 16, 1989:

ΔP Trigger = 26.0" WC
Pulse Cleaning - 290 psig/0.1 sec
0234 - dust off
Depressurize vessel, dust added
0311 - dust on
Occasional erratic dust feed

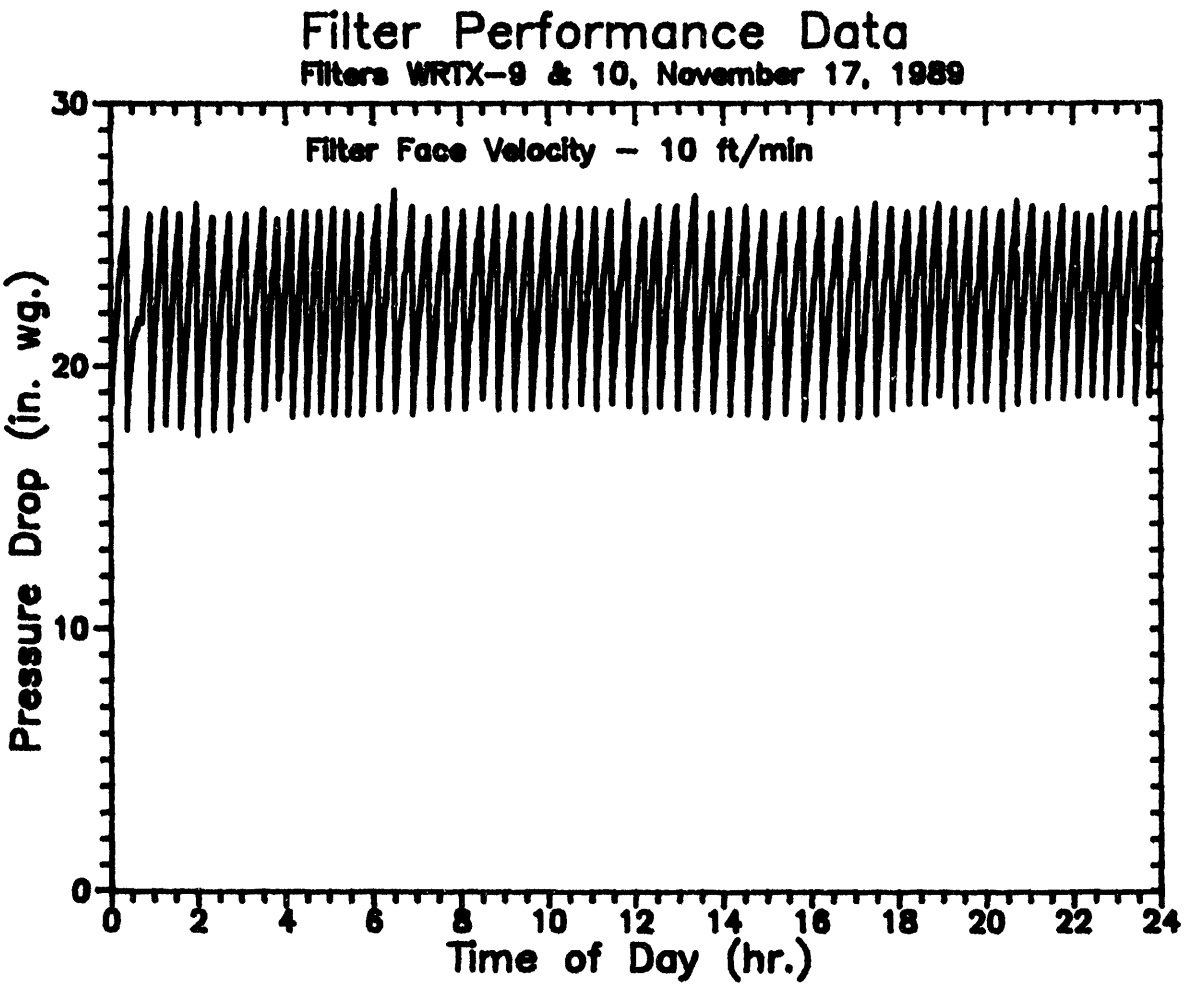

Operation Notes for November 17, 1989:
ΔP Trigger = 26.0" WC
Pulse Cleaning 290 psig/0.1 sec

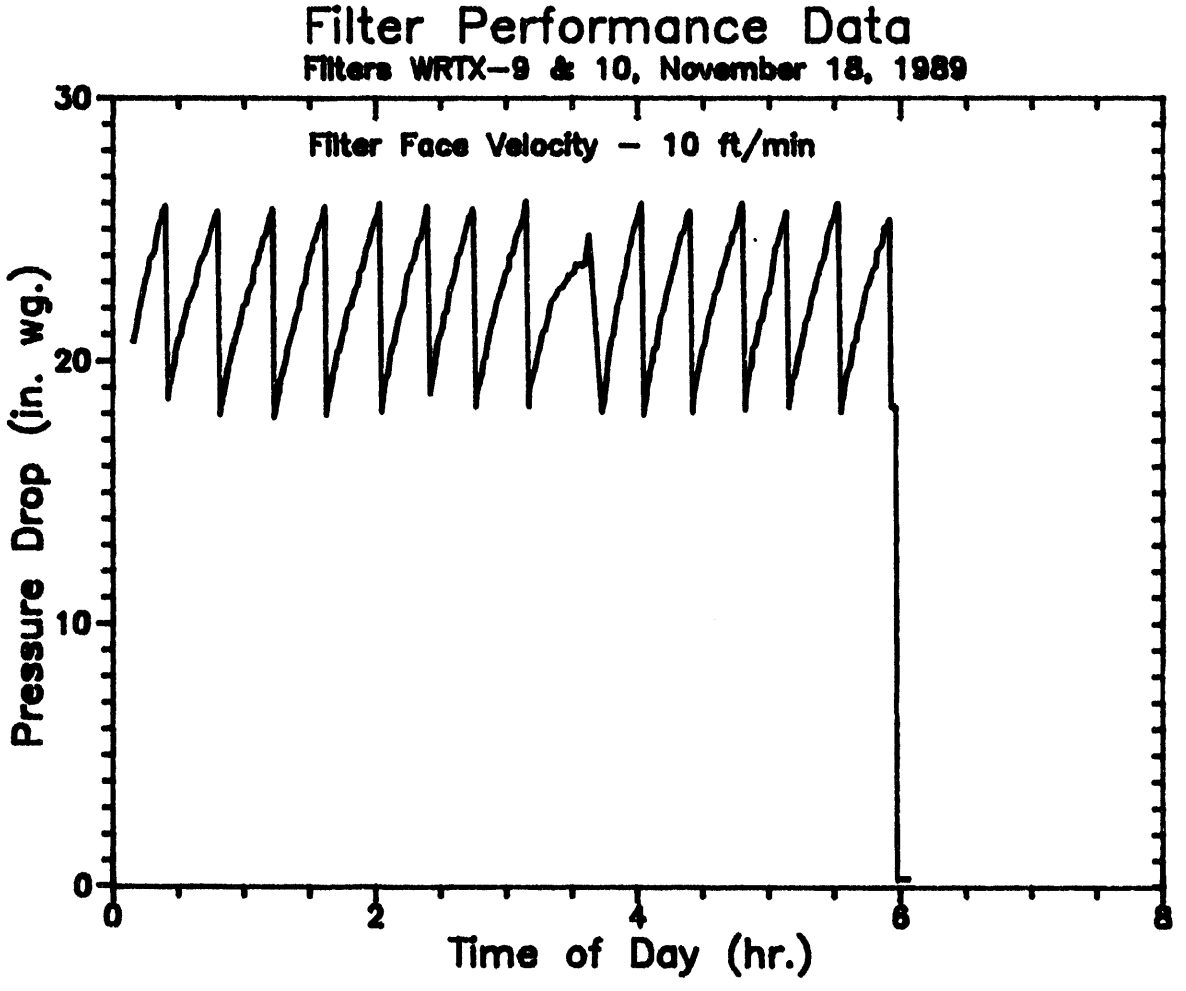

Operation Notes for November 18, 1989:

End of week long test
Scheduled shutdown
ΔP Trigger = 26.0" WC
Pulse Cleaning - 290 psig/0.1 sec

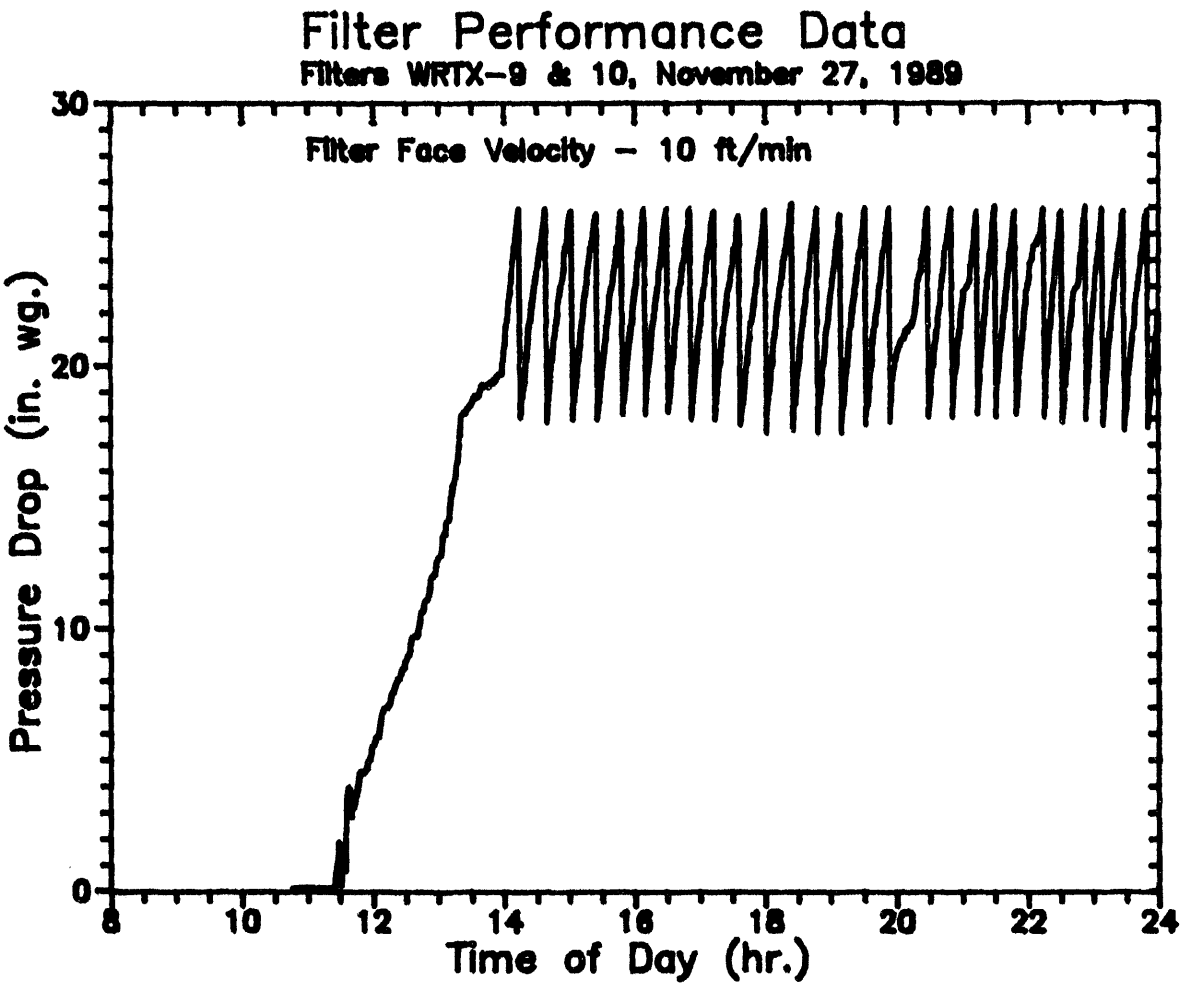

Operation Notes for November 27, 1989:

Begin week long test
Startup
ΔP Trigger = 26.0" WC
Pulse Cleaning - 290 psig/0.1 sec

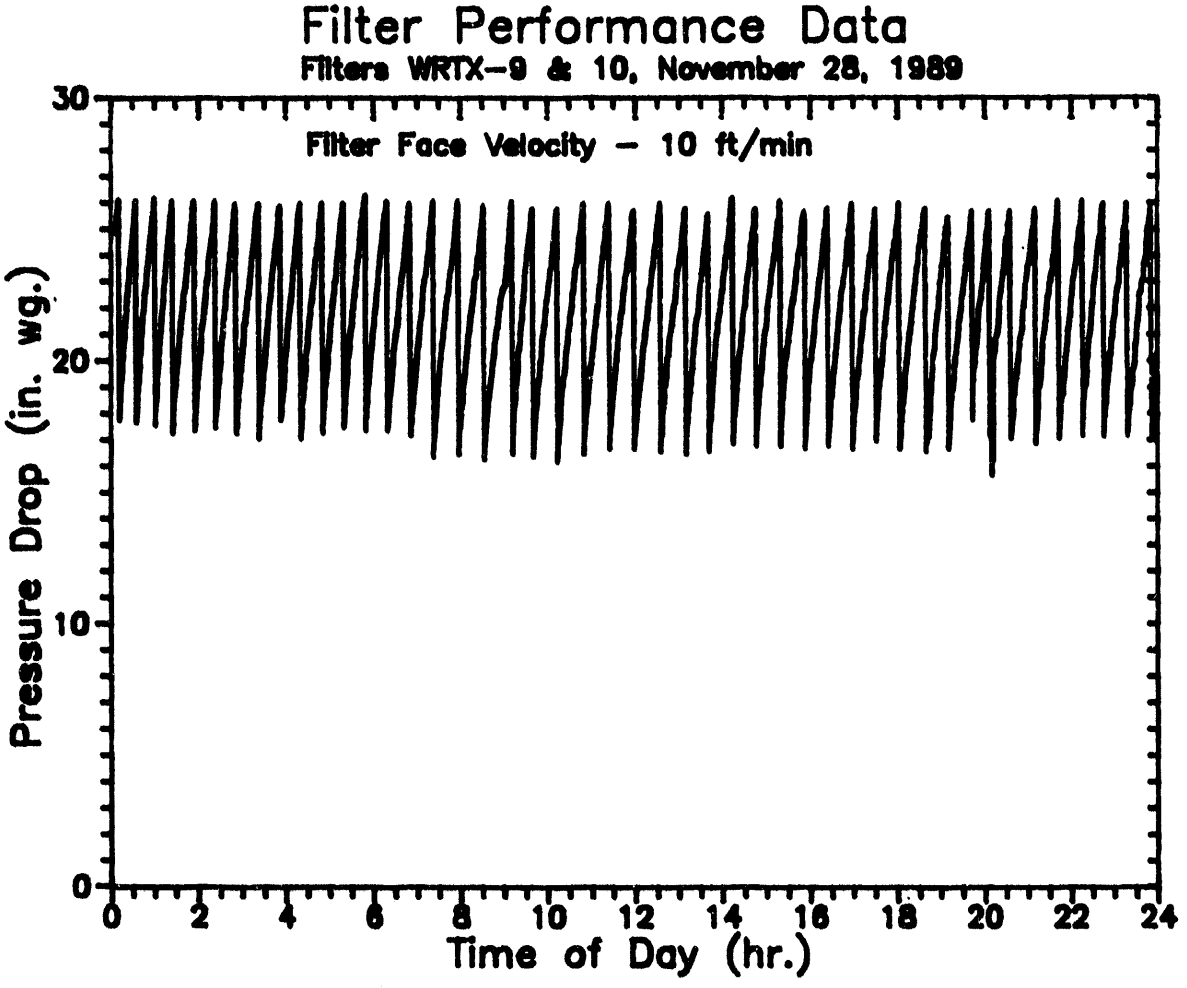

Operation Notes for November 28, 1989:
ΔP Trigger = 26.0" WC
Pulse Cleaning - 290 psig/0.1 sec

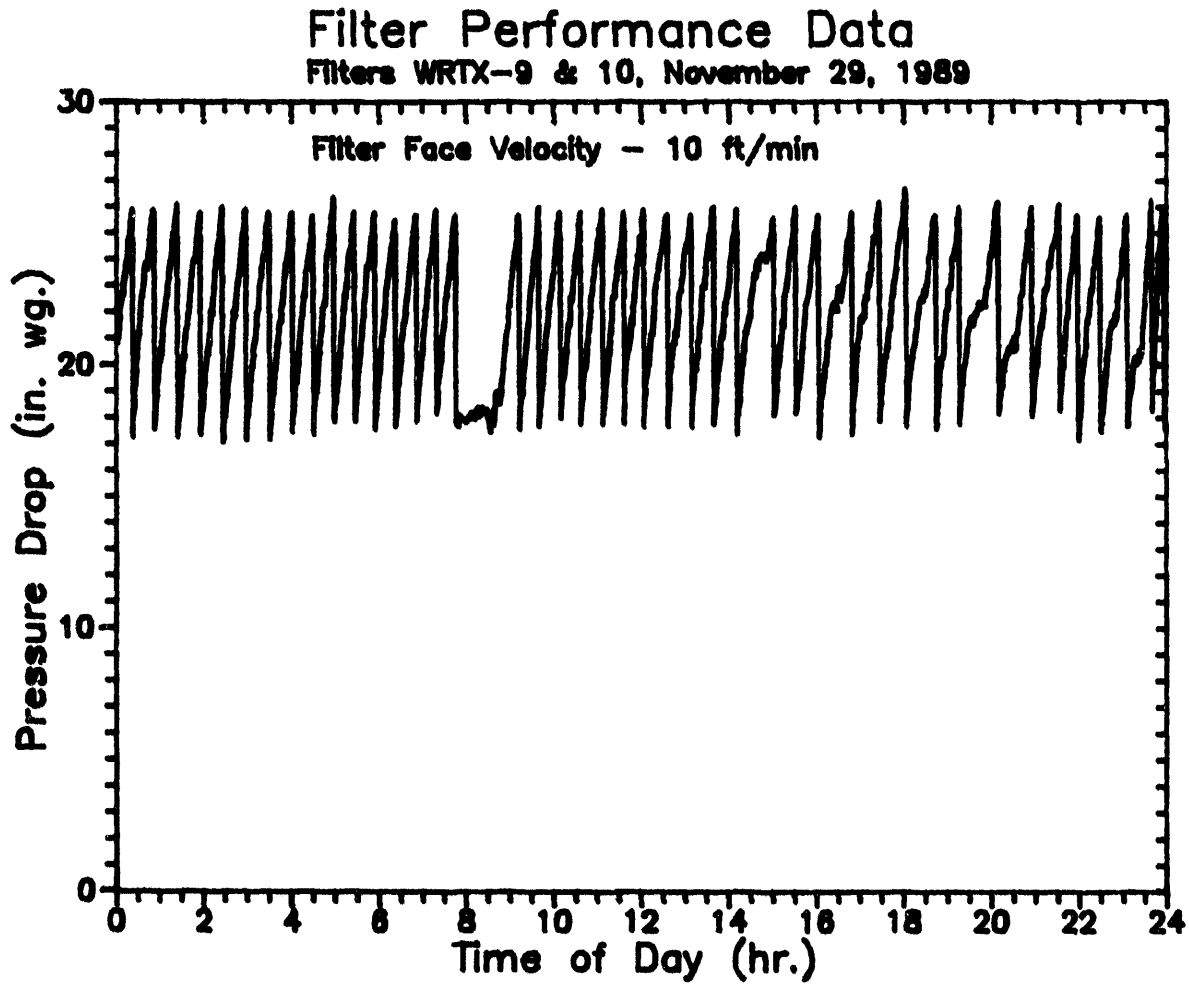

Operation Notes for November 29, 1989:

ΔP Trigger = 28.0" WC
Pulse Cleaning - 290 psig/0.1 sec
0747 - dust off, dust added to vessel
0846 - dust on
1400 - erratic feed

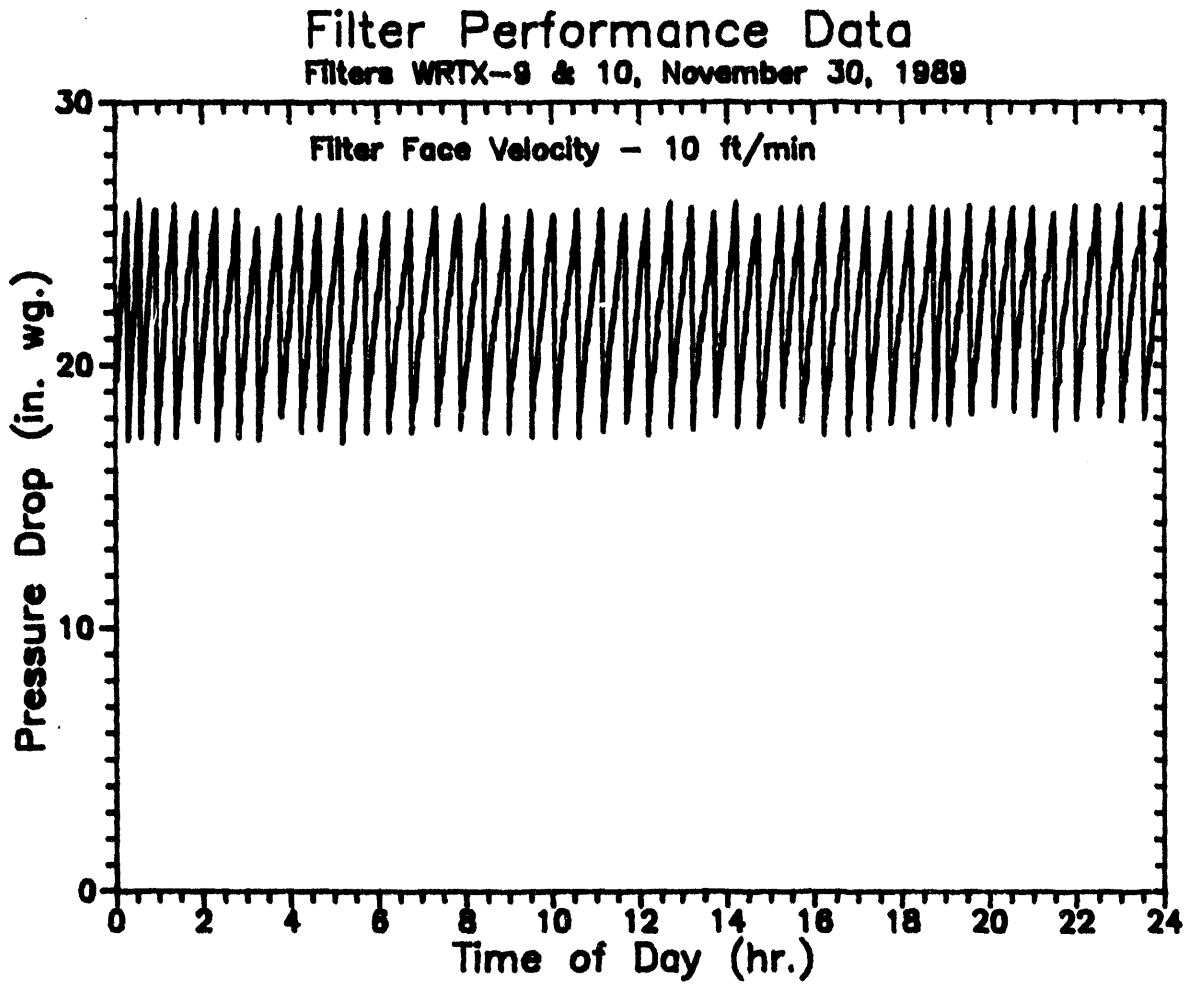

Operation Notes for November 30, 1989:
ΔP Trigger = 26.0" WC
Pulse Cleaning - 290 psig/0.1 sec

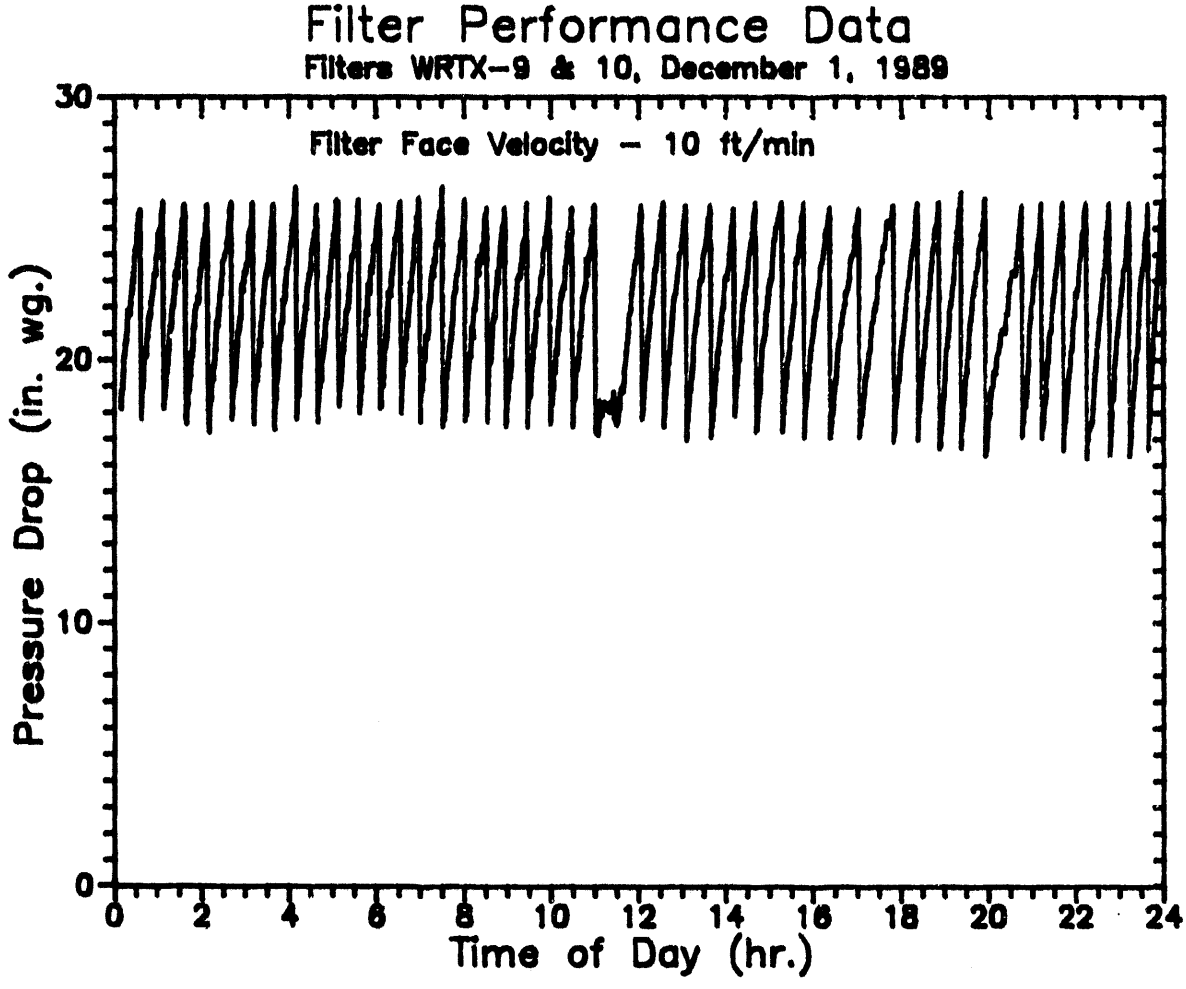

Operation Notes for December 1, 1989:

ΔP Trigger = 26.0" WC
Pulse Cleaning - 290 psig/0.1 sec
11:00 dust off, dust added to vessel
11:37 dust on

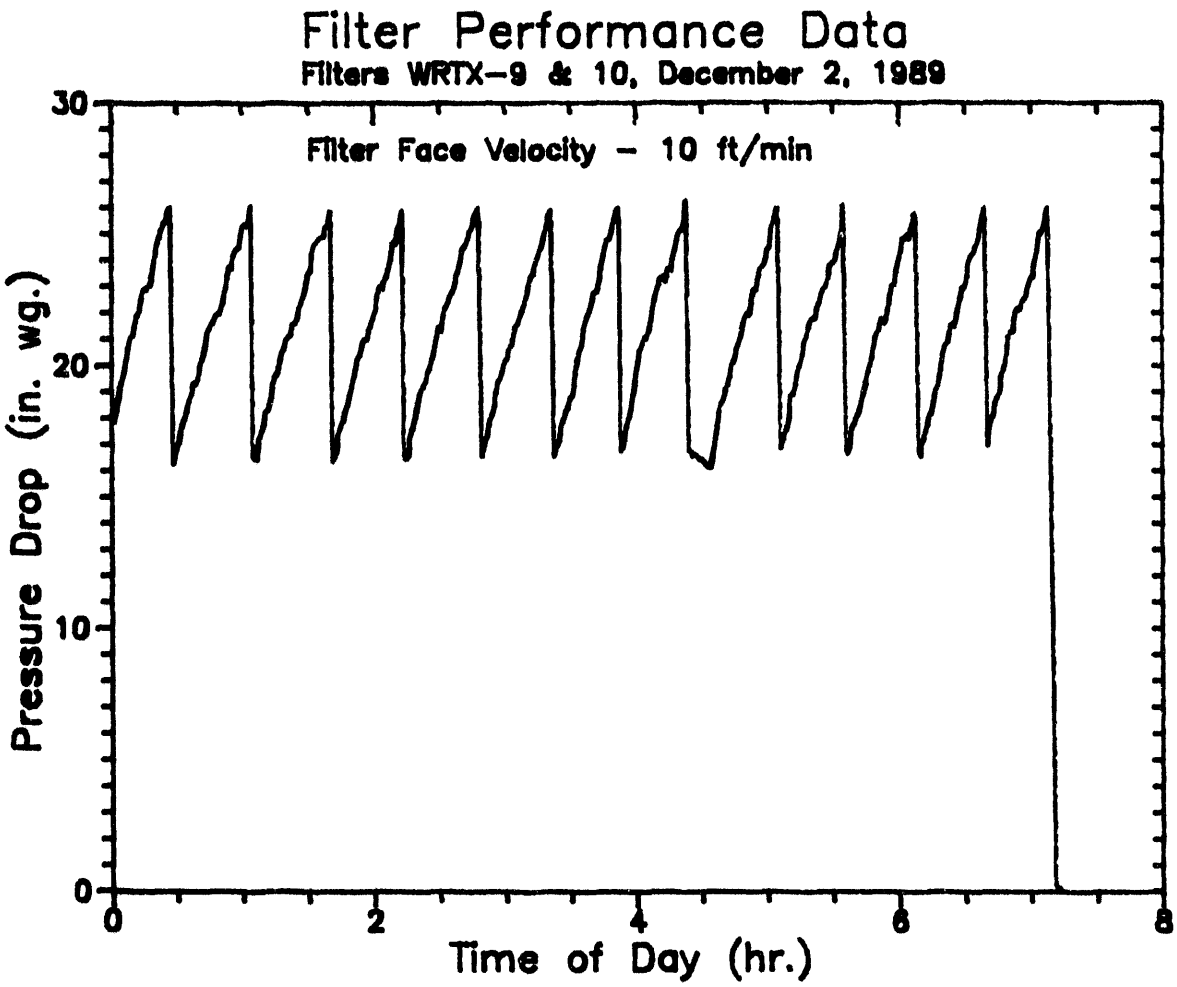

Operation Notes for December 2, 1989:

End week long test
Scheduled shutdown
ΔP Trigger = 26.0" WC
Pulse Cleaning - 290 psig/0.1 sec
0424 to 0435 Dust feed off

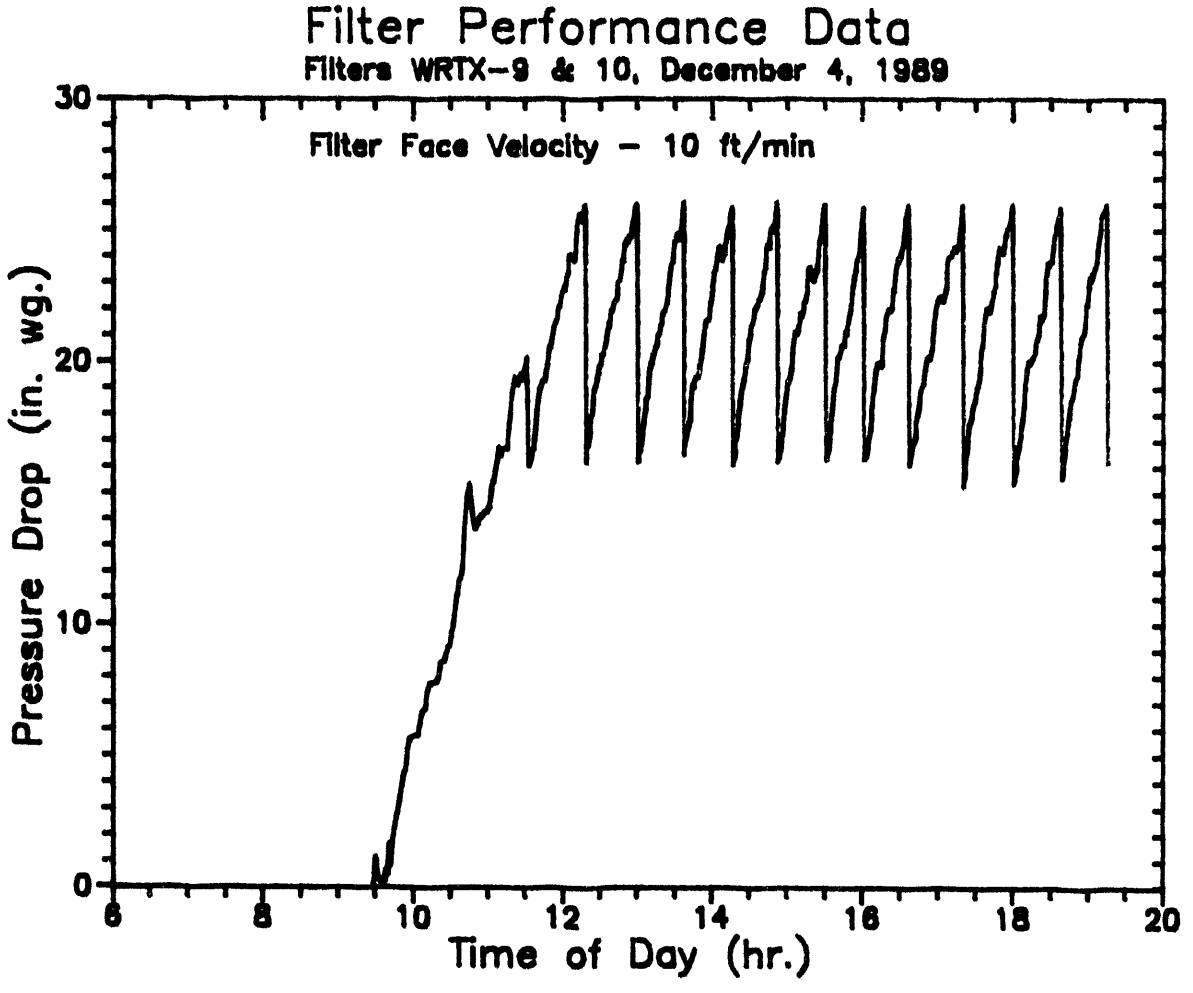

Operation Notes for December 4, 1989:

Begin week long test
Startup
ΔP Trigger = 26.0" WC
Pulse Cleaning - 290 psig/0.1 sec
~2400 - Data acquisition off
0608 - Unscheduled shutdown - flame out
Hot spot at combustor

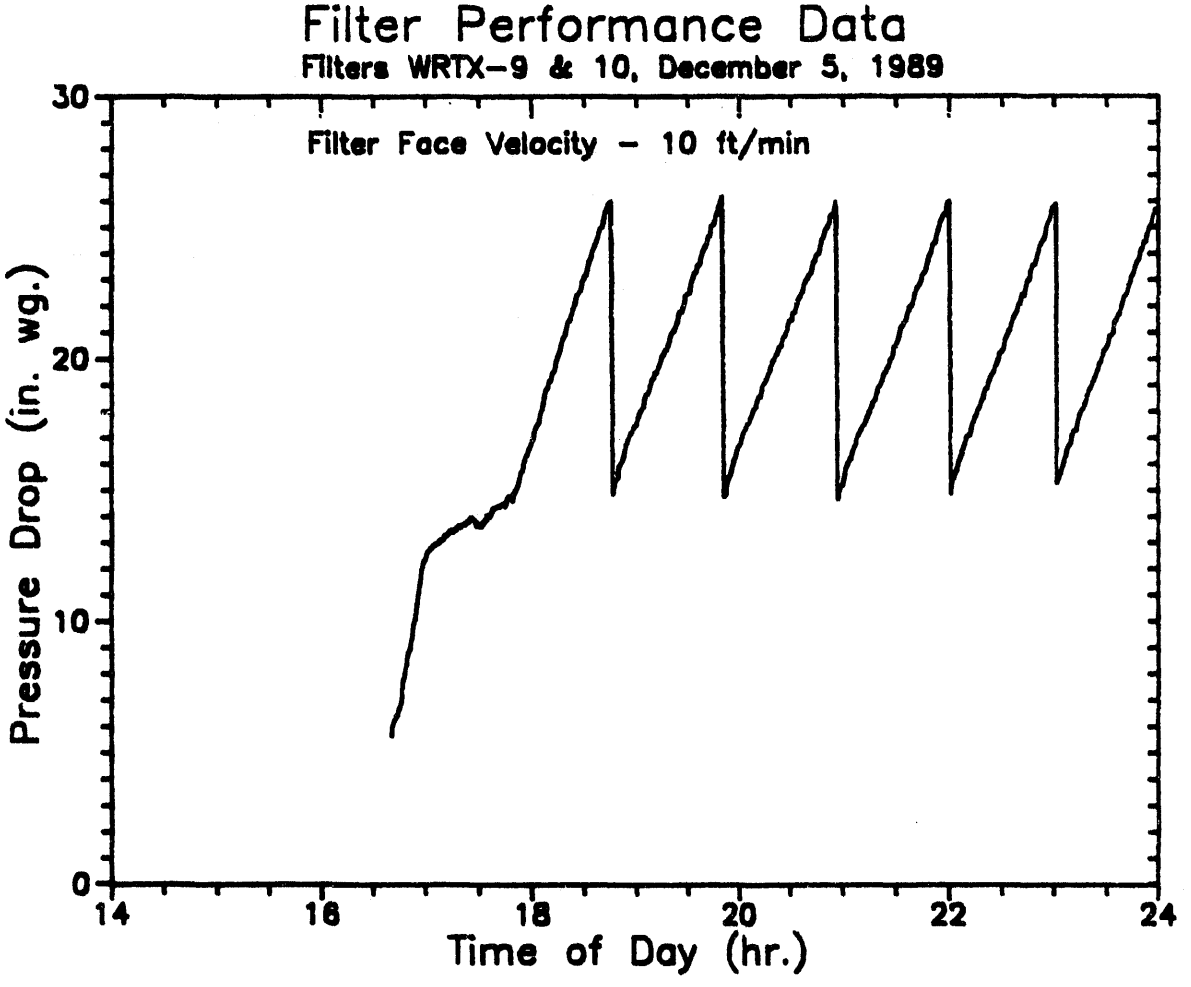

Operation Notes for December 5, 1989:
Combustor liner replaced
Restart week long test
ΔP Trigger = 26.0" WC
Pulse Cleaning - 290 psig/0.1 sec

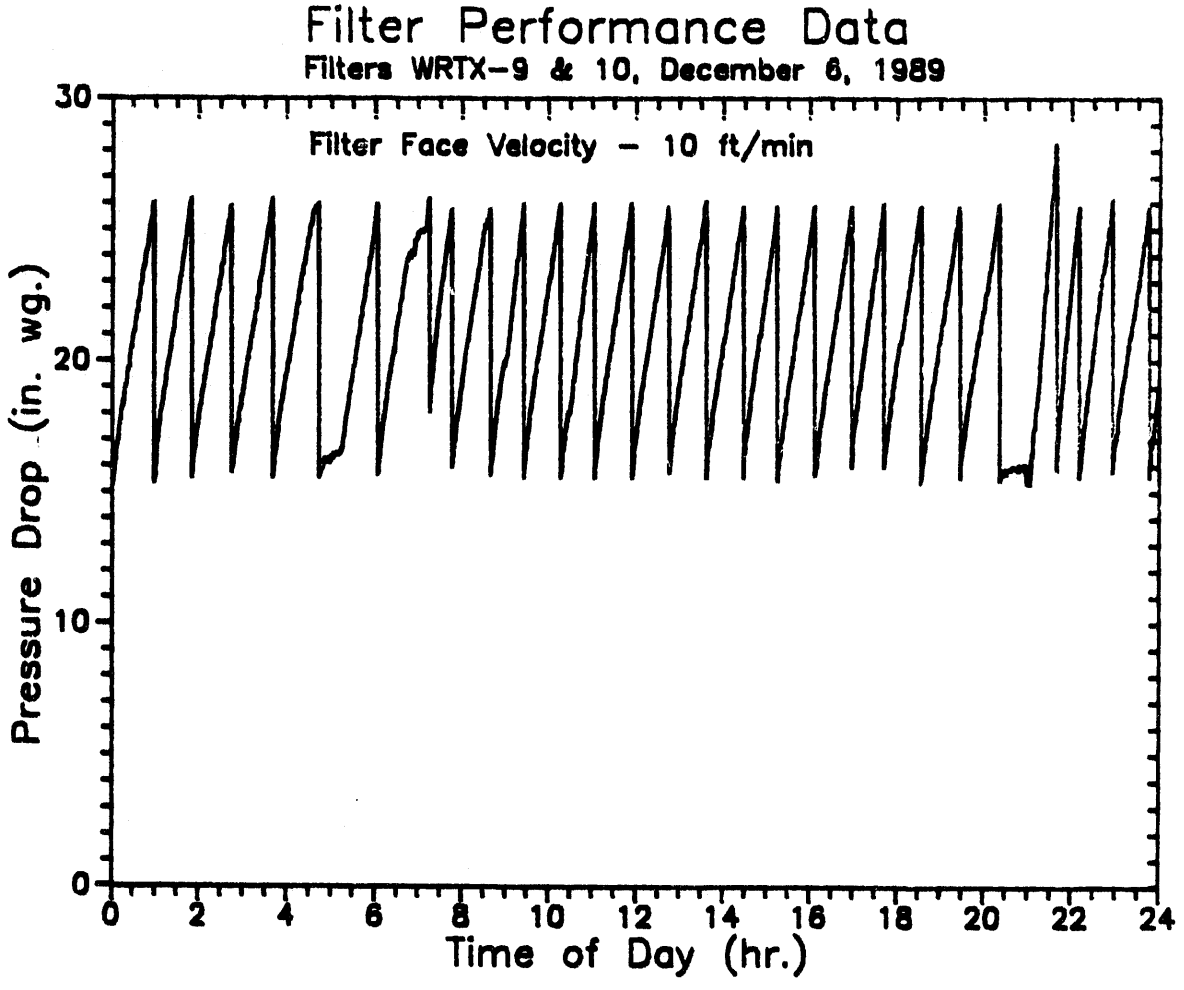

Operation Notes for December 6, 1989:

ΔP Trigger = 26.0" WC
Pulse Cleaning - 290 psig/0.1 sec
2023 - dust off, dust added to vessel
2105 - dust on

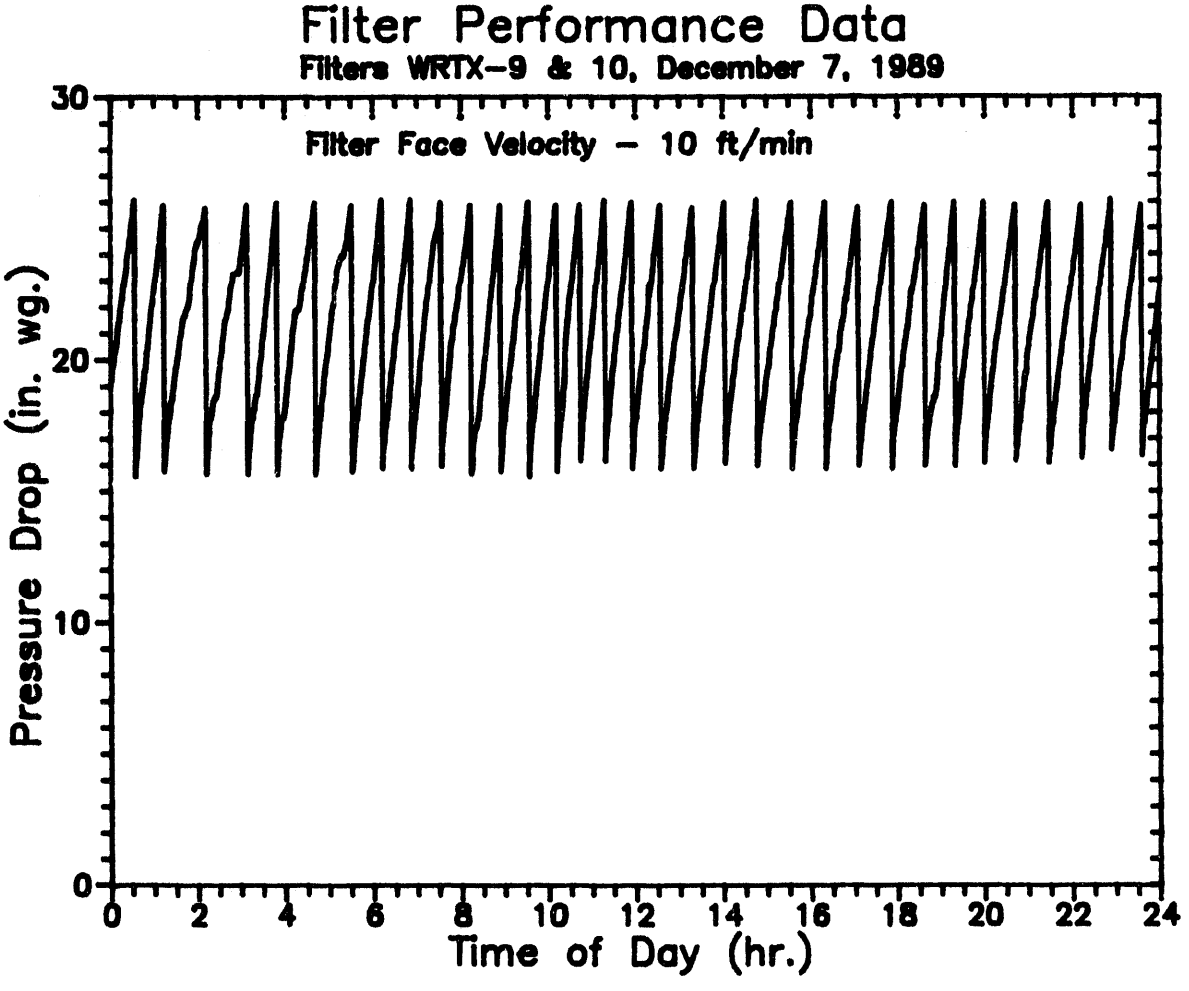

Operation Notes for December 7, 1989:
ΔP Trigger = 26.0" WC
Pulse Cleaning - 290 psig/0.1 sec

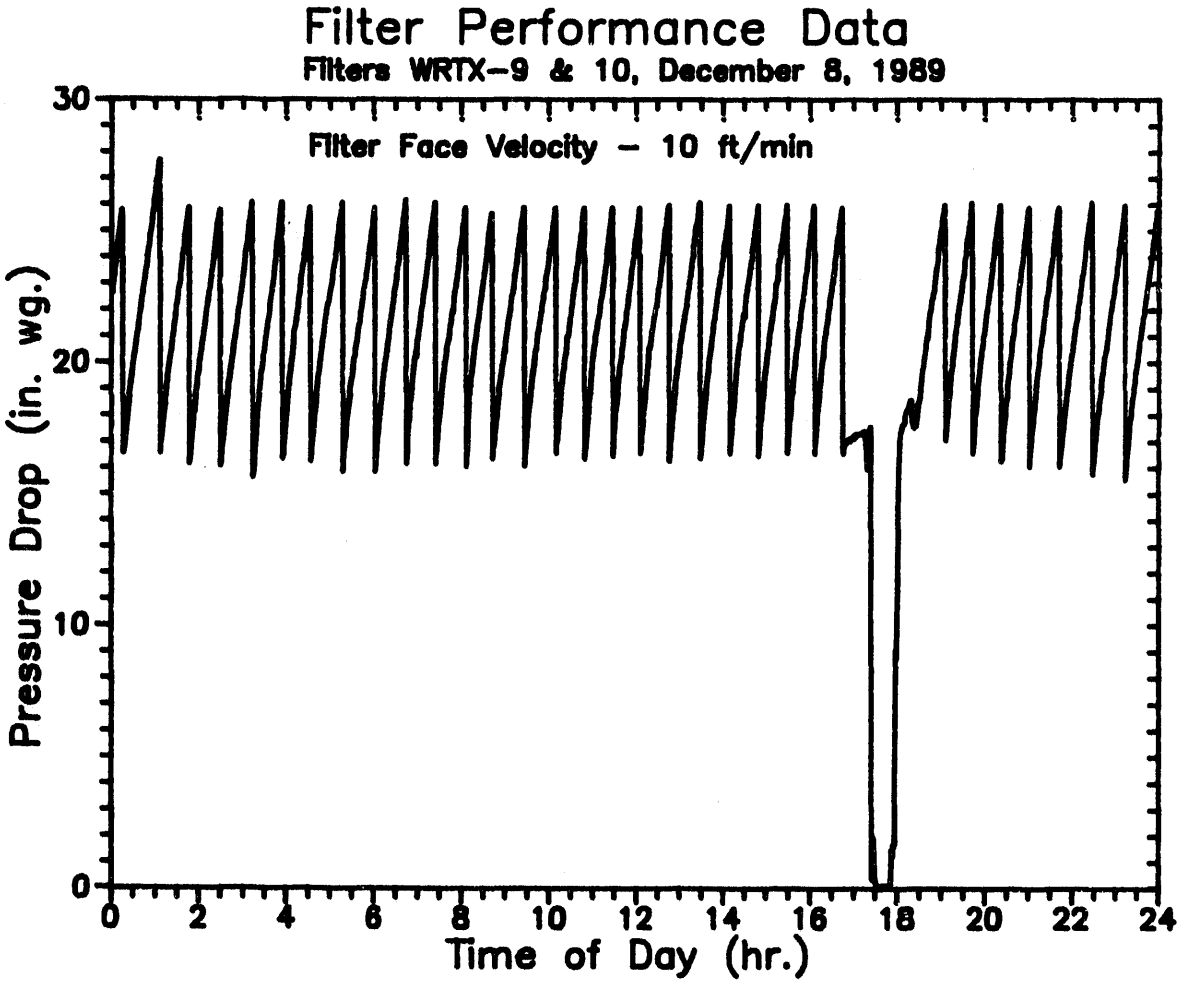

Operation Notes for December 8, 1989:

ΔP Trigger = 26.0" WC
Pulse Cleaning - 290 psig/0.1 sec
1644 - Dust off, dust added to vessel
1725 - Unscheduled shutdown - repair dust feed line
1753 - Retart

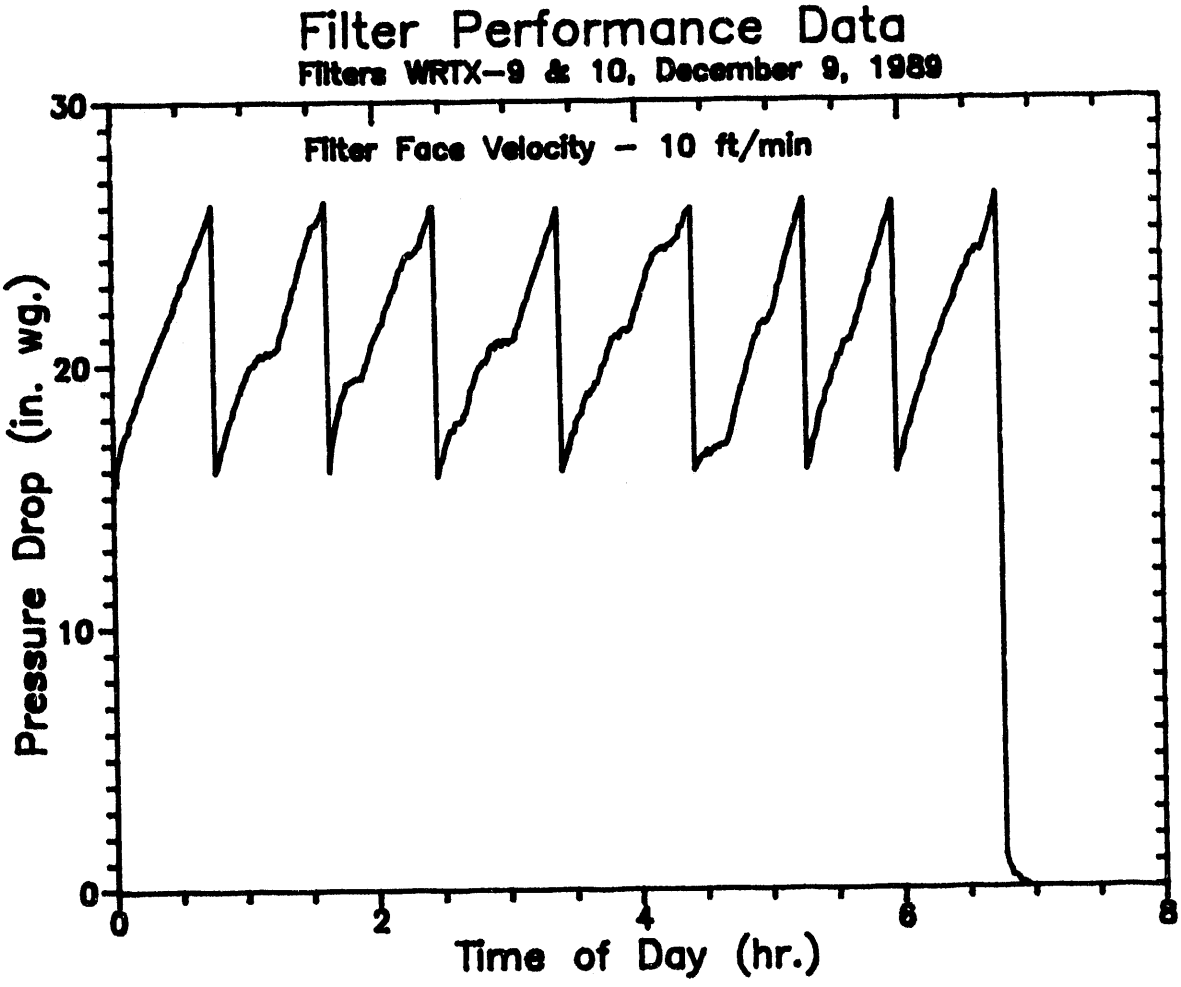

Operation Notes for December 9, 1989:

End week long test
Scheduled shutdown
ΔP Trigger = 26.0" WC
Pulse Cleaning - 290 psig/0.1 sec

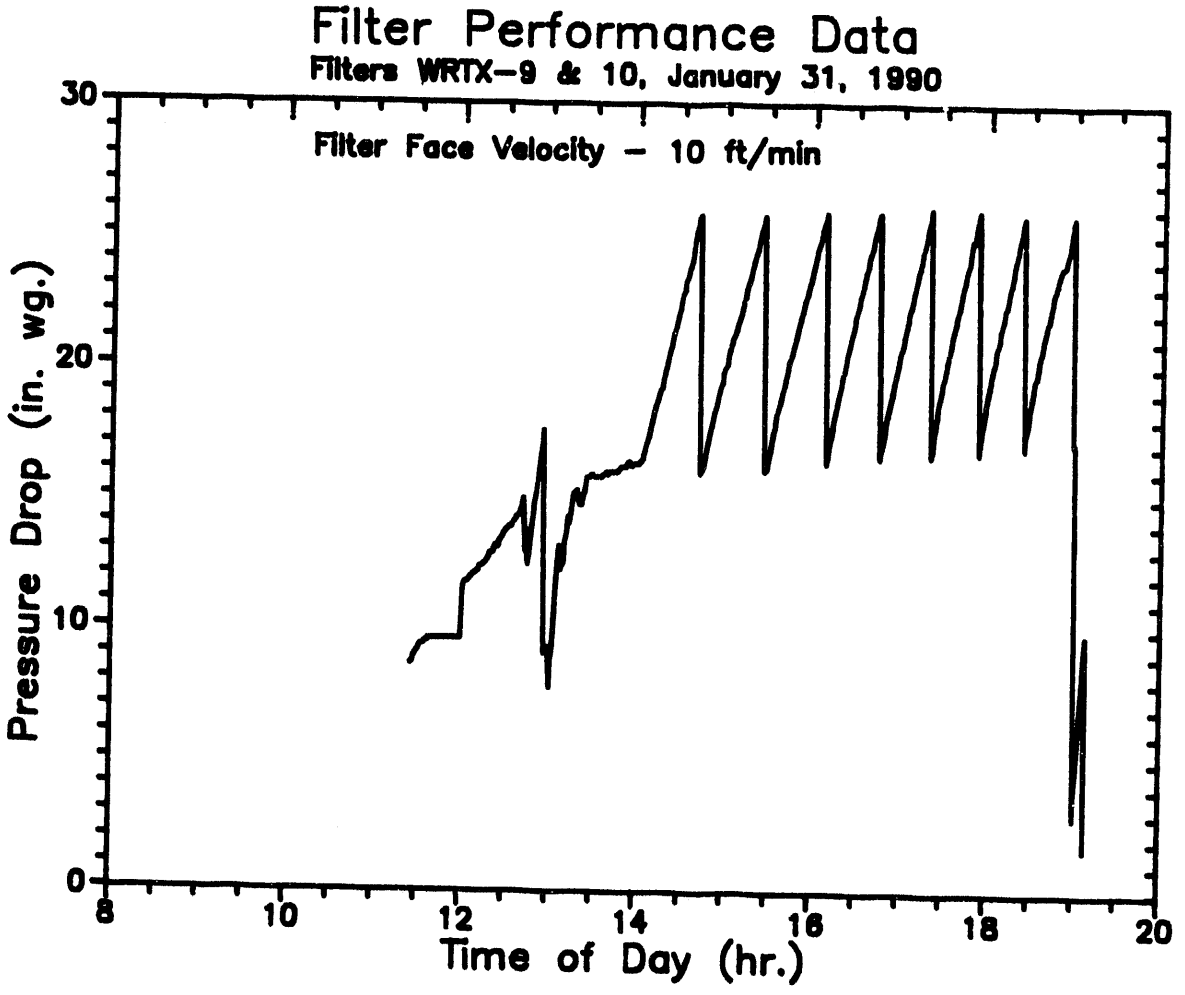

Operation Notes for January 31, 1990:

12 hour test, includes startup and shutdown
1300 - Lost house air supply
Shut down
Restarted
ΔP Trigger = 26.0" WC
Pulse Cleaning 290 psig/0.1 sec

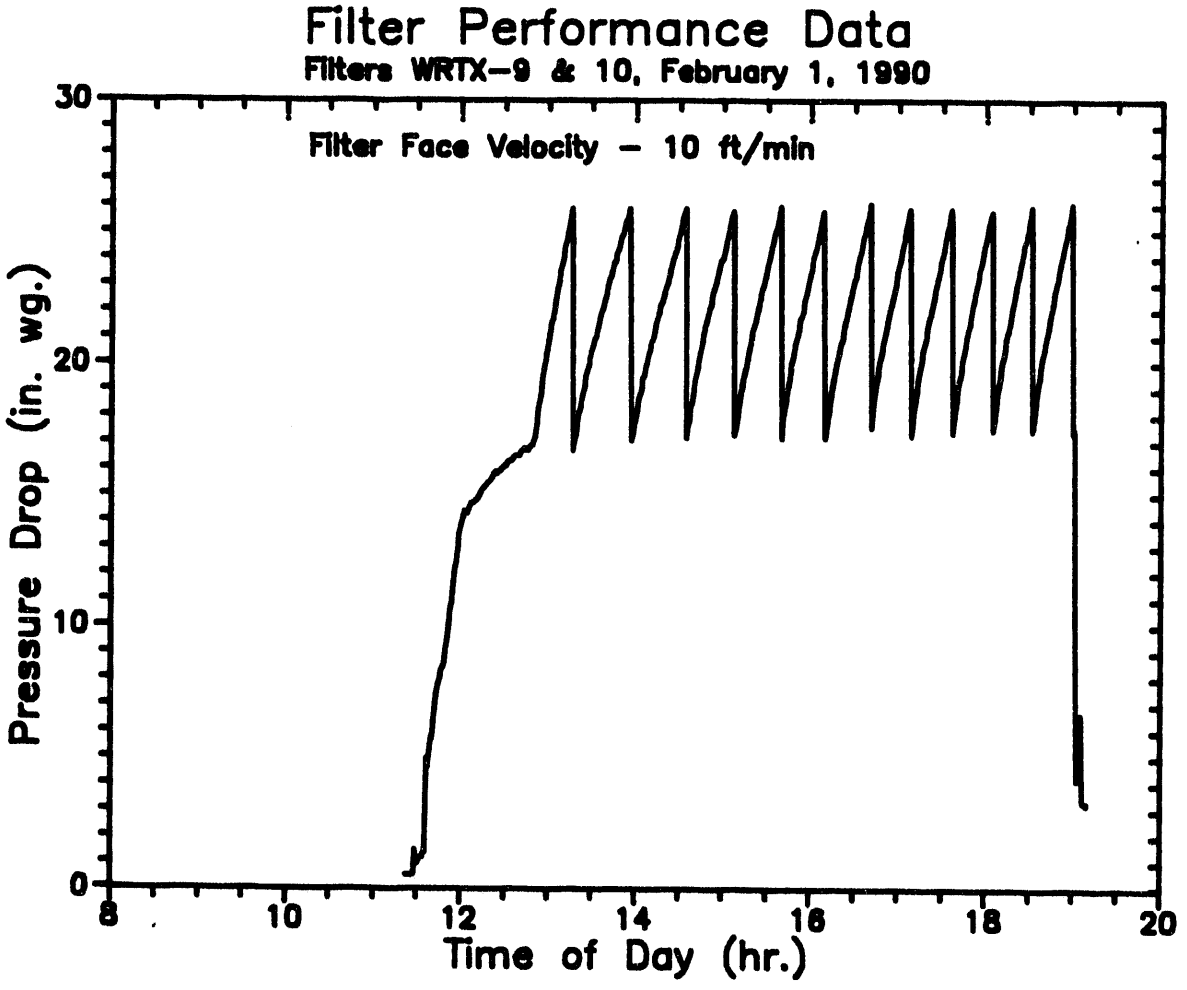

Operation Notes for February 1, 1990:
12 hour test, includes startup and shutdown
ΔP Trigger = 26.0" WC
Pulse Cleaning - 290 psig/0.1 sec

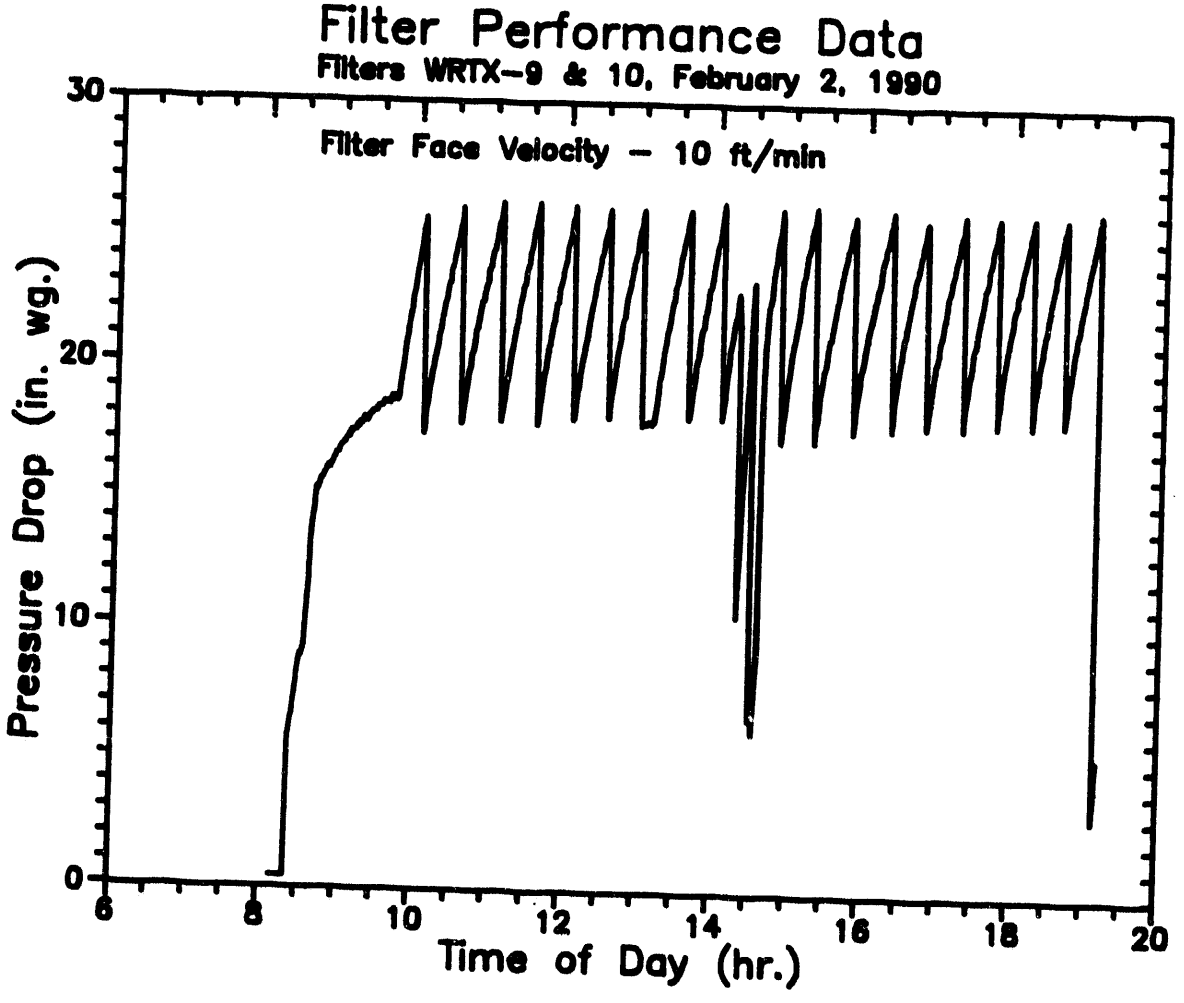

Operation Notes for February 2, 1990:

12 hour test, includes startup and shutdown
1430 Lost cooling water to air compressor
Shutdown & restart
ΔP Trigger = 26.0" WC
Pulse Cleaning - 290 psig/0.1 sec

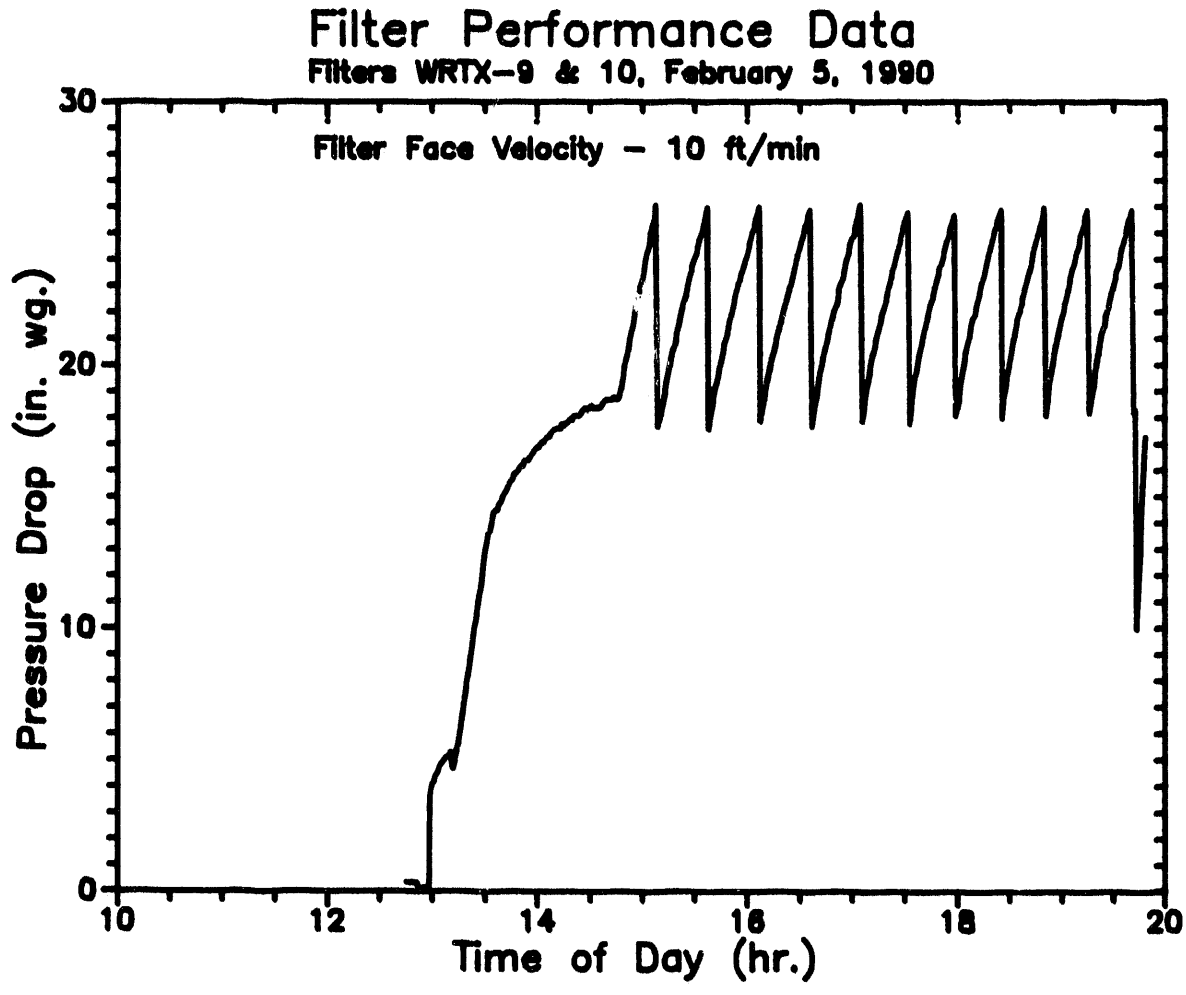

Operation Notes for February 5, 1990:

8 hour test, includes startup and shutdown
ΔP Trigger = 26.0" WC
Pulse Cleaning - 290 psig/0.1 sec

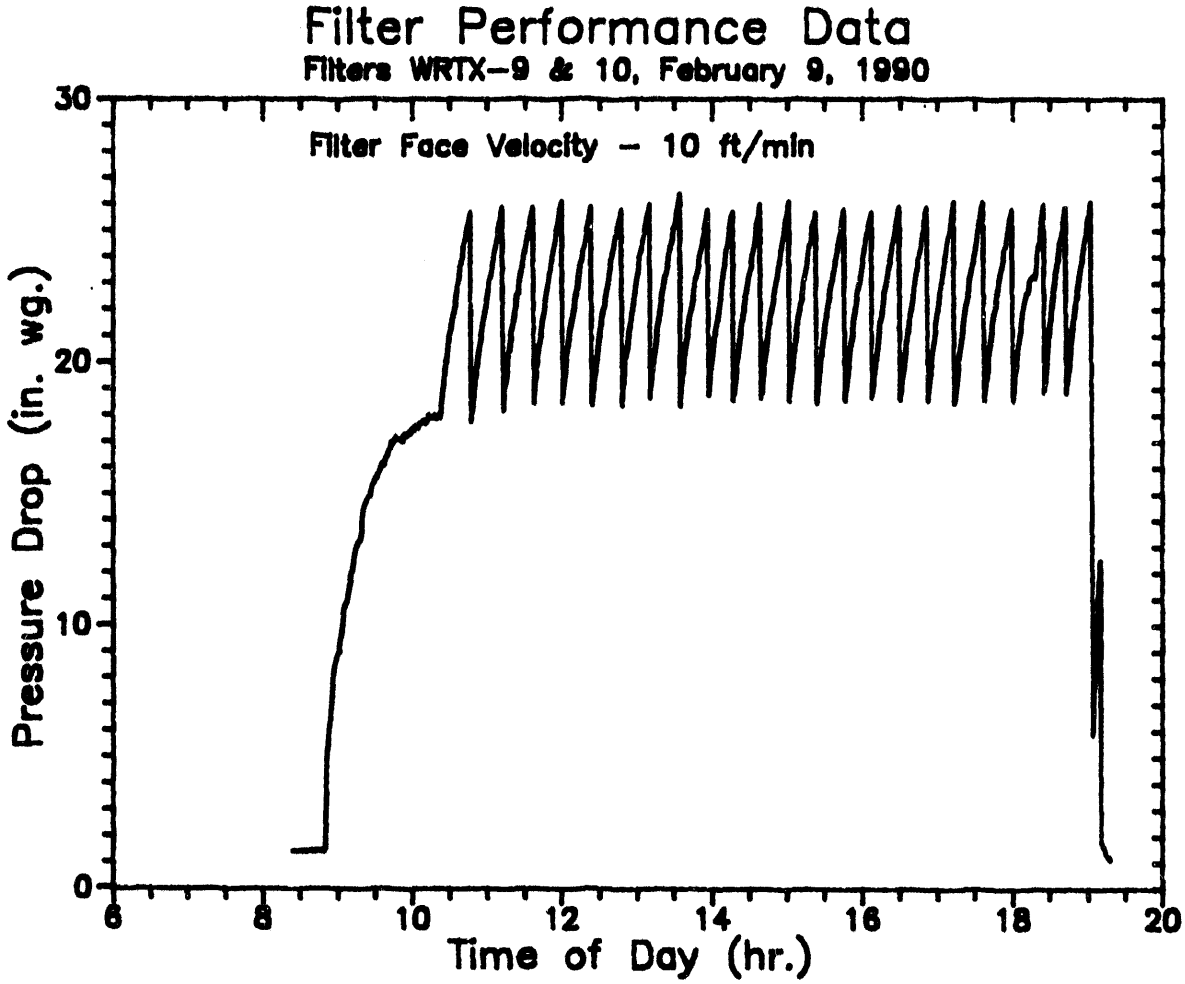

Operation Notes for February 9, 1990:
12 hour test, includes startup and shutdown
ΔP Trigger = 26.0" WC
Pulse Cleaning - 290 psig/0.1 sec

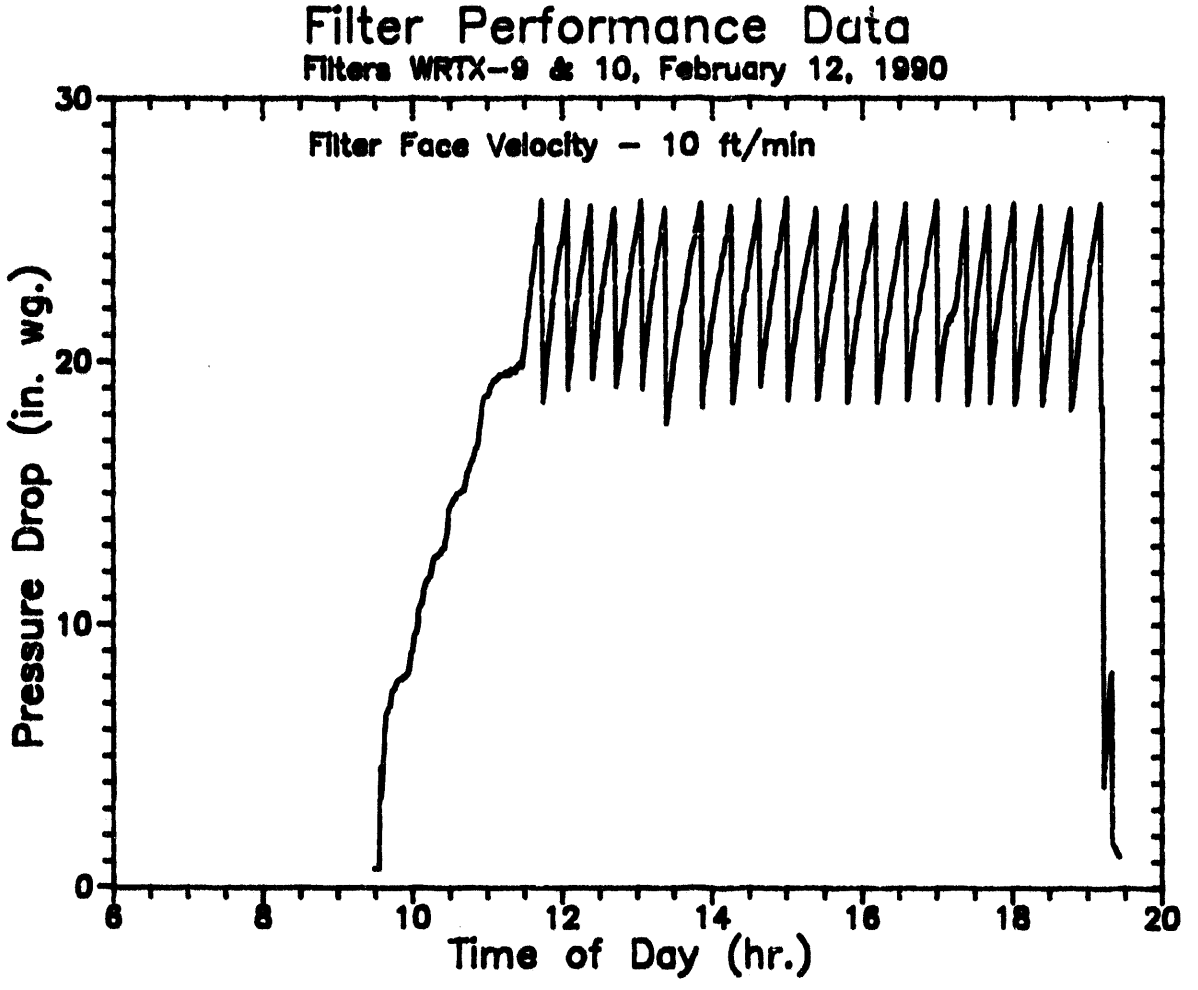

Operation Notes for February 12, 1990:
12 hour test, includes startup and shutdown
ΔP Trigger = 26.0" WC
Pulse Cleaning - 290 psig/0.1 sec

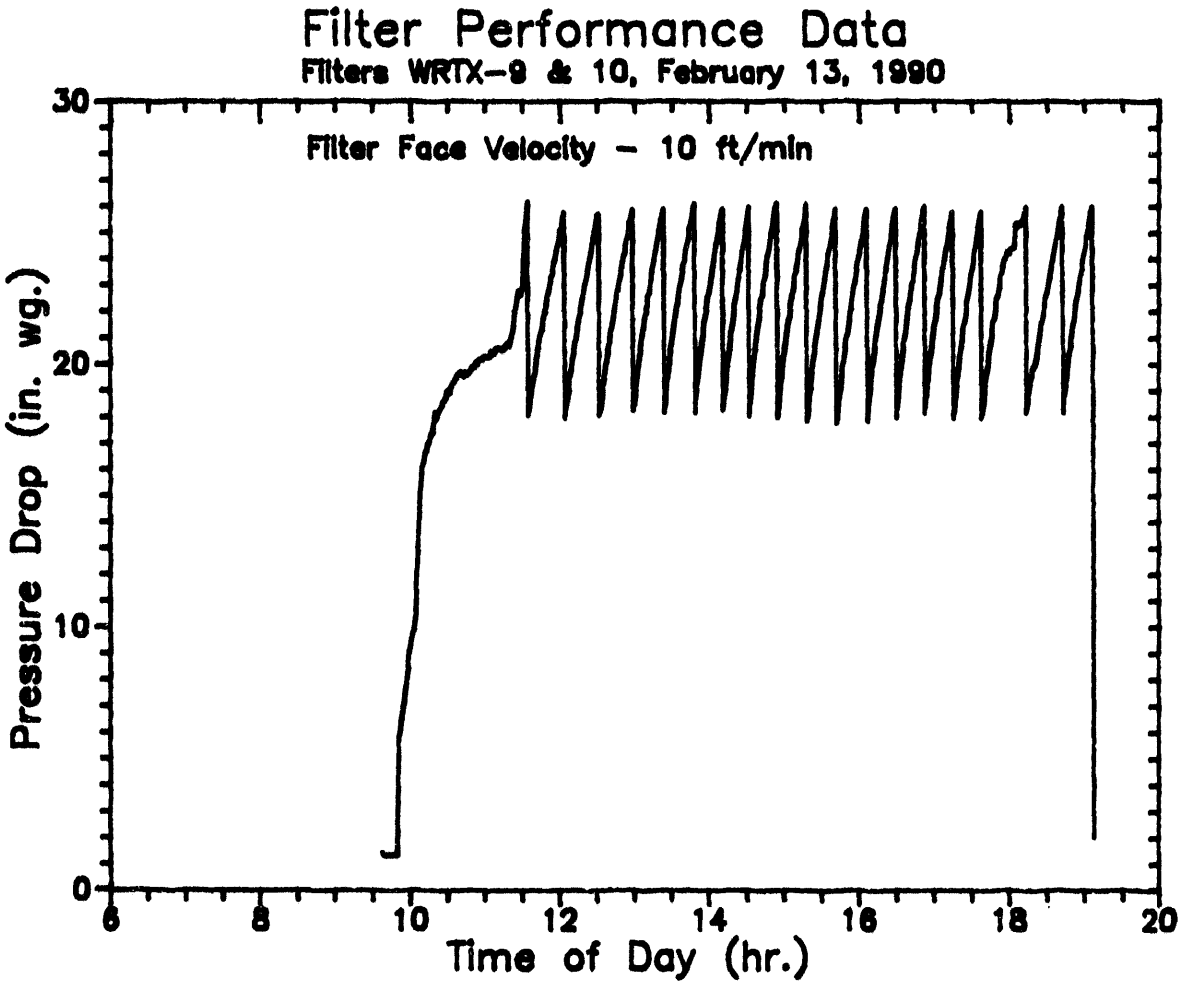

Operation Notes for February 13, 1990:
12 hour test, includes startup and shutdown
ΔP Trigger = 26.0" WC
Pulse Cleaning - 290 psig/0.1 sec

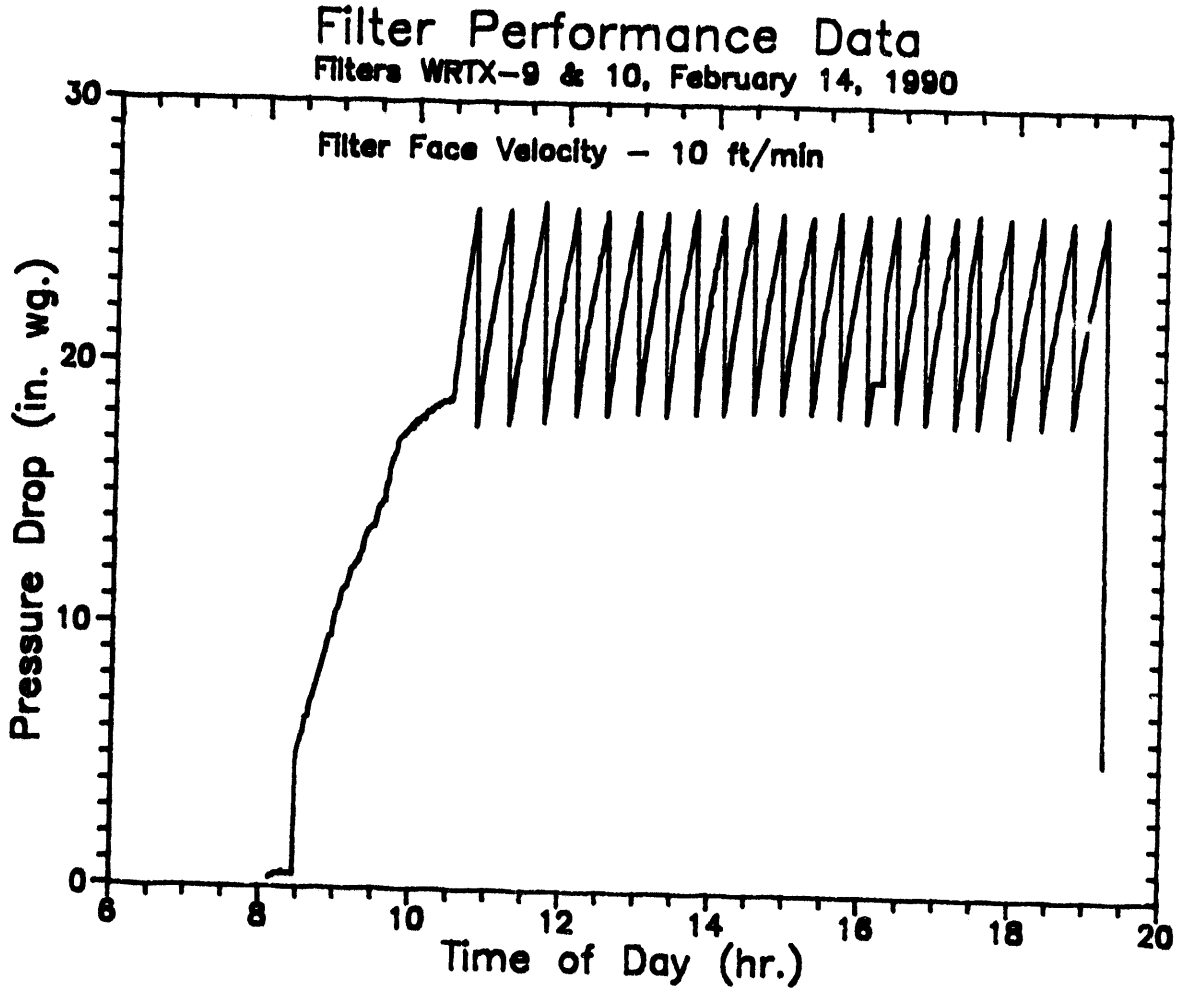

Operation Notes for February 14, 1990:
12 hour test, includes startup and shutdown
ΔP Trigger = 26.0" WC
Pulse Cleaning - 290 psig/0.1 sec

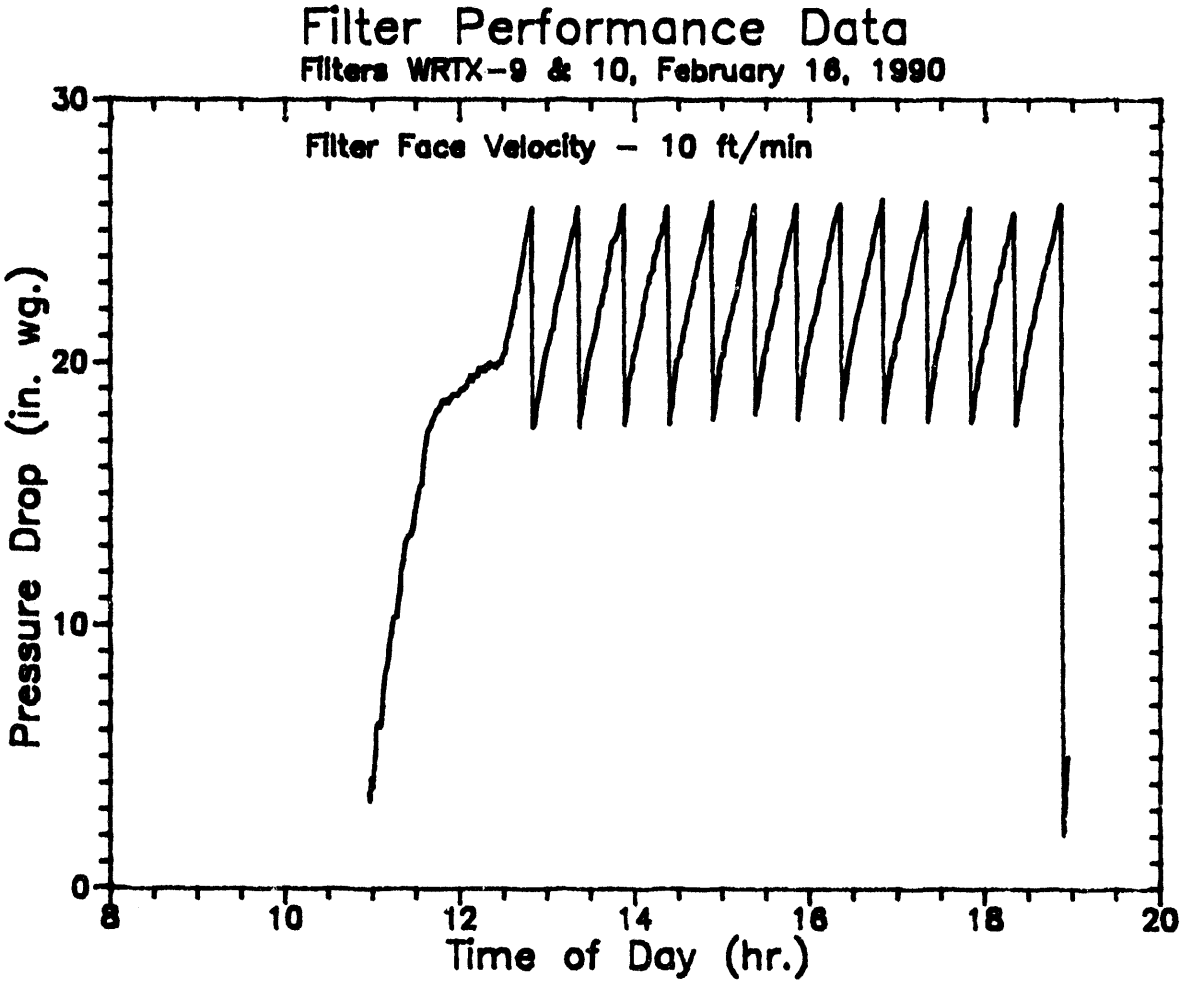

Operation Notes for February 16, 1990:
12 hour test, includes startup and shutdown
ΔP Trigger = 26.0" WC
Pulse Cleaning - 290 psig/0.1 sec

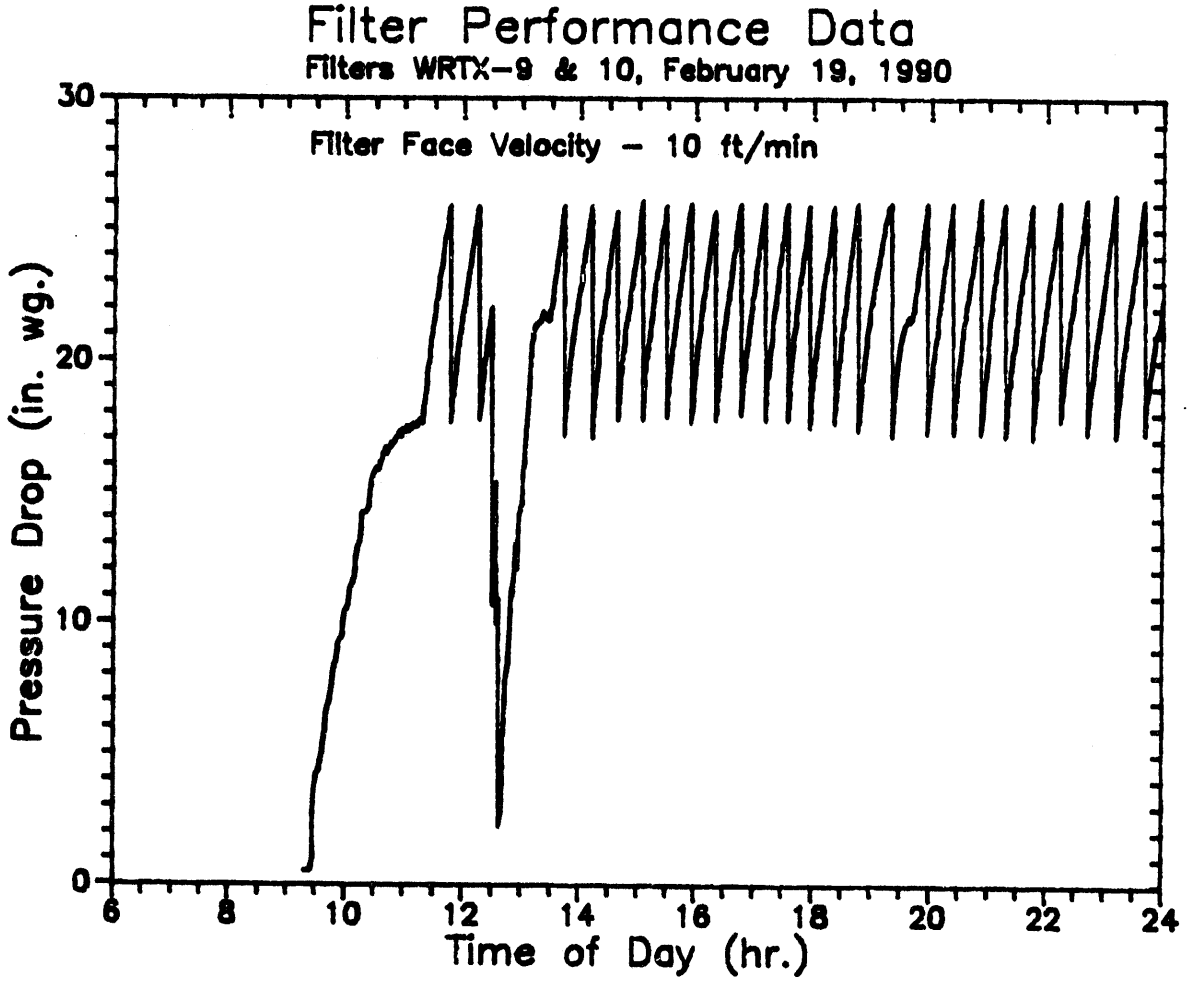

Operation Notes for February 19, 1990:

Start of week long test
1230 Flame out - unscheduled
Restarted
ΔP Trigger = 26.0" WC
Pulse Cleaning - 290 psig/0.1 sec

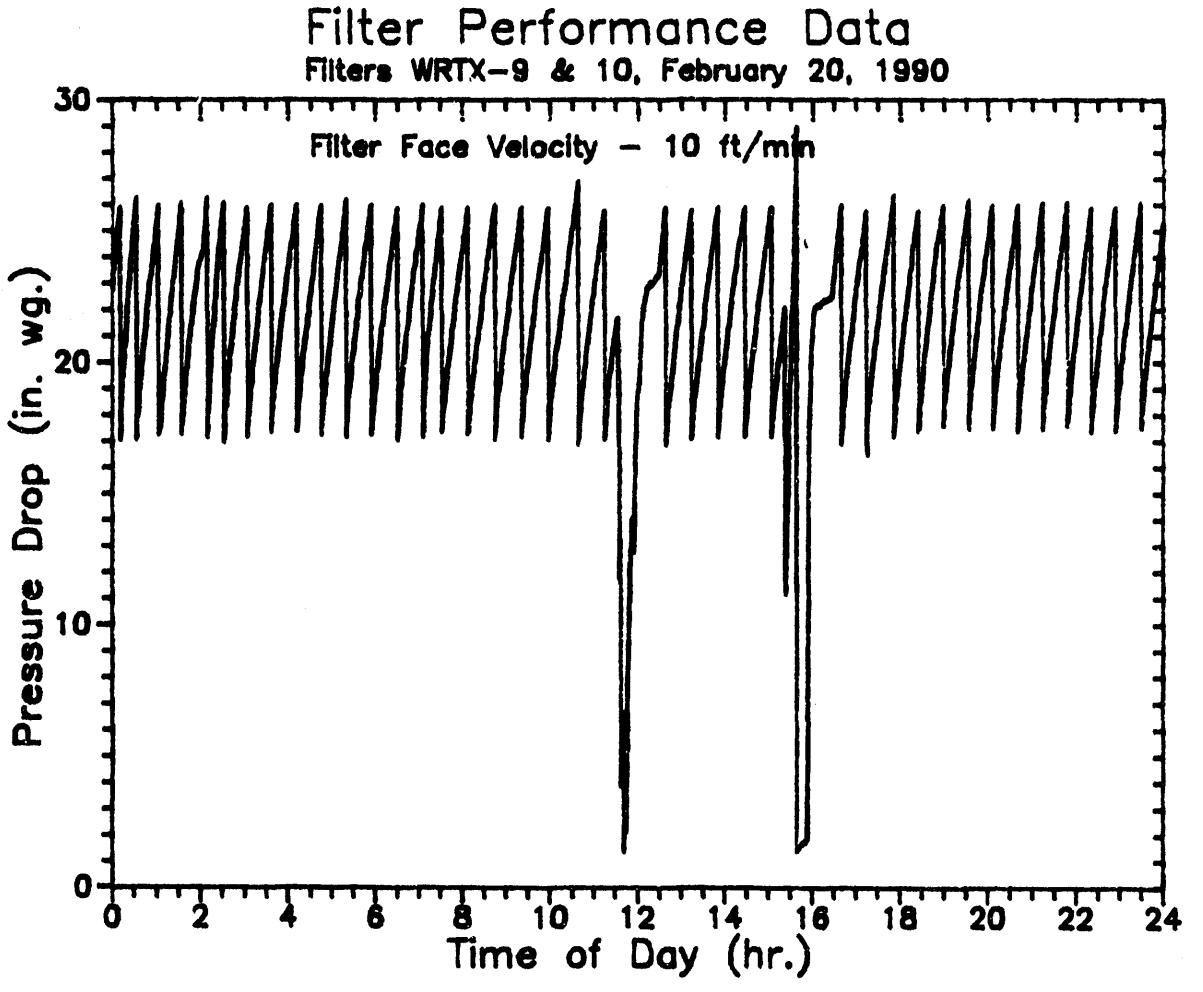

Operation Notes for February 20, 1990:

1130 Flame out - unscheduled
1520 Flame out - unscheduled
Restarted
ΔP Trigger = 26.0" WC
Pulse Cleaning - 290 psig/0.1 sec

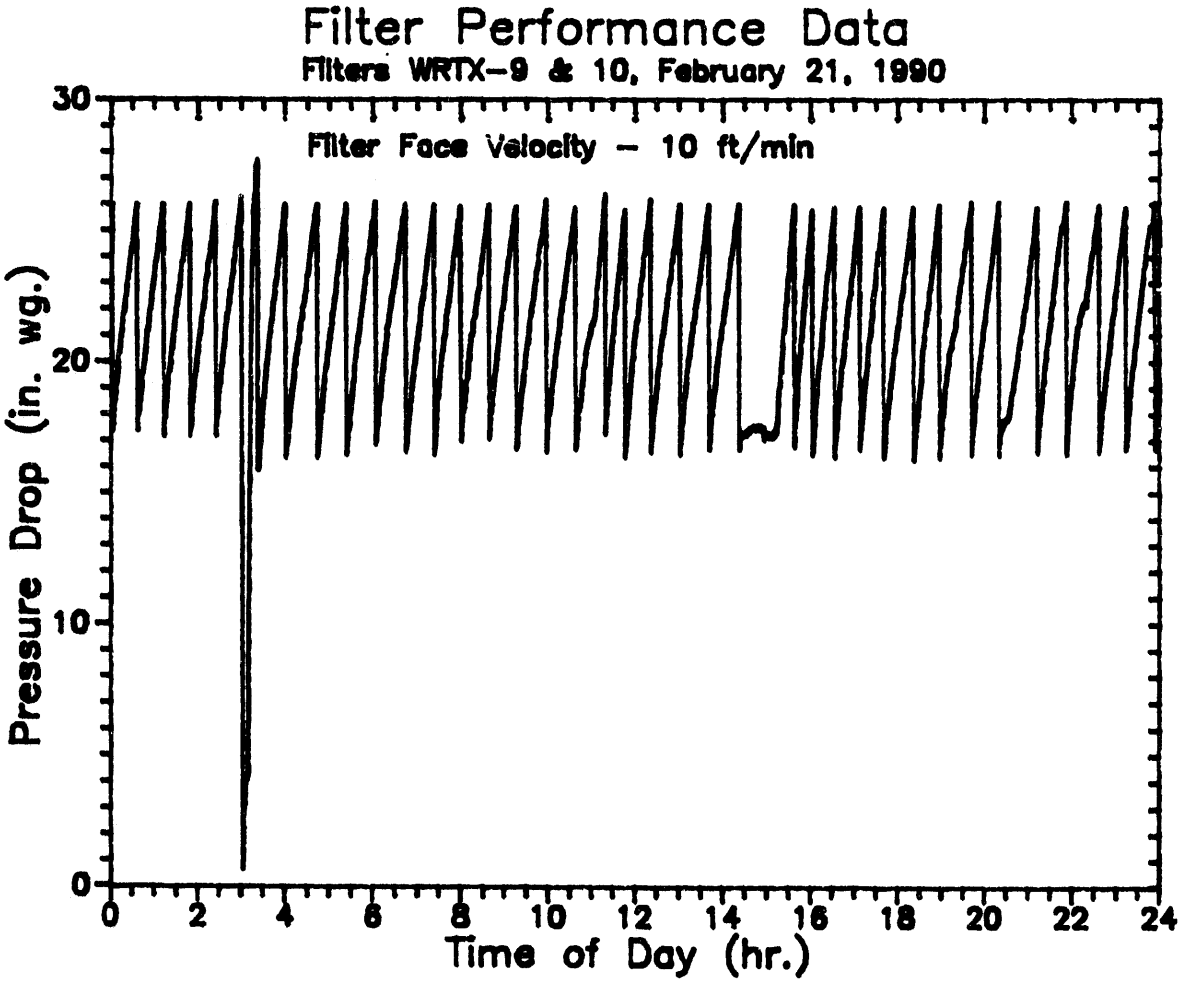

Operation Notes for February 21, 1990:

0300 Flame out - unscheduled
Restart
1430 Dust Added
Pulse Cleaning - 290 psig/0.1 sec

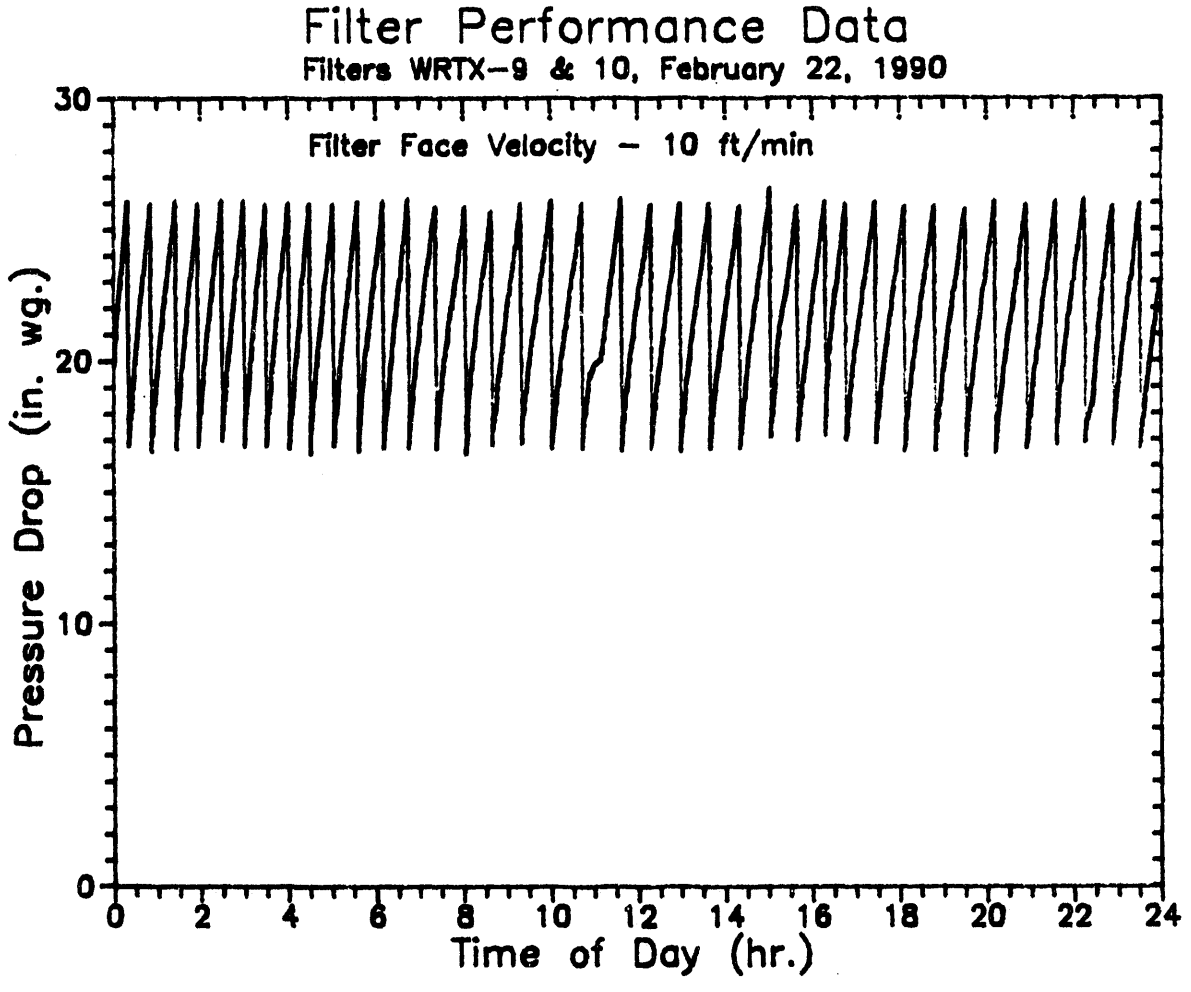

Operation Notes for February 22, 1990:
ΔP Trigger = 26.0" WC
Pulse Cleaning - 290 psig/0.1 sec

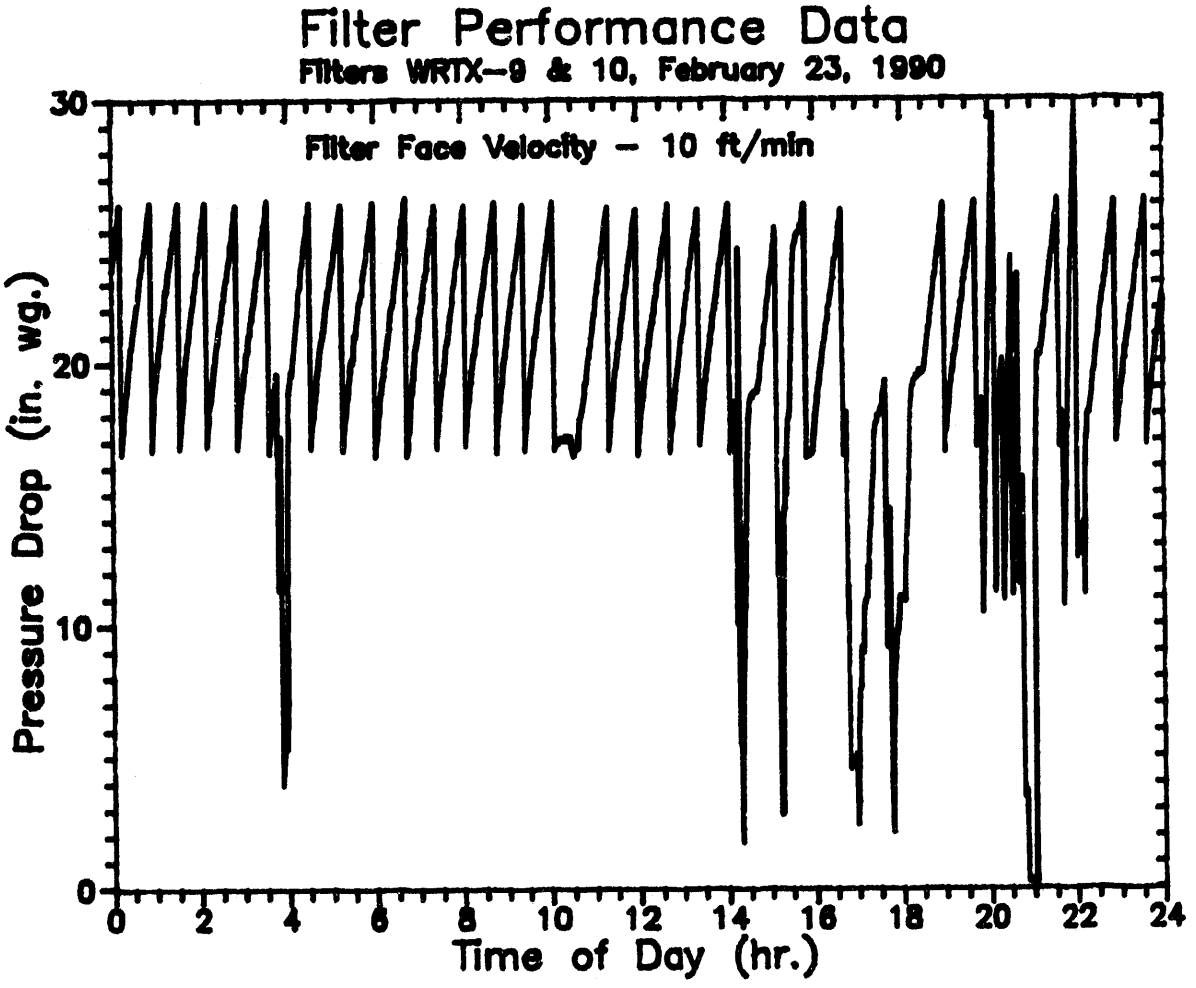

Operation Notes for February 23, 1990:

0345 Flame out - unscheduled
Restart
1000 Dust Added
1415 - 2200 Multiple Flame outs - unscheduled
Restarted each time
ΔP Trigger = 26.0" WC
Pulse Cleaning - 290 psig/0.1 sec

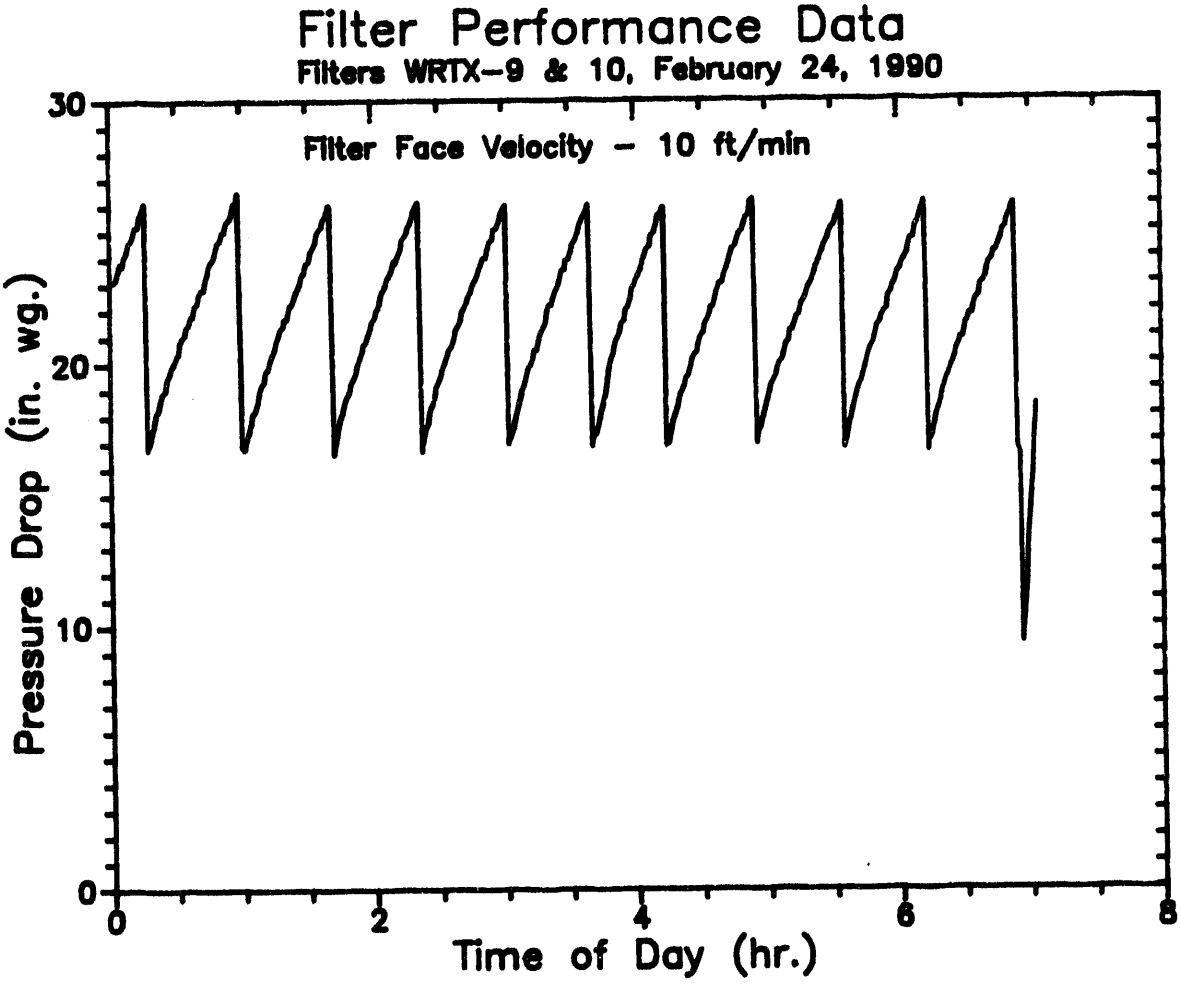

Operation Notes for February 24, 1990:
End of week long test
0700 scheduled shutdown
ΔP Trigger = 26.0" WC
Pulse Cleaning - 290 psig/0.1 sec

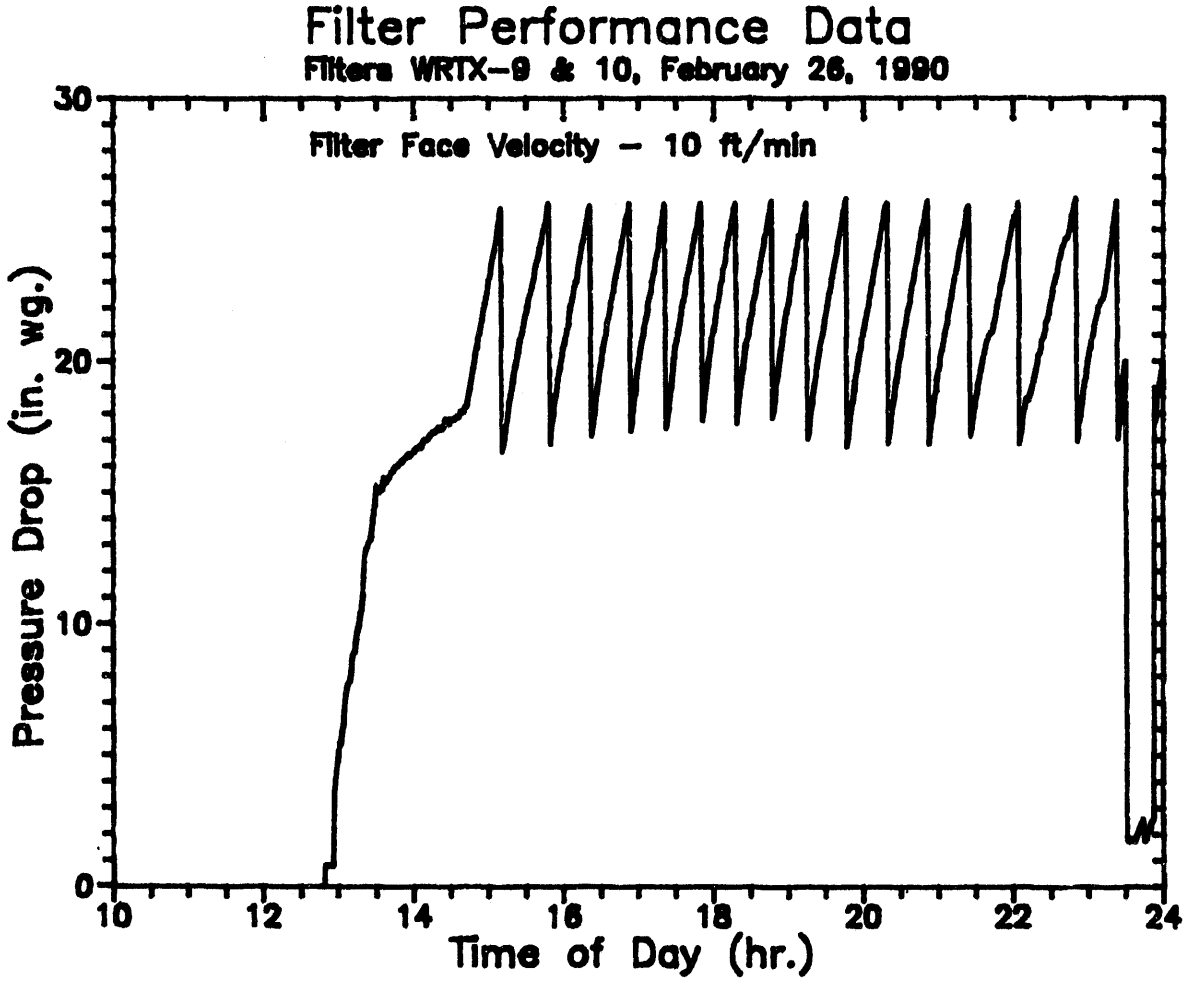

Operation Notes for February 26, 1990:

Start of week long test
Changed to Grimethorpe PFBC flyash for dust injection
2330 Flame out - unscheduled
Restart
ΔP Trigger = 26.0" WC
Pulse Cleaning - 290 psig/0.1 sec

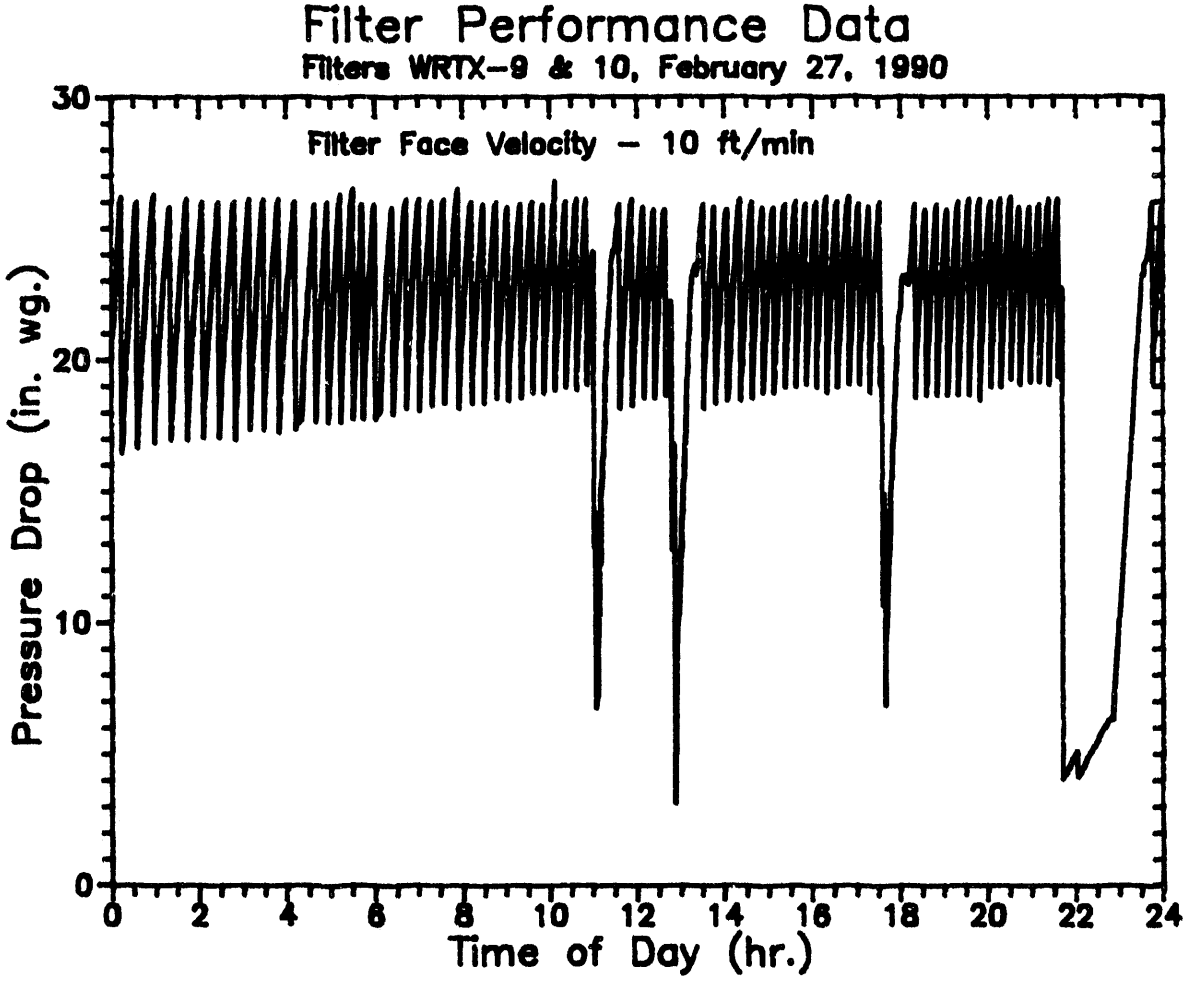

Operation Notes for February 27, 1990:

1100-2145 Multiple Flame outs - unscheduled
Restarted each time
ΔP Trigger = 26.0" WC
Pulse Cleaning - 290 psig/0.1 sec

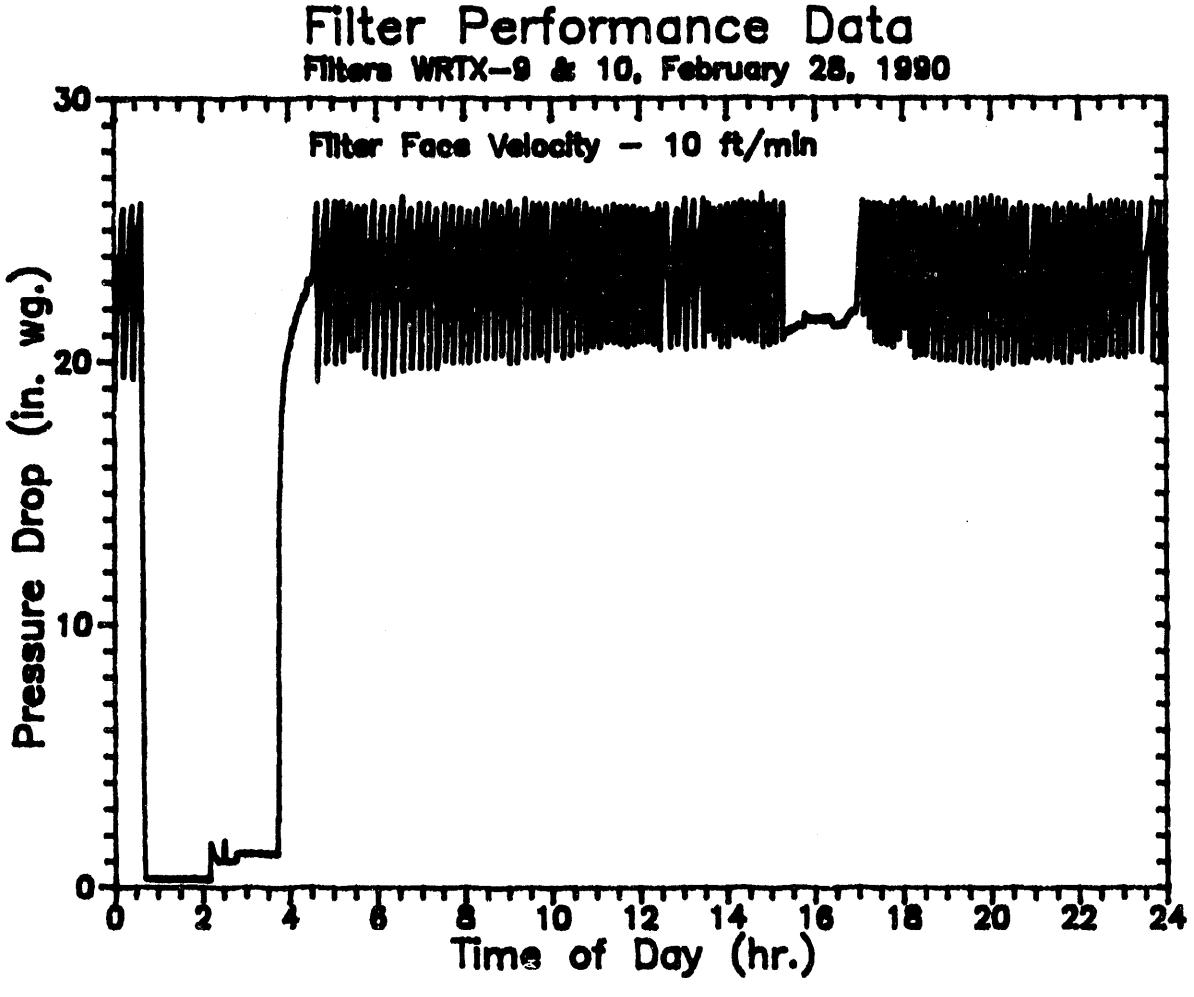

Operation Notes for February 28, 1990:

0040 Flame out - unscheduled
Temperature controller malfunction - repaired
Restarted
1515 Dust Added
ΔP Trigger = 26.0" WC
Pulse Cleaning - 305 psig/0.1 sec

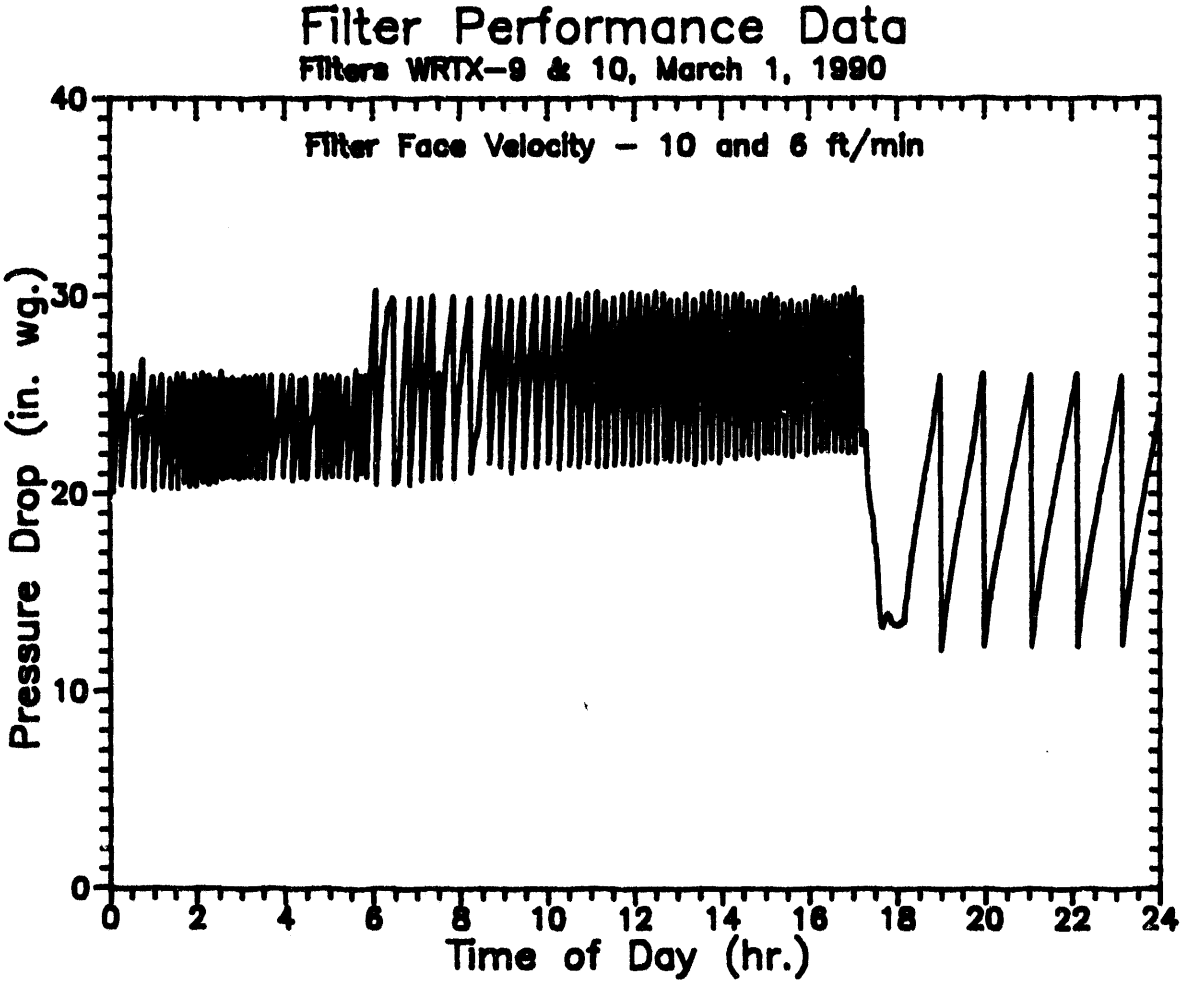

Operation Notes for March 1, 1990:

0600 Changed ΔP Trigger to 30.0 "WC
1800 Conditions changed from 10 ft/min to 6 ft/min face velocity, ΔP Trigger changed back to 26.0" WC
Pulse Cleaning - 315 psig/0.1 sec

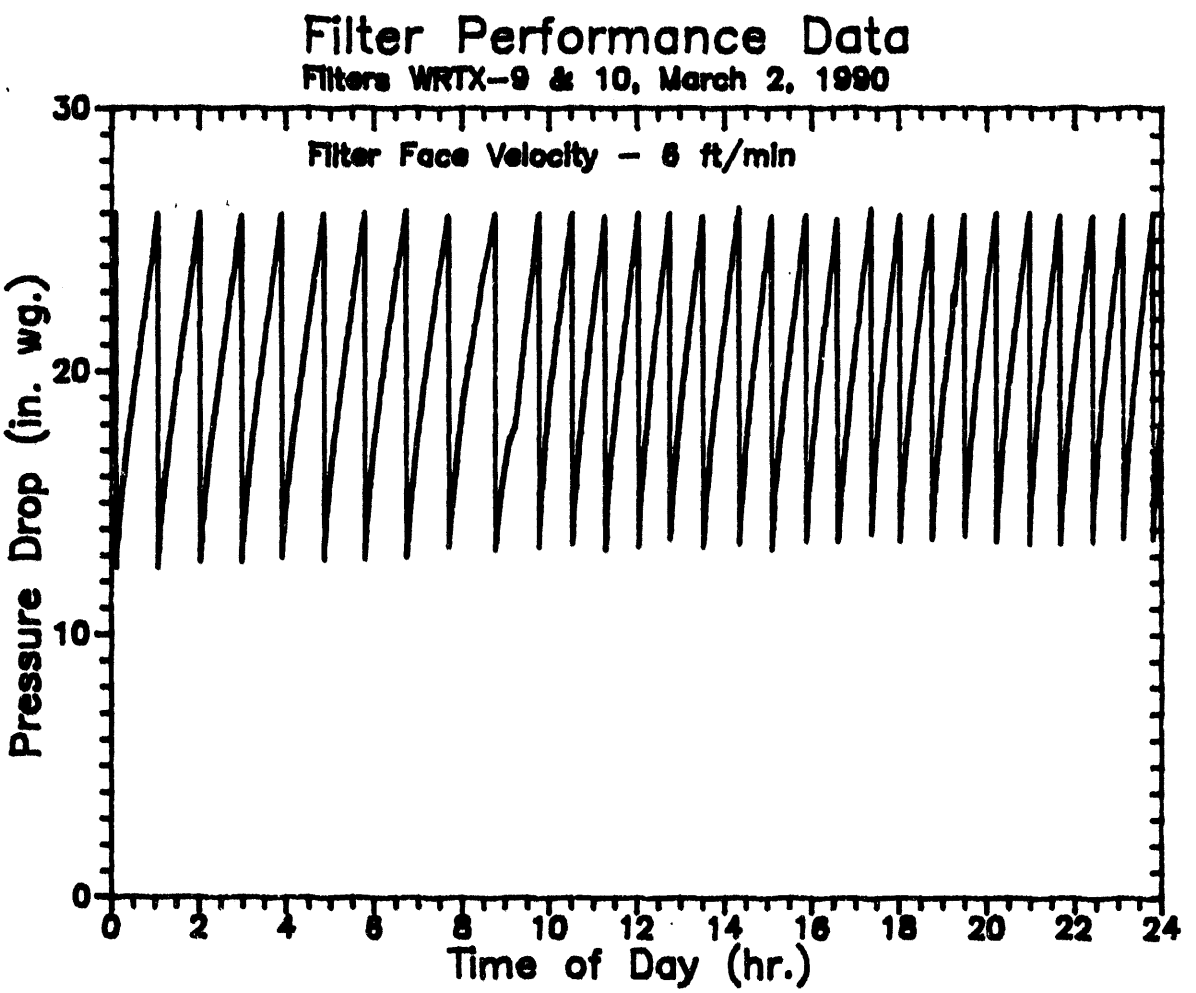

Operation Notes for March 2, 1990:
ΔP Trigger = 26.0" WC
Pulse Cleaning - 315 psig/0.1 sec

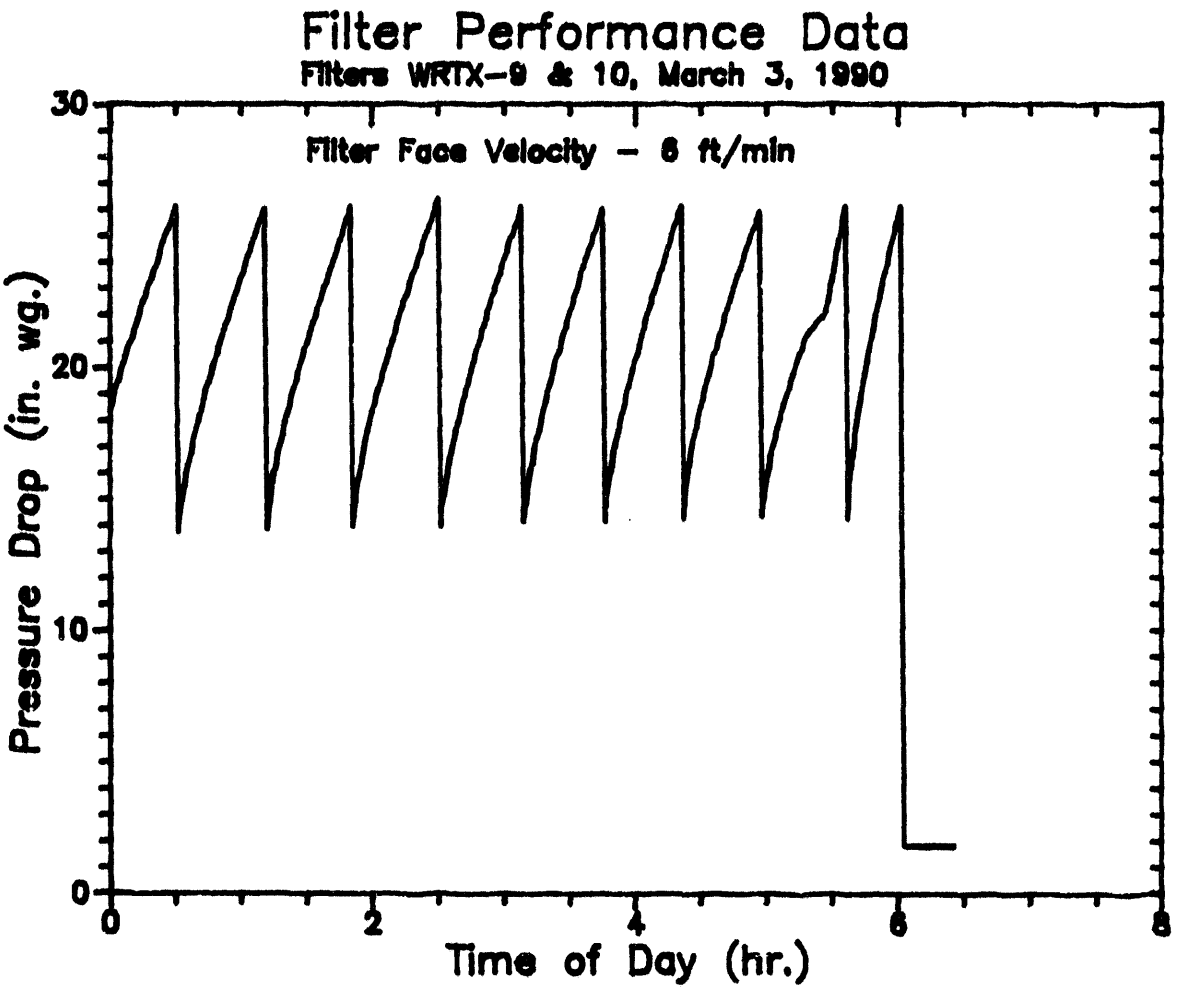

Operation Notes for March 3, 1990:
End of week long test
0600 scheduled shutdown
ΔP Trigger = 26.0" WC
Pulse Cleaning - 315 psig/0.1 sec

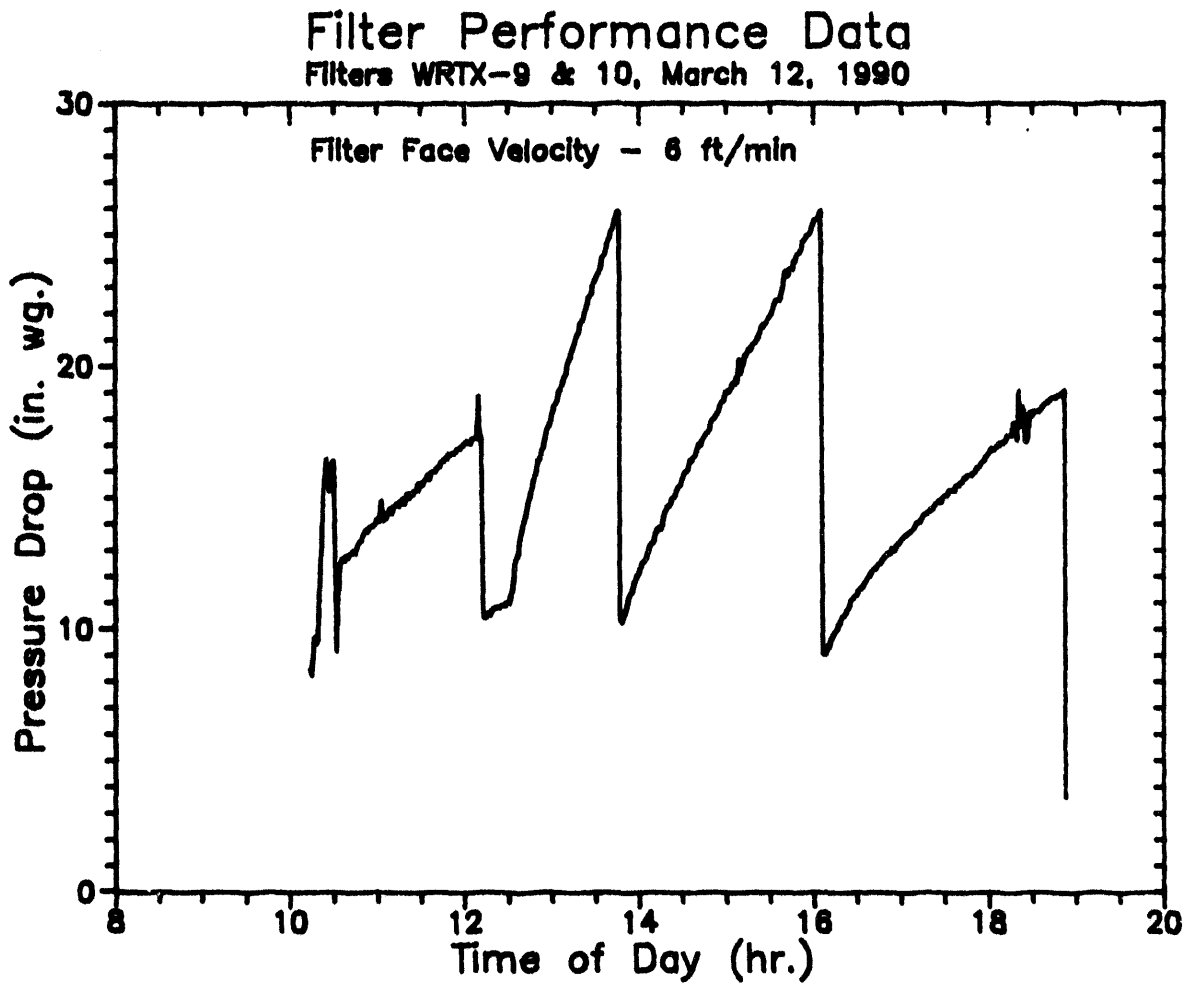

Operation Notes for March 12, 1990:

Dust out concentration higher than usual
Shutdown for inspection
ΔP Trigger = 26.0" WC
Pulse Cleaning - 315 psig/0.1 sec

APPENDIX E

ASSESSMENT OF CROSS FLOW FILTER MOUNTING DESIGN

FILTER SYSTEM STATUS

1.0 SUMMARY

Two cross flow filter elements were successfully tested under simulated PFBC conditions for over 1300 hours, thus representing the longest successful test campaign on this barrier filter technology. The filter operation was terminated when the dust loading on the filter outlet increased up to 100 ppm and the system permeability profiles suggested that a breach had developed on at least one of the elements. Post test inspection of the filter system revealed that one of the elements had developed a longitudinal crack on the ceramic flange, and the flange corners of both elements were crushed by the metal clamping plates. Neither filter showed any signs of delamination failure which had historically plagued the first generation of cross flow filters.

A comprehensive fractographic evaluation and a mechanical design analysis were undertaken to investigate and correct the cause of this failure. The flange failure ıttributed to three principal deficiencies in the current ıg apparatus, namely,

- Non-uniform loading of the ceramic flange imparting point or line stresses which ultimately lead to brittle fracture failure,

- Relaxation of the filter clamping bolts causing up to 90% reduction of the seating forces on the filter and gasket after about 1000 hours of hot testing such that the element could either vibrate, or in the extreme, levitate during reverse pulse cleaning,

- Imposition of differential contraction stresses on the ceramic flange during shutdown periods caused by the accumulation of dust in the cavities outside the element seating area.

A retrofit design has been proposed to eliminate the deficiencies in the current mounting apparatus. It is recommended that this retrofit be implemented on the PFBC simulator facility and other cross flow filter prototypical test facilities to ensure long term operational reliability of this cleanup system.

2.0 DESCRIPTION OF CURRENT SYSTEM

The PFBC long term durability test rig can accommodate up to four commercial scale cross flow filter elements which are distributed on two metal plenum pipes suspended from an uncooled metal tubesheet. During the 1304 hours of simulated PFBC testing only one active plenum with two filter elements was used. The second plenum was installed with blank metal plates covering the filter seating areas of the plenum fixtures. The following discussion provides background information on the filter elements and the current assembly procedure.

2.1 Element Geometry

The two filter elements tested in the PFBC rig, labelled WRTX-9 and WRTX-10, featured the use of the mid rib bond and radiused flanges for enhancing the mechanical strength of the ceramic flange and filter body. Prior to installation these elements were characterized for their permeability at ambient conditions and found to be within the Westinghouse acceptance criteria for pressure drop, namely less than 5 in. wc. at a face velocity of 10 fpm. The elements were dimensionally checked to verify fitup inside the metal fixture. During this inspection one of the elements was found to be oversized along the length, causing an interference with the fixture. Therefore a small

section of the end plate 5 inches wide by 0.5 inch high and 0.2 inch deep was cut using a diamond saw. Per normal practice the seams between the individual plates were painted with a ceramic glue as a precautionary measure against dust infiltration through any gaps left in the manufacturing process. In addition the clean side channel rows on the two outer edges of the element (near the 12x4 end plates) were filled with the ceramic cement because these channels are otherwise blocked by the gasket material.

The flanges of the two elements were inspected to verify that the radiused fillet on each flange met the Westinghouse specification and that there were no residual sharp edges or corners on the flange and fillet surface.

2.2 Element Mount Configuration

Figure E.1 is an engineering drawing of a typical element mount configuration. The element rests on a stainless steel ledge which is welded to the support fixture. After installation the ceramic flanges on the element are nearly flush with the upper surface of the fixture. The filter flanges are clamped to the fixture by means of stainless steel plates, 13 inches long by 1.25 inches wide and 0.375 inch thick. Each plate is held by four 0.25 inch 316 stainless steel bolts.

Figure E.2 shows an end view of a fully assembled "ideal" filter element (i.e., an element that meets all dimensional tolerances). The clamping plate would rest flat and parallel with the top surface of the flange with a compliant layer of gasketing material between the metal and the ceramic. Note also the position of the compressed gasket under the filter which functions as a dust seal during filtration (forward flow) periods and a partial gas seal during any pulse cleaning event (reverse flow).

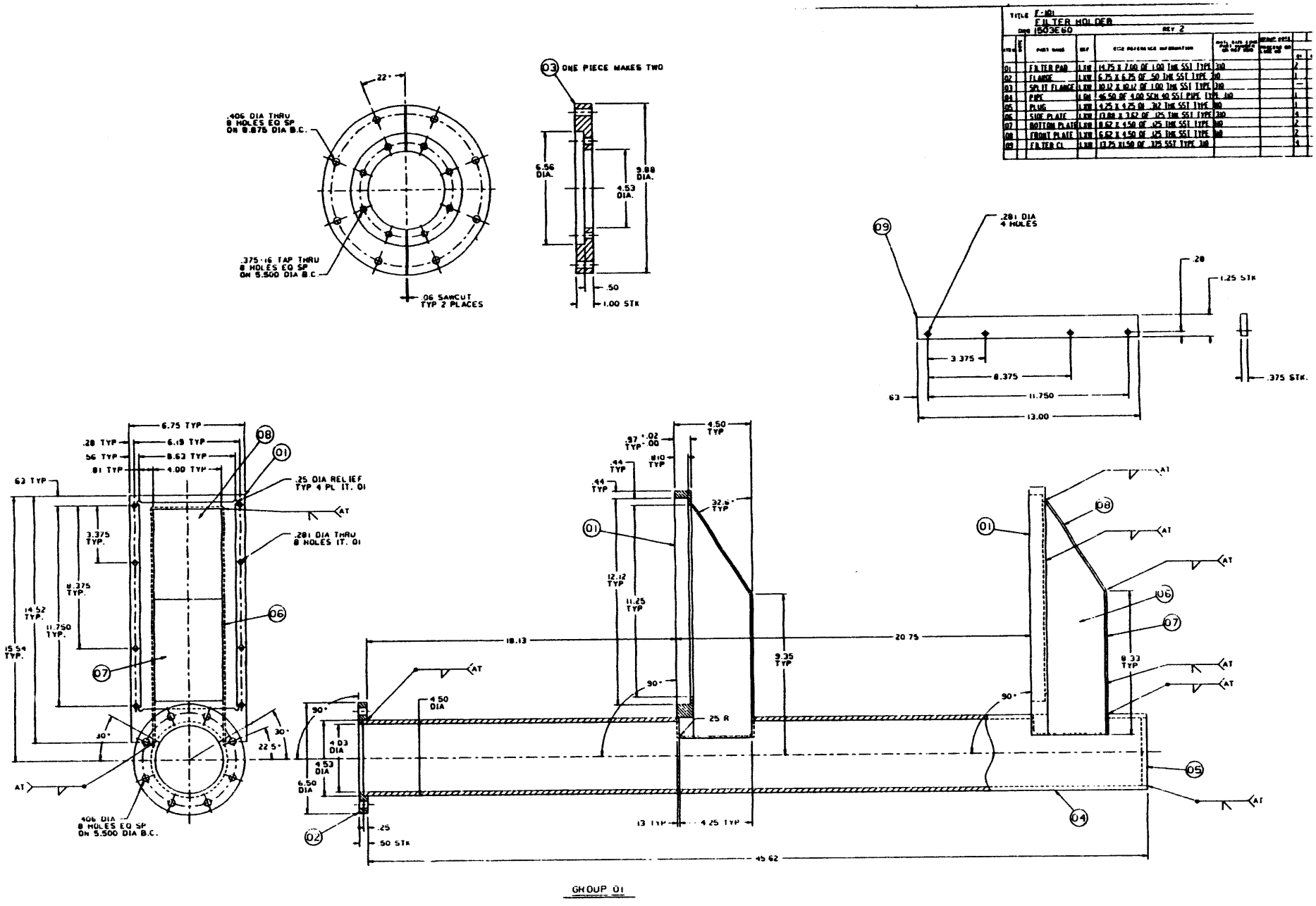

Figure E.1 - Typical Element Mount Configuration

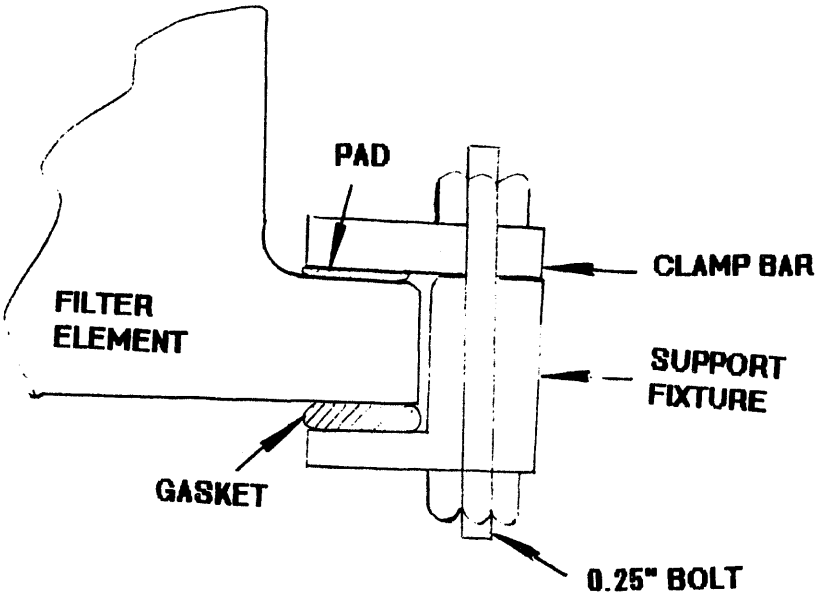

Figure E.2 - End View of an "Ideal" Assembled Filter Element

2.3 Gasketing Materials

As shown above there are two gasketing materials used for fixing the ceramic element inside the metal fixture. The top layer is essentially a compliant pad to fill the asperities on the ceramic flange surface. The material used for this purpose on the PFBC test rig was a 0.15 inch thick layer of Interam Brand Mat Mount made by the 3M Company. This material is made of alumina silicate fibers interspersed with an intumescent or heat expandable layer of vermiculite. While this material has found commercial use as a gasket on catalytic converters, the upper temperature limit is only 1300°F. Figure E.3 shows a photograph of an Interam pad after exposure to a temperature of 1600°F for 8 hours. Note that the pad completely disintegrates into powder after exposure to PFBC type conditions, which indicates that the material has marginal resilient properties and, at best, only provides a residual granular layer sandwiched between the clamping plate and the ceramic flange.

The bottom gasket, on which the element rests and which actually functions as the dust seal, is a Westinghouse assembled pad made of 3M's commercially available Nextel fabric and a silica-boria-alumina fiber blanket, shown in Figure E.4. After exposure to the PFBC simulator conditions for 1304 hours and 2068 pulse cleaning cycles, there was virtually no damage or distortion sustained by this gasket. The load-deflection characteristics for the unused and the exposed gasket, as measured on a standard testing machine, were found to be identical; thus indicating that the gasket does not experience any long term deterioration in its resiliency properties.

2.4 Assembly Methods

During assembly the dust seal gasket is first installed on the metal ledge inside the fixture. The filter is then seated on the dust seal and loaded with a 400 lbs. weight placed on top of the element,

Figure E.3 - Interam Gasket After Exposure to 1600°F for 8 Hours.

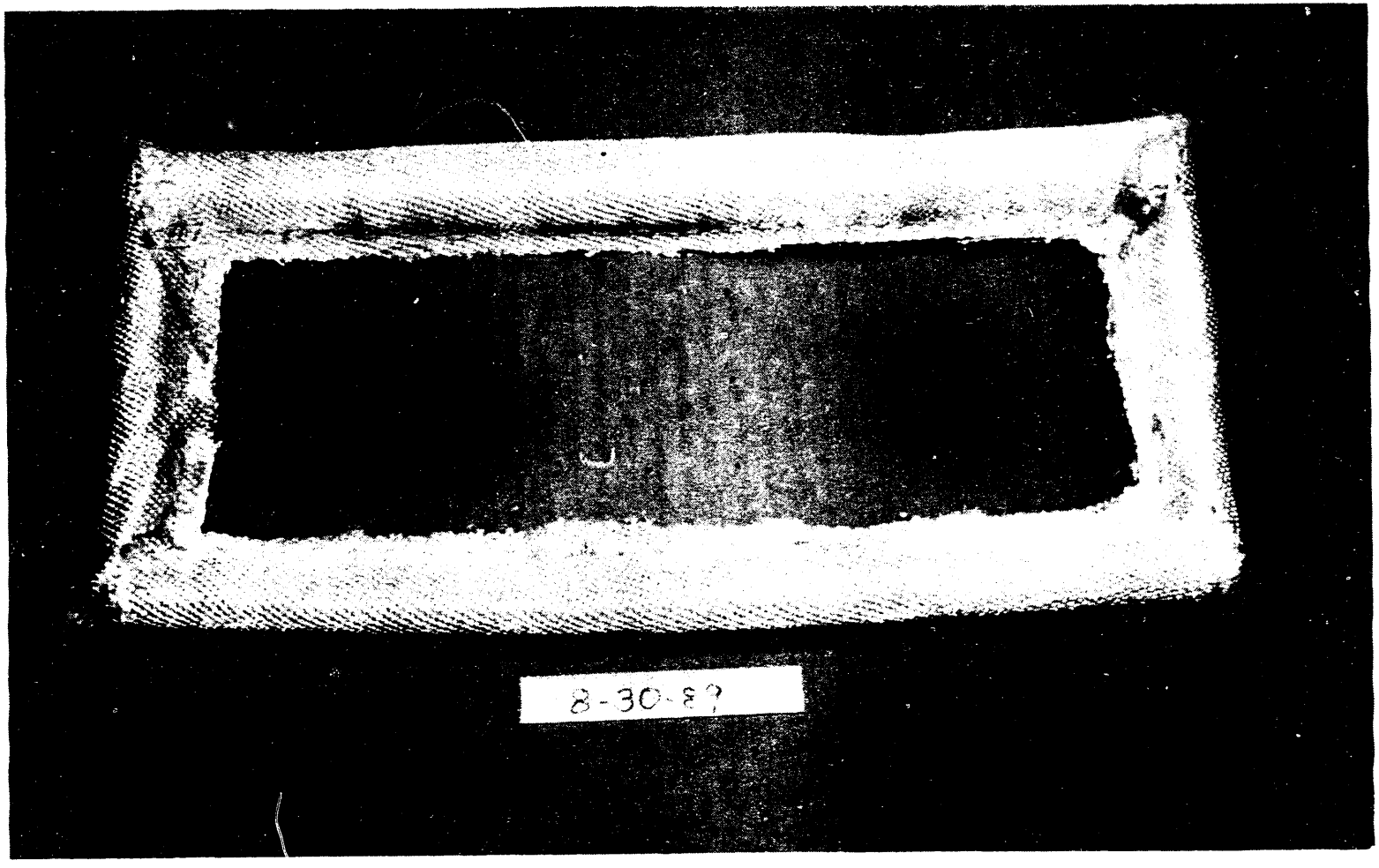

Figure E.4 - Photograph of Nextel Reinforced Fiber Blanket Pad Used as Dust Seal.

thereby uniformly compressing the gasket. Two strips of Interam pads are then placed on the ceramic flanges which are then covered by the clamping plates. The eight bolts are assembled finger-tight and subsequently torqued to 15 in-lbs. The weights are now removed thus providing a total nominal gasket seating force of 2430 lbs.

Each element is then mounted with side compression plates to provide precautionary reinforcement against element delamination. These plates are made of 4 inch by 12 inch by 0.25 inch thick 316 stainless steel plates, which are assembled using metal tie-rods to provide a compressive force of approximately 1400 lbs. Six ceramic rods are then fitted into corresponding slots on the sides of the parallel plates, these rods are held in place by compression collars. After assembling the ceramic rods the metal rods are removed. Interam pads are used as cushioning material between the metal end plates and the ceramic side walls of the filter. Figure E.5 shows a photograph of a typical fully assembled filter element.

3.0 ASSESSMENT OF SYSTEM RELIABILITY

The PFBC simulator rig containing the two ceramic filter elements was operated for a total of 1304 hours. The system was subjected to 43 warm standby to startup cycles and 6 cold shutdown to startup cycles. The filter pressure vessel was first disassembled at the end of the 1304 hours when the dust mass loadings at the exit of the filter showed a dramatic increase from a nominal 3 ppm to over 100 ppm. This excursion was diagnosed as a serious breach in at least one of the filters, hence the testing was thereafter discontinued. The results of the operational analysis, system inspection and failure analysis are reported below.

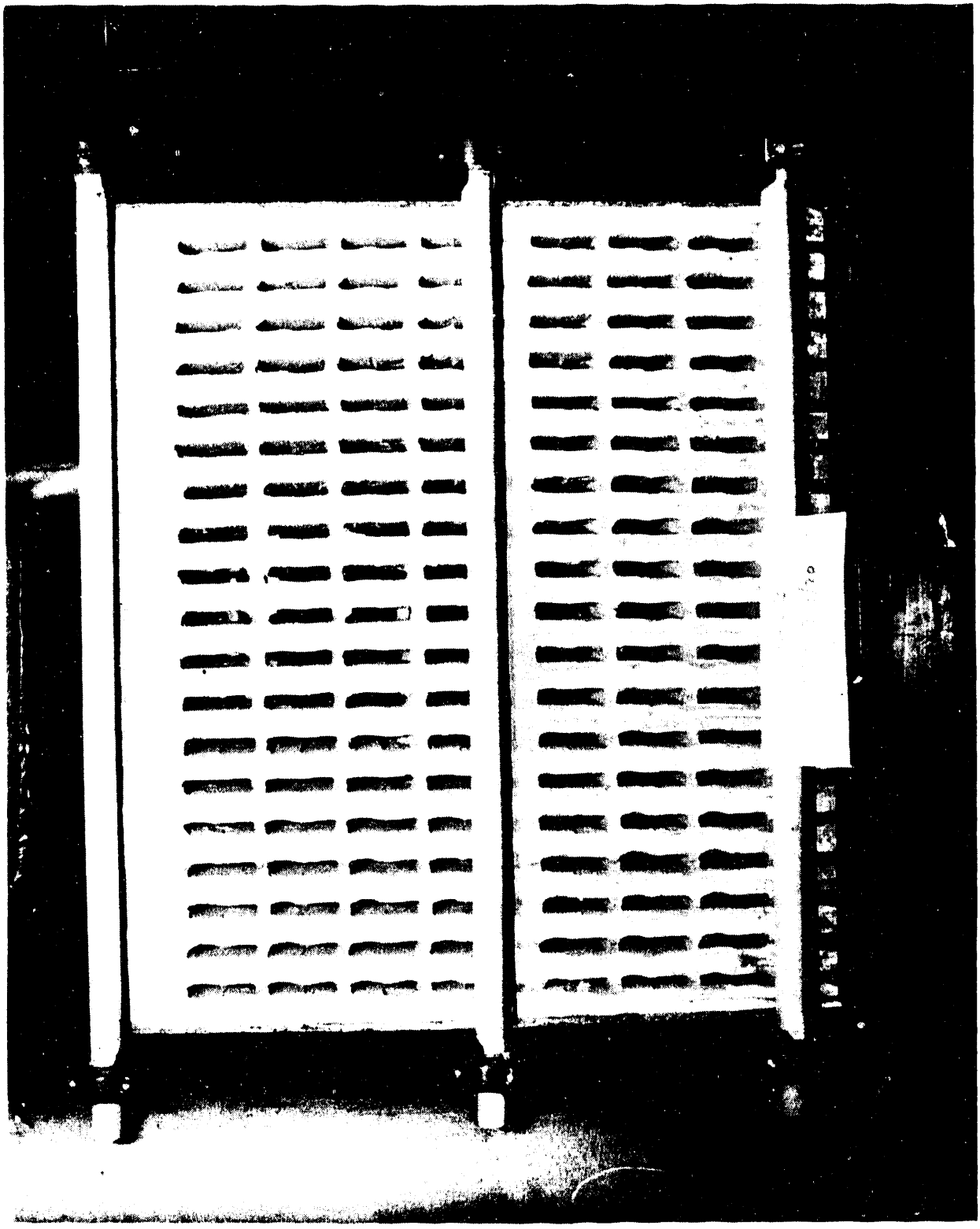

Figure E.5 - Photograph of an Assembled Filter Element

3.1 Operational Analysis

The test campaign of 1304 hours represented the longest successful test exposure of cross flow filters to the high temperature and high pressure PFBC conditions. During the first 1300 hours of testing the system operated as a barrier filter releasing trace quantities of PFBC dust. The system pressure drop profiles showed consistent recovery after each pulse cleaning action, indicating efficient removal of dust cake. As discussed elsewhere in this report, the residual or baseline pressure drop showed a normal stabilization behavior at a value approaching 20% of the unused filter permeability. In an attempt to identify the sequence of operational events that may have triggered the filter failures, the operational behavior of the filter system was closely examined.

The outlet dust loading profiles for the entire test campaign are shown in Figure E.6, wherein the test interruptions are marked by the "S" and "C" symbols designating the warm startups (from a warm standby condition at 600°F temperature) and cold startups (from ambient temperature conditions) respectively. It is interesting to note in this chart that, with the exception of C7, all other startups were marked by a 10 ppm spike in the outlet loading (not necessarily dust) which subsides to less than 1 ppm within a few hours of hot operation. Figure E.7 shows a typical sequence of dust samples extracted by the sample probe following an interim shutdown. The initial samples consistently show a black patch on the filter paper, the samples subsequently become lighter and after about 10 hours show a faint smearing of the beige color which is characteristic of the PFBC ash. This trend in the dust profile indicates that the internal 316 stainless steel components develop corrosion scale from exposure to the damp shutdown conditions. After the system has been reheated the black scale is released. It is concluded that the 10 ppm spikes occurring over the

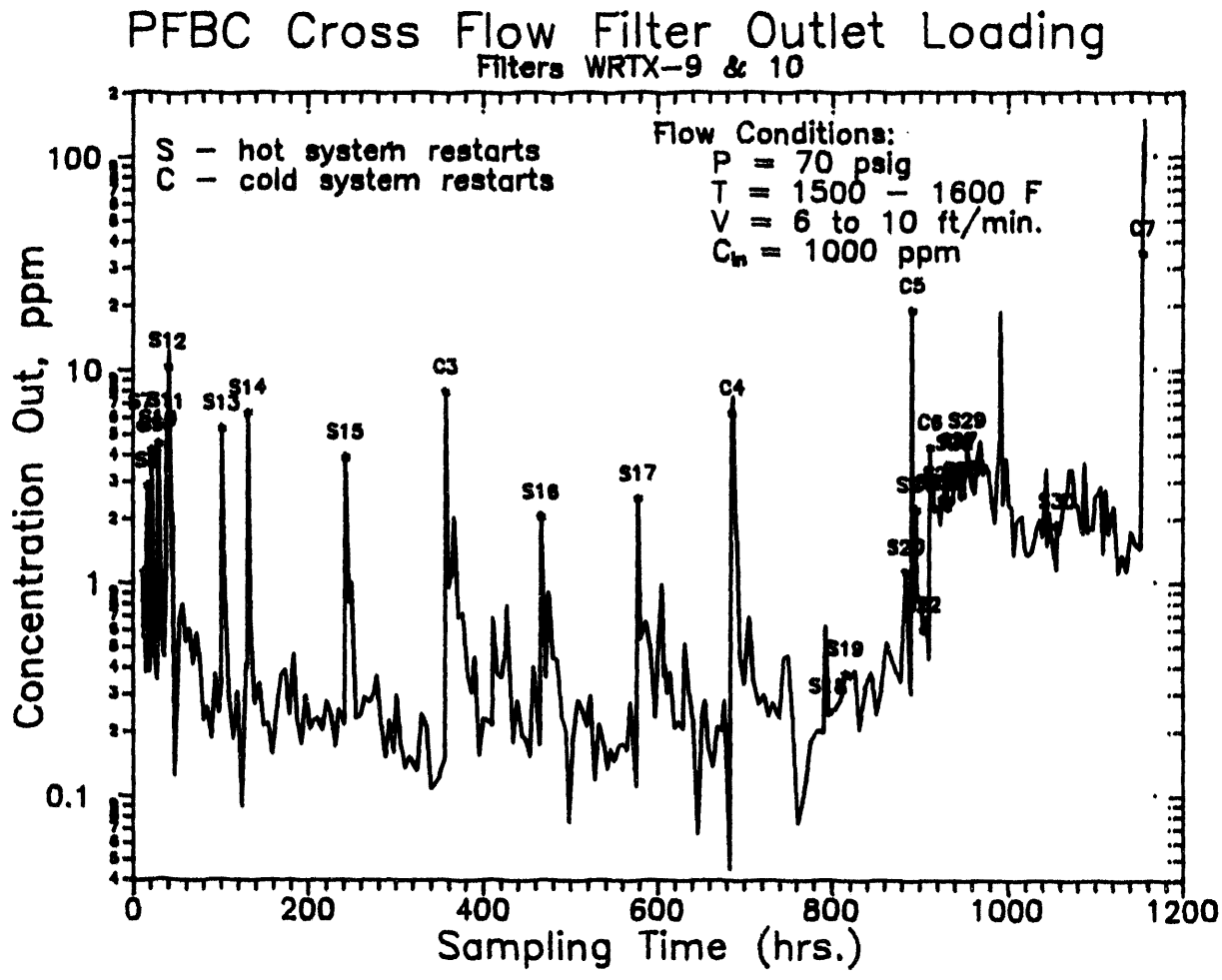

Figure E.6 - Filter Outlet Loading Profiles During PFBC Simulator Test

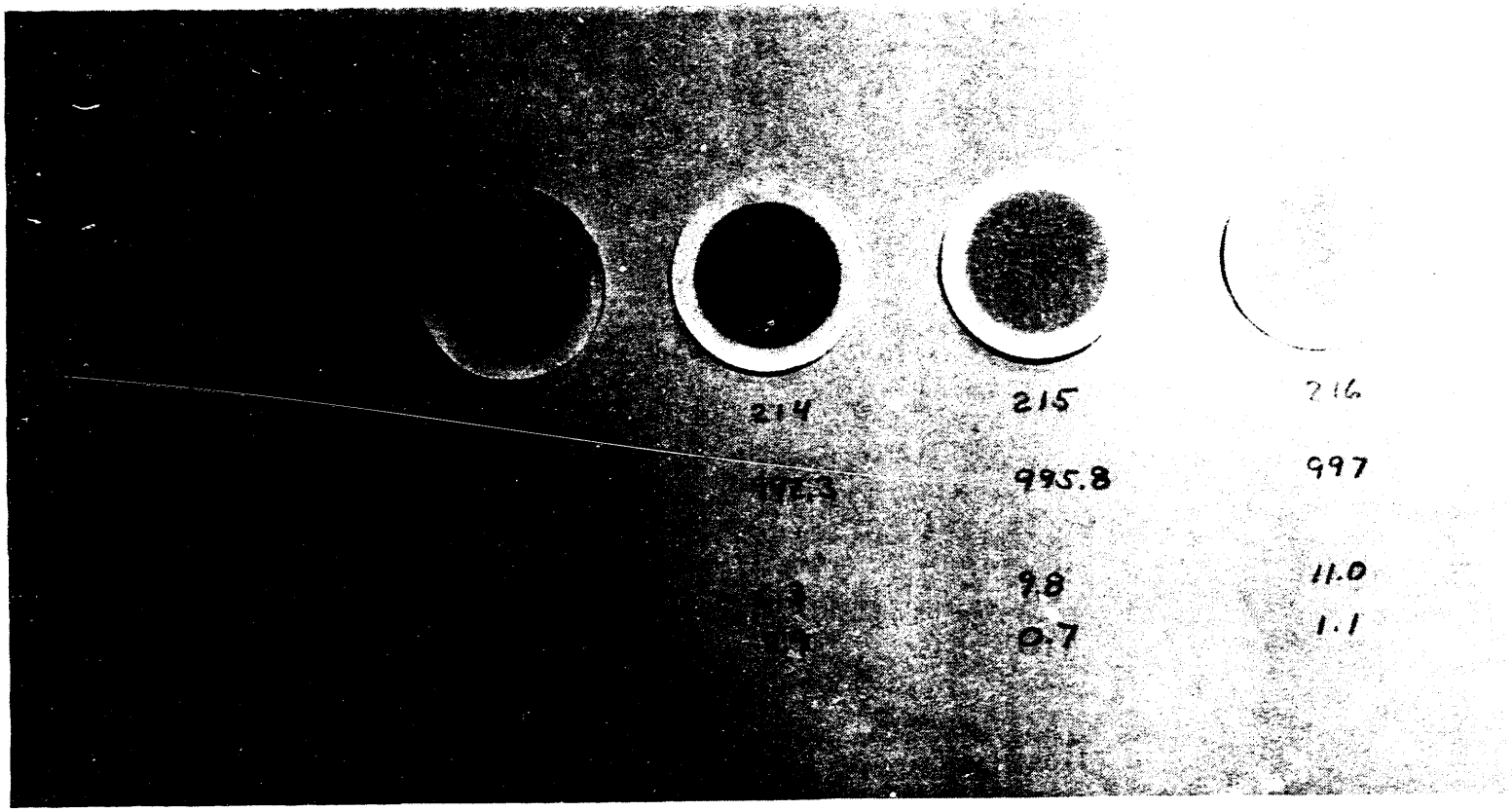

Figure E.7 - Progression of Outlet Dust Samples Following Interim Shutdown.

first 1300 hours of testing are, in fact, the corrosion scale released by the internal steel lining, and the actual PFBC dust penetration throughout the bulk of the test campaign was less than 1 ppm.

From the dust loading traces in Figure E.6 it appears that the filter elements developed an initial breach after shutdown C6 (increase from less than 1 ppm to about 4 ppm) which increased in severity after shutdown C7 when the loadings exceeded 100 ppm. The overall system permeability, defined as the reciprocal of the normalized pressure drop, was analyzed for the post C6 shutdown test periods. As shown in Figure E.8 the permeability did not show an increase until after shutdown C7 suggesting that the first stage of failure after C6 was a small crack which only allowed seepage of dust cake, whereas the second stage of failure was a large crack which permitted significant bypassing of dust laden gases into the clean side of the system.

3.2 Inspection and Fractographic Examination

The tubesheet and plenums were removed from the vessel and first inspected with a borescope inserted from the top open end of the plenum pipe. The internal cavities of the two fixtures showed some accumulation of the beige colored PFBC dust; it appeared that the top fixture with element WRTX-10 contained more dust than the lower fixture with WRTX-9. The compression braces on both elements were found to be loosely connected, and one of the end plates had actually become detached from the ceramic rods. The elements were securely seated in their respective fixture cavities and did not show any outward indication of breakage or cracking.

The clamping plates on both filters appeared to be tilted such that the inside edges of the plates actually impinged on the ceramic flange surface. Cracks emanated from the contact point and appeared to have propagated into the fillet of the flange.

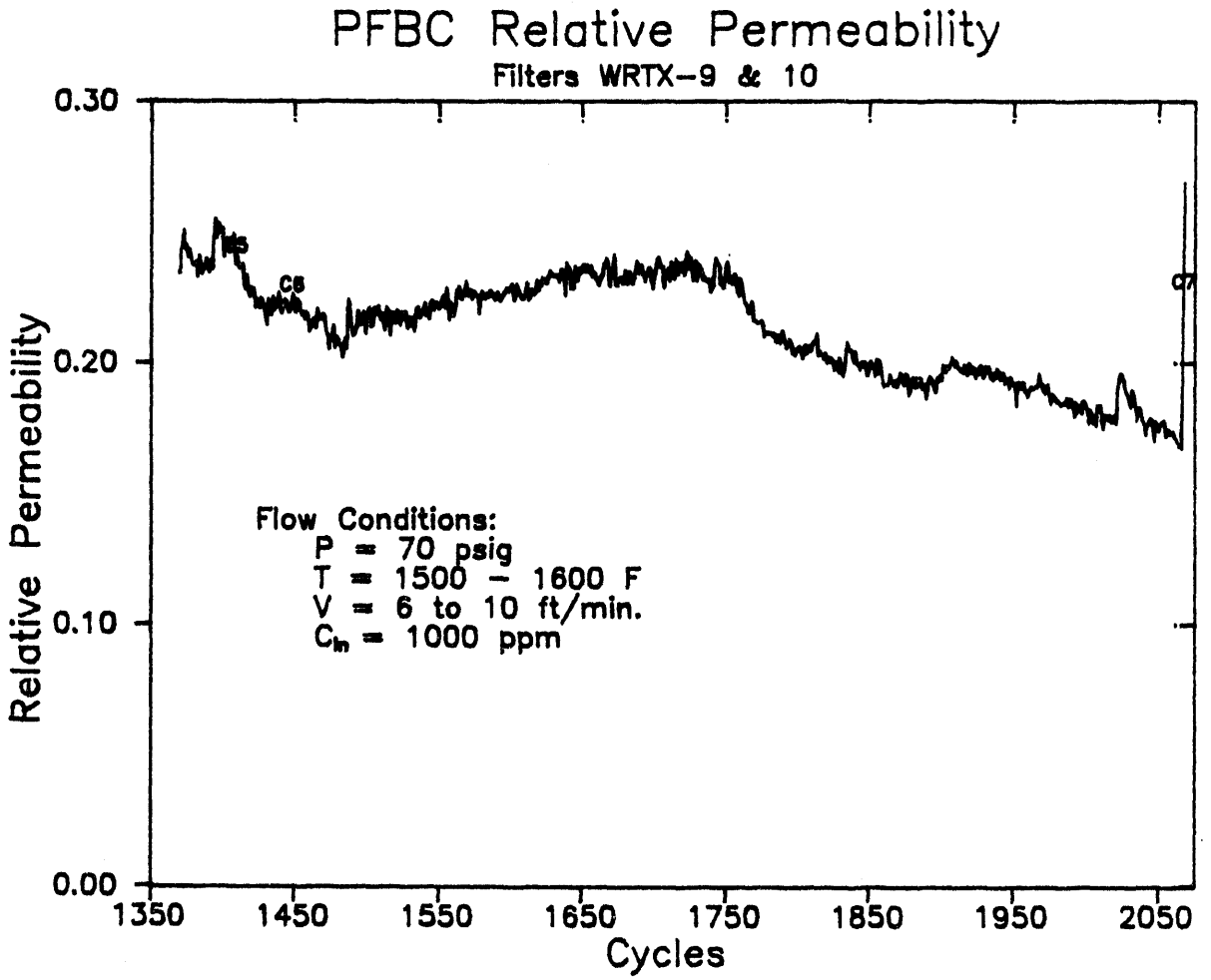

Figure E.8 - Filter Permeability Trends During PFBC Simulator Test

The side plate of filter WRTX-10 (which was machined prior to installation) showed cracking and spalling along the bottom face as shown in Figure E.9. The cracking and spalling may have been caused by the thinning of the end plate during the machining process.

The flange surfaces were examined after removal of all four clamping plates. The flange corners of both filters showed severe crushing and/or cracking damage, as typified in Figure E.10. The gaps between the flanges and the metal fixture were completely filled with fly ash.

The most significant failure was a longitudinal crack along one of the flanges on filter WRTX-10, as shown in Figure E.11. The crack appeared to have started at the corners and propagated through the fillet and caused a separation of the filter body from the flange.

The bottom filter WRTX-9 was wedged firmly into the fixture by the fly ash and, during disassembly, a part of the flange was sheared off. Figure E.12 shows a remnant of this flange and the gasket after removal of the element. The fly ash present on the corners of the gasket indicates that the corners of the flanges were crushed during operation, allowing dust penetration.

Figure E.13 describes, in schematic form, the shapes of the various fractures formed on these filters during operation.

3.3 Failure Mechanisms

- The clamping bars rested partly on the fillets between the flanges and the body of each filter, and partly on the edges of the flanges. This caused concentrated pressures on the filters and bending of the flanges, as well as bending of the bolts.

Figure E.9 - End View of Filter WRTX-10, Shows Cracking and Spalling in the Area Which Was Machined Prior to Installation

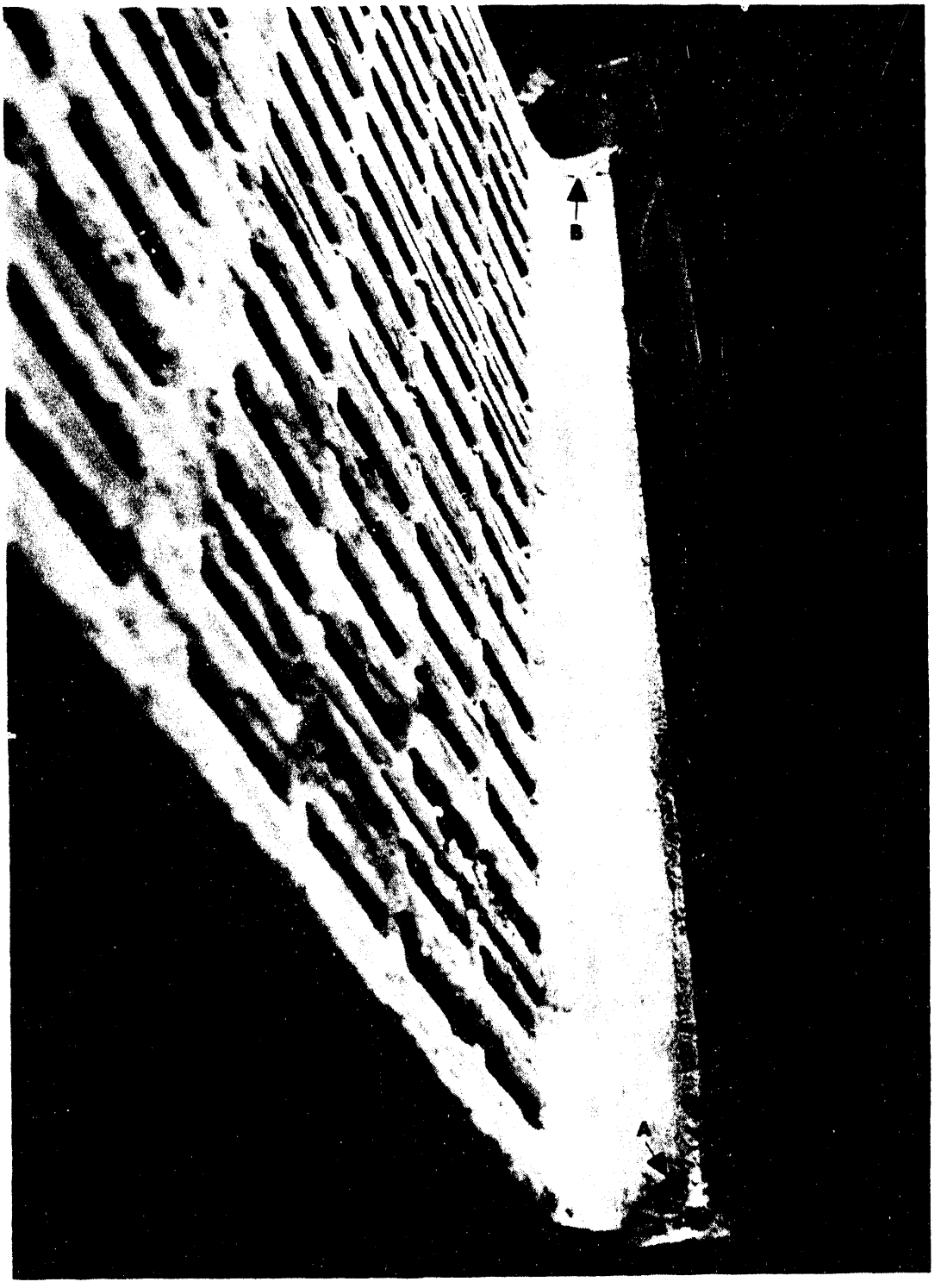

Figure E.10 - Top View of Filter, Shows Crushing and Cracking on Flange Corners and Accumulation of Dust in the Fixture Cavity

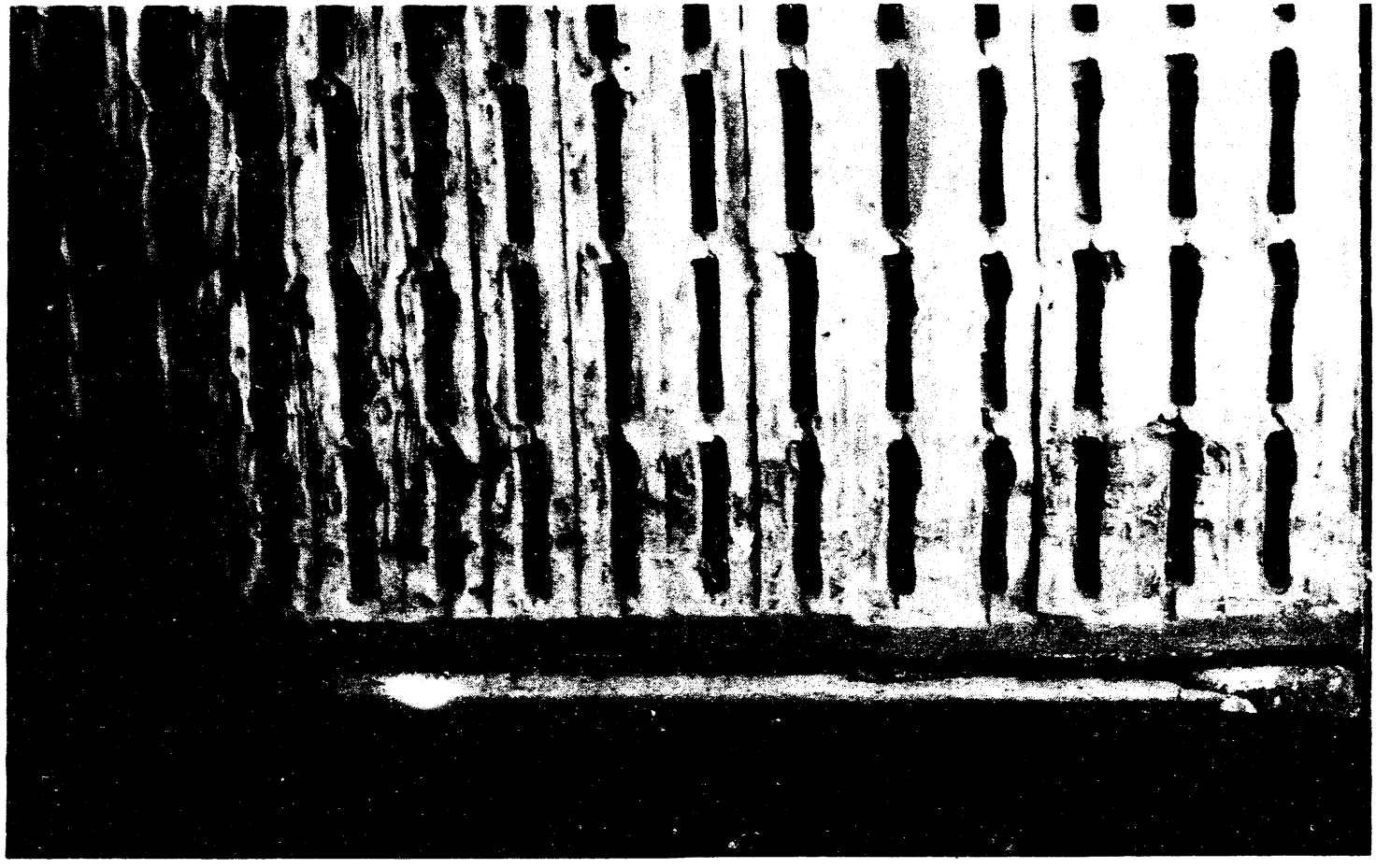

Figure E.11 - Frontal View of Filter WRTX-10, Shows Longitudinal Crack Along the Fillet of the Flange

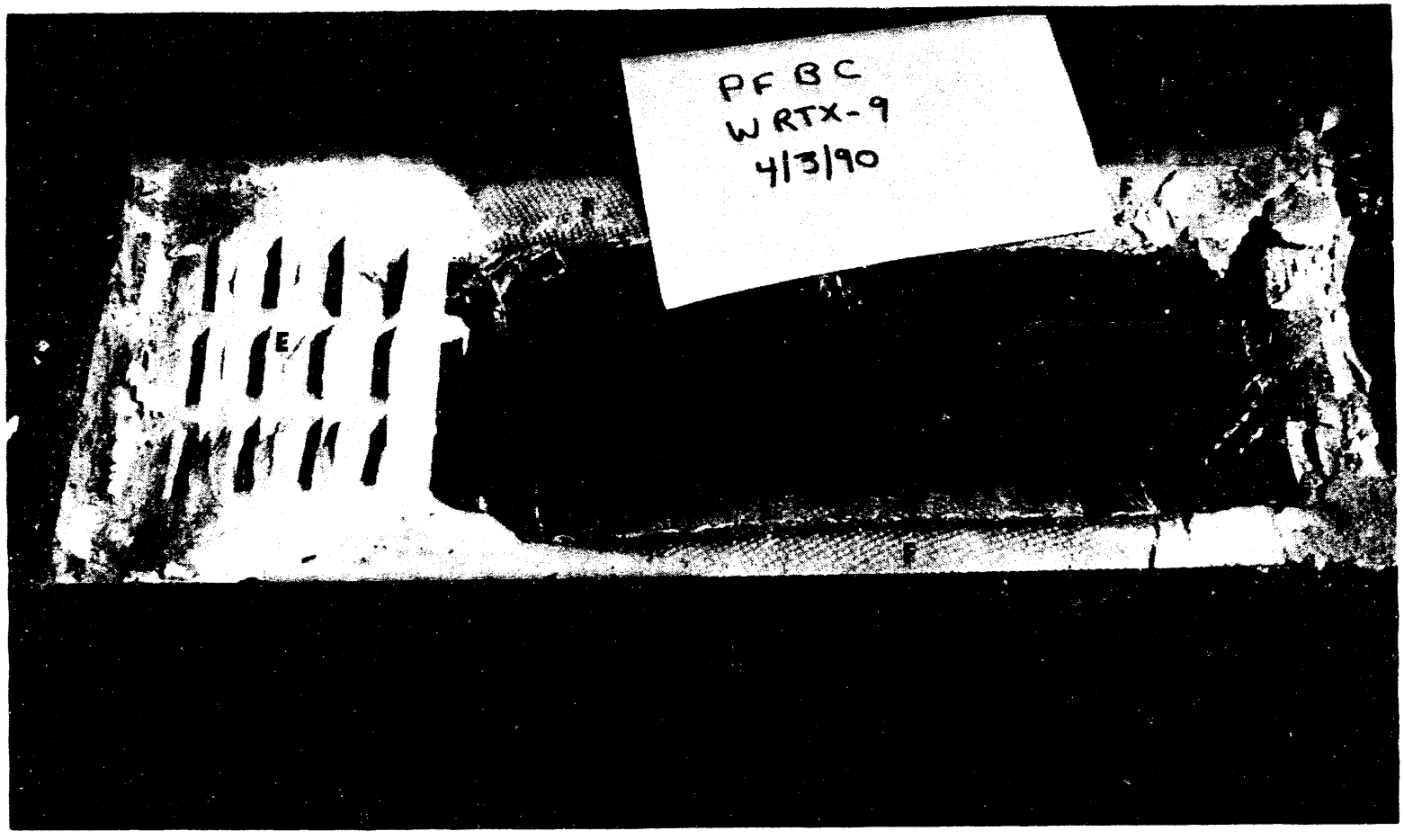

Figure E.12 - Remnant of Filter WRTX-9 Which Broke During the Element Removal; Note the Collection of Dust on Corners of Mount Indicating Flange Cracks During Service

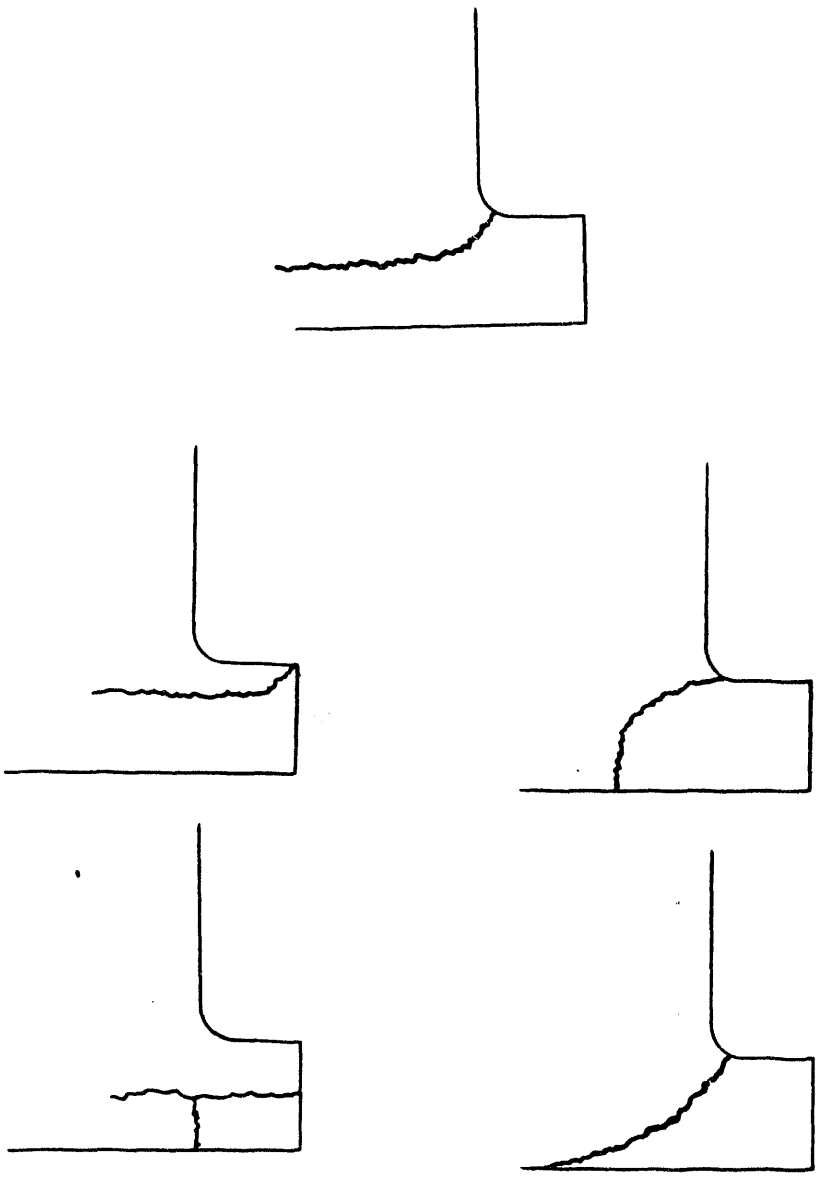

Figure E.13 - Fracture Profiles on WRTX-9 and WRTX-10 Filters

- Grinding of the end walls of the filters prior to the installation may have contributed to the cracking and spalling of the lower portions of the end walls.

- The location of the end bolts of the clamping bars next to the end corners of the flanges may have contributed to the crushing of the surface of the corners.

- The fractures in the flanges and in the bases of the filters appear to have always started in the regions of the end corners of the flanges.

- The holder appears to have exerted considerable loads on each filter by "pinching" tight its base via fly-ash compressed between the vertical walls of the holder and the sides of the filter.

- In general, the cracking of the filters appears to have been caused by concentrated stresses, some constant, some cyclic (including thermal fatigue), resulting from the methods of supporting and clamping the filters. Grinding of the filters prior to the installation might have been a contributing factor to some additional spalling.

3.4 Drawbacks of Current Design

Judging from the results of the operational analysis and the fractographic evaluation, the primary cause of the filter failure appears to be the design of the filter mounting apparatus and the assembly procedure. The characteristics of the flange fractures indicate that the crack initiation occurred primarily on the flange edges and that the crack growth was accelerated by the imposition of point and/or line stresses on the interface between the ceramic flange

and the metal clamping plates. Notably, these fractures did not result in any filter delaminations, as previously experienced on the first generation of cross flow filters. The absence of delamination in the second generation elements is attributed to the use of the radiused fillet between the flange and the filter body, the mid-rib bond structure and the overall improvement made by Coors in the element fabrication and sintering procedures. Once initiated, these cracks did not propagate laterally into the filter body as a delamination, but instead proceeded longitudinally across the flange.

Specific deficiencies in the current mount design are discussed below.

A. Non-uniform Loading of Filter Flanges

The filter support ledge is recessed inside the metal fixture so that the clamping plates are normally flat and horizontal in the assembled state. Such a perfect fitup of the element is seldom achieved in practice because the flange dimensions vary by 150 mils in thickness and 30 mils in flatness. Therefore, after installation, the clamp becomes tilted and imposes a direct crushing load on the longitudinal edges and corners of the flanges as shown in Figure E.14(a). Alternatively, shims are used to raise the outboard side of the clamping plates to achieve a horizontal fitup as shown in Figure E.14(b). The end result is that when the bolts are torqued the compression force only acts on the shim; the clamp transfers marginal compression to the ceramic flange again in the form of an edge load or moment. It is virtually impossible to (a) achieve uniform distribution of load along the flat surface of the flange, (b) to preclude any interference of the flange corners and

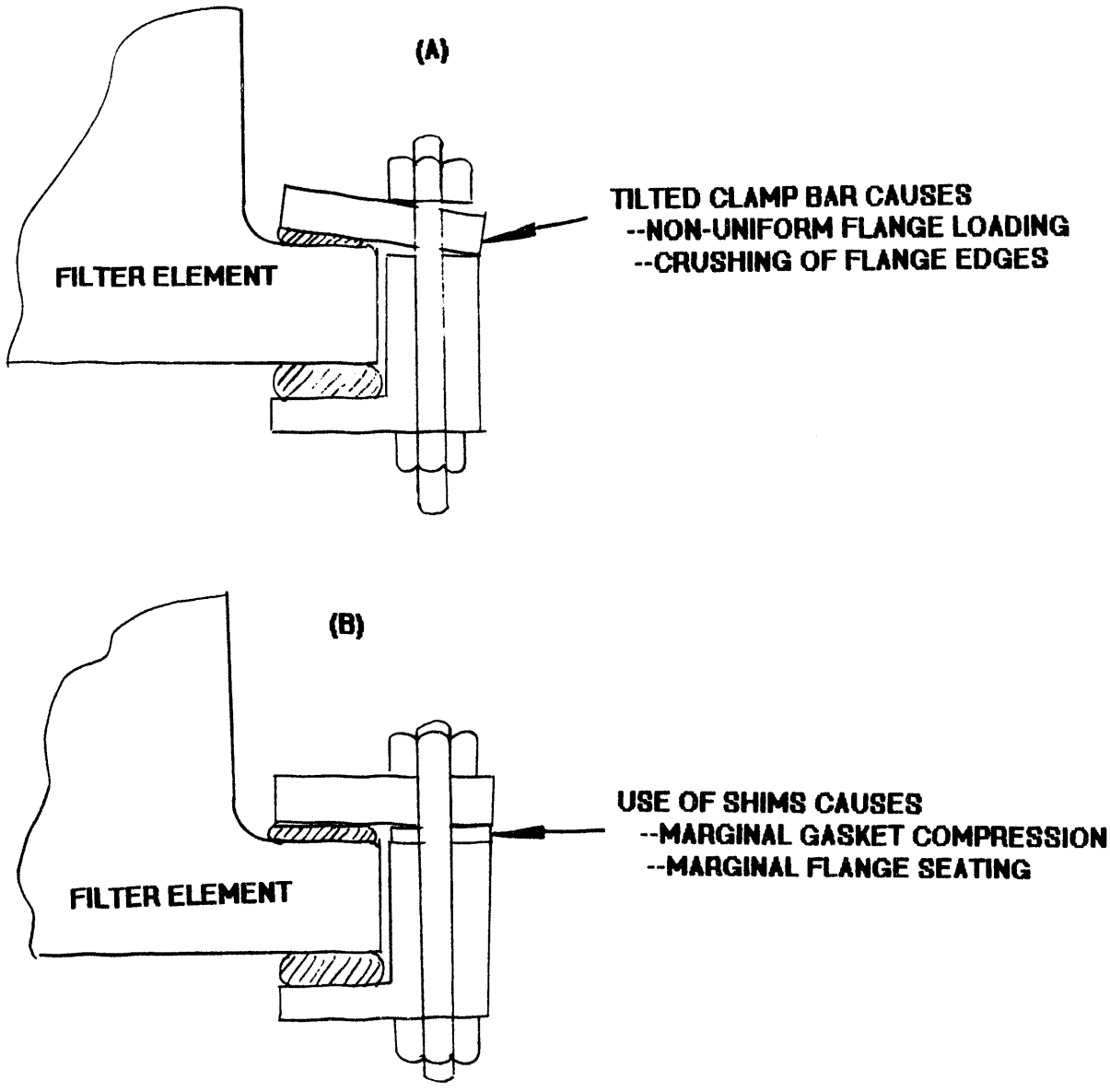

Figure E.14 - Typical Element Installation Problems with Current Mount Design

edges with the clamp plates, and, (c) to reliably translate the bolt loads into an equivalent seating force on the filter.

B. Bolt Relaxation due to Creep Effects

As described previously, the filter gasket is preloaded with an initial seating force of 2430 lbs. The 0.25 inch 316 stainless steel bolts, however, relax at high temperature causing a reduction in the effective seating force on the gasket. Using the isochronous stress-strain curves for 316 stainless steel the gasket seating force was calculated for various exposure times at 1500°F temperature. As shown in Figure E.15, the actual seating force deteriorates to about 10% of the initial value after 1000 hours or about 260 lbs. Given the non uniform loading characteristics of the clamp discussed above and the closeness of the residual seating force to the reverse hydrostatic force generated during pulse cleaning, it is probable that the elements are partially lifted and/or severely vibrated during each pulse. Because the Interam pad placed between the clamp and the flange crumbles to powder at high temperature there is virtually no resilient layer to absorb any impact of the ceramic flange with the metal plate.

C. Lateral Loads due to Dust Accumulation

Because of the differential thermal expansion between the ceramic flange and the metal ledge, the 0.125 inch gap is opened during high temperature operation. After 1000 hours the creep relaxation behavior of the bolts substantially reduces the gas sealing characteristics of the gaskets allowing dust laden gas to permeate through the gasket and

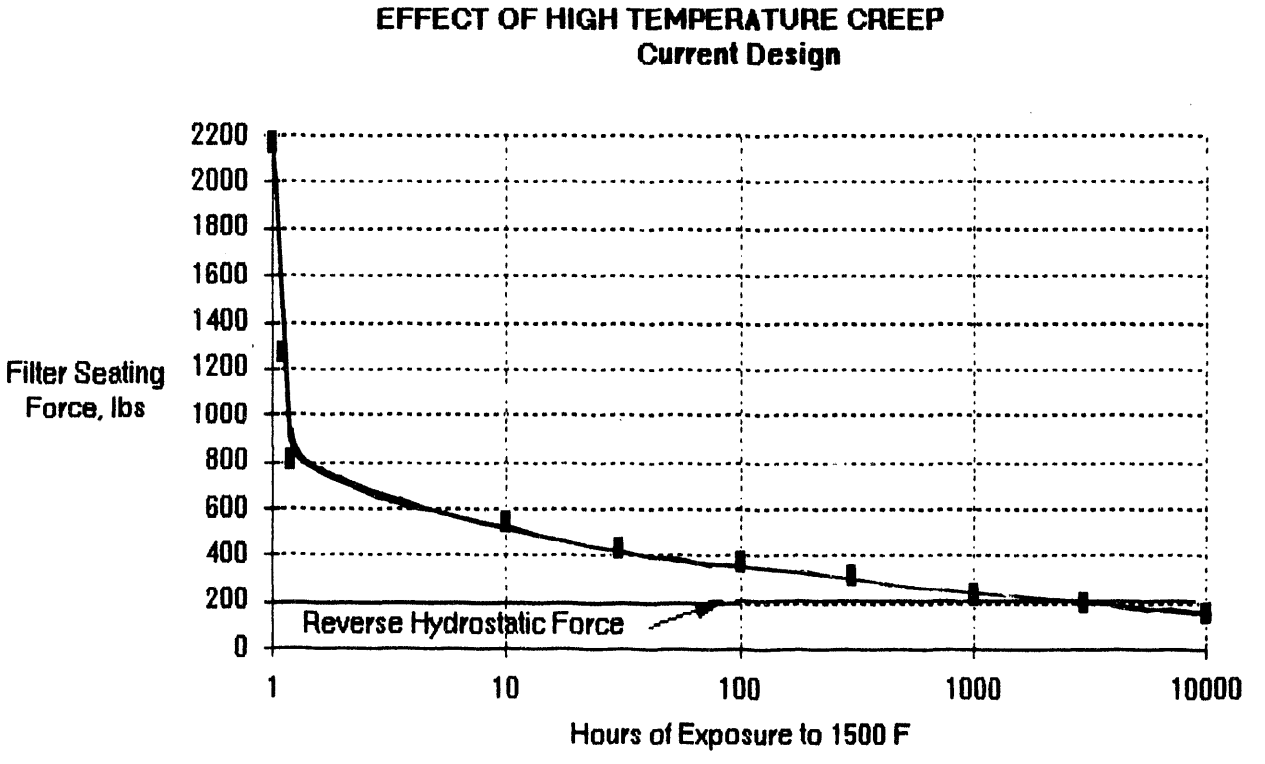

Figure E.15 - Effect of Bolt Relaxation on Filter Seating (Current Design)

form a dust cake in the cavities outside the gasket and in the gaps between the flanges and the metal fixture. Because this cake is normally thicker than the cake depositing on the filter walls, it is unlikely to be removed during on-line pulse cleaning. Upon shutdown when the metal cavity contracts a residual stress is exerted laterally into the flange body. The wedging effect of the fines was particularly visible on the bottom element which had to be forcibly ejected out of the metal fixture causing a cleavage of the flange during disassembly. The lateral forces would principally be manifested during the cold shutdown periods after about 1000 hours of hot operation when the seating forces on the gasket have substantially relaxed allowing the buildup of dust in the cavities.

3.5 Proposed System Retrofit

In an effort to eliminate the deficiencies in the current filter mounting apparatus a retrofit design has been developed as shown in Figure E.16. The salient features of this retrofit are now outlined.

1. The Nextel reinforced gaskets are used on the upper and lower surfaces of the ceramic flange. Note that the upper gasket after compression now provides a compliant layer to smooth out the seating forces imposed by the flange loading plate and also ensures a resilient shock-absorbing layer to cushion the vibrational forces generated during pulse cleaning.

2. The single clamp plate is now substituted by a flange loading plate and a separate loading bar with a swivel action. This type of clamping arrangement ensures that,

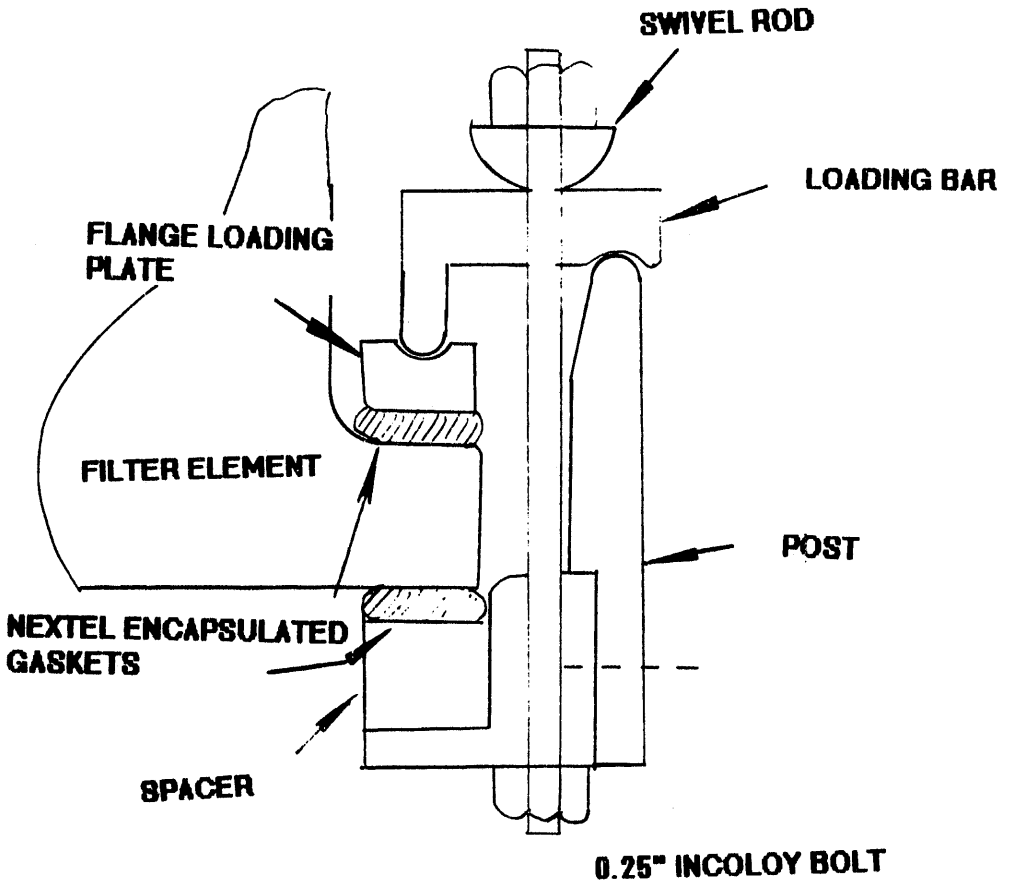

Figure E.16 - End View of Retrofitted Element Mount Fixture

regardless of the ceramic flange geometric variations, the loading plate will remain parallel and horizontal whereas the loading bar can rotate as necessary without actually interfering with the edge of the ceramic flange.

3. A metal post is attached to the outside of the existing fixture such that the loading bar is simply supported on either side of the bolting axis. Thus the bolting forces are directly transferred into an equivalent seating force on the filter, without the use of shims.

4. The eight 316 stainless steel bolts are substituted by 14 bolts made of creep resistant Incoloy 800 alloy. During the assembly procedure a 270 lbs weight is placed on the element to pre-compress the bottom gasket. The clamping device is now mounted and the 14 bolts are sequentially torqued up to 10 in-lbs. After removal of the 270 lbs weight, the two gaskets will be loaded in series to approximately 2700 lbs of seating force. For the retrofit design Figure E.17 shows the effect of long duration bolt creep on the seating forces acting on the filter. Comparing with Figure E.15 it is clear that the seating forces are held to a relatively steady value with a substantial margin over the hydrostatic reverse forces generated during pulse cleaning. Note also that this high seating force is calculated to prevail over at least a 4 year operating period.

5. The filter seating area is elevated by the use of a spacer such that no dust can accumulate between the flange and the metal fixture. Notwithstanding the rugged gasket seating properties of the modified design, this feature ensures that no residual transverse stresses can act on the flange during shutdown conditions.

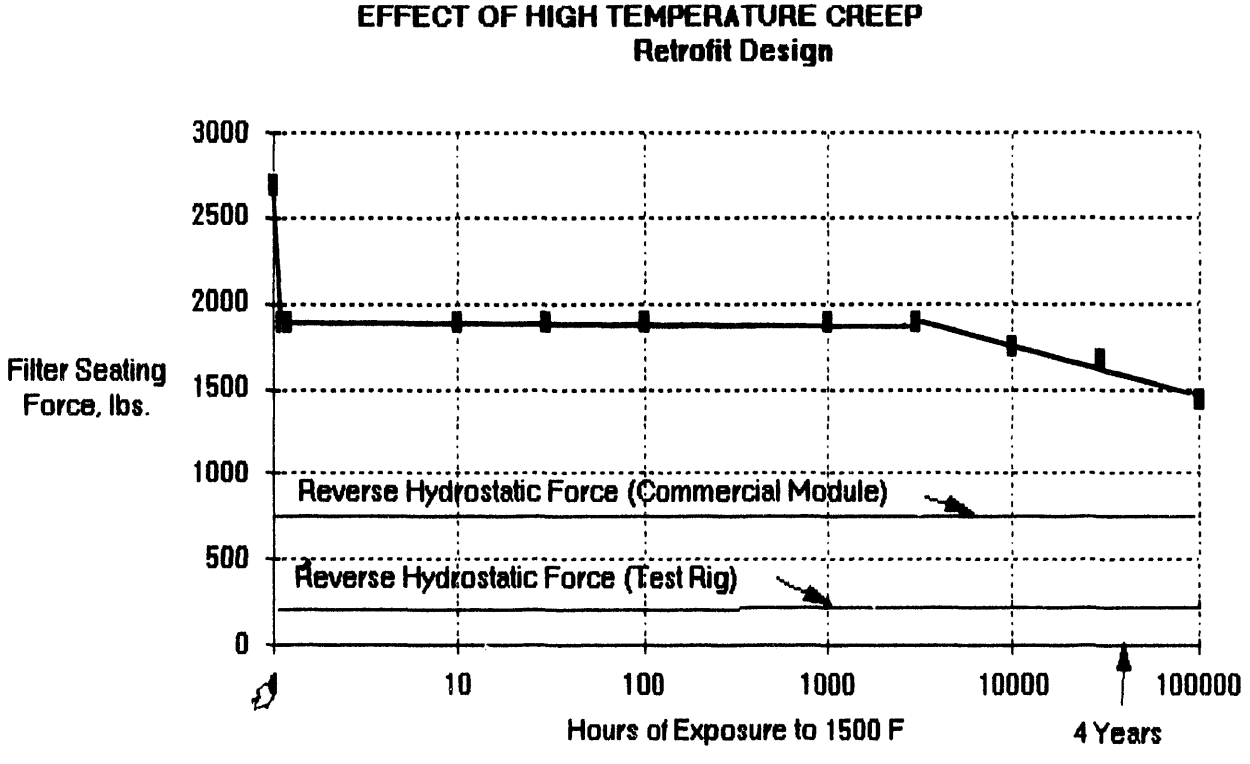

Figure E.17 - Filter Seating Characteristics of Retrofit Mount Design

Whereas, these modifications can be easily implemented in the current filter support structure, the retrofit mount blocks off the bottom two rows of filtering surface, thus reducing the overall filtration area from 8.4 to approximately 7.0 ft^2. This penalty, however, can be easily eliminated in a "clean sheet" mount design which incorporates all of the improved features associated with the retrofit design.

It is recommended that the element mount modifications be implemented on the long term durability test rigs as well as on pilot scale filter systems integrated with the Texaco gasifier and the Foster Wheeler second generation PFBC system. Additionally, it is recommended that the filter compression braces, which were hitherto used to guard against delamination, be omitted in future testing. The results of the 1300 hour test campaign have shown significantly improved resistance to delamination and that delamination may no longer be an operational issue with cross flow filter elements. It is also clear that these braces become easily detached during high temperature operation and provide negligible compressive forces on the element.

APPENDIX F

PRESSURE DROP AND GAS TEMPERATURE TRACES RECORDED DURING PFBC PLANT THERMAL TRANSIENT TESTING WRTX-76, WRTX-77, WRTX-78, WRTX-81 (WRTX-80, AND WRTX-84)

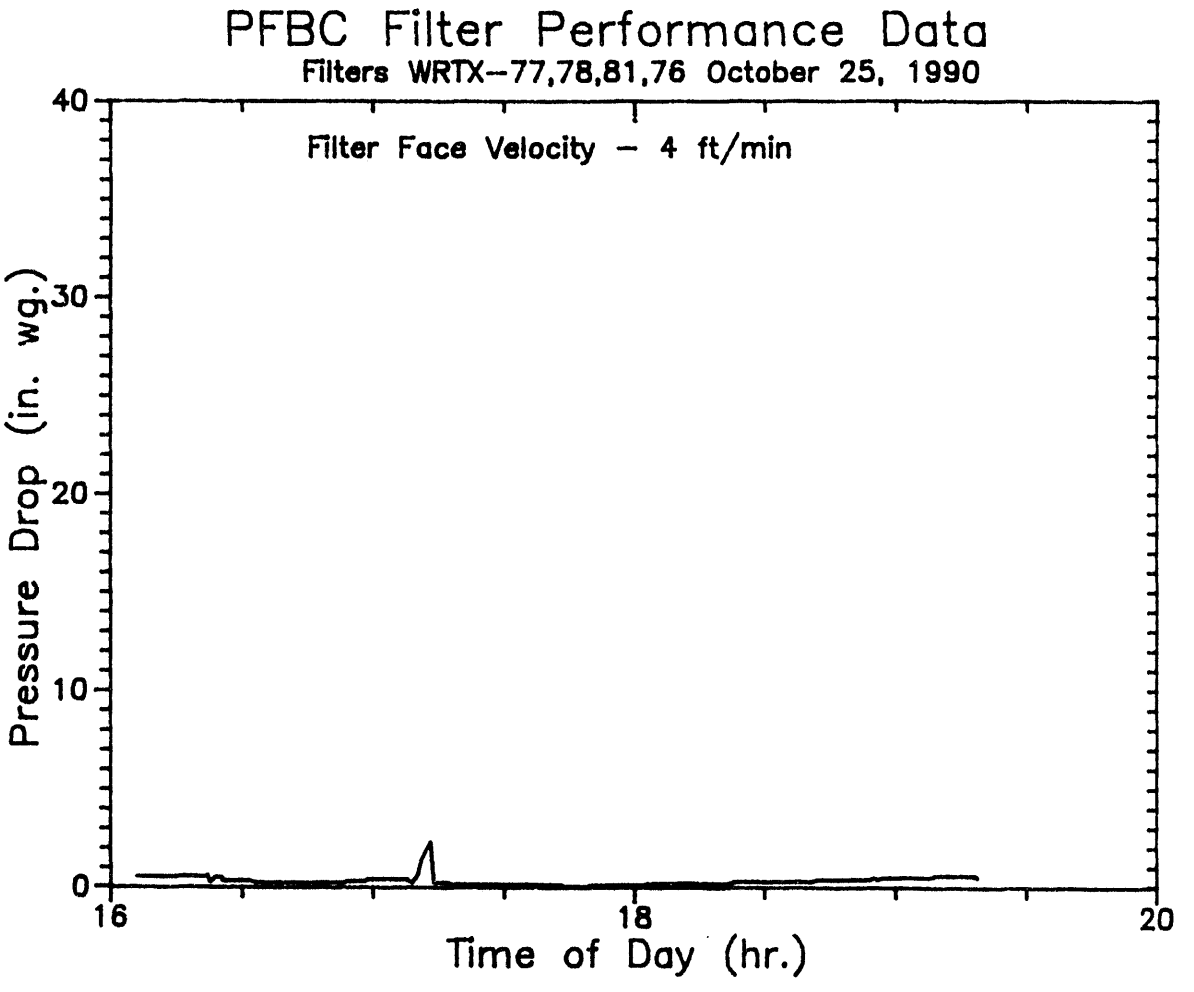

OPERATION NOTES FOR
OCTOBER 25, 1990

4 NEW FILTERS

PLENUM 1 - TOP - WRTX-77
BOTTOM - WRTX-78

PLENUM 2 - TOP - WRTX-81
BOTTOM - WRTX-76

COLD START
INITIAL HEAT UP

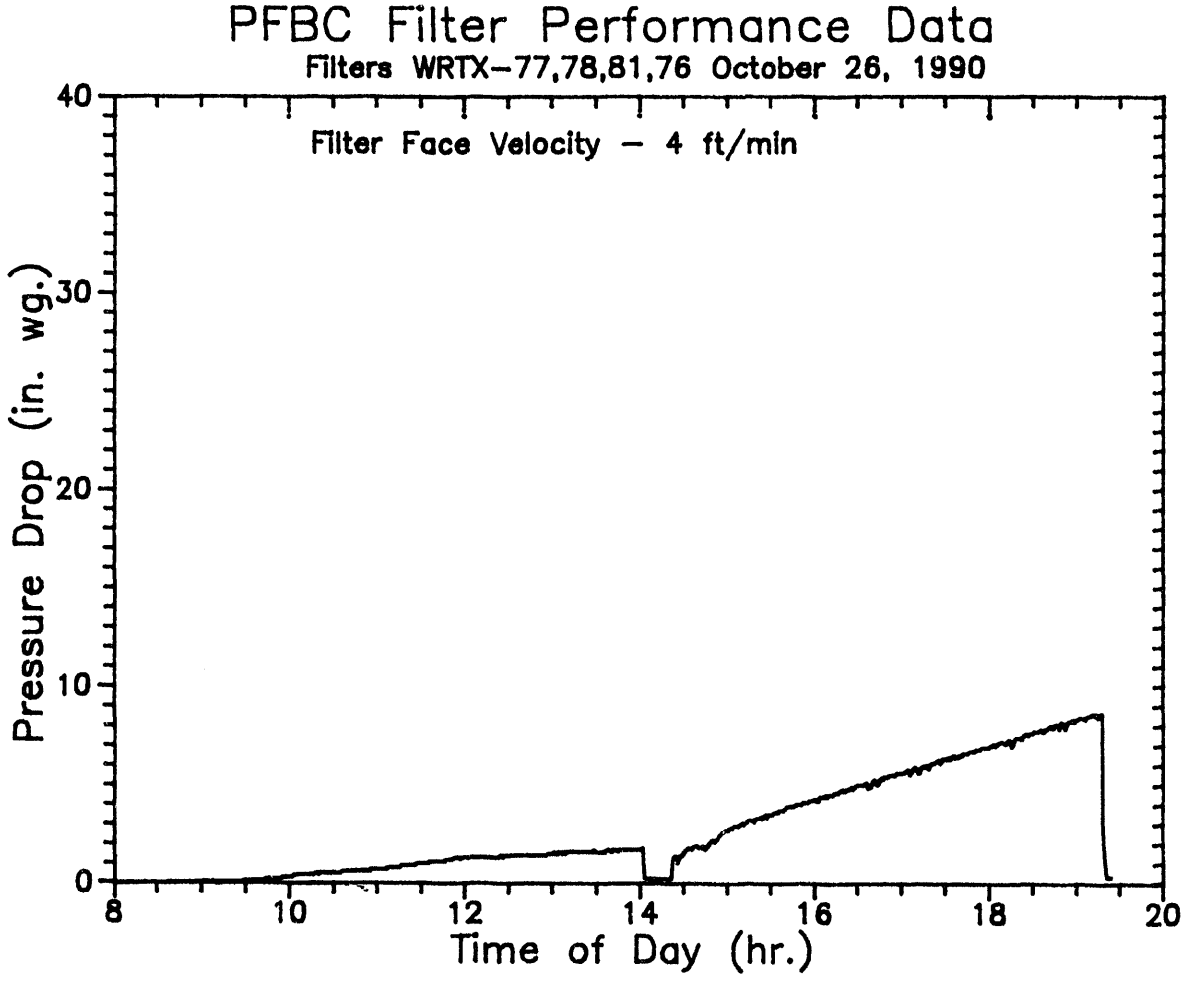

OPERATION NOTES FOR
October 26, 1990
12 hour test, includes
start up and shutdown
1400 FLAME OUT - UNSCHEDULED
RESTART
INITIAL CYCLE

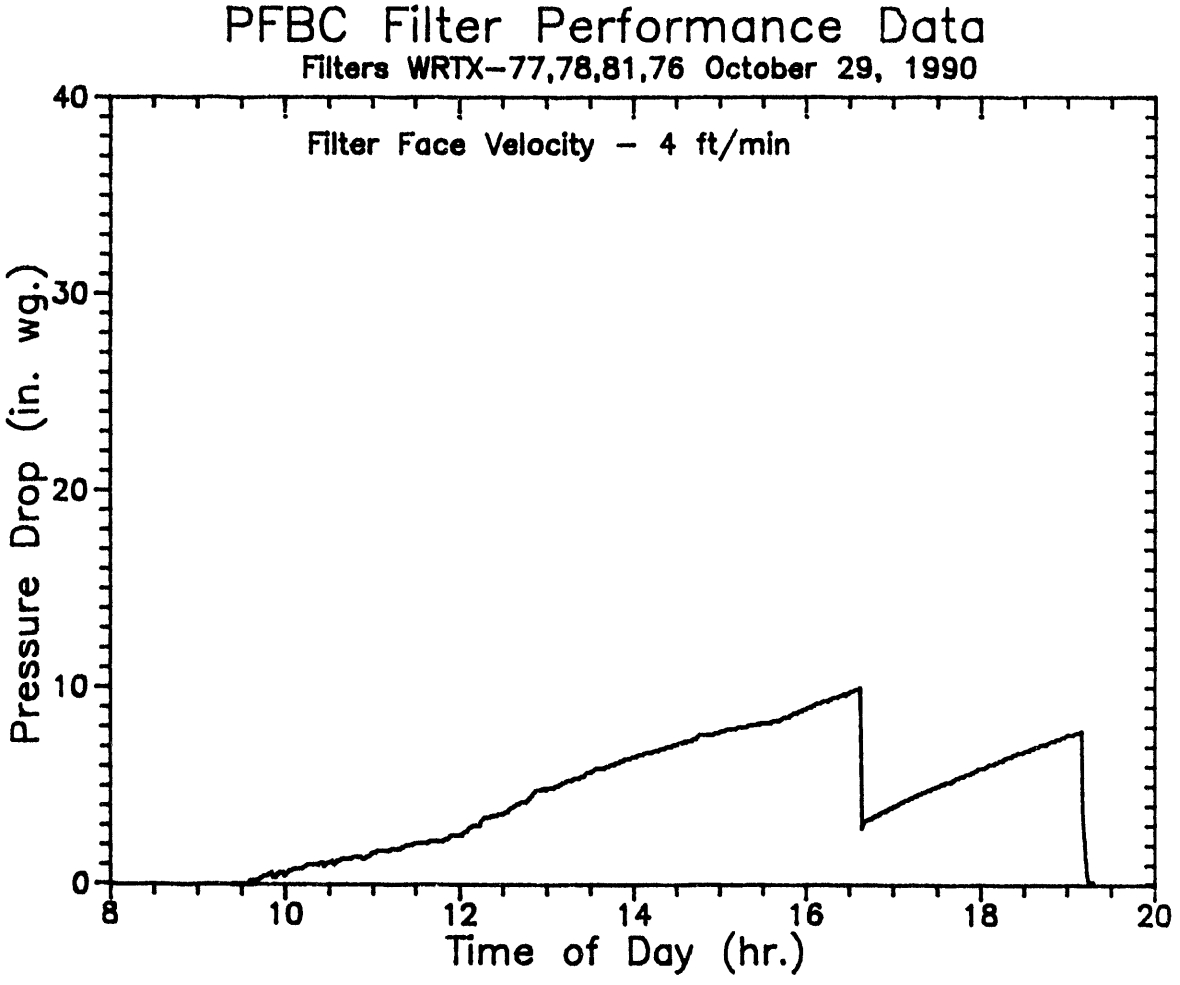

OPERATION NOTES FOR
OCTOBER 29, 1990

12 hour test, INCLUDES
Cold startup and shutdown

ΔP Trigger = 10" wc

Pulse Cleaning = 295 psig/sec

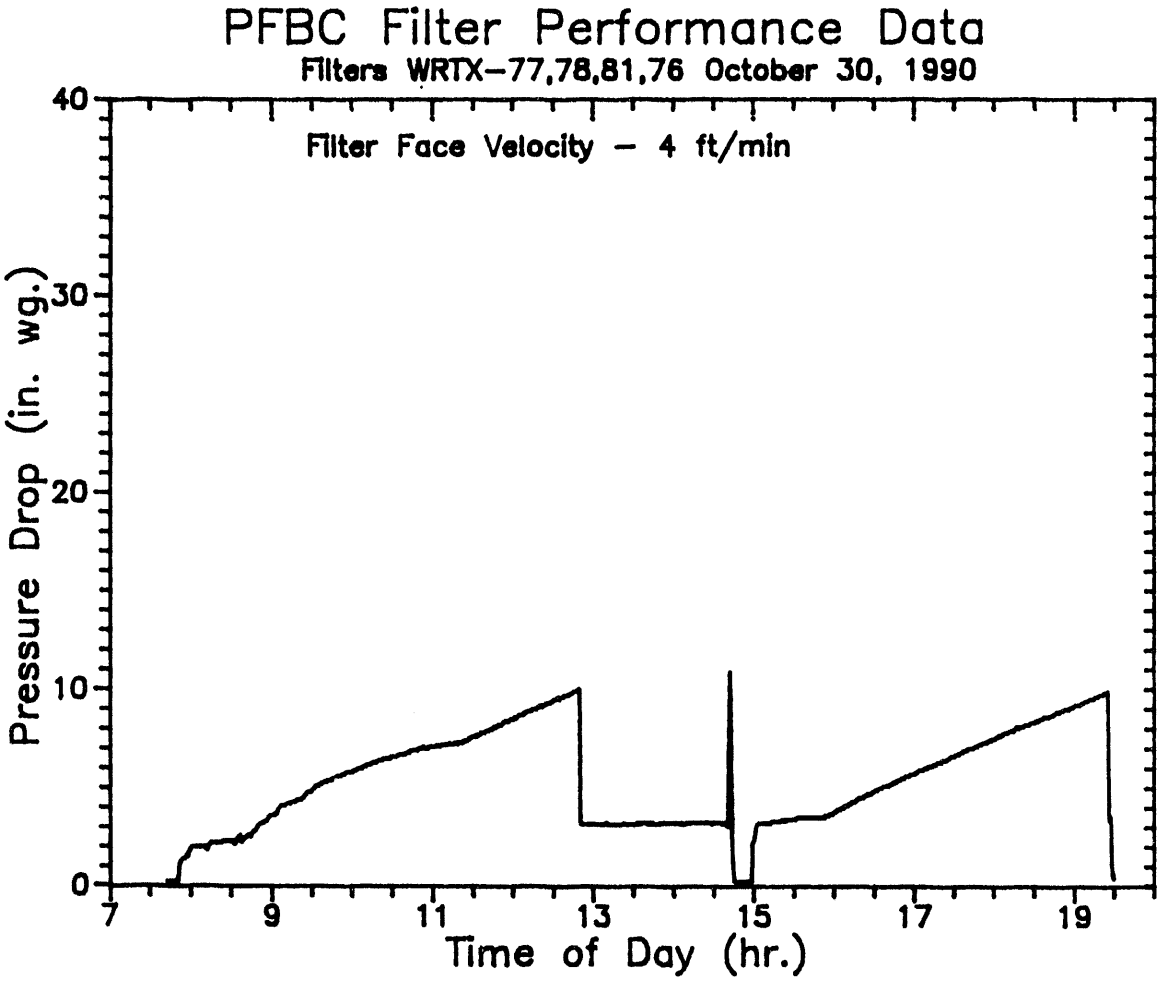

Operation Notes for
October 30, 1990

12 hour test, includes
startup and shutdown

Δ P TRIGGER = 10" WC
PULSE CLEANING - 300 psig/0.1sec

1430 Turbine trip SIMULATION
ATTEMPT
FLAME OUT - SCHEDULED
RESTART

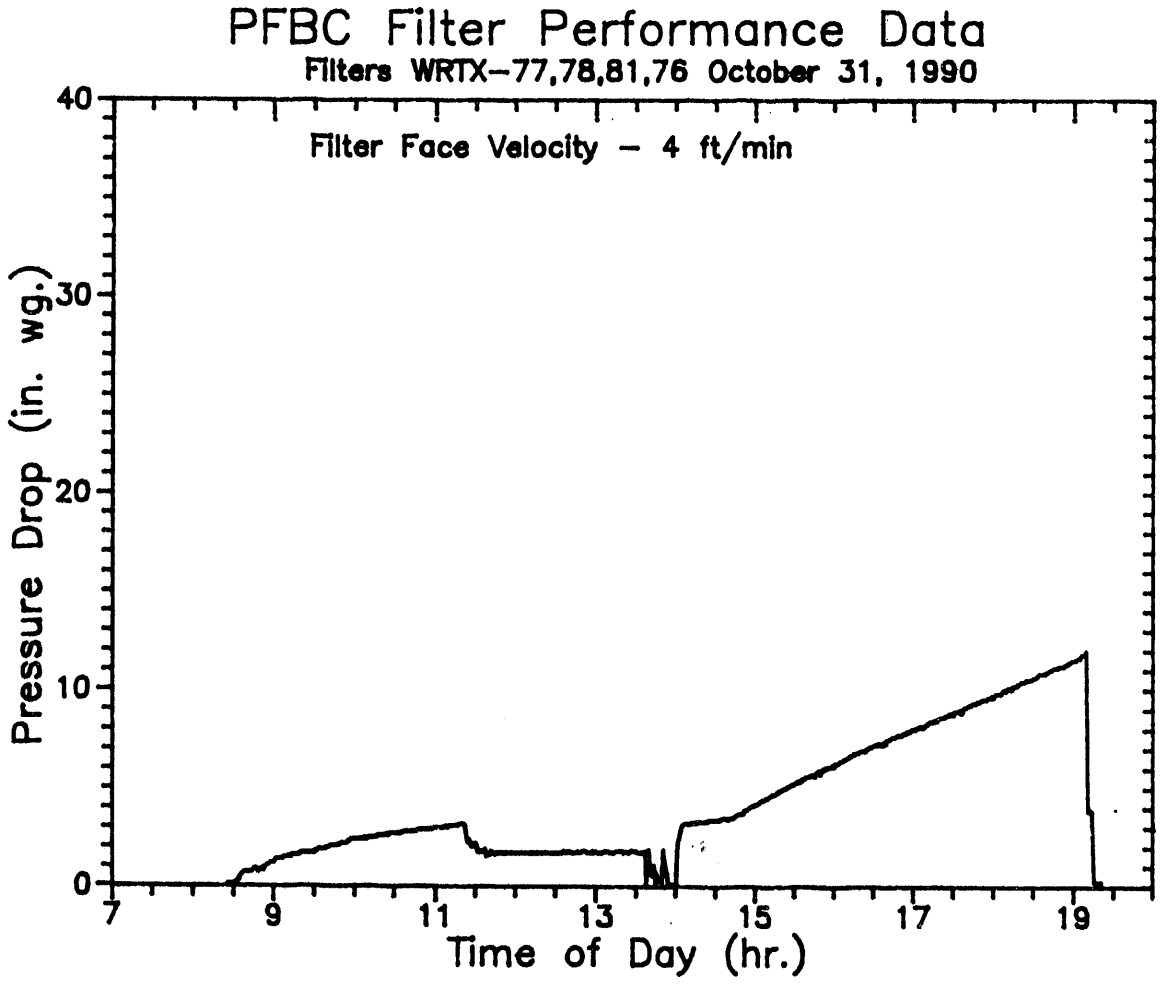

OPERATION NOTES FOR
OCTOBER 31, 1990
12 hour test, includes
Startup and shutdown
ΔP TRIGGER = 12" WC
PULSE CLEANING = 300 psig/0.1sec
1130 - Increased system pressure
to 150 psig prior to
1340 TURBINE TRIP SIMULATION
FLAME OUT – SCHEDULED
RESTART

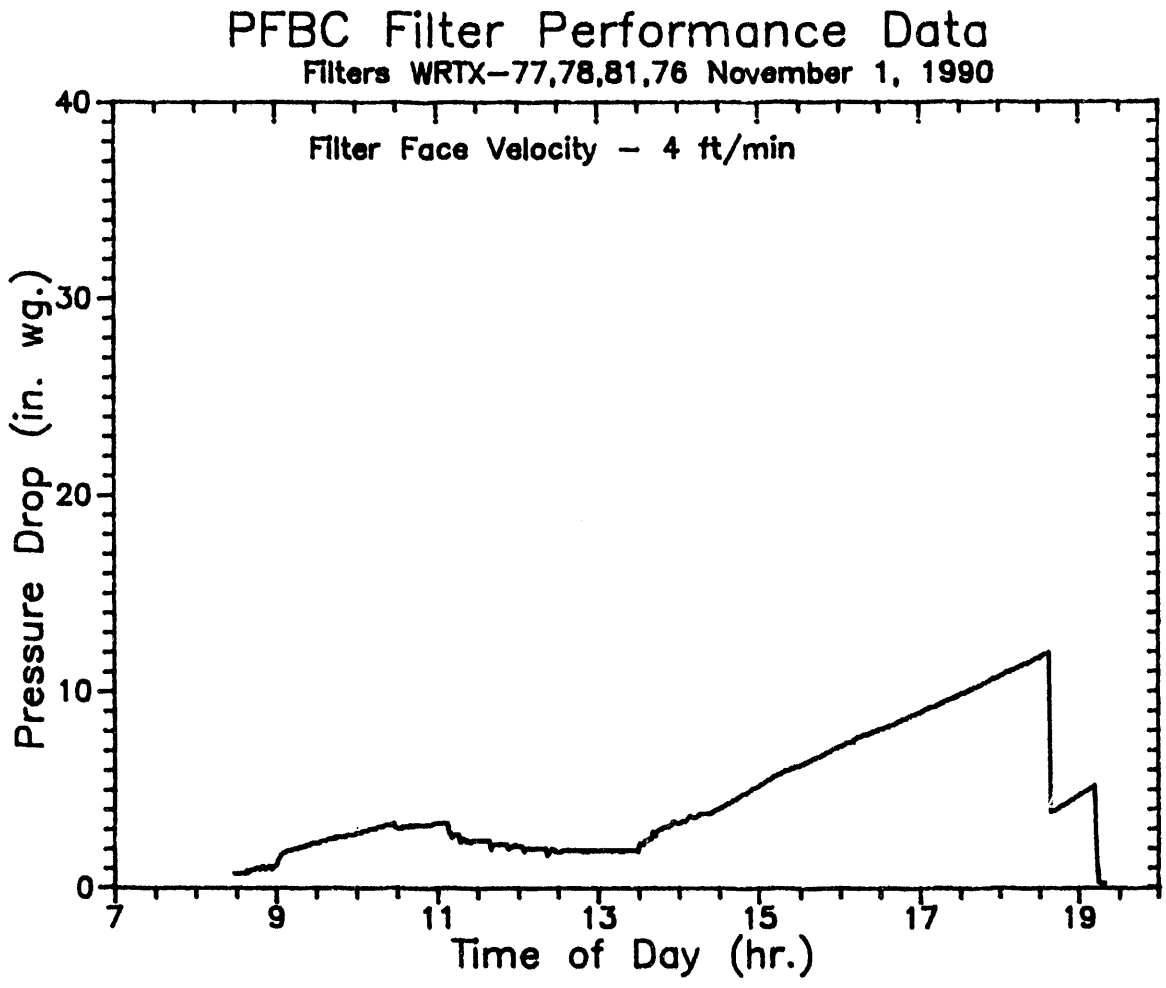

OPERATION NOTES FOR
November 1, 1990

12 hour test, includes
Startup and shutdown

ΔP TRIGGER = 12" WC

Pulse Cleaning - 300psig/0.1sec

1030 - 1330 - SYSTEM PRESSURE
AT 150 PSIG

1330 - SYSTEM PRESSURE
REDUCED TO 75 PSIG

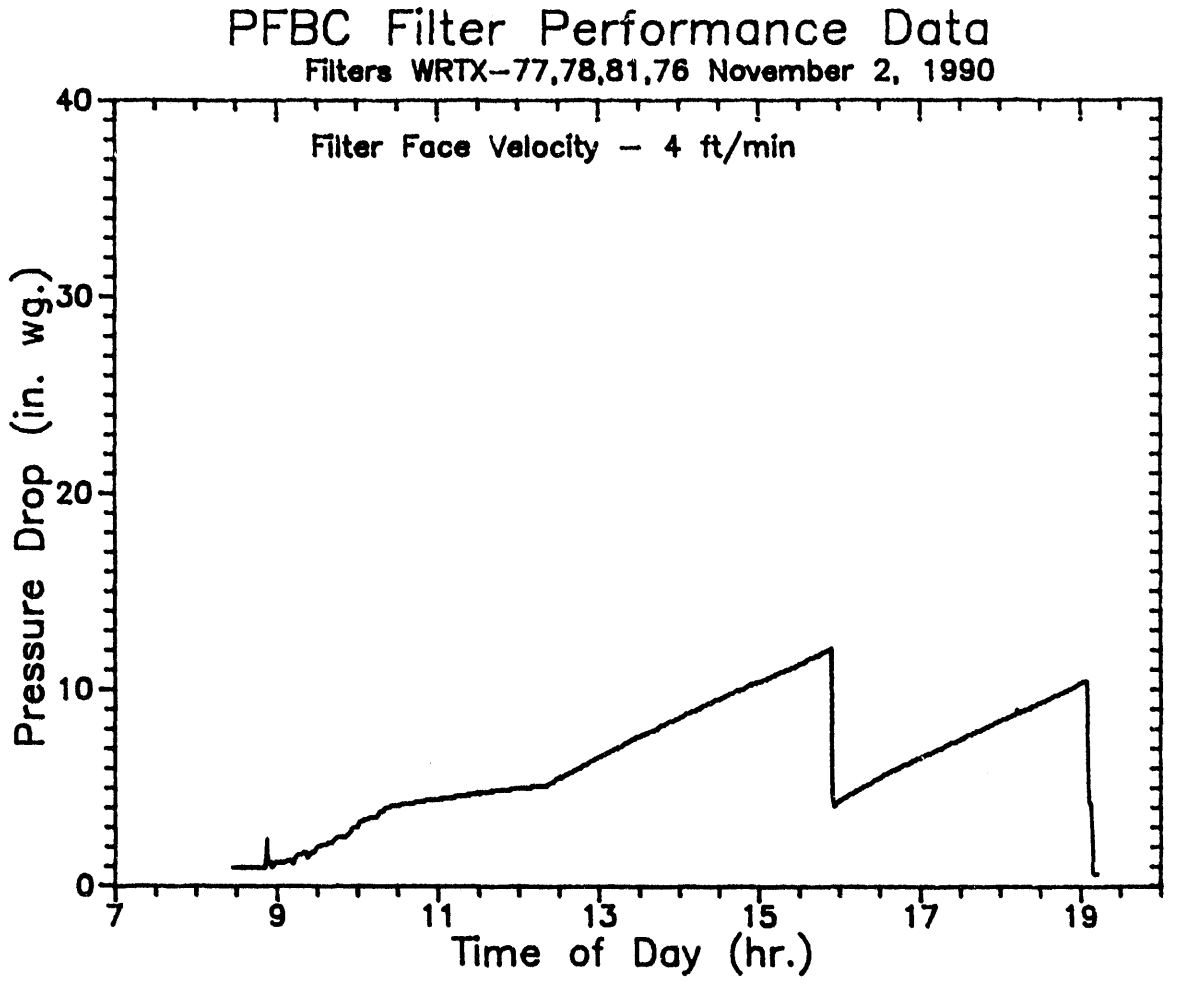

OPERATION NOTES FOR
NOVEMBER 2, 1990
12 hour test, includes
startup and shutdown
ΔP TRIGGER = 12 "WC
PULSE CLEANING -300psig/0.1sec

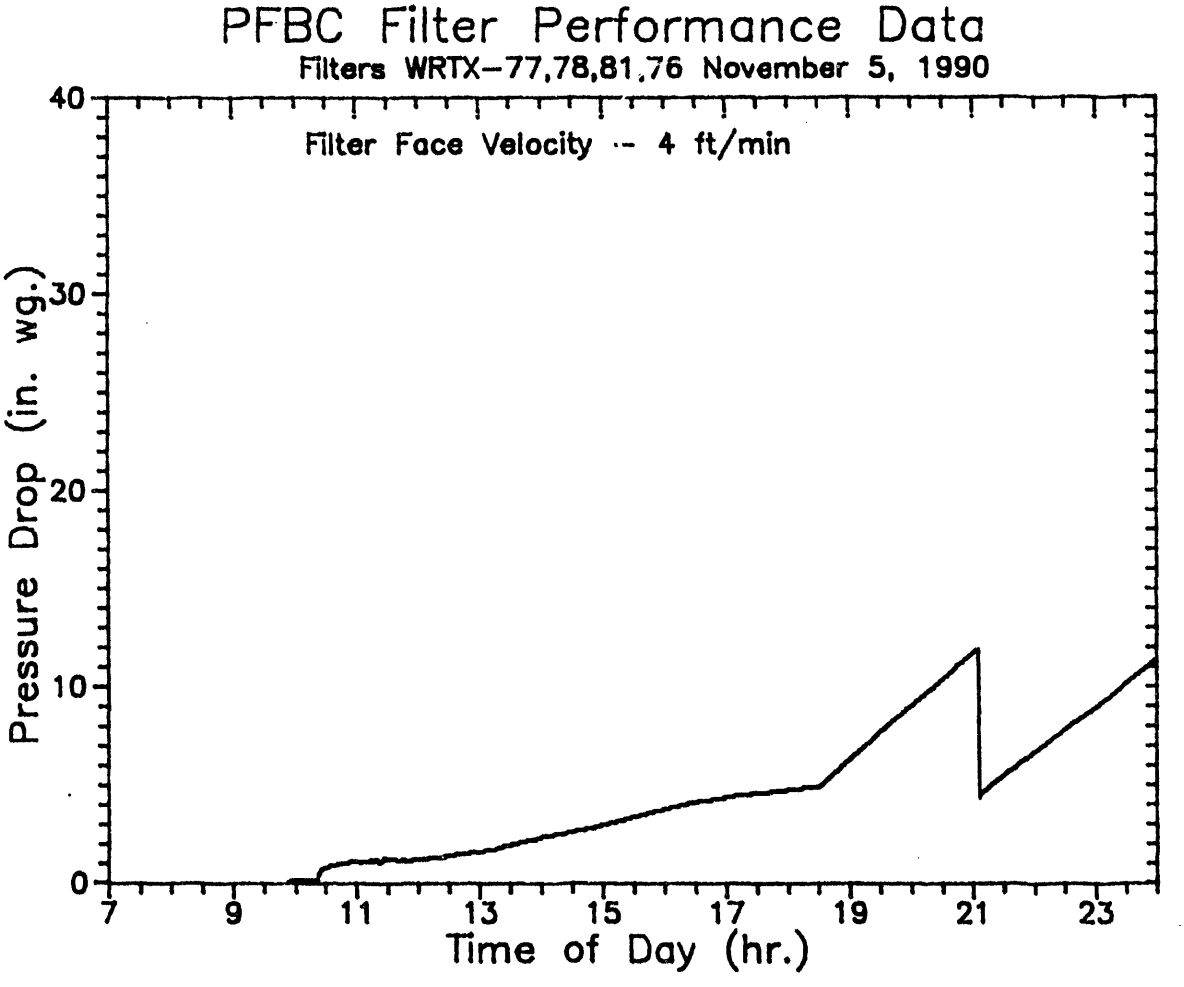

OPERATION NOTES FOR
NOVEMBER 5, 1990
START OF WEEK LONG TEST
COLD START
ΔP TRIGGER = 12" WC
PULSE CLEANING = 300 psig/0.1sec

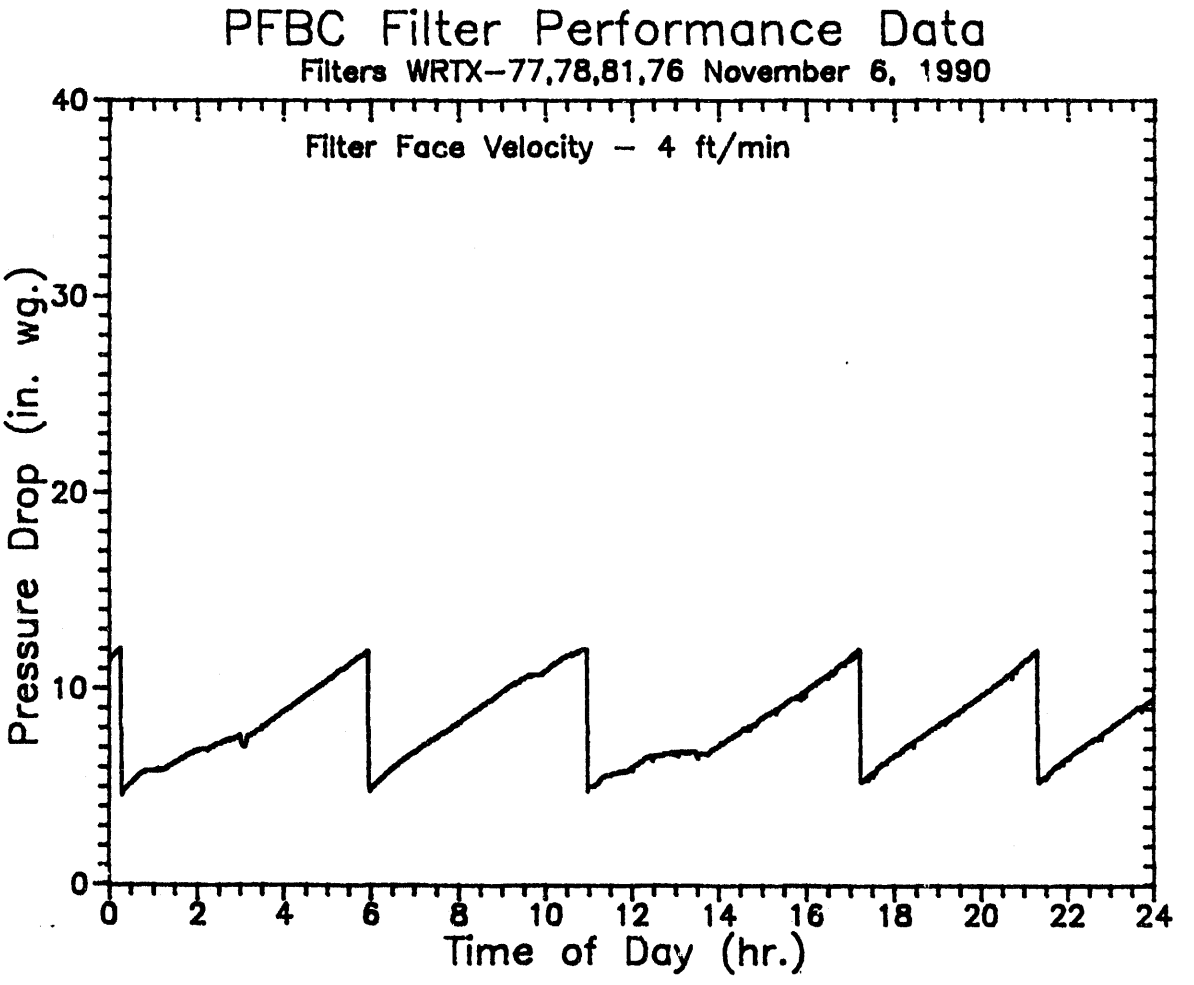

OPERATION NOTES FOR
November 6, 1990

ΔP TRIGGER = 12" WC

PULSE CLEANING - 320 psig/0.1sec

1100 - 1395 - DUST FEED ERRATIC, DUST VESSEL DEPRESSURIZED and DUST STIRRED

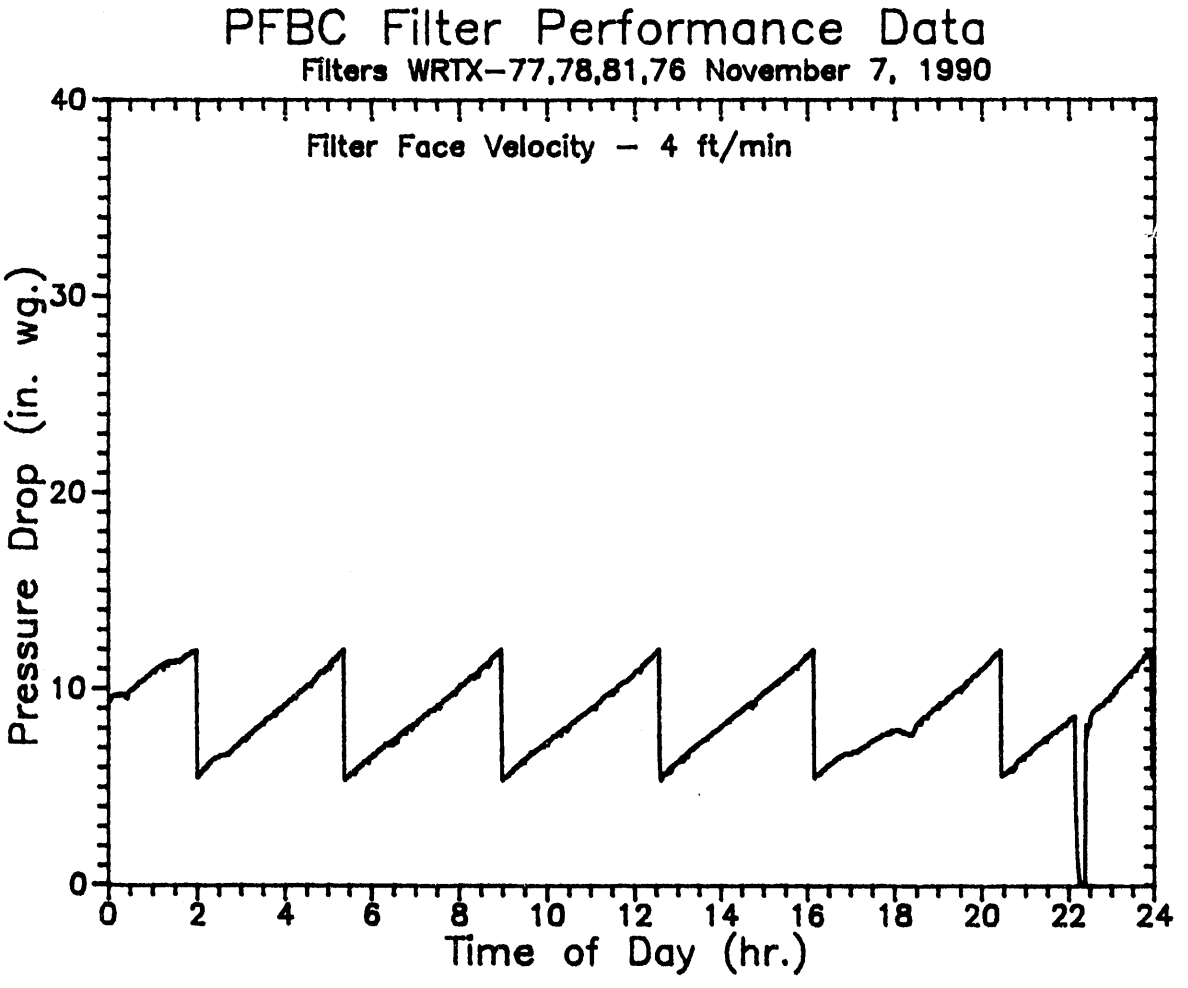

OPERATION NOTES FOR
NOVEMBER 7, 1990
ΔP TRIGGER = 12" WC
PULSE CLEANING - 320psig/0.1 sec
2210 FLAME OUT - UNSCHEDULED - RESTART

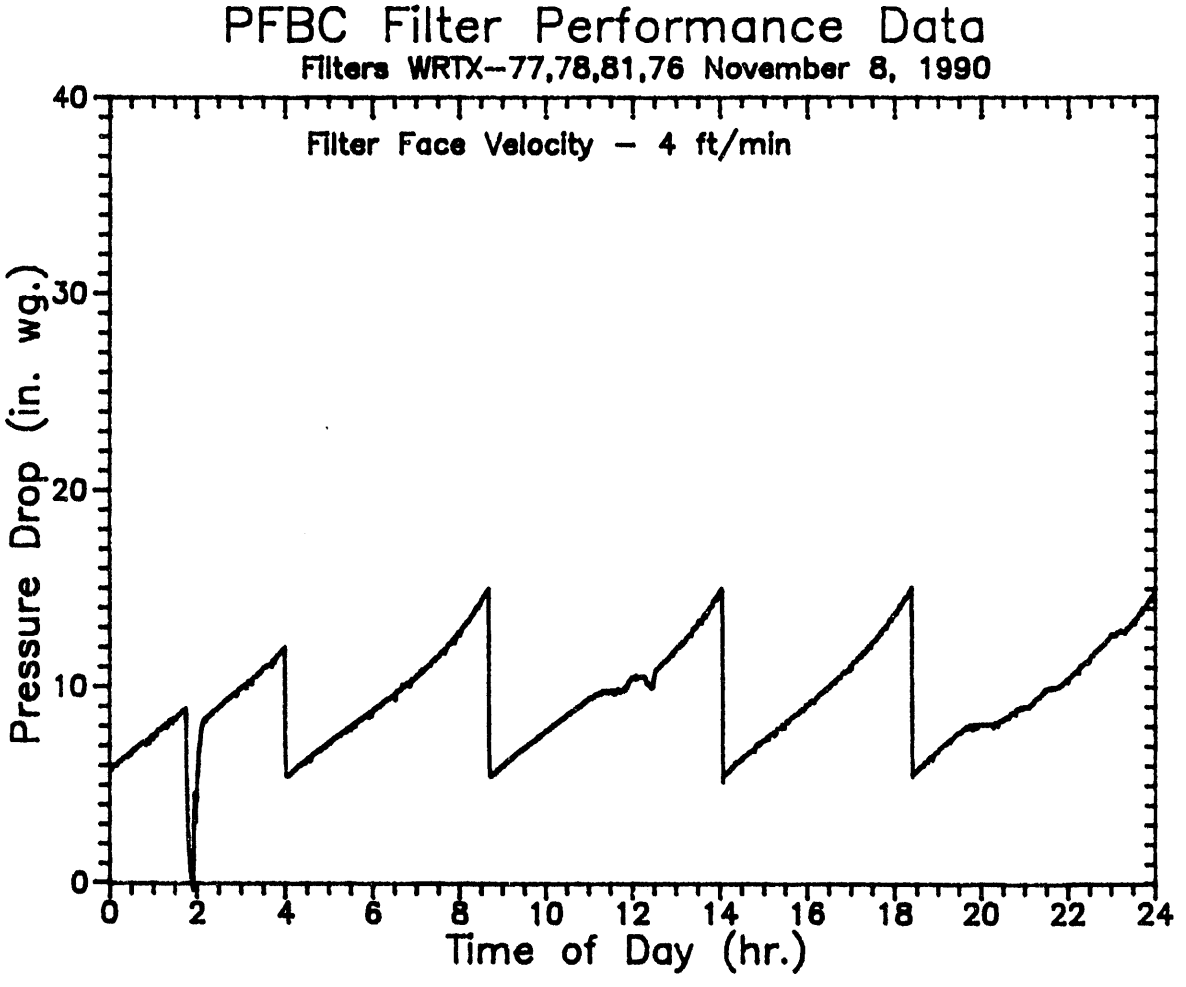

OPERATION NOTES FOR NOVEMBER 8, 1990

0145 FLAME OUT – UNSCHEDULED RESTART

0840 CHANGED Δ P TRIGGER FROM 12" wc to 15" wc

PULSE CLEANING - 320psig/0.1sec

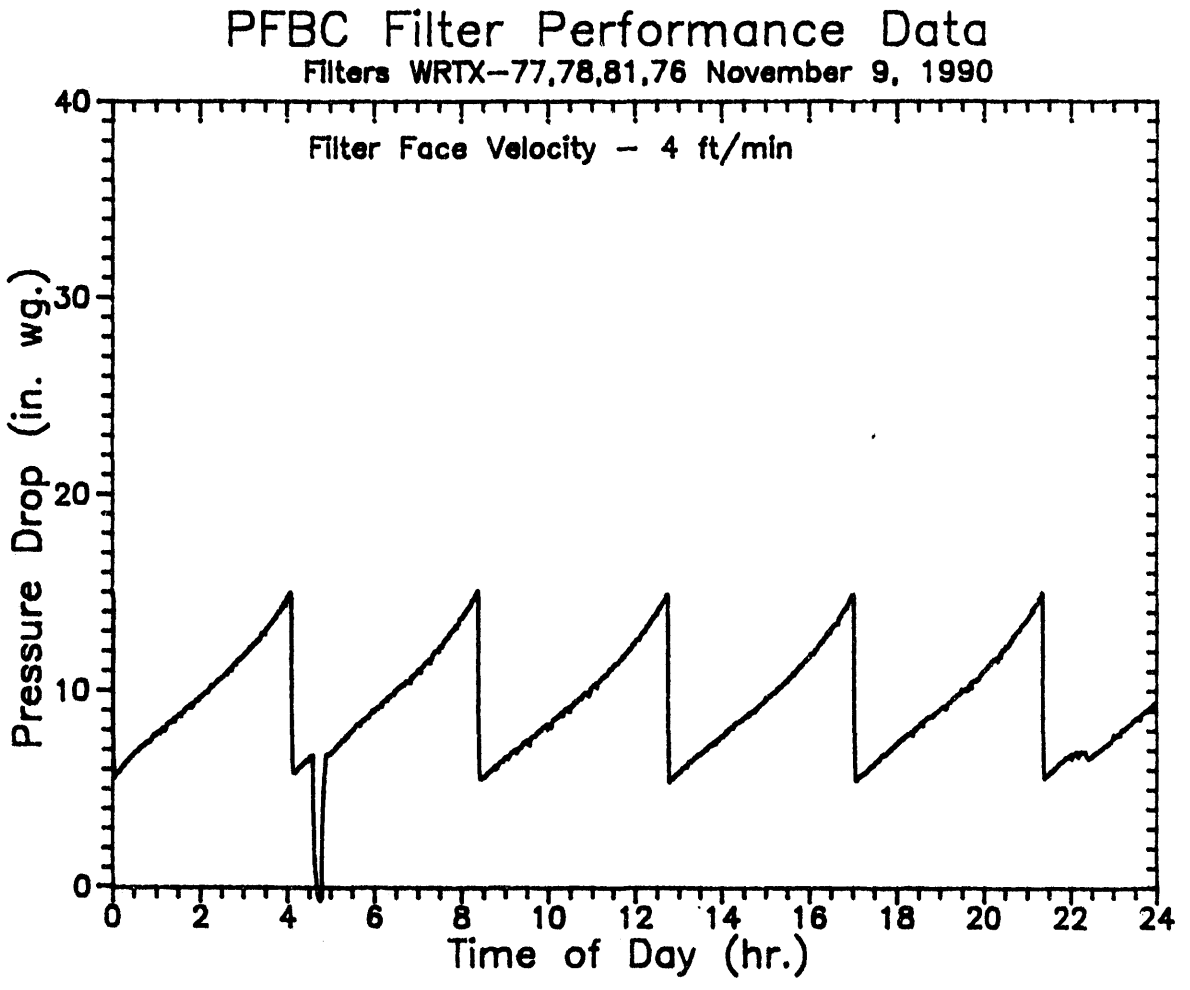

OPERATION NOTES FOR
NOVEMBER 9, 1990
0430 FLAME OUT - UNSCHEDULED
RESTART
Δ P TRIGGER = 15" WC
PULSE CLEANING - 320psig/0.1sec
2200 - DUST LOADED

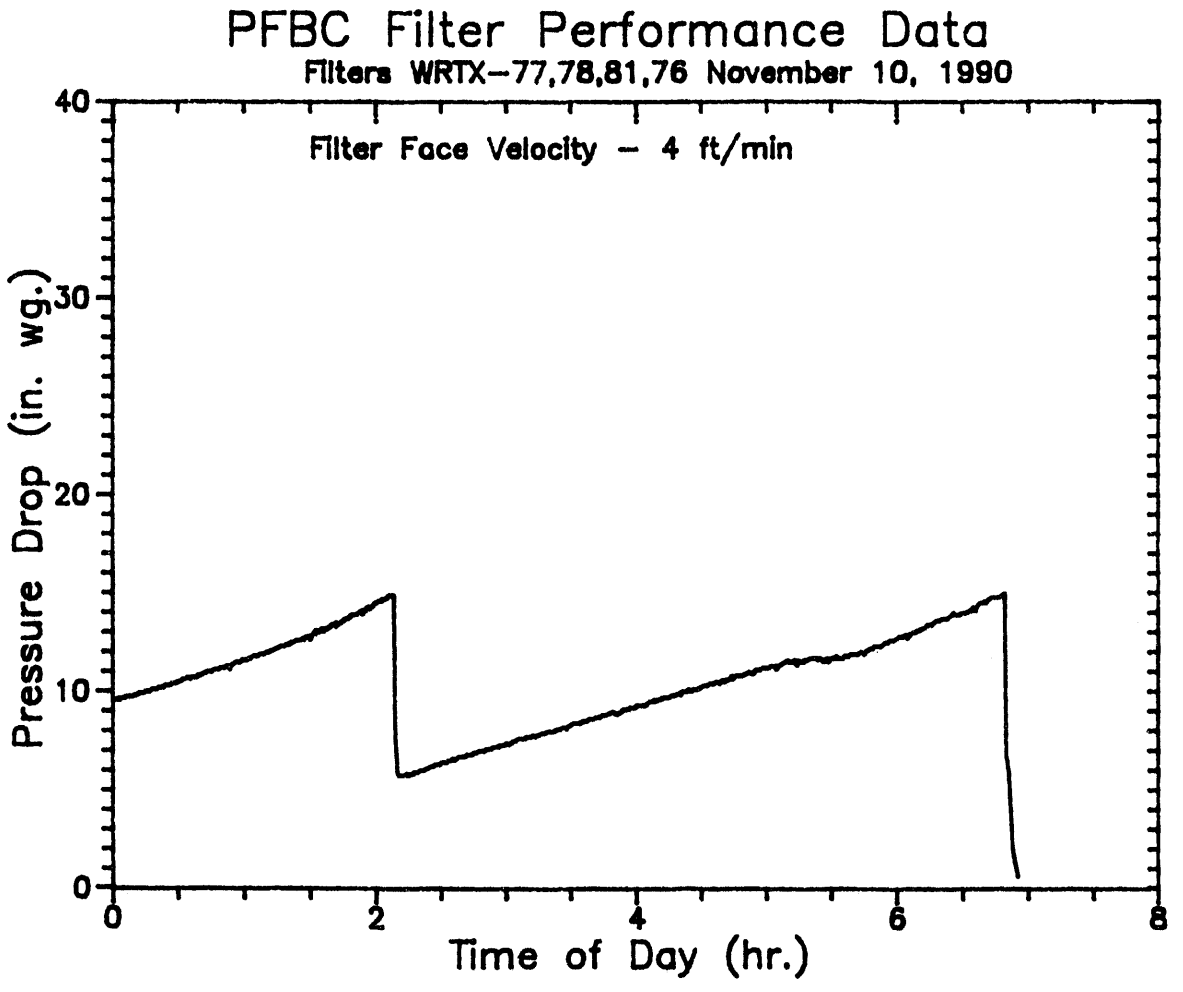

OPERATION NOTES FOR
NOVEMBER 10, 1990
END OF WEEK LONG TEST
0650 SCHEDULED
SHUTDOWN
ΔP TRIGGER = 15" WC
PULSE CLEANING - 320psig/0.1 sec

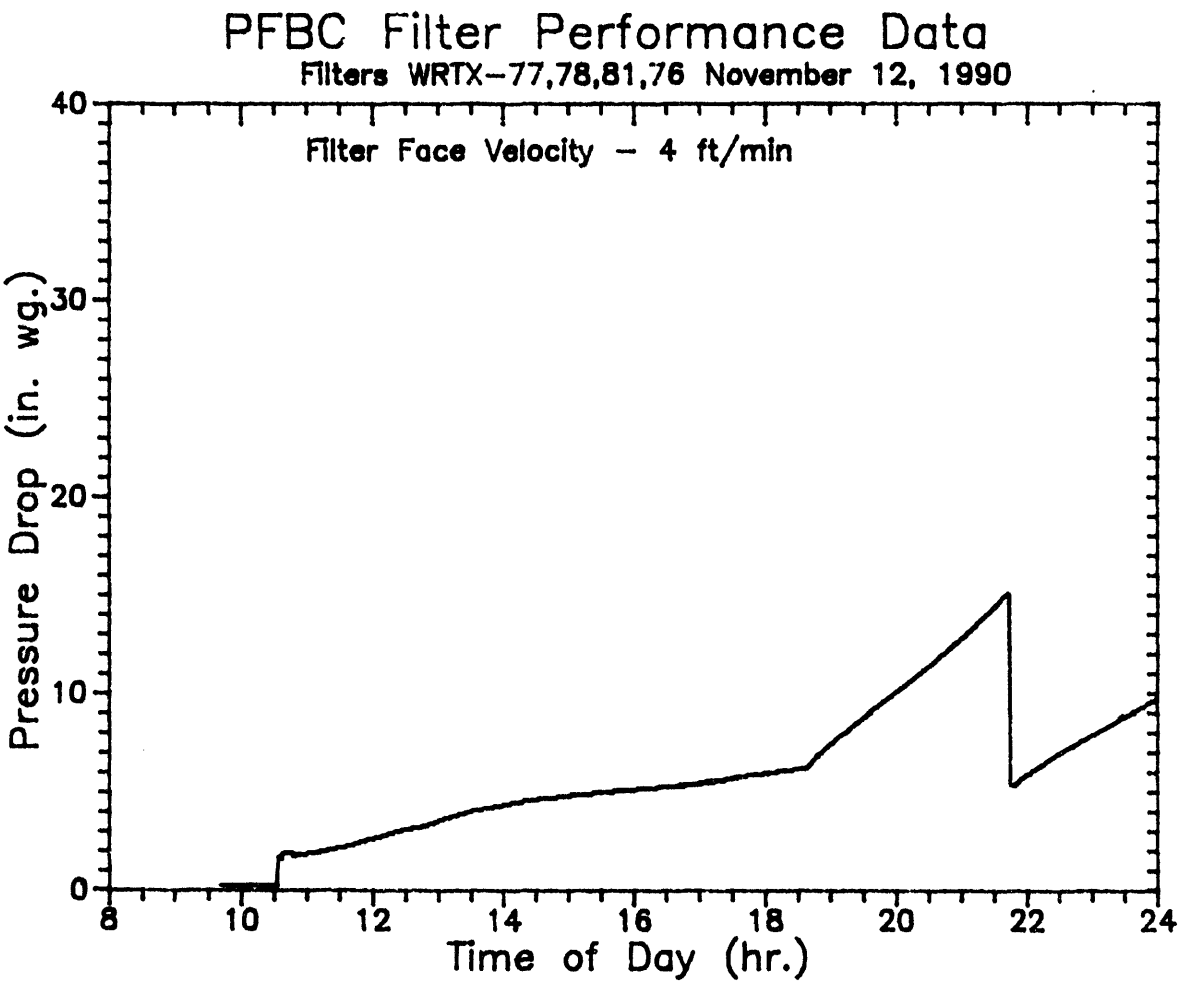

OPERATION NOTES FOR
NOVEMBER 12, 1990
START OF WEEK LONG TEST
ΔP TRIGGER = 15" WC
PULSE CLEANING -
320 psig / 0.1 sec.

COLD START

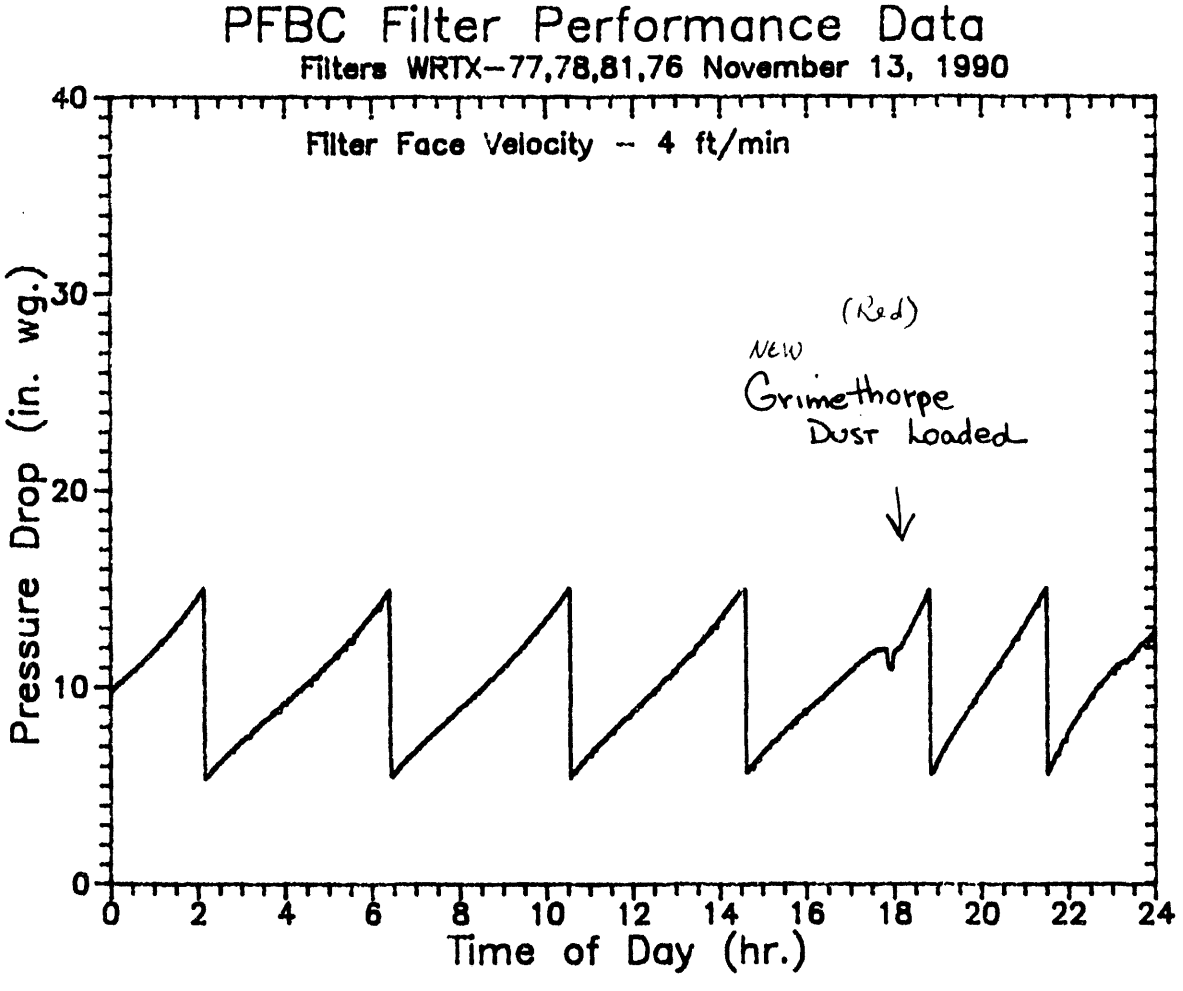

OPERATION NOTES FOR
NOVEMBER 13, 1990
ΔP TRIGGER = 15" WC
PULSE CLEANING - 320psig/0.1 sec
1715 - DUST LOADED

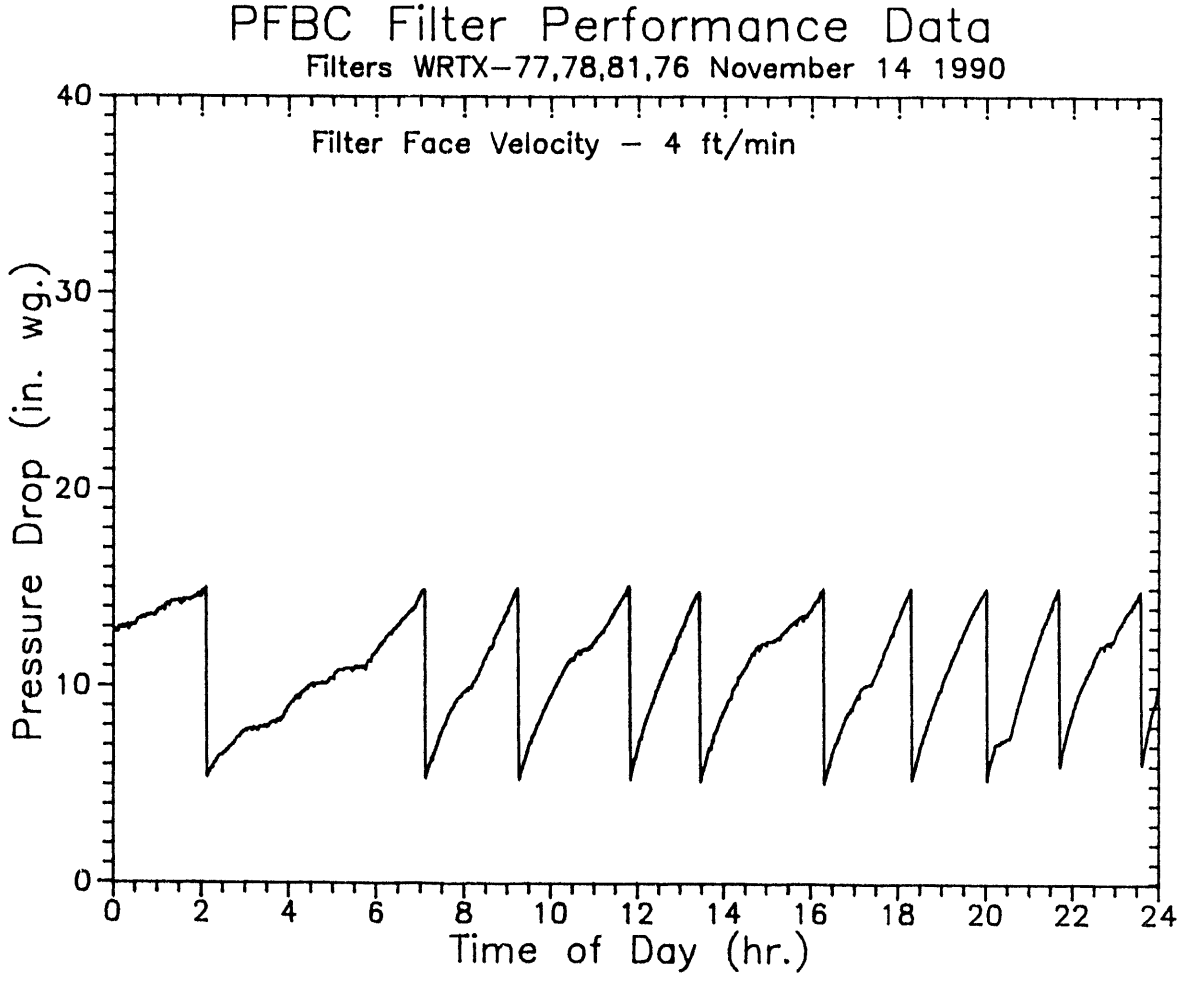

OPERATION NOTES FOR
NOVEMBER 14, 1990

Δ P TRIGGER = 15 "WC

PULSE CLEANING – 320psig/0.1 sec

DUST FEED ERRATIC

0200 - 0530
1030 - 1100
1430 - 1545
2000 - 2030
2230 - 2300

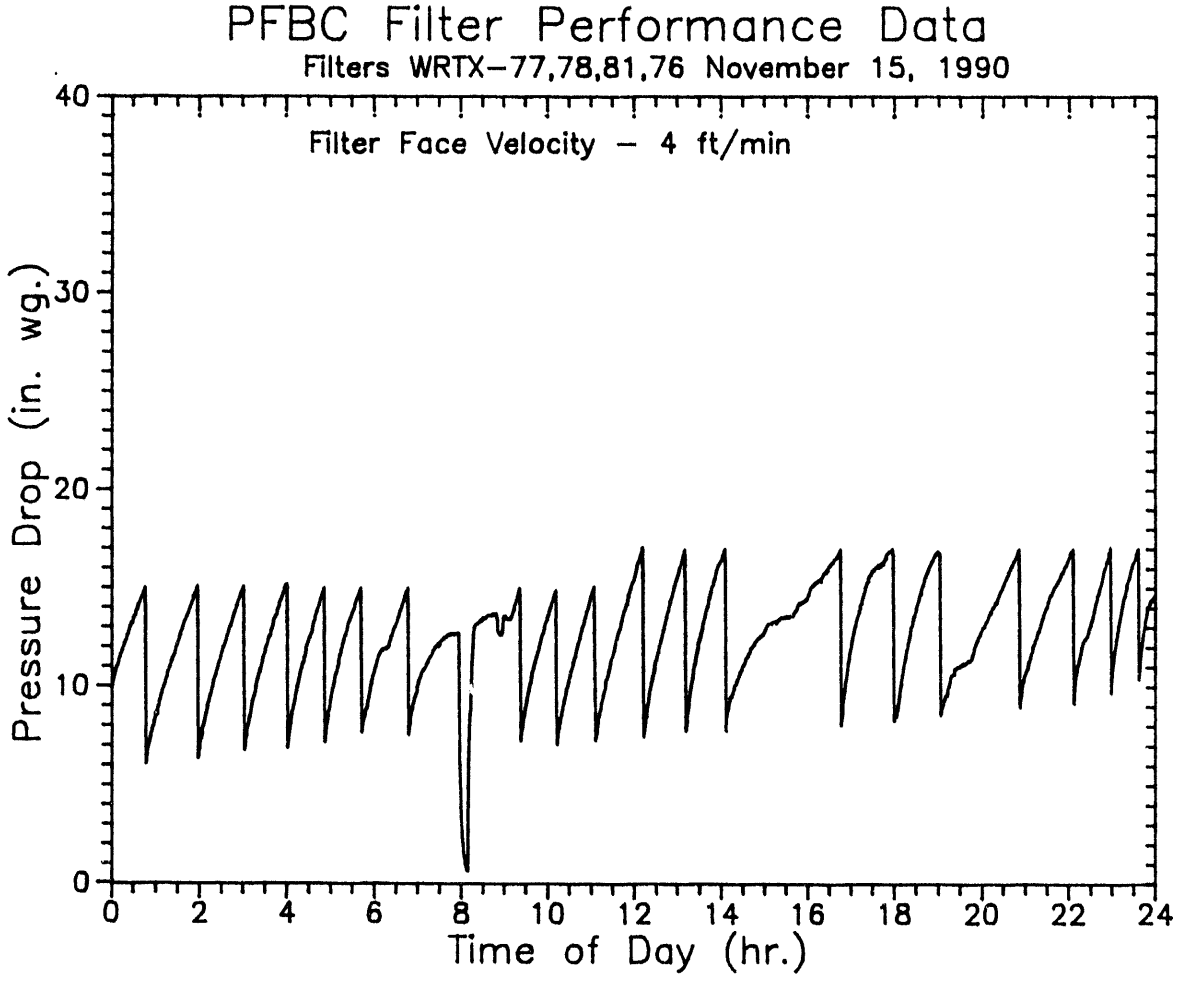

OPERATION NOTES FOR
NOVEMBER 15, 1990

0800 FLAME OUT-UNSCHEDULED RESTART
0850 - DUST LOADED
1210 - CHANGED ΔP TRIGGER FROM 15" WC to 17" WC
PULSE CLEANING:
320 psig/0.1 sec
1010 330 psig/0.1 sec
1100 340 psig/0.1 sec

Nov 15, 1990
CONT.

ERRATIC DUST FEED
1500 – 1540
1920 – 1945

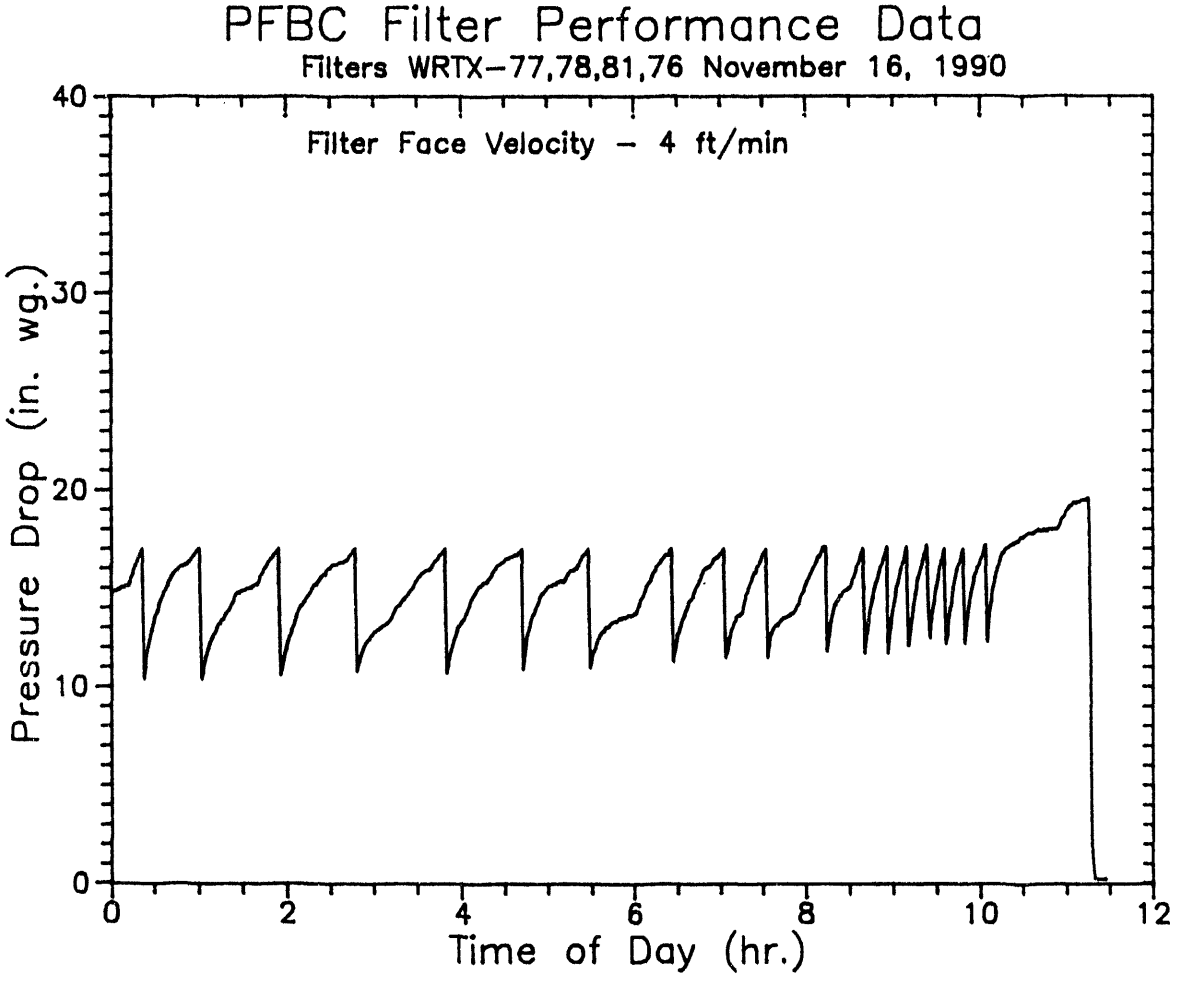

OPERATION NOTES FOR NOVEMBER 16, 1990

1115 - UNSCHEDULED SHUTDOWN
BACK PRESSURE CONTROL VALVE HOUSING LEAK
END OF TEST

1000 - CHANGE ΔP TRIGGER FROM 17"WC to 19.5"WC

pulse cleaning - 11-16-90 cont.
340 psig 0.1 sec

Dust Not Feeding PROPERLY
0000 → 0830
1000 → 1115

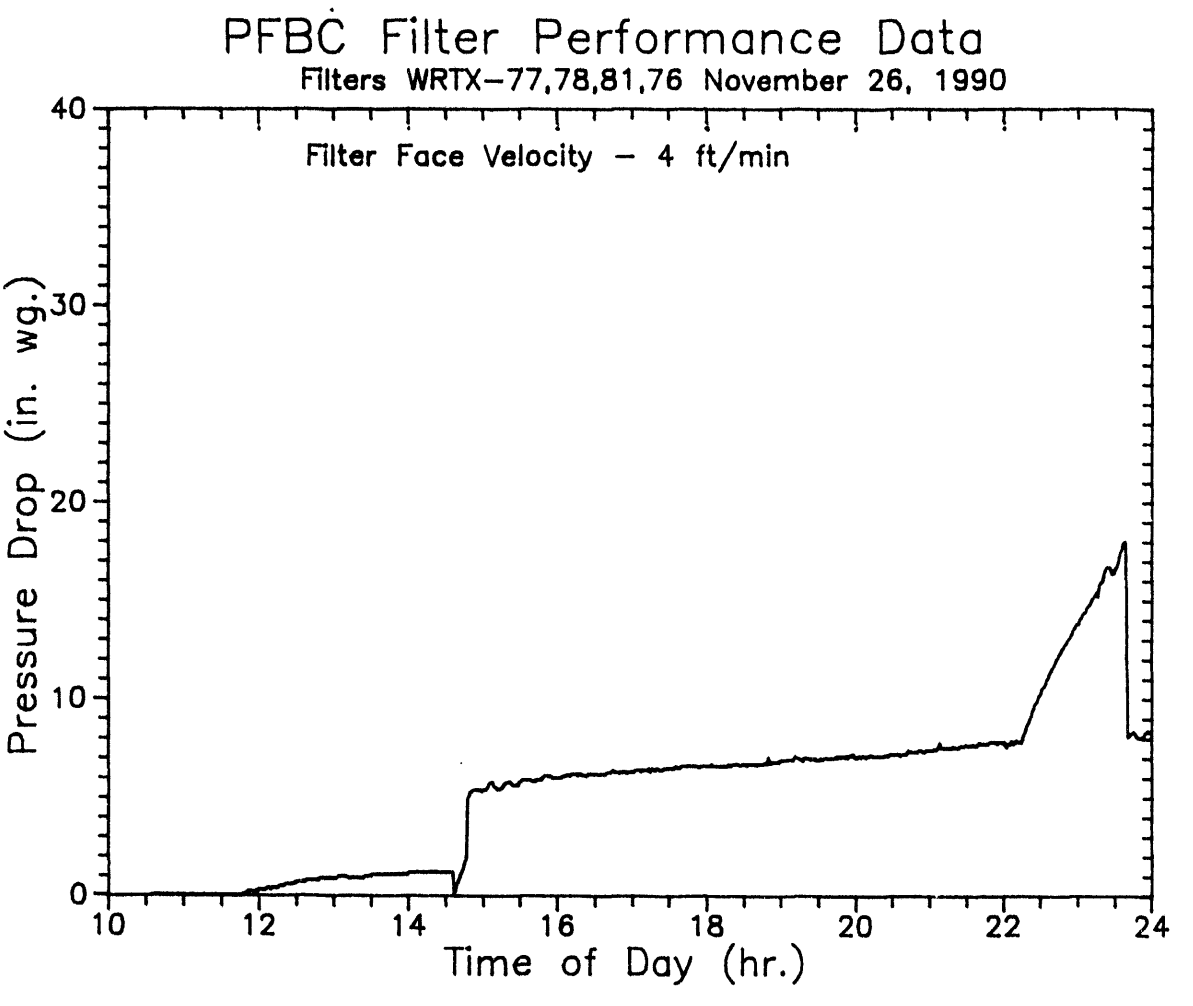

OPERATION NOTES FOR
NOVEMBER 26, 1990
START WEEK LONG TEST
INCLUDING TURBINE
TRIP SIMULATIONS
ΔP TRIGGER = 18" WC
PULSE Cleaning - 340 psig/0.1 sec

PFBC Filter Performance Data

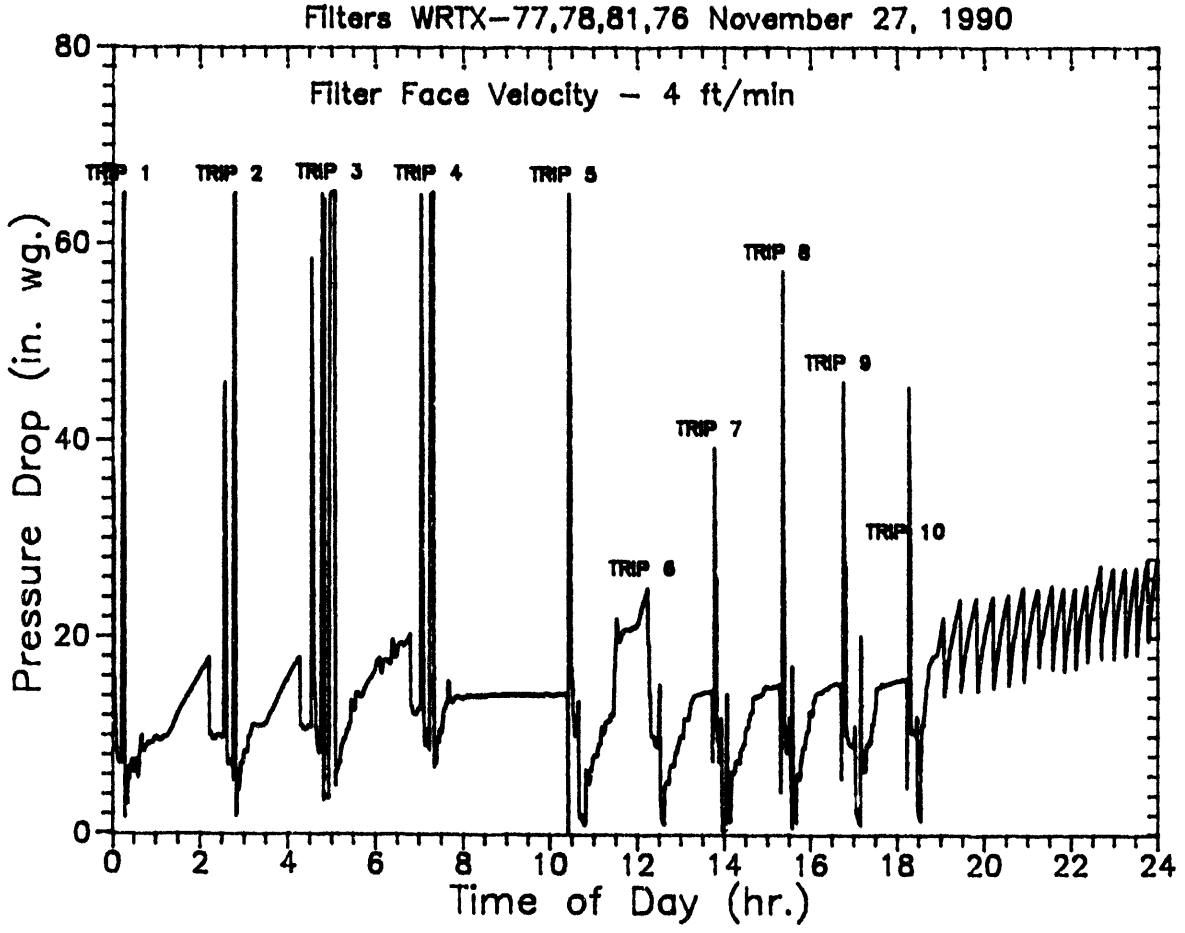

OPERATION NOTES FOR NOVEMBER 27, 1990

TURBINE TRIP SIMULATIONS 1–10

0645 change ΔP TRIGGER from 18" wc to 20" wc

1210 change ΔP TRIGGER From 20" wc to 25" wc

1830 - Decrease System Pressure to 75 psig

11/27/90 cont.

1900 change ΔP TRIGGER FROM 25" wc to 22" wc

1925 change ΔP TRIGGER FROM 22" wc to 24" wc

2100 change ΔP TRIGGER FROM 24" wc to 25" wc

2230 change ΔP TRIGGER FROM 25" wc to 27" wc

2330 change ΔP TRIGGER from 27" wc to 28" wc

11/27/90 Cont.

pulse cleaning – 340 psig/0.1sec

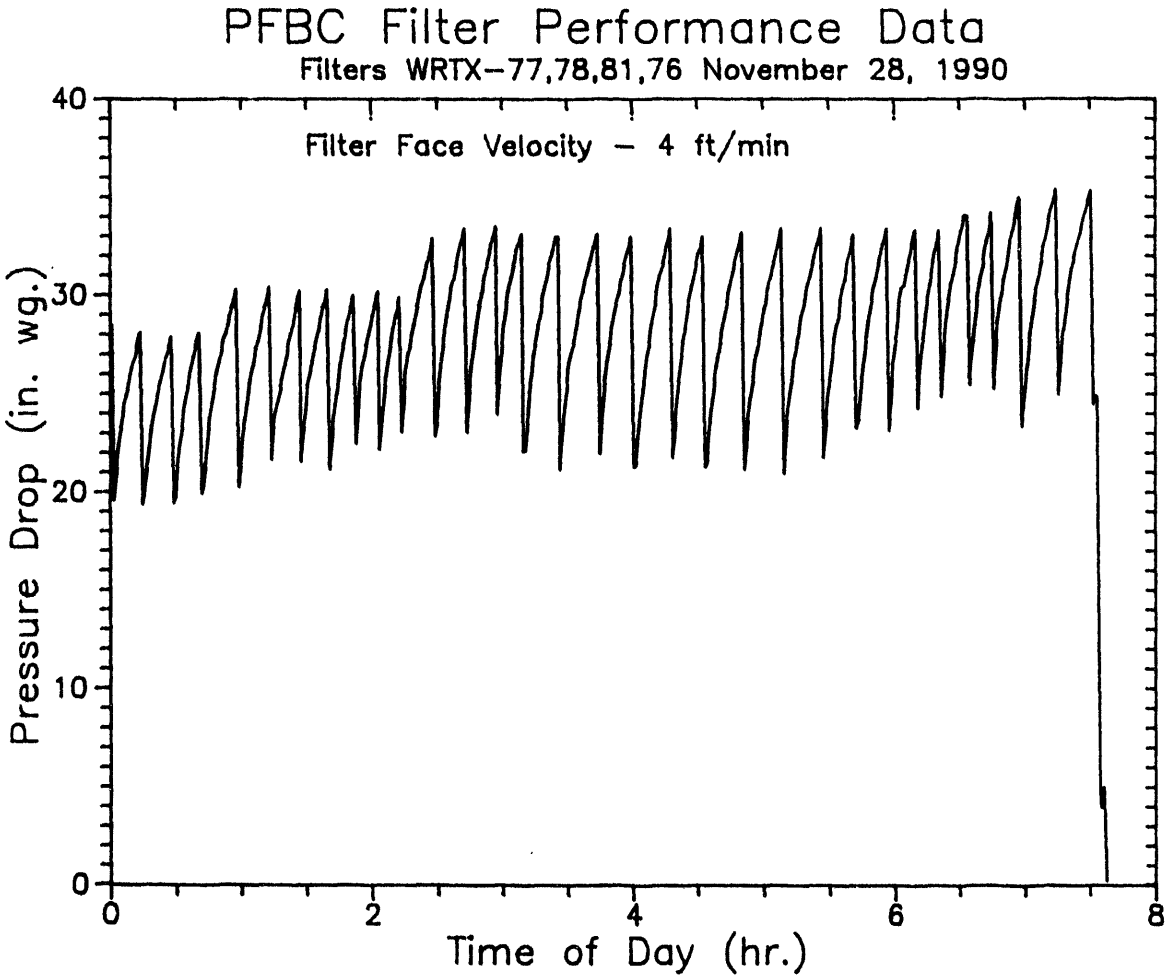

OPERATION Notes FOR
November 28, 1990

0100 Change ΔP TRIGGER
FROM 28 "wc to 30" wc.
0230 Change ΔP TRIGGER
FROM 30 "wc to 33" WC
0630 Change ΔP TRIGGER
FROM 33 "wc to 34 "wc
0700 Change ΔP TRIGGER
FROM 34" wc to 35 " WC

11/28/90
CONT.

0820 PULSE CLEANING
CHANGED FROM 340 TO
360 PSIG/0.1SEC
0940 PULSE CLEANING
CHANGED FROM 360 TO
370 PSIG/0.1SEC
0730 Dust Leak
>10ppm Concentration
OUT
SHUT DOWN FOR INSPECTION

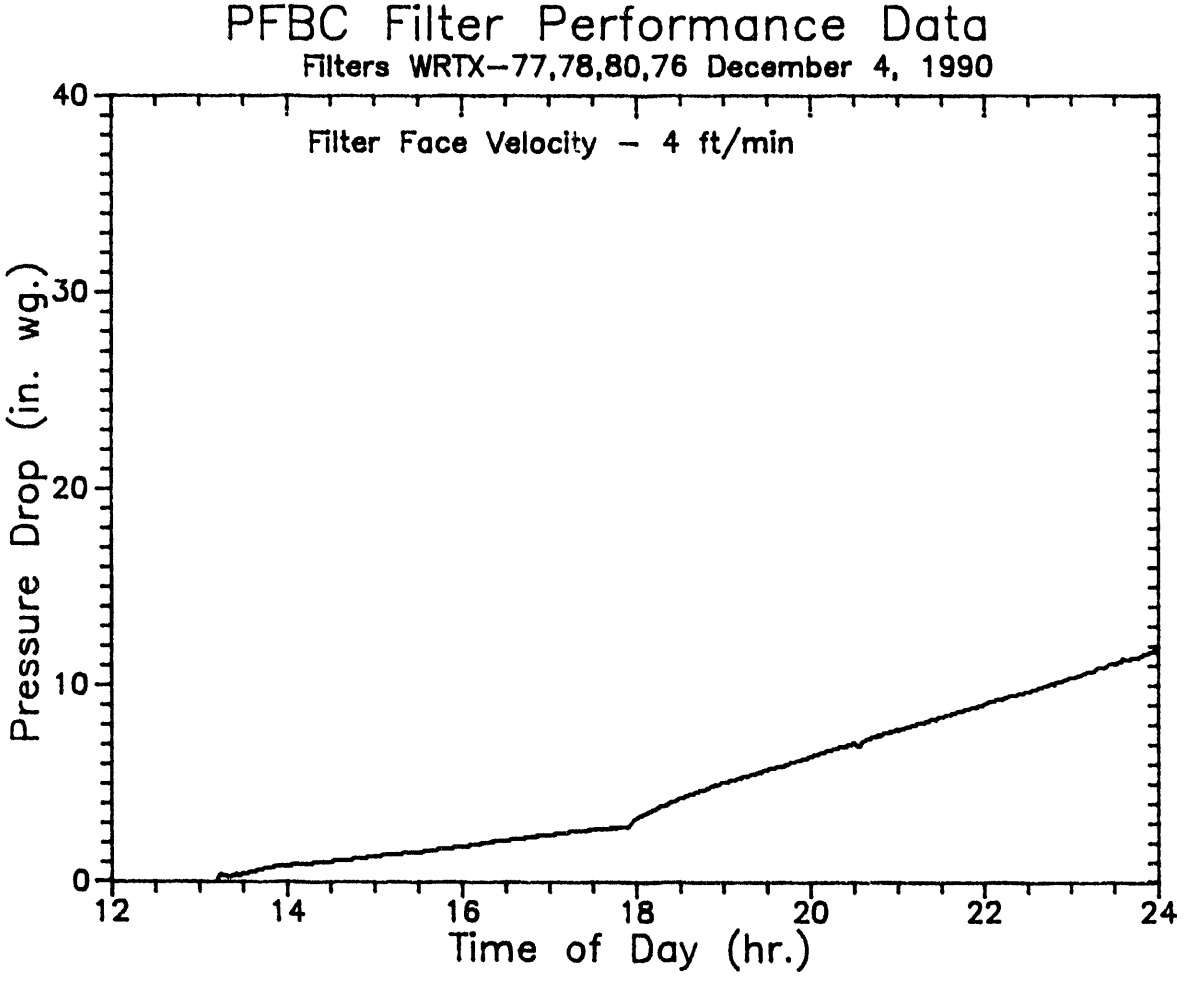

OPERATION NOTES FOR
December 4, 1990
WRTX-81 REPLACED WITH
WRTX-80

START WEEK LONG TEST
1750 - DUST FEED ON
ΔP TRIGGER = 13" WC.
COLD START

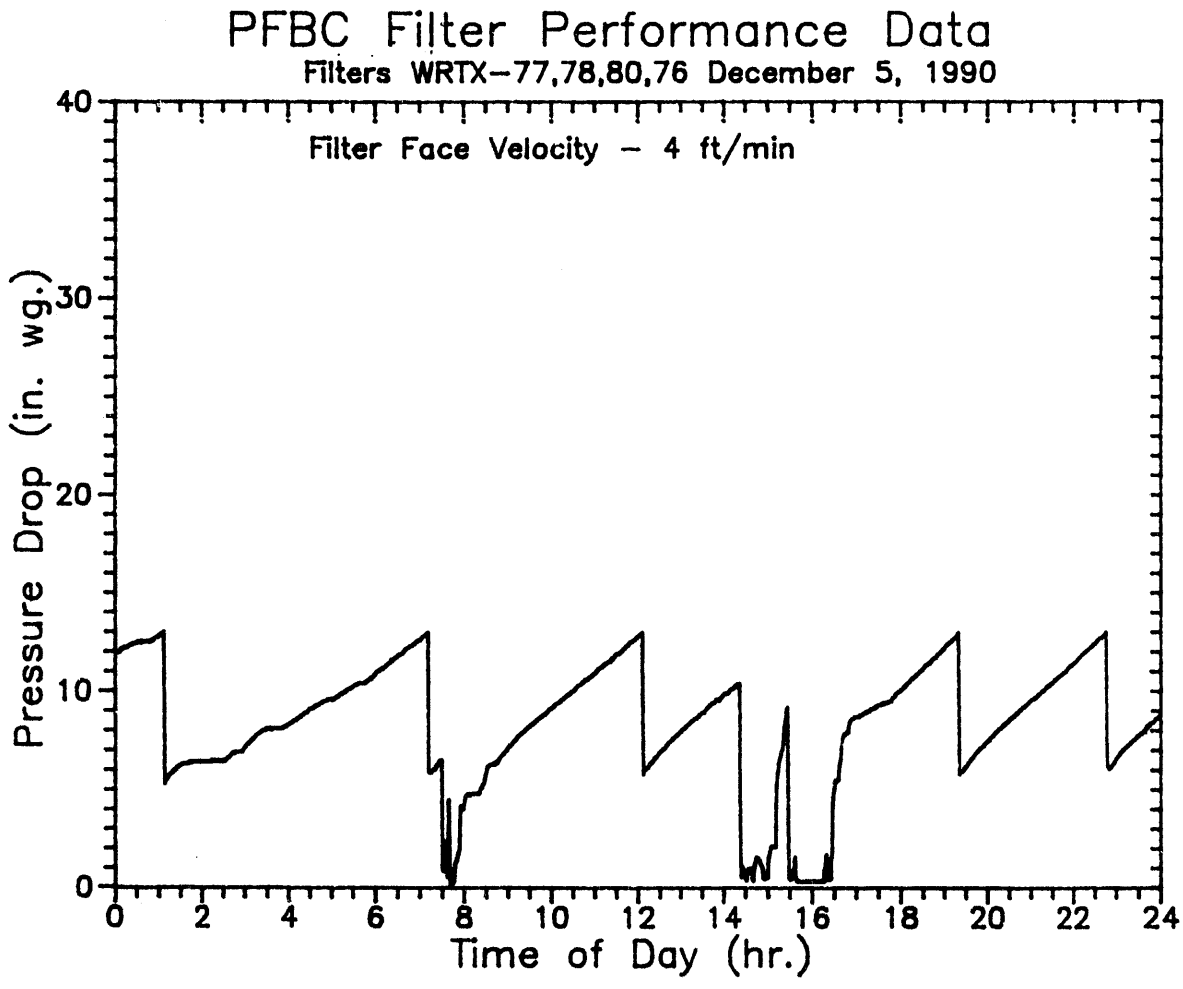

OPERATION NOTES FOR DECEMBER 5, 1990

A P TRIGGER = 13" WC

PULSE CLEANING - 310 psig/0.1 sec

ERRATIC DUST FEED
0130 - 0400

0725 FLAME OUT-UNSCHEDULED
RESTART

1420-FLAME OUT- UNSCHEDULED

1500 RESTART

1525 FLAME OUT - UNSCHEDULED (12/5/90 CONT.)

1615 RESTART

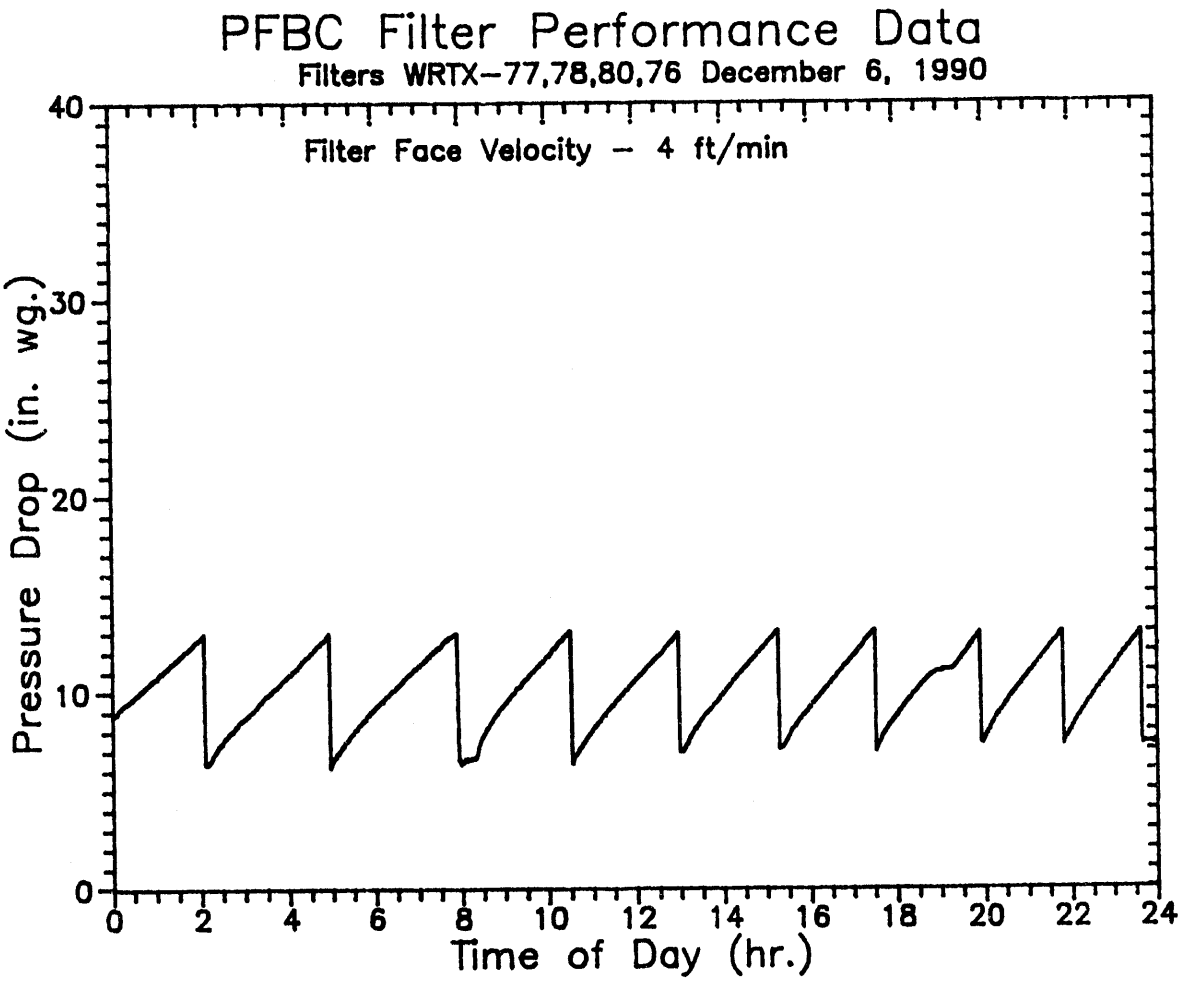

OPERATION NOTES FOR
DECEMBER 6, 1990
ΔP TRIGGER = 13" WC
PULSE CLEANING - 310psig/0.1 sec.

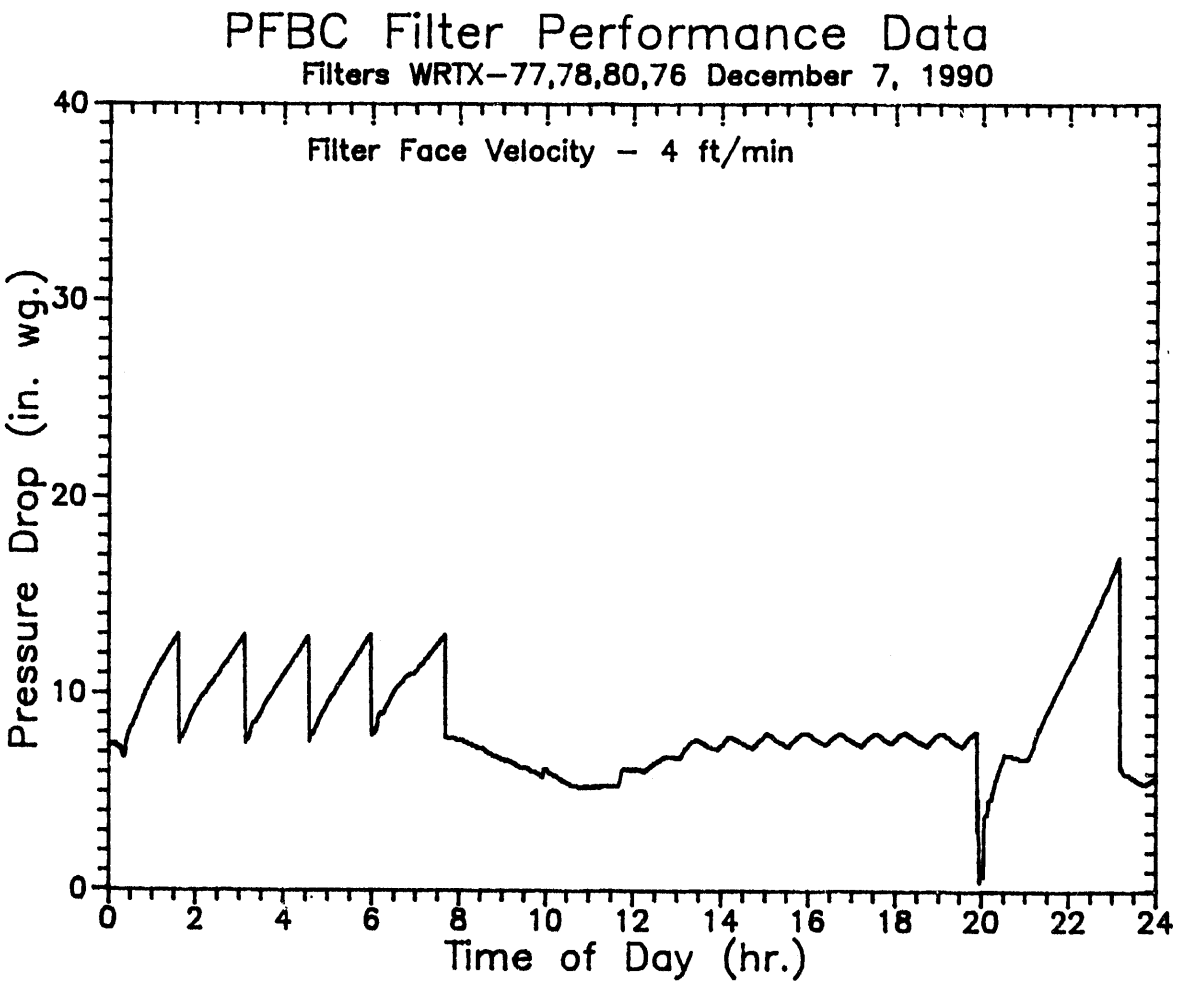

OPERATION NOTES FOR
DECEMBER 7, 1990
0800 - DECREASE FILTER
TEMPERATURE TO 950°F
1300-2100 TEMPERATURE
RAMP CYCLES (950°F-1250°F)
#1-10
1950 FLAME OUT - UNSCHEDULED
RESTART
2300 Change ΔP TRIGGER
FROM 13" WC TO 17" WC.
PULSE CLEANING - 310 PSIG/0.1sec

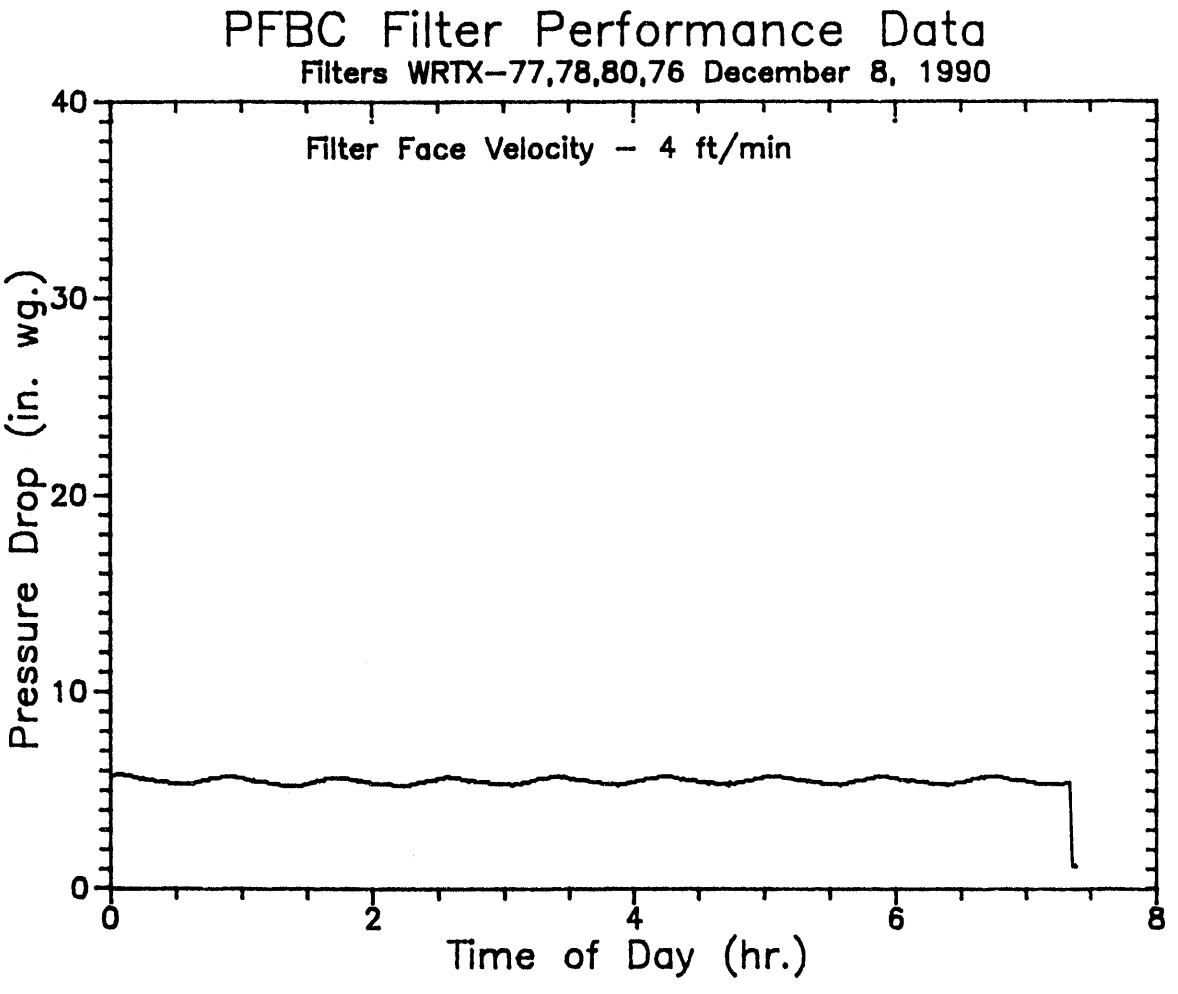

OPERATION NOTES FOR
DECEMPER 8, 1990

TEMPERATURE RAMP
CYCLES 11 - 20 (950-1250°F)

0720 SCHEDULED
SHUTDOWN

NO DUST FED

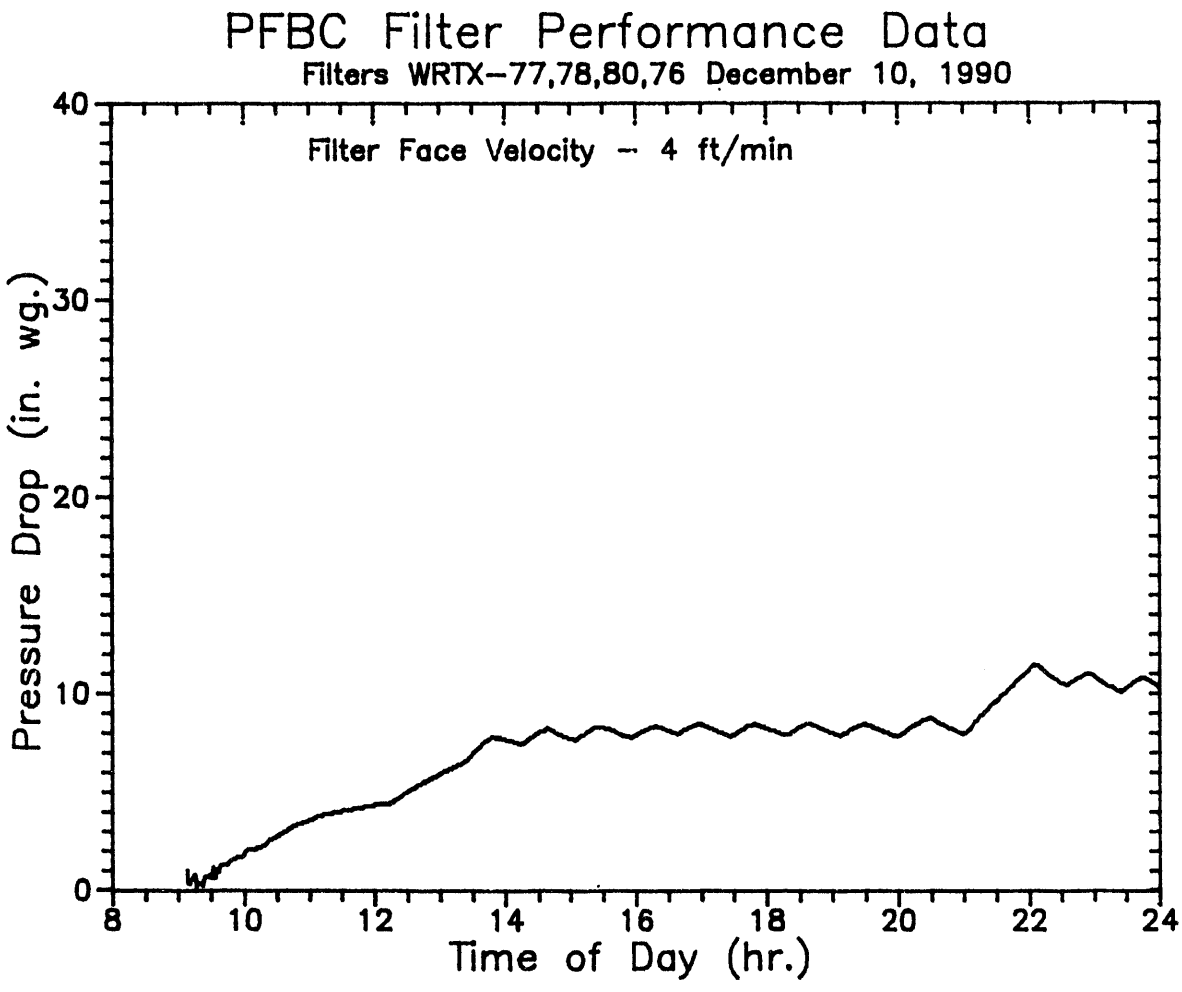

OPERATION NOTES FOR
DECEMBER 10, 1990
START WEEK LONG TEST
TEMPERATURE RAMP CYCLES
21 - 32 (950-1250°F)

DUST FED + SAMPLES
1210 – 1320
2100 – 2200

COLD START

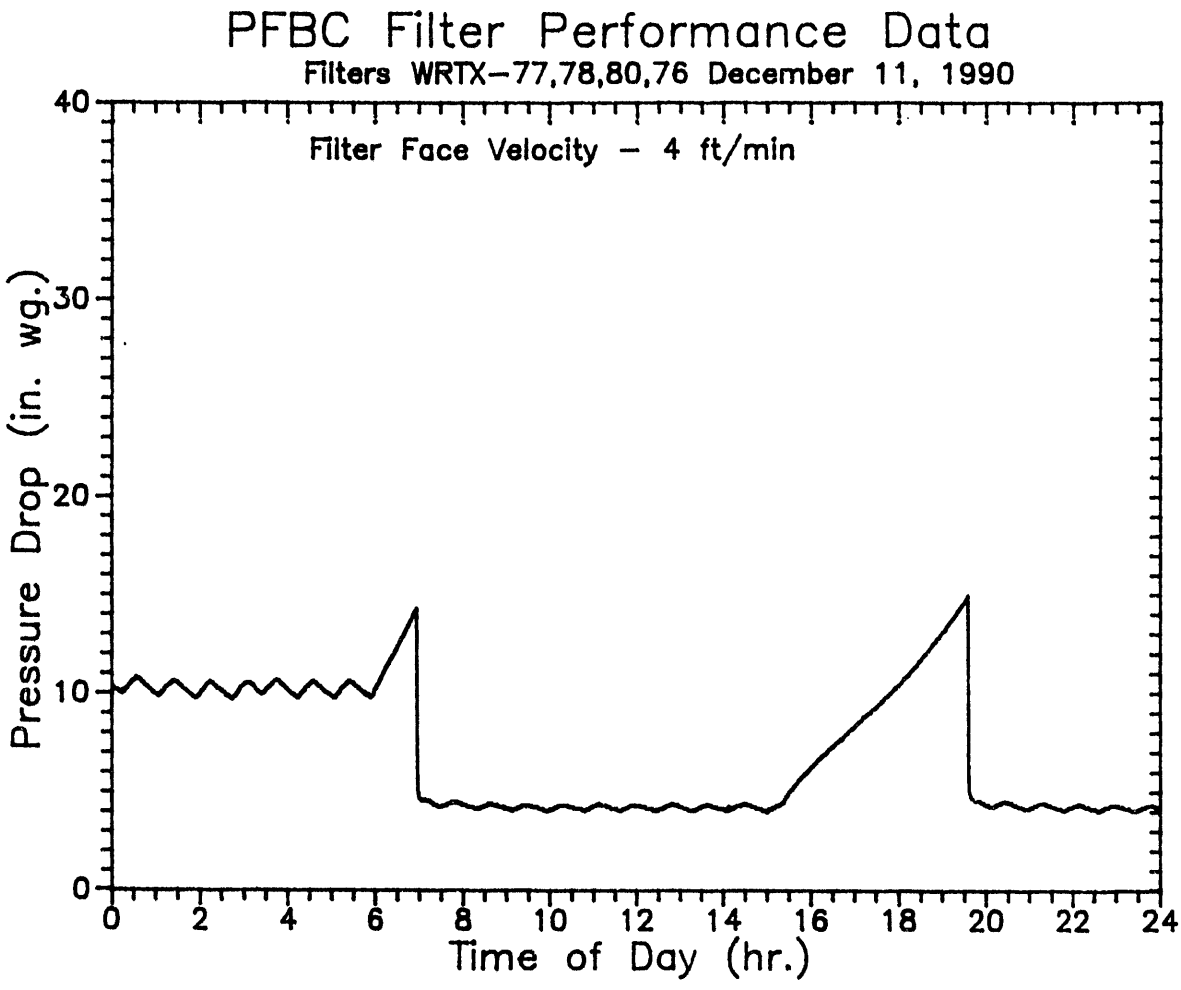

OPERATION NOTES FOR
DECEMBER 11, 1990

TEMPERATURE RAMP CYCLES
33 – 55 (950-1250°F)

0650 ΔP TRIGGER = 14.3" wc
PULSE CLEANING - 310psig/0.1 sec.

1930 ΔP TRIGGER = 15.0" wc
PULSE CLEANING - 310psig/0.1 sec.

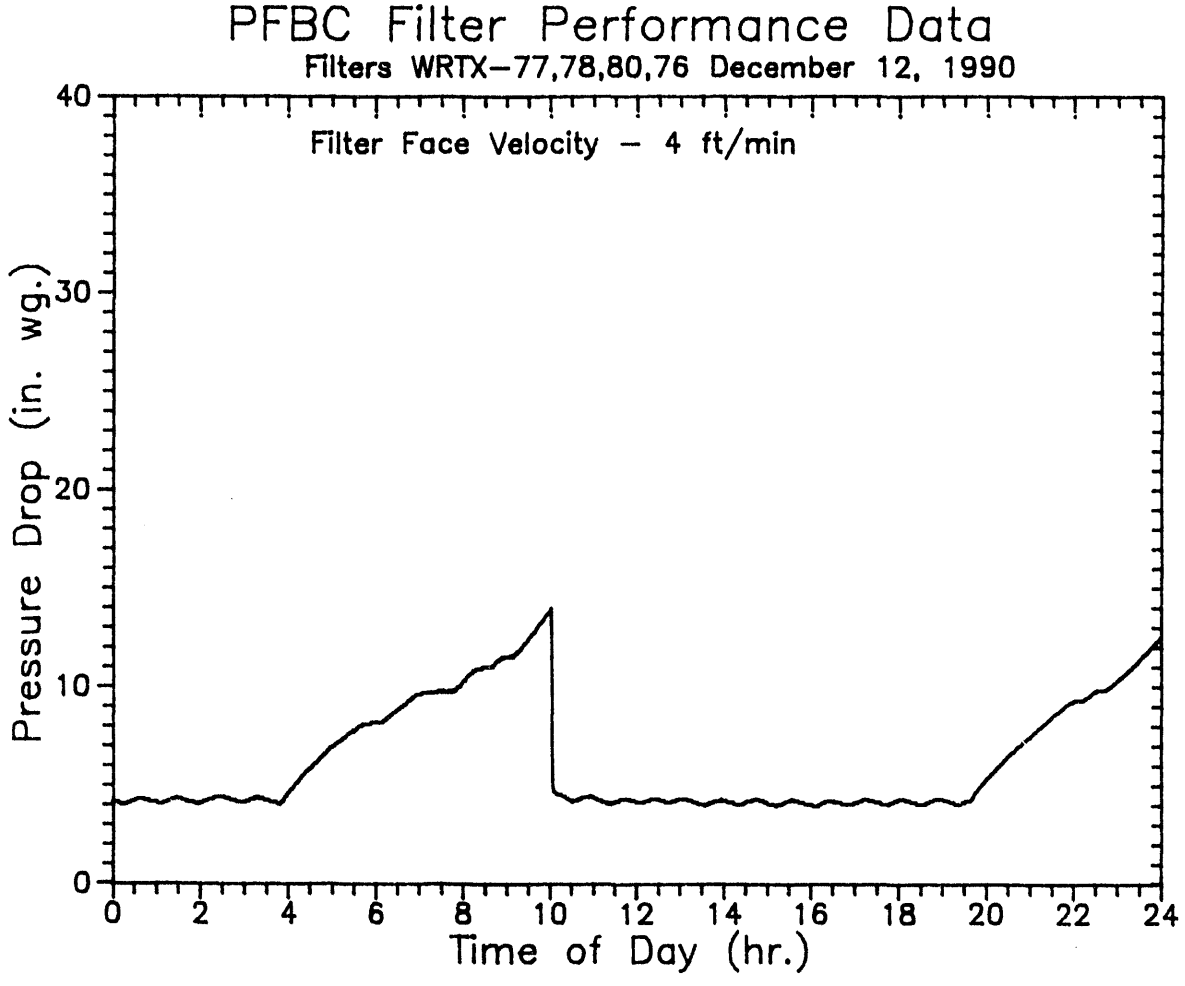

OPERATION NOTES FOR
DECEMBER 12, 1990

TEMPERATURE RAMP
CYCLES 56-72 (950-1250°)

ΔP TRIGGER = 14 "WC
PULSE CLEANING - 310psig/0.15sec

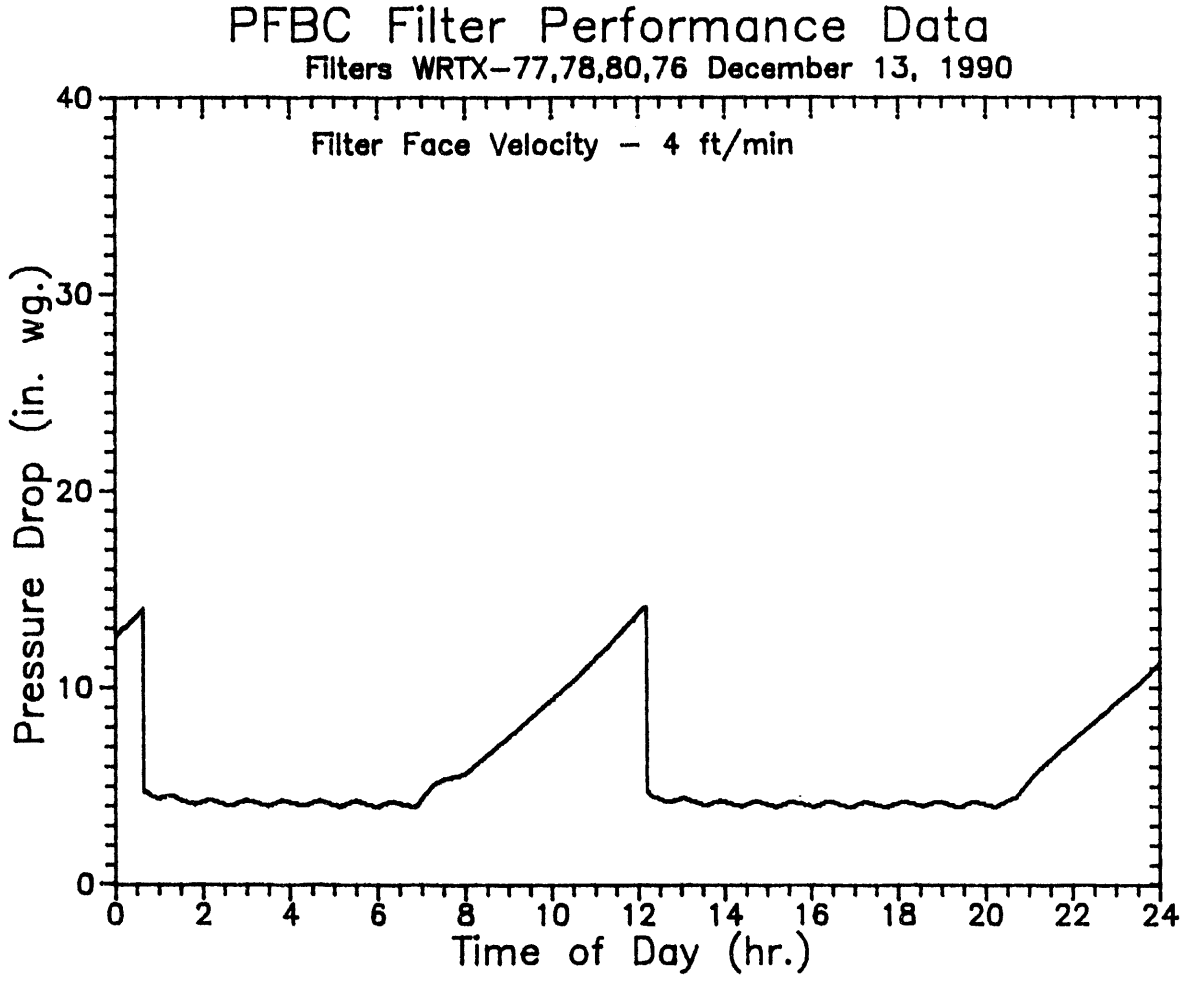

OPERATION NOTES FOR
DECEMBER 13, 1990
TEMPERATURE RAMP
CYCLES 73-90 (950-1260°F)
Δ P TRIGGER = 14" WC
PULSE CLEANING - 310 psig / 0.1 Sec

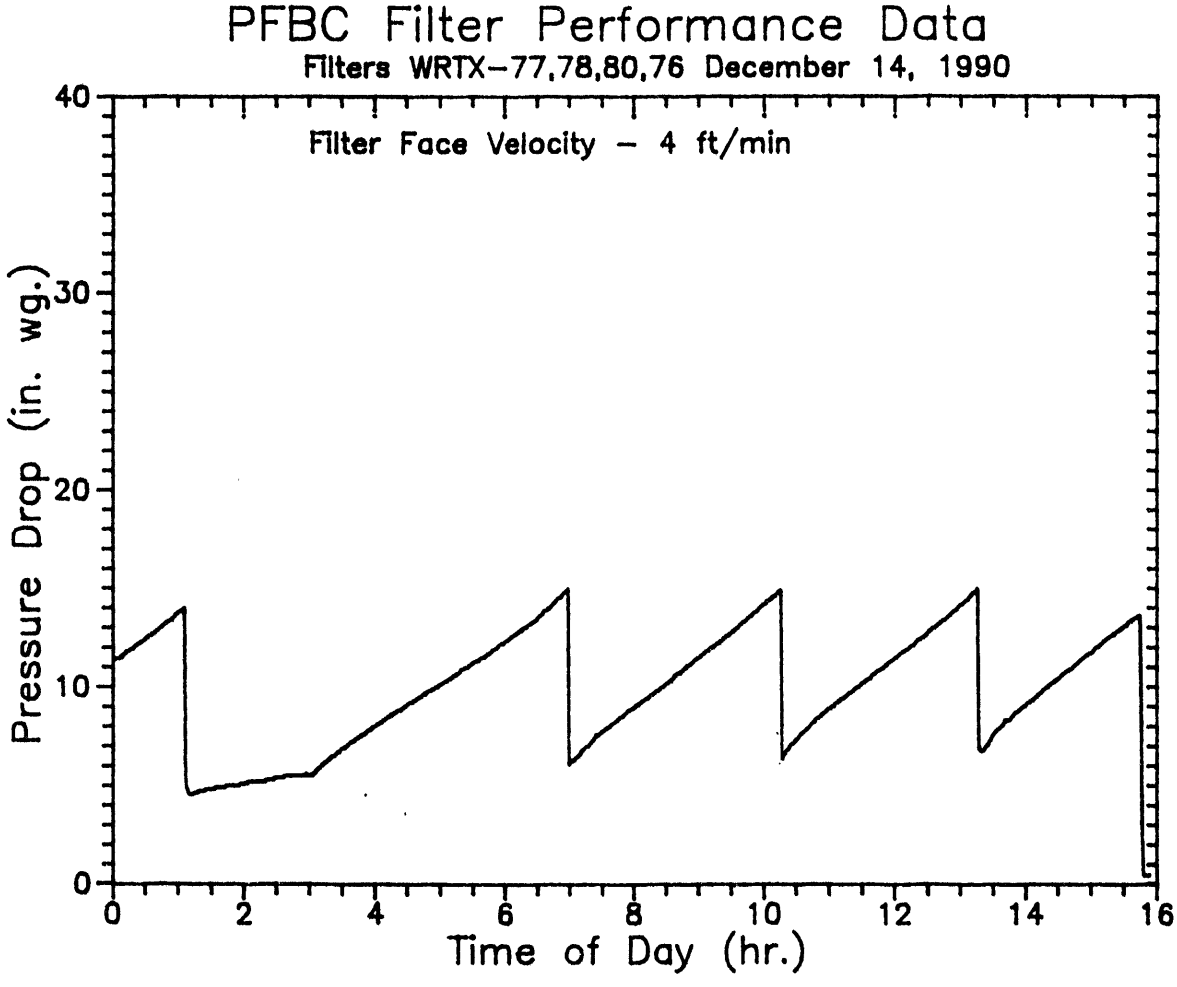

OPERATION NOTES FOR
DECEMBER 14, 1990
0100 INCREASE FILTER
TEMPERATURE TO 1550°F
0700 Change ΔP TRIGGER
FROM 14" WC to 15" WC.
PULSE CLEANING - 310 psig/0.1
SEC.
1540 DUST LEAK, 7.14ppm
Concentration out
SHUT DOWN FOR INSPECTION

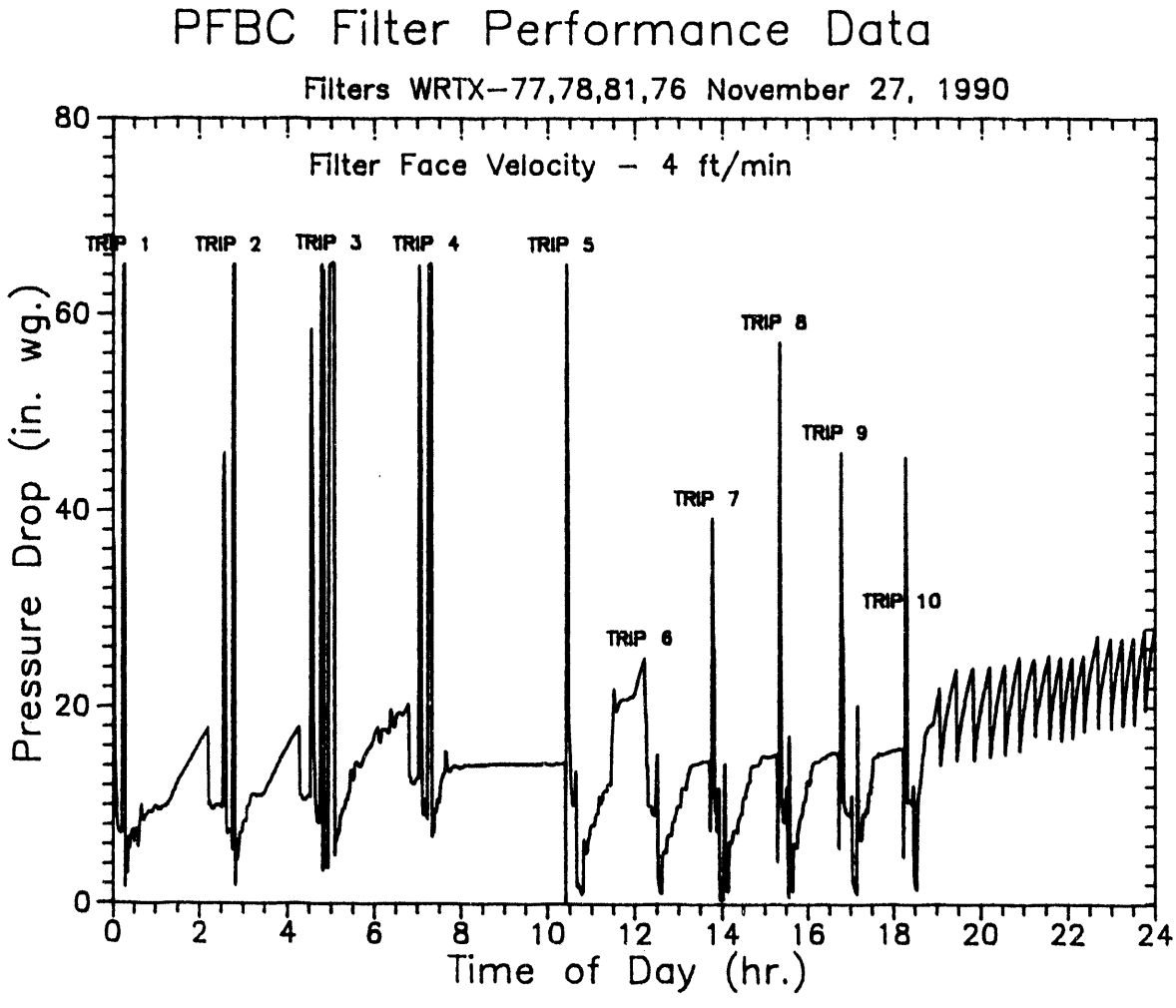

OPERATION NOTES FOR NOVEMBER 27, 1990

TURBINE TRIP SIMULATION #1 - #10

900 lb/hr passage flow
160 psig system pressure
1500 - 1550 °F - PASSAGE TEMPERATURE
FLAME OUT FOR EACH SIMULATION

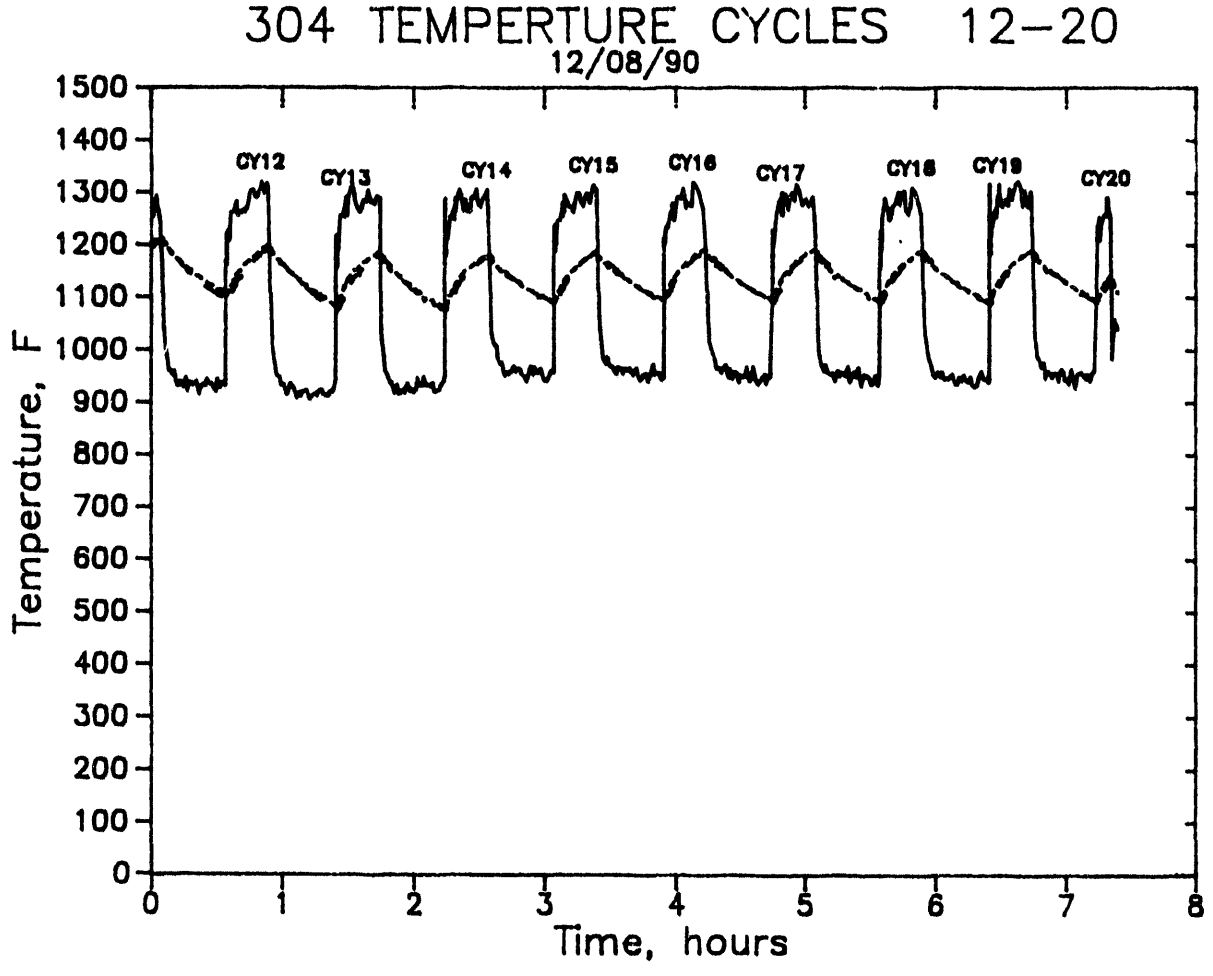

OPERATION NOTES FOR
DECEMBER 8, 1990

——— INLET TEMP.
— — FILTER TEMP.
- - - - VESSEL TEMP.

TEMPERATURE RAMPS
950°F to 1250°F
0720 SCHEDULED SHUTDOWN

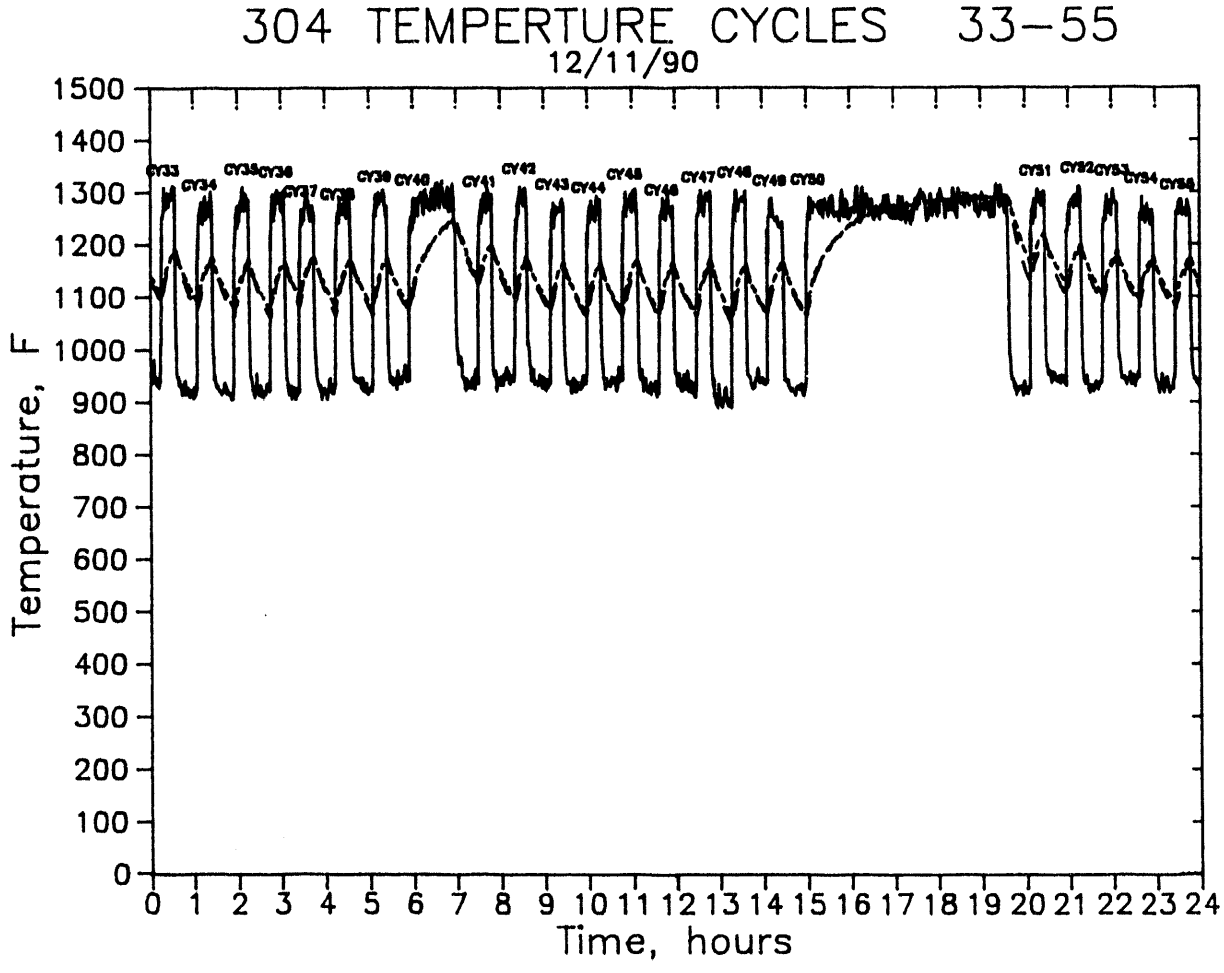

OPERATION NOTES FOR
DECEMBER 11, 1990

—— INLET TEMP.
— — FILTER TEMP
- - - - VESSEL TEMP

TEMPERATURE RAMPS
950 °F - 1250 °F
DUST FED AND SAMPLES TAKEN
AFTER CYCLES 40 AND 50

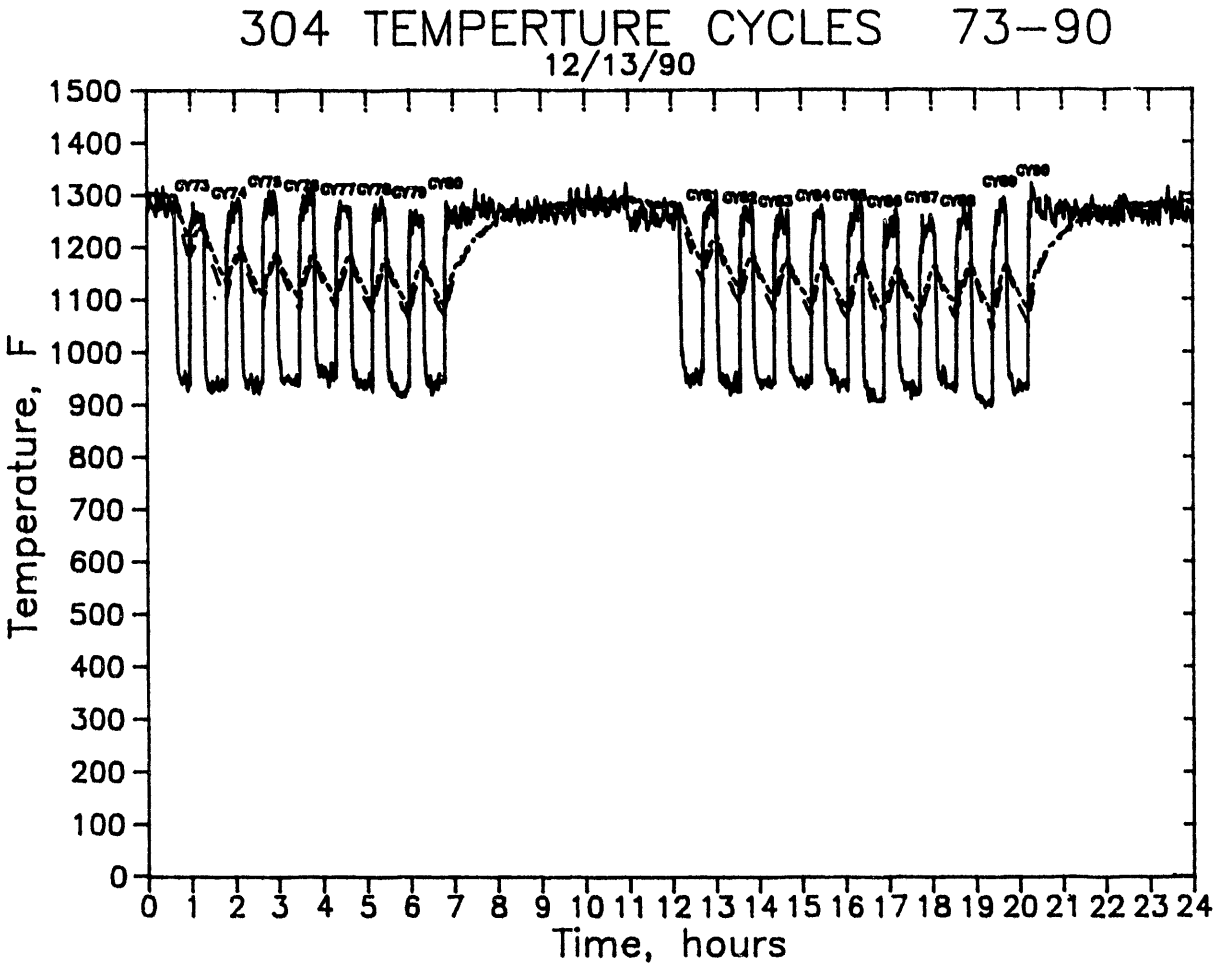

OPERATION NOTES FOR
DECEMBER 13, 1990

——— INLET TEMP.
— — FILTER TEMP
- - - - - VESSEL TEMP.

TEMPERATURE RAMPS
850°F – 1250°F
Dust fed and samples
taken after cycles 80 and
90

APPENDIX G

PRESSURE DROP TRACES FROM PFBC SIMULATOR FILTER TESTS WRTX-76, WRTX-77, WRTX-78 AND WRTX-21 STEADY STATE OPERATION

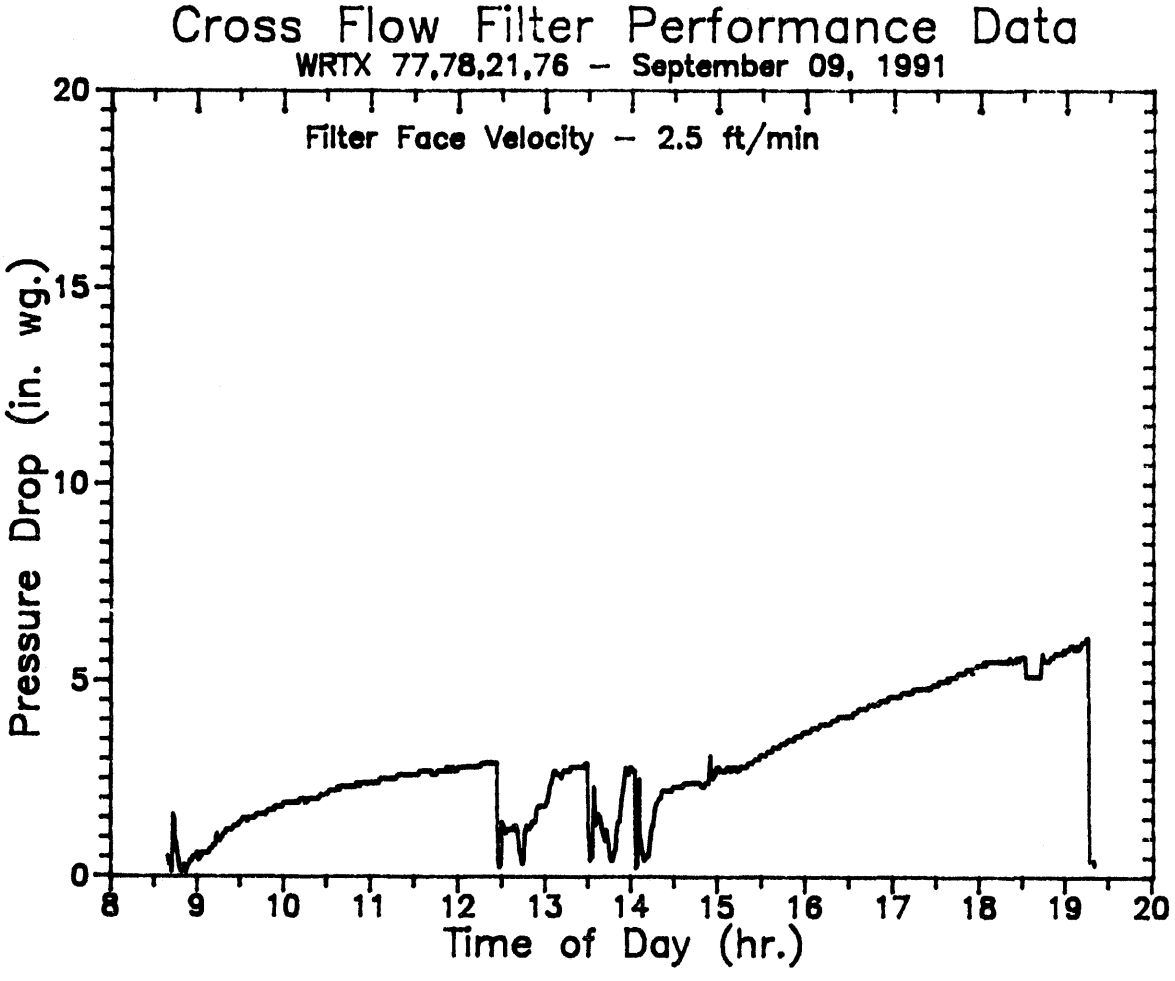

Operation Notes for September 09, 1991
delta–P Trigger = 13 in wc
Pulse Cleaning – 300 psig/0.1 sec
0849 Flame On system to temperature and pressure
1225 Flame out – Unscheduled
1330 Flame out – Unscheduled
1402 Flame out – Unscheduled
1755 Dust off, dust covering funnel in dust vessel, corrected
1916 Scheduled Shutdown

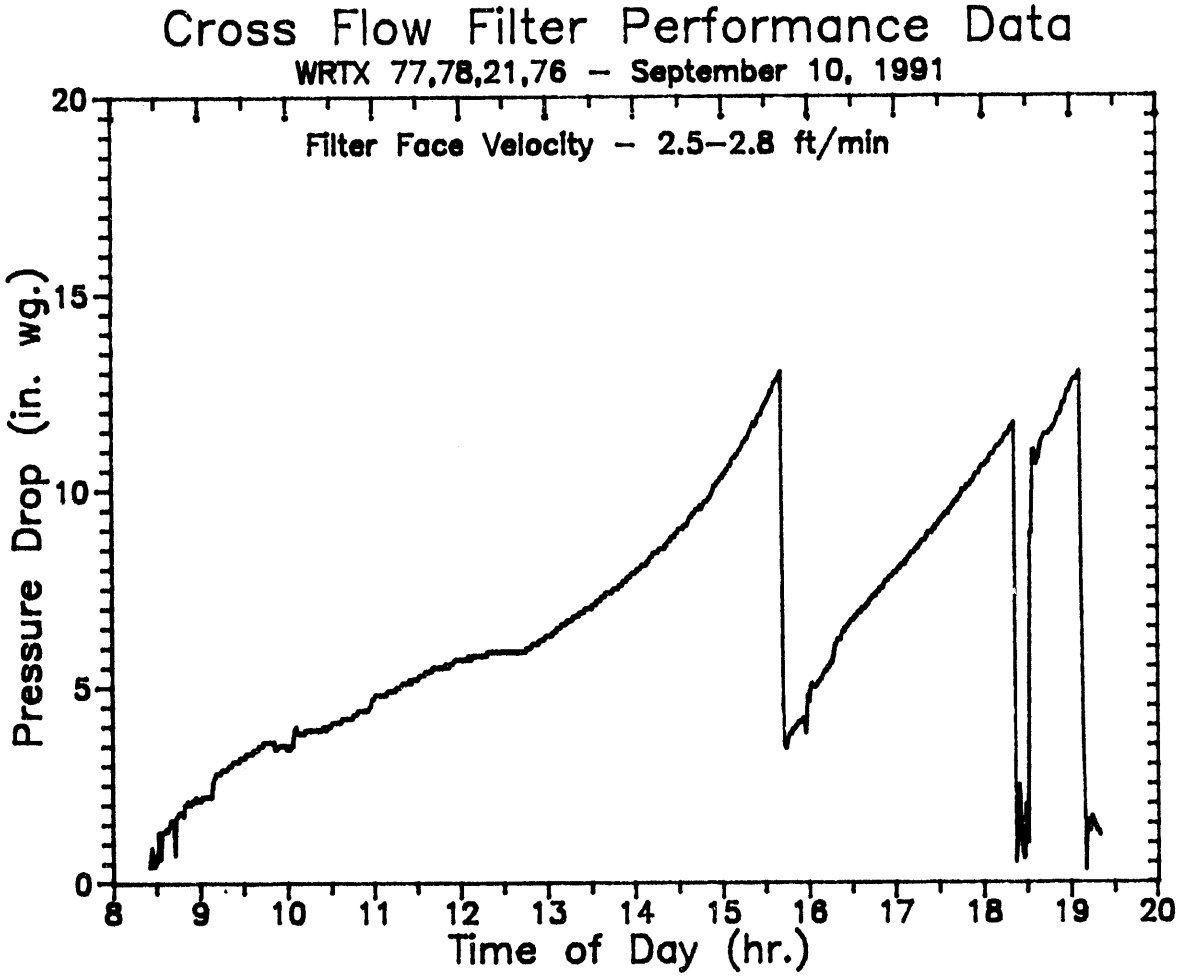

Operation Notes for September 10, 1991
delta–P Trigger = 13 in wc
Pulse Cleaning – 300 psig/0.1 sec
0825 Flame On system to temperature and pressure
1555 System Pressure lowered to 90 psig
1615 System Flow raised to 800 PPH
1820 Flame out – Unscheduled
1835 System Pressure raised to 95 psig
1908 Scheduled Shutdown

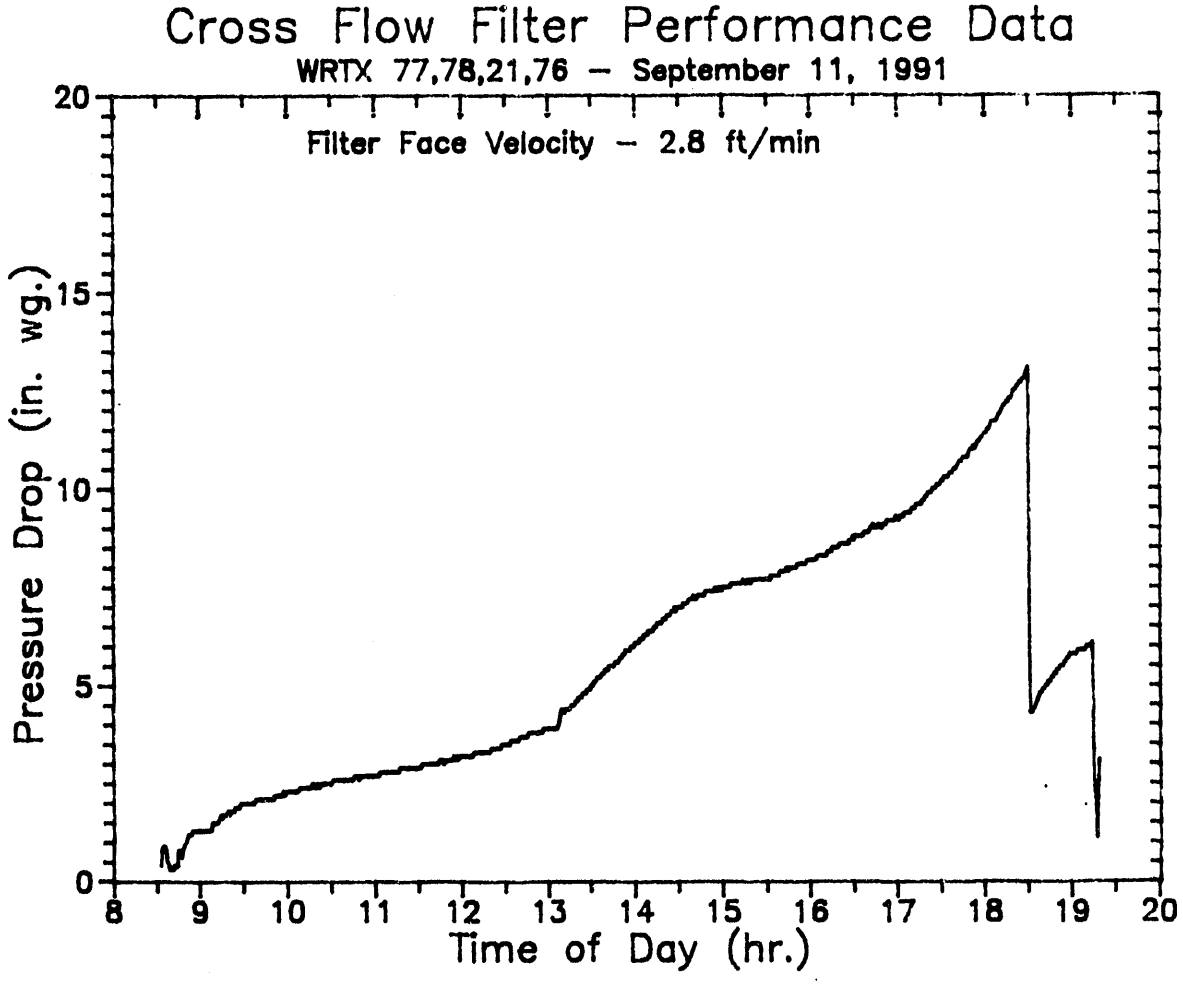

Operation Notes for September 11, 1991
delta–P Trigger = 13 in wc
Pulse Cleaning – 300 psig/0.1 sec
0835 Flame On system to temperature and pressure
1915 Scheduled Shutdown

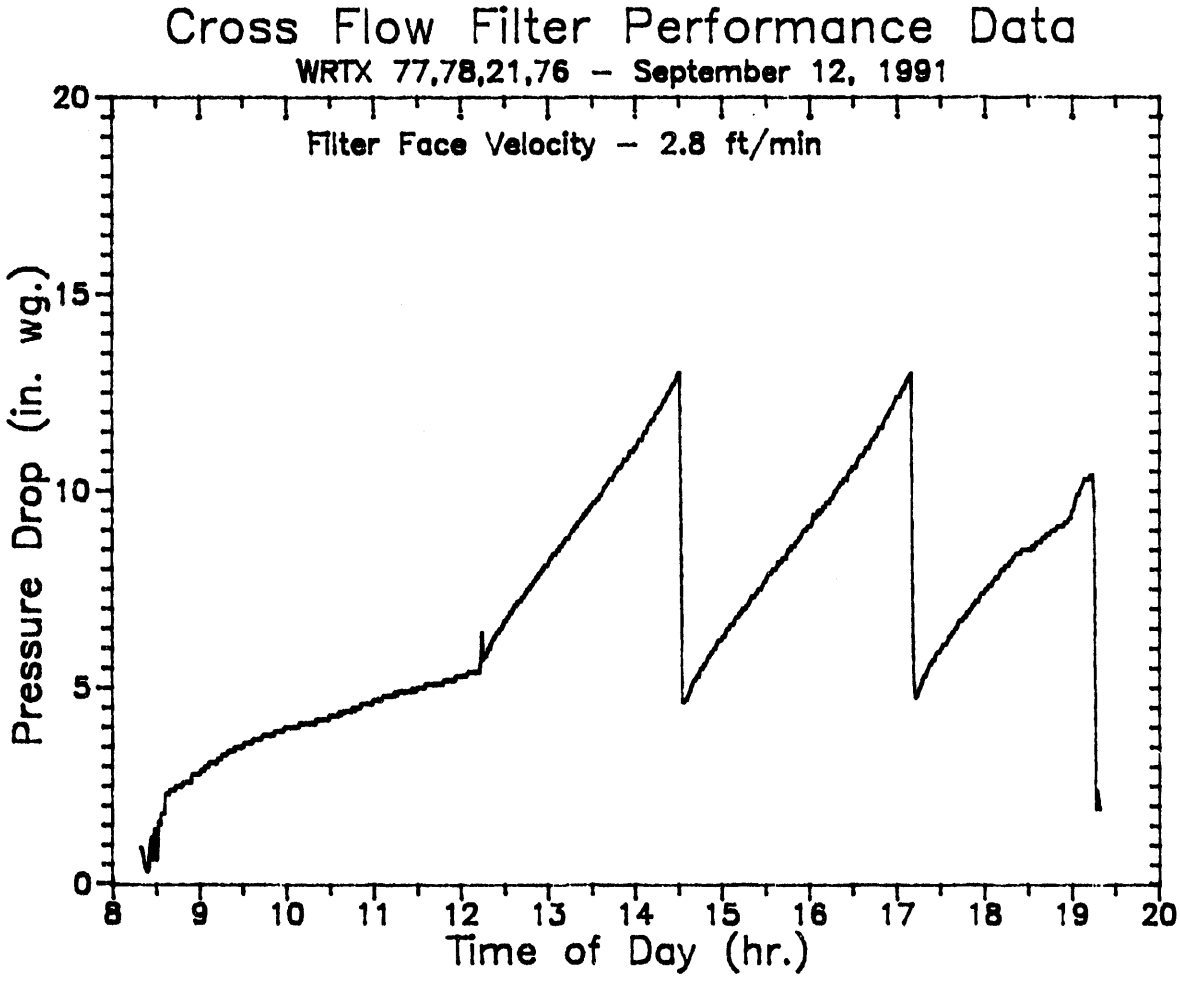

Operation Notes for September 12, 1991
delta–P Trigger = 13 in wc
Pulse Cleaning – 300 psig/0.1 sec
0820 Flame On system to temperature and pressure
1916 Scheduled Shutdown

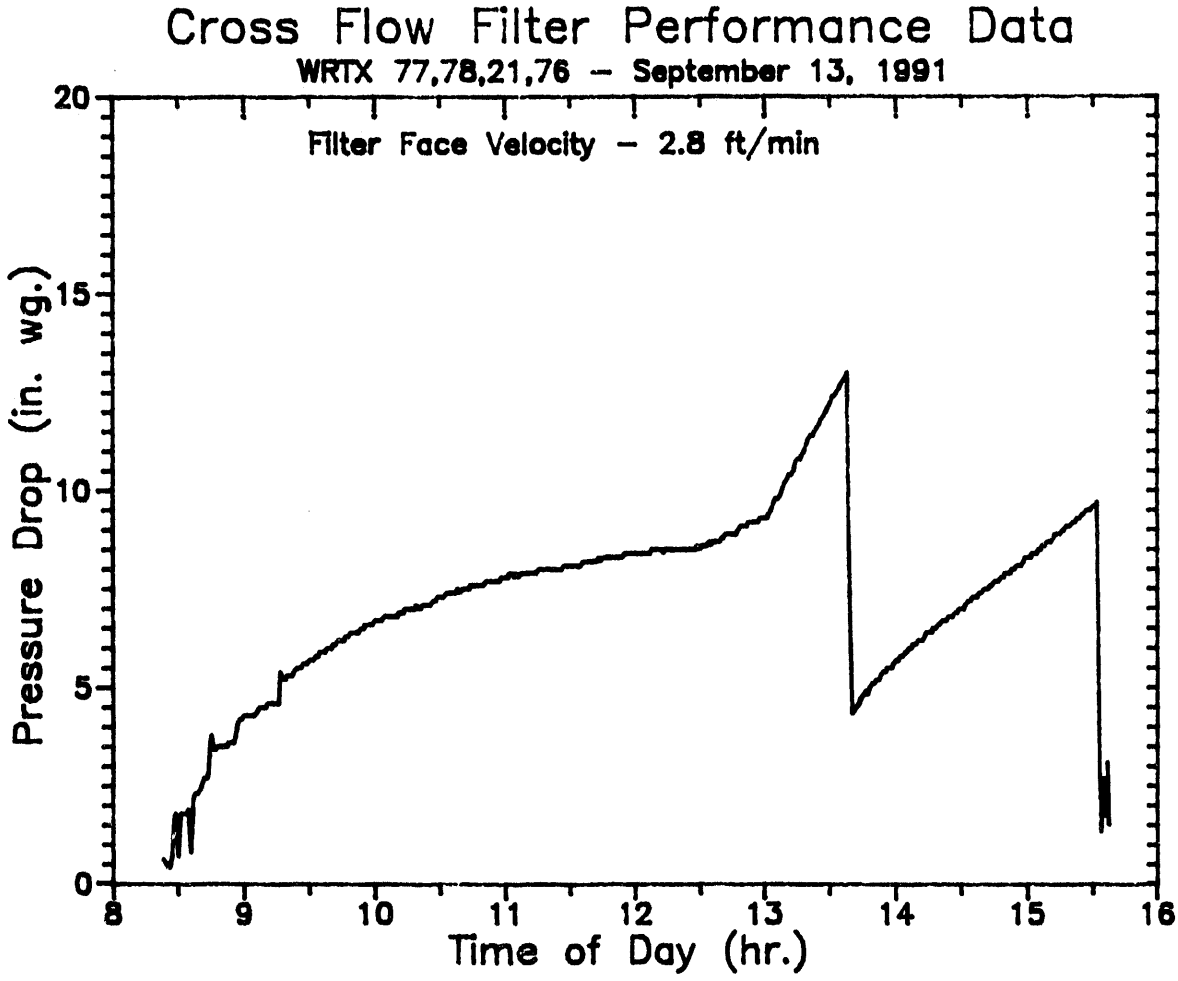

Operation Notes for September 13, 1991
delta–P Trigger = 13 in wc
Pulse Cleaning – 300 psig/0.1 sec
0822 Flame On system to temperature and pressure
1533 Scheduled Shutdown

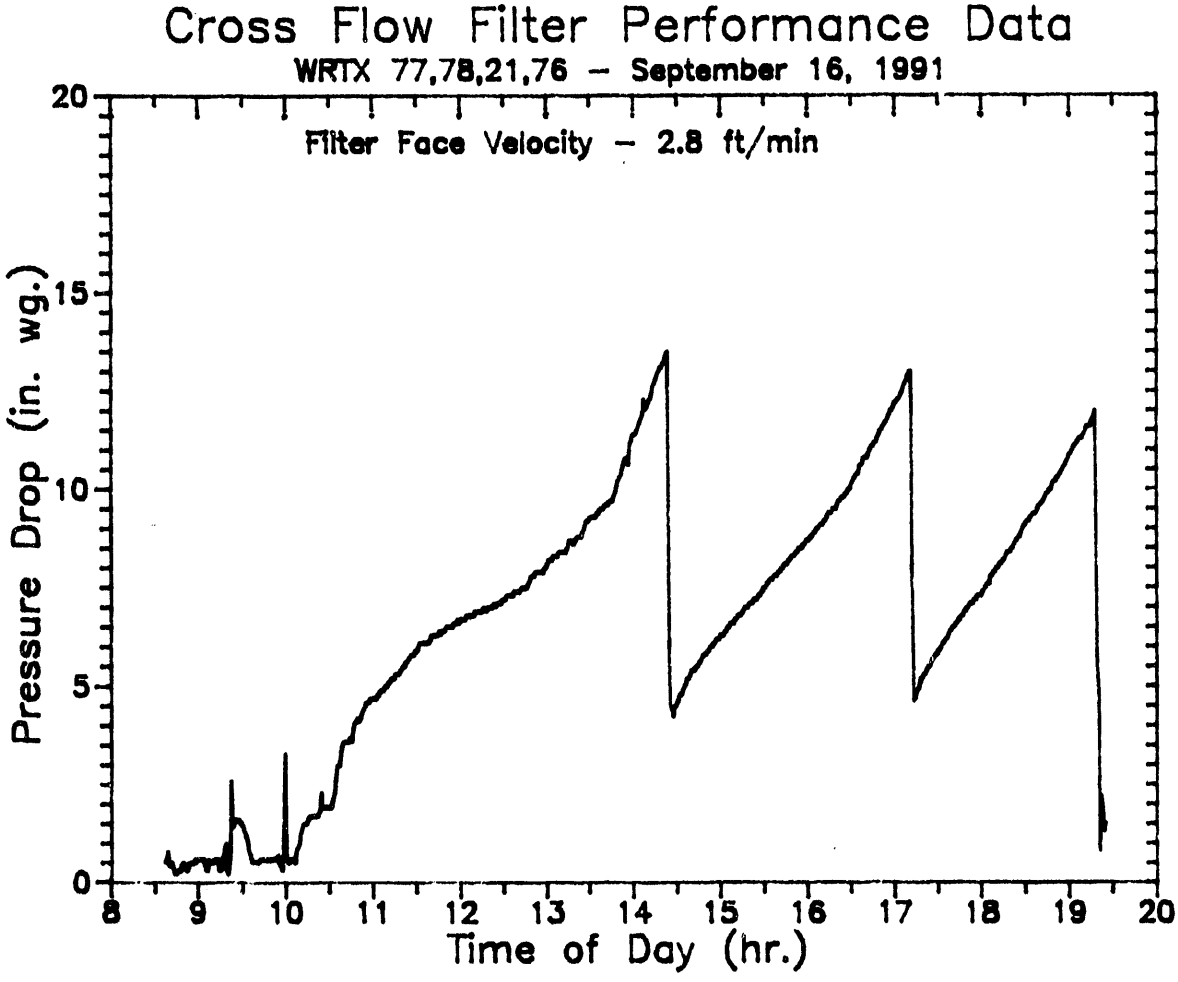

Operation Notes for September 16, 1991
delta–P Trigger = 13 in wc
Pulse Cleaning – 300 psig/0.1 sec
0838 Flame On system to temperature and pressure
0920 Uncheduled Shutdown, main vessel gasket leak, bolts tightened
1000 Flame On
1920 Scheduled Shutdown

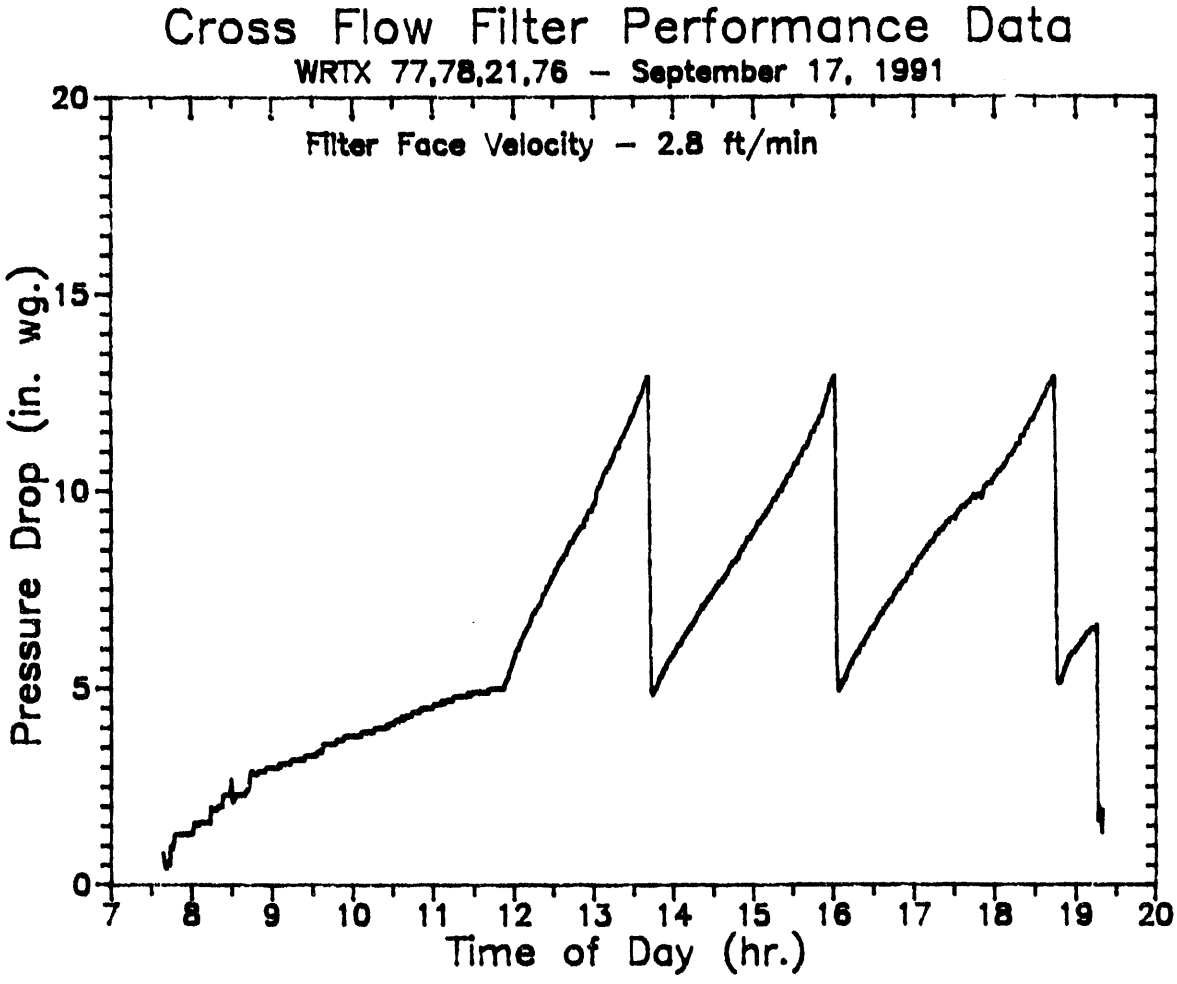

Operation Notes for September 17, 1991
delta–P Trigger = 13 in wc
Pulse Cleaning – 300 psig/0.1 sec
0737 Flame On system to temperature and pressure
1915 Scheduled Shutdown

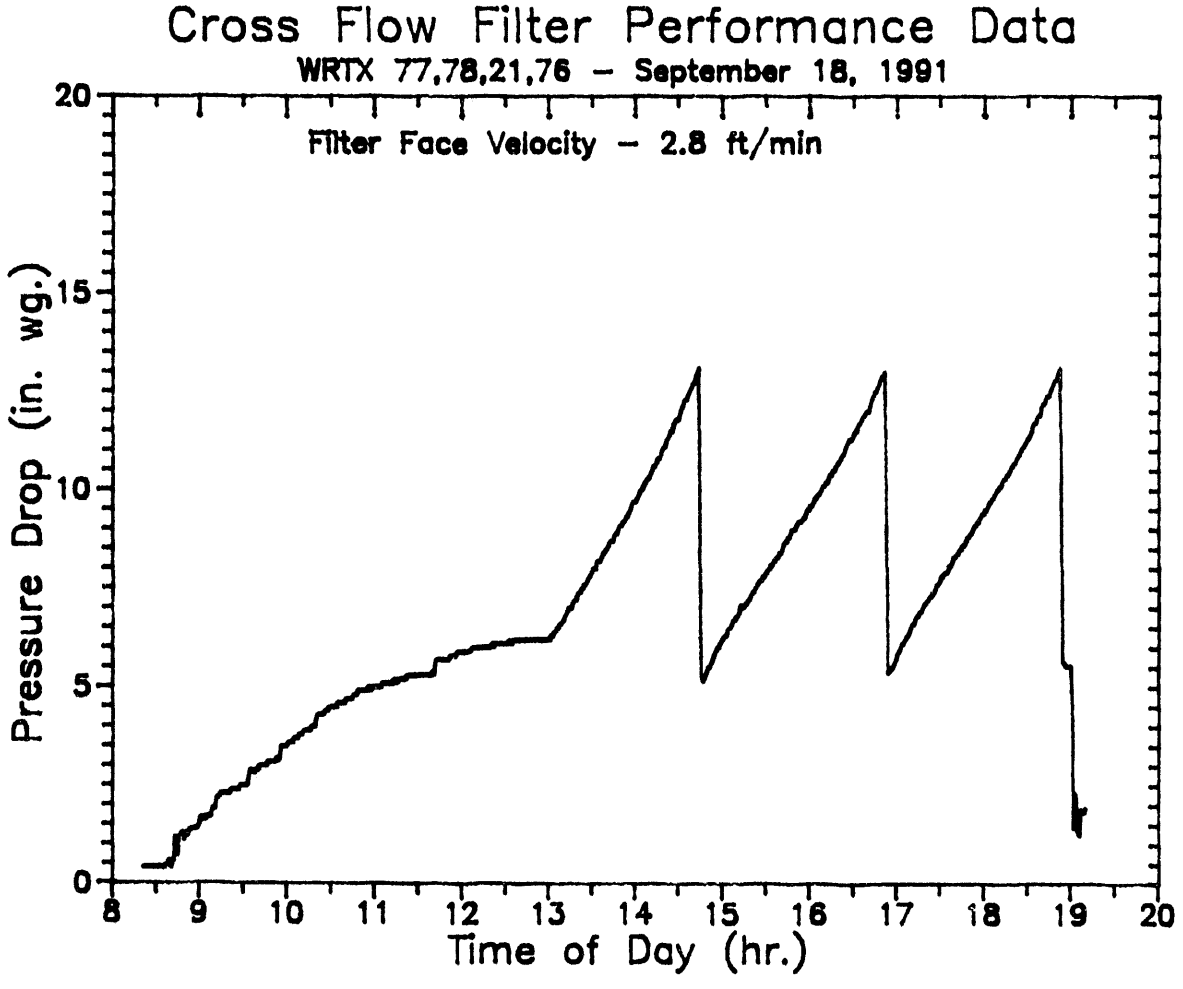

Operation Notes for September 18, 1991
delta–P Trigger = 13 in wc
Pulse Cleaning – 300 psig/0.1 sec
0837 Flame On system to temperature and pressure
1901 Scheduled Shutdown

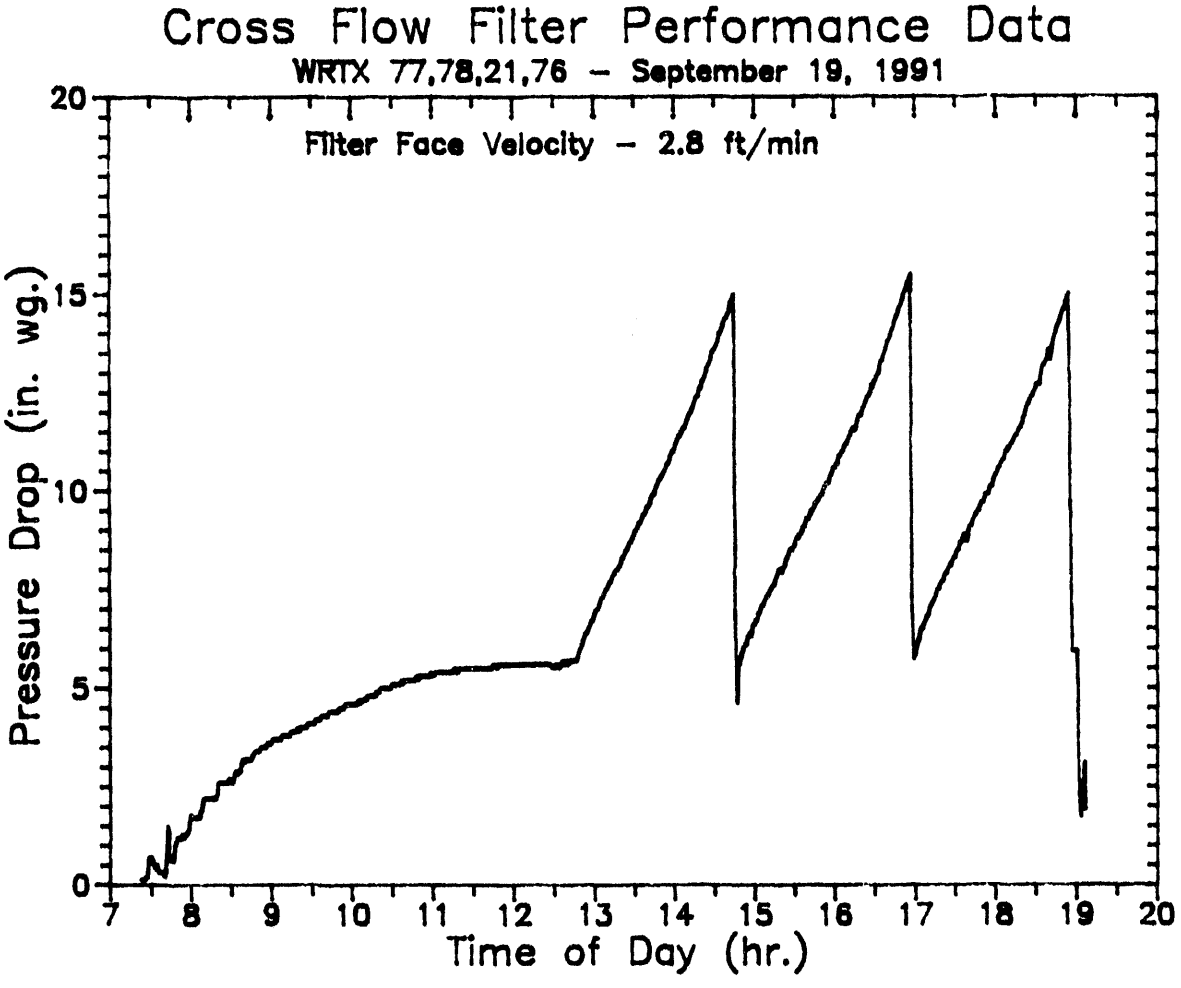

Operation Notes for September 19, 1991
delta–P Trigger = 15 in wc
Pulse Cleaning – 300 psig/0.1 sec
0728 Flame On system to temperature and pressure
0739 Unscheduled Flame Out
0743 Flame On
1902 Scheduled Shutdown

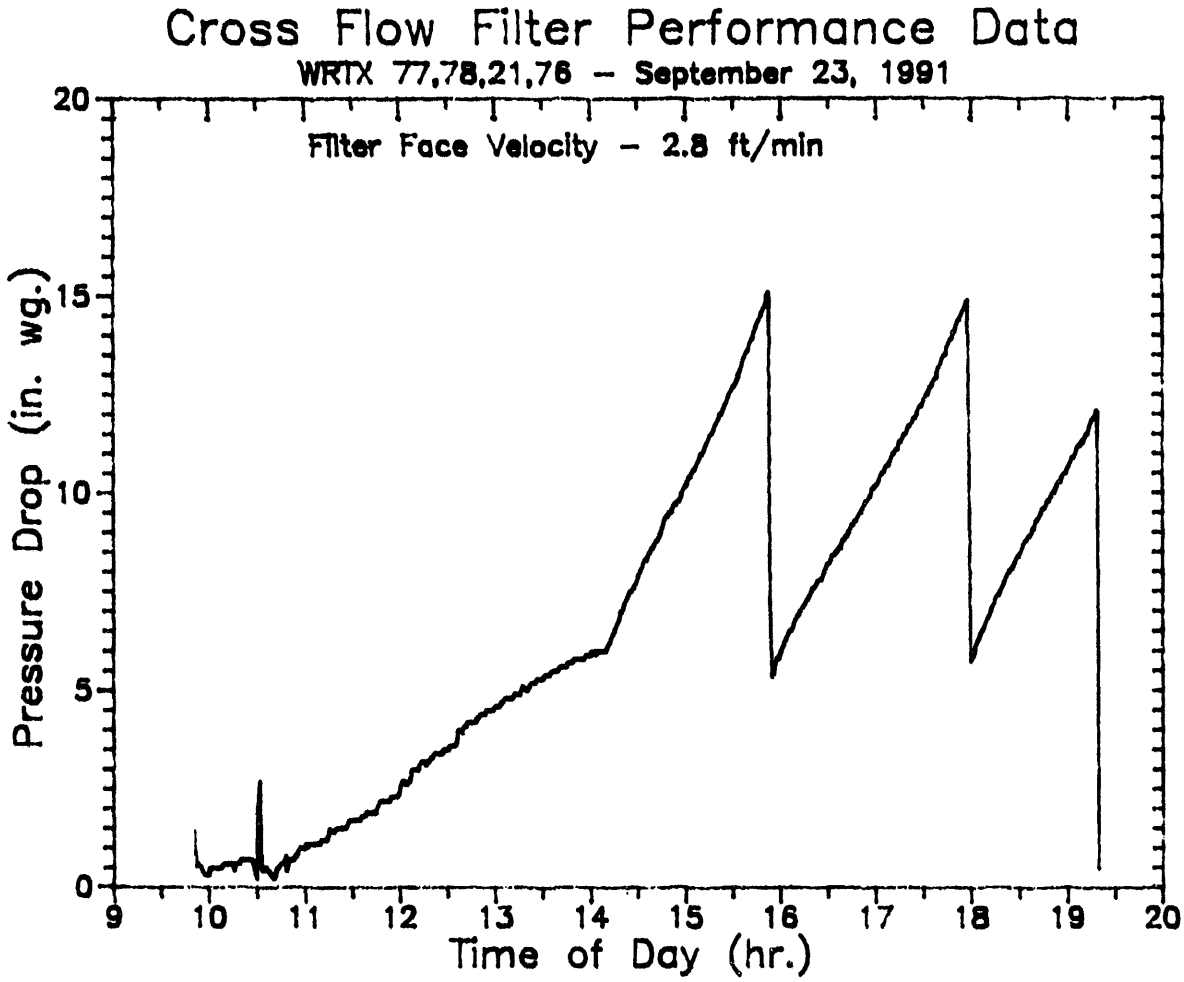

Operation Notes for September 23, 1991
delta–P Trigger = 15 in wc
Pulse Cleaning – 300 psig/0.1 sec
0951 Flame On system to temperature and pressure
1027 Unscheduled Flame Out
1032 Flame On
1918 Scheduled Shutdown

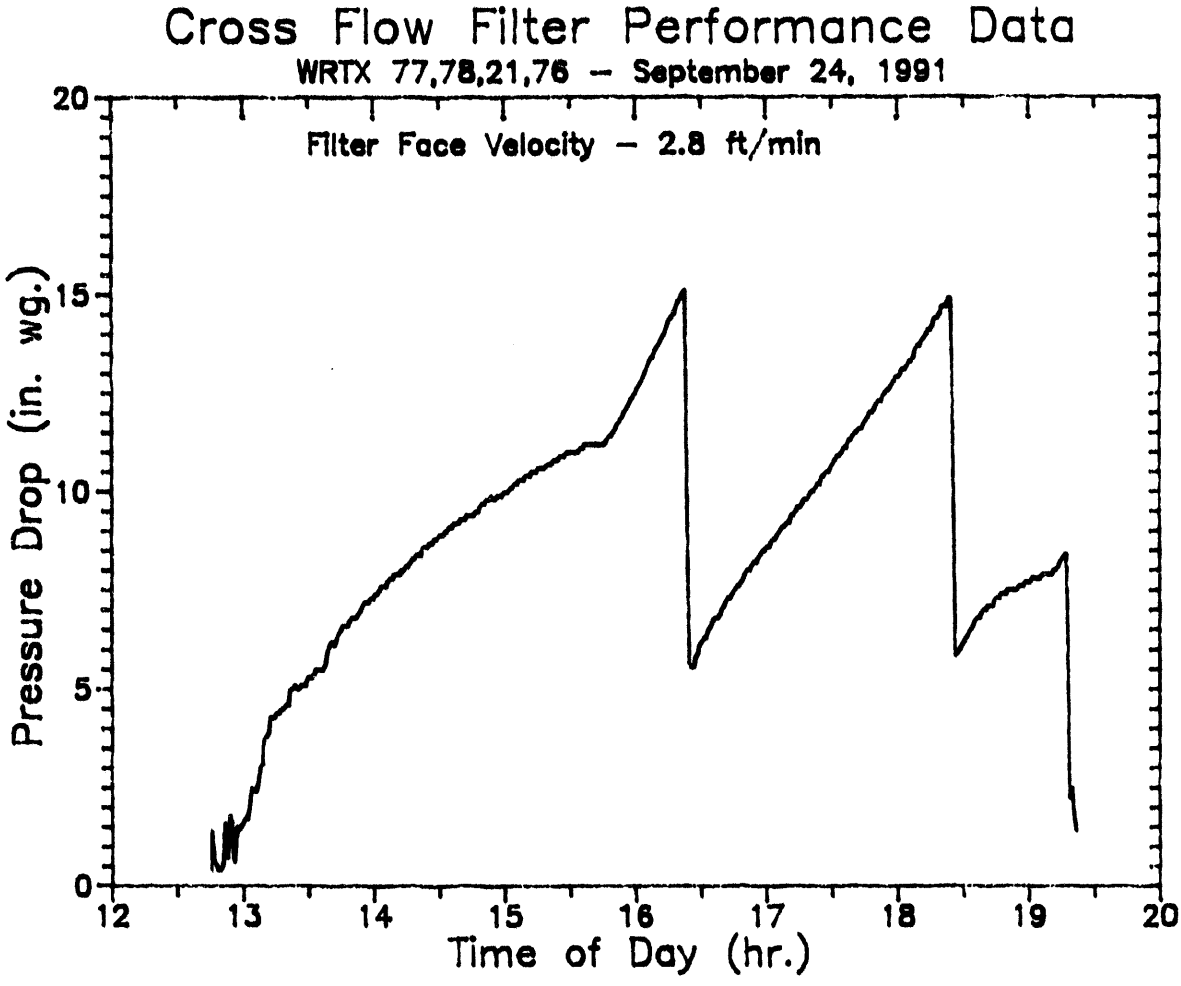

Operation Notes for September 24, 1991
delta–P Trigger = 15 in wc
Pulse Cleaning – 300 psig/0.1 sec
1245 Flame On system to temperature and pressure
1918 Scheduled Shutdown

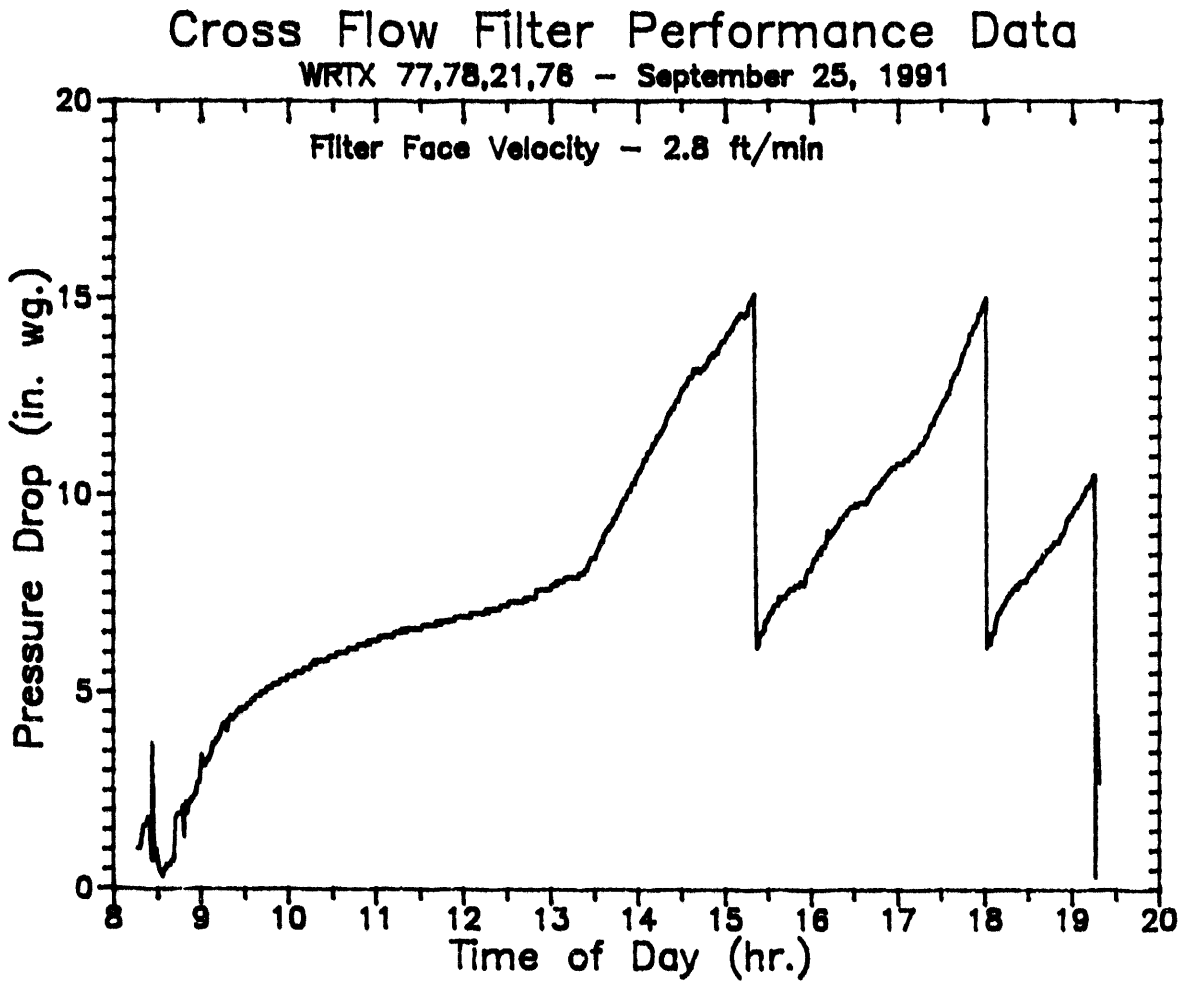

Operation Notes for September 25, 1991
delta–P Trigger = 15 in wc
Pulse Cleaning – 300 psig/0.1 sec
0829 Flame On system to temperature and pressure
1916 Scheduled Shutdown

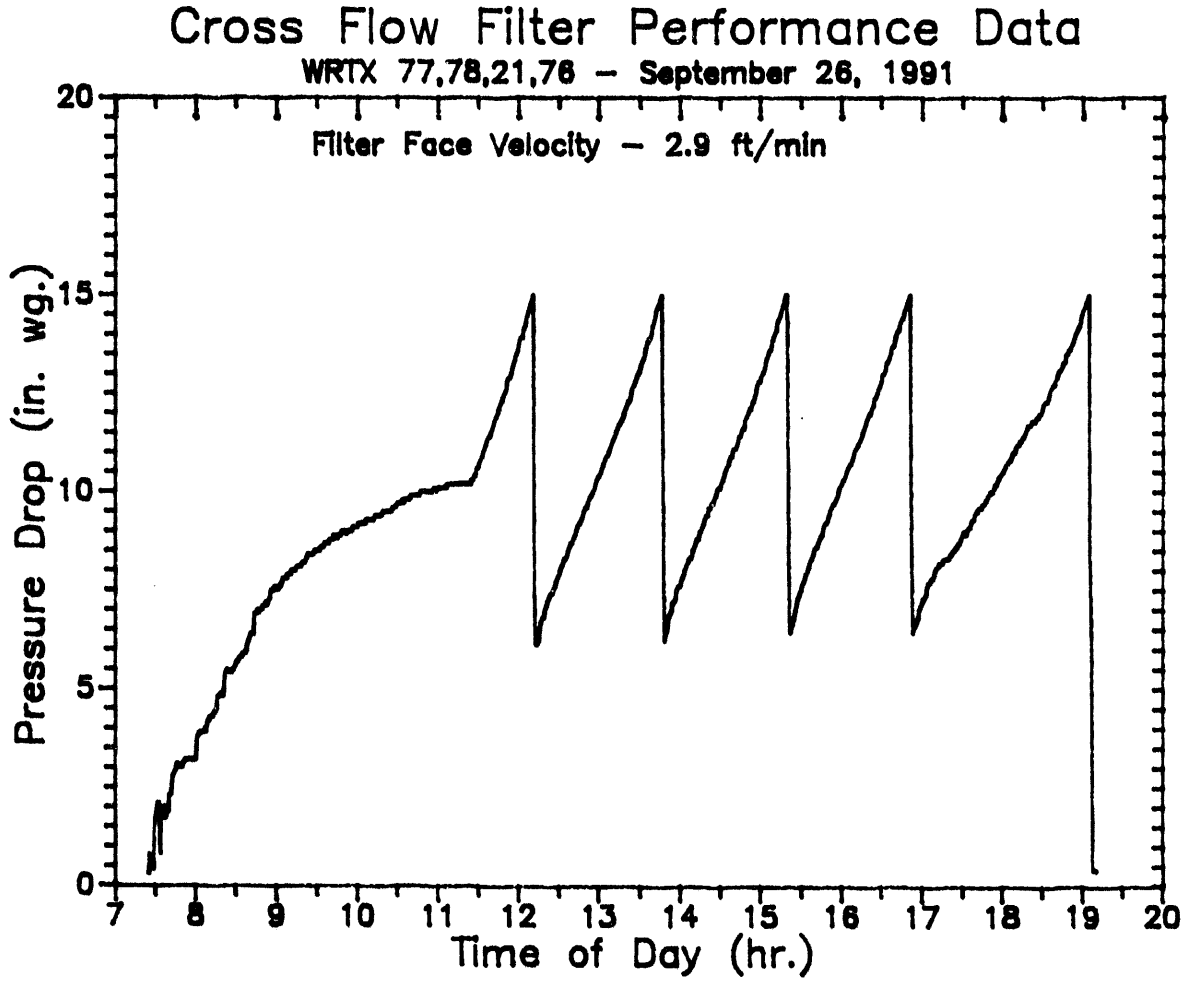

Operation Notes for September 26, 1991
delta–P Trigger = 15 in wc
Pulse Cleaning – 300 psig/0.1 sec
0724 Flame On system to temperature and pressure
1906 Scheduled Shutdown

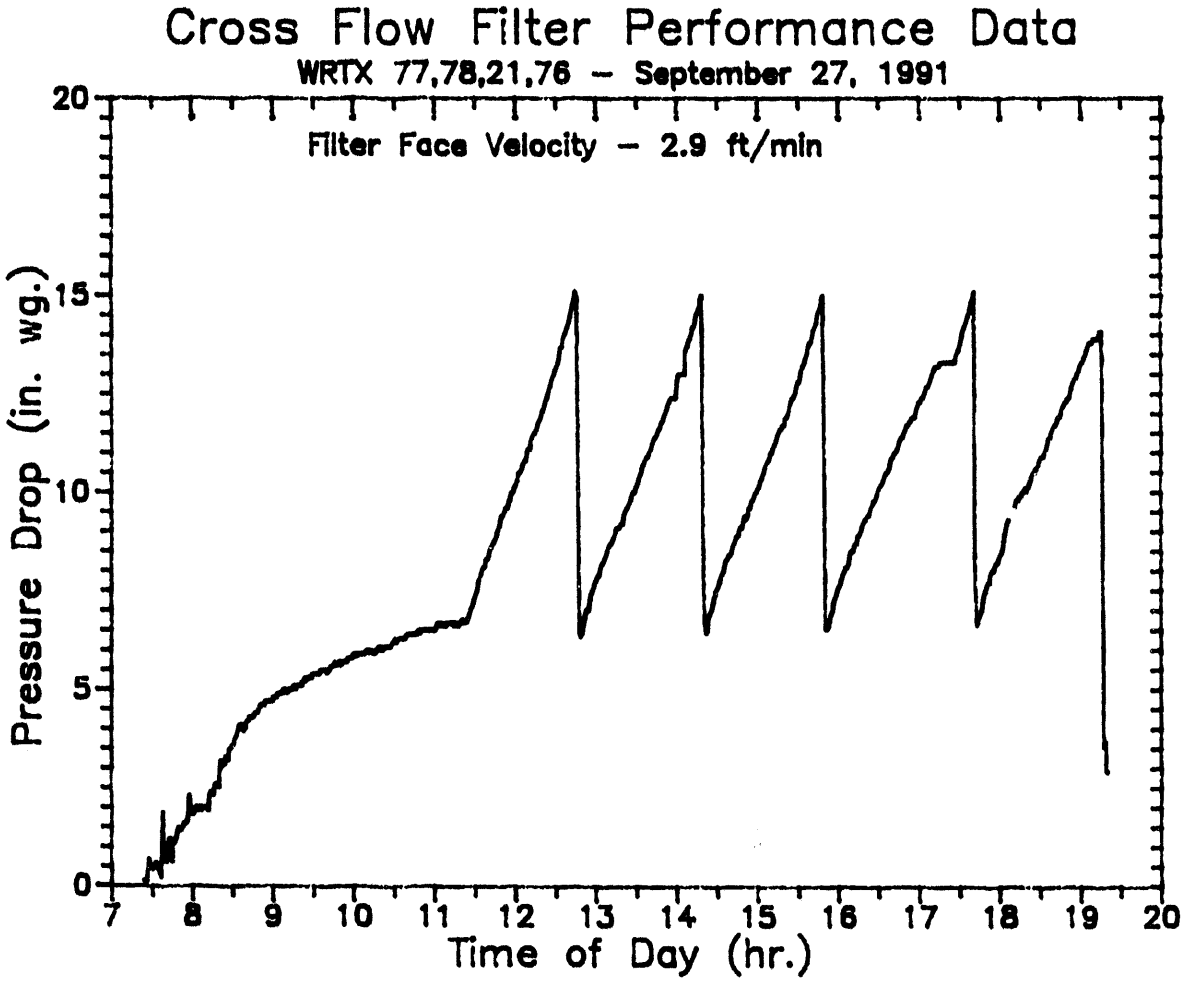

Operation Notes for September 27, 1991
delta–P Trigger = 15 in wc
Pulse Cleaning – 300 psig/0.1 sec
0725 Flame On system to temperature and pressure
0732 Flame Out, Unscheduled
0736 Flame On
1916 Scheduled Shutdown

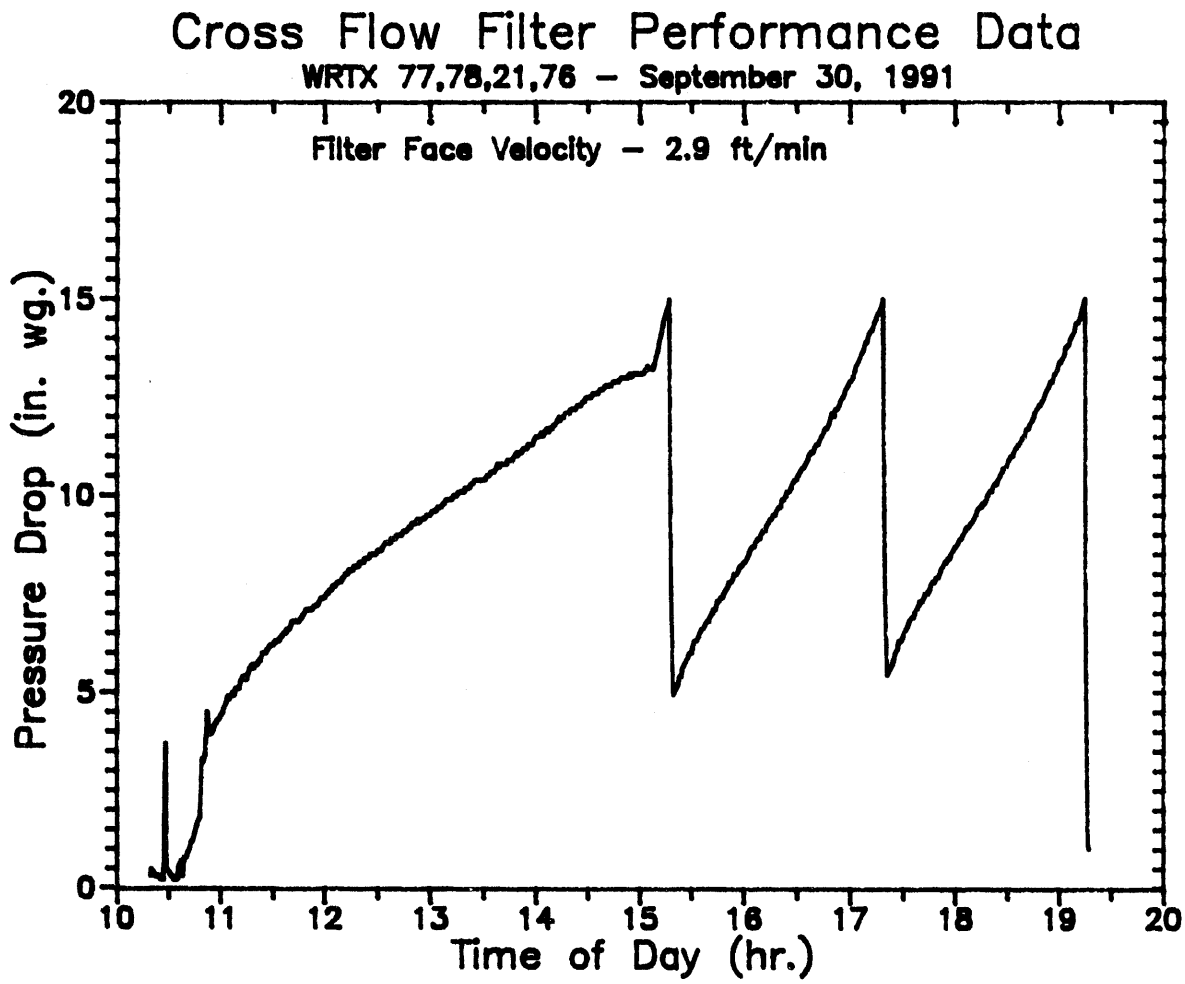

Operation Notes for September 30, 1991
delta–P Trigger = 15 in wc
Pulse Cleaning – 325 psig/0.1 sec
1020 Flame On system to temperature and pressure
1026 Flame Out, Unscheduled
1027 Flame On
1916 Scheduled Shutdown

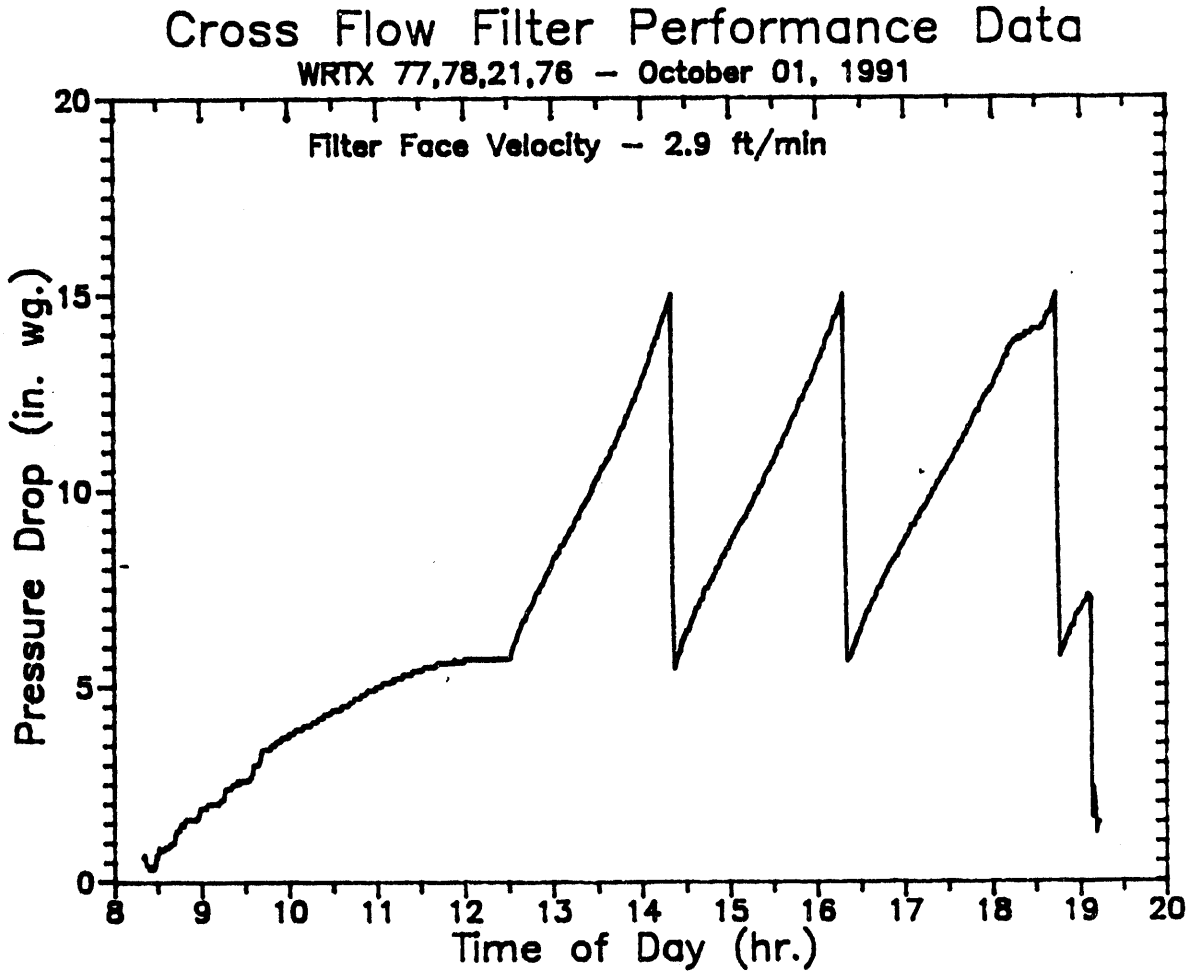

Operation Notes for October 01, 1991
delta–P Trigger = 15 in wc
Pulse Cleaning – 330 psig/0.1 sec
0819 Flame On system to temperature and pressure
1907 Scheduled Shutdown

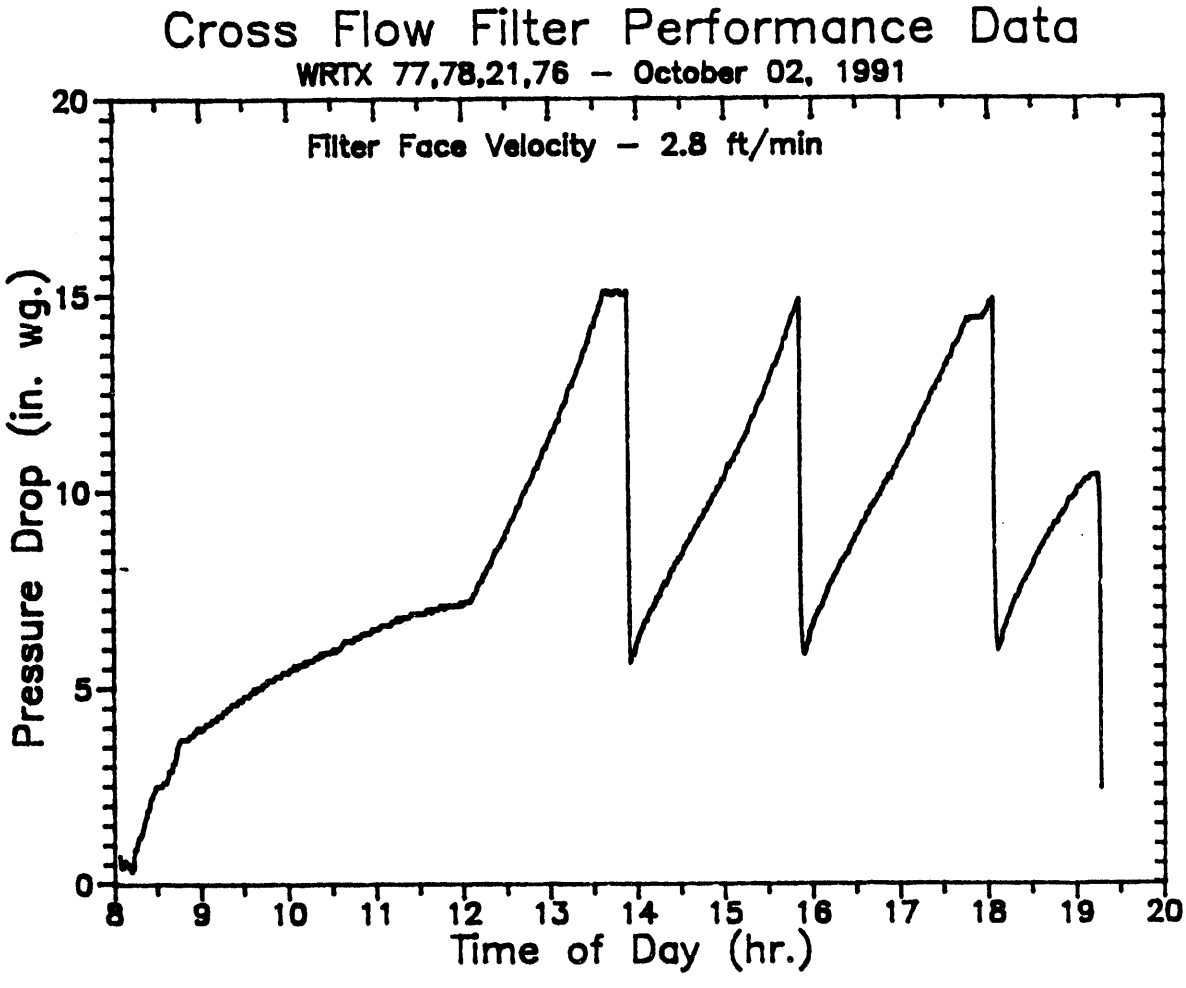

Operation Notes for October 02, 1991
delta–P Trigger = 15 in wc
Pulse Cleaning – 330 psig/0.1 sec
0802 Flame On system to temperature and pressure
1337 Pulse Blowback pressure stabilizing
initially low, adjusted – Pulse Cleaning at 340 psig/0.1 sec
1917 Scheduled Shutdown

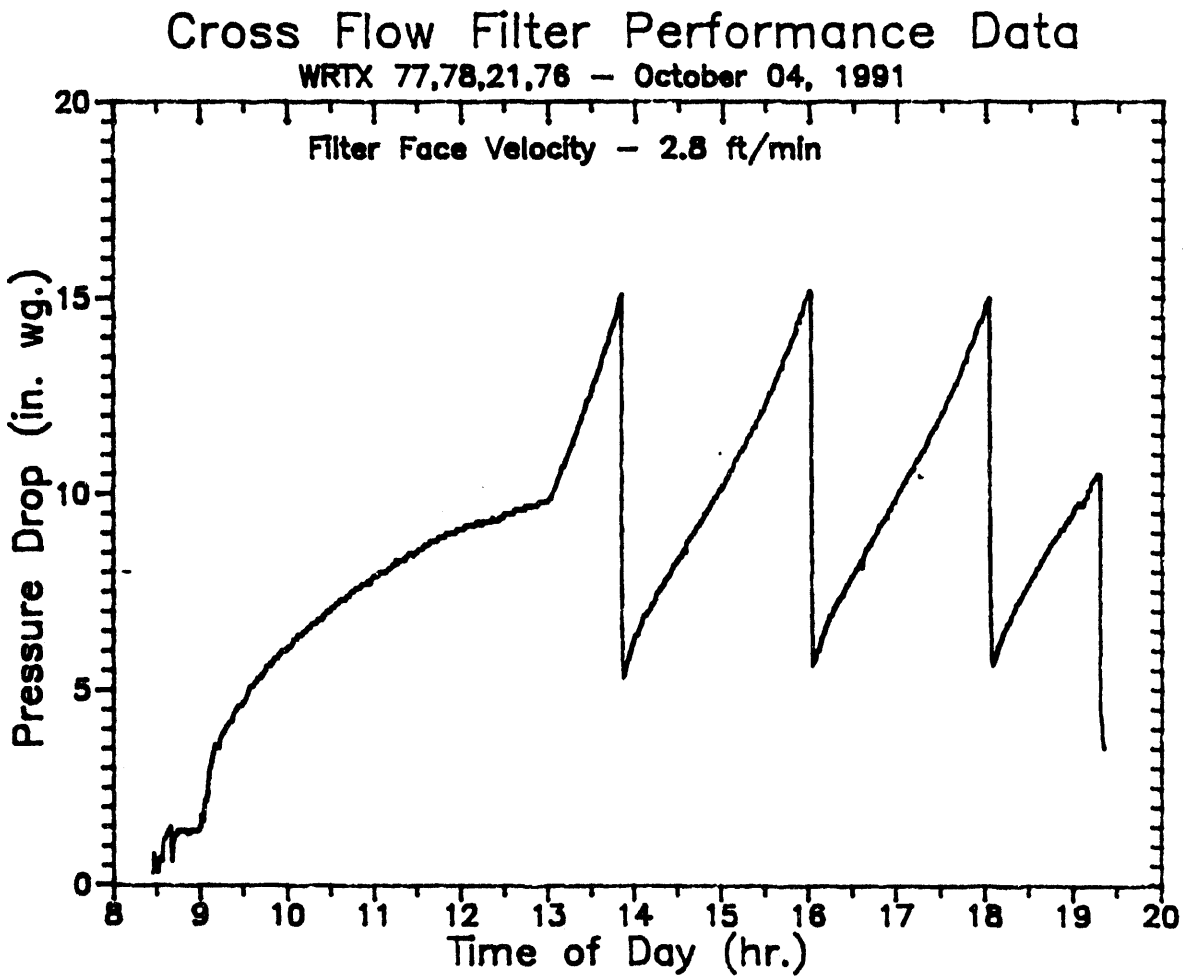

Operation Notes for October 04, 1991
delta-P Trigger = 15 in wc
Pulse Cleaning – 330 psig/0.1 sec
0827 Flame On system to temperature and pressure
1917 Scheduled Shutdown

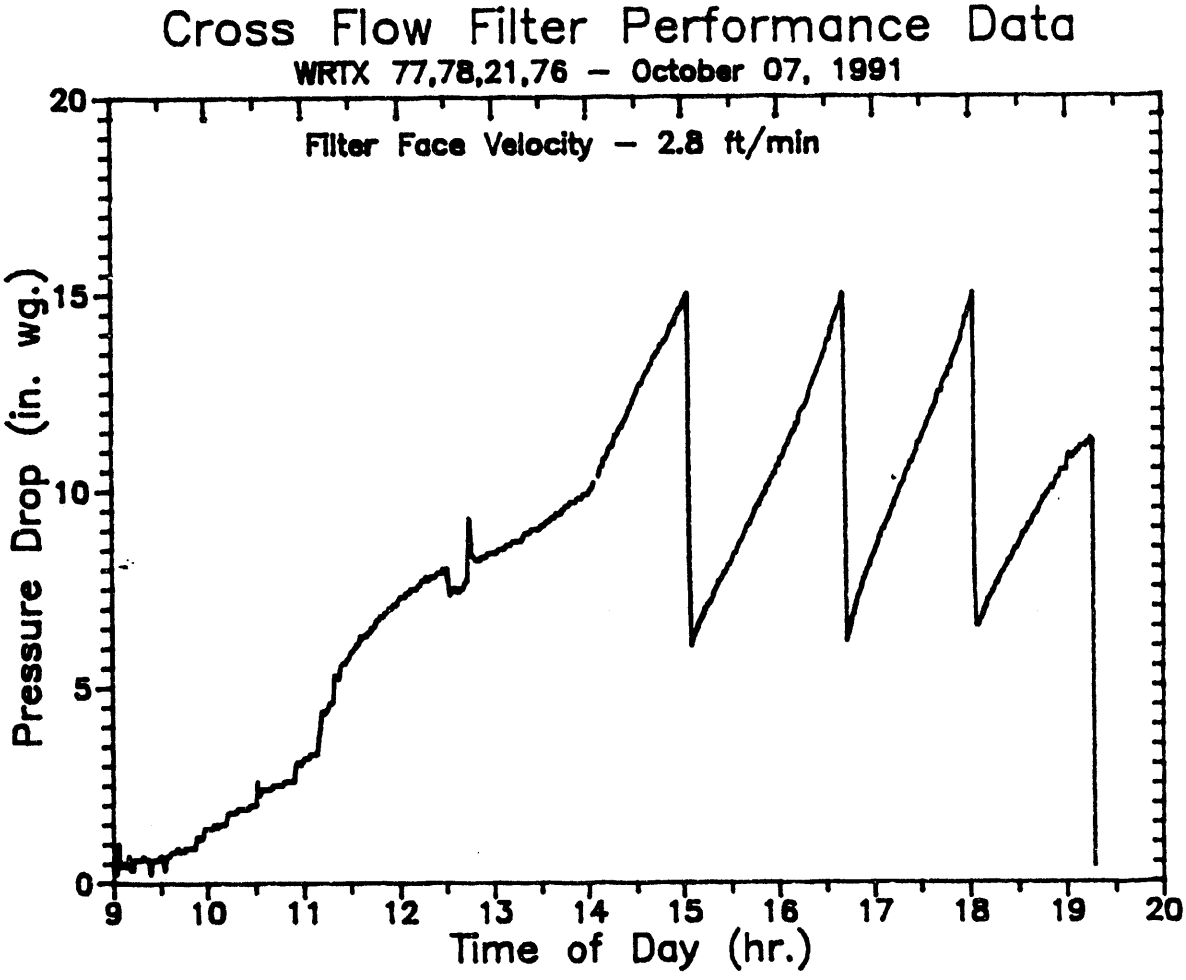

Operation Notes for October 07, 1991
delta–P Trigger = 15 in wc
Pulse Cleaning – 300 psig/0.1 sec
0902 Flame On system to temperature and pressure
1915 Scheduled Shutdown

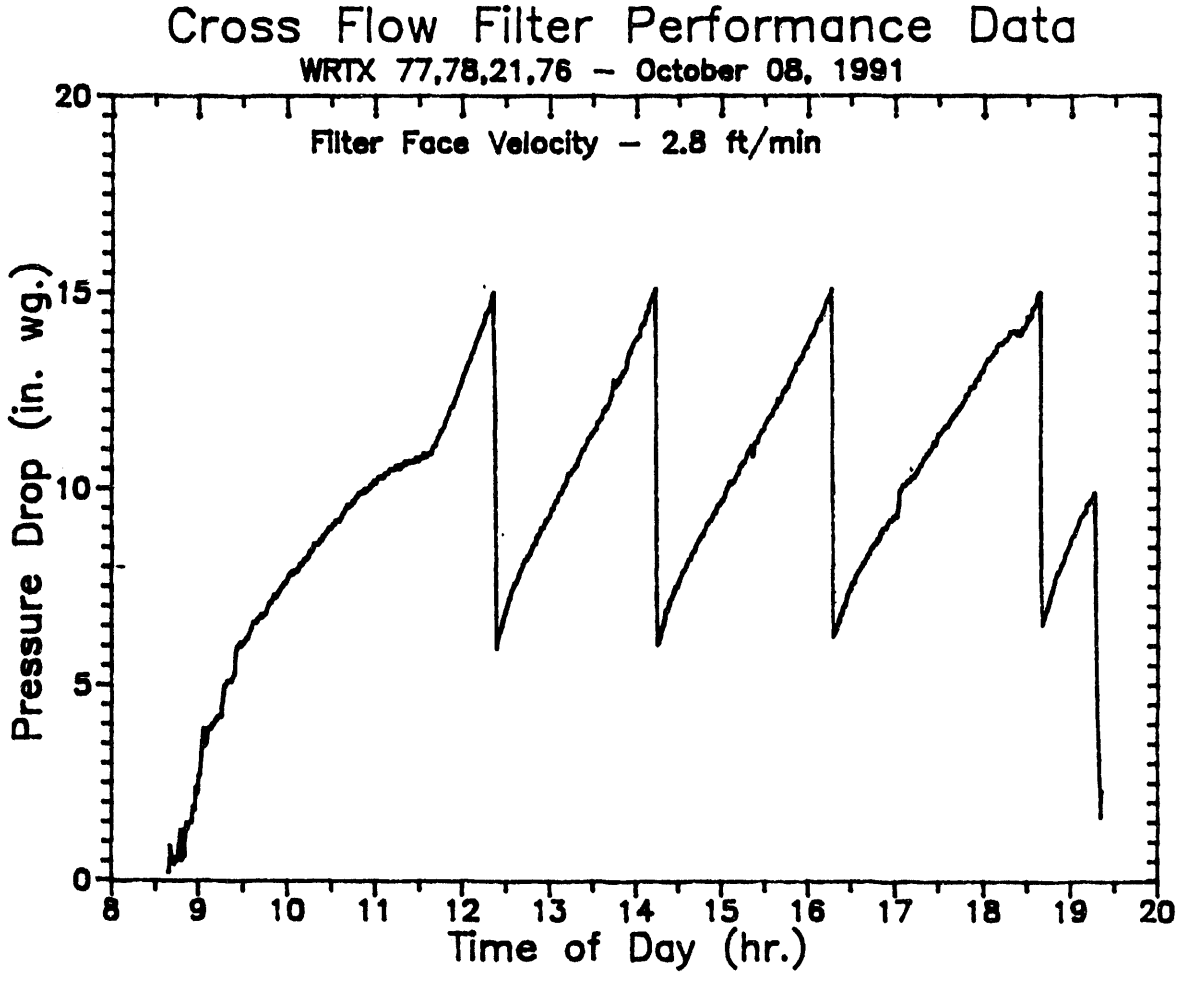

Operation Notes for October 08, 1991
delta–P Trigger = 15 in wc
Pulse Cleaning – 310 psig/0.1 sec
0839 Flame On system to temperature and pressure
1614 Pulse Cleaning – 300 psig/0.1 sec
1701–1716 Dust feeder speed reset, vibrator on
1916 Scheduled Shutdown

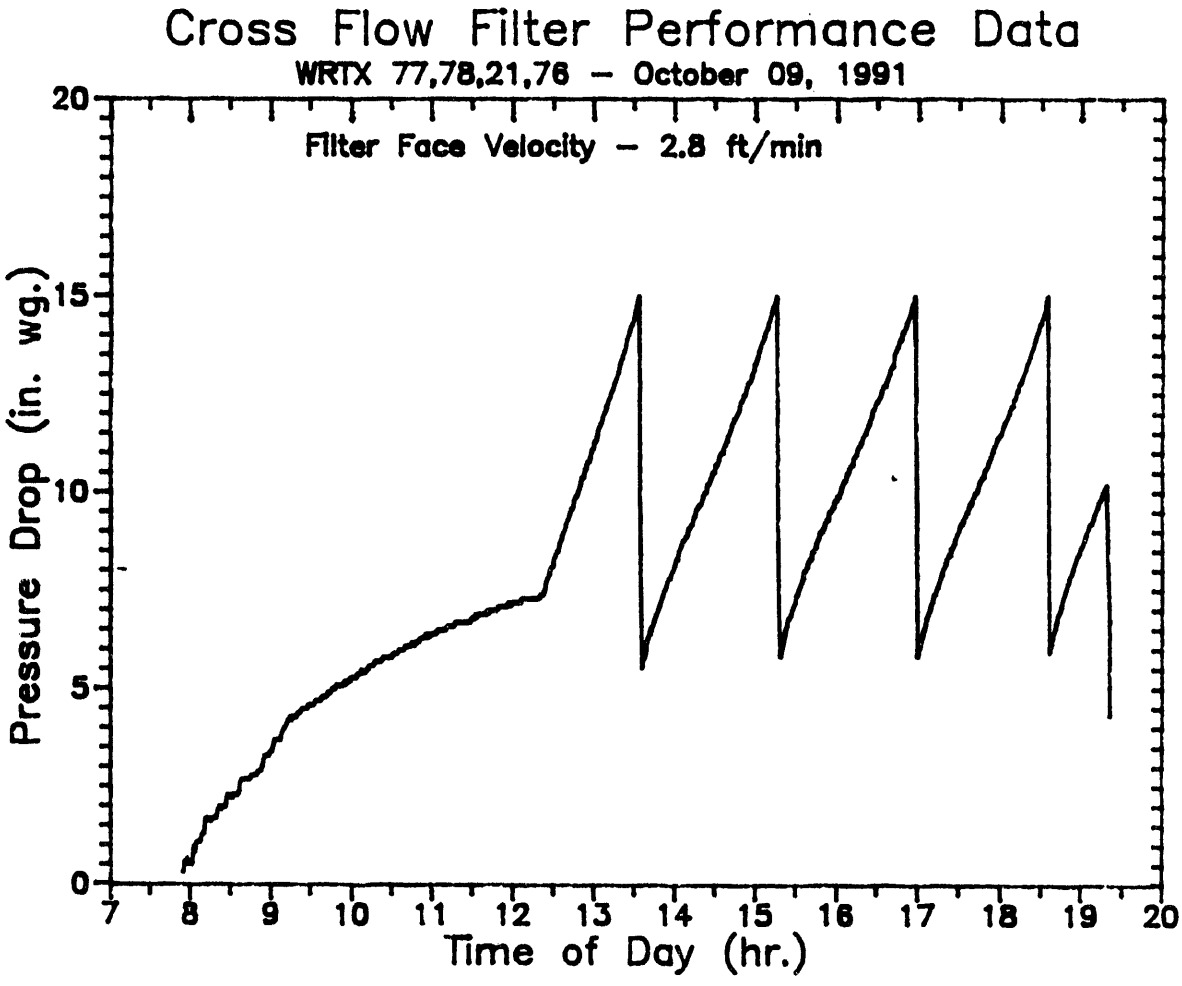

Operation Notes for October 09, 1991
delta–P Trigger = 15 in wc
Pulse Cleaning – 300 psig/0.1 sec
0754 Flame On system to temperature and pressure
1920 Scheduled Shutdown

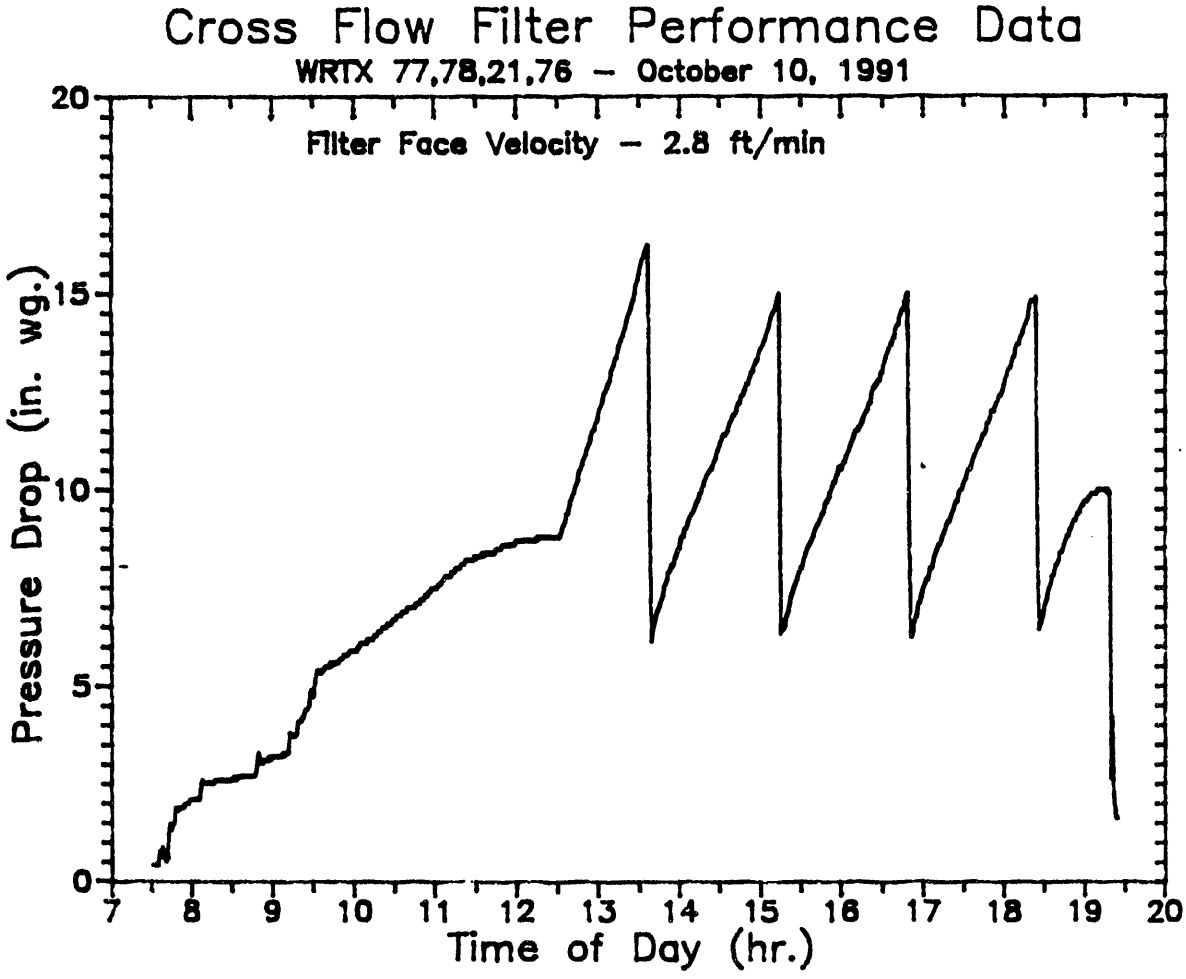

Operation Notes for October 10, 1991
delta–P Trigger = 15 in wc
Pulse Cleaning – 315 psig/0.1 sec
0734 Flame On system to temperature and pressure
1920 Scheduled Shutdown

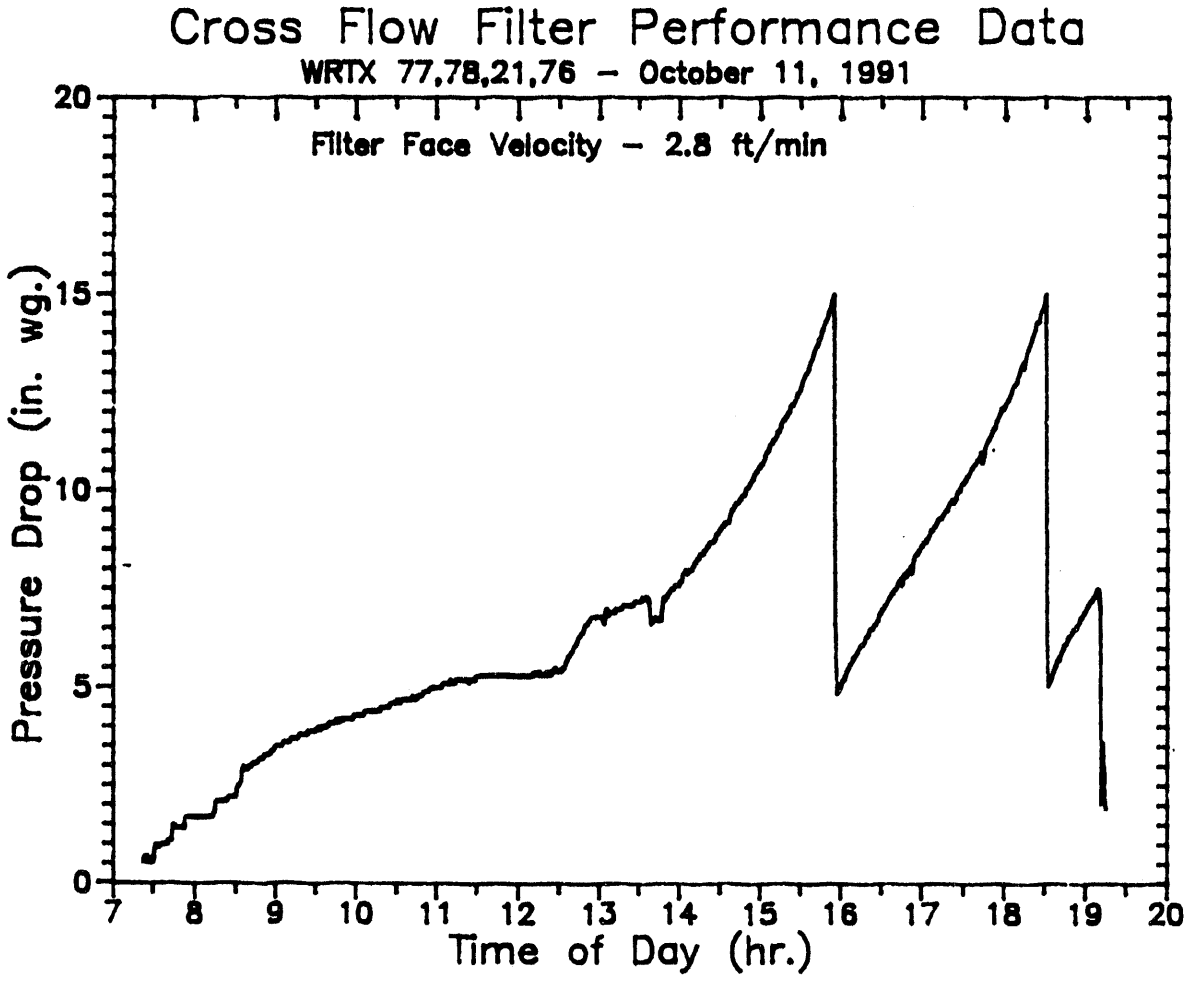

Operation Notes for October 11, 1991
delta–P Trigger = 15 in wc
Pulse Cleaning – 320 psig/0.1 sec
0723 Flame On system to temperature and pressure
1301 Dust not feeding due to electrical service disruption
1911 Scheduled Shutdown

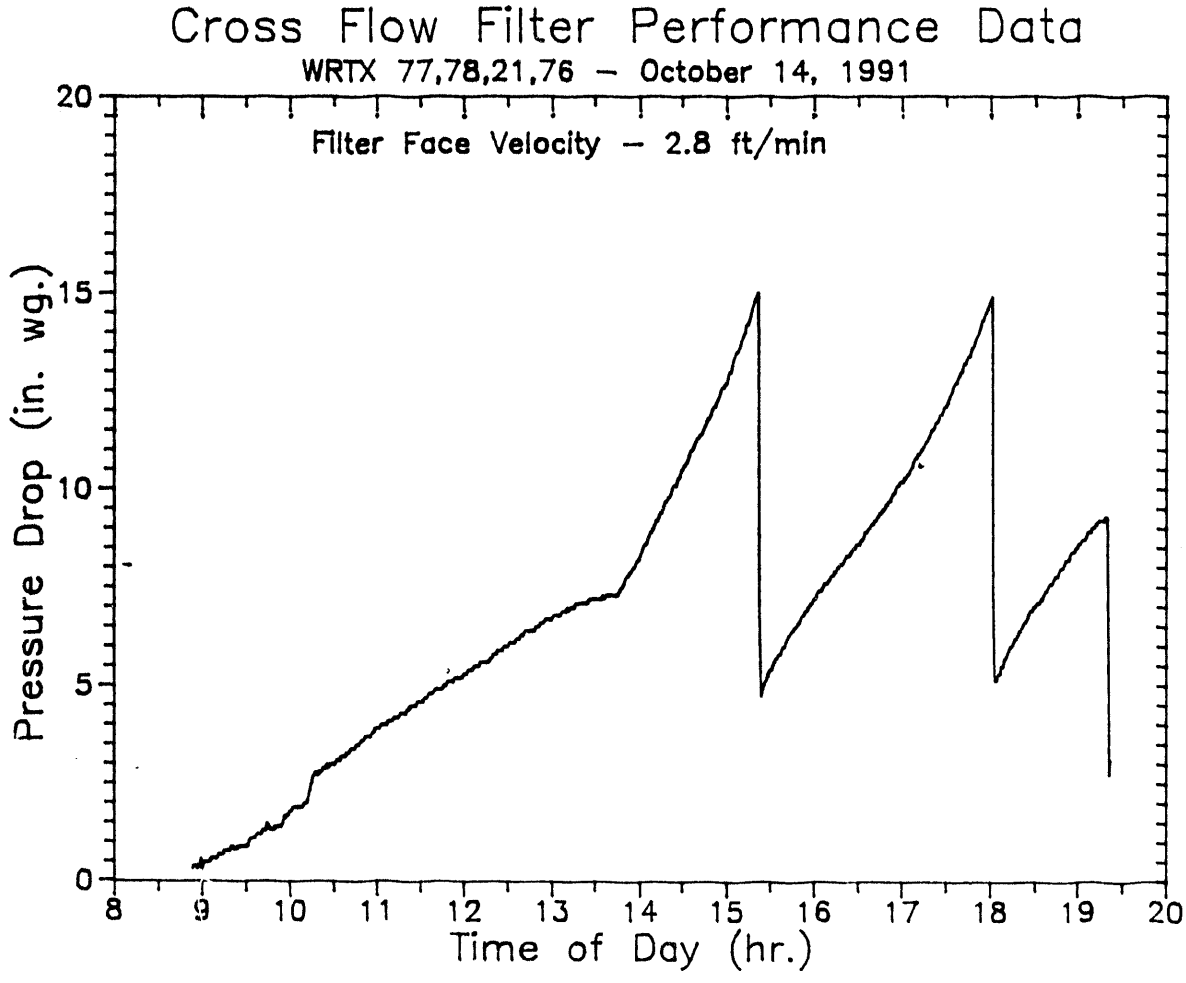

Operation Notes for October 14, 1991
delta–P Trigger = 15 in wc
Pulse Cleaning – 310 psig/0.1 sec
0849 Flame On system to temperature and pressure
1920 Scheduled Shutdown

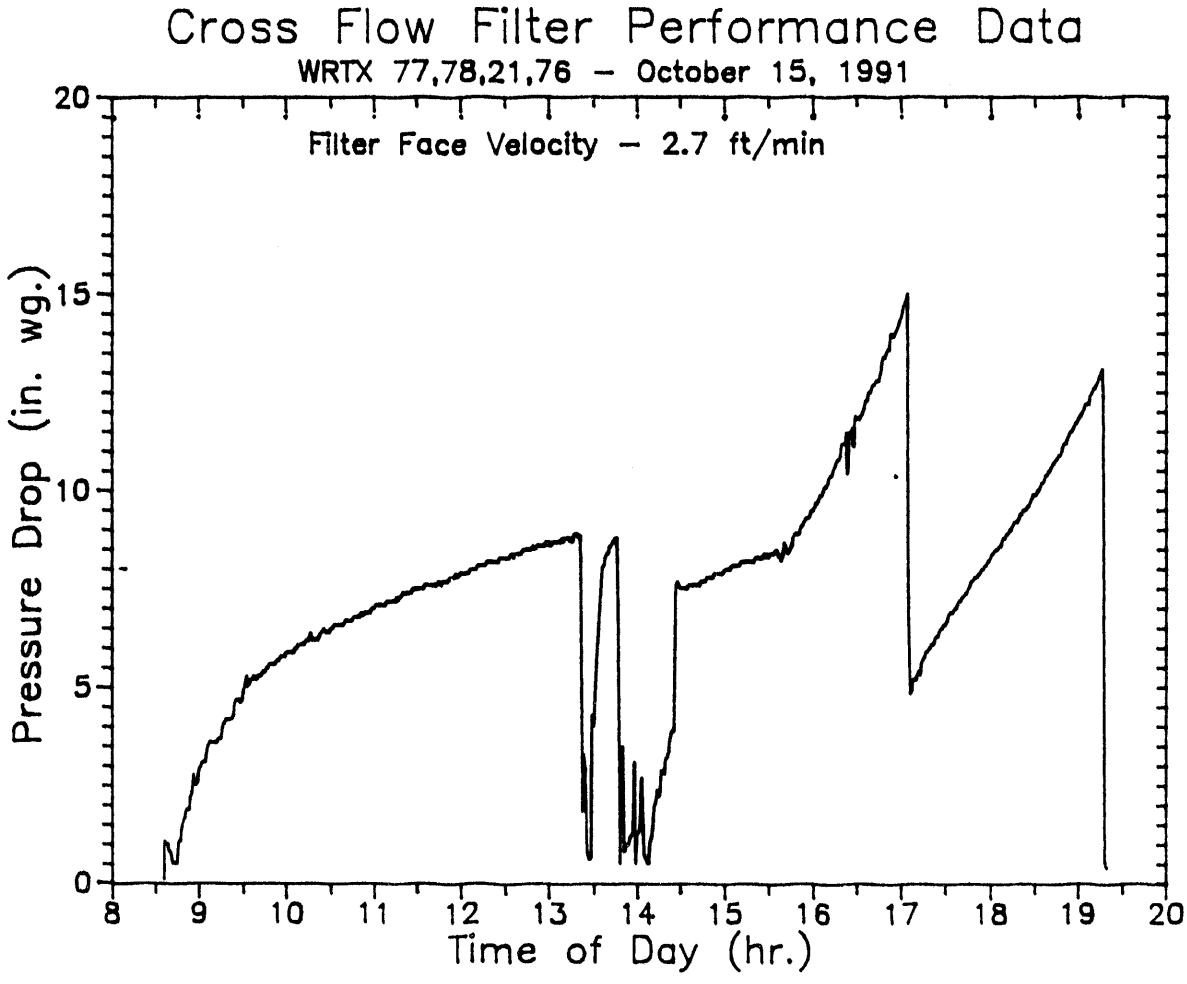

Operation Notes for October 14, 1991
delta–P Trigger = 15 in wc
Pulse Cleaning – 320 psig/0.1 sec
0835 Flame On system to temperature and pressure
1320 Flame Out, Unscheduled
1323 Flame On
1346 Flame Out, Unscheduled, Fire Eye Cleaned
1402 Flame On
1915 Scheduled Shutdown

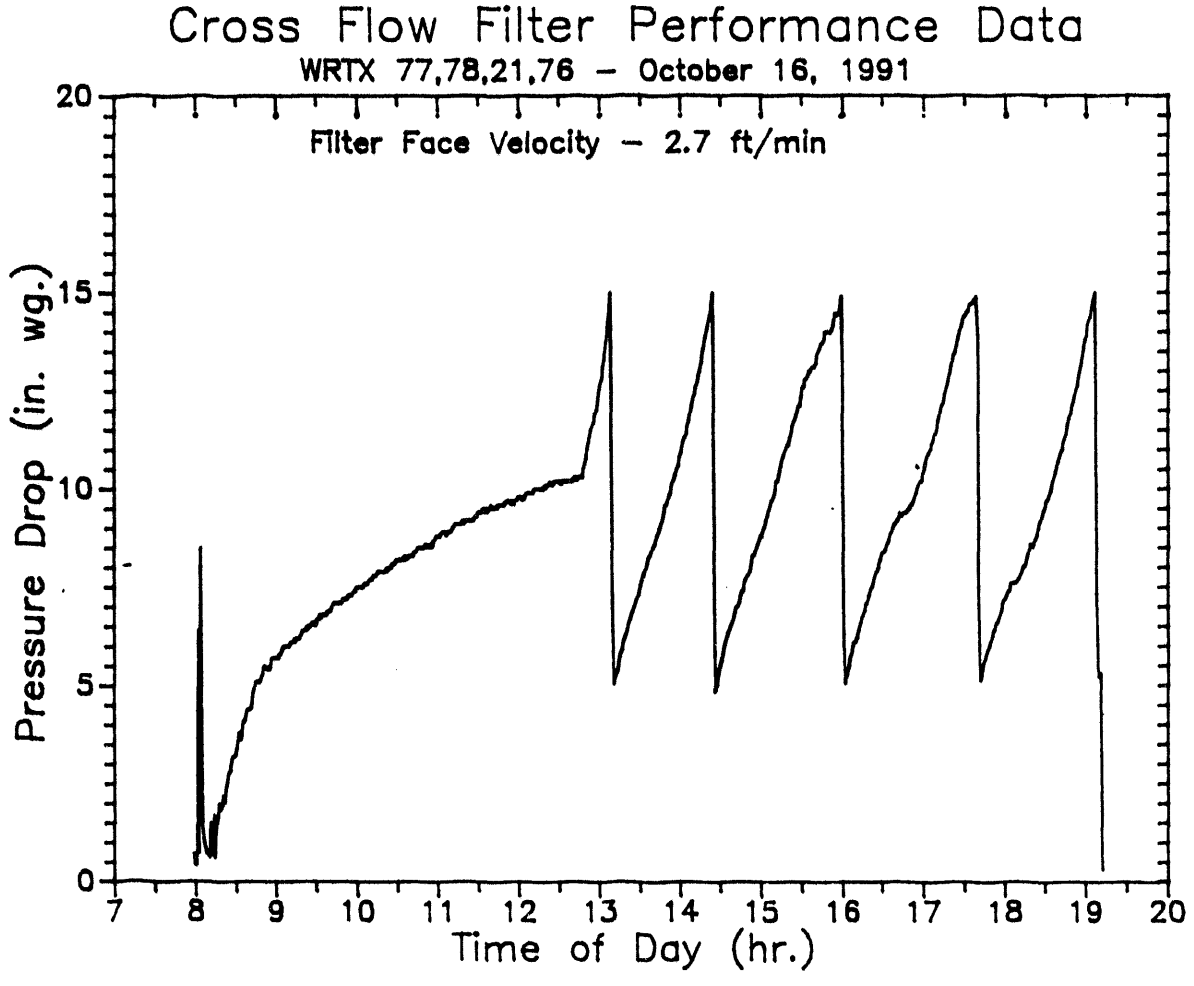

Operation Notes for October 16, 1991
delta–P Trigger = 15 in wc
Pulse Cleaning – 318 psig/0.1 sec
0756 Flame On system to temperature and pressure
0801 Flame Out, Unscheduled
0803 Flame On
1258 Dust Feed increased to 2000 ppm Concentration In
1910 Scheduled Shutdown

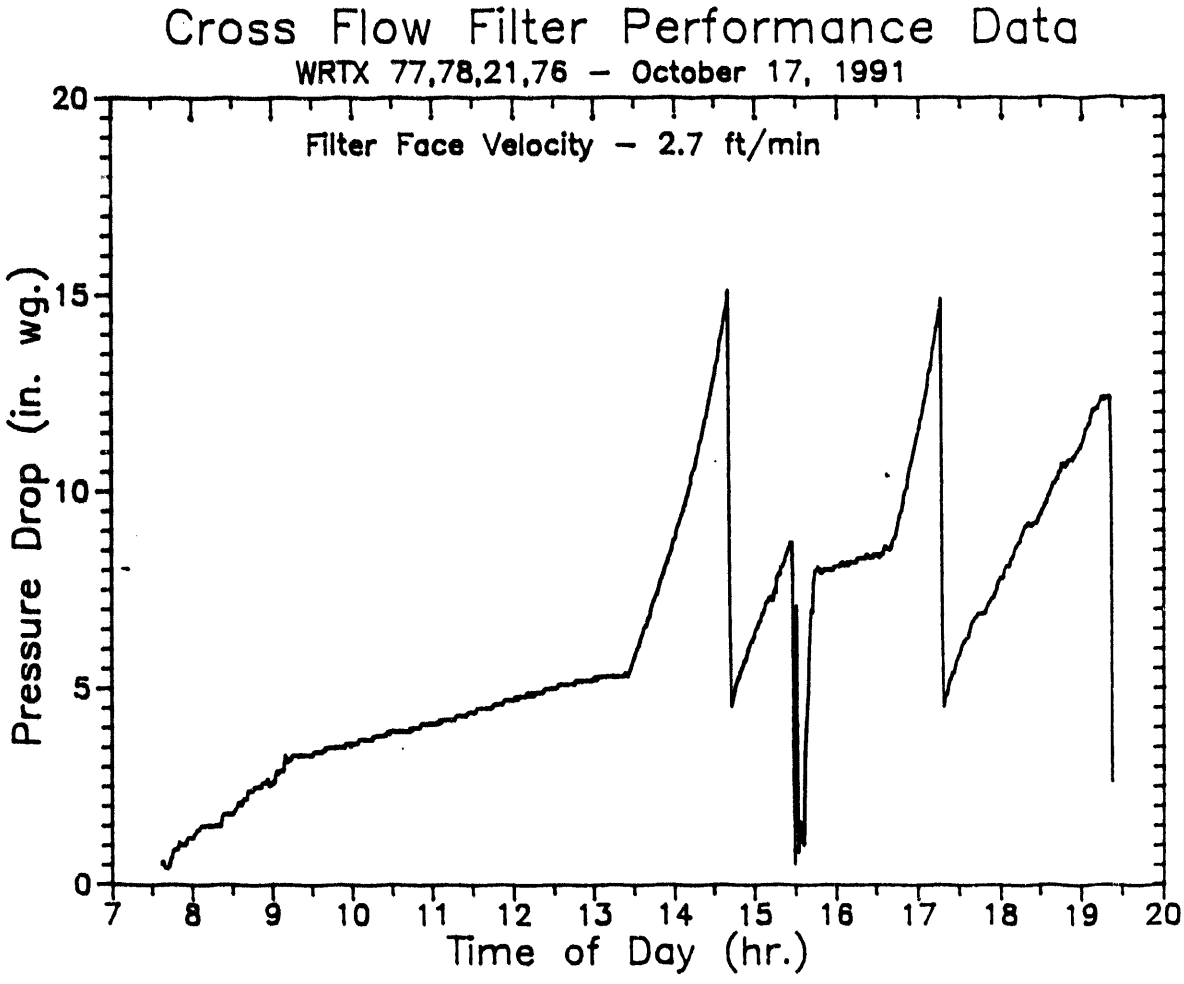

Operation Notes for October 17, 1991
delta–P Trigger = 15 in wc
Pulse Cleaning – 320 psig/0.1 sec
0732 Flame On system to temperature and pressure
1526 Flame Out, Unscheduled
1530 Flame On
1716 Dust not feeding properly
1920 Scheduled Shutdown

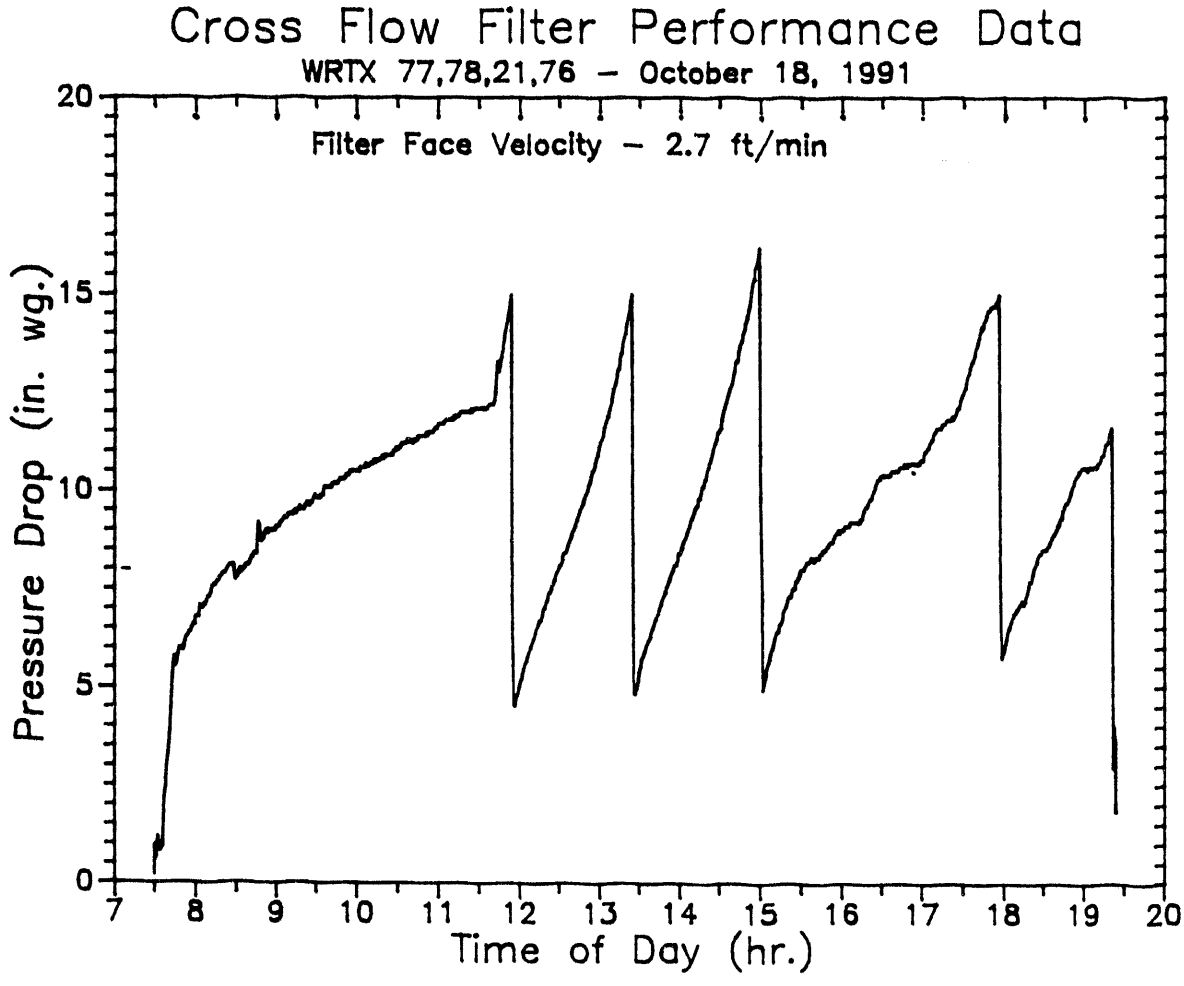

Operation Notes for October 18, 1991
delta–P Trigger = 15 in wc
Pulse Cleaning – 320 psig/0.1 sec
0730 Flame On system to temperature and pressure
1457–1920 Dust not feeding properly
1920 Scheduled Shutdown

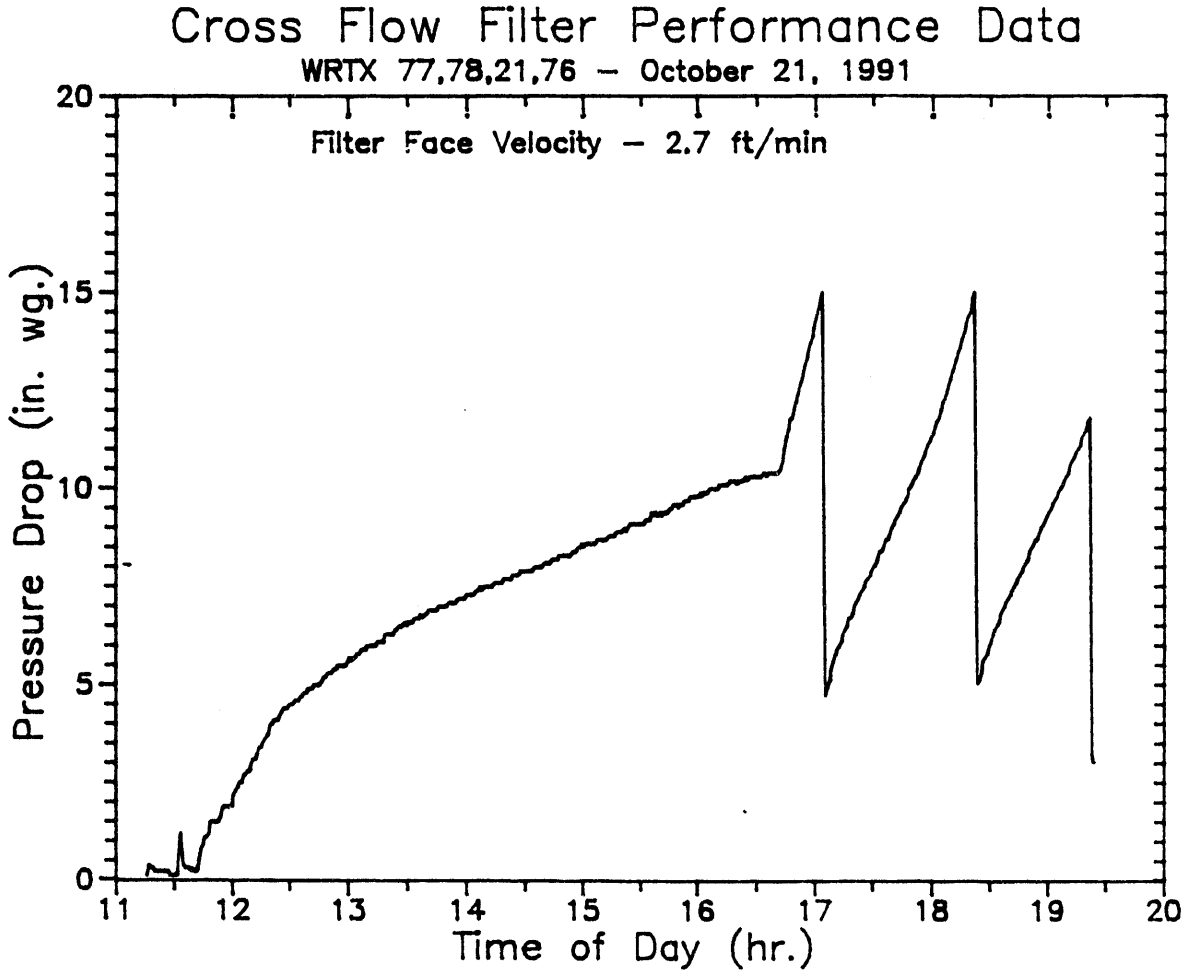

Operation Notes for October 21, 1991
delta–P Trigger = 15 in wc
Pulse Cleaning – 320 psig/0.1 sec
1114 Flame On system to temperature and pressure
1129 Flame Out, Unscheduled, over pressure
1132 Flame On
1920 Scheduled Shutdown

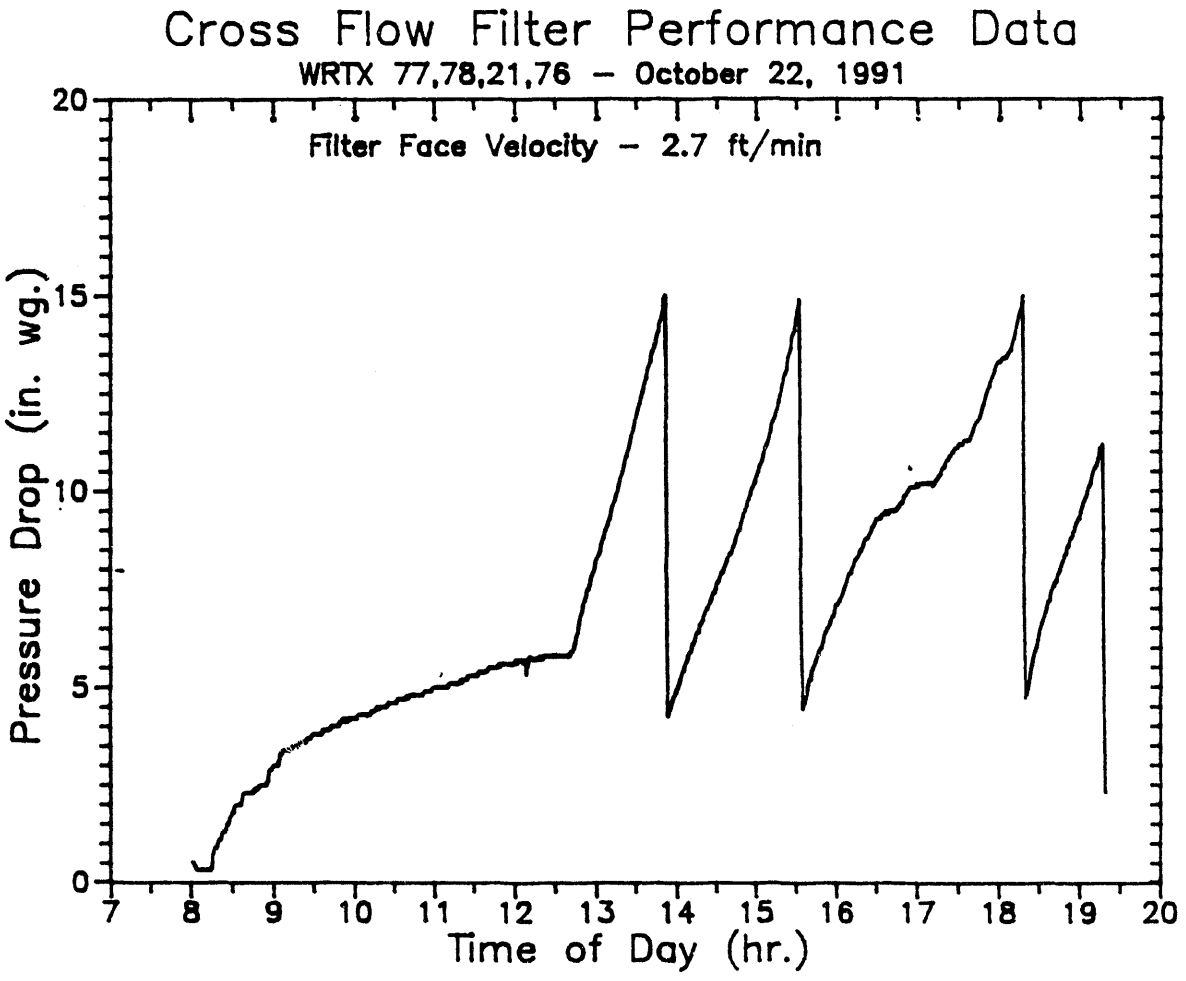

Operation Notes for October 22, 1991
delta–P Trigger = 15 in wc
Pulse Cleaning – 320 psig/0.1 sec
0758 Flame On system to temperature and pressure
1633–1800 Dust not feeding properly
1918 Scheduled Shutdown

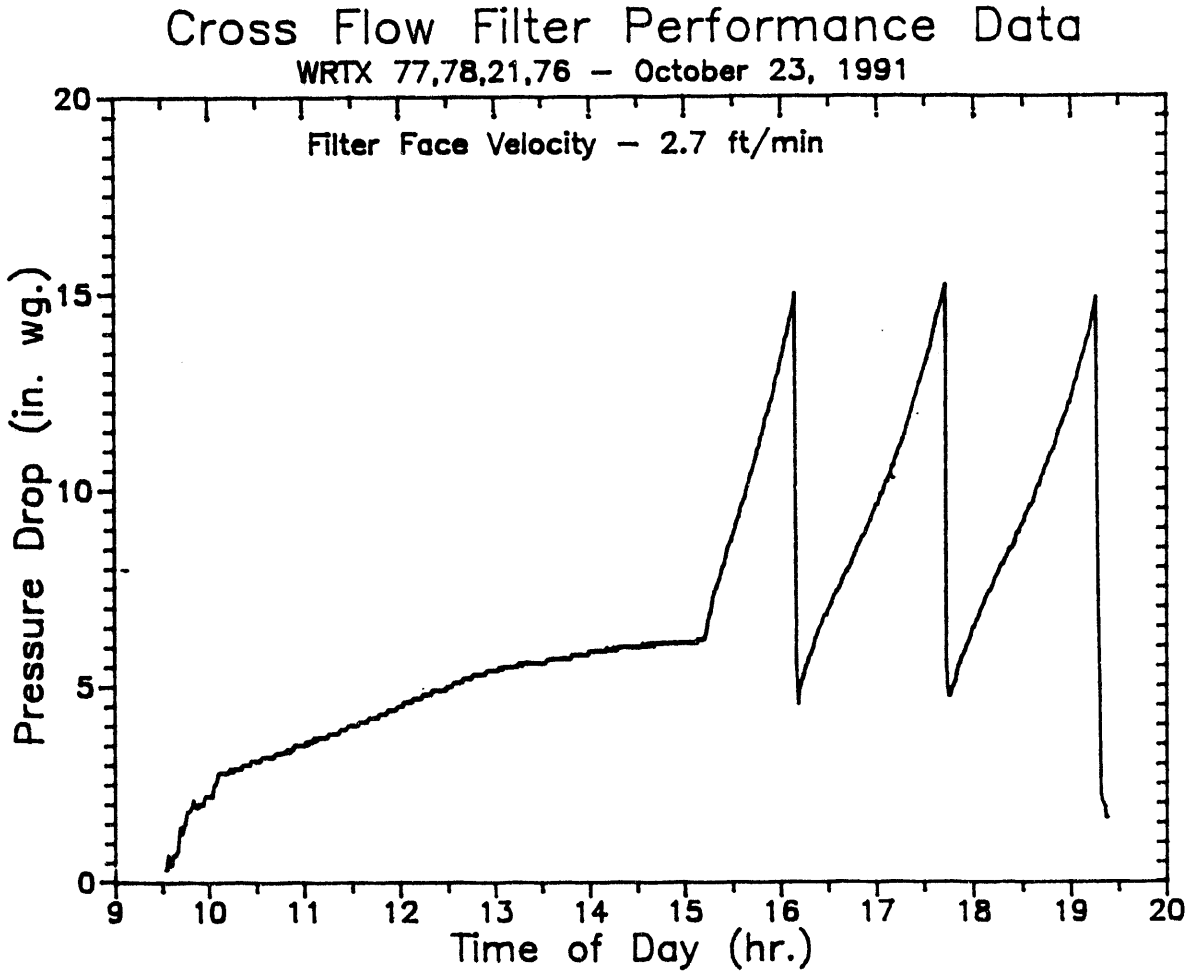

Operation Notes for October 23, 1991
delta–P Trigger = 15 in wc
Pulse Cleaning – 320 psig/0.1 sec
0930 Flame On system to temperature and pressure
1919 Scheduled Shutdown

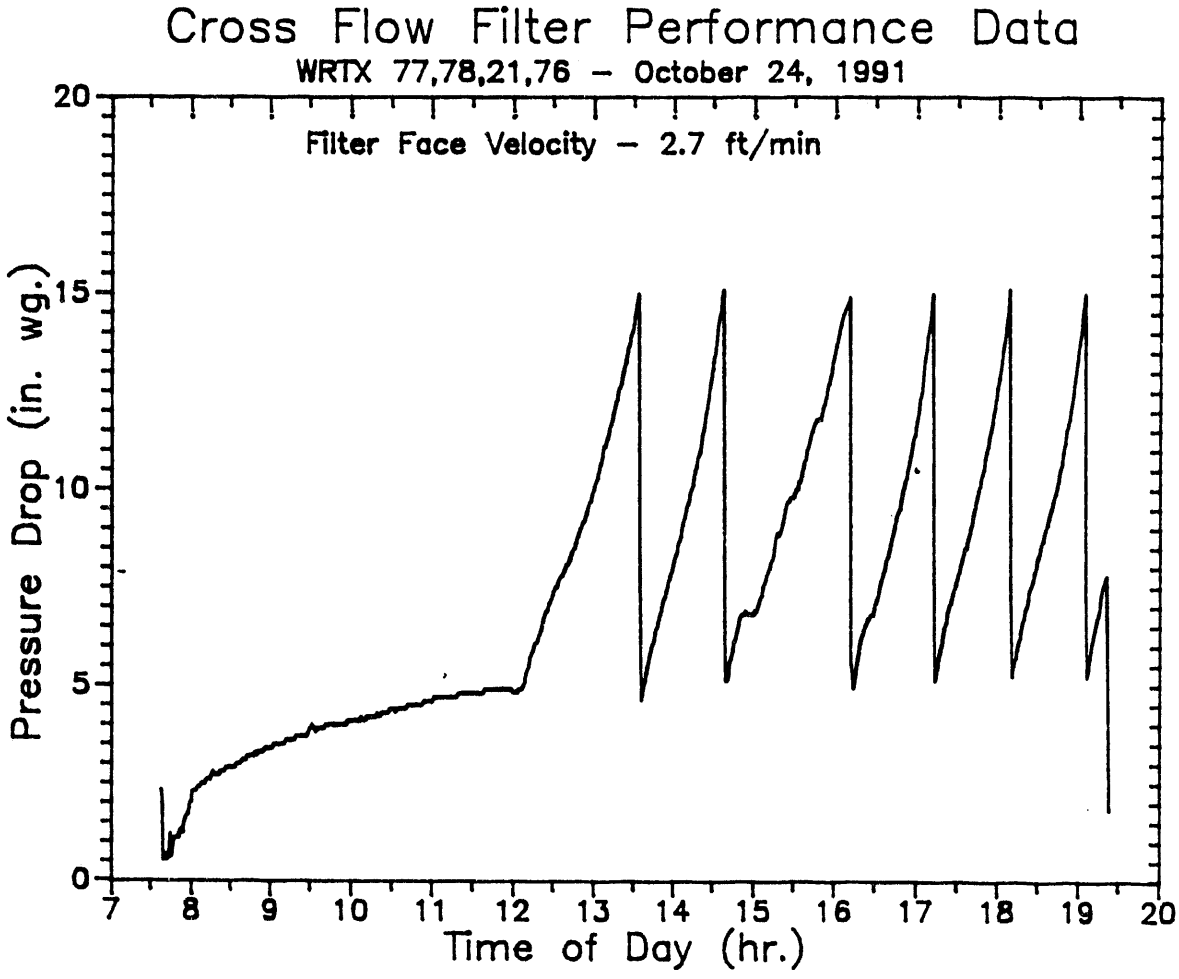

Operation Notes for October 24, 1991
delta–P Trigger = 15 in wc
Pulse Cleaning – 330 psig/0.1 sec
0735 Flame On system to temperature and pressure
1334 Dust Concentration in increased to 3000 ppm
1450 Dust not feeding properly
1920 Scheduled Shutdown

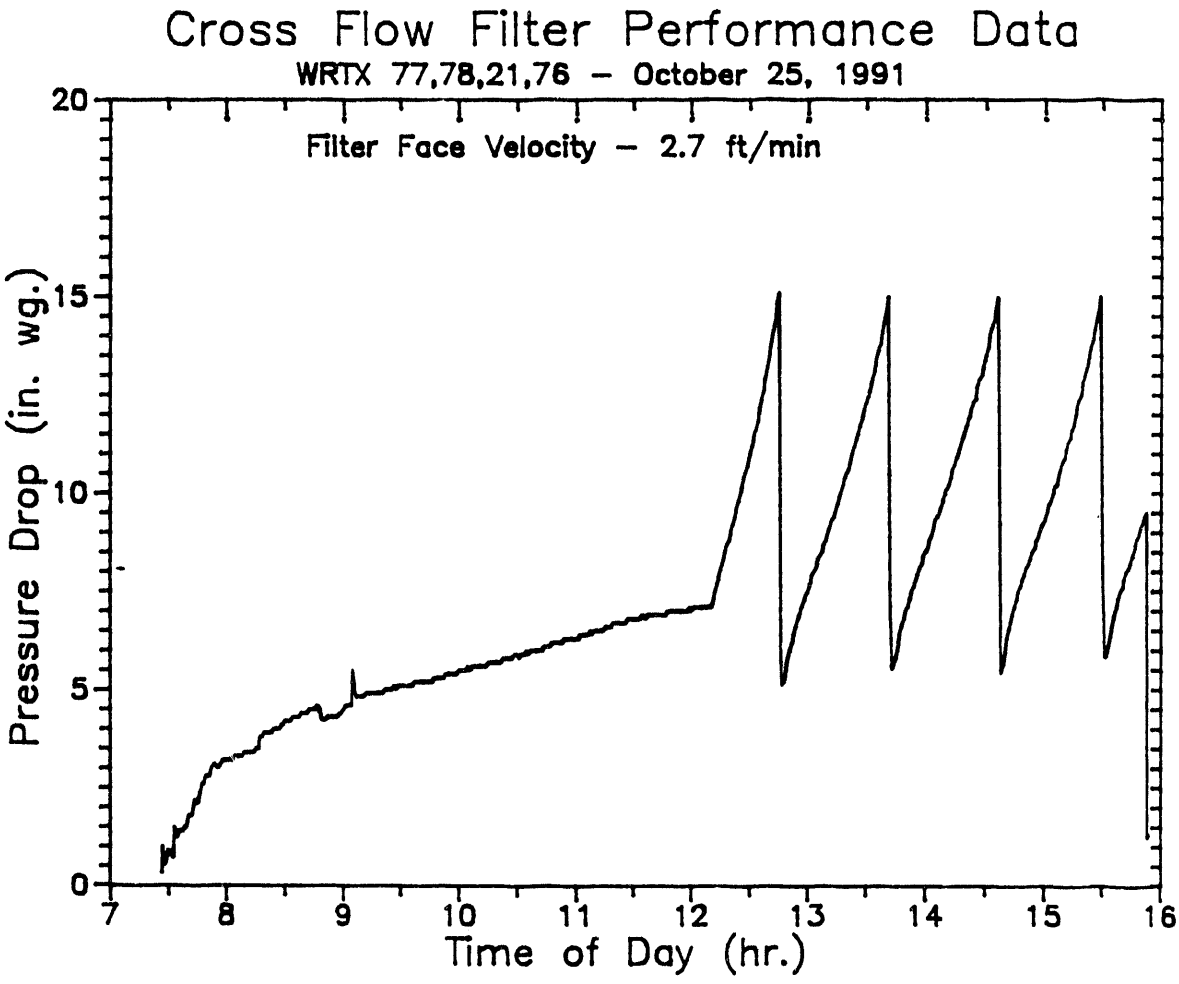

Operation Notes for October 25, 1991
delta–P Trigger = 15 in wc
Pulse Cleaning – 320 psig/0.1 sec
0724 Flame On system to temperature and pressure
1550 Scheduled Shutdown

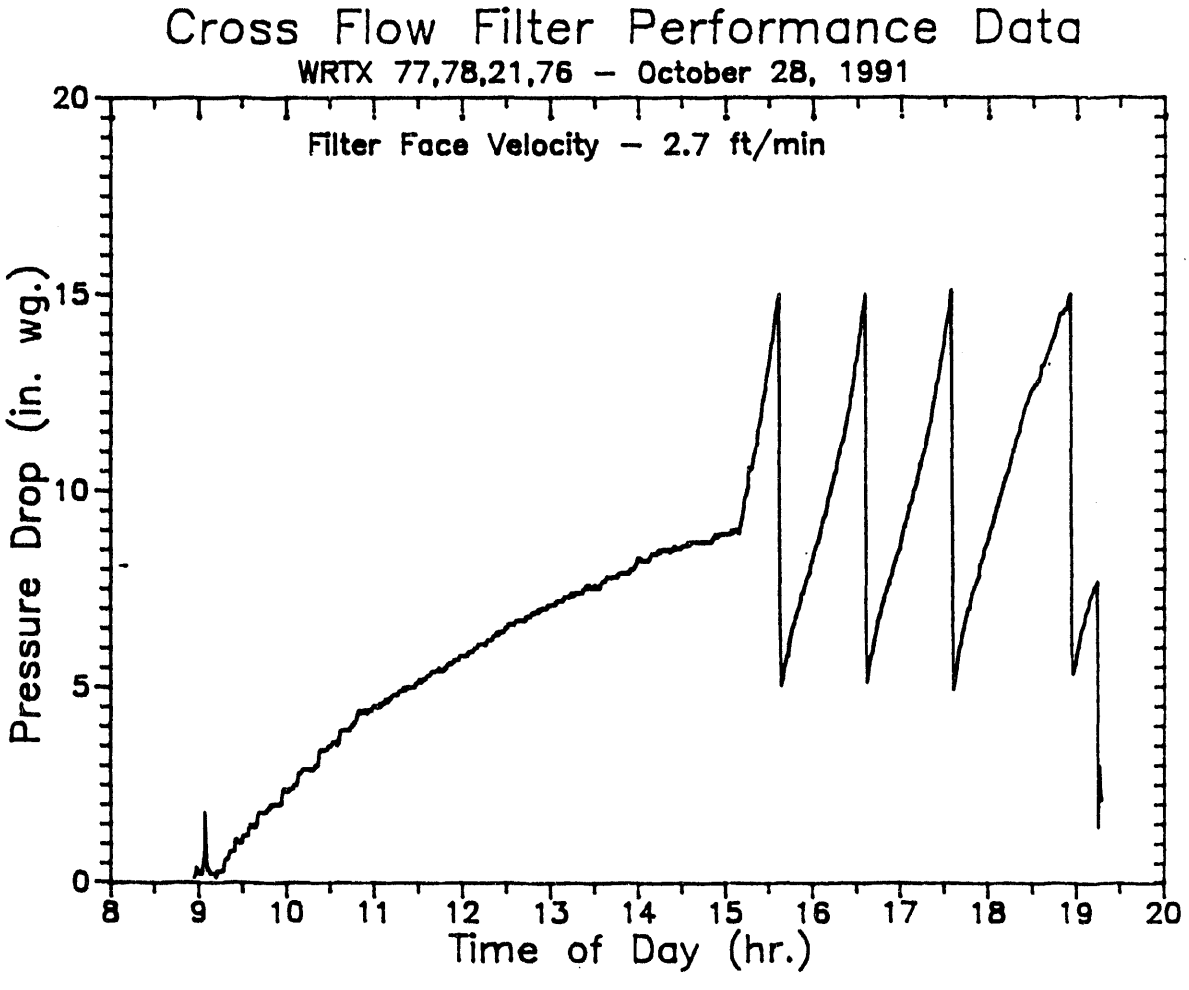

Operation Notes for October 28, 1991
delta–P Trigger = 15 in wc
Pulse Cleaning – 320 psig/0.1 sec
0858 Flame On system to temperature and pressure
0903 Flame Out, Unscheduled
0905 Flame On
1835 Dust not feeding properly
1915 Scheduled Shutdown

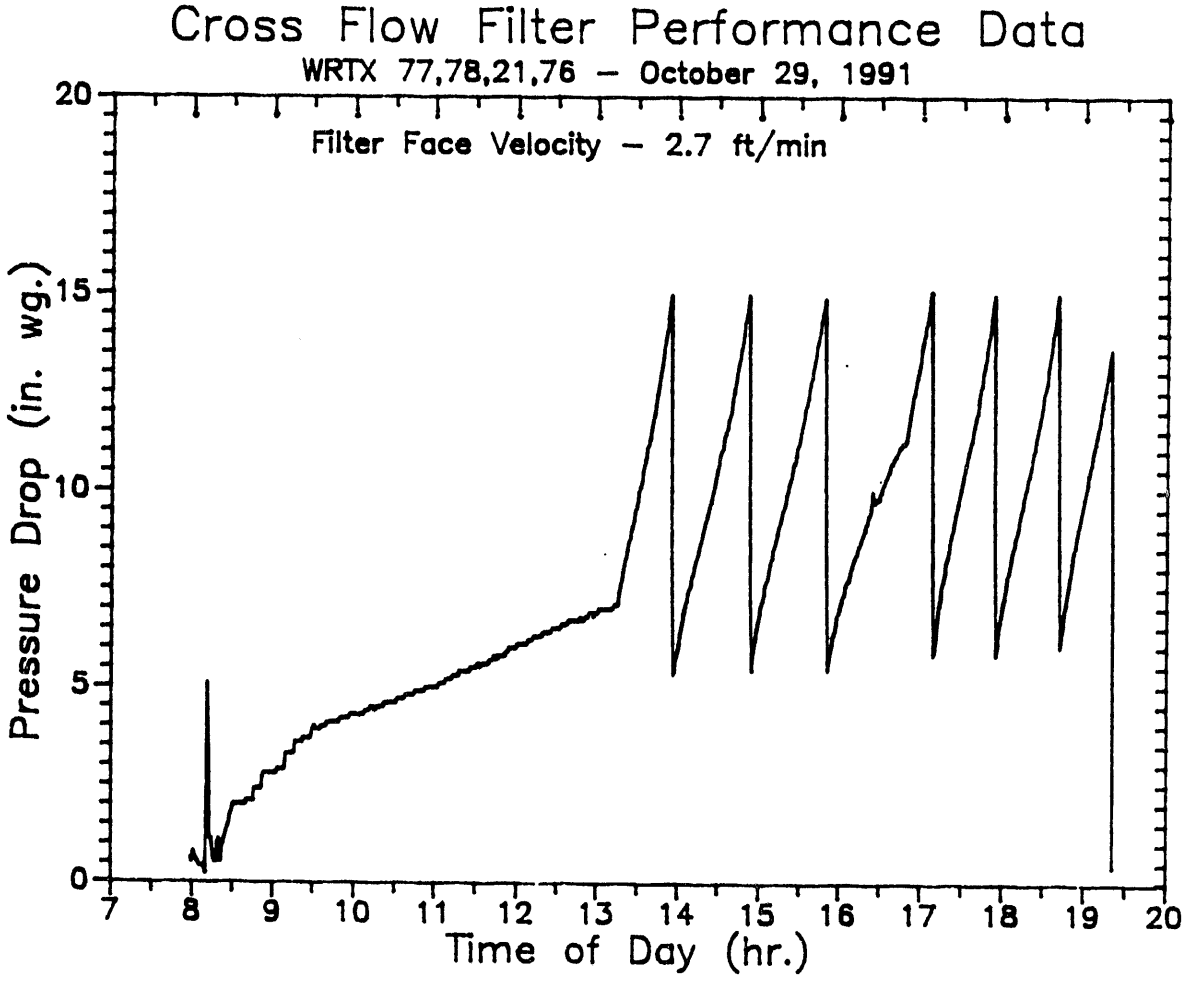

Operation Notes for October 29, 1991
delta–P Trigger = 15 in wc
Pulse Cleaning – 320 psig/0.1 sec
0759 Flame On system to temperature and pressure
0810 Flame Out, Unscheduled
0813 Flame On
1920 Scheduled Shutdown

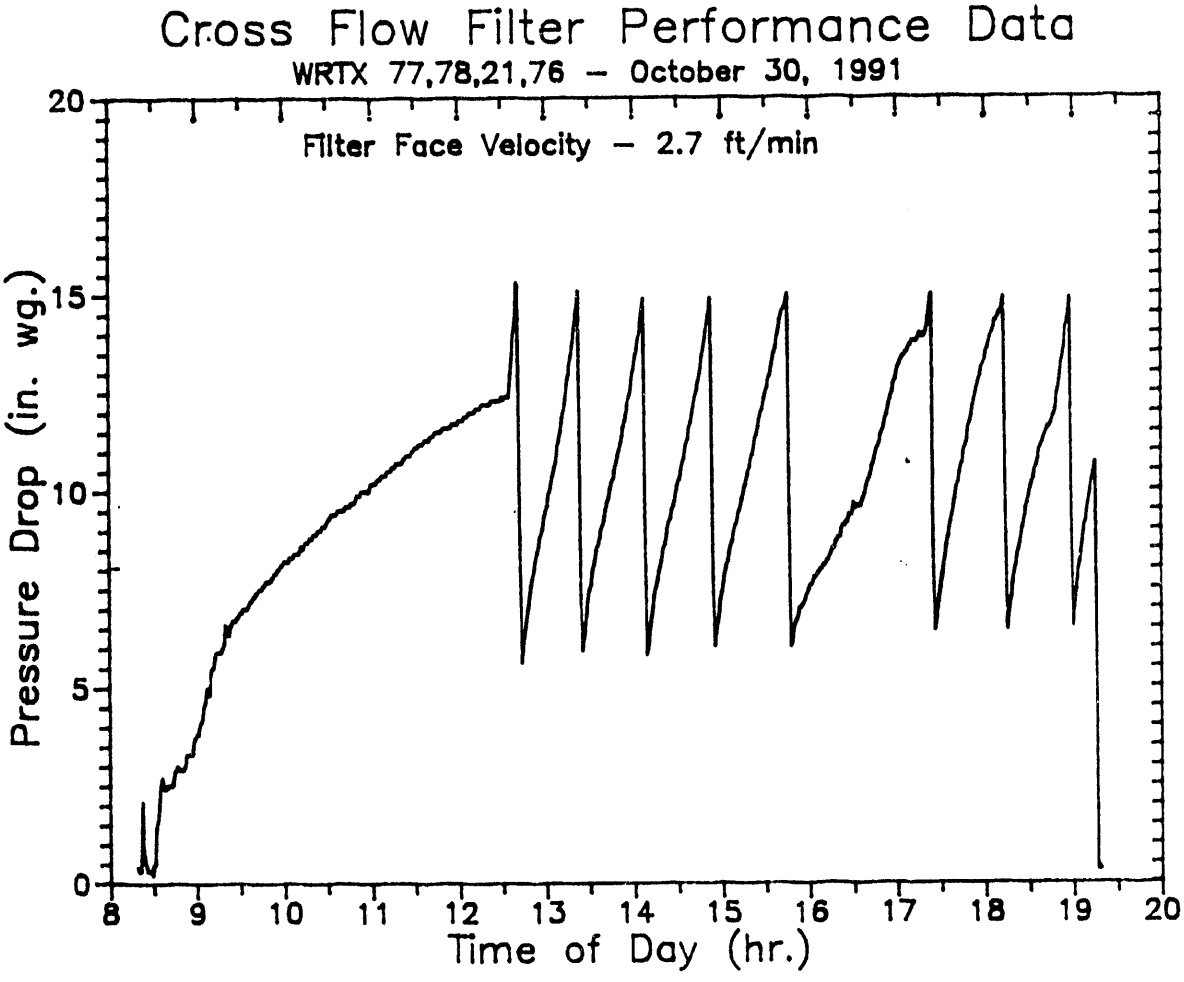

Operation Notes for October 30, 1991
delta–P Trigger = 15 in wc
Pulse Cleaning – 325 psig/0.1 sec
0816 Flame On system to temperature and pressure
0821 Flame Out, Unscheduled
0823 Flame On
1630 Dust not feeding properly
1916 Scheduled Shutdown

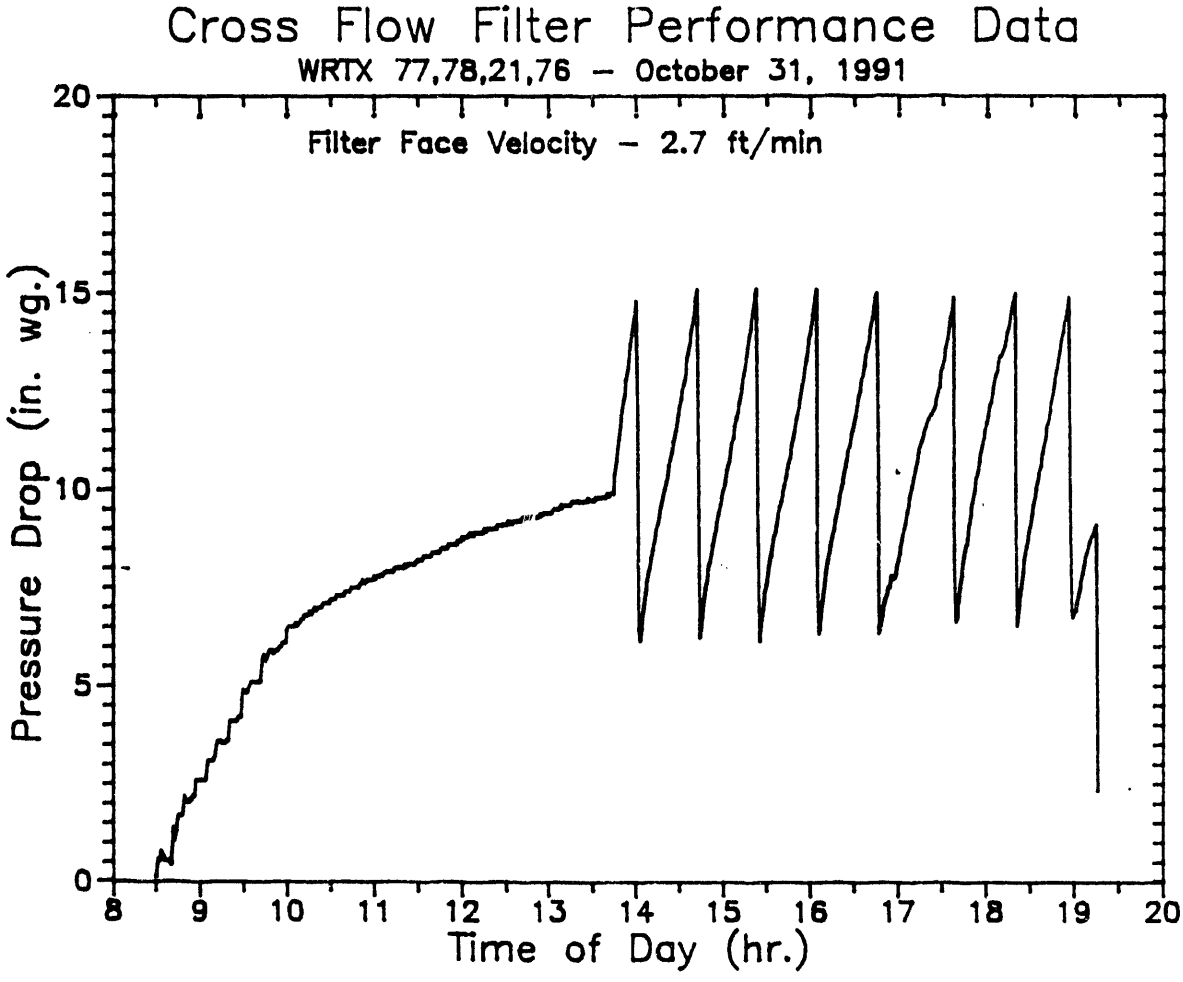

Operation Notes for October 31, 1991
delta–P Trigger = 15 in wc
Pulse Cleaning – 328 psig/0.1 sec
0831 Flame On system to temperature and pressure
1916 Scheduled Shutdown

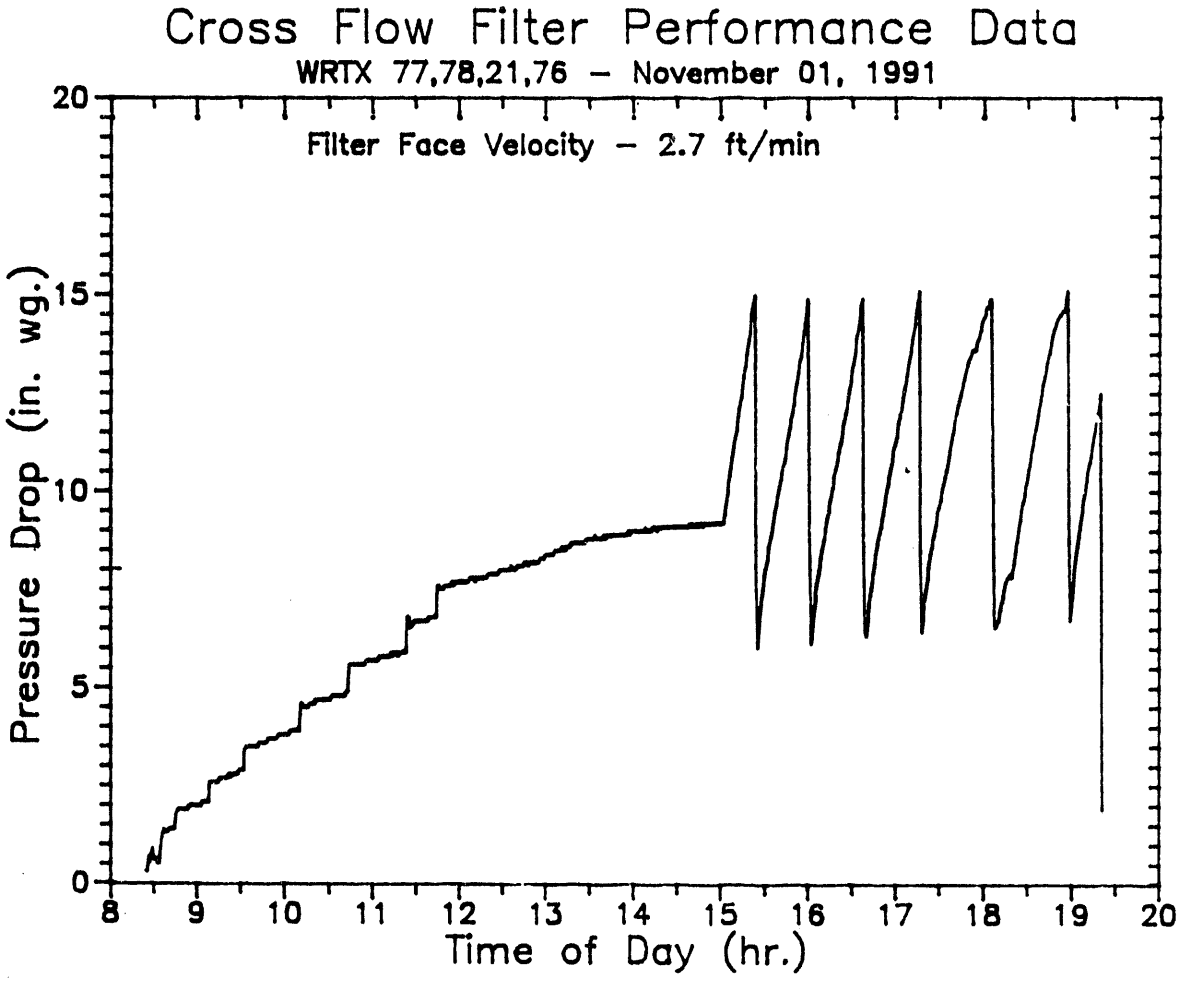

Operation Notes for November 01, 1991
delta–P Trigger = 15 in wc
Pulse Cleaning – 330 psig/0.1 sec
0826 Flame On system to temperature and pressure
1920 Scheduled Shutdown

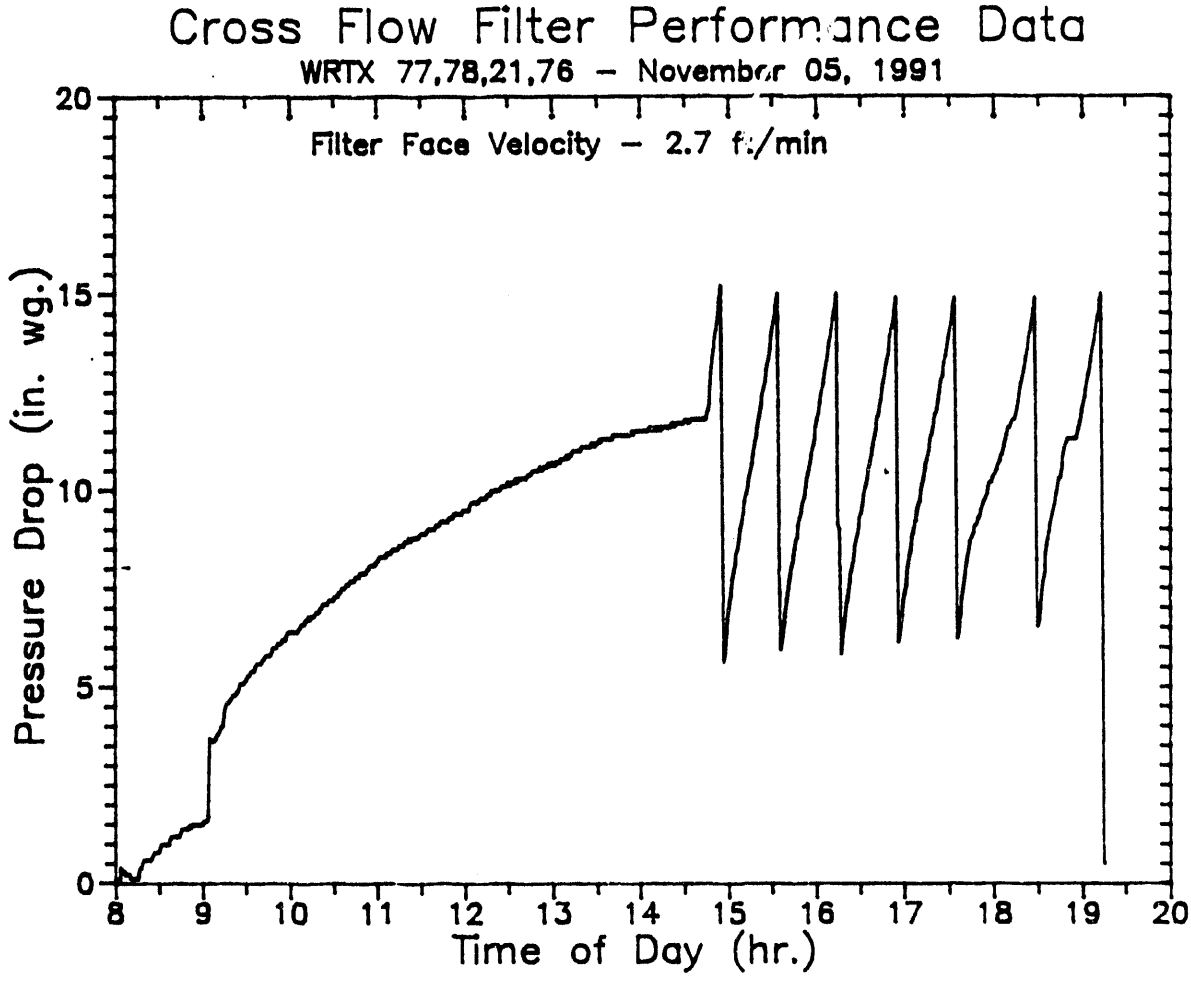

Operation Notes for November 05, 1991
delta–P Trigger = 15 in wc
Pulse Cleaning – 305 psig/0.1 sec
0803 Flame On system to temperature and pressure
1813 Dust not feeding properly
1855 Dust not feeding properly
1913 Scheduled Shutdown

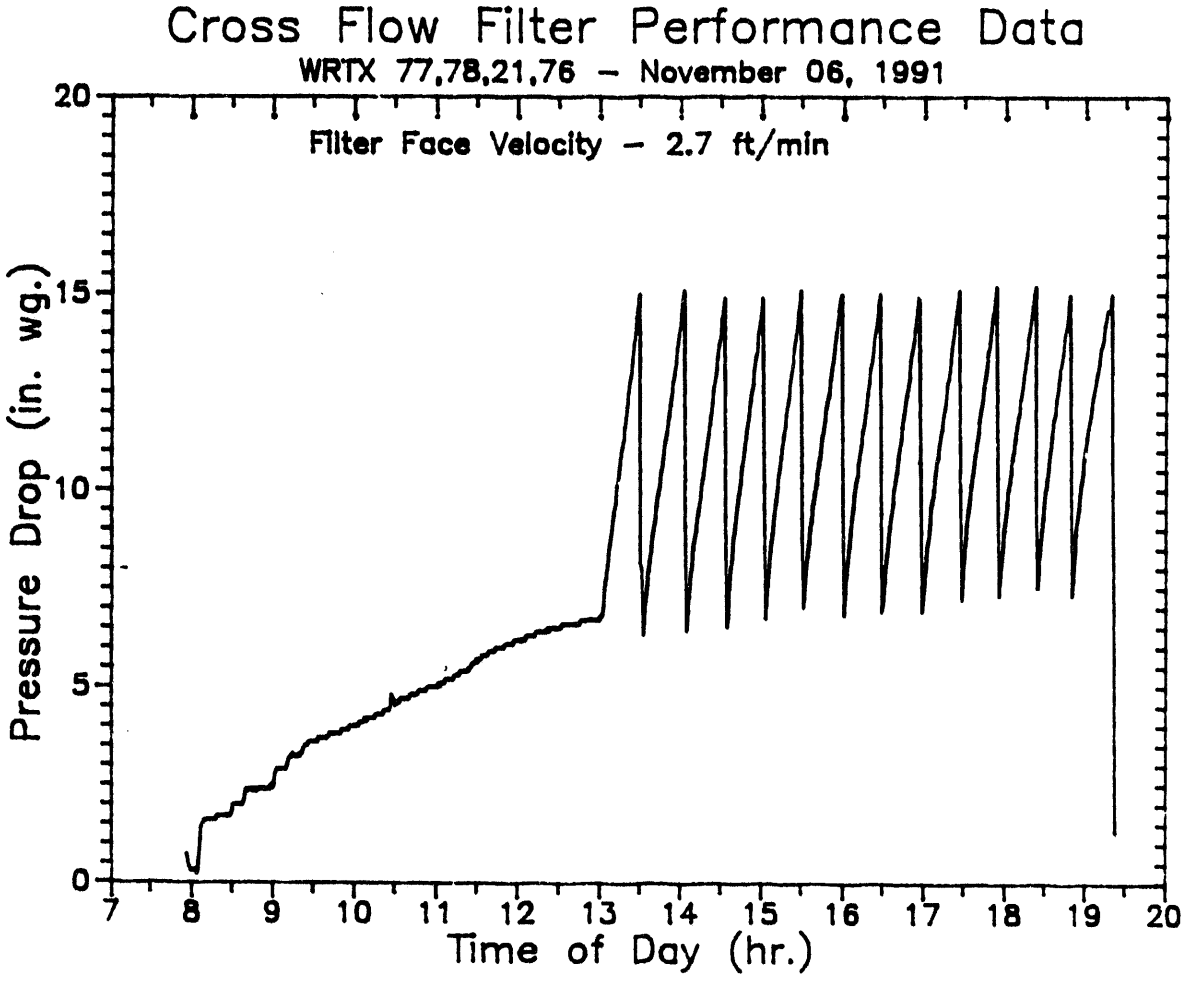

Operation Notes for November 06, 1991
delta–P Trigger = 15 in wc
Pulse Cleaning – 305 psig/0.1 sec
0755 Flame On system to temperature and pressure
1922 Scheduled Shutdown

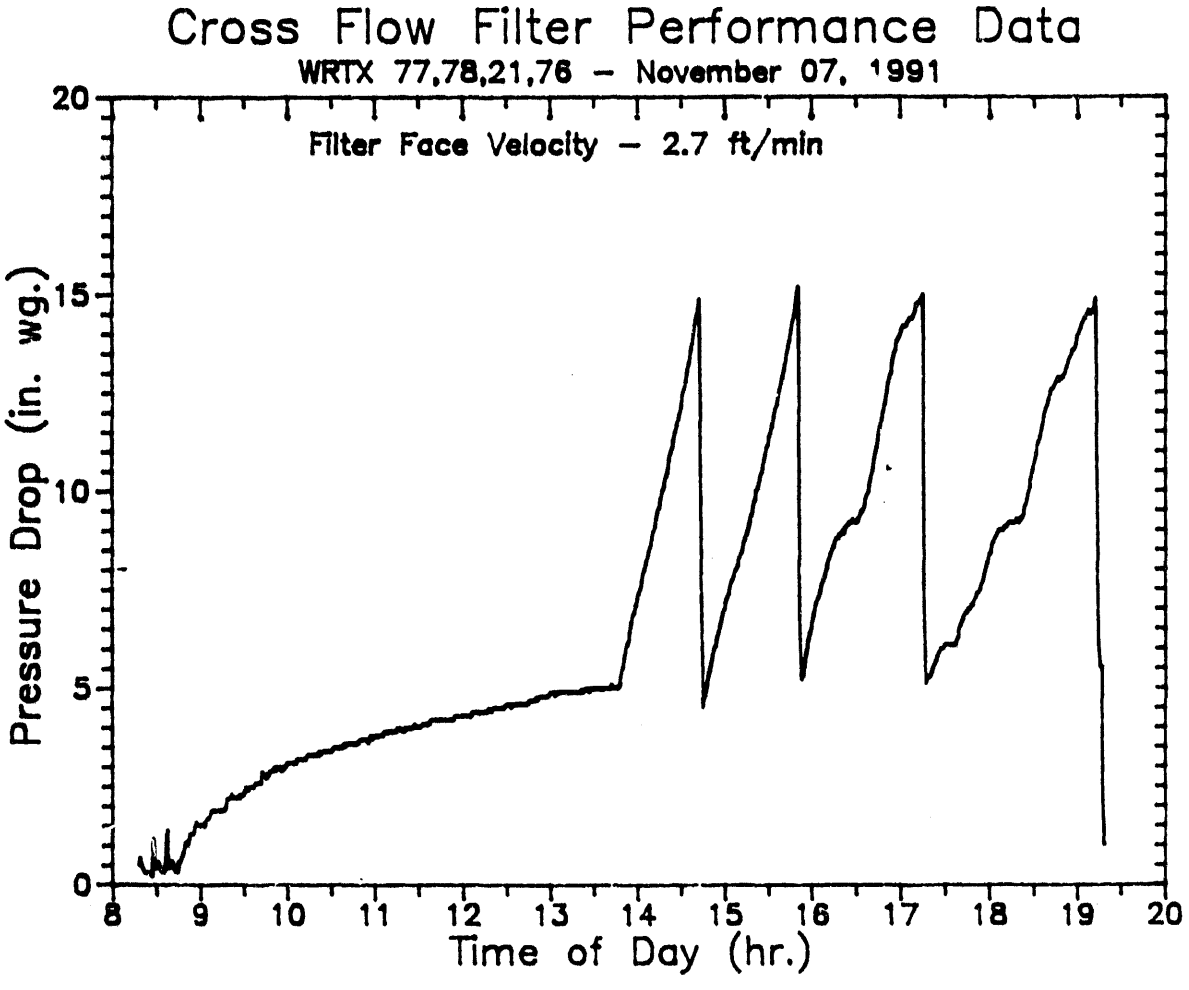

Operation Notes for November 07, 1991
delta–P Trigger = 15 in wc
Pulse Cleaning – 317 psig/0.1 sec
0818 Flame On system to temperature and pressure
1551 – 1913 Dust not feeding properly
1917 Scheduled Shutdown

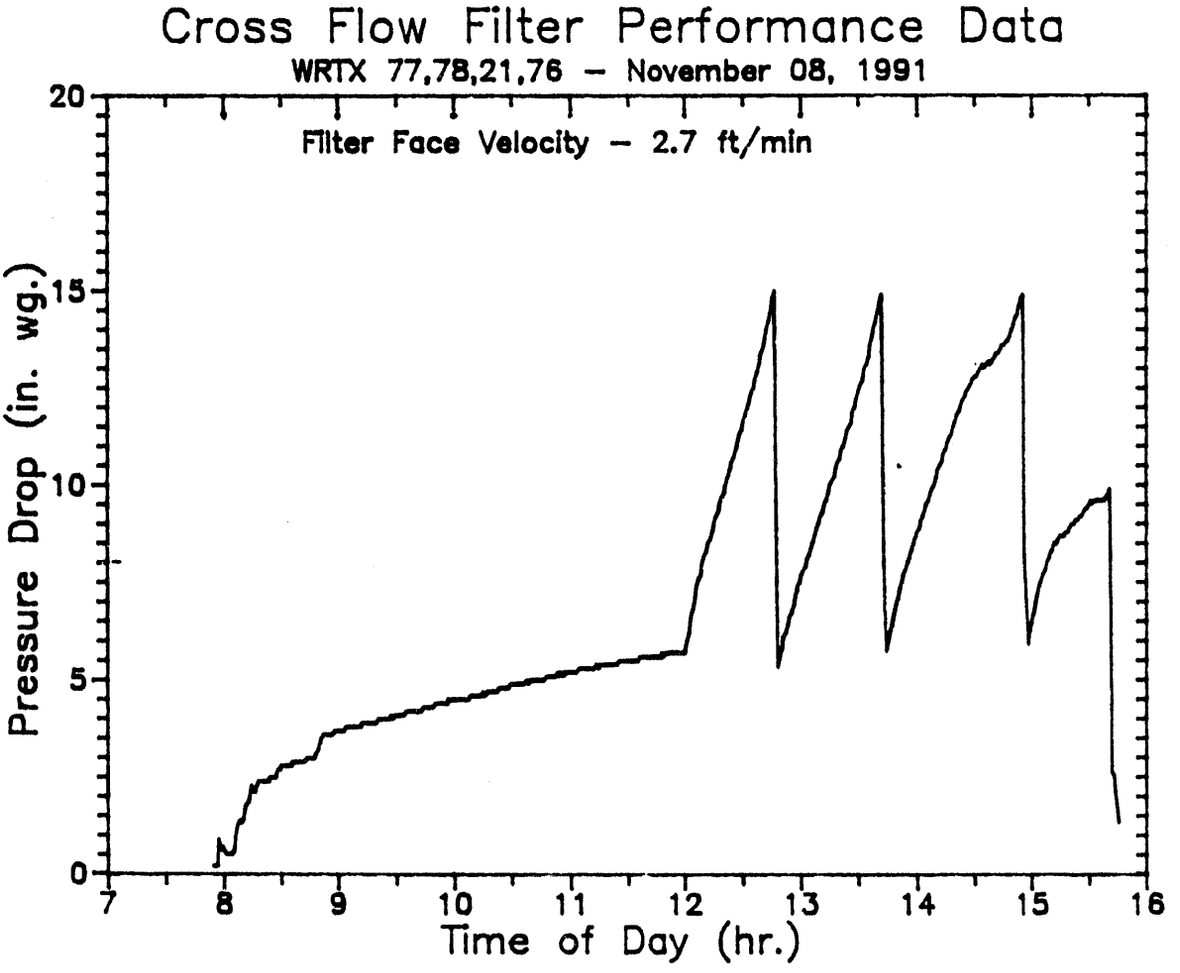

Operation Notes for November 08, 1991
delta–P Trigger = 15 in wc
Pulse Cleaning – 315 psig/0.1 sec
0755 Flame On system to temperature and pressure
1438 – 1542 Dust not feeding properly
1542 Scheduled Shutdown

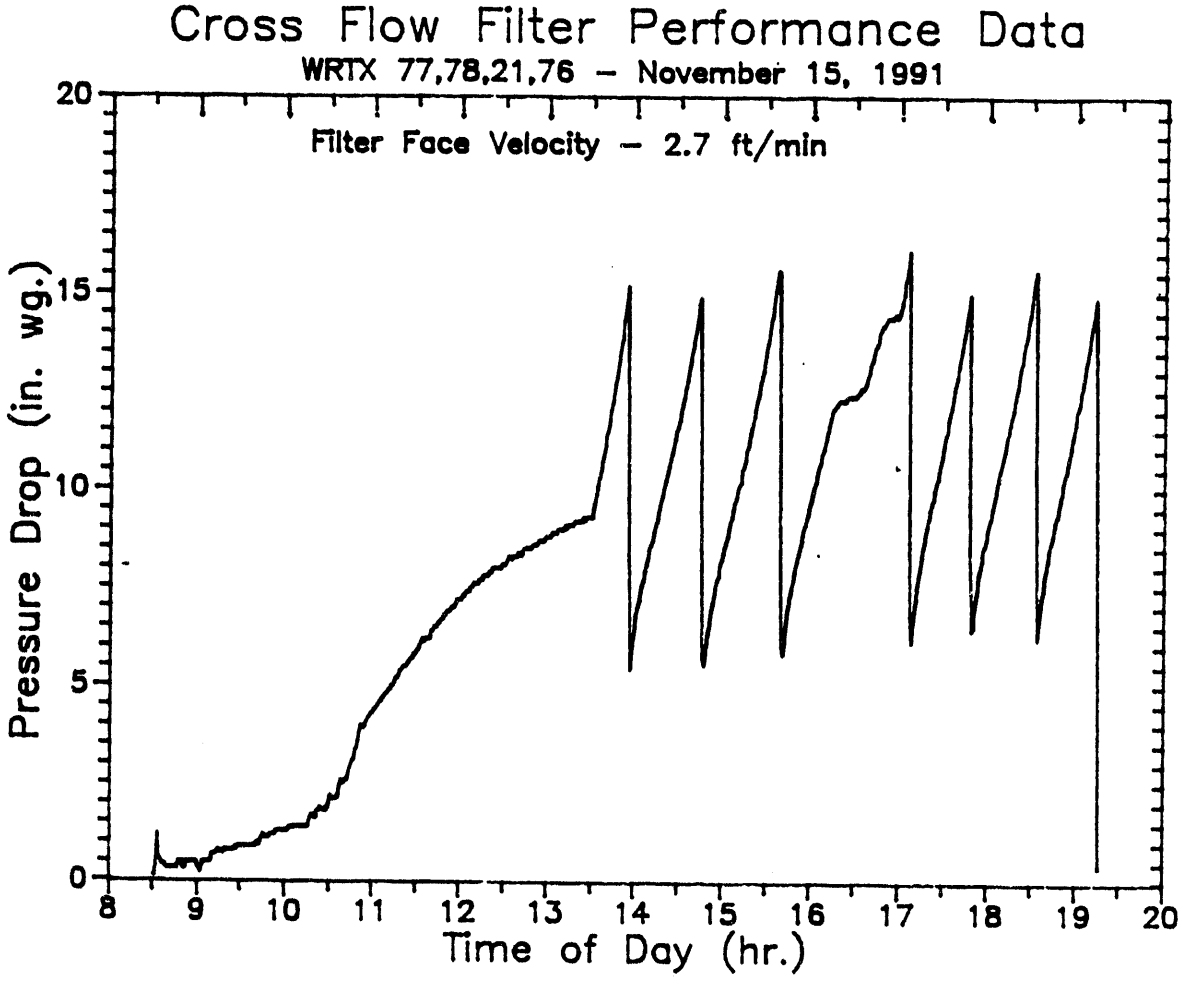

Operation Notes for November 15, 1991
delta–P Trigger = 15 in wc
Pulse Cleaning – 305 psig/0.1 sec
0832 Flame On system to temperature and pressure
1550 Dust not feeding properly
1912 Scheduled Shutdown

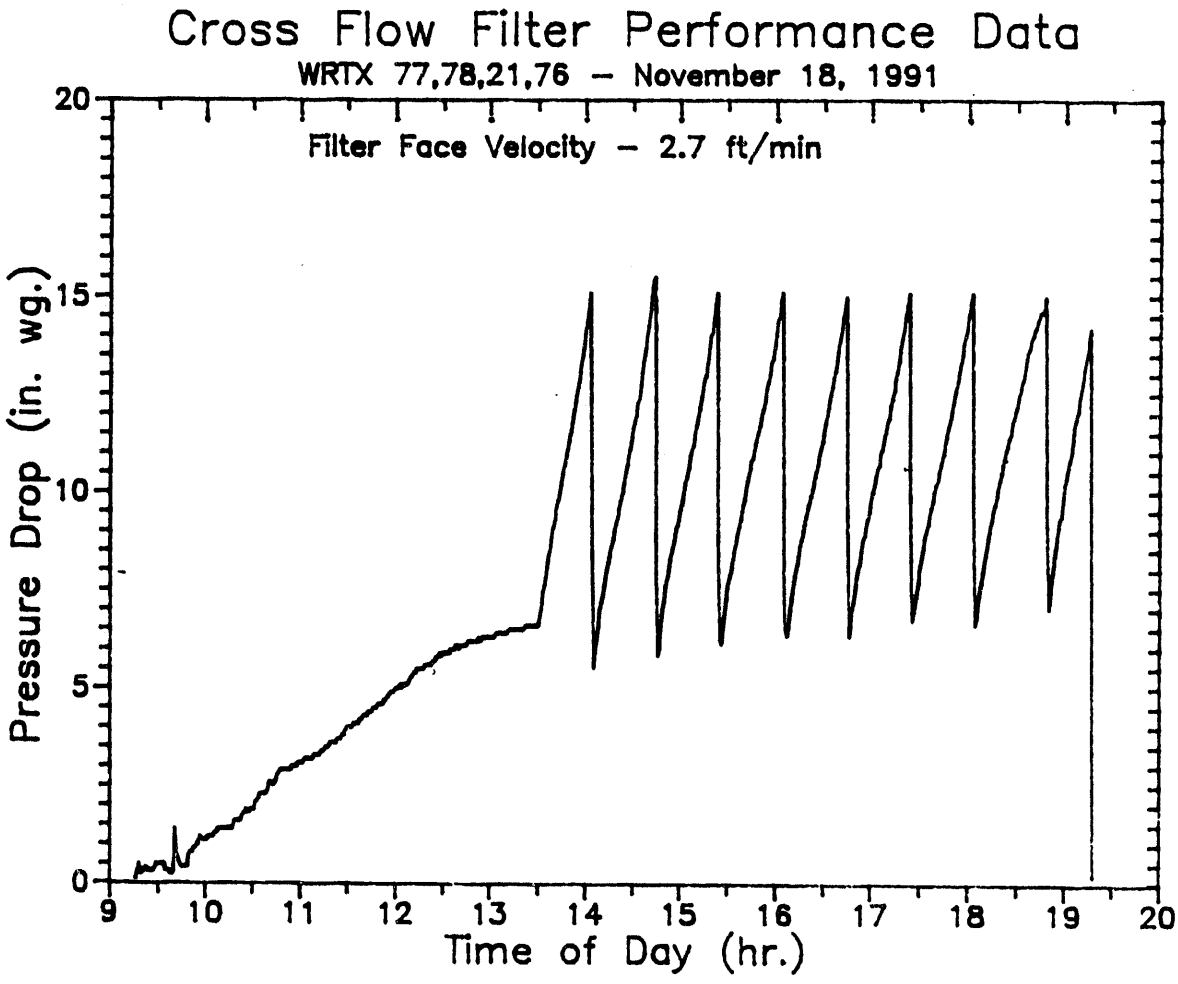

Operation Notes for November 18, 1991
delta–P Trigger = 15 in wc
Pulse Cleaning – 305 psig/0.1 sec
0916 Flame On system to temperature and pressure
0935 Flame Out, Unscheduled
0938 Flame On
1916 Scheduled Shutdown

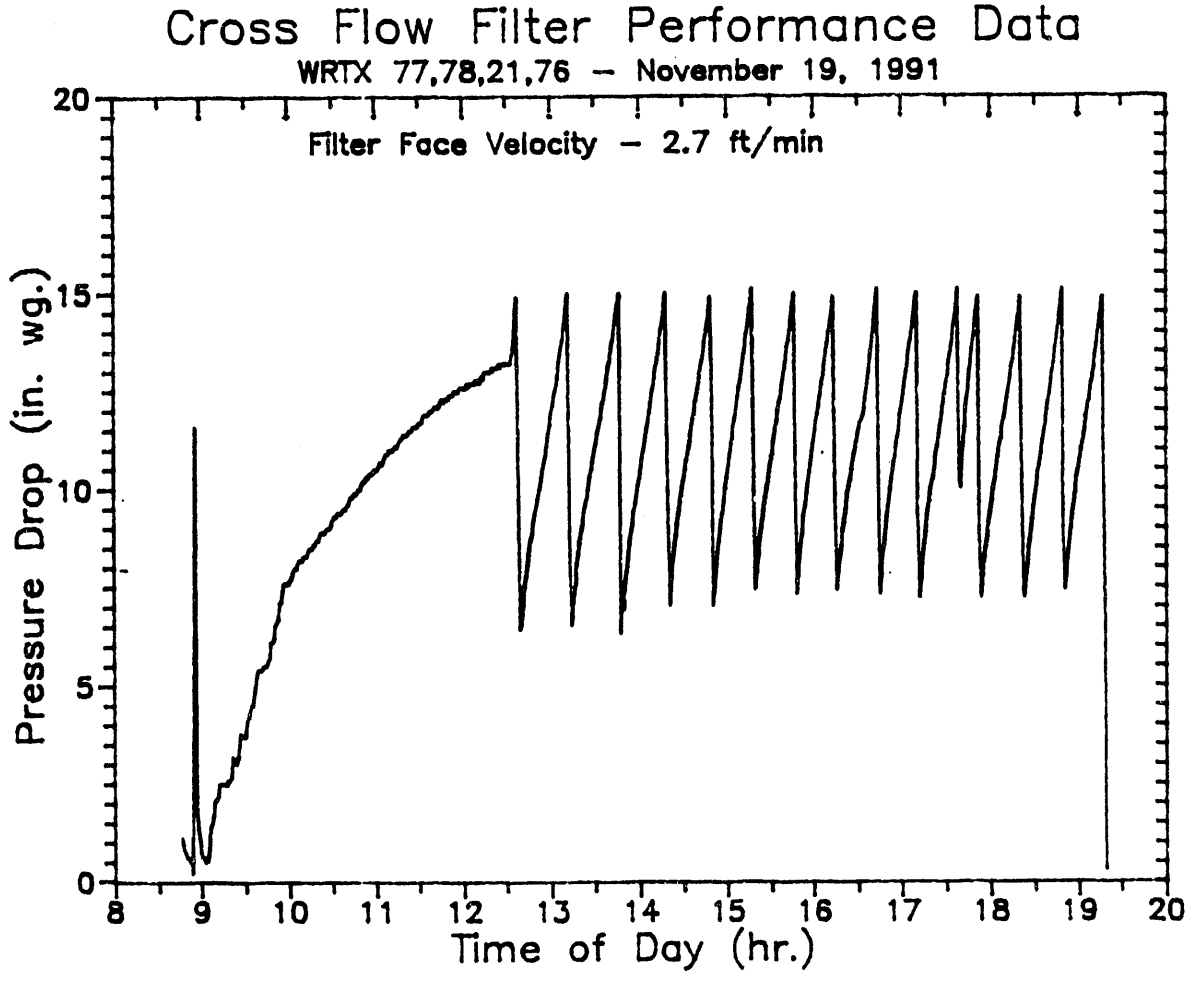

Operation Notes for November 19, 1991
delta–P Trigger = 15 in wc
Pulse Cleaning – 305 psig/0.1 sec
0842 Flame On system to temperature and pressure
0852 Flame Out, Unscheduled
0855 Flame On
1630 Blow back tank pressure increased to 320 psig
1736 Plenum selector switch did not completely engage
1916 Scheduled Shutdown

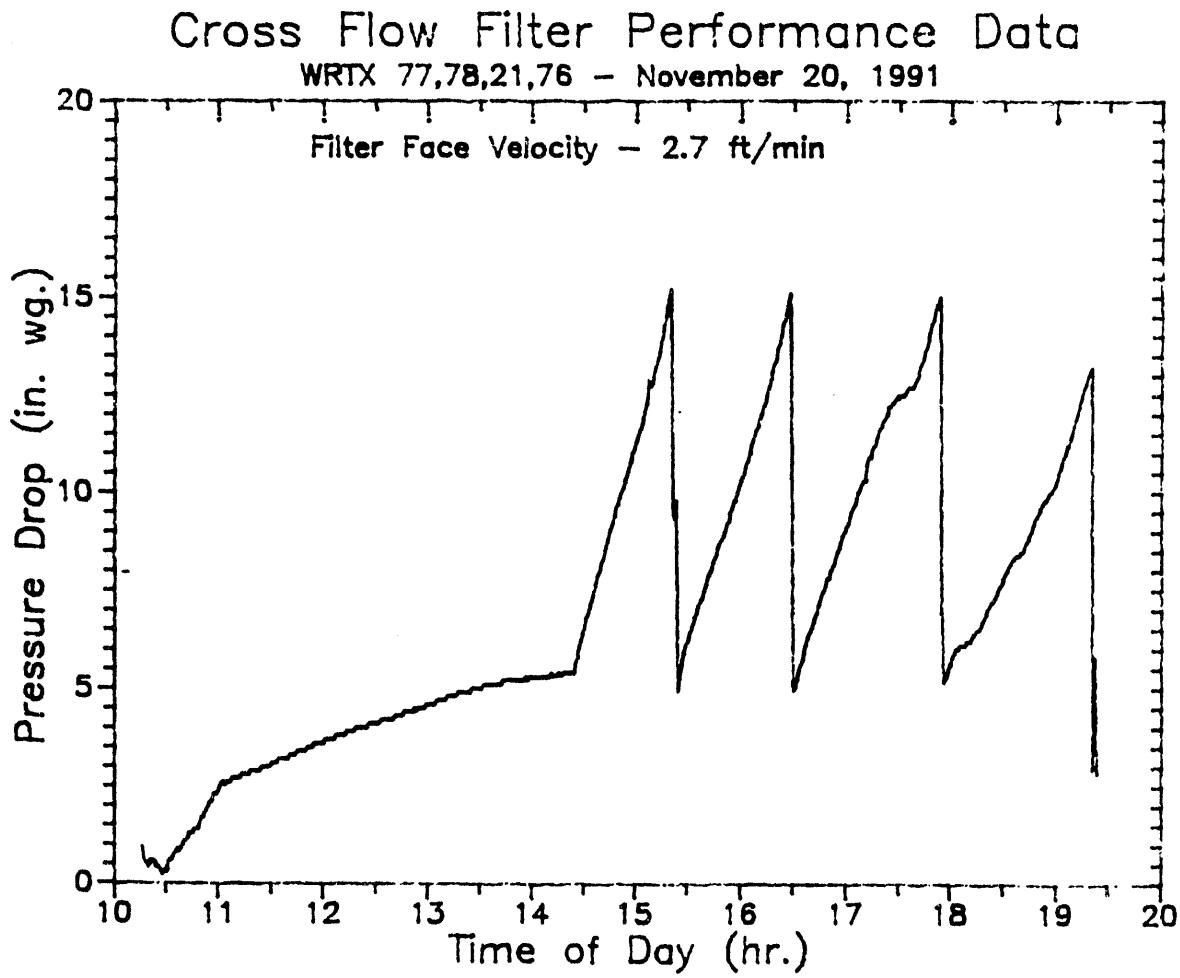

Operation Notes for November 20, 1991
delta–P Trigger = 15 in wc
Pulse Cleaning – 320 psig/0.1 sec
1014 Flame On system to temperature and pressure
1018 Flame Out, Unscheduled
1020 Flame On
1920 Scheduled Shutdown

APPENDIX H

FILTER PRESSURE DROP TRACES FROM SELECTED TEST PERIODS DURING GASIFIER SIMULATOR TESTING

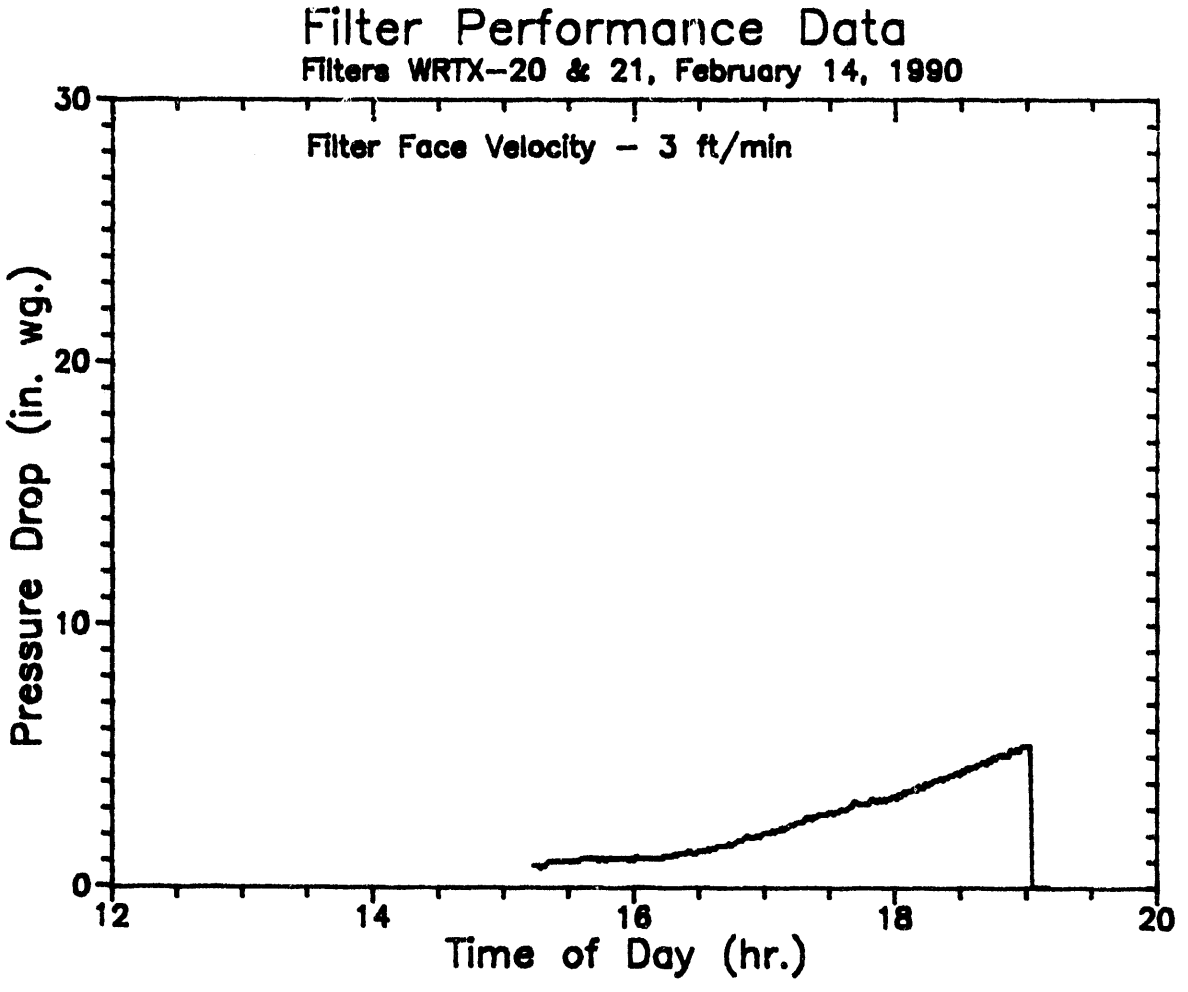

Operation Notes for February 14, 1990:

Start of testing in recirculating gas test loop

Dust - Texaco Char

Pulse Cleaning - 200 psig/0.1 sec

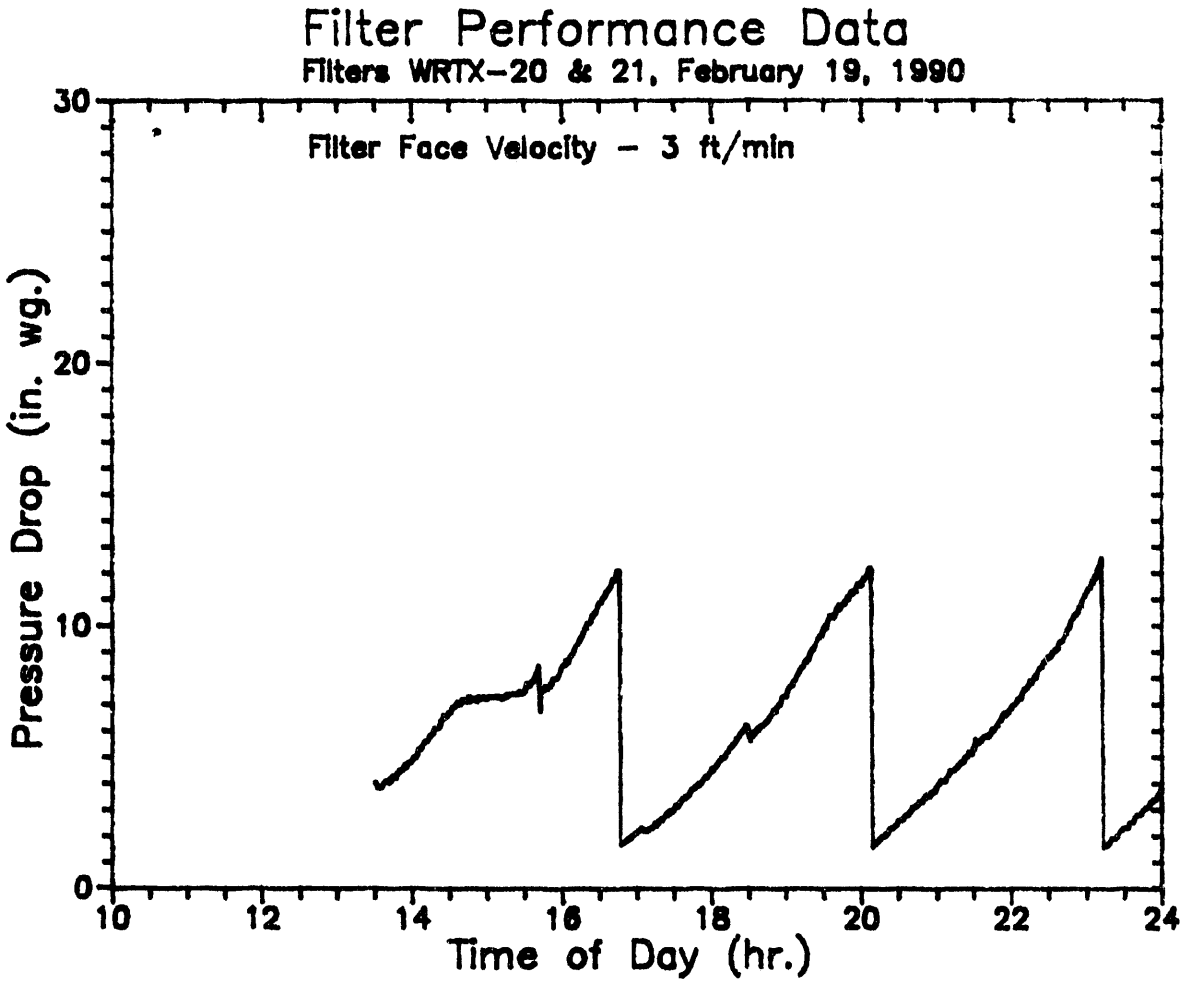

Operation Notes for February 19, 1990:

Start of week long test

ΔP Trigger = 12.0" WC

Pulse Cleaning - 198 psig/0.1 sec

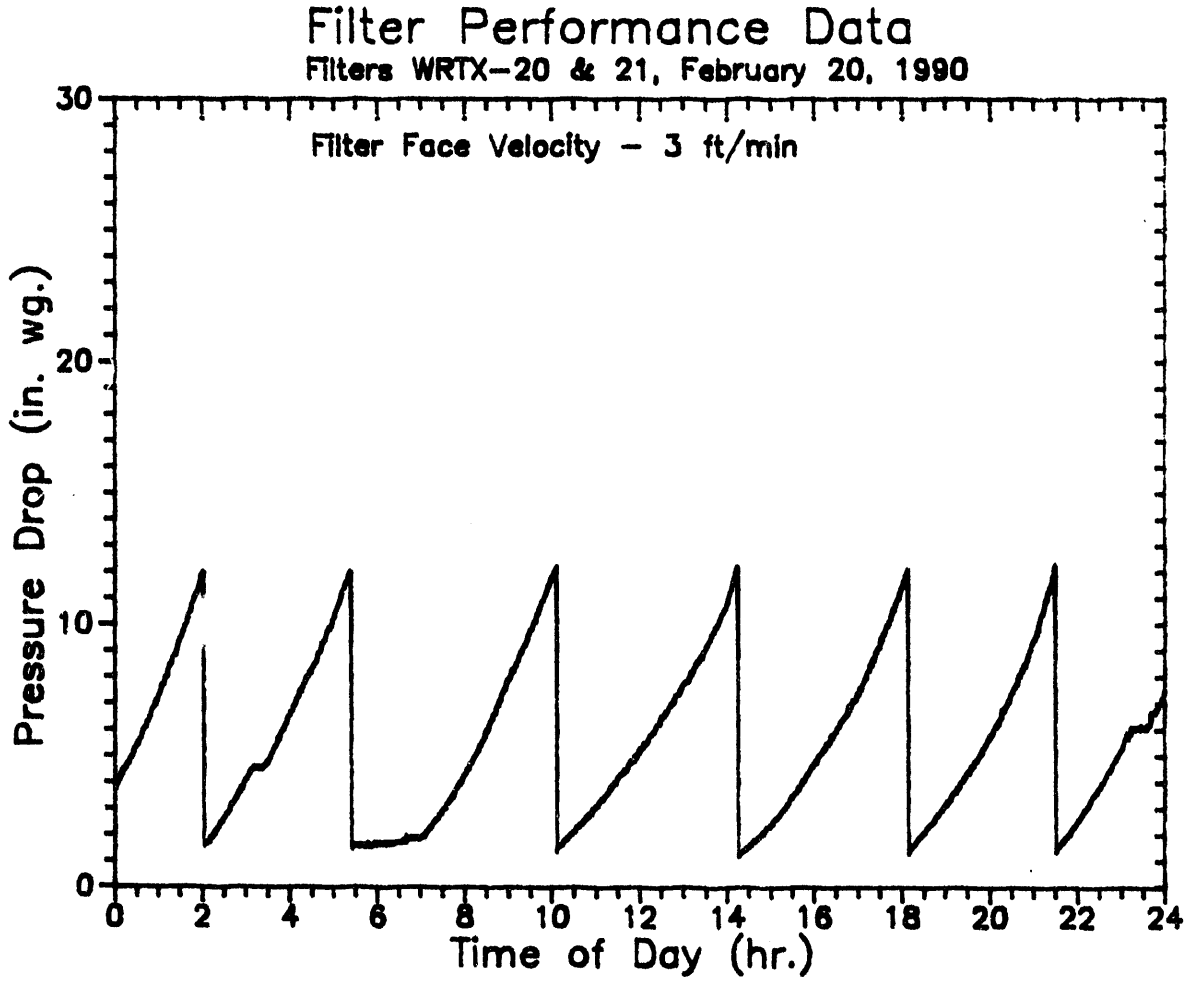

Operation Notes for February 20, 1990:

0600 Dust Added

ΔP Trigger = 12.0" WC

Pulse Cleaning - 195 psig/0.1 sec

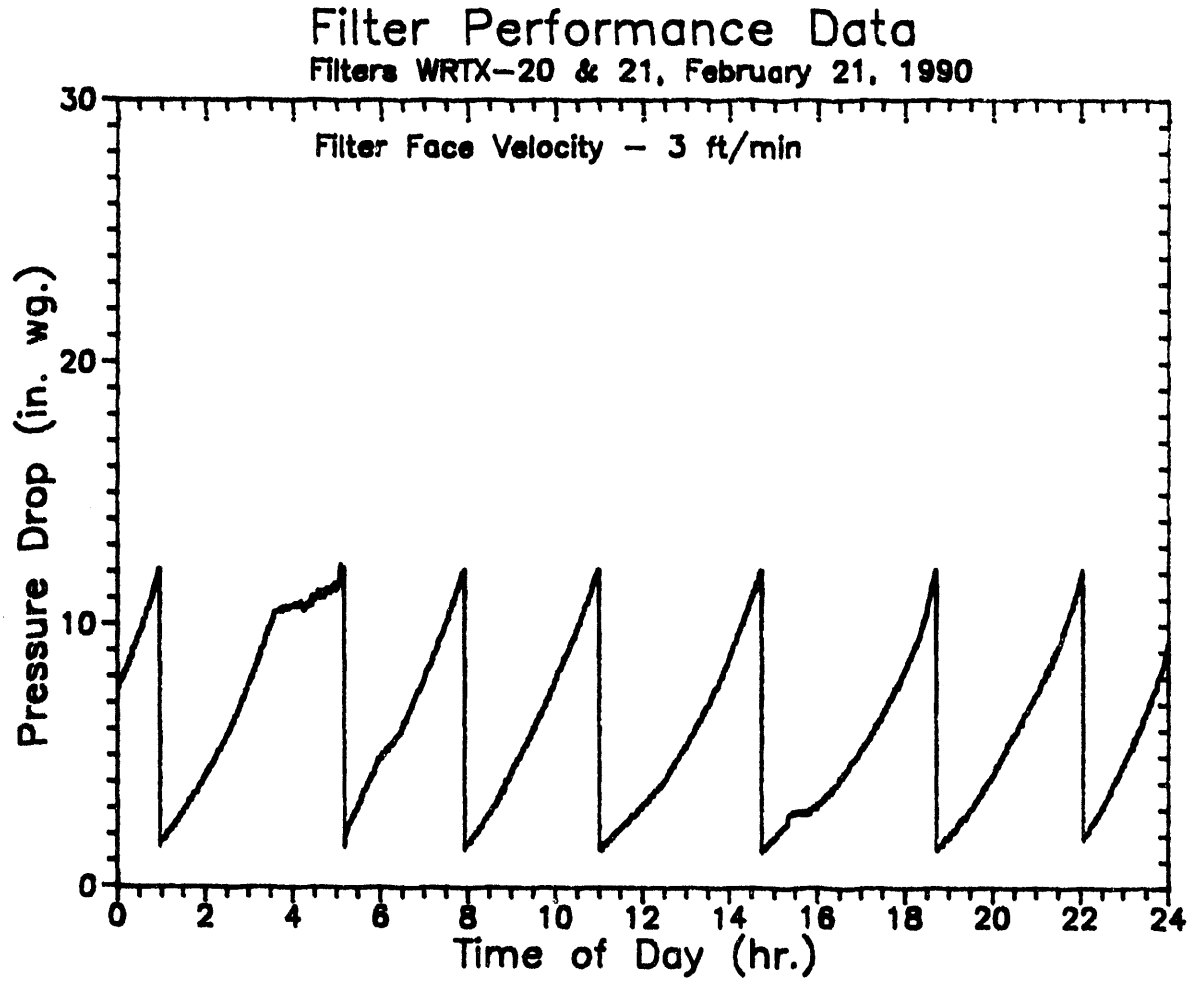

Operation Notes for February 21, 1990:

0340 Dust Feed off

0430 Dust Feed on

ΔP Trigger = 12.0" WC

Pulse Cleaning - 198 psig/0.1 sec

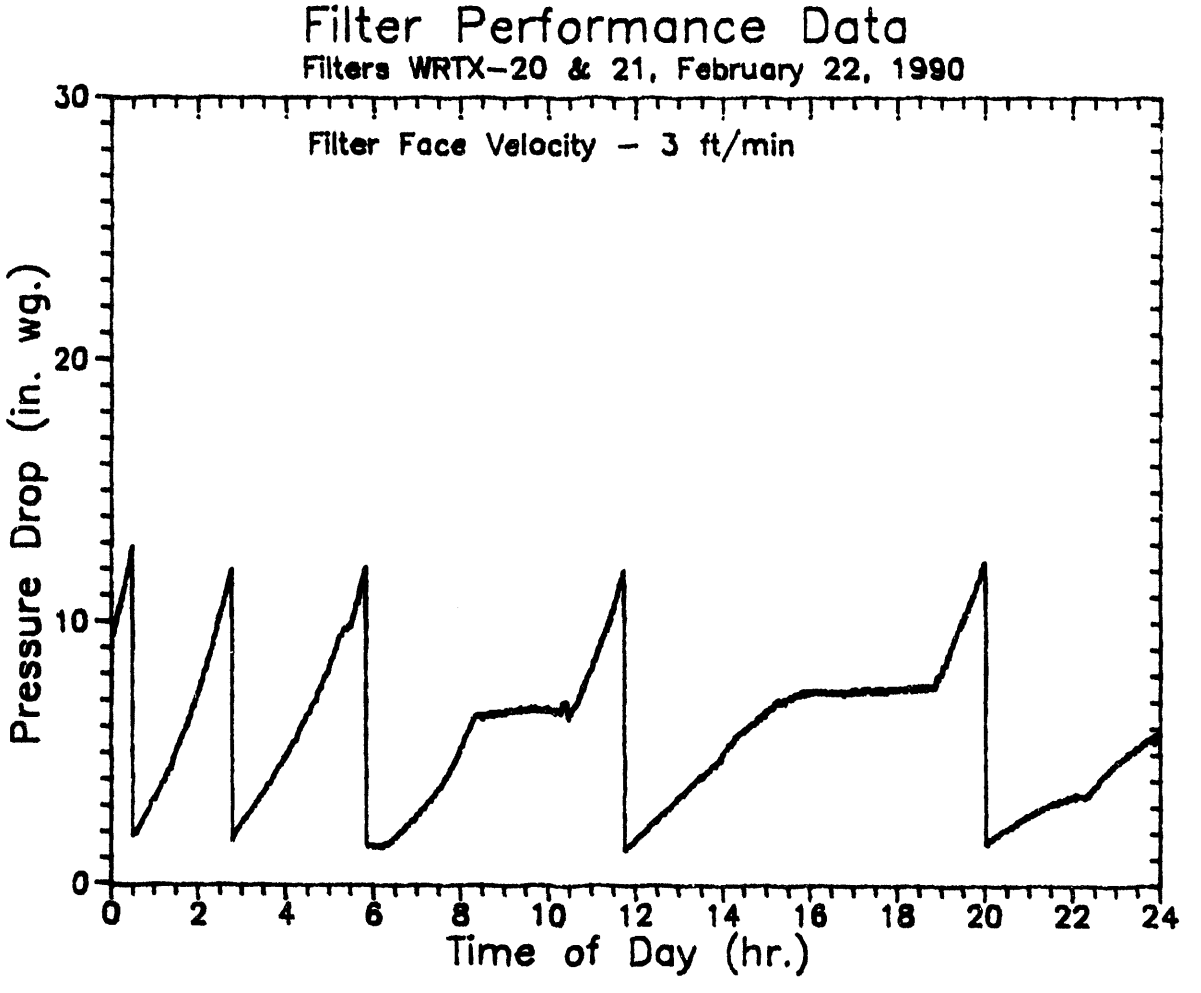

Operation Notes for February 22, 1990:

0830 Dust Added

1530 Dust Feed Motor failure

ΔP Trigger = 12.0" WC

Pulse Cleaning - 195 psig/0.1 sec

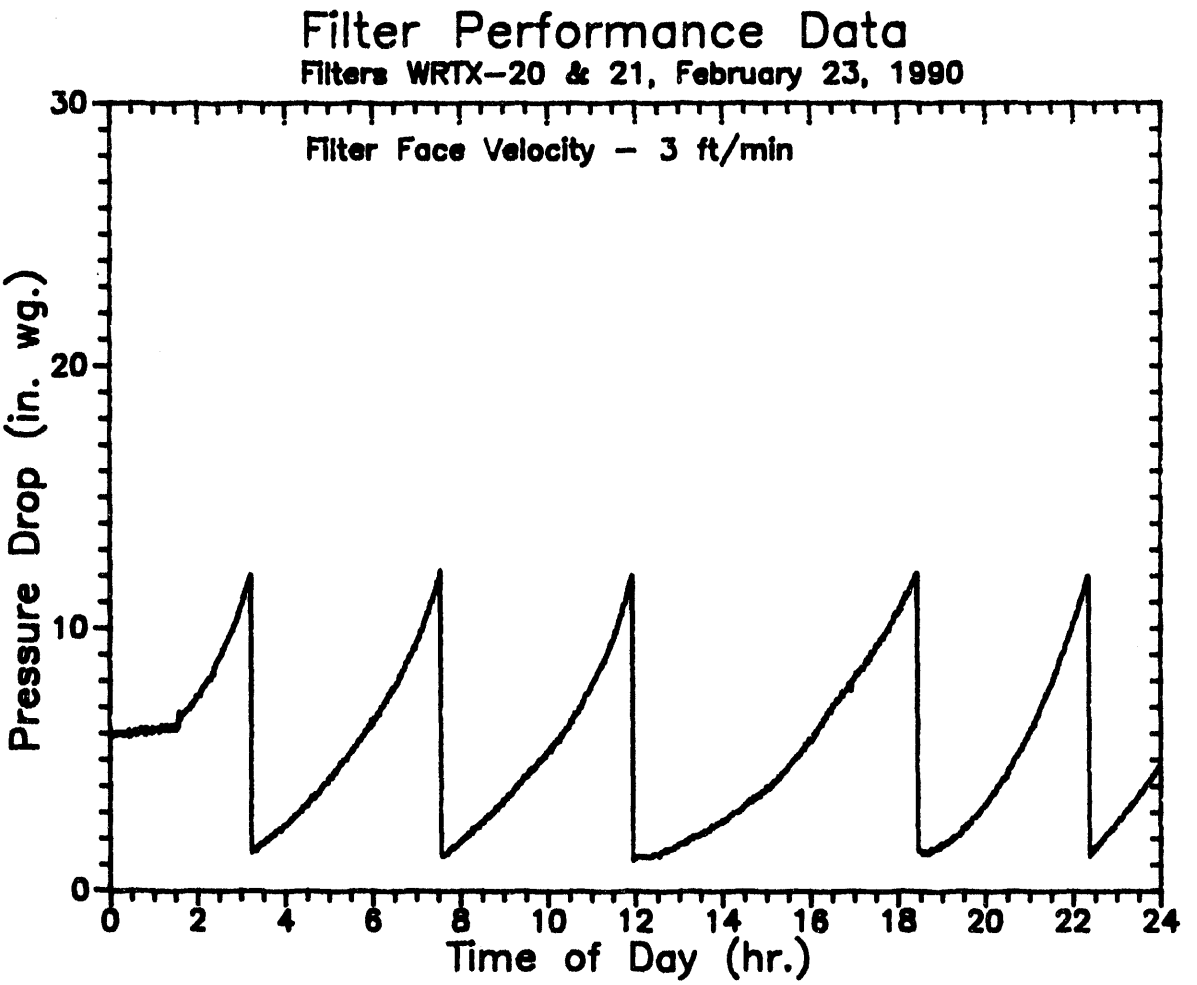

Operation Notes for February 23, 1990:

0130 Dust feed restarted

ΔP Trigger = 12.0" WC

Pulse Cleaning - 195 psig/0.1 sec

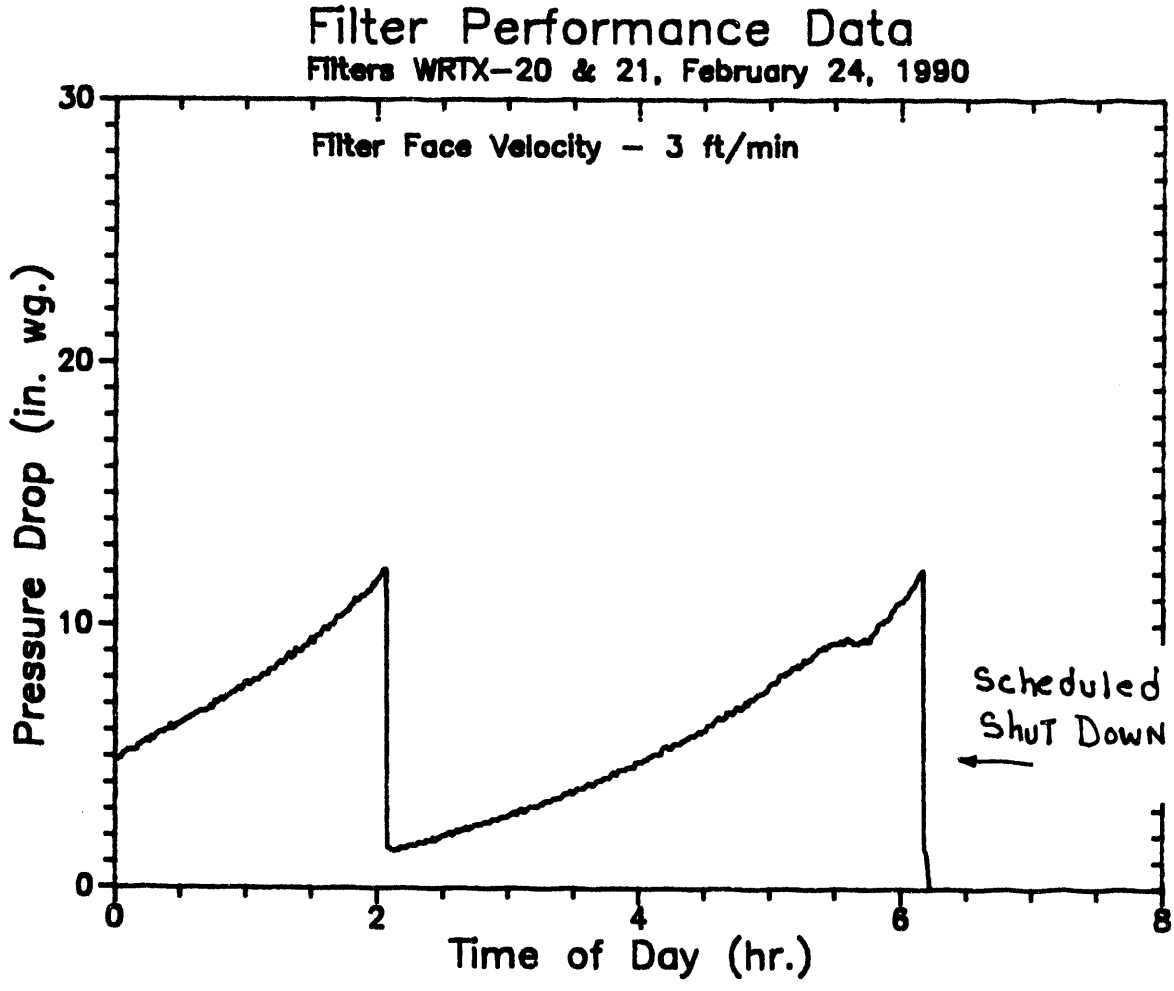

Operation Notes for February 24, 1990:

0615 End of week long test scheduled shut down

ΔP Trigger = 12.0" WC

Pulse Cleaning - 195 psig/0.1 sec

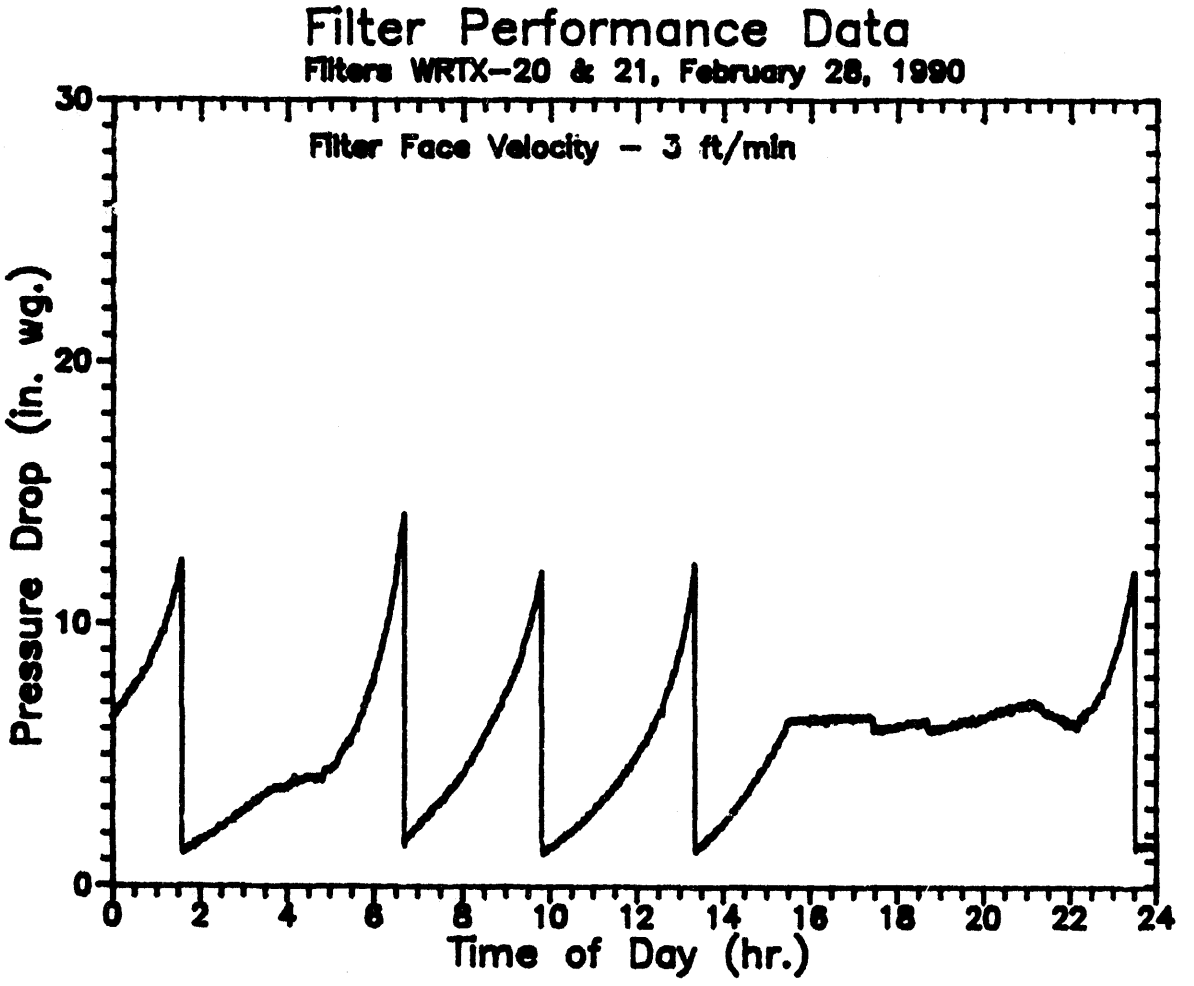

Operation Notes for February 28, 1990:

0345 Loaded dust

1530 Dust Feed Motor Failure

2215 Restarted Dust Feed

ΔP Trigger = 12.0" WC

Pulse Cleaning - 200 psig/0.1 sec

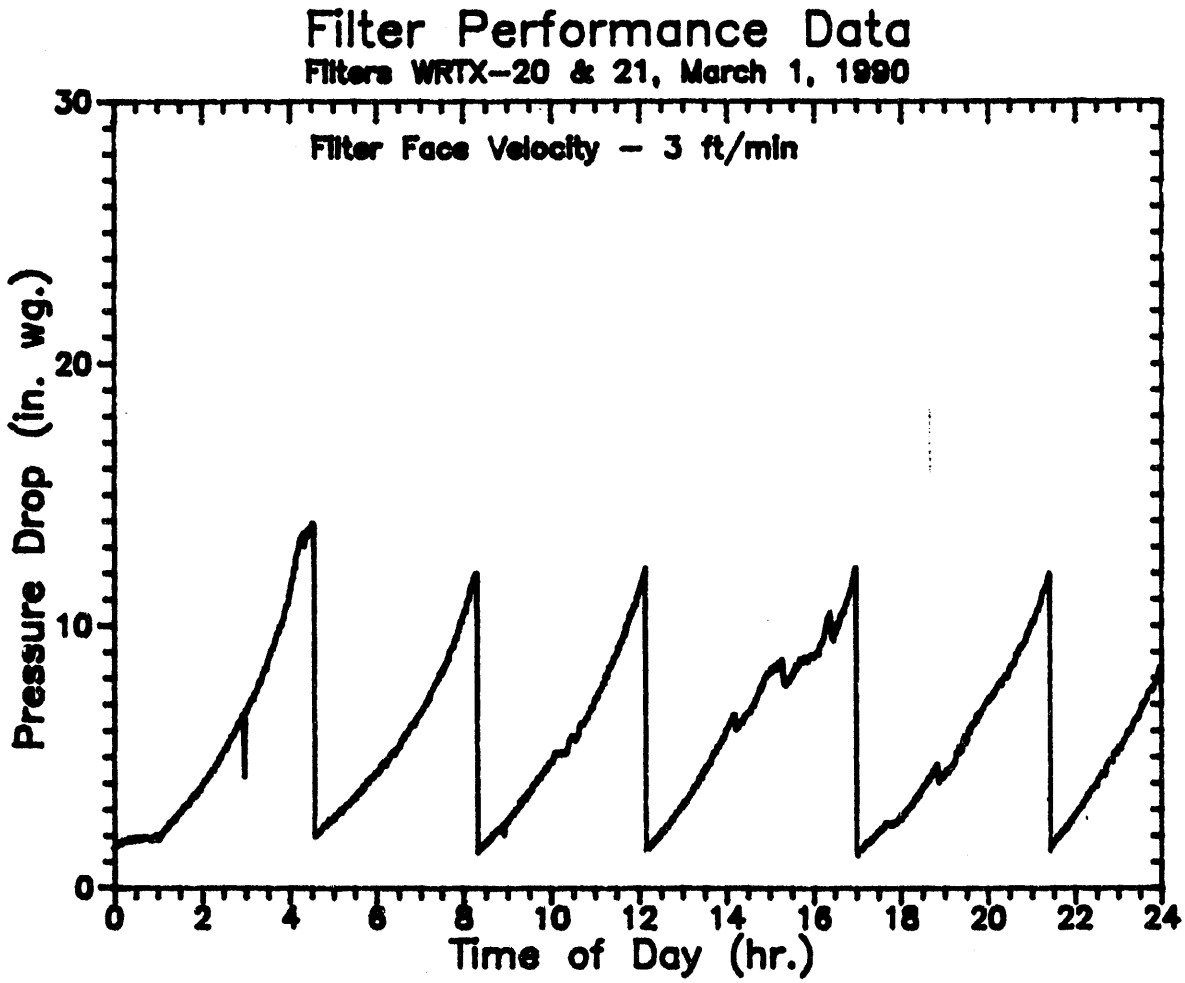

Operation Notes for March 1, 1990:

0000 Load Dust

1400-1900 Pressure fluctuations

ΔP Trigger = 12.0" WC

Pulse Cleaning - 200 psig/0.1 sec

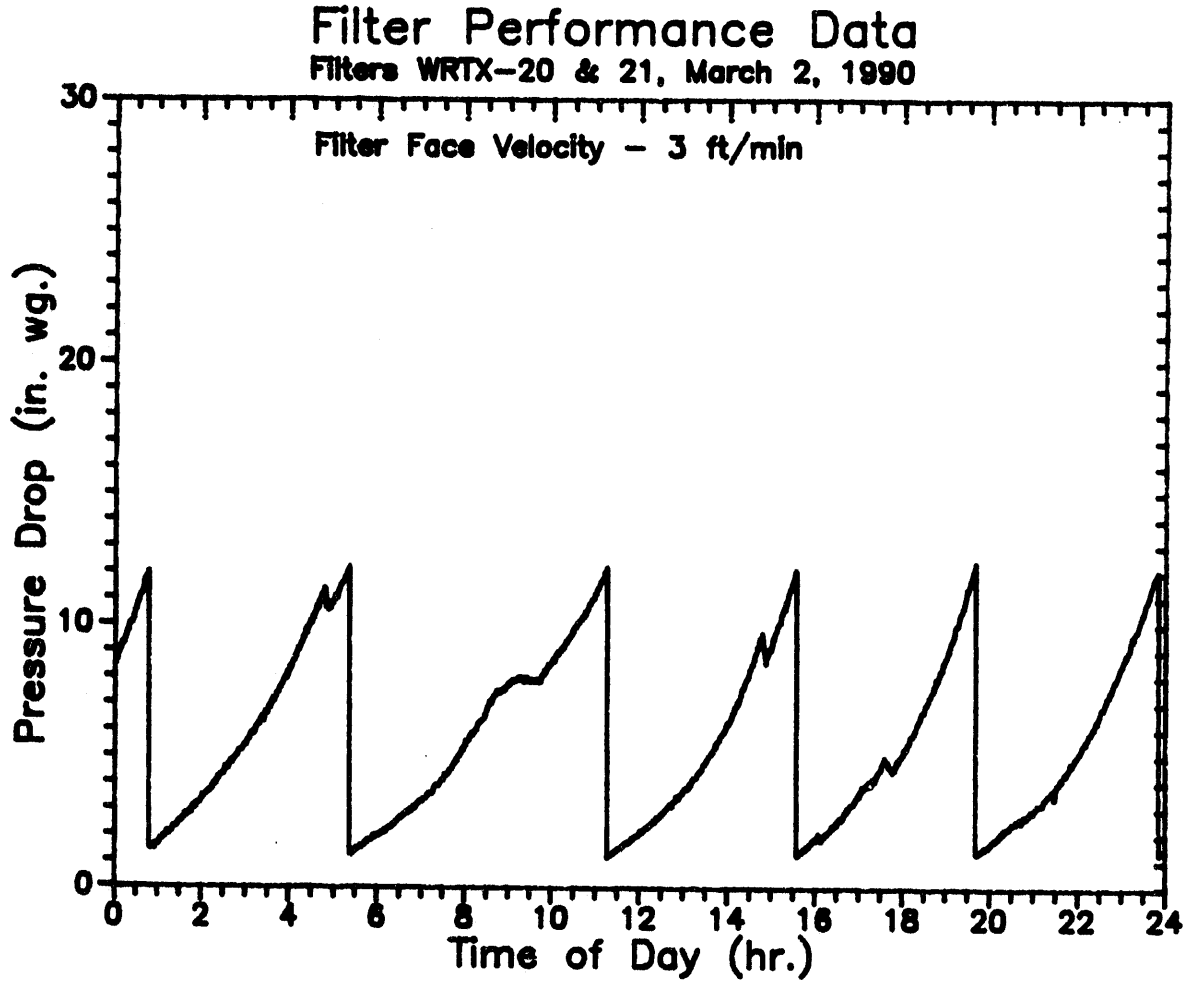

Operation Notes for March 2, 1990:

0900 Dust loaded

ΔP Trigger = 12.0" WC

Pulse Cleaning - 200 psig/0.1 sec

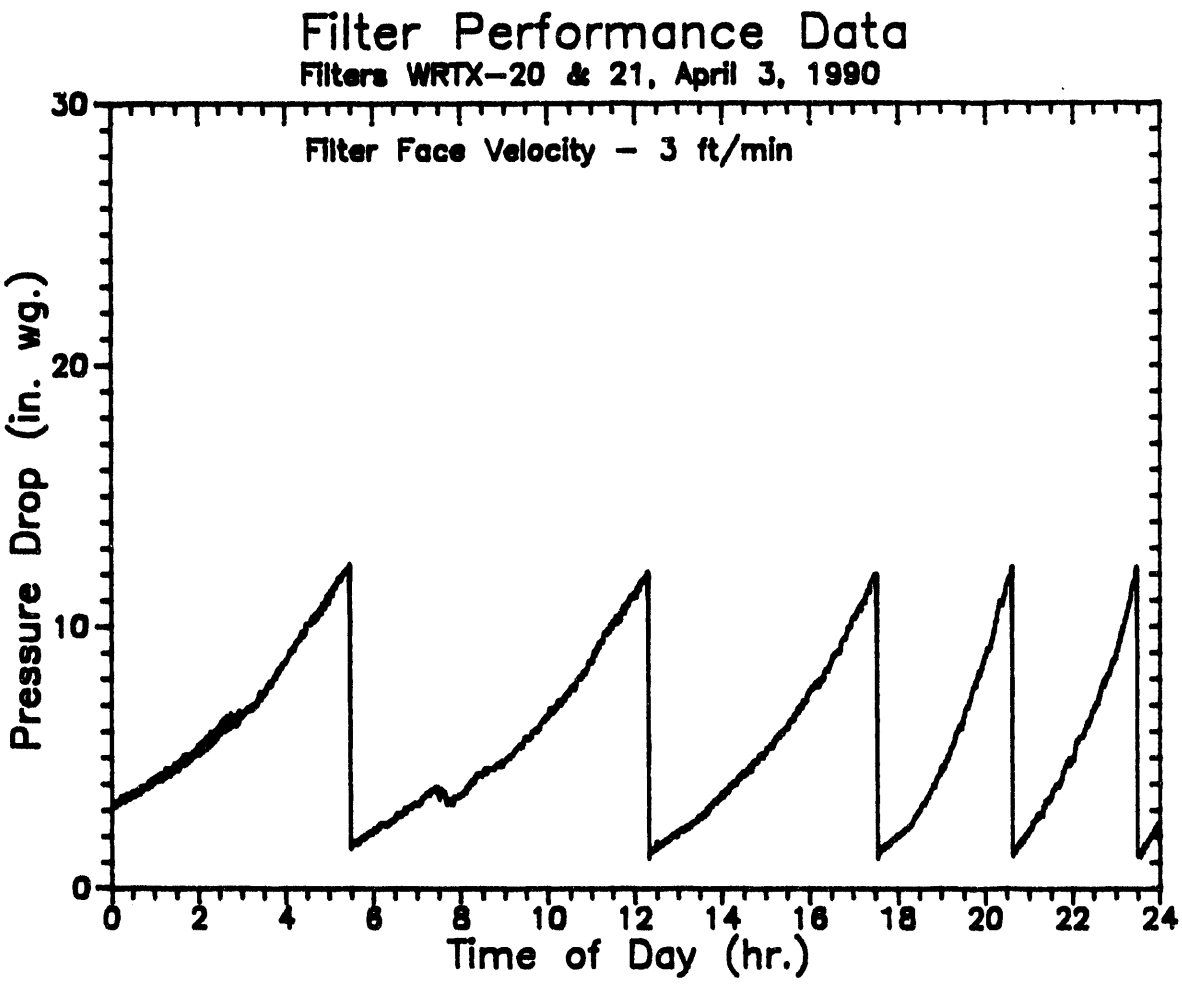

Operation Notes for April 3, 1990:

ΔP Trigger = 12" wc

Pulse Cleaning - 200 psig/0.1 sec

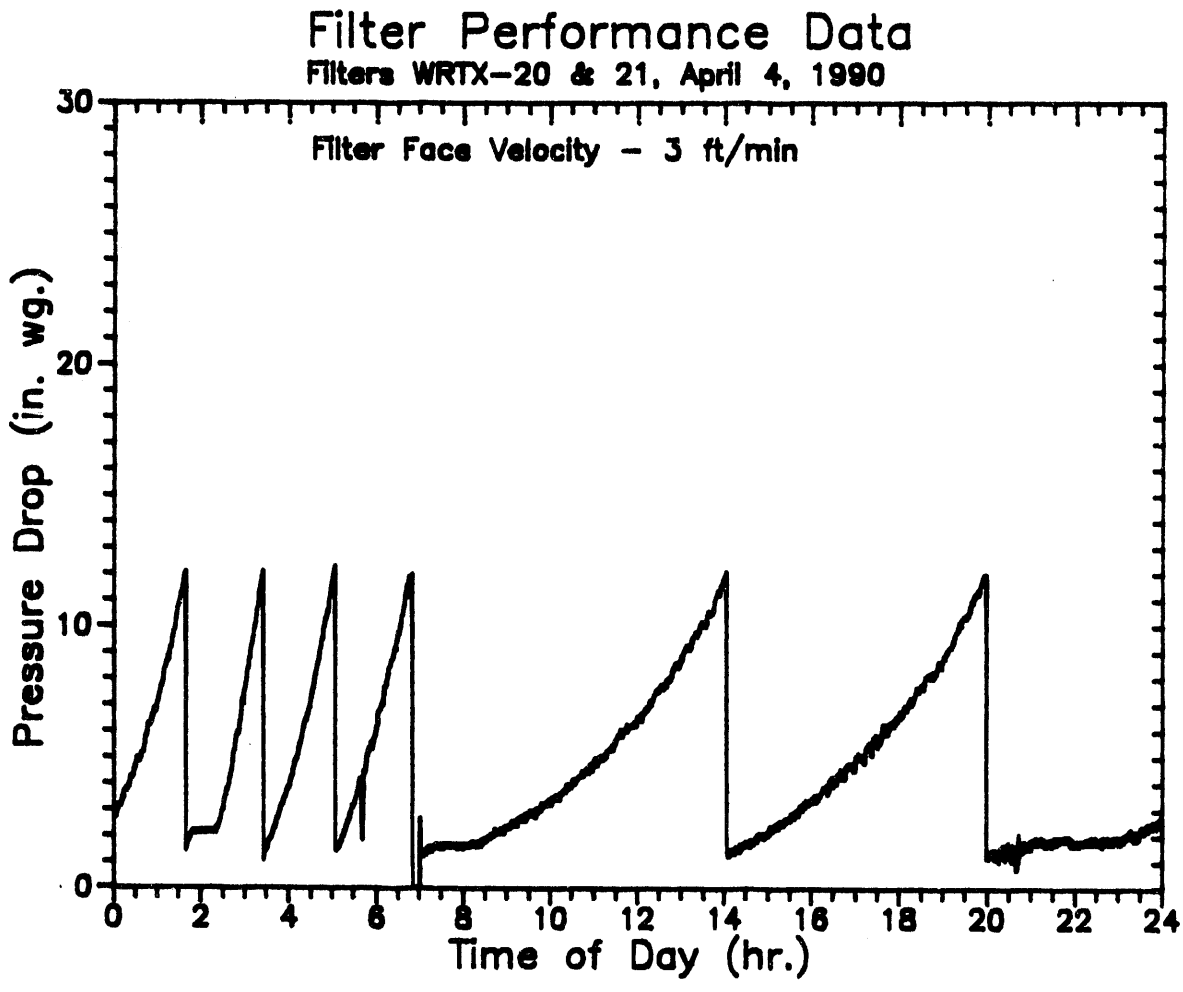

Operation Notes for April 4, 1990:

0700 Load Dust

2030 Dust feeder failed

ΔP Trigger = 12" wc

Pulse Cleaning - 200 psig/0.1 sec

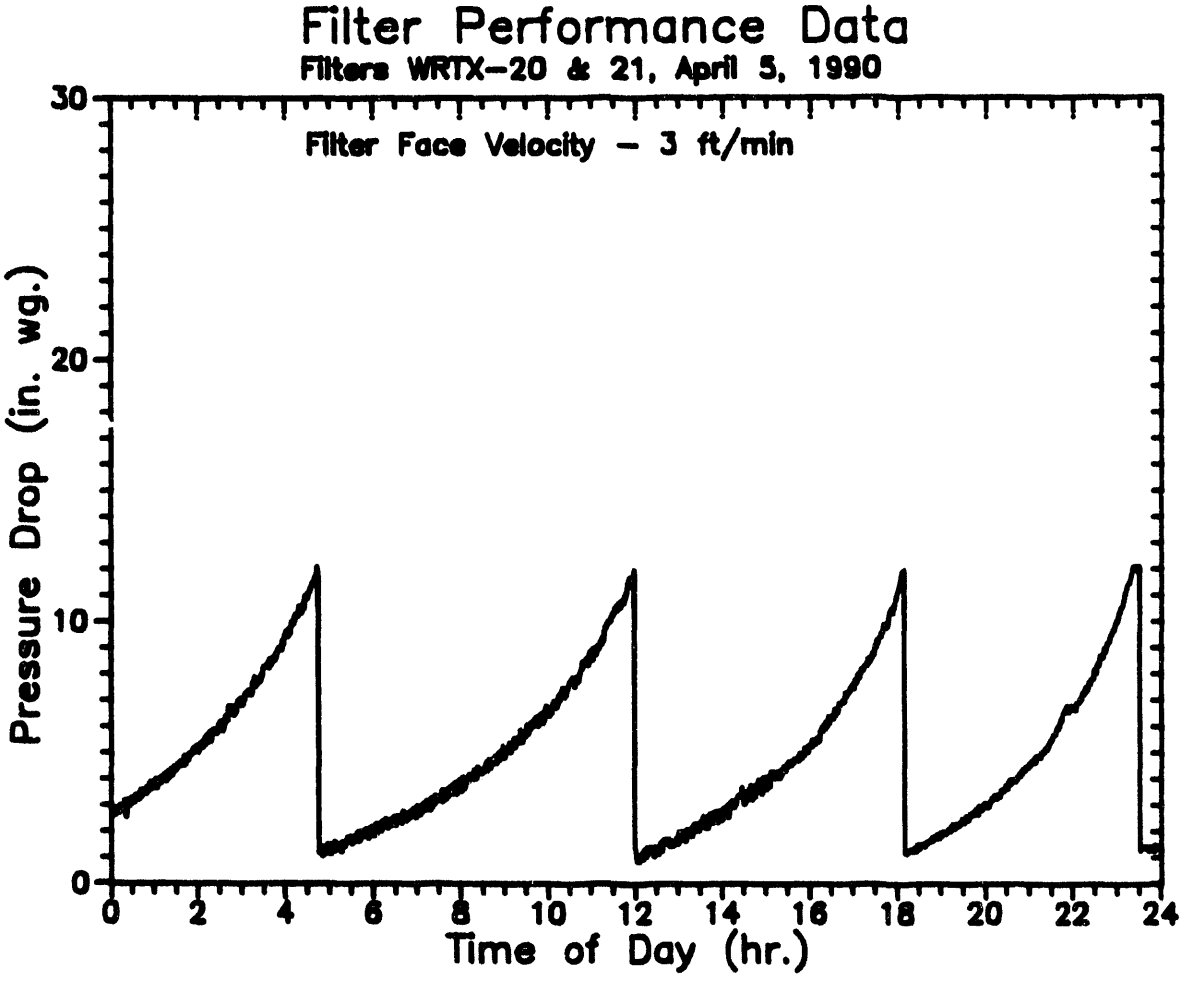

Operation Notes for April 5, 1990

2153 Changed Process Gas make-up to N_2

ΔP Trigger = 12" wc

Pulse Cleaning - 200 psig/0.1 sec

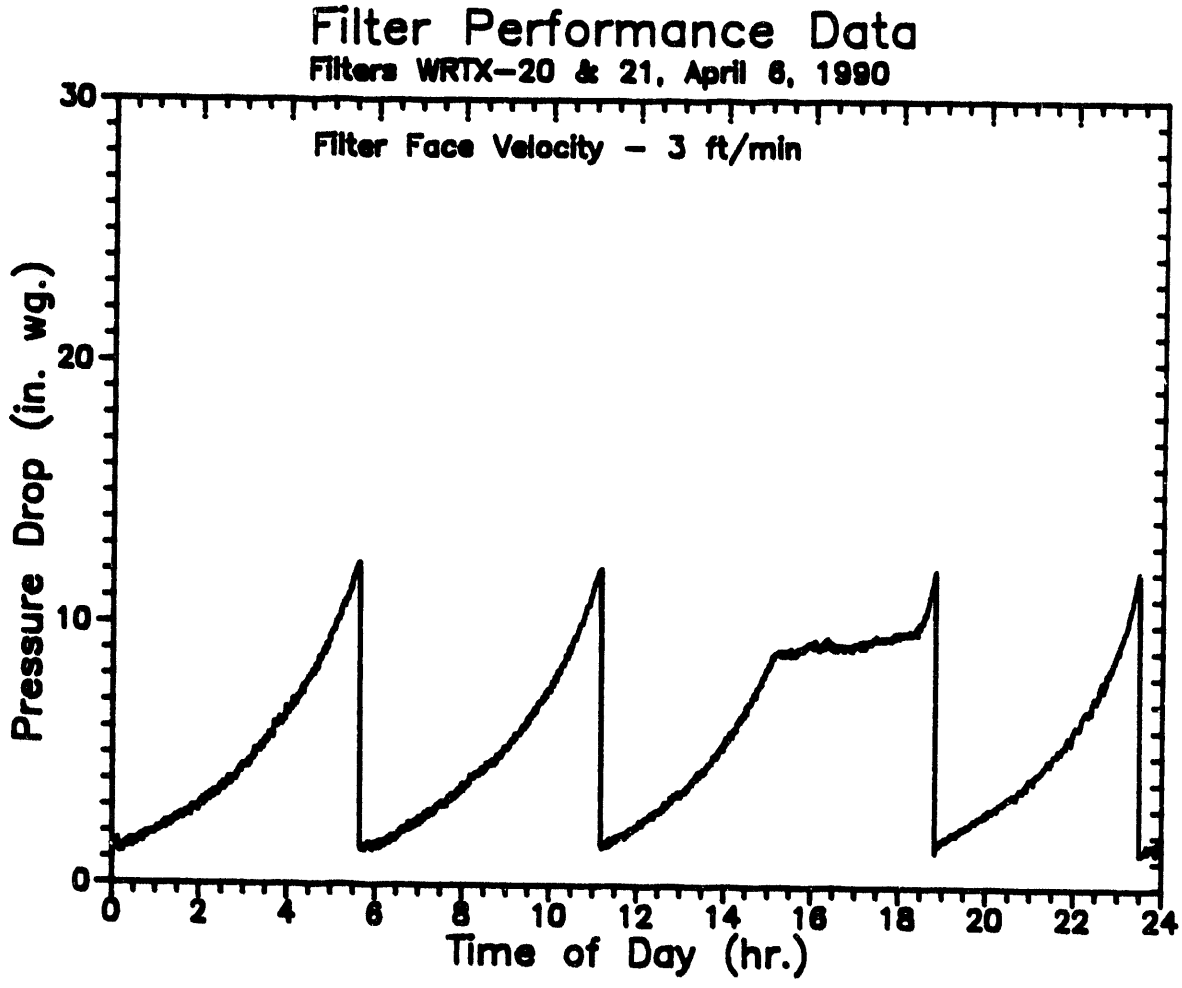

Operation Notes for April 6, 1990:

1500 Load dust

ΔP Trigger = 12" wc

Pulse Cleaning - 200 psig/0.1 sec

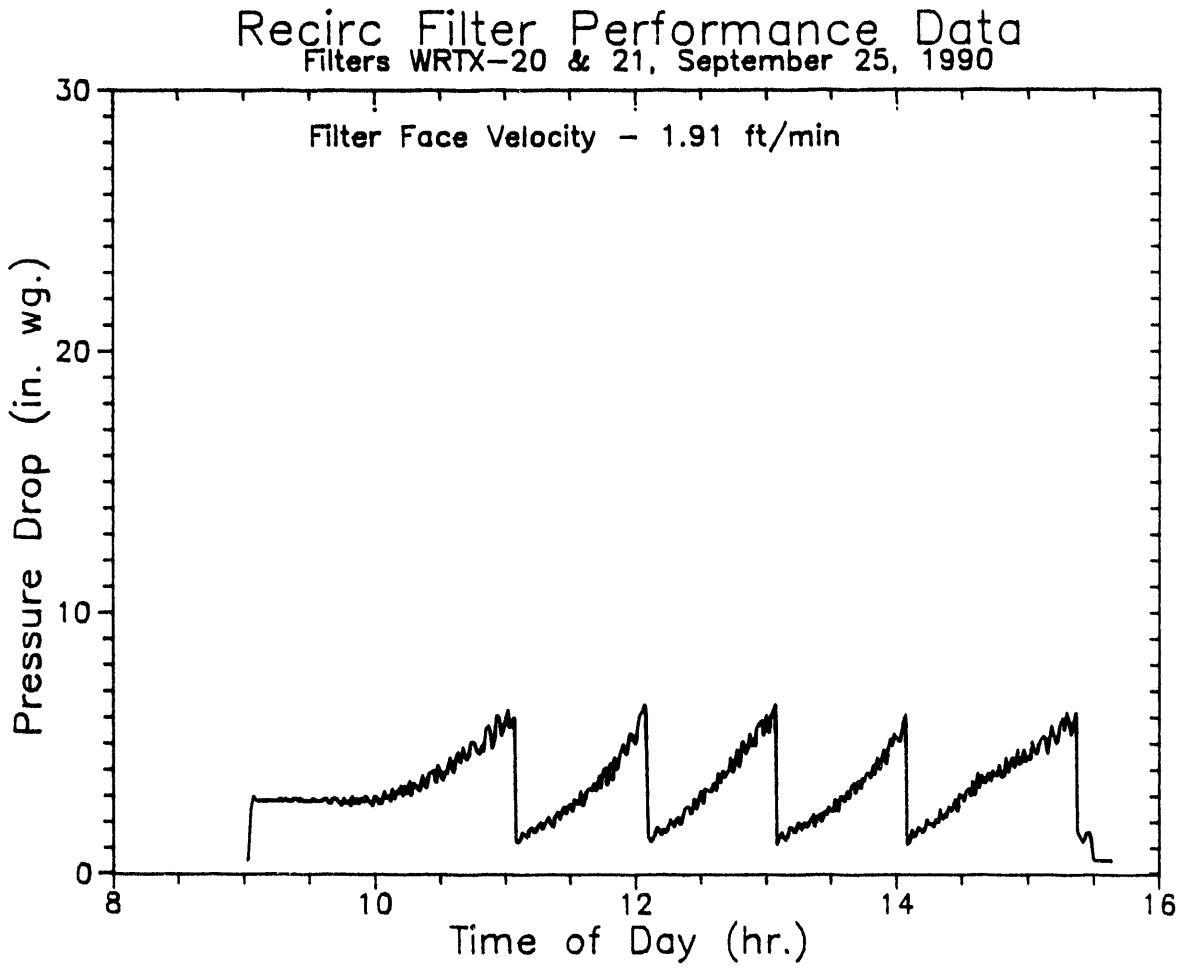

Operation Notes for September 24, 1990:

8 hour test

ΔP Trigger = 6" wc

Pulse Cleaning - 300 psig/0.1 sec

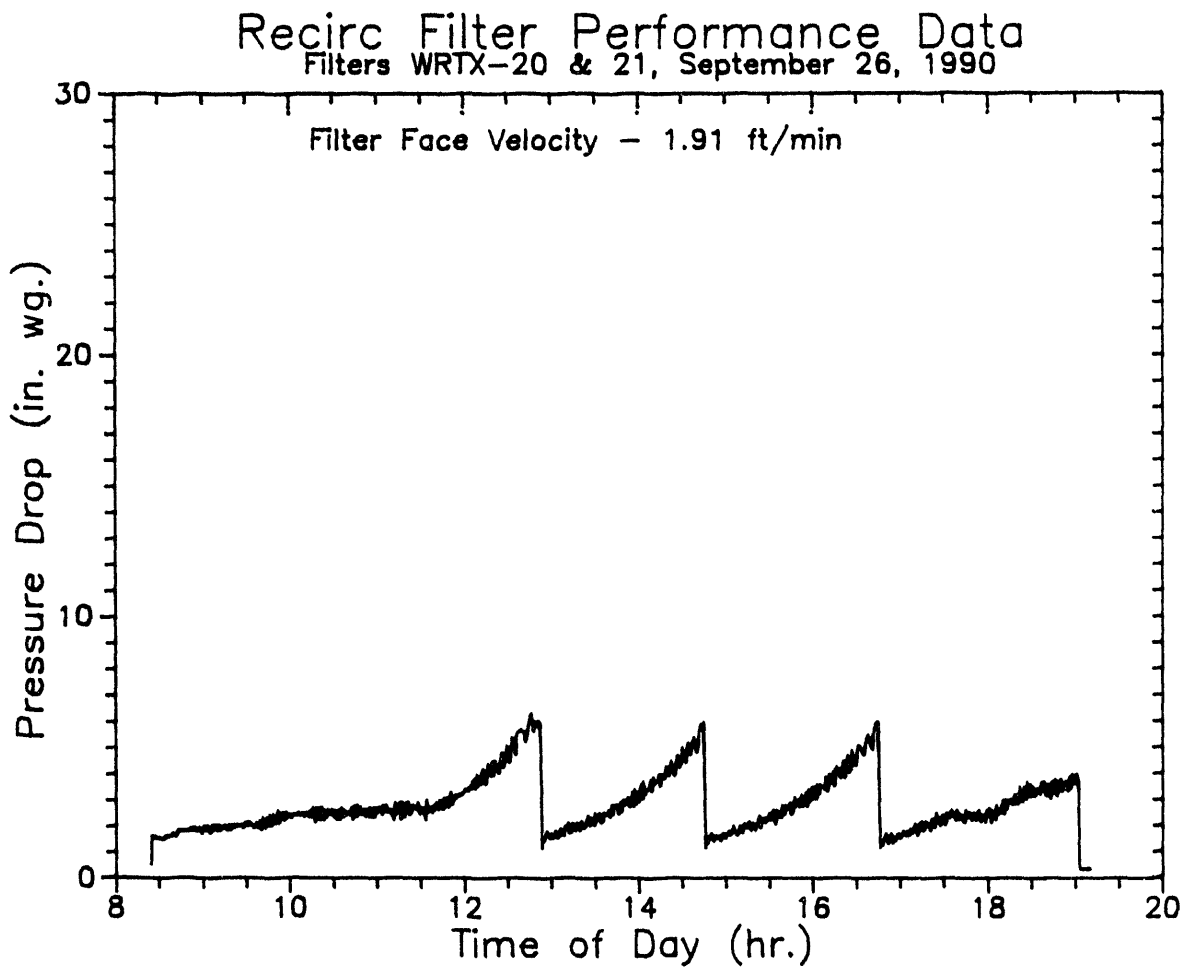

Operation Notes for September 26, 1990:

12 hour test

ΔP Trigger = 6" wc

Pulse Cleaning - 300 psig/0.1 sec

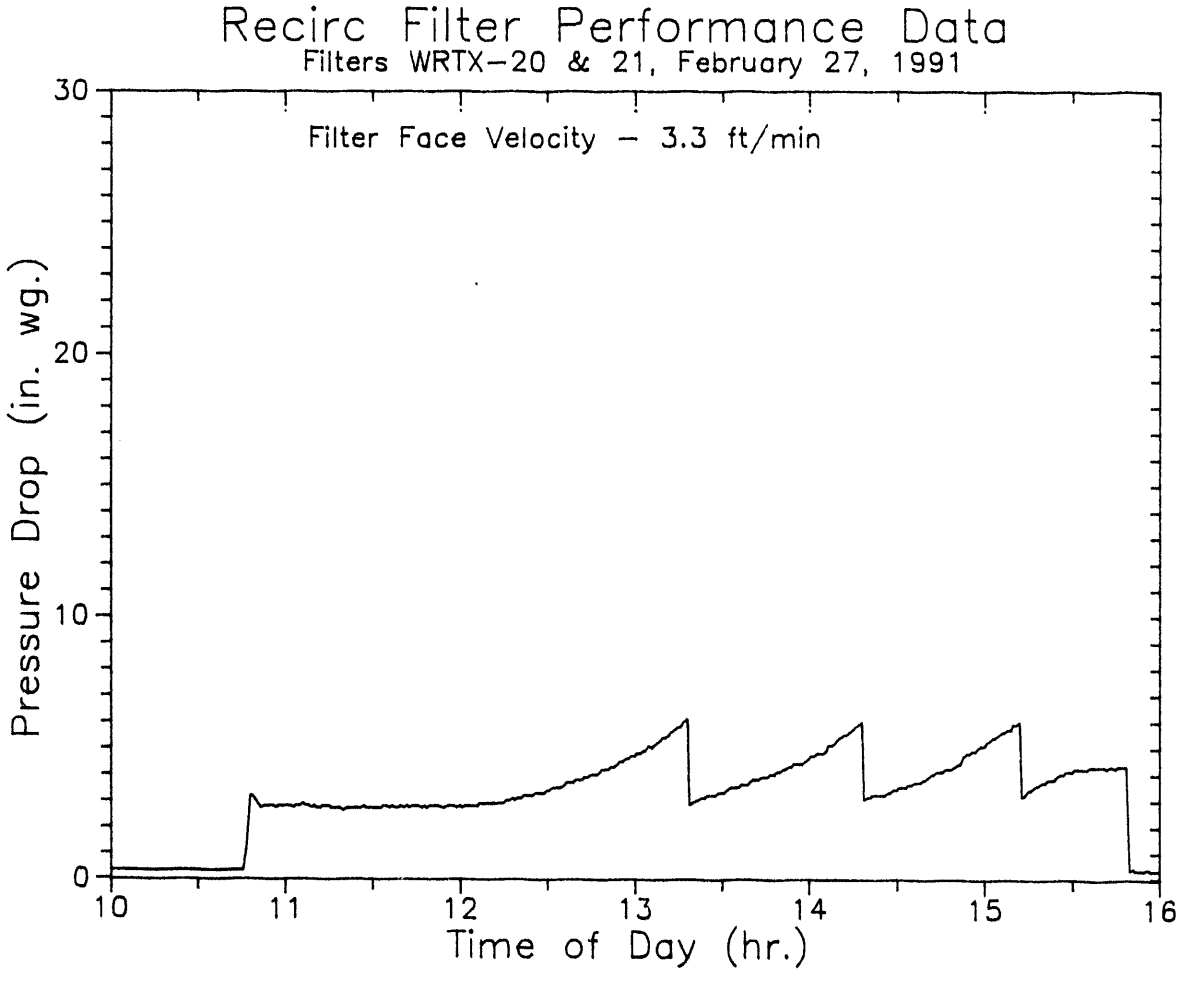

Operation Notes for February 27, 1991
1500 lb/hr. flow, 132 psig system pressure
Texaco char
delta-P Trigger = 6 in. wc
Pulse Cleaning - 300 psig/0.1 sec
1550 Scheduled Shutdown

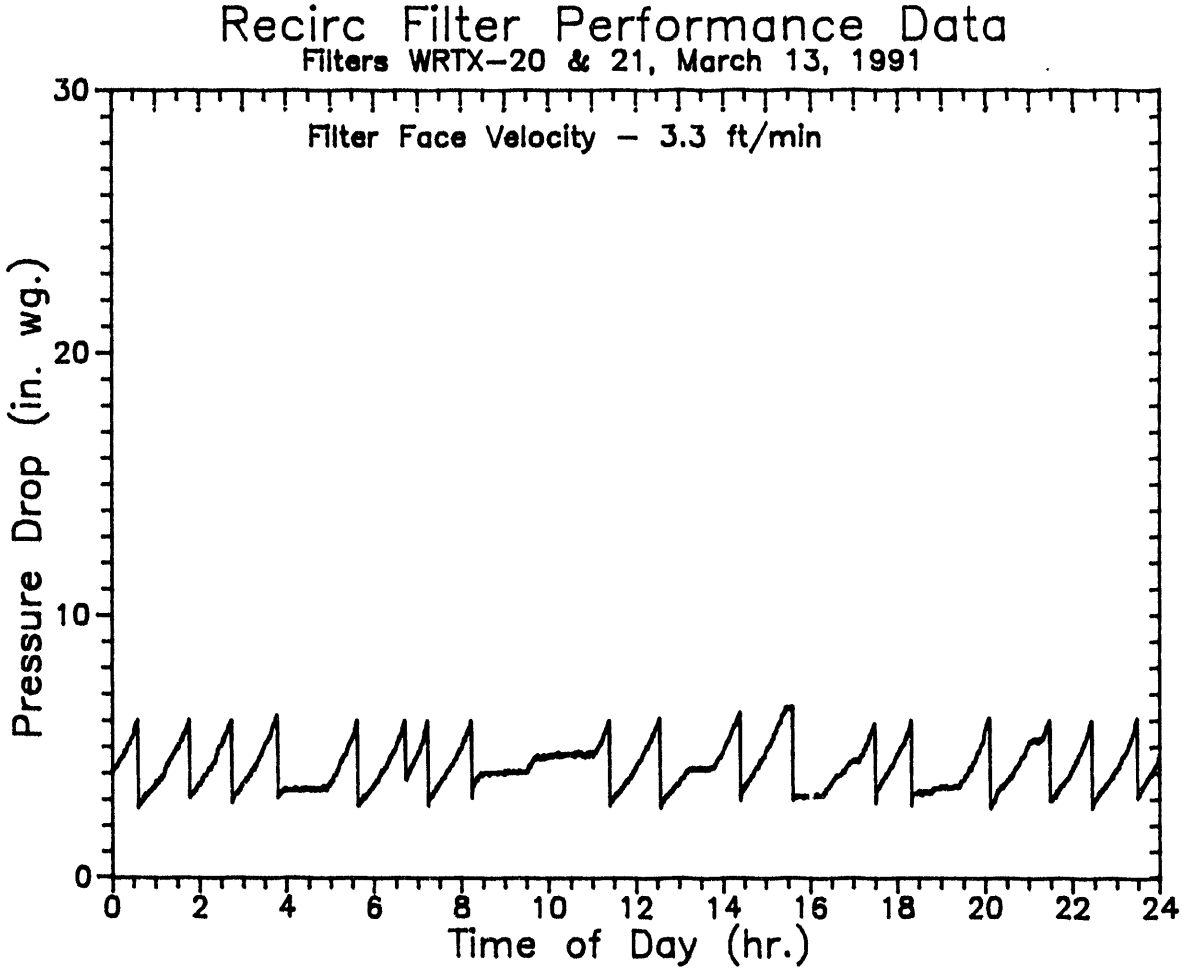

Operation Notes for March 13, 1991
delta-P Trigger = 6 in wc
Pulse Cleaning - 300 psig/0.1 sec
2127 Pulse Cleaning changed - 310 psig/0.1 sec
0430 - 0450 Char loaded
0940 - 1100 Char loaded
1850 - 1920 Char loaded

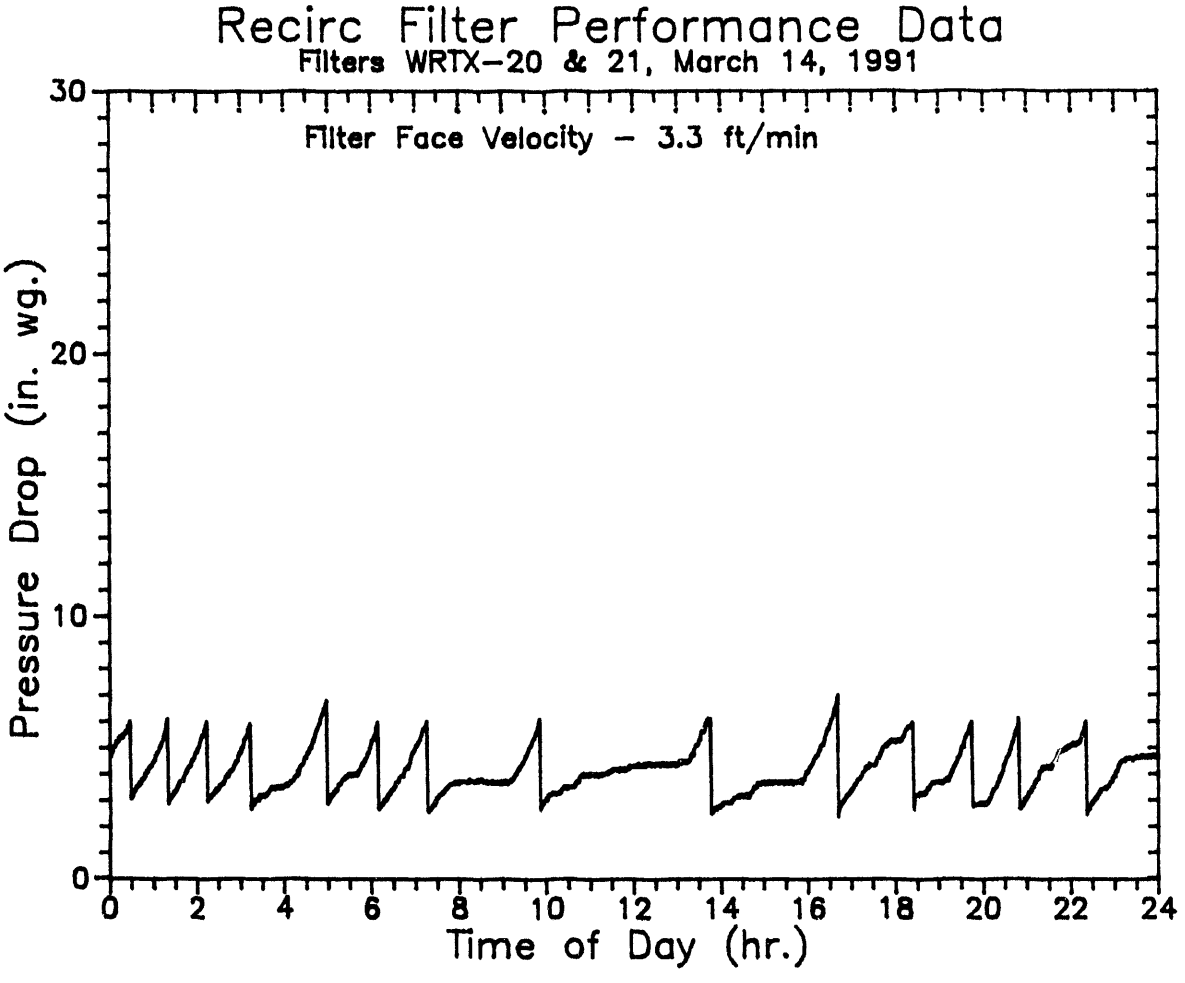

Operation Notes for March 14, 1991
delta-P Trigger = 6 in wc
Pulse Cleaning - 310 psig/0.1 sec
0340 - 0404 Char loaded
1236 - 1314 Char loaded

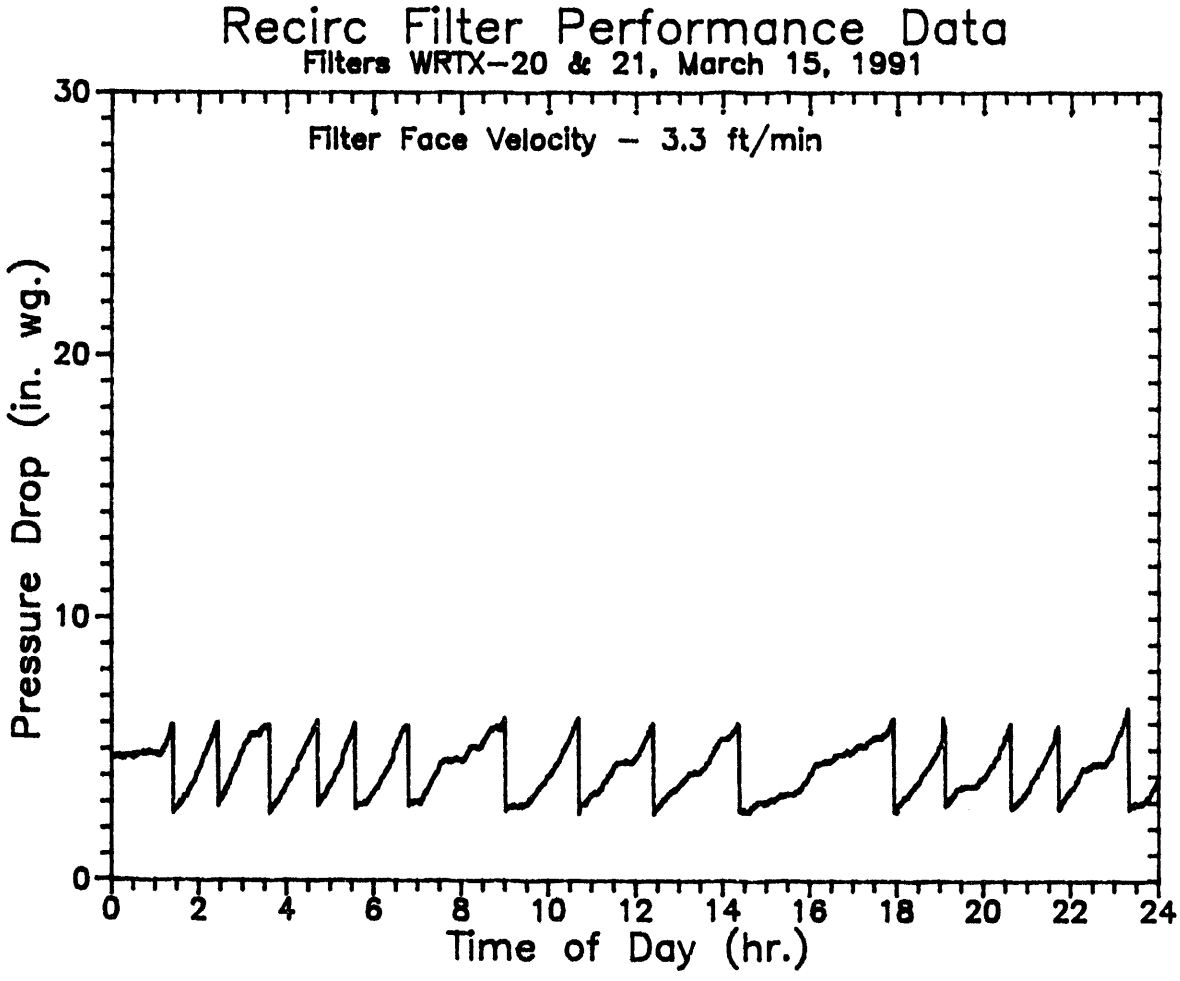

Operation Notes for March 15, 1991
delta-P Trigger = 6 in wc
Pulse Cleaning - 310 psig/0.1 sec
0022 - 0107 Char loaded
0900 - 0928 Char loaded
1722 - 1741 Char loaded

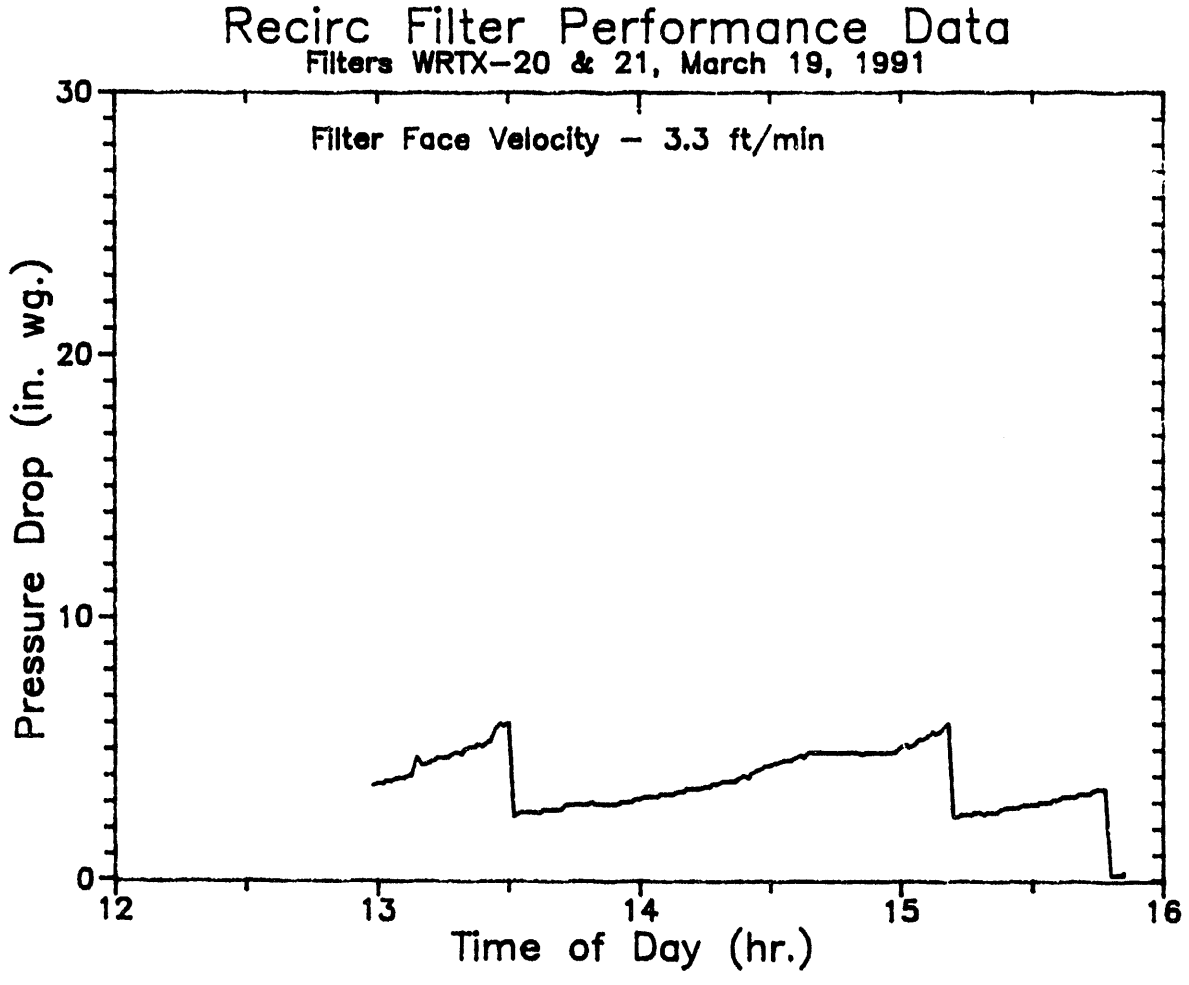

Operation Notes for March 19, 1991
delta-P Trigger = 6 in wc
Pulse Cleaning - 310 psig/0.1 sec

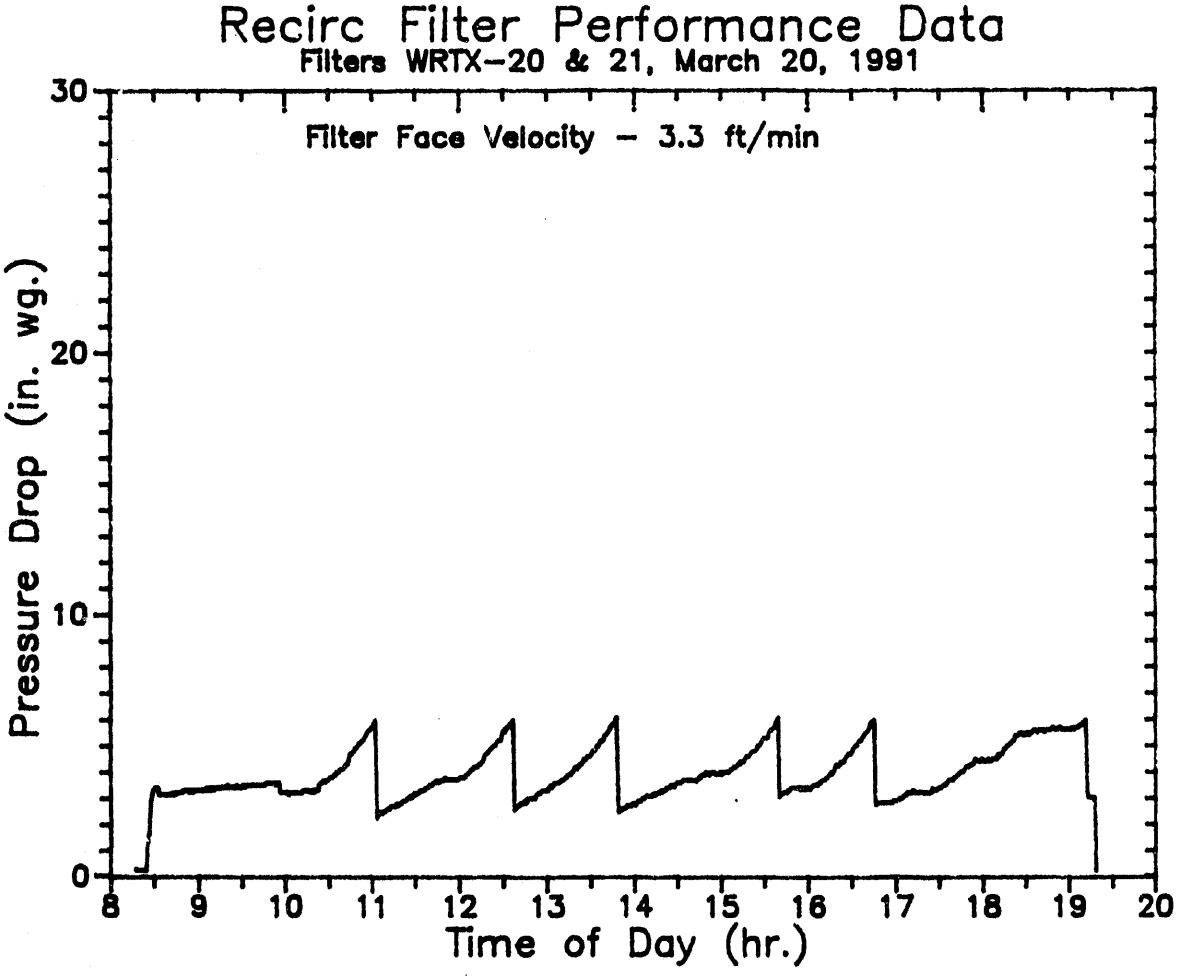

Operation Notes for March 20, 1991
delta-P Trigger = 6 in wc
Pulse Cleaning - 310 psig/0.1 sec
1839 - 1908 Char loaded

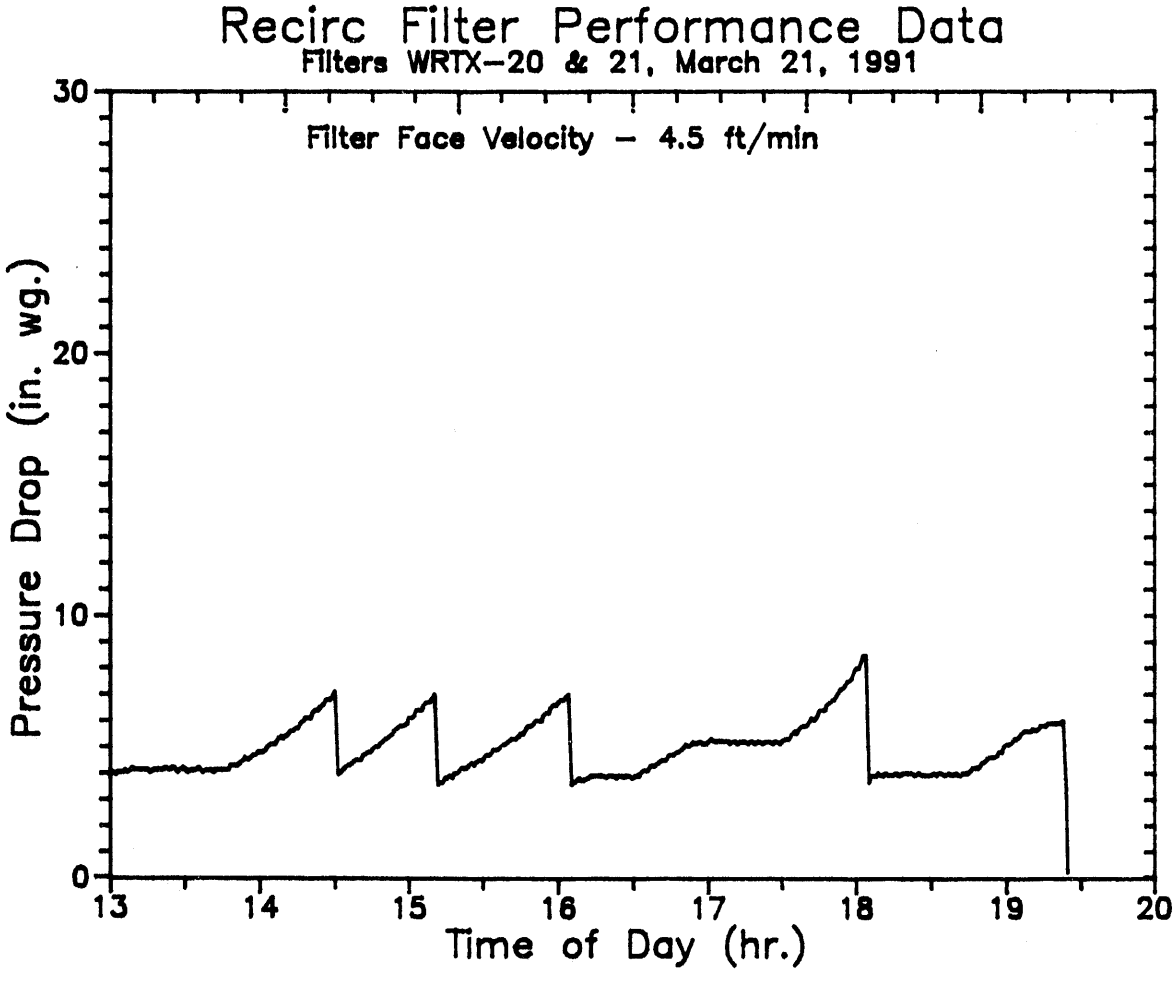

Operation Notes for March 21, 1991
4.5 ft/min face velocity
delta-P Trigger = 7 in wc
Pulse Cleaning - 170 psig/0.1 sec

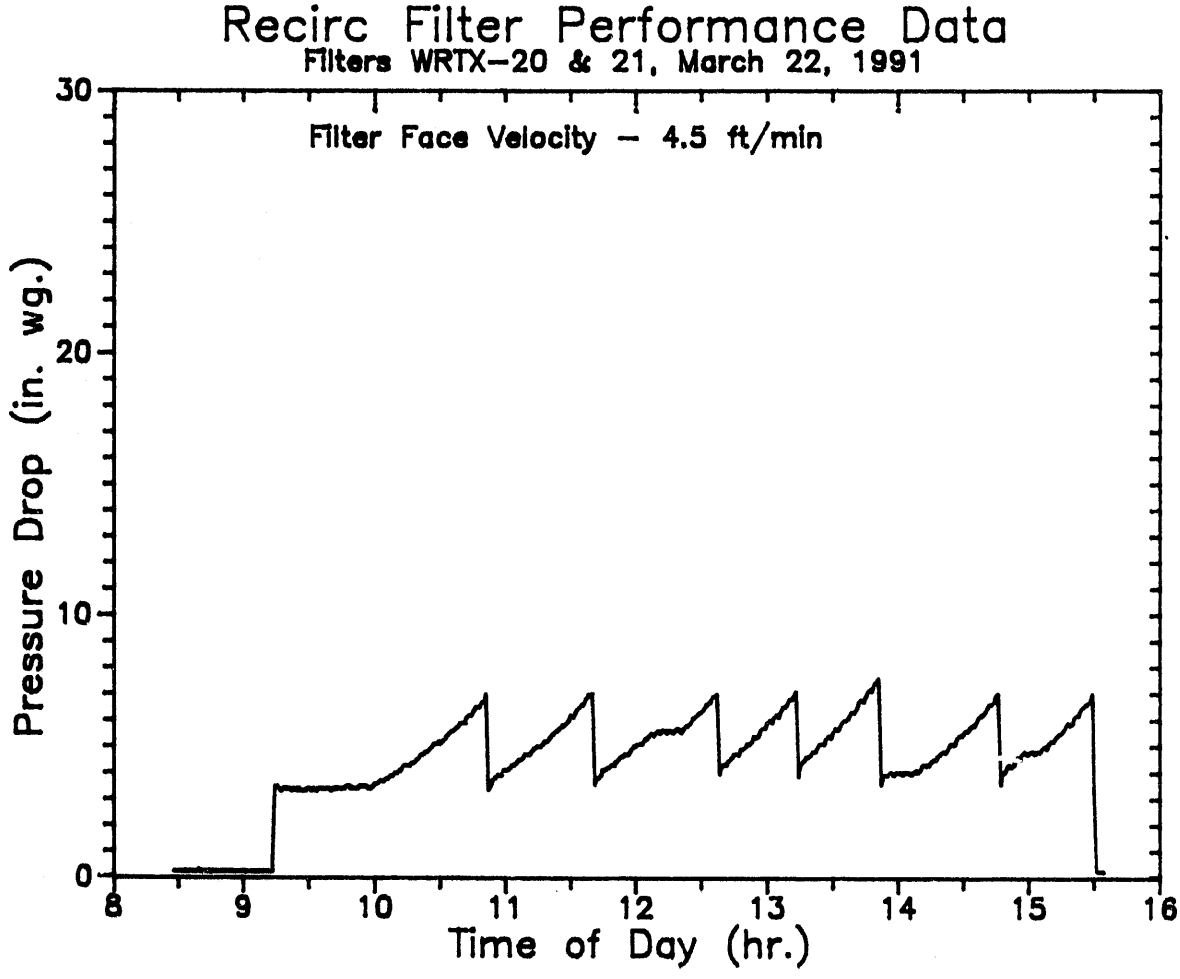

Operation Notes for March 22, 1991
delta-P Trigger = 7 in wc
Pulse Cleaning - 170 psig/0.1 sec

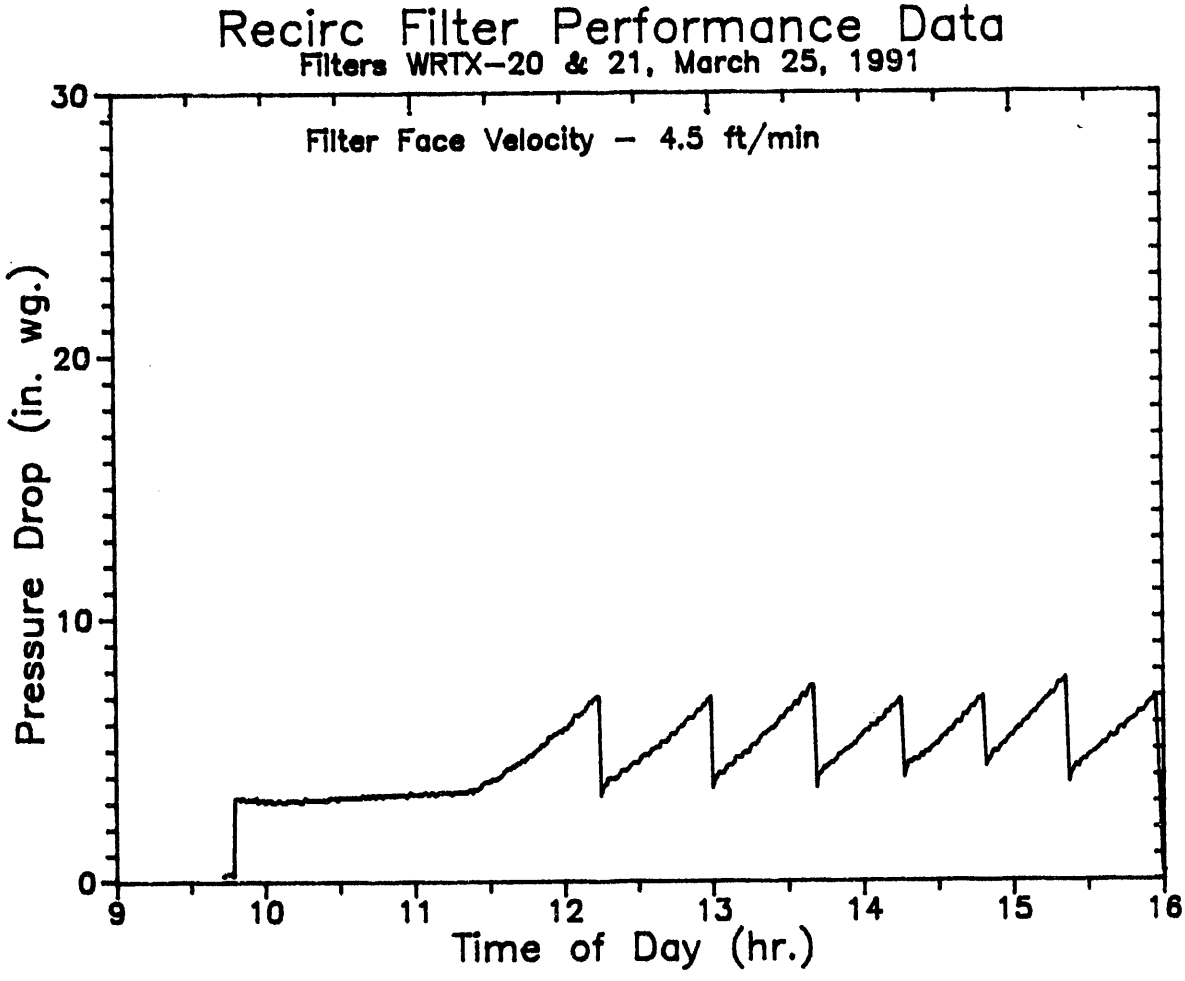

Operation Notes for March 25, 1991
delta–P Trigger = 7 in wc
Pulse Cleaning – 170 psig/0.1 sec
1000 –1100 Char loaded

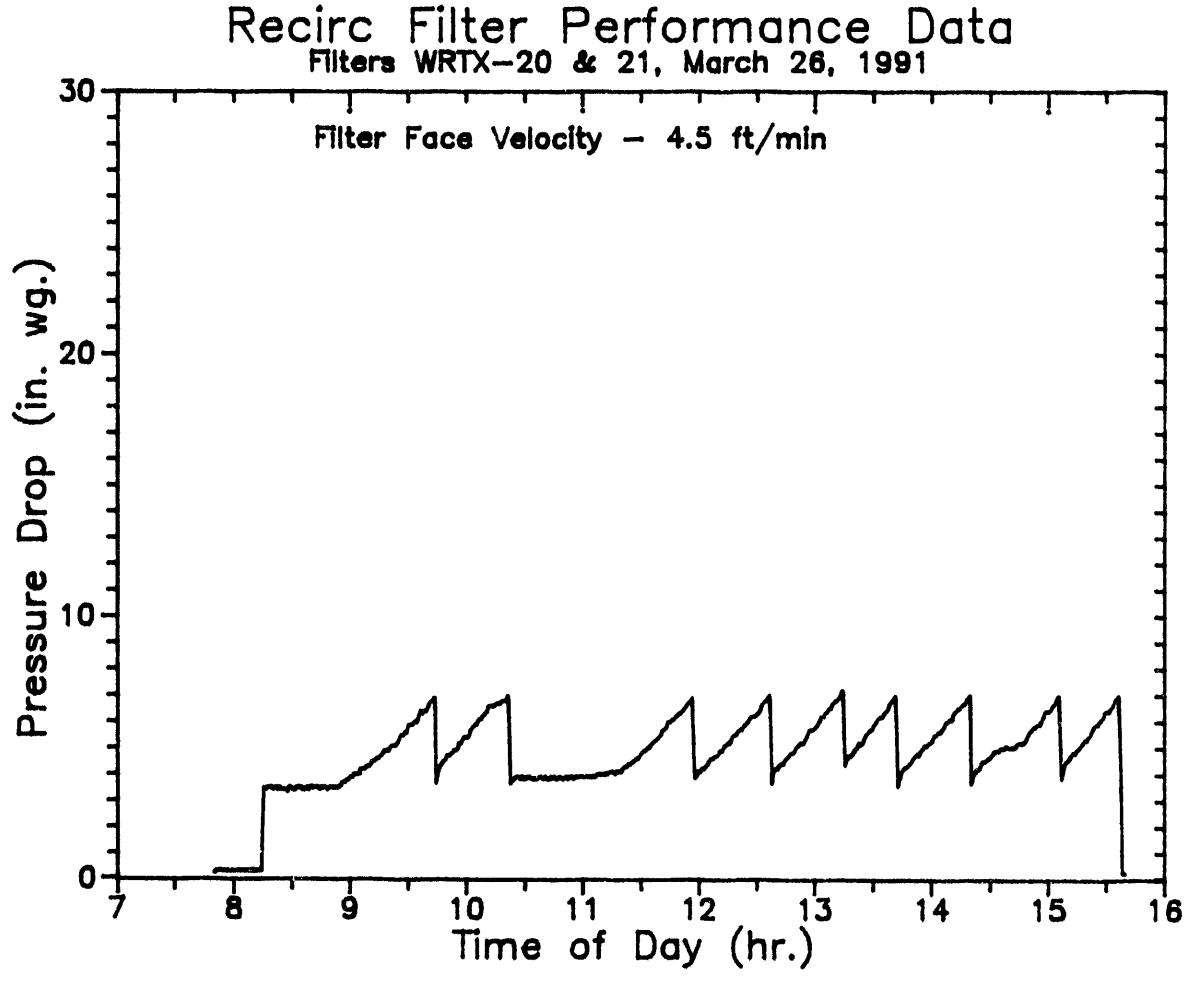

Operation Notes for March 26, 1991
delta-P Trigger = 7 in wc
Pulse Cleaning - 170 psig/0.1 sec
1018 -1115 Char loaded

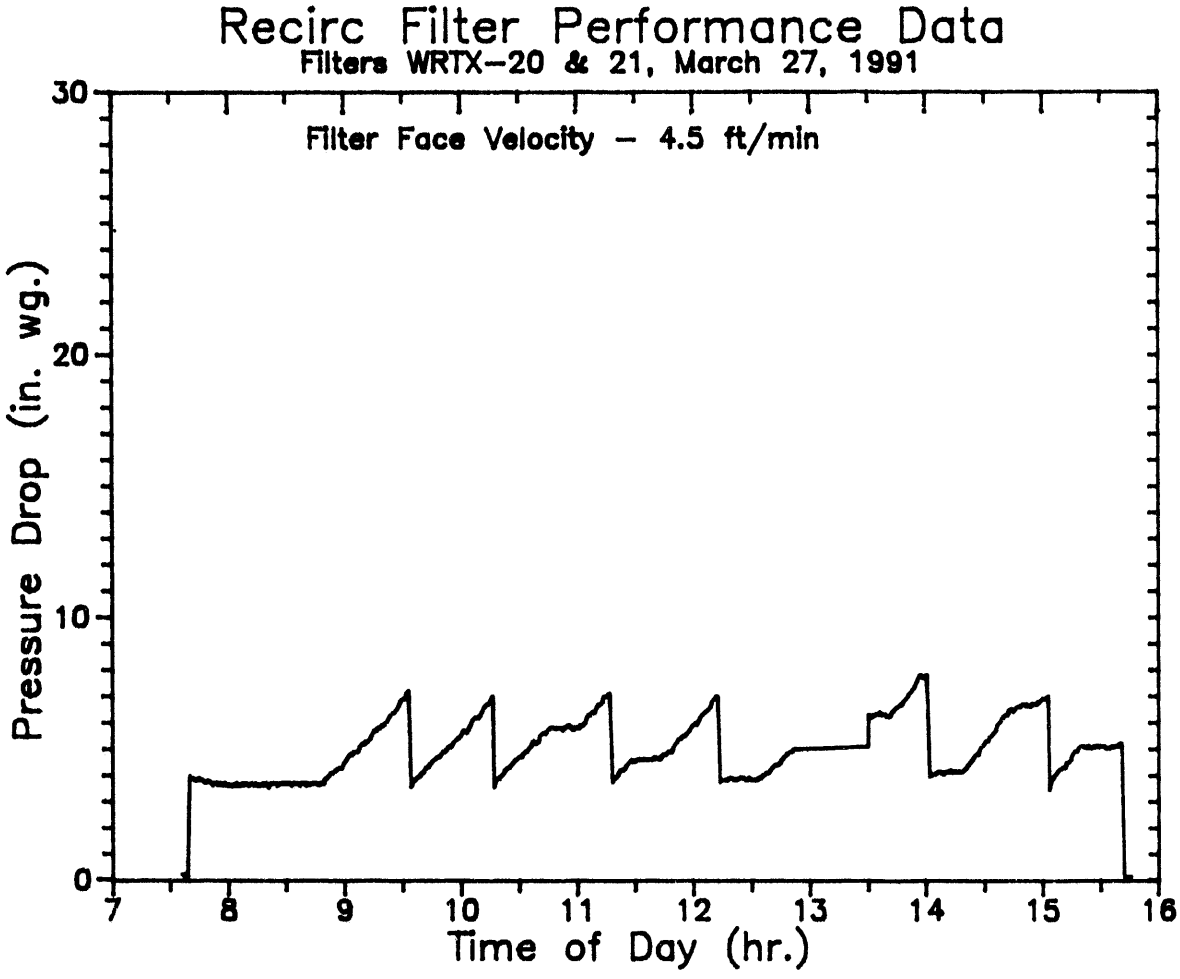

Operation Notes for March 27, 1991
delta-P Trigger = 7 in wc
Pulse Cleaning - 170 psig/0.1 sec
1245 - 1330 Char not feeding properly
1515 - 1538 Char not feeding properly

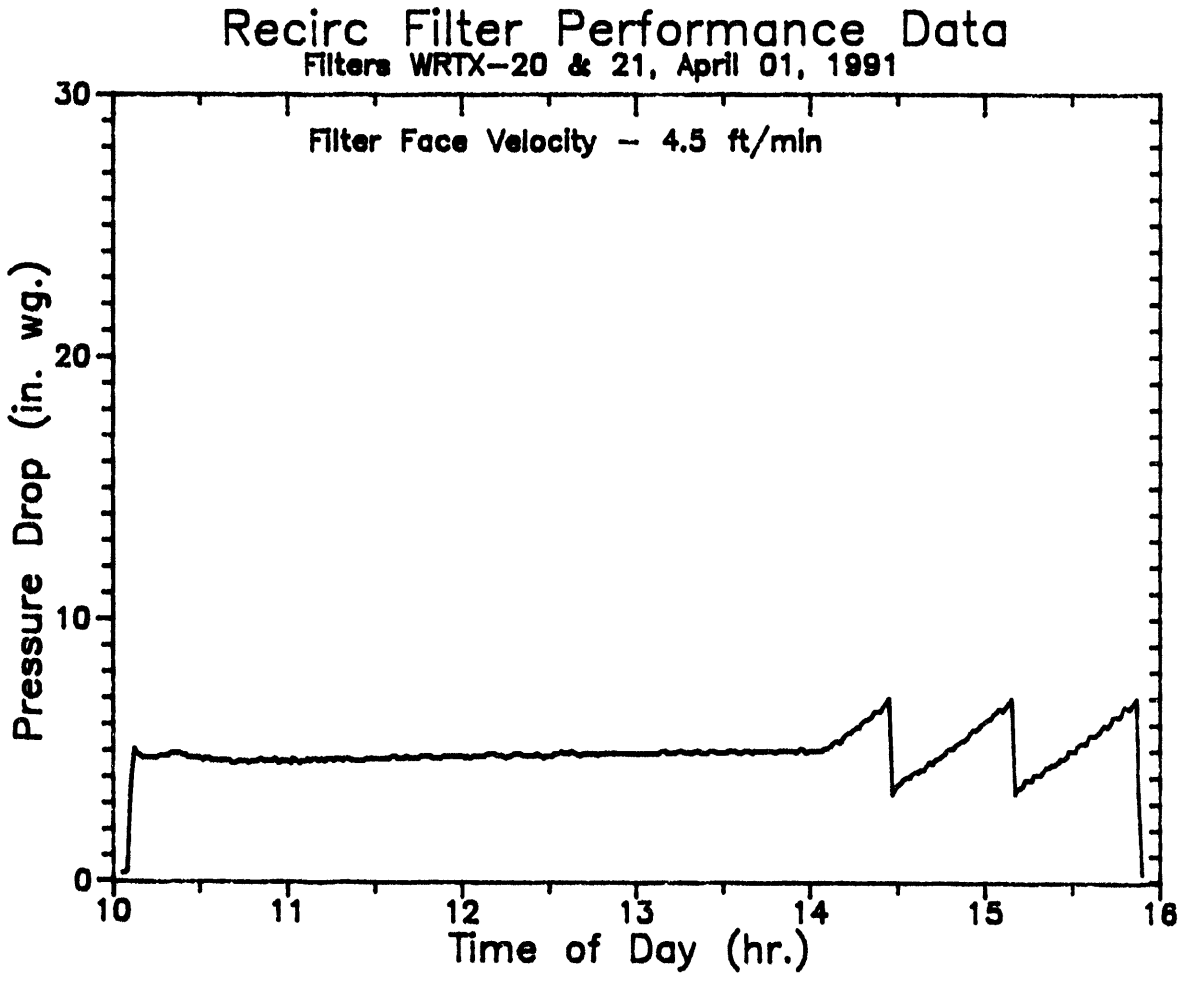

Operation Notes for April 01, 1991
delta–P Trigger = 7 in wc
Pulse Cleaning – 170 psig/0.1 sec
0800 –1400 Char loaded and system to pressure and temperature

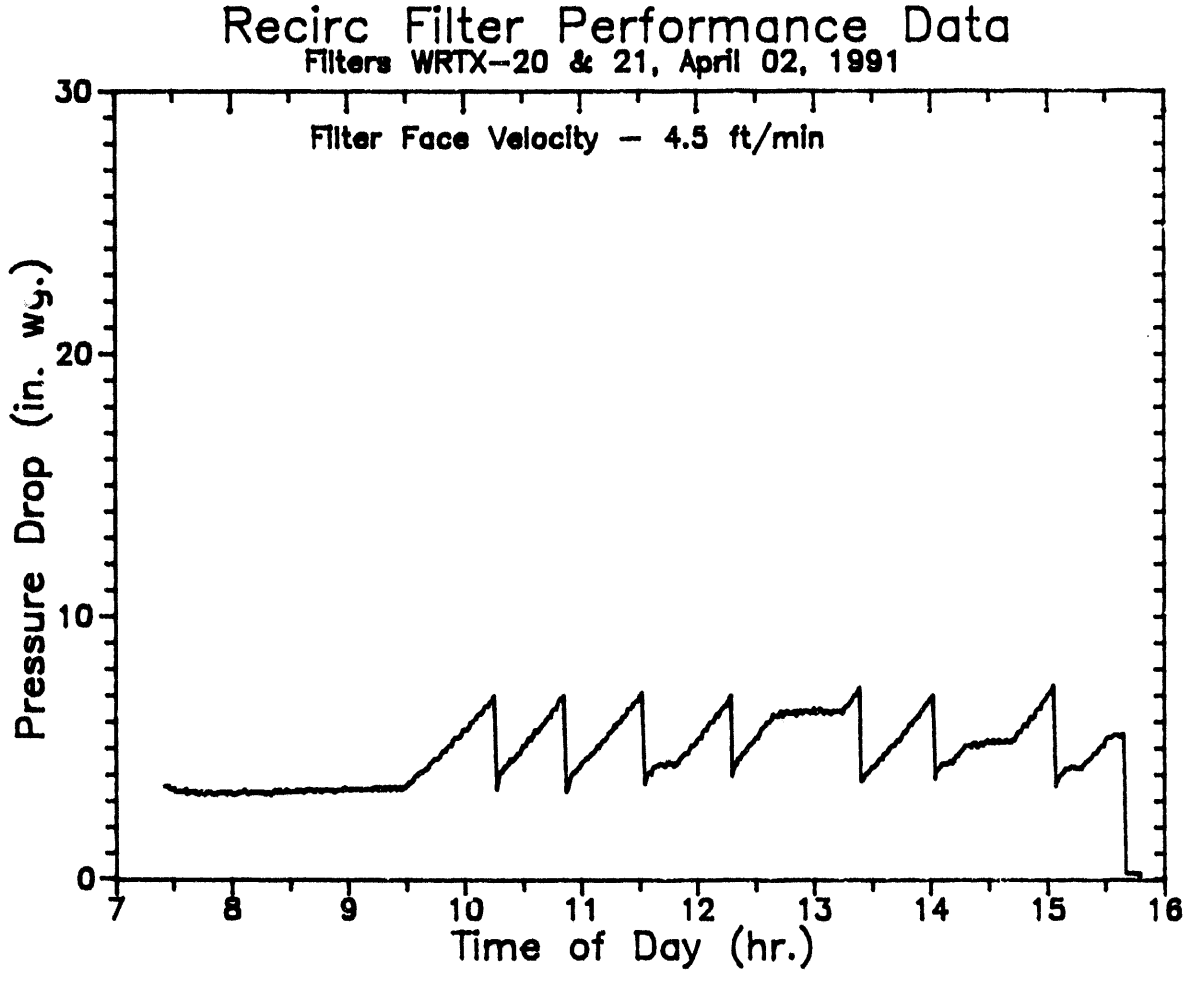

Operation Notes for April 02, 1991
delta-P Trigger = 7 in wc
Pulse Cleaning - 170 psig/0.1 sec
0722 - 0925 system to temperature
1132 - 1149 Char not feeding properly
1245 - 1315 Char not feeding properly
1420 - 1445 Char not feeding properly

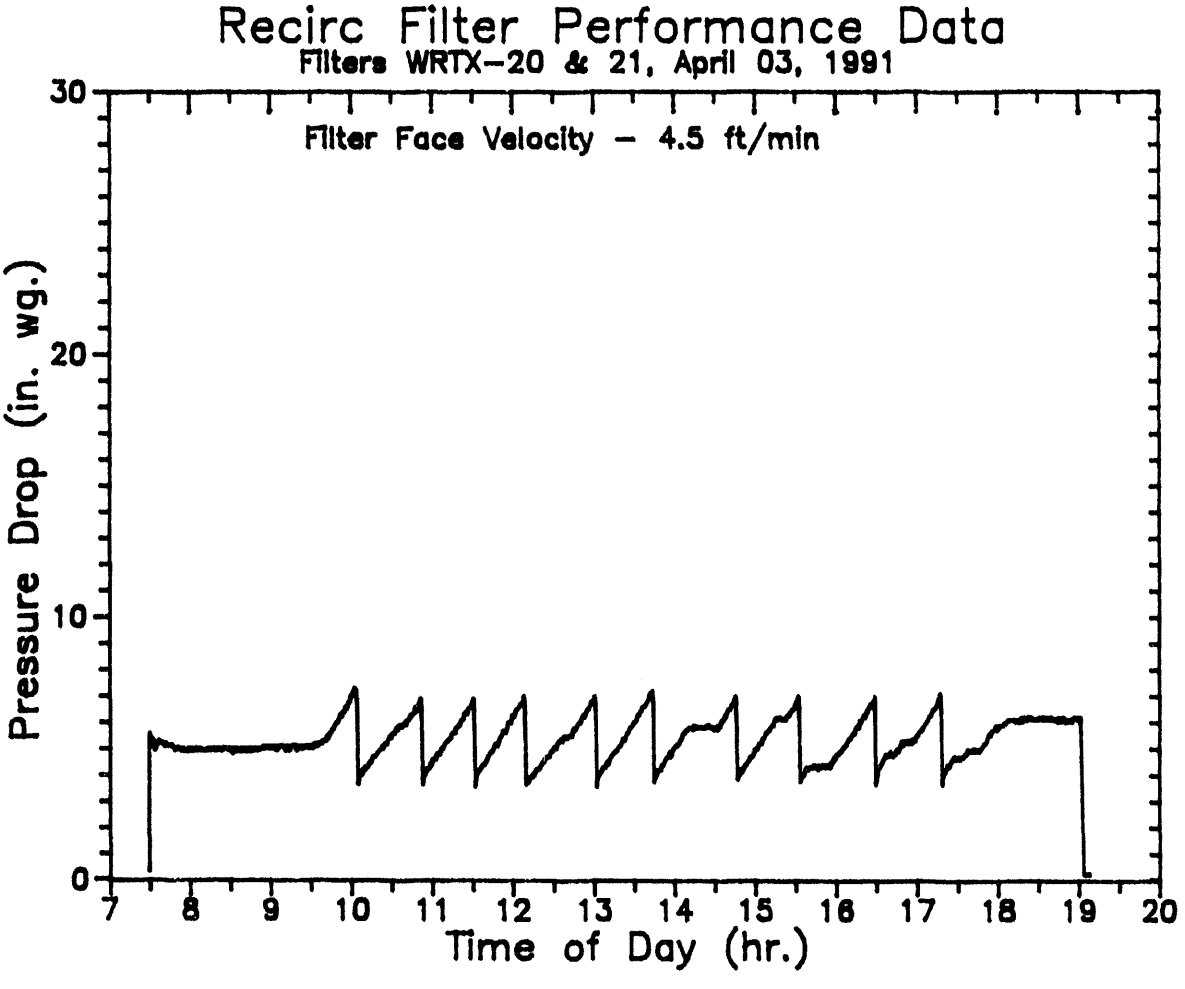

Operation Notes for April 03, 1991
delta-P Trigger = 7 in wc
Pulse Cleaning - 170 psig/0.1 sec
0726 - 0935 Char added, system to temperature
1405 - 1433 Char not feeding properly
1539 - 1555 Char not feeding properly
1812 - 1902 Out of Char

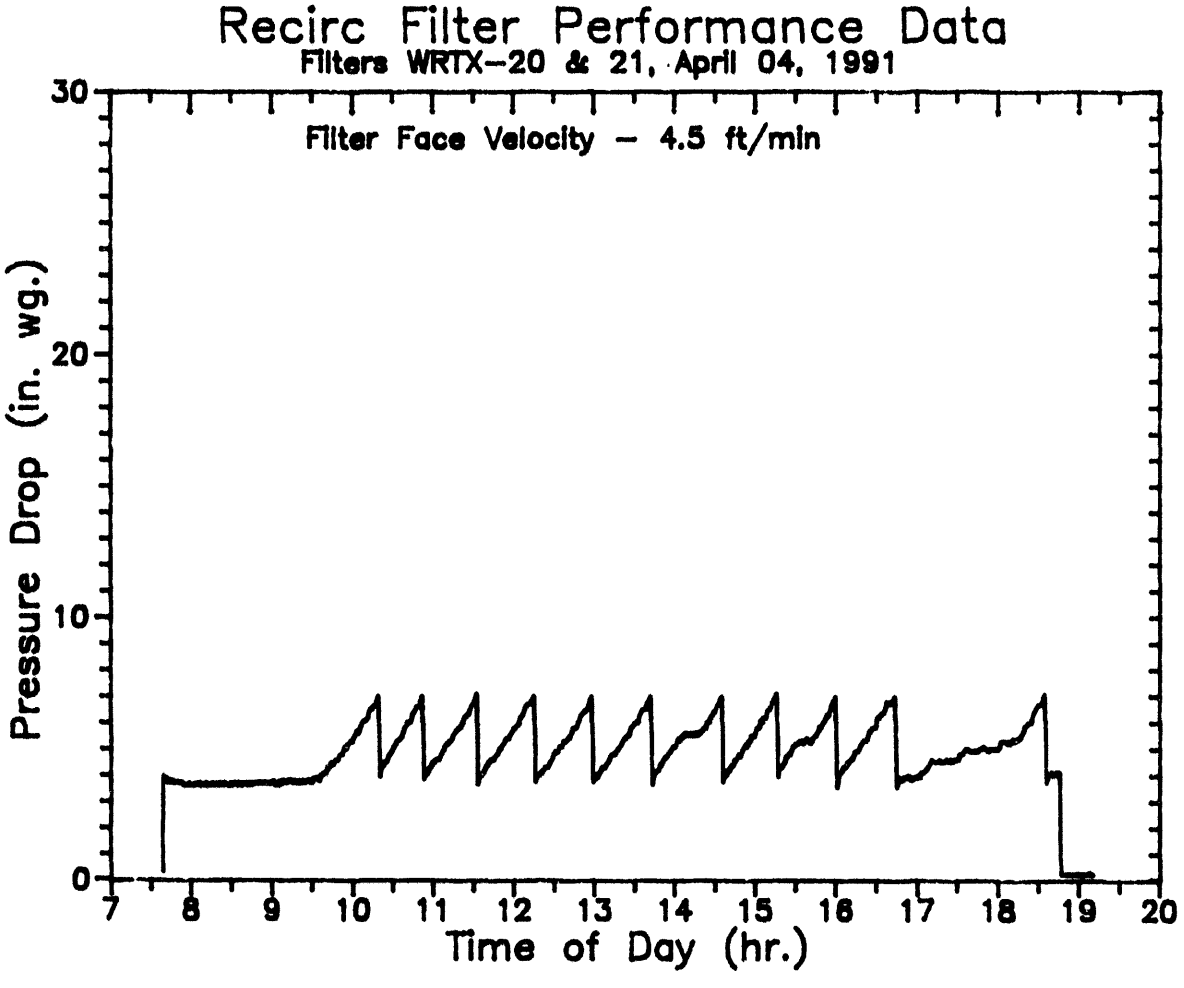

Operation Notes for April 04, 1991
delta-P Trigger = 7 in wc
Pulse Cleaning -- 170 psig/0.1 sec
0736 - 0931 Char added, system to temperature
1645 - 1815 Char not feeding properly

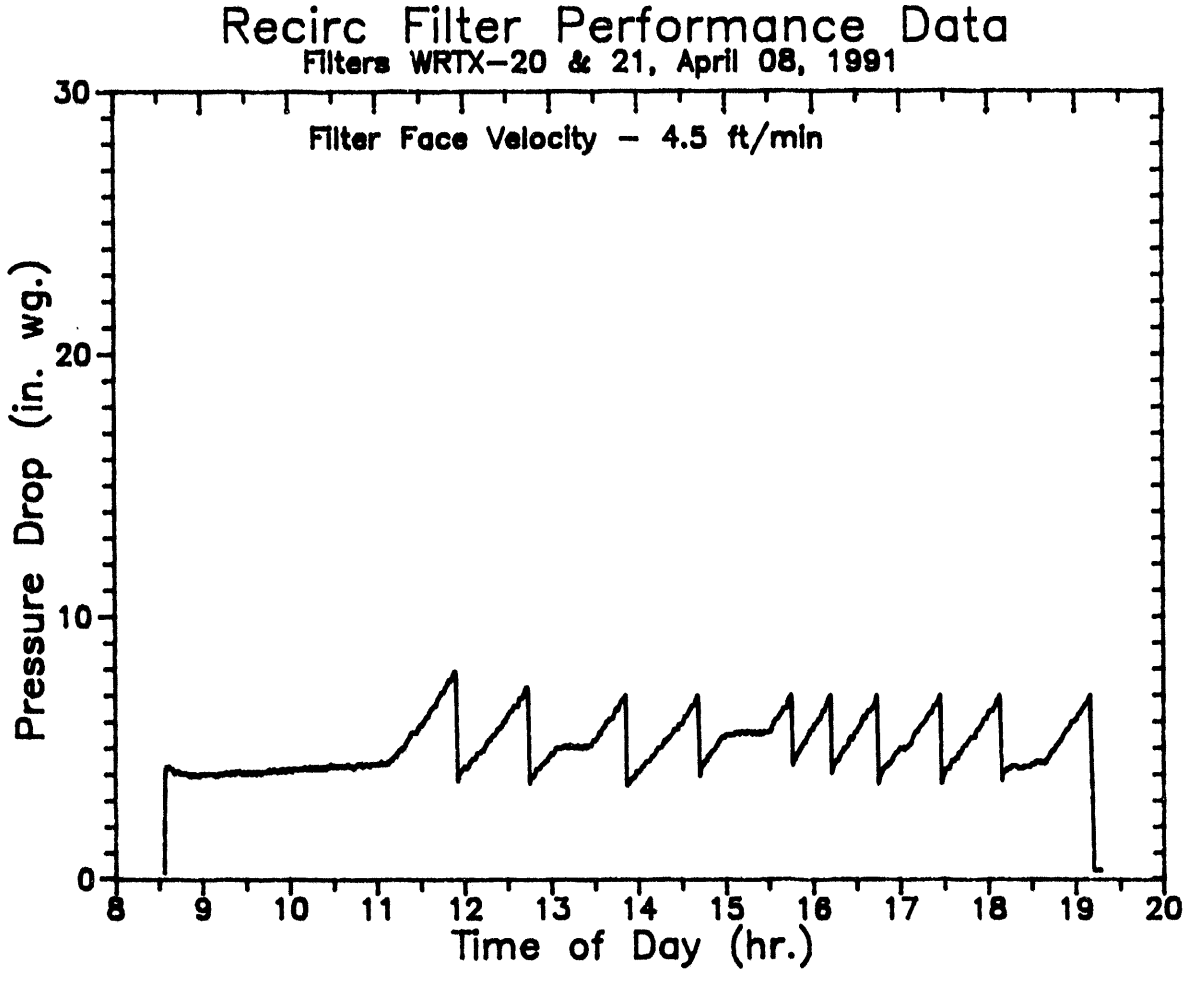

Operation Notes for April 08, 1991
delta-P Trigger = 7 in wc
Pulse Cleaning - 170 psig/0.1 sec
0835 - 1110 Char added, system to temperature
1300 - 1330 Char not feeding properly
1500 - 1530 Char not feeding properly
1810 - 1840 Char not feeding properly

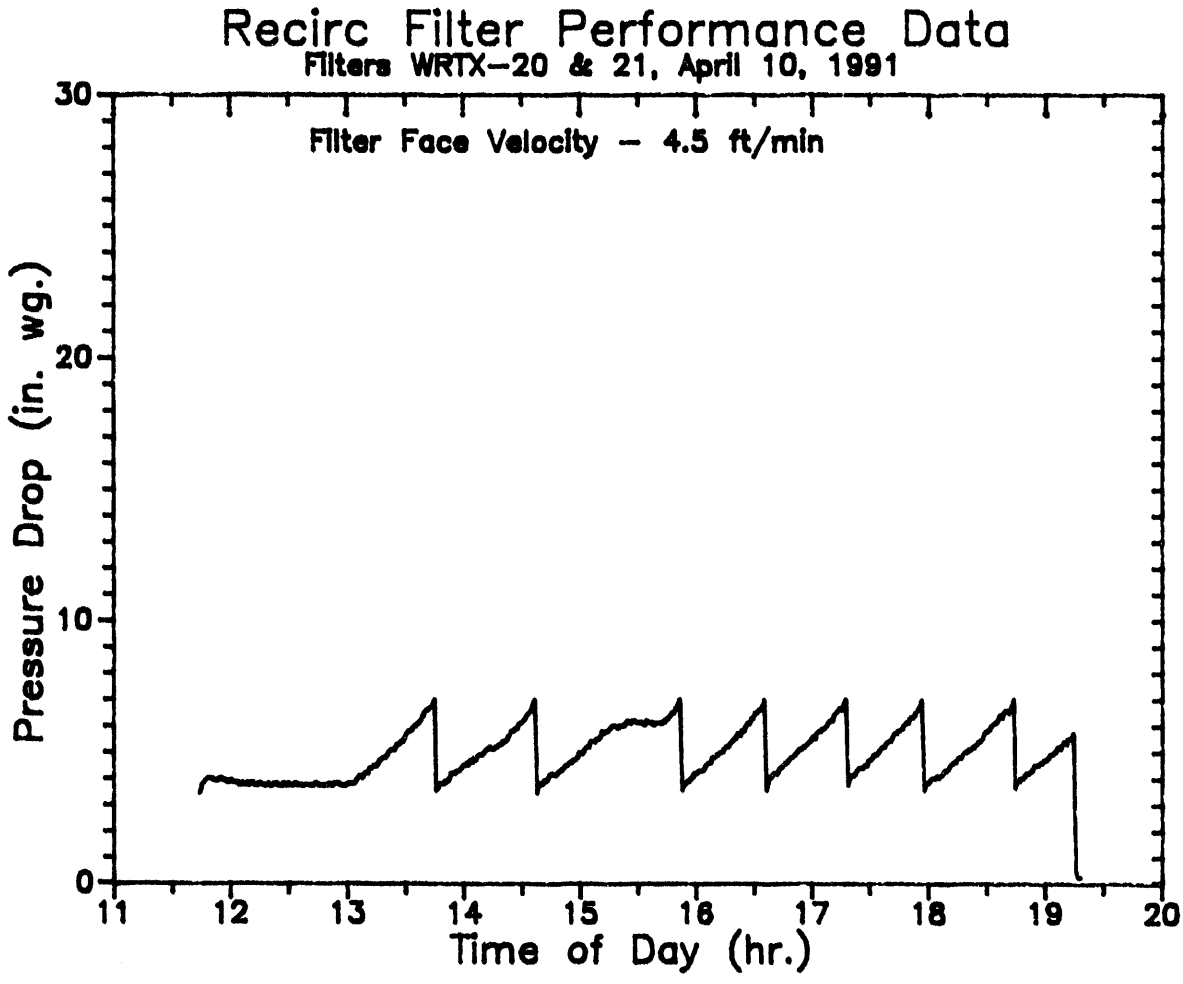

Operation Notes for April 10, 1991
delta-P Trigger = 7 in wc
Pulse Cleaning - 170 psig/0.1 sec
0730 - 1140 system emptied, refilled and repressurized
1140 - 1300 system to temperature
1510 - 1540 Char not feeding properly

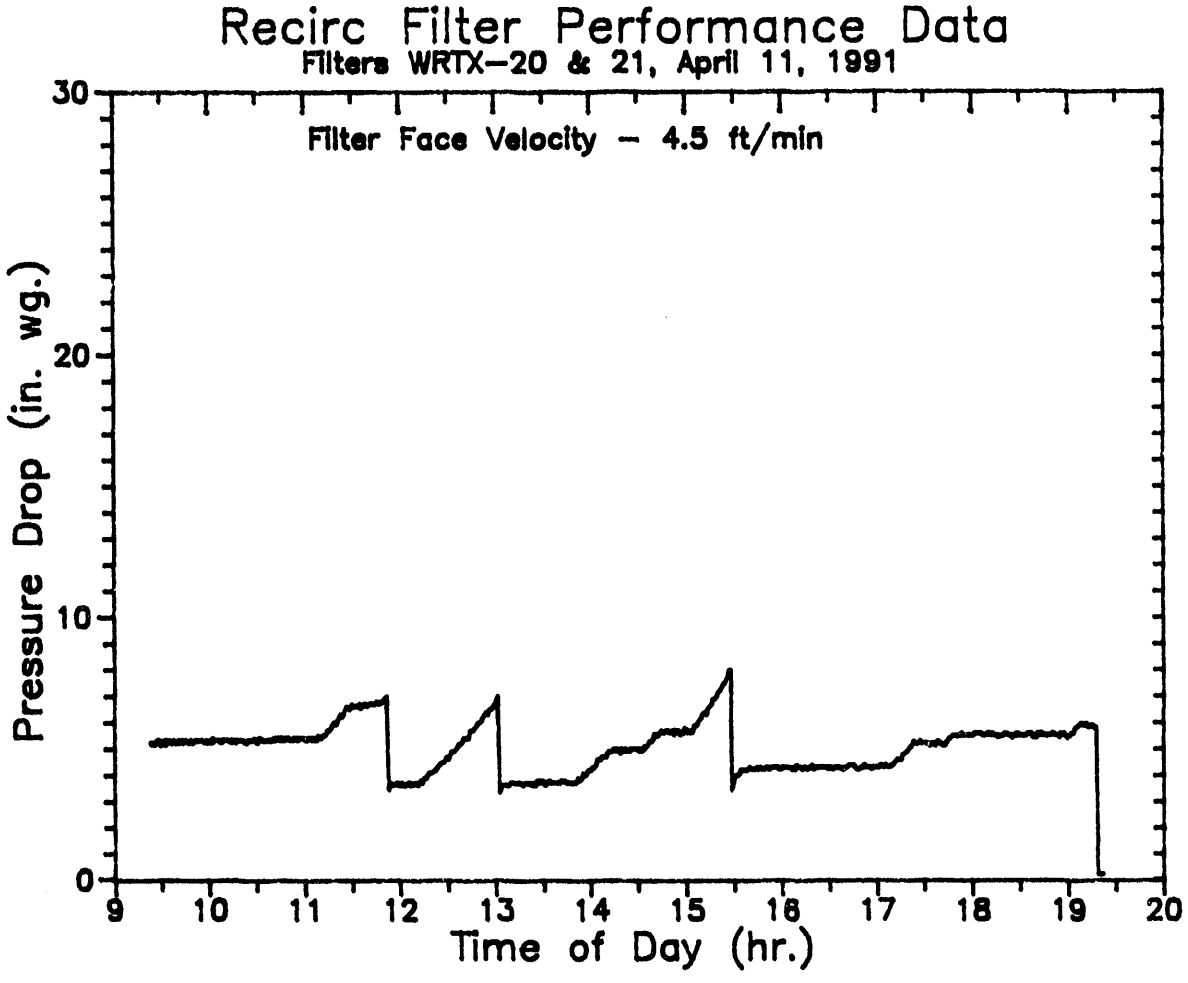

Operation Notes for April 11, 1991
delta-P Trigger = 7 in wc
Pulse Cleaning - 170 psig/0.1 sec
0857 - 1109 system to temperature
1300 - 1500 Char not feeding properly
1530 - 1917 Char not feeding properly

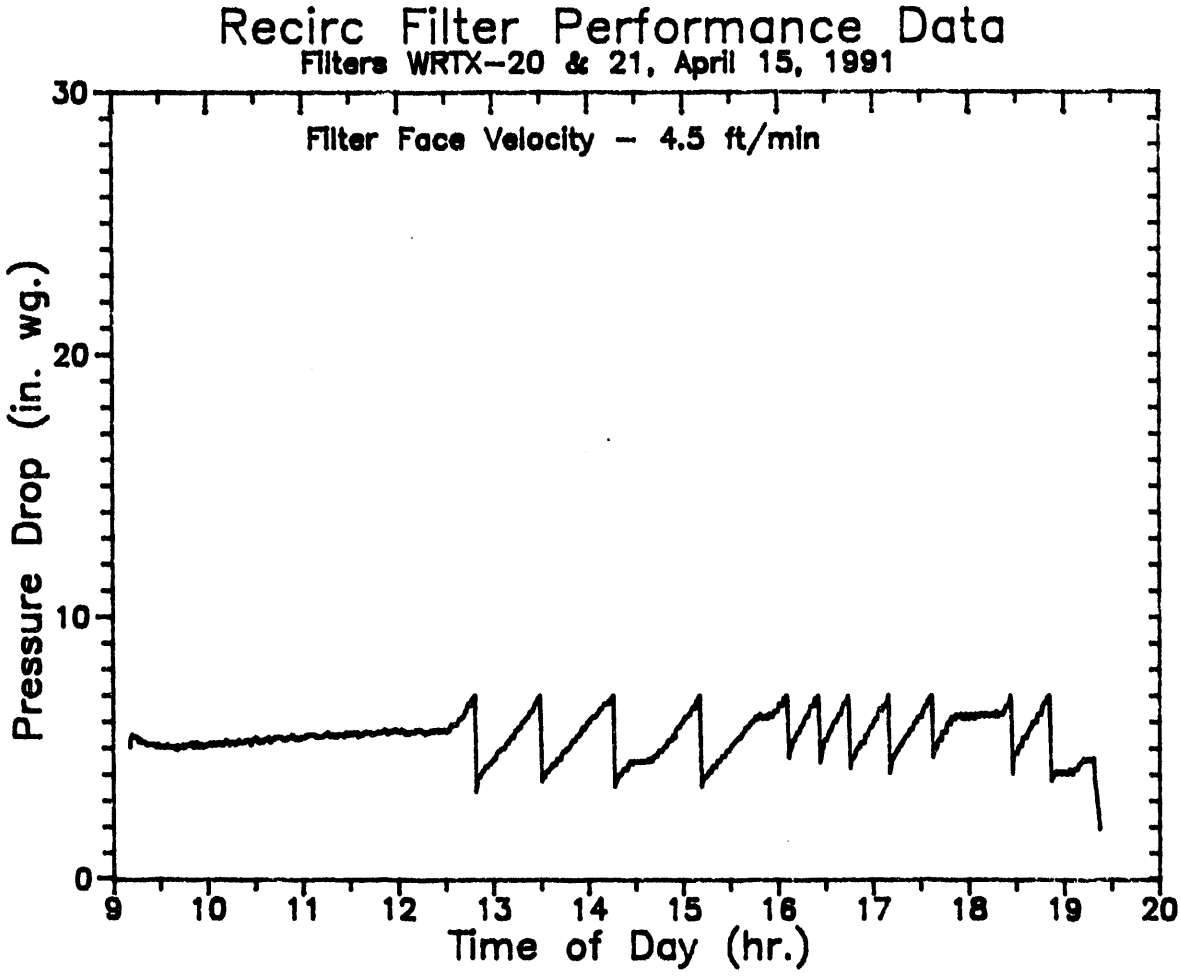

Operation Notes for April 15, 1991
delta-P Trigger = 7 in wc
Pulse Cleaning - 170 psig/0.1 sec
0910 - 1230 Char loaded, system to pressure and temperature
1918 Scheduled Shutdown

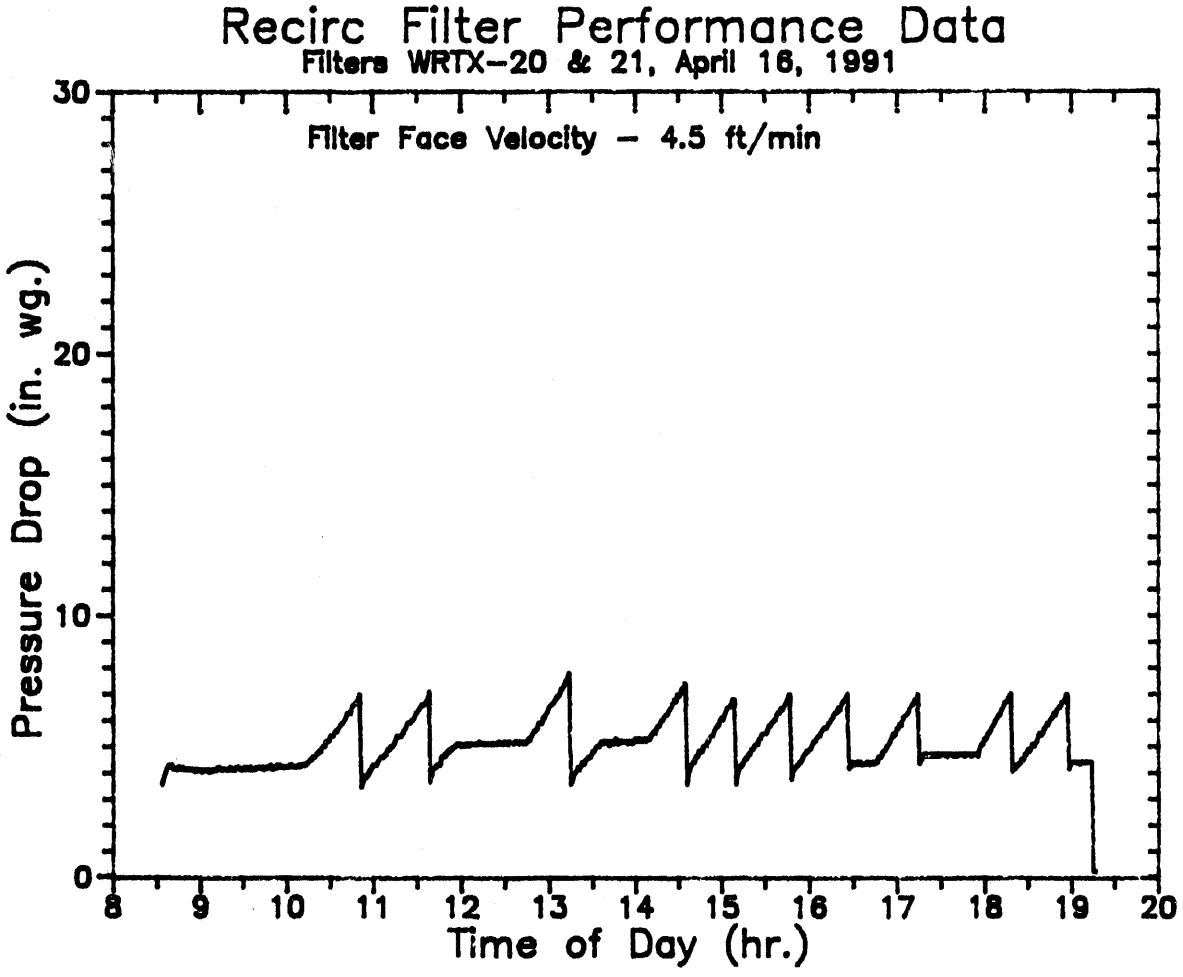

Operation Notes for April 16, 1991
delta–P Trigger = 7 in wc
Pulse Cleaning – 170 psig/0.1 sec
0745 – 1013 Char loaded, system to pressure and temperature
1913 Scheduled Shutdown
Plateaus in delta–P indicate dust feed malfunction

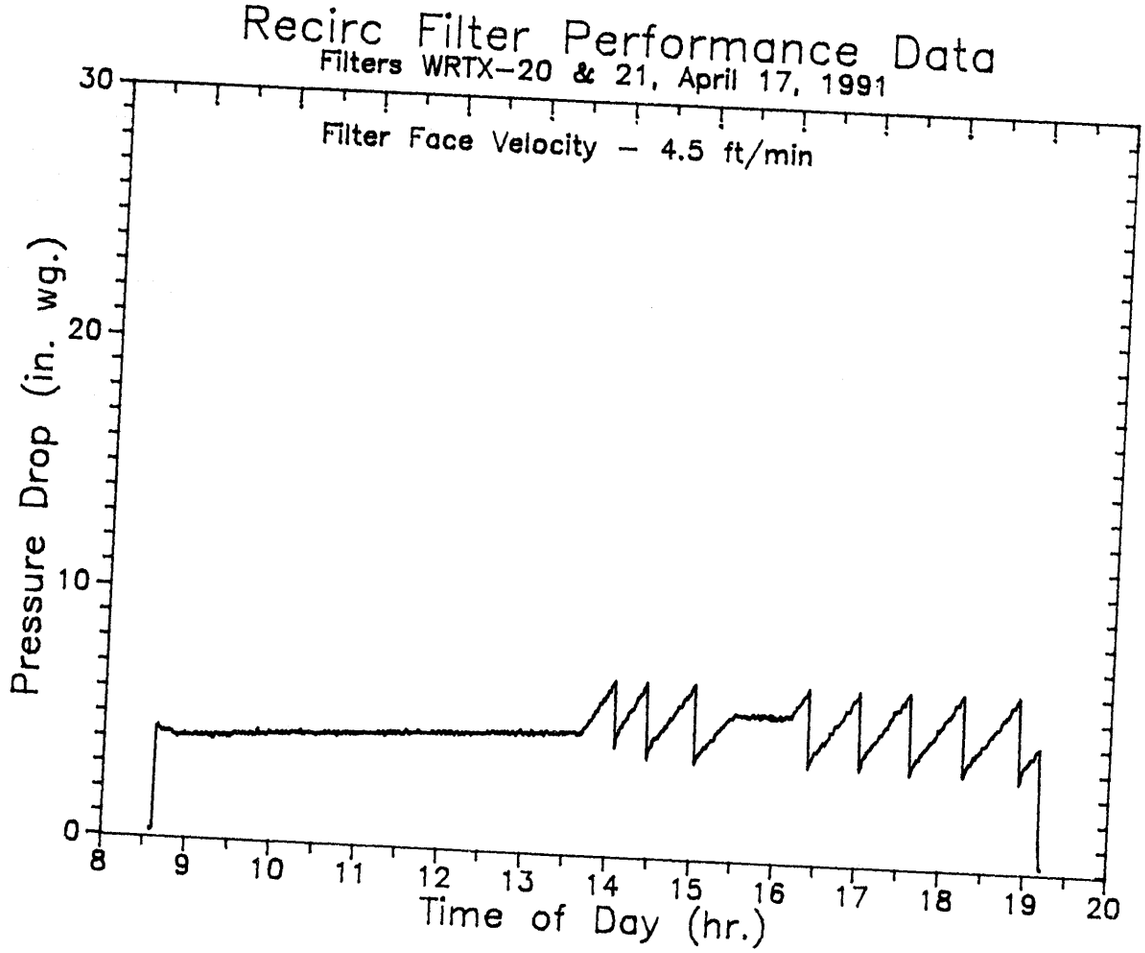

Operation Notes for April 17, 1991
delta-P Trigger = 7 in wc
Pulse Cleaning - 170 psig/0.1 sec
0830 - 1340 Char loaded, system to pressure and temperature
1910 Scheduled Shutdown
Plateau in delta-P indicates dust feed malfunction

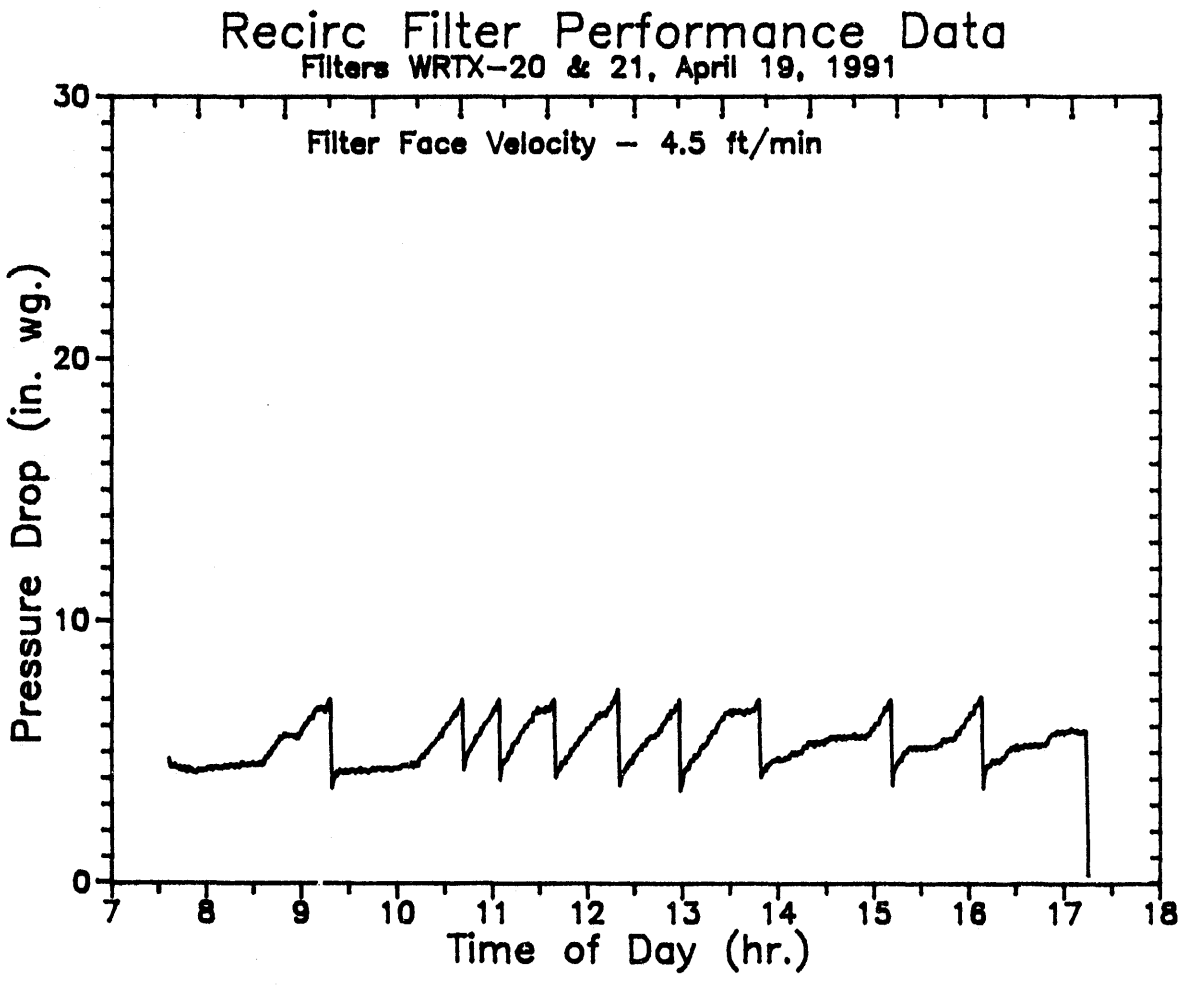

Operation Notes for April 19, 1991
delta–P Trigger = 7 in wc
Pulse Cleaning – 170 psig/0.1 sec
0734 – 0834 System to pressure and temperature
0922 – 1010 Char loaded
1713 Scheduled Shutdown
Plateaus in delta–P due to inconsistent dust feed

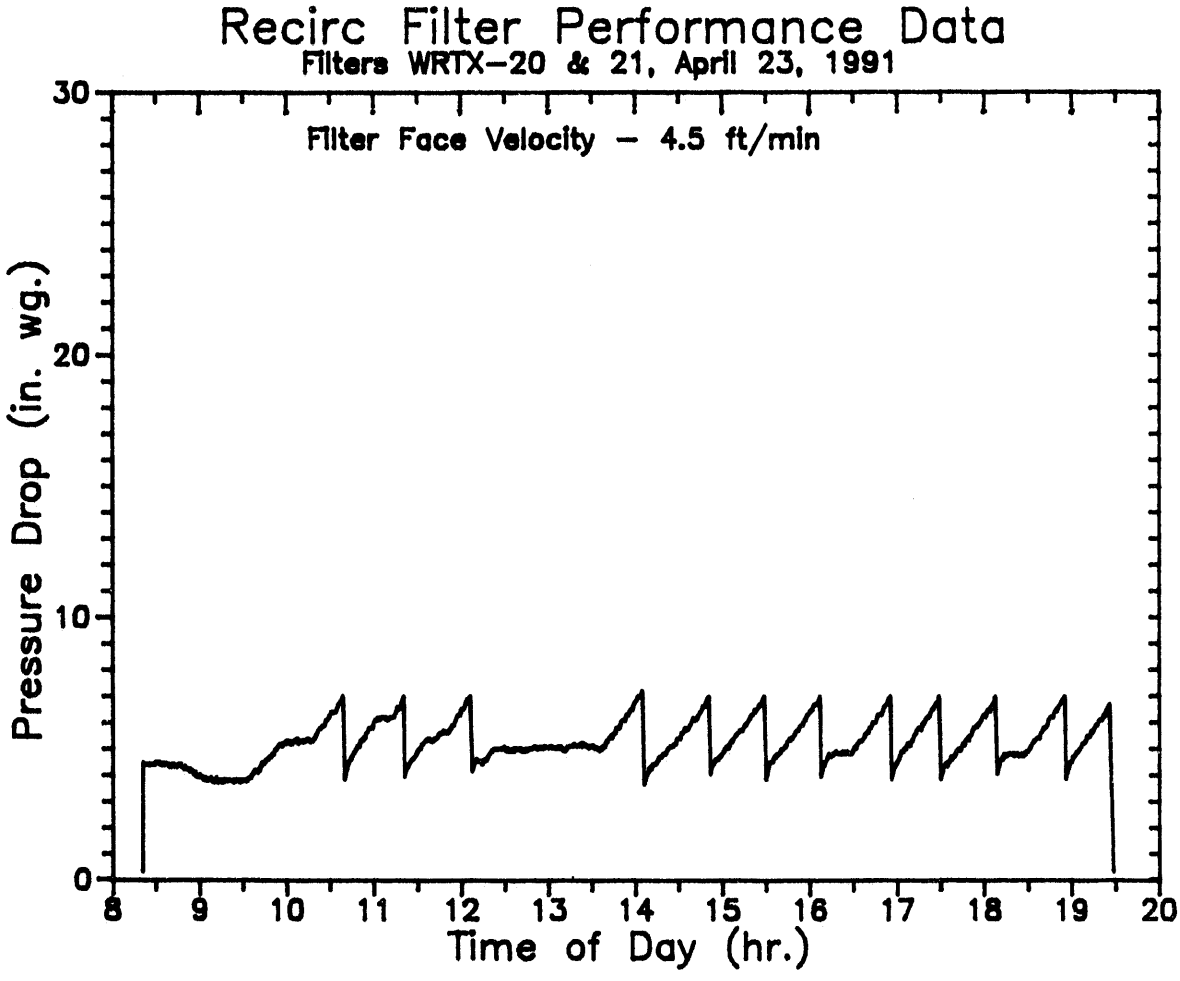

Operation Notes for April 23, 1991
delta-P Trigger = 7 in wc
Pulse Cleaning - 170 psig/0.1 sec
0730 - 0930 System to pressure and temperature
1227 - 1400 Char loaded
1926 Scheduled Shutdown
Plateaus in delta-P due to inconsistent dust feed

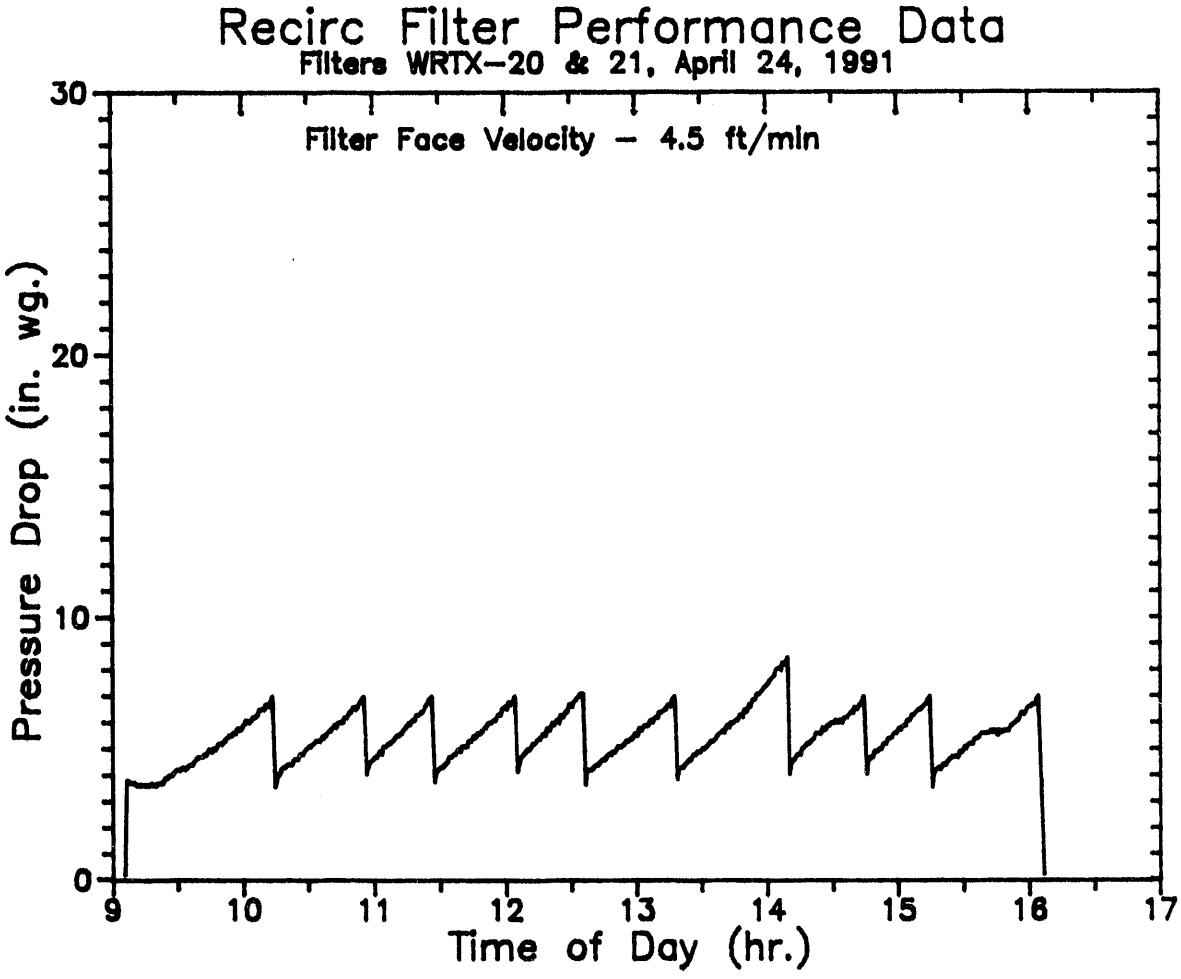

Operation Notes for April 24, 1991
delta-P Trigger = 7 in wc
Pulse Cleaning - 170 psig/0.1 sec
0730 - 0918 Char loaded, system to pressure and temperature
1603 Scheduled Shutdown
Plateaus in delta-P due to inconsistent dust feed

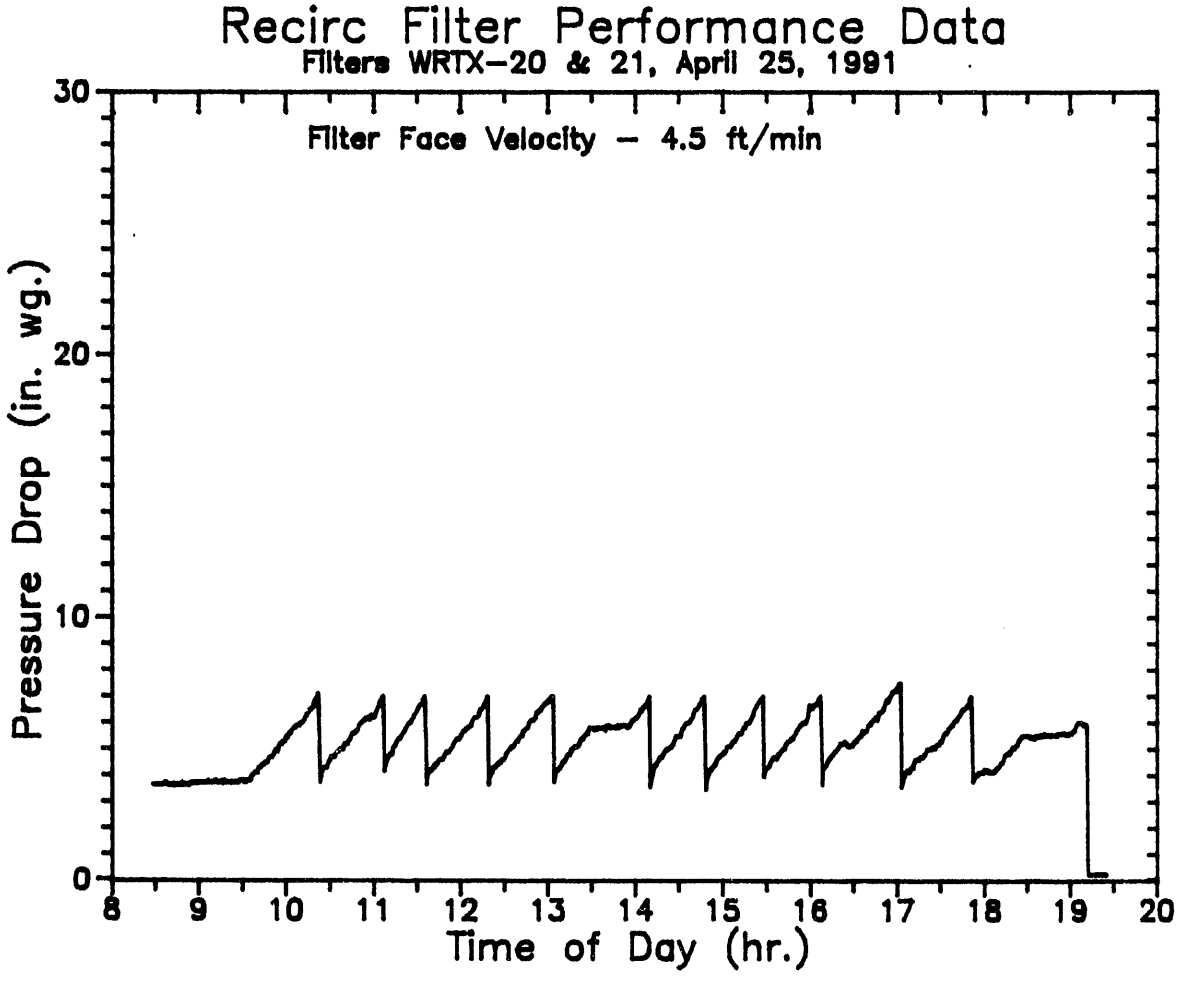

Operation Notes for April 25, 1991
delta-P Trigger = 7 in wc
Pulse Cleaning - 170 psig/0.1 sec
0810 - 0930 Char loaded, system to pressure and temperature
1910 Scheduled Shutdown
Plateaus in delta-P due to inconsistent dust feed, or low char level

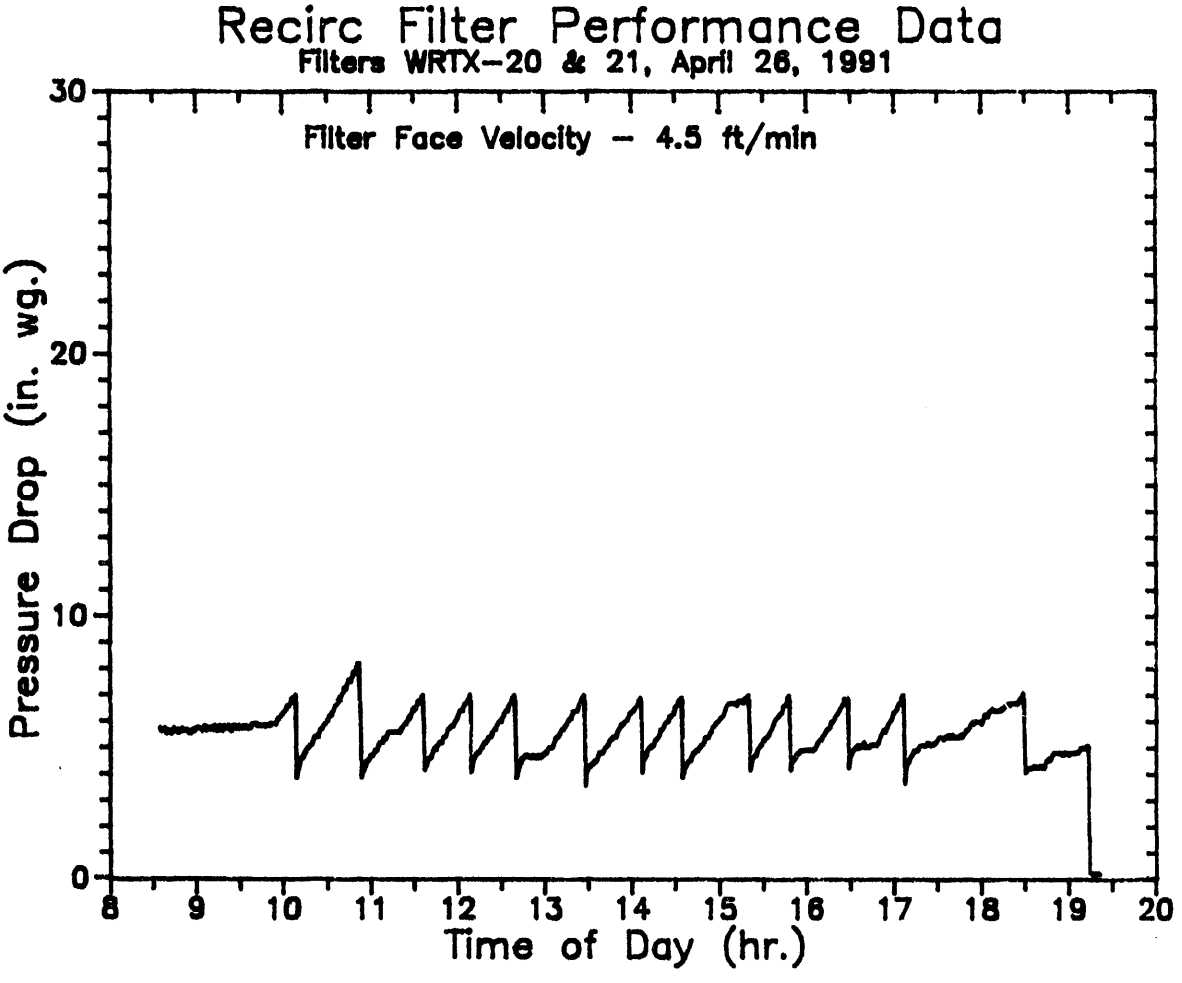

Operation Notes for April 26, 1991
delta-P Trigger = 7 in wc
Pulse Cleaning - 170 psig/0.1 sec
0831 - 0950 Char loaded, system to pressure and temperature
1911 Scheduled Shutdown
Plateaus in delta-P due to inconsistent dust feed, or low char level

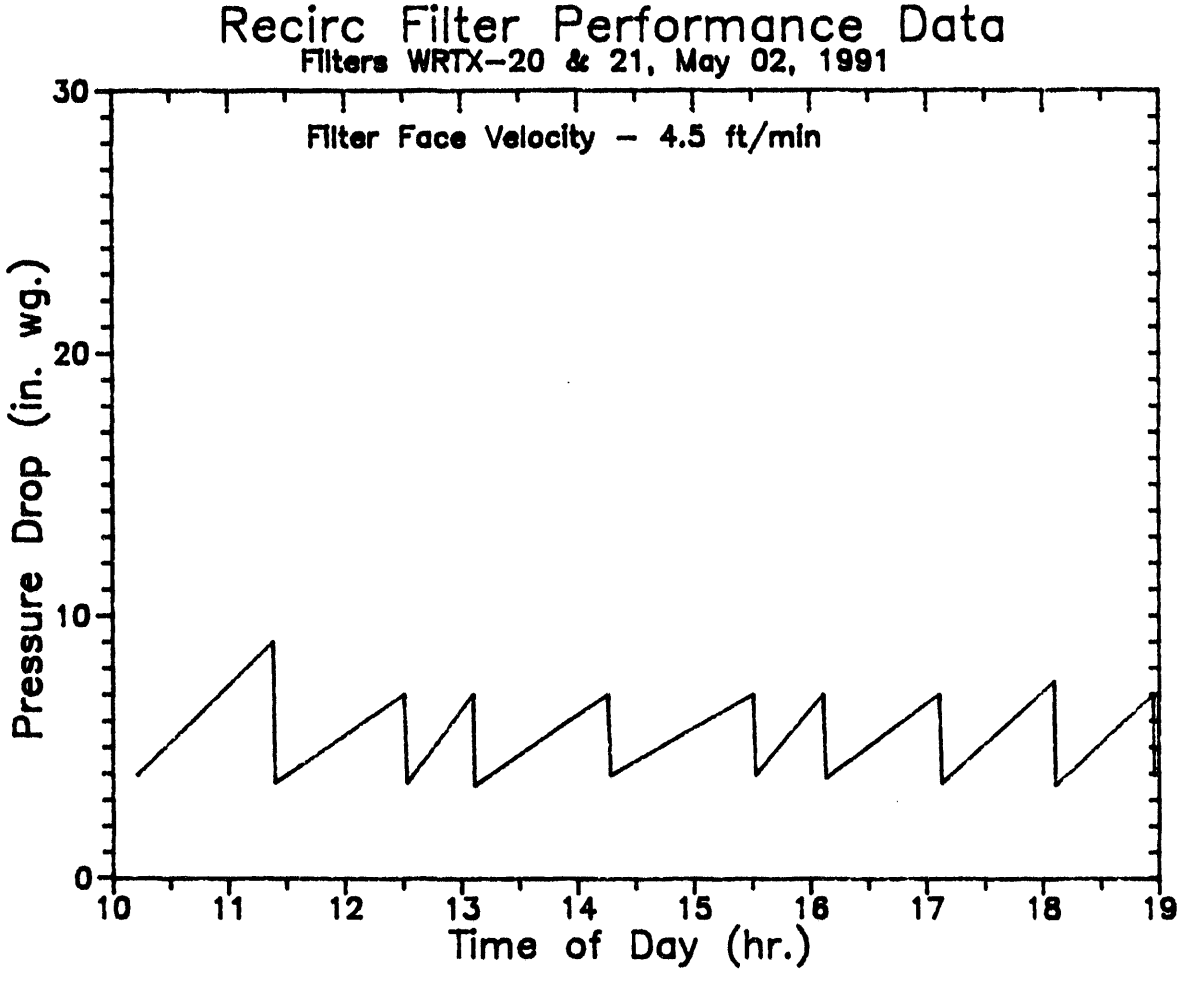

Operation Notes for May 02, 1991
delta-P Trigger = 7 in wc
Pulse Cleaning - 170 psig/0.1 sec
0850 - 1015 Char loaded, system to pressure and temperature
1857 Scheduled Shutdown
Plateaus in delta-P due to inconsistent dust feed, or low char level

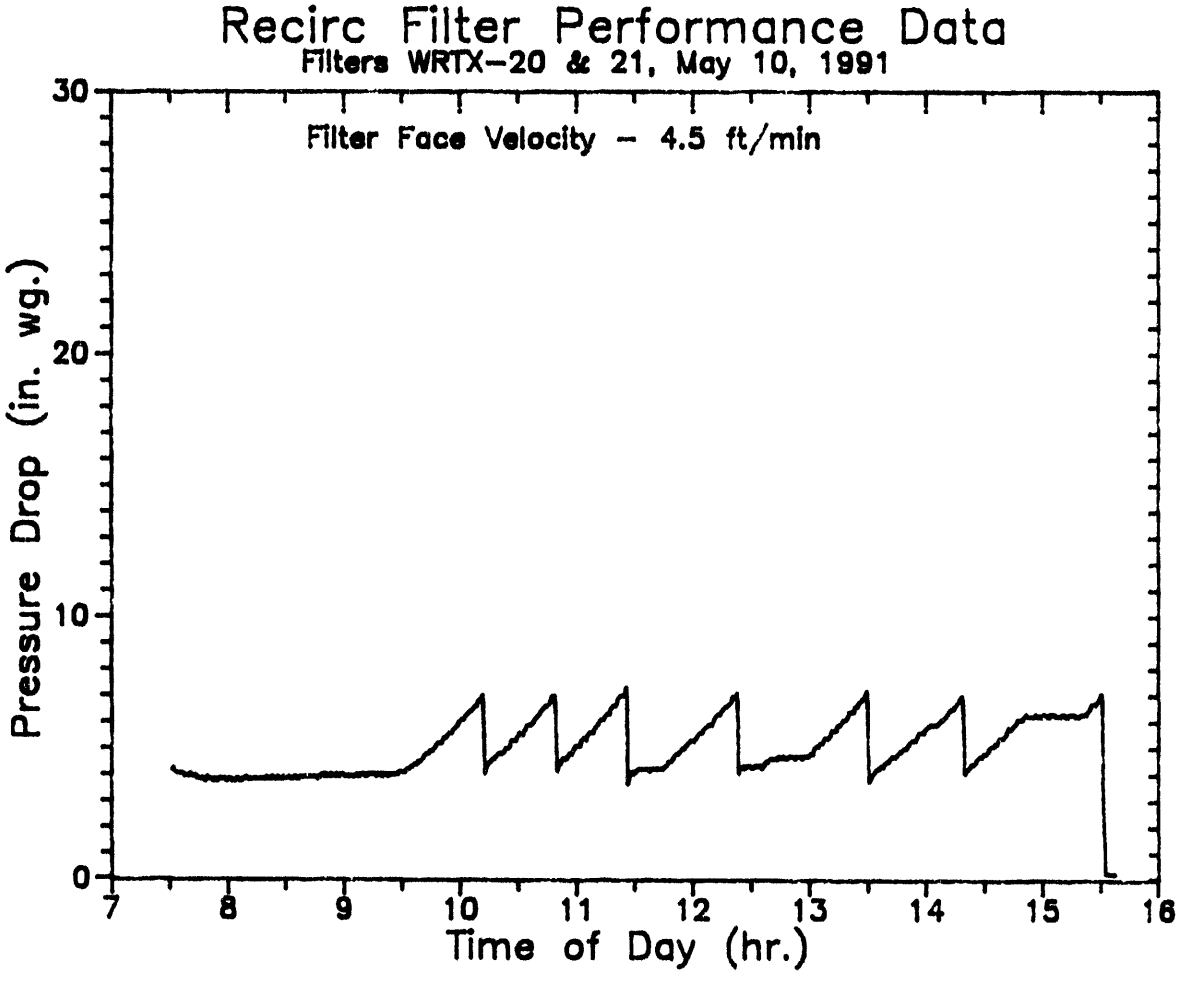

Operation Notes for May 10, 1991
delta-P Trigger = 7 in wc
Pulse Cleaning - 170 psig/0.1 sec
0729 - 0930 Char loaded, system to pressure and temperature
1532 Scheduled Shutdown
Plateaus in delta-P due to inconsistent dust feed, or low char level

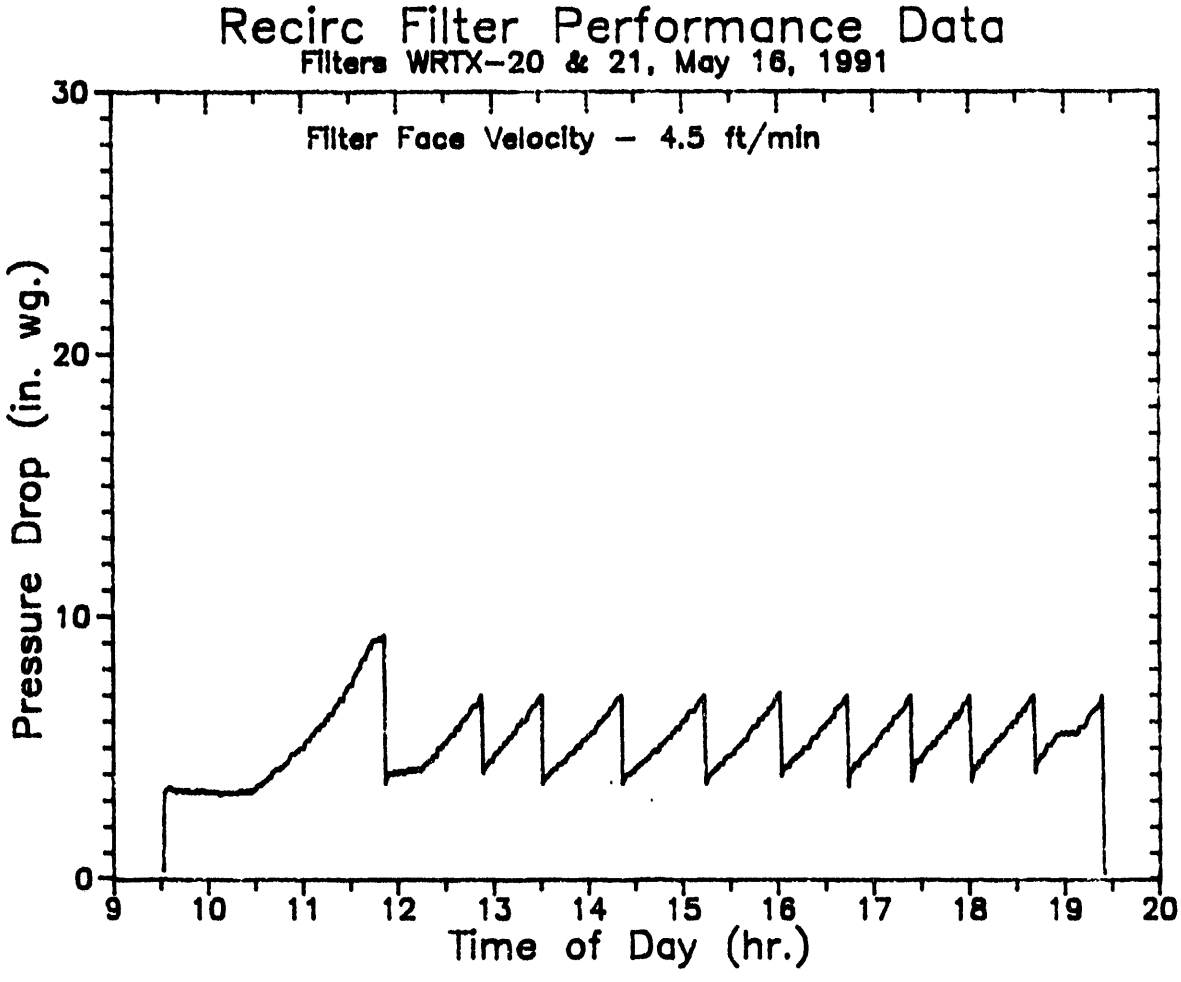

Operation Notes for May 16, 1991
delta–P Trigger = 7 in wc
Pulse Cleaning – 170 psig/0.1 sec
0930 – 1027 Char loaded, system to pressure and temperature
1923 Scheduled Shutdown
Plateaus in delta–P due to inconsistent dust feed, or low char level

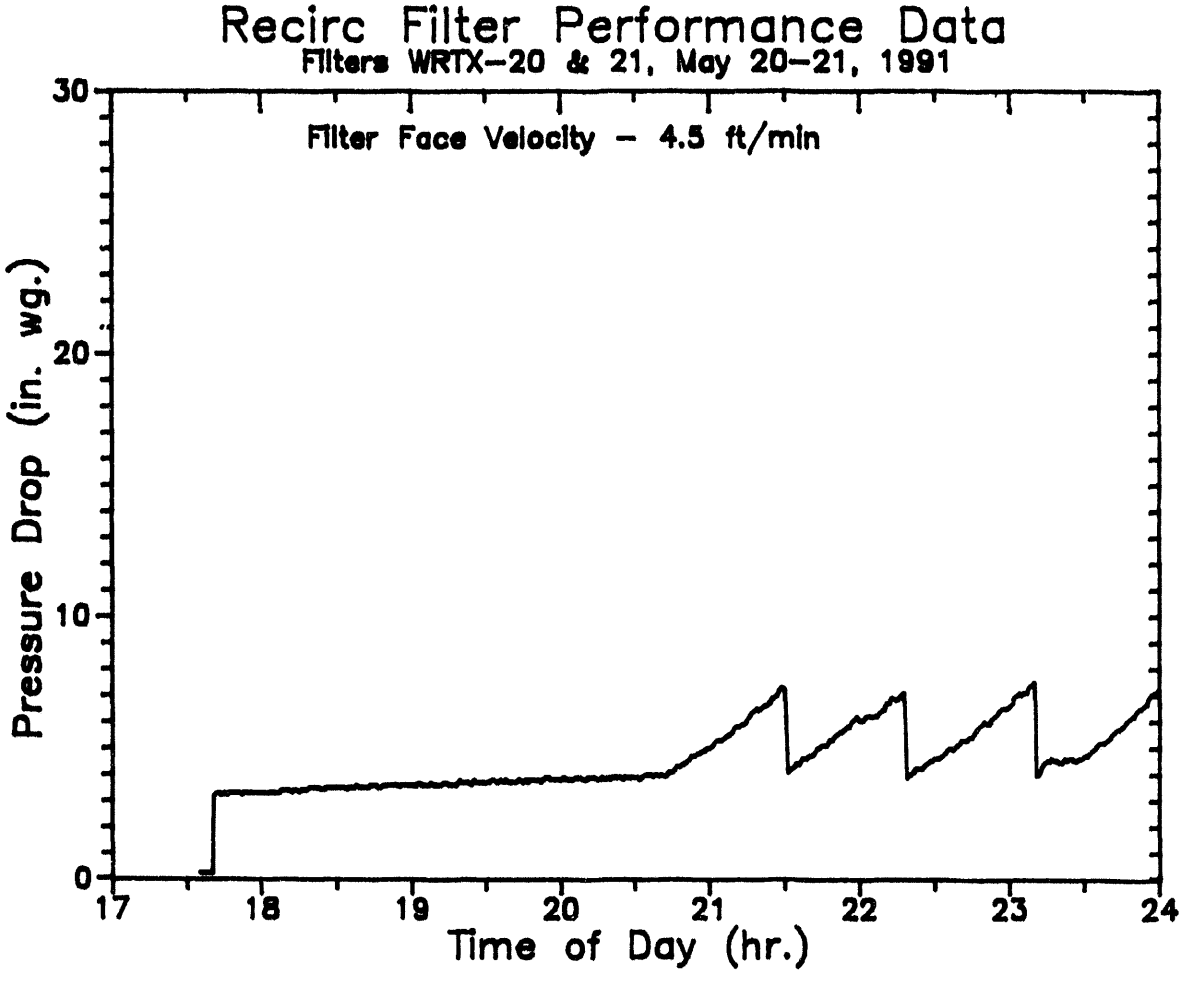

Operation Notes for May 20-21, 1991
delta-P Trigger = 7 in wc
Pulse Cleaning - 170 psig/0.1 sec
1738 - 2040 Char loaded, system to pressure and temperature
0353 Scheduled Shutdown (May 21, 1991)
Plateaus in delta-P due to inconsistent dust feed, or low char level

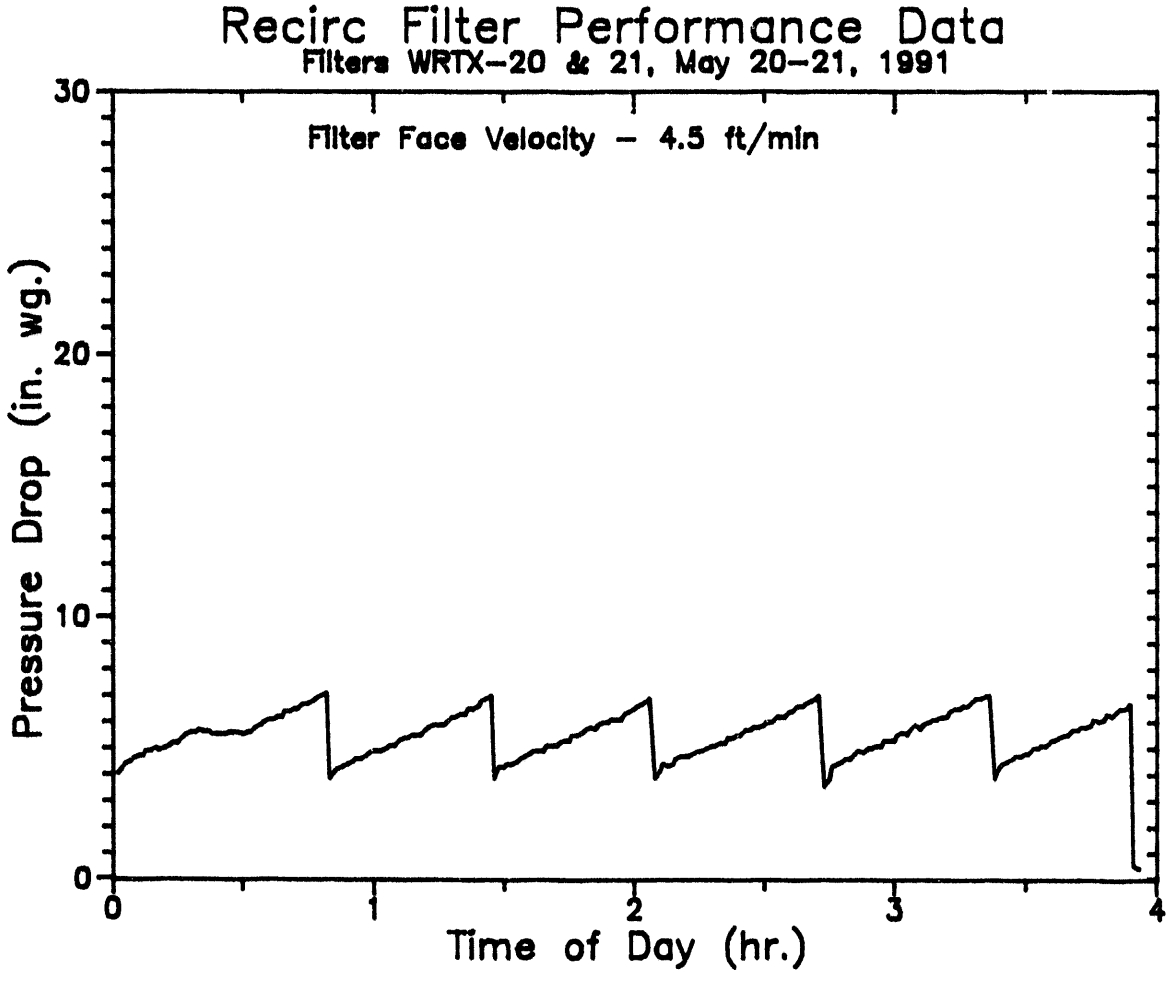

Operation Notes for May 20-21, 1991
delta-P Trigger = 7 in wc
Pulse Cleaning - 170 psig/0.1 sec
1739 - 2040 Char loaded, system to pressure and temperature
0353 Scheduled Shutdown (May 21, 1991)
Plateaus in delta-P due to inconsistent dust feed, or low char level

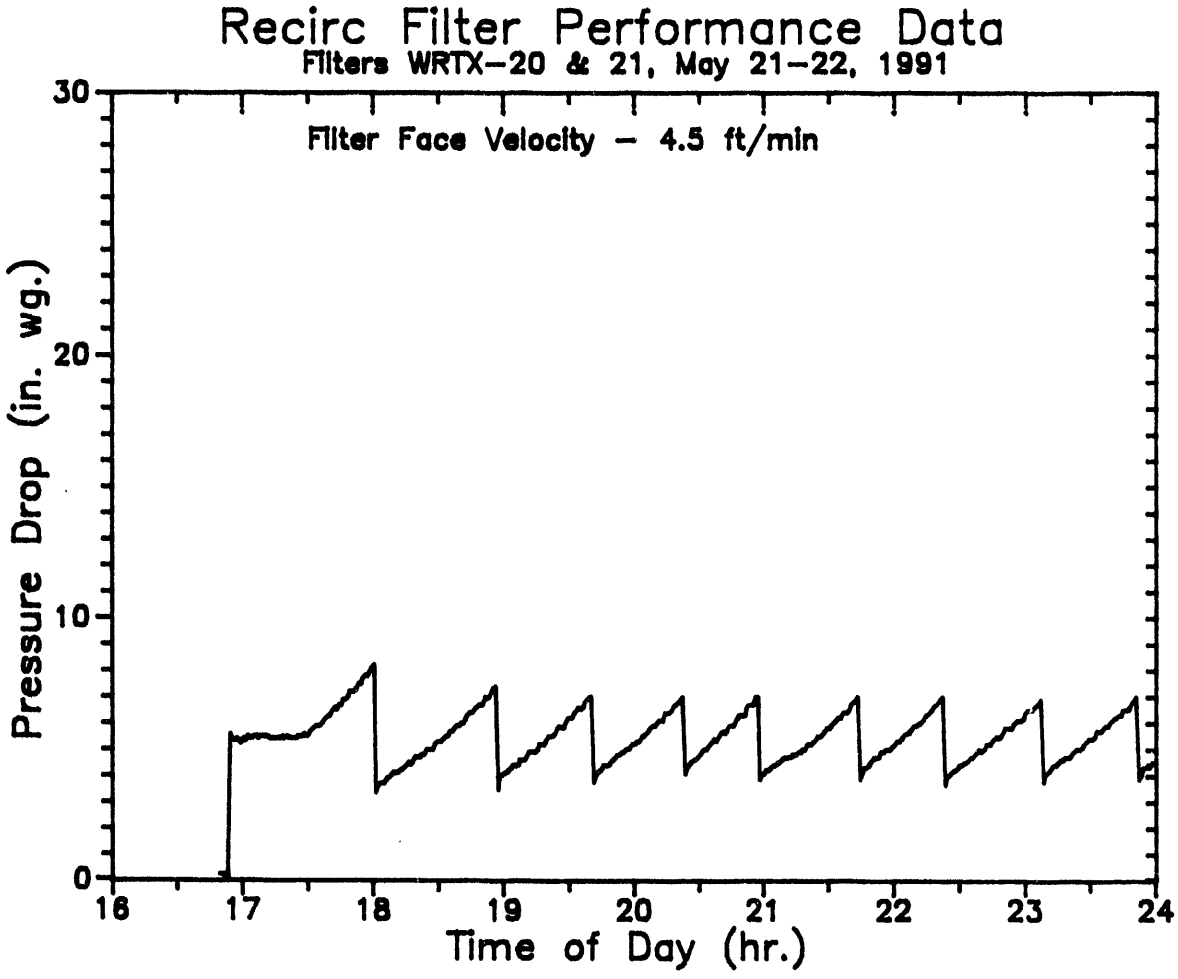

Operation Notes for May 21-22, 1991
delta-P Trigger = 7 in wc
Pulse Cleaning - 170 psig/0.1 sec
1652 - 1725 Char loaded, system to pressure and temperature
0347 Scheduled Shutdown (May 22, 1991)
Plateaus in delta-P due to inconsistent dust feed, or low char level

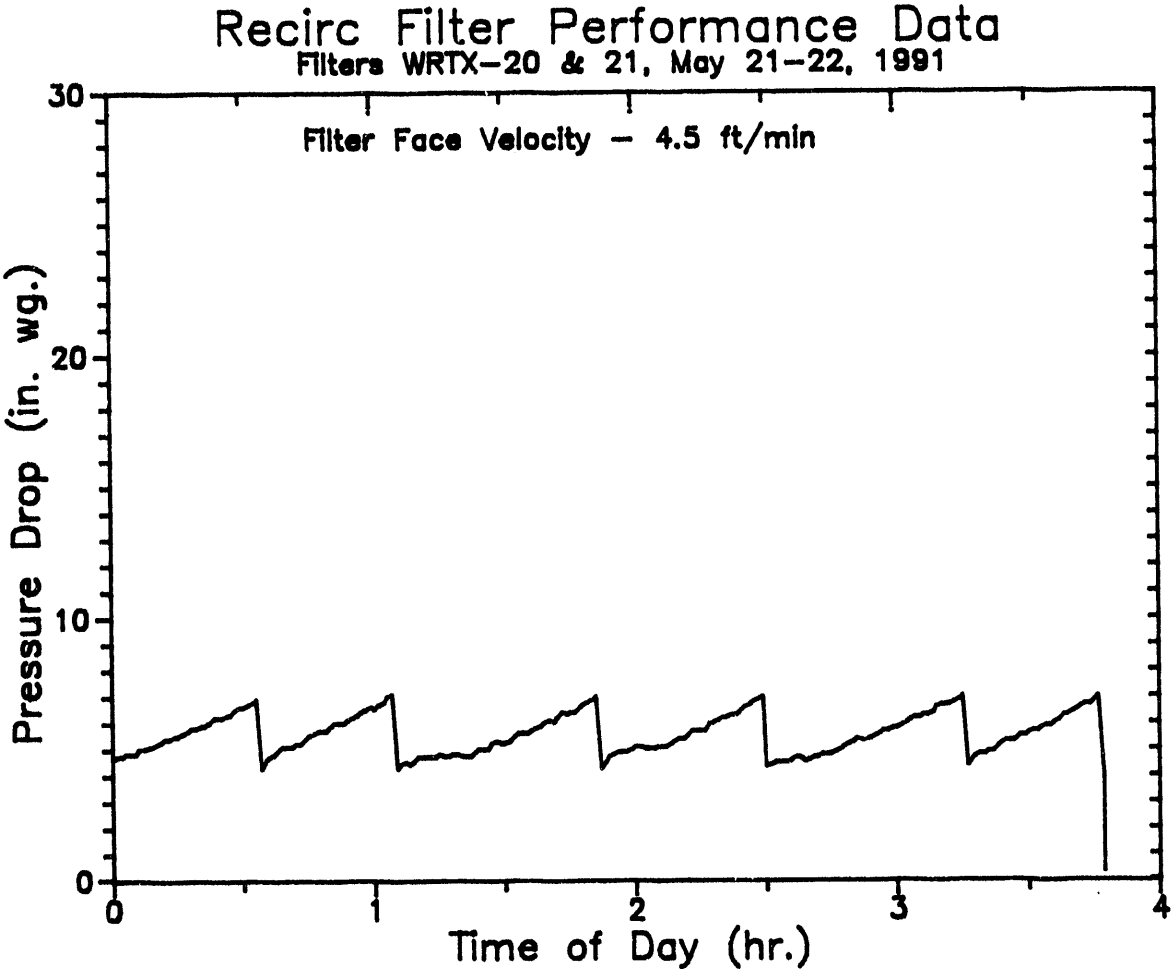

Operation Notes for May 21-22, 1991
delta-P Trigger = 7 in wc
Pulse Cleaning - 170 psig/0.1 sec
1652 - 1725 Char loaded, system to pressure and temperature
0347 Scheduled Shutdown (May 22, 1991)
Plateaus in delta-P due to inconsistent dust feed, or low char level

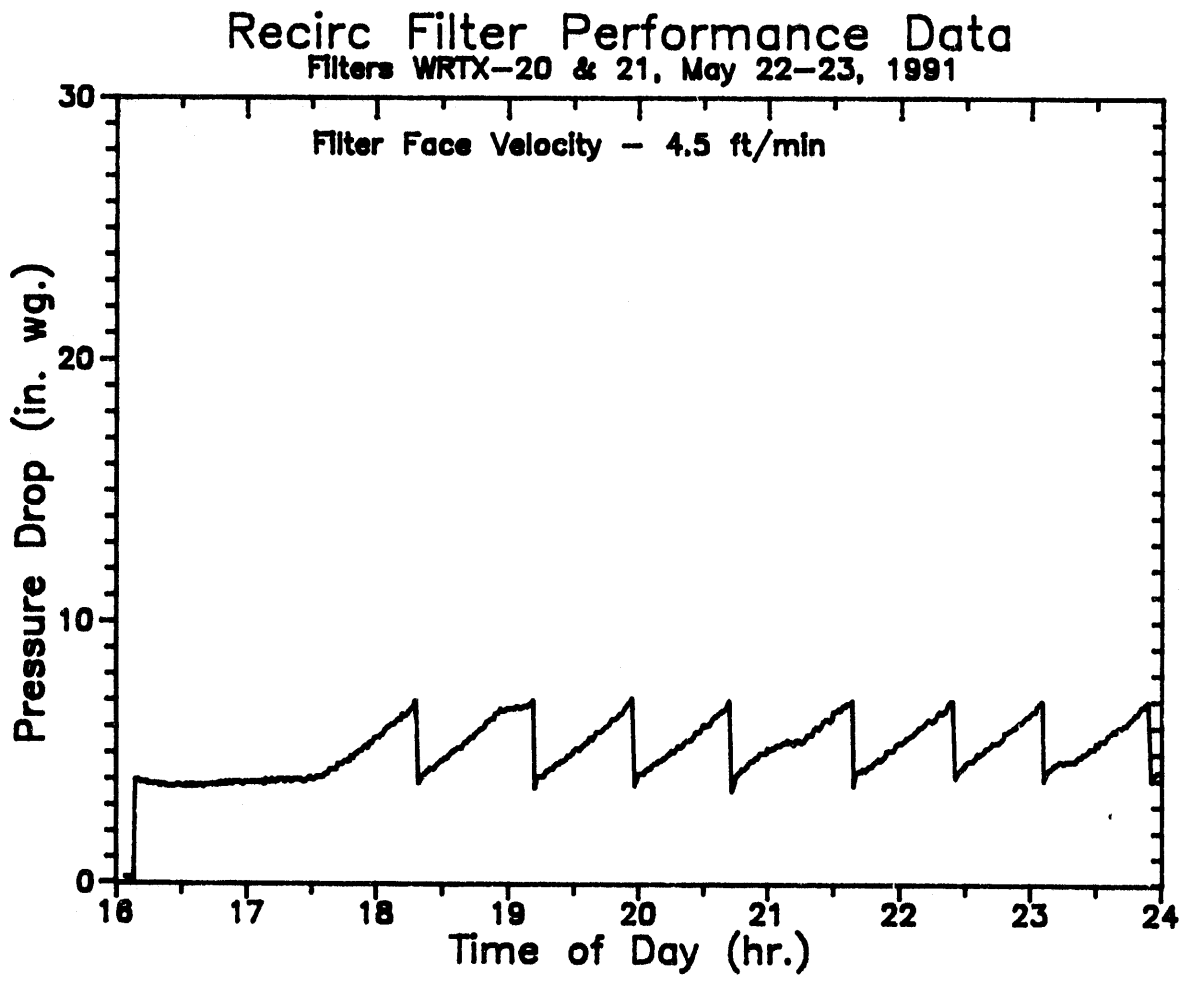

Operation Notes for May 22-23, 1991
delta-P Trigger = 7 in wc
Pulse Cleaning - 170 psig/0.1 sec
1607 - 1730 Char loaded, system to pressure and temperature
0349 Scheduled Shutdown (May 23, 1991)
Plateaus in delta-P due to inconsistent dust feed, or low char level

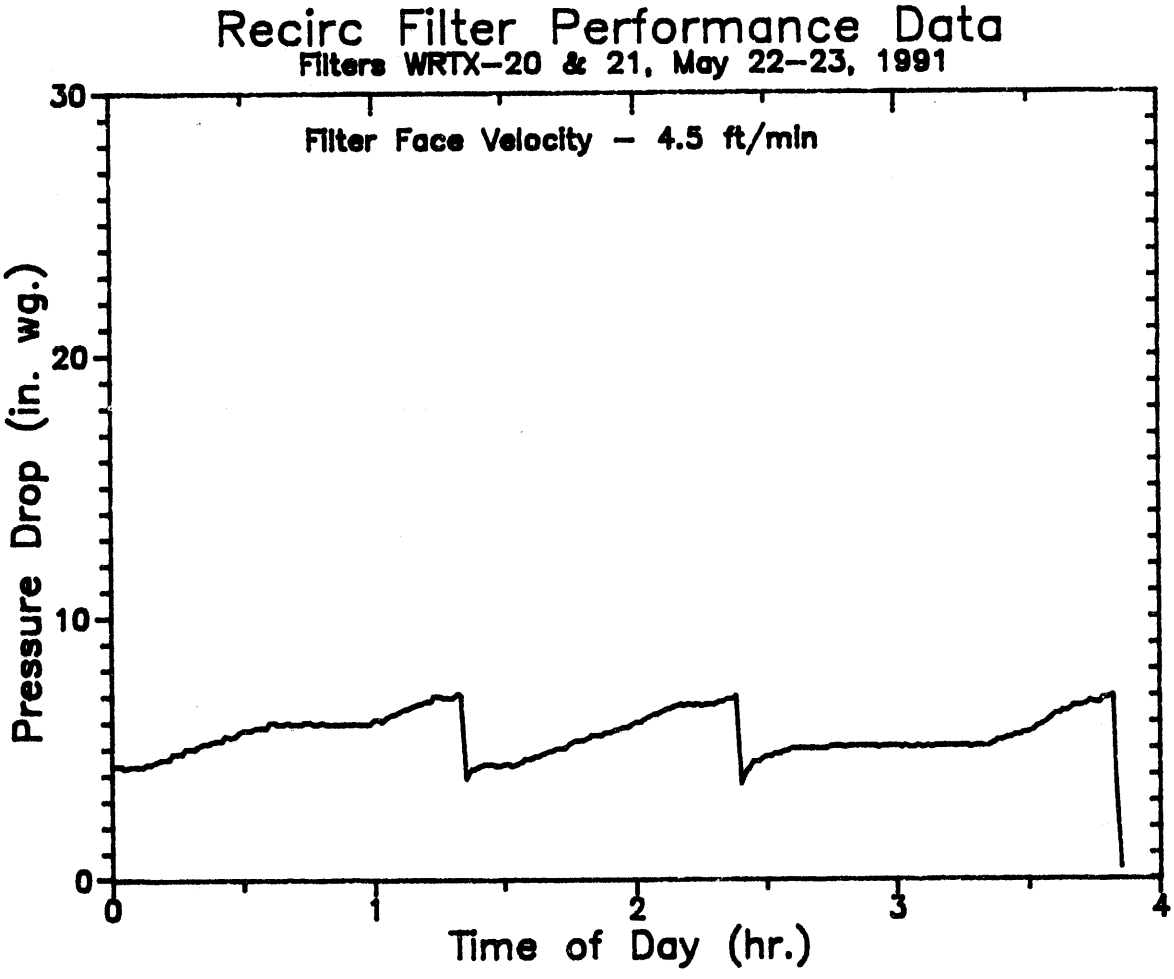

Operation Notes for May 22-23, 1991
delta-P Trigger = 7 in wc
Pulse Cleaning - 170 psig/0.1 sec
1607 - 1730 Char loaded, system to pressure and temperature
0349 Scheduled Shutdown (May 23, 1991)
Plateaus in delta-P due to inconsistent dust feed, or low char level

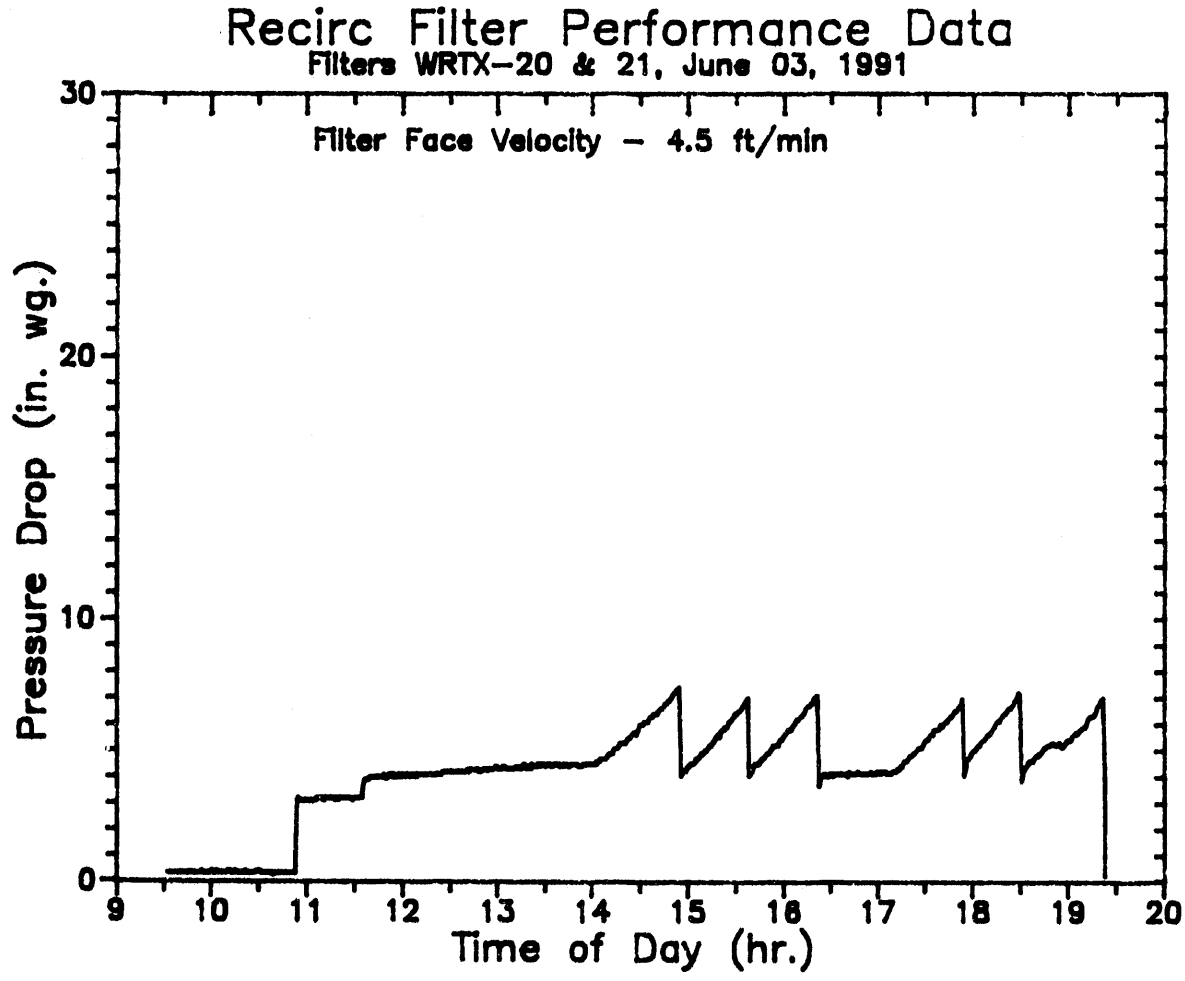

Operation Notes for June 03, 1991
delta-P Trigger = 7 in wc
Pulse Cleaning - 170 psig/0.1 sec
0730 - 1050 Char loaded, System to pressure and temperature
1920 Scheduled Shutdown
Plateaus in delta-P due to inconsistent dust feed, or low char level

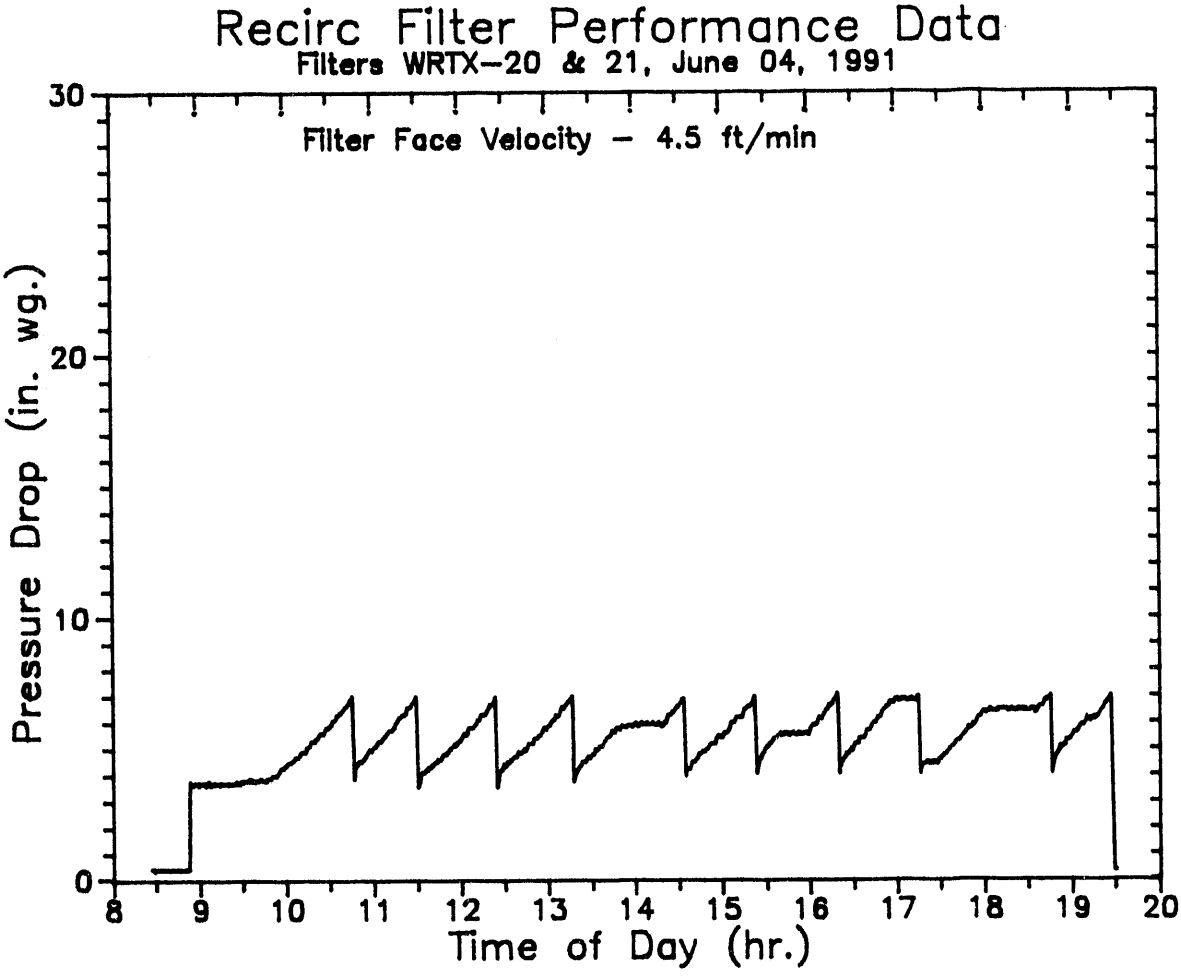

Operation Notes for June 04, 1991
delta-P Trigger = 7 in wc
Pulse Cleaning - 170 psig/0.1 sec
0730 - 0850 Char loaded, System to pressure and temperature
1926 Scheduled Shutdown
Plateaus in delta-P due to inconsistent dust feed, or low char level

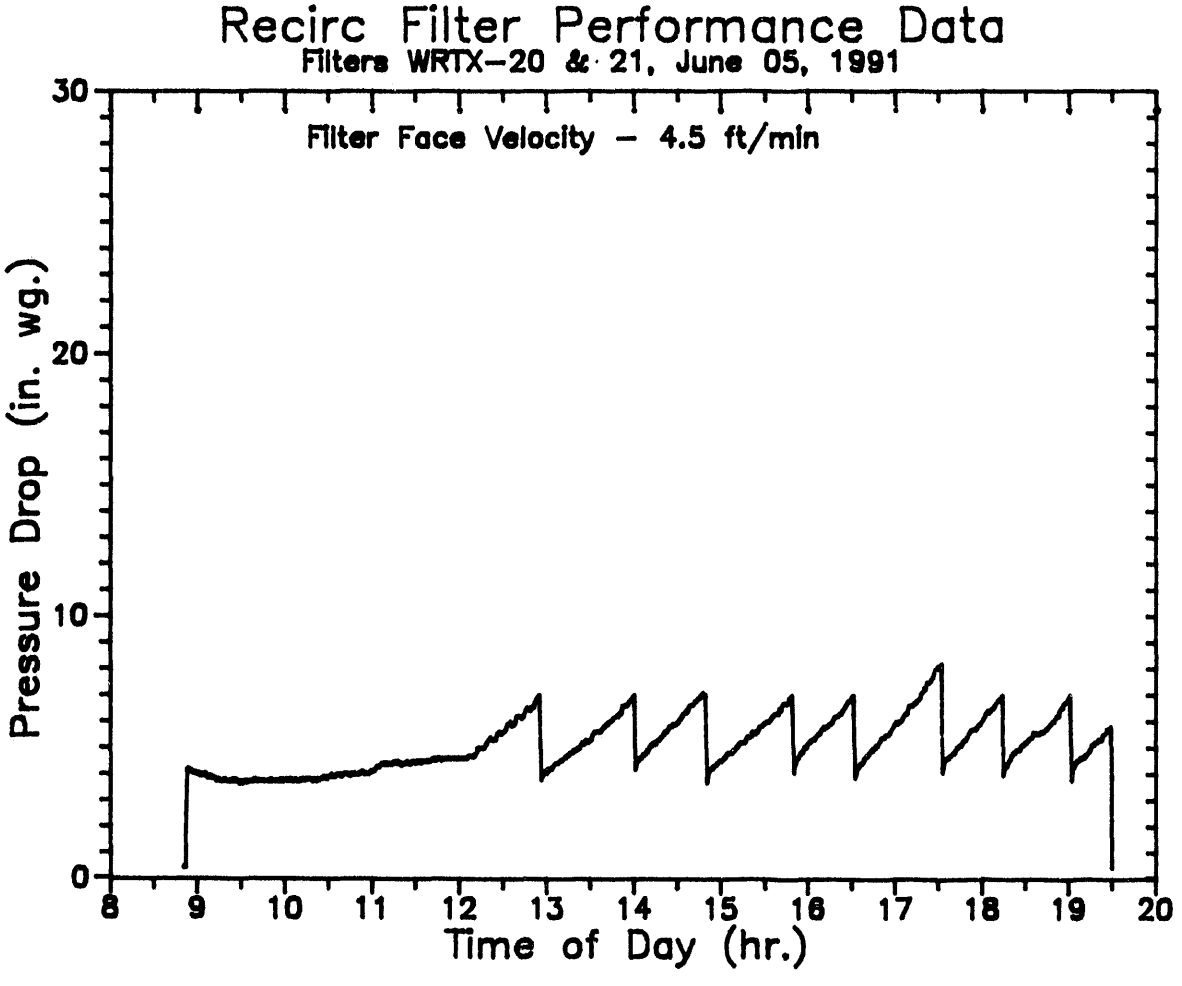

Operation Notes for June 05, 1991
delta-P Trigger = 7 in wc
Pulse Cleaning - 170 psig/0.1 sec
0730 - 0850 System to pressure and temperature
1112 - 1200 Char loaded
1927 Scheduled shutdown
Plateaus in delta-P due to inconsistent dust feed, or low char level

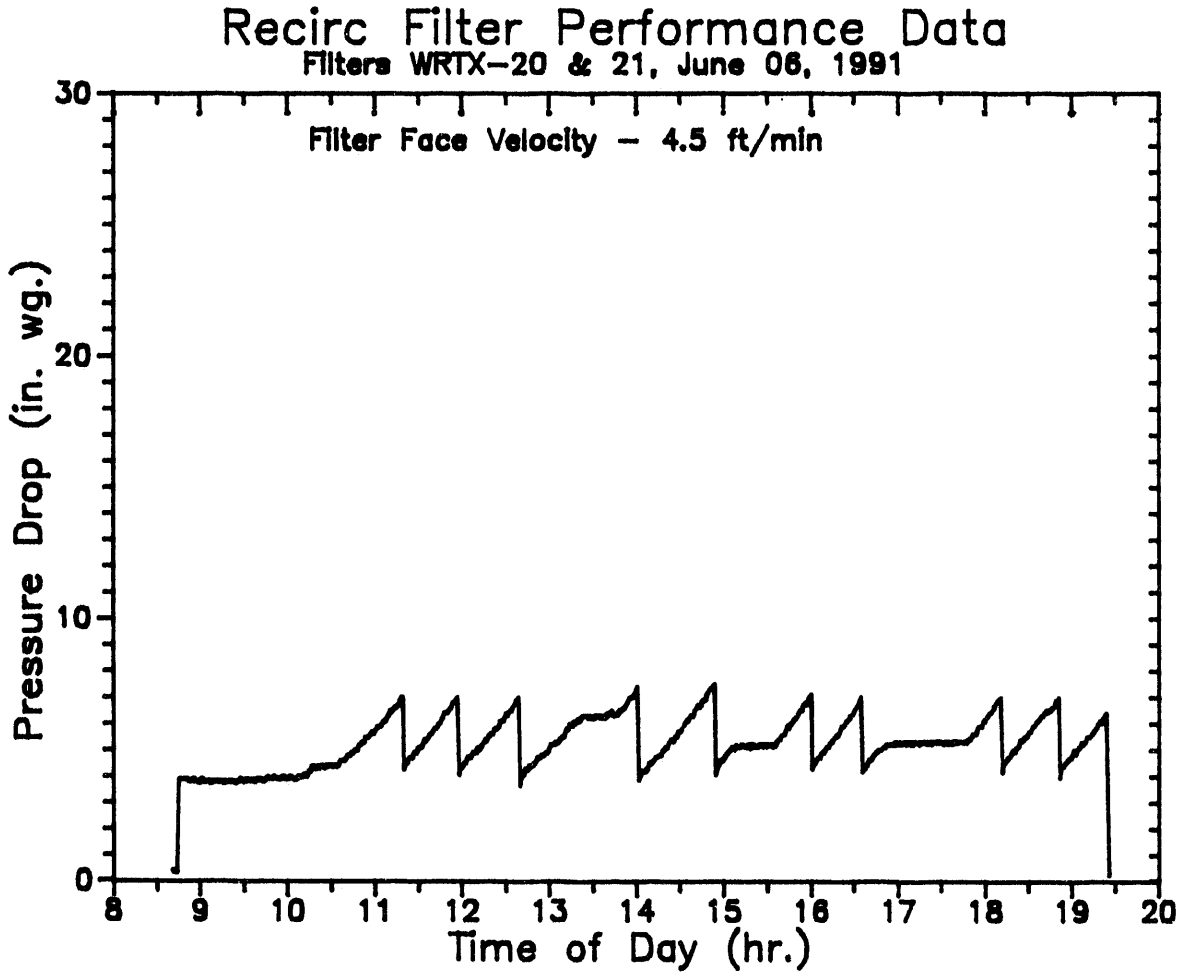

Operation Notes for June 06, 1991
delta-P Trigger = 7 in wc
Pulse Cleaning - 170 psig/0.1 sec
0841 - 1027 Char loaded, System to pressure and temperature
1923 Scheduled Shutdown
Plateaus in delta-P due to inconsistent dust feed, or low char level

APPENDIX I

1. CHARACTERIZATION OF THE ASH AND CHAR FINES USED IN SIMULATOR TESTING

2. CHARACTERIZATION OF ALUMINA/MULLITE FILTERS EXPOSED IN THE WESTINGHOUSE PFBC DURABILITY TEST FACILITY

1. MORPHOLOGY AND SIZE VARIATION OF PROCESS FINES

The morphology of the ash and char fines which were generated at the Exxon and Grimethorpe pressurized fluidized bed combustion (PFBC) facilities, Kellogg Rust-Westinghouse (KRW) fluid bed gasifier, and Texaco entrained bed gasifier are shown in Figures I.1.1 and I.1.2. All fines with the exception of the Exxon ash were collected by ceramic barrier filter systems. Since the Exxon ash was collected by cyclones, the material was pulverized prior to use in the W-HTHP long-term durability test facility. The small particle size distribution was considered to more closely represent fines that would have been carried over and collected by ceramic barrier filters.

The cenosphere formations shown in Figure I.1.1 are typical of ash formed under combustion gas environments. The 10-20 μm cenospheres contain micron and submicron fines which frequently are released during processing. Interdispersed in the Exxon ash are irregularly shaped particles, agglomerates, and infrequently larger (>20 μm) particles. As determined by coulter counter analysis, the 50% mass mean diameter of the pulverized Exxon fines and Grimethorpe filter catch fines is 6.1 and 5μm, respectively (Figure I.1.3).

In contrast with the spherical ash formations are the jagged and irregularly shaped char particles formed in the KRW fluidized bed gasifier (Figure I.1.2). Greater than 97% of the rather nondescript, mottled KRW fines are less than 20 μm. As identified by coulter counter analysis, the 50% mass mean diameter of the KRW filter catch char is 4 μm. Cascade impactor data for fines carried to the filter during testing at KRW were identified to have a drag equivalent diameter of 0.46 μm. Unfortunately we are not able to identify whether the coulter counter sample material is representative of the cascade impactor material.

Exxon

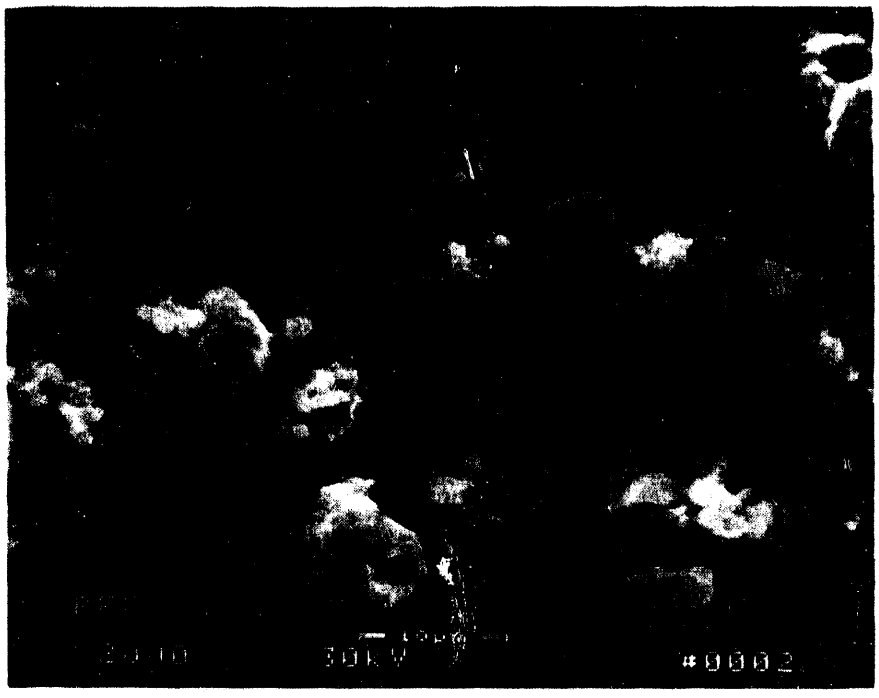

Grimethorpe

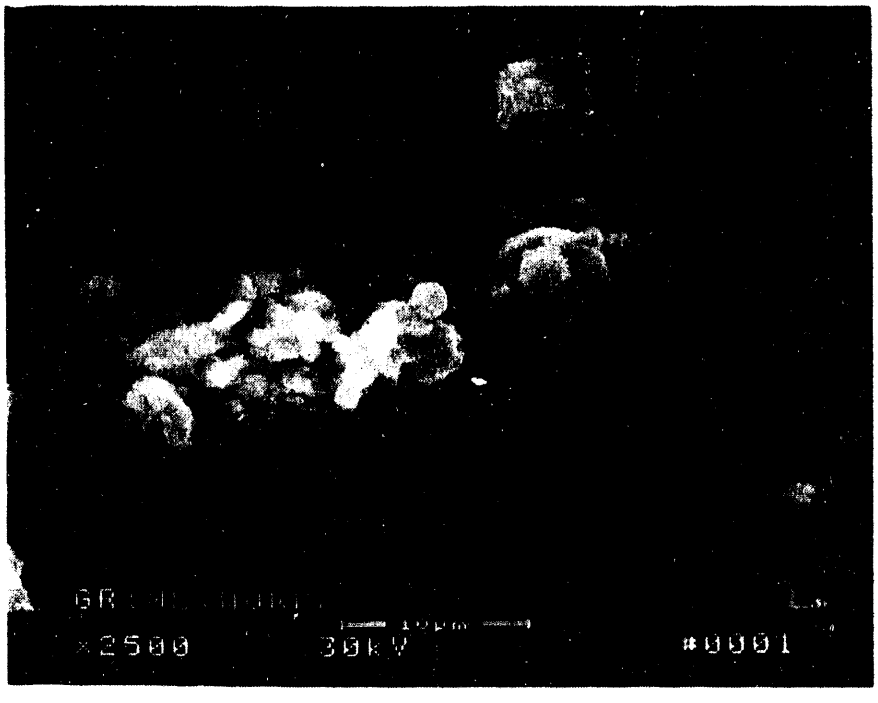

Figure I.1.1 - Scanning Electron Micrographs of the Exxon and Grimethorpe PFBC Ash Fines

KRW

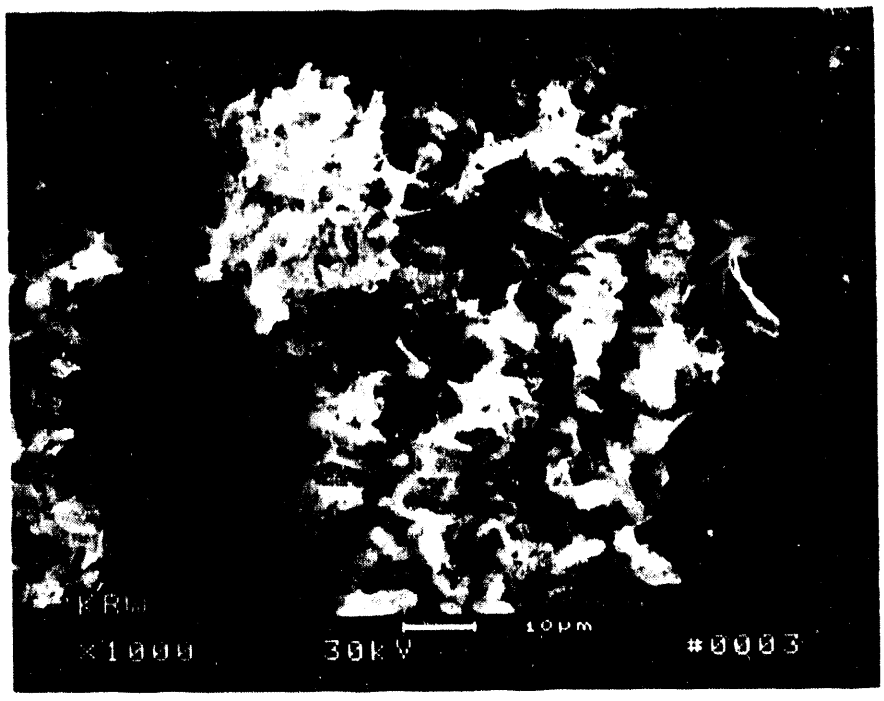

Texaco

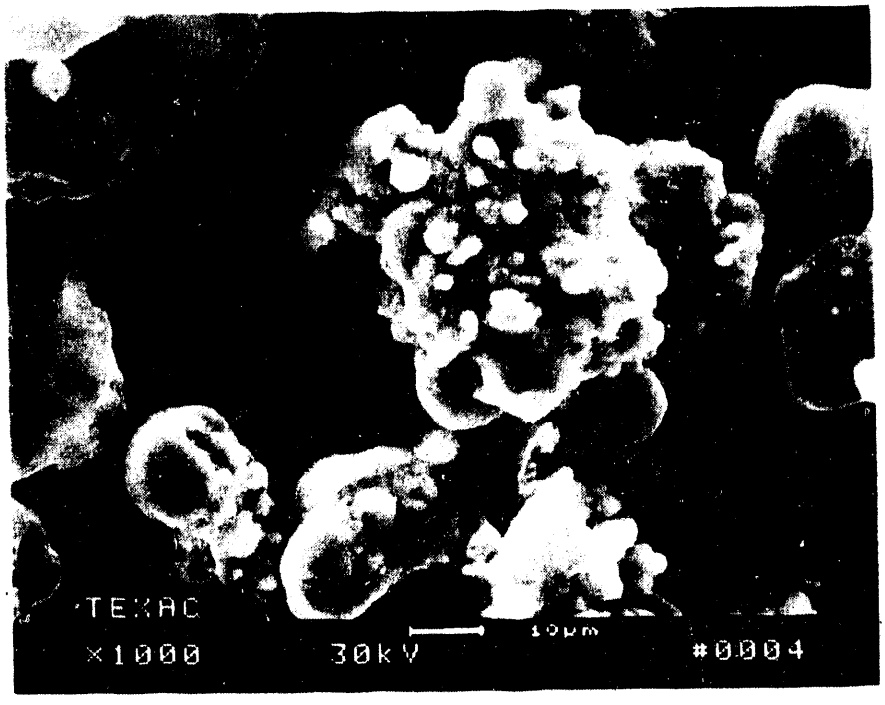

Figure I.1.2 - Scanning Electron Micrographs of the KRW Fluid Bed and Texaco Entrained Bed Gasifier Char Fines.

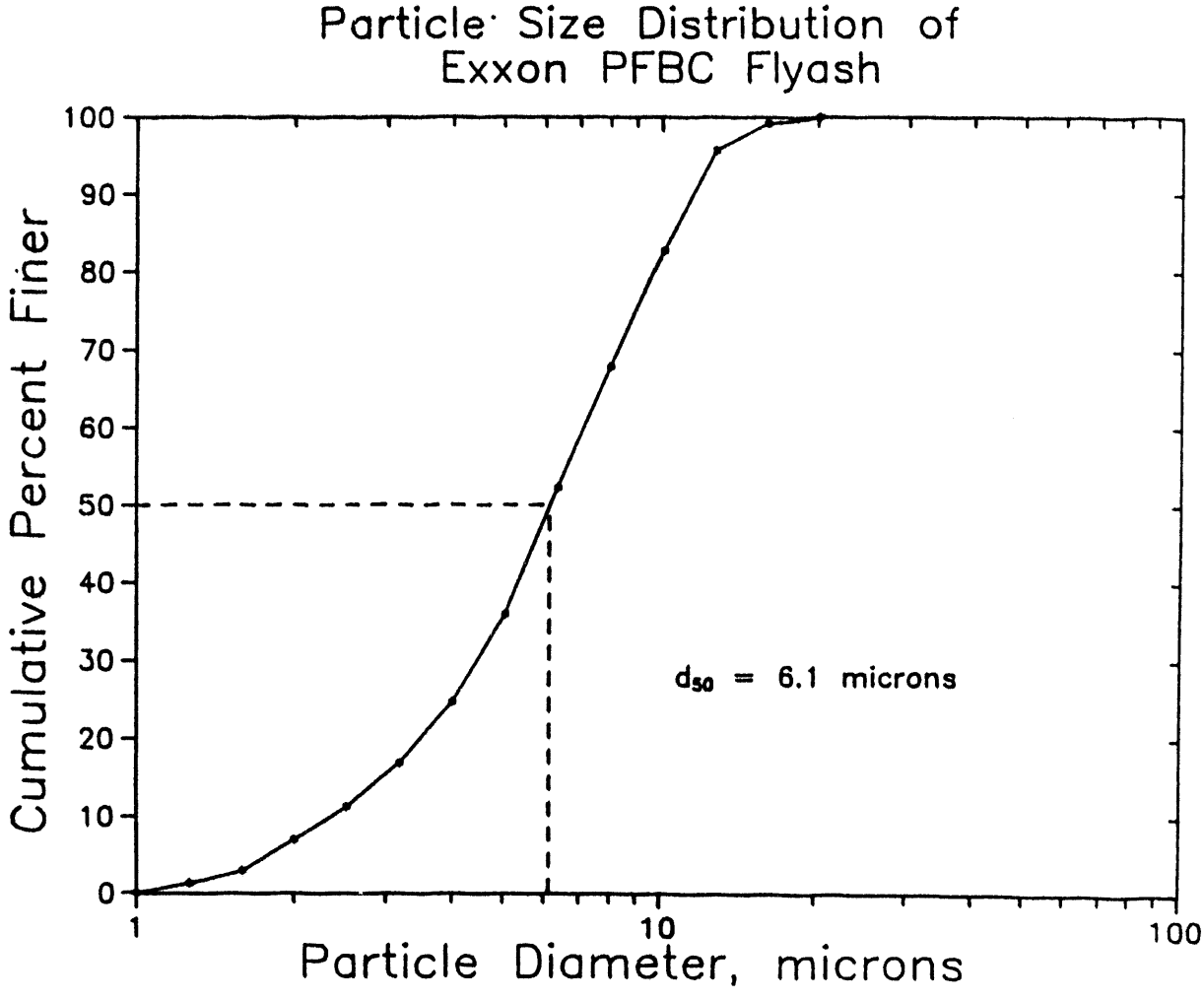

Figure I.1.3a - Ash and Char Particle Size Distribution.

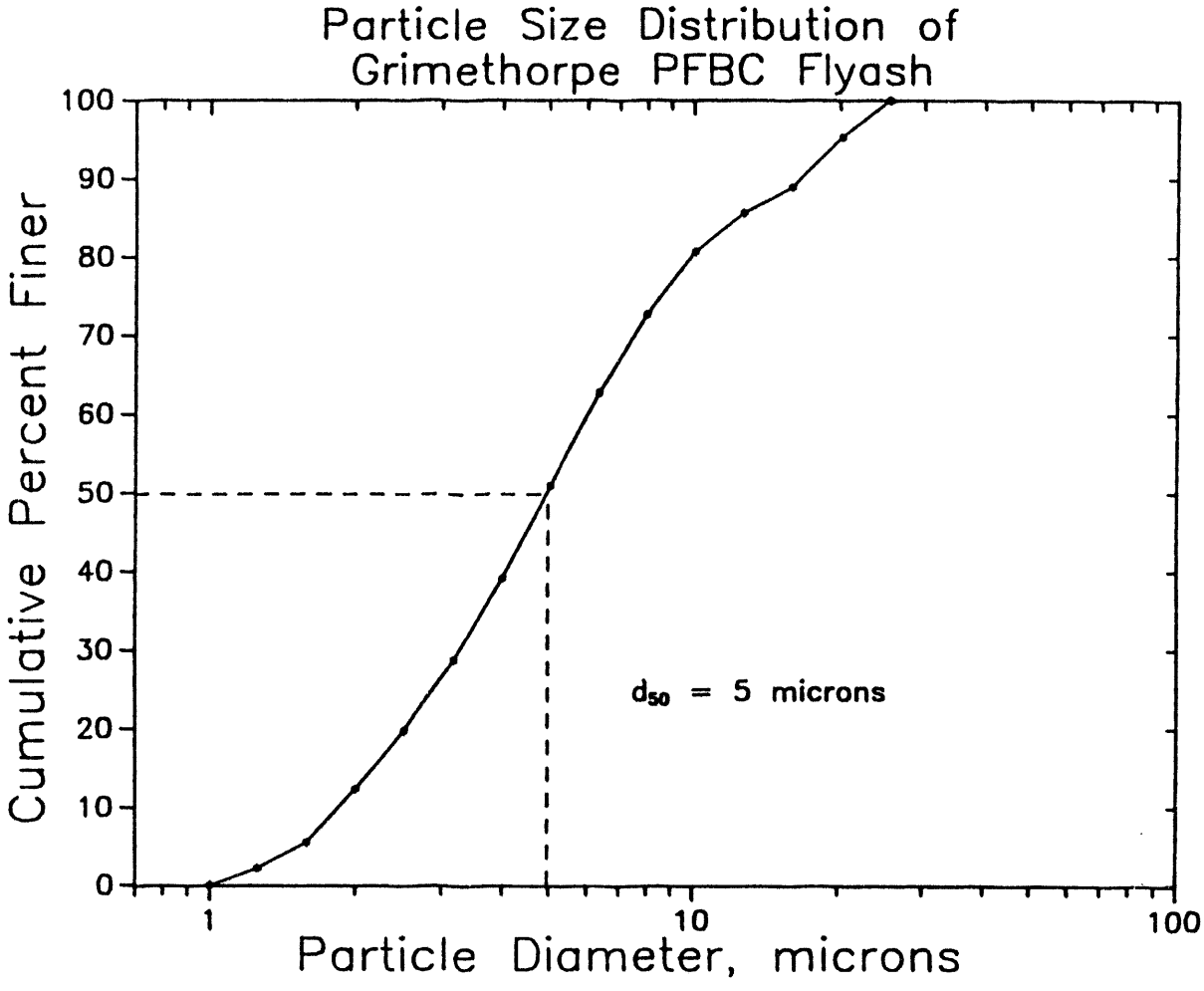

Figure I.1.3b - Ash and Char Particle Size Distribution.

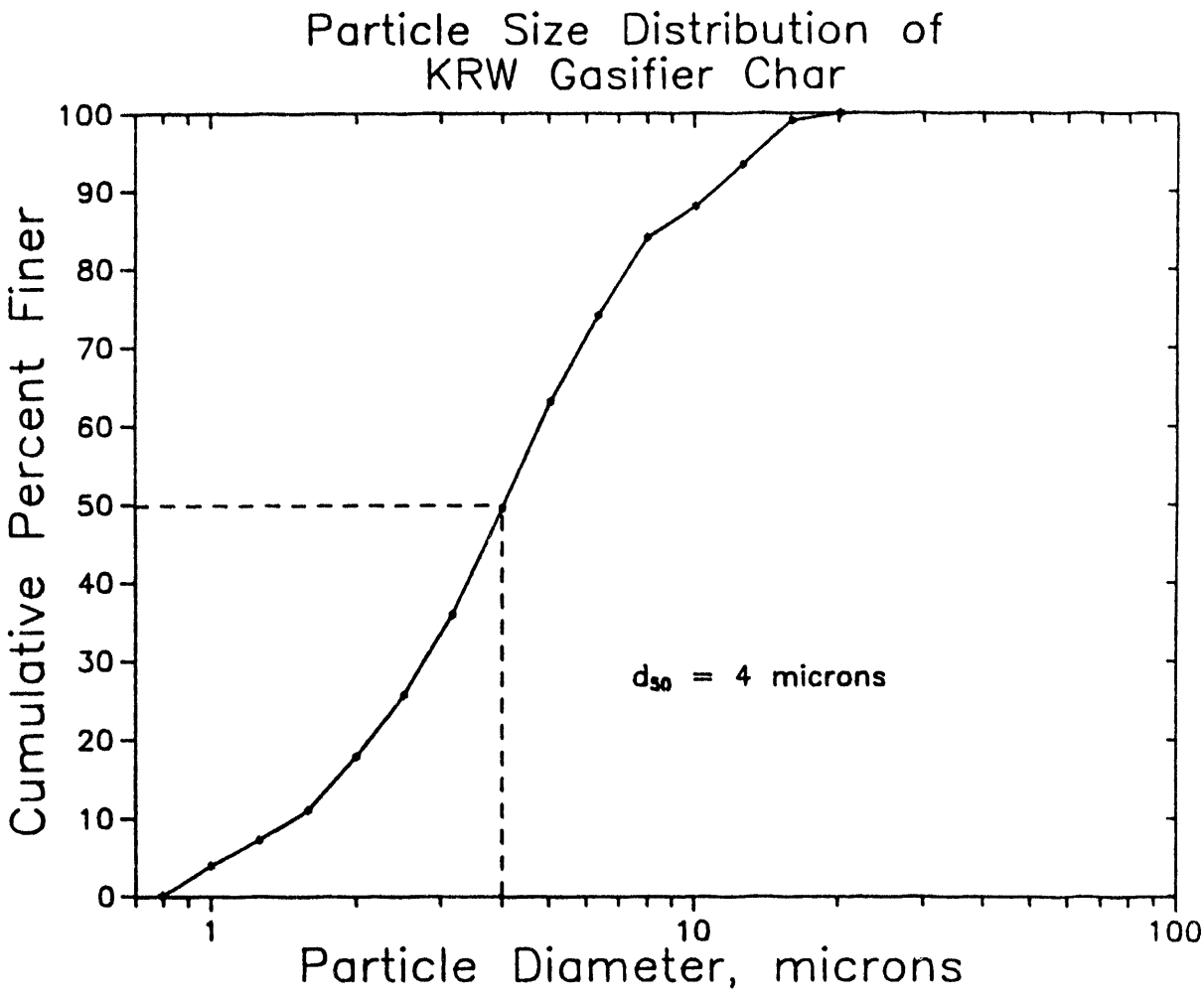

Figure I.1.3c - Ash and Char Particle Size Distribution.

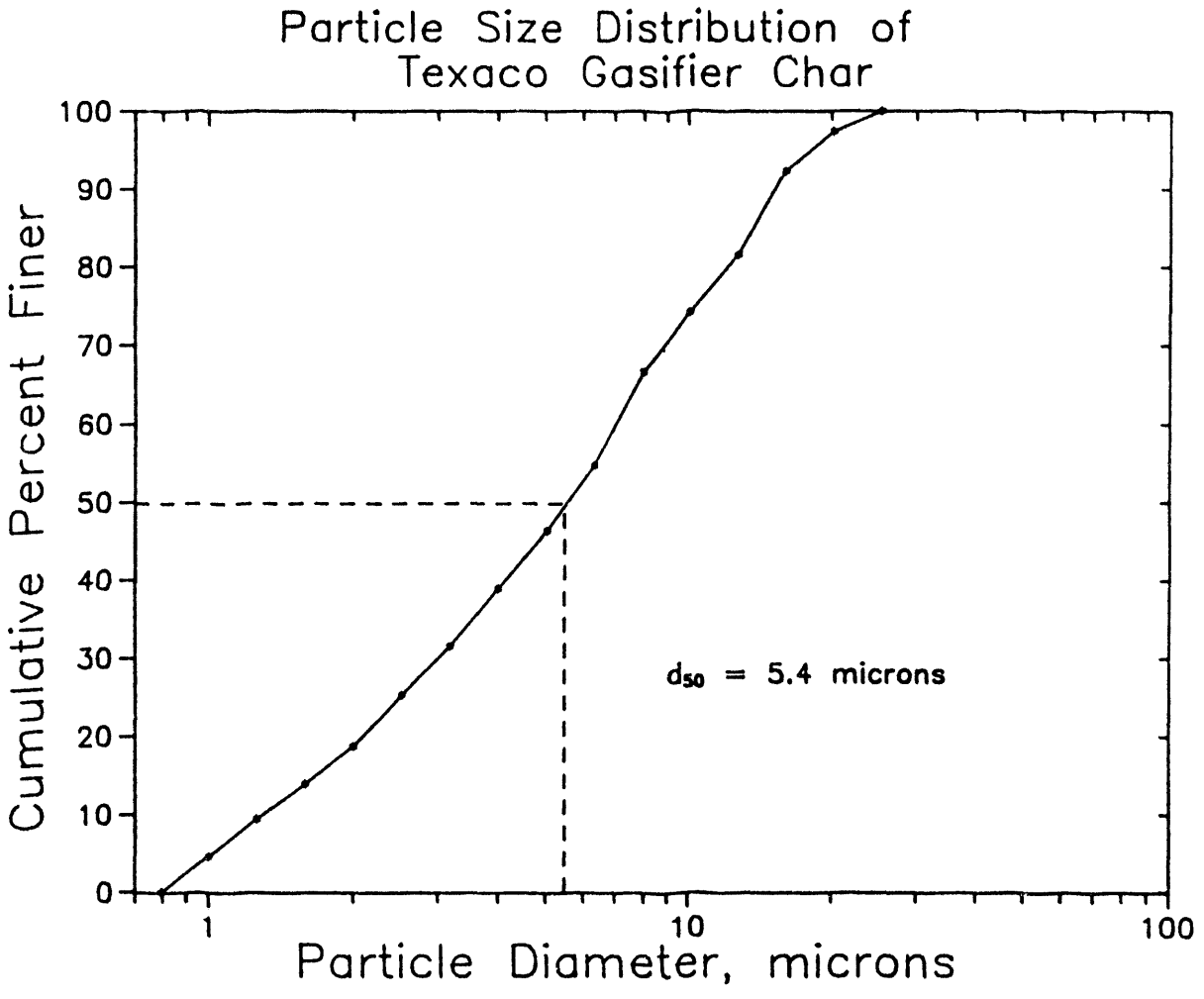

Figure I.1.3d - Ash and Char Particle Size Distribution.

Unlike the KRW gasifier fines, the char formation which results during entrained bed gasification at Texaco is morphologically similar to the ash fines formed under PFBC conditions. Cenosphere formations and agglomerates can be identified in the Texaco fines, as well as submicron fines and particles which exceed 20 μm in diameter. The 50% mass mean diameter of the Texaco filter catch material is 5.3 μm. Again the mass mean diameter is based on coulter counter analysis.

2. CHARACTERIZATION OF ALUMINA/MULLITE FILTERS EXPOSED IN THE WESTINGHOUSE PFBC DURABILITY TEST FACILITY

Sections from an alumina/mullite filter (WRTX-1) which had been exposed for 366 hours in the Westinghouse HTHP (high temperature, high pressure) durability test facility were removed for characterization. This filter had experienced temperatures of 815-843°C (1500-1550°F), pressures of 50-150 psi, and 1500-4400 ppm loadings of Exxon ash, simulating pressurized fluidized bed combustion conditions (6% O_2, 73% N_2, 14% H_2O, 7% CO_2). Testing of this filter was terminated when a crack developed horizontally, near the thick mid-ribbed bond support section. An uneven crack line resulted, traversing all of the clean and dirty gas channels.

Sections were also removed from an alumina/mullite filter (WRTX-10) which had been exposed for approximately 1300 hours in the Westinghouse HTHP durability test facility. This filter had experienced temperatures of 815-870°C (1500-1600°F), pressures of 70 psi, and 1000 ppm loadings of dust fines. Exxon ash fines were used during the first 1188 hours of filtration, while Grimethorpe ash was used during the later part of the test. Testing of this filter was terminated when dust outlet loadings exceeded 149 ppm. Although the filter had not delaminated during operation, a break was evident across the entire length of the flange section.

Figures I.2.1 and I.2.2 illustrate the cross-sectional morphology of the alumina/mullite filter matrix near the dirty gas channel surface. Neither accumulation of fines within the surface pores, nor significant penetration of fines which fill or "plug" internal pores or interconnecting channels are evident in either of these filters. Since both filters had been fabricated in the same

Westinghouse PFBC Test Facility

Filter WRTX-1 - 366 Hours

SEM

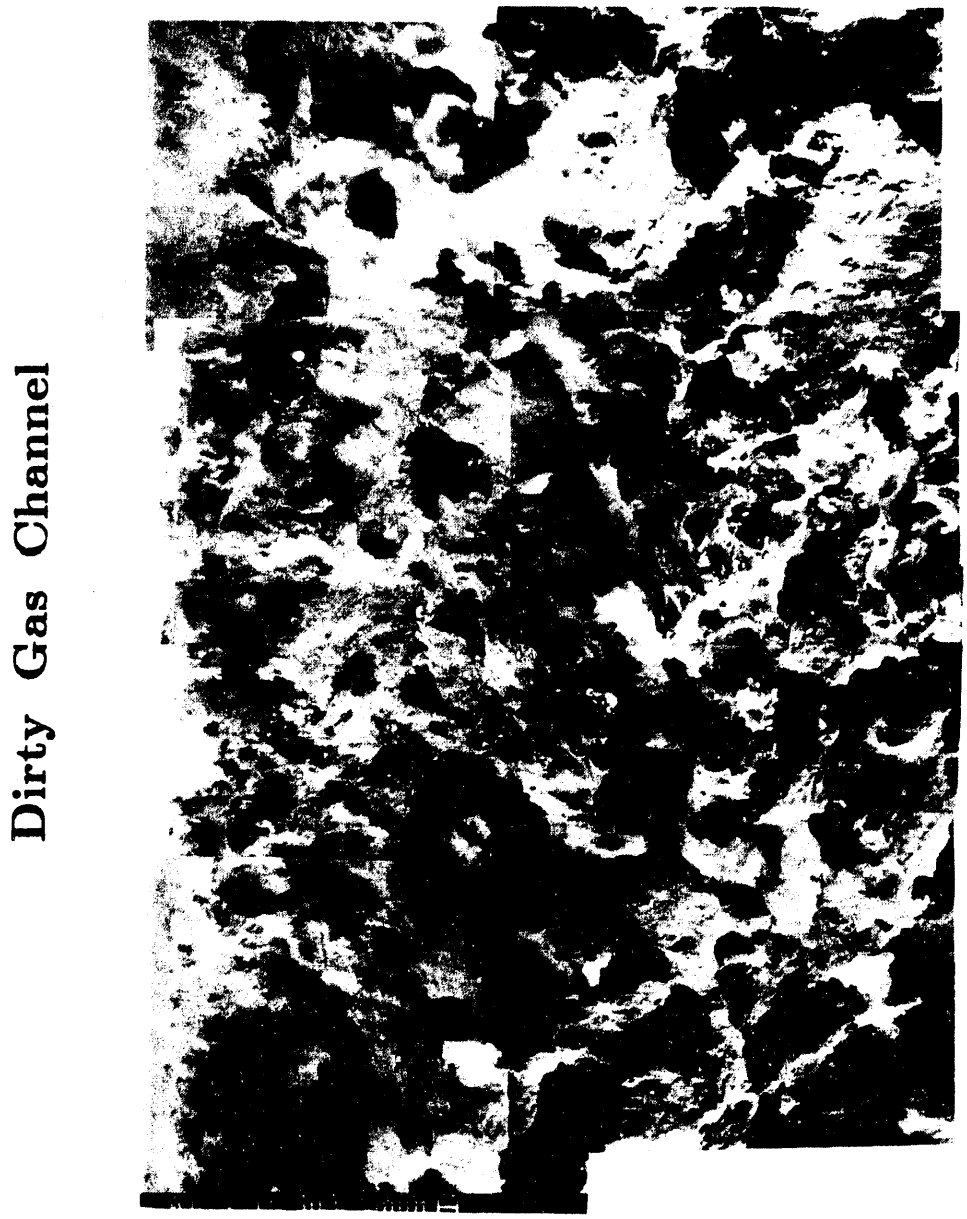

Figure I.2.1 - Scanning Electron Micrograph Illustrating Depth of Fines Penetration Along the Dirty Gas Channel of an Alumina/ Mullite Filter Which Had Experienced 366 Hours of Operation in the Westinghouse PFBC Durability Test Facility

Westinghouse PFBC Test Facility

Filter WRTX-10 - 1300 Hours

SEM

Figure I.2.2 - Scanning Electron Micrograph Illustrating Depth of Fines Penetration Along the Dirty Gas Channel of an Alumina/ Mullite Filter Which Had Experienced 1300 Hours of Operation in the Westinghouse PFBC Durability Test Facility

filter lot, porosity appears to be relatively similar. Both filters appear to contain a uniform pore size, and do not contain large (i.e., 300-500 μm) voids. The relatively high conditioned permeability of both filters (WRTX-1 = 27%; WRTX-10 = 27%) reflects the absence of fines and subsequently negligible surface pore closure after 366 or 1300 hours of exposure to simulated PFBC test conditions.

An alternate scanning electron microscope was used to more clearly identify the morphology of the alumina/mullite filter matrix after 366 and 1300 hours of exposure in the simulated PFBC environment, as well as the possible location for adherence of fines. Figure I.2.3 illustrates the cross-sectioned morphology of the 366 hour filter plate, near the dirty channel surface, while Figure I.2.4 illustrates the morphology of the 1300 hour filter plate. Intermittent in both materials are mullite rod-like formations embedded in the "amorphous" phase. Fines in both filter matrices adhere to the "amorphous" pore cavity wall. Pore plugging was not observed in either filter. Fines are identified to contain silicon, calcium, magnesium, and iron.

The actual surface of the alumina/mullite dirty gas channel from the 1300 hour exposed filter was characterized, and is shown in Figure I.2.5. Note the relative abundance of "blunted" crystals which are considered to be the ends of the mullite rods which are embedded in the "amorphous" phase. After 1300 hours in the simulated PFBC environment, the dirty channel surface "amorphous" phase is retained, while mullite appears to be surfacing.

After 1300 hours of exposure in the simulated PFBC test environment, the majority of the edges along the dirty gas filter channels, close to where the Eremco paint is applied at the seams, appear to have been removed. One last analysis was attempted along these regions to identify possible changes in the filter matrix which may have attributed to cracking or erosion of the matrix. The matrix

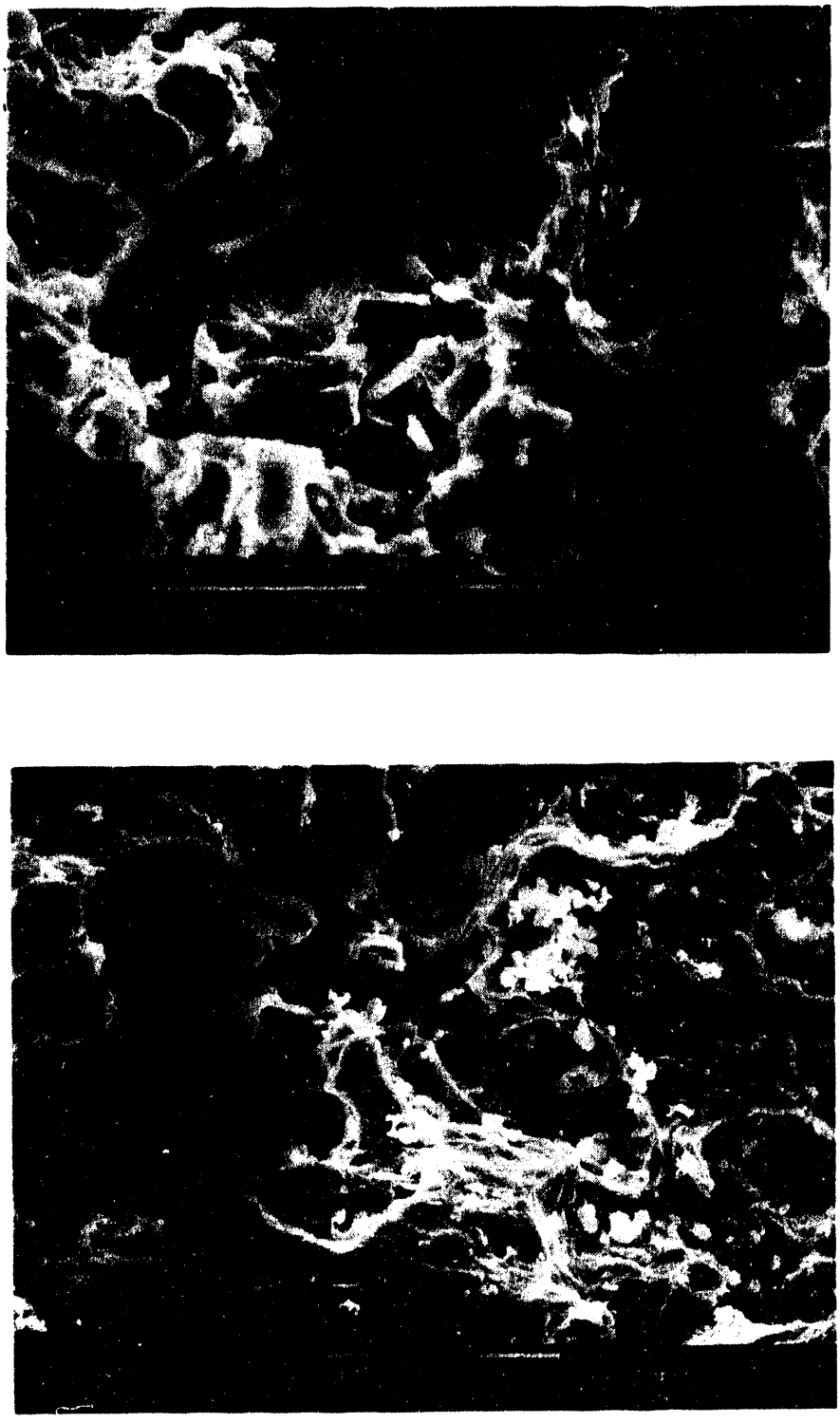

Figure I.2.3a - Scanning Electron Micrographs Illustrating the Morphology of the Alumina/Mullite Filter Matrix After 366 Hours of Exposure in the Westinghouse PFBC Durability Test Facility

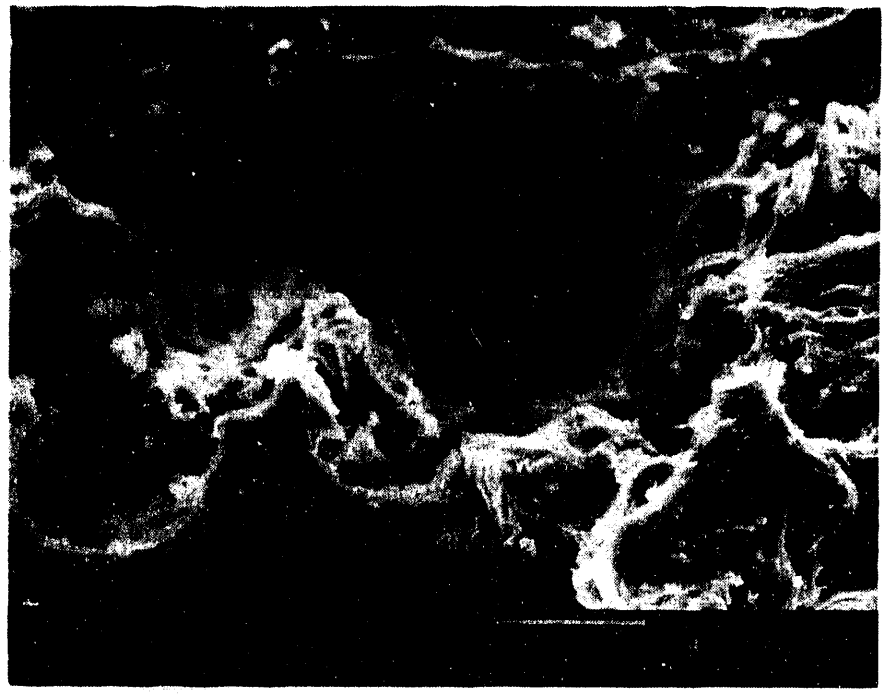

Figure I.2.3b - Scanning Electron Micrograph Illustrating the Morphology of the Alumina/Mullite Filter Matrix After 366 Hours of Exposure in the Westinghouse PFBC Durability Test Facility

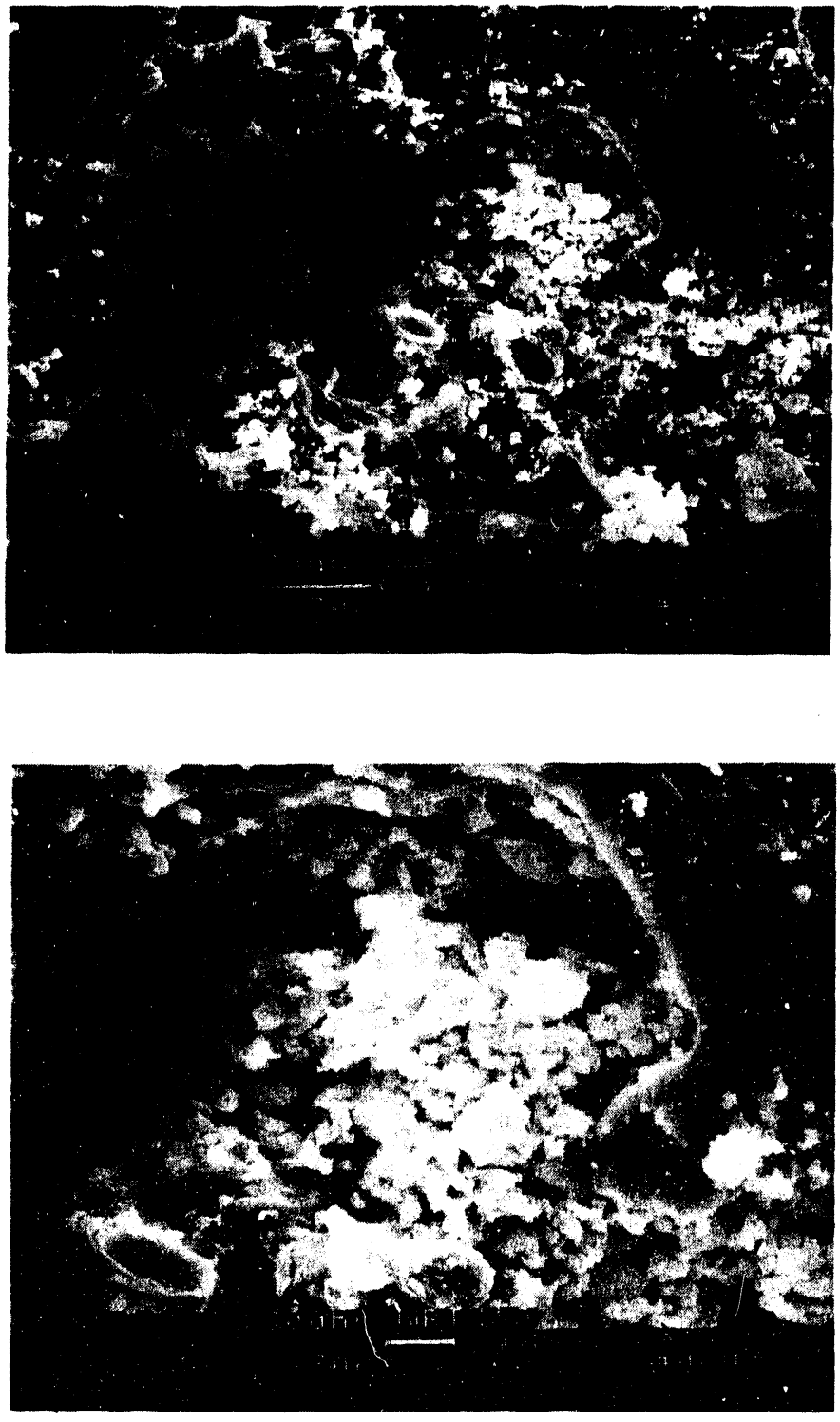

Figure I.2.4a - Scanning Electron Micrographs Illustrating the Morphology of the Alumina/Mullite Filter Matrix After 1300 Hours of Exposure in the Westinghouse PFBC Durability Test Facility

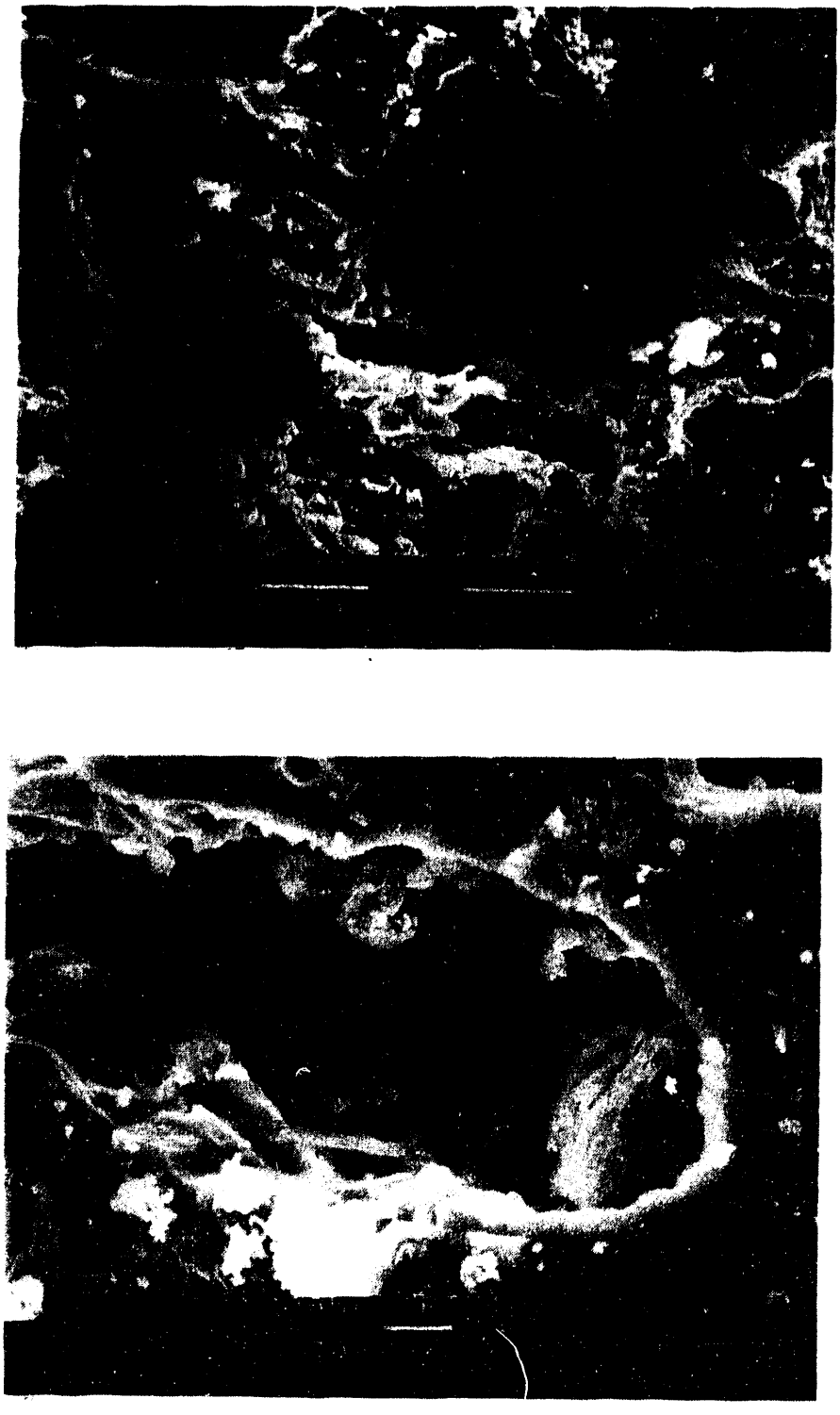

Figure I.2.4b - Scanning Electron Micrographs Illustrating the Morphology of the Alumina/Mullite Filter Matrix After 1300 Hours of Exposure in the Westinghouse PFBC Durability Test Facility

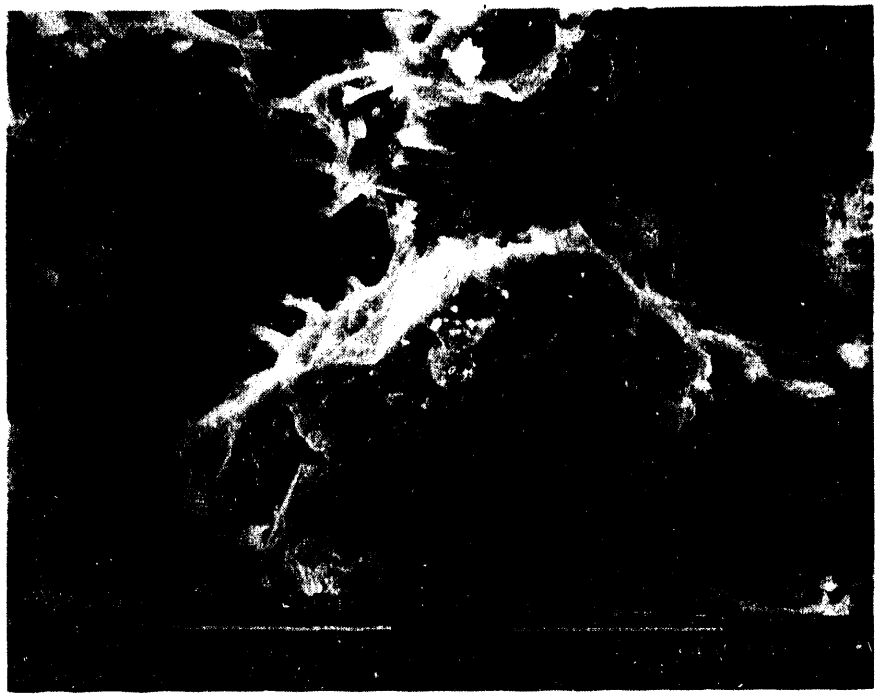

Figure I.2.4c - Scanning Electron Micrograph Illustrating the Morphology of the Alumina/Mullite Filter Matrix After 1300 Hours of Exposure in the Westinghouse PFBC Durability Test Facility

Figure I.2.5 - Surface Morphology of the 1300 Hour PFBC Exposed Alumina/Mullite Filter Dirty Gas Channel

morphology is comparable with that of sections removed from various locations within the filter. At this time we feel that either cracking of the Aremco paint has occurred, pulling with it a portion of the underlying matrix, or that after long term exposure to dust fines, erosion at the sharp corners of the dirty channels may have occurred. Further effort will be necessary to resolve this issue.

Additional characterization of the 1300 hour exposed alumina/mullite filter will include strength testing along both the filter flange, as well as within the webbed section, similar to the work conducted by Argonne on the Texaco exposed filters. Data will be compared with as-fabricated material strength.

APPENDIX J

DESCRIPTION OF CROSS FLOW FILTER DURABILITY DURING PFBC SIMULATOR THERMAL TRANSIENT TESTING

THERMAL TRANSIENT TESTS

The existing gas-fired HTHP (high temperature, high pressure) pressurized fluidized bed combustor (PFBC) simulator filter test loop was used in this series of tests to demonstrate whether cross flow filter elements can withstand heat-up and cool-down system transients, similar to those projected for a PFBC plant. In the first thermal transient test, four cross flow filters (WRTX-48 and WRTX-53 were fabricated in April 1990, and had been used in prior durability testing; WRTX-66 and WRTX-70 were fabricated in September 1990, and were only used in this segment of testing) were subjected to 900 lb/hr gas flow, 165 psia pressure, and temperatures of 1550°F. Simulated turbine trip transients were accomplished by:

- Turning off the fuel flow to the combustor
- Dropping the pressure from 165 psia to 15 psia
- Increasing the gas flow to 1100 lb/hr.

Cross flow filters WRTX-48 and WRTX-53 acquired a total of 335 hours of testing with 472 pulse cycles, two mild and one severe transient, using Grimethorpe dust[a] (see Appendix B) prior to detection of a 25 ppm dust outlet loading. Alternately cross flow filters WRTX-66 and WRTX-70 acquired a total of 38 hours of testing, 3 pulse cleaning cycles, prior to detection of the dust outlet loading increase. Based on the outlet dust loadings throughout the test, all four cross flow filters were considered to be intact up to the time of the severe

a. Two different Grimethorpe dust compositions were used in the initial turbine trip transient test. The compositional differences of the dust generally include variation in the iron and sorbent content, as related to the processing conditions (i.e., coal feed and sorbent used) at Grimethorpe. In the second turbine trip test, as well as the heat-up transient test, the lower iron content Grimethorpe ash was used. The lower iron content ash is representative of the dust previously used in the long-term durability studies, where 1800 hours of operating life was demonstrated for two cross flow filter elements. These two cross flow filters were fabricated at the vendor site in February 1989. A comparison of the various Grimethorpe dust compositions, and their influence on filter cleaning will be provided in the next Quarterly Report.

transient event. After system shutdown and removal of the filters, all four filters were observed to have developed partial or complete delamination cracks. A description of each filter after testing, including the location of the various cracks or delaminations, and their relation to filter position within the HTHP vessel are provided in Section 1.

After a step-wise (Runge-Kutta method) dynamic mass and energy balance was performed to project the temperature versus time profile of the gas in the filter vessel during the simulated turbine trip transient, we concluded that the initial four cross flow filters were subjected to more severe conditions than those projected to occur at a PFBC plant (Figure J.1). In an attempt to subject the cross flow filters to a more representative set of test conditions, four new cross flow filters were selected and installed in the Westinghouse HTHP test facility (WRTX-76, WRTX-77, WRTX-78, and WRTX-81; October 1990 fabrication lot). Test conditions again included exposure of the cross flow filters to 900 lb/hr gas flow, 165 psia, and temperatures of 1550°F. In this test turbine transients were simulated by:

- Turning off the flow to the combustor
- Immediately reducing the gas flow to 400 lb/hr
- Ramping pressure from 165 psia to 110 psia over the first 100 sec
- At t = 100 sec, reducing flow to 300 lb/hr
- Ramping pressure from 110 to 55 psia over the next 100 sec
- At t = 200 sec, reducing flow to 100 lb/hr
- Ramping pressure to 20 psia over the next 400 sec.

After 320 hours of testing, including 10 simulated turbine trip transients (Appendix E), approximately 11 ppm of the Grimethorpe dust was detected in the outlet gas loading. Inspection of the filters after cool-down of the system indicated that three of the four cross flow filters remained intact, and only one filter (WRTX-81) had developed both a partial and complete delamination crack. A description of the location of these cracks within the filter, as well as the position of the filter within the HTHP vessel are provided in Section 2.

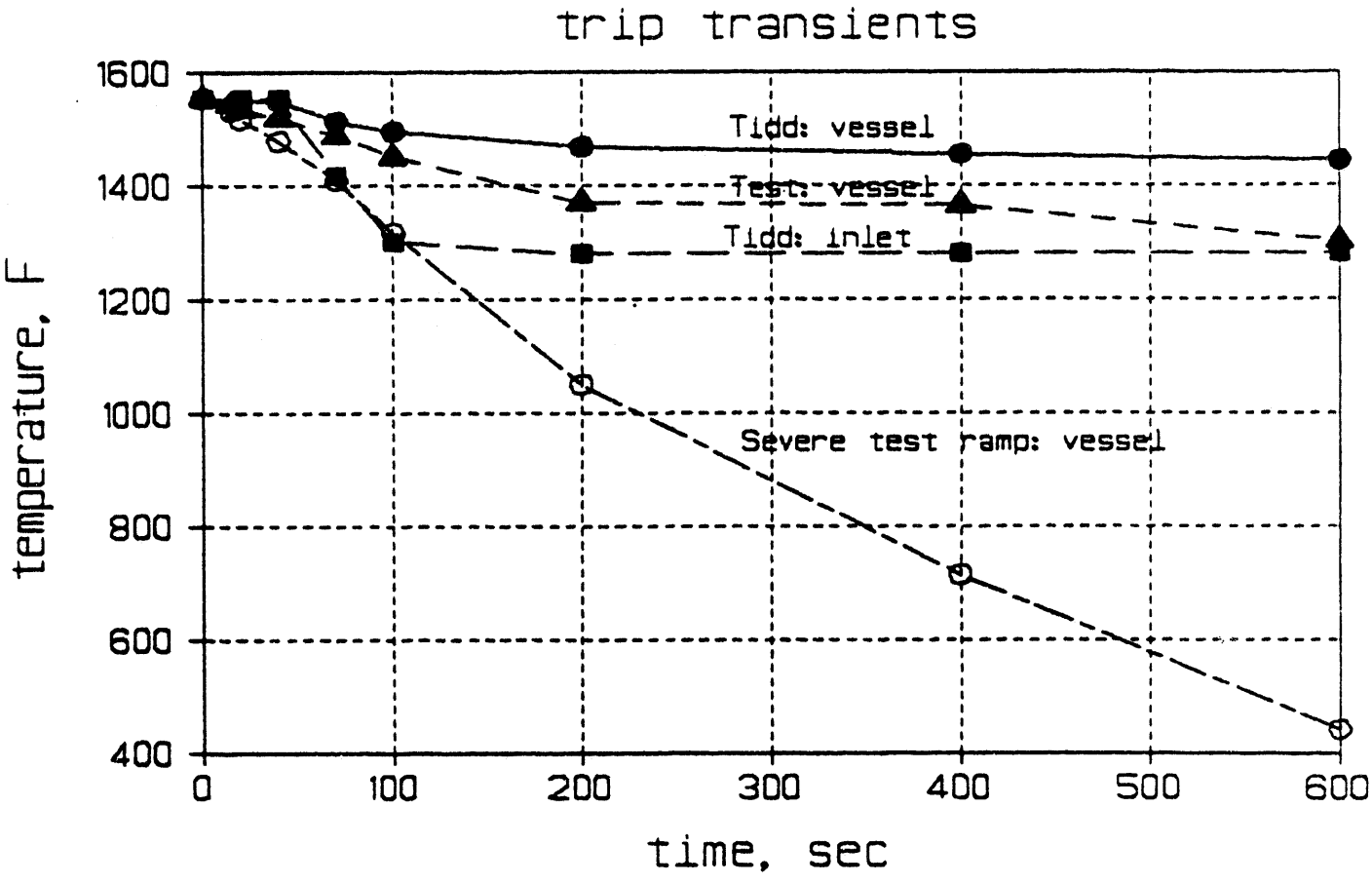

Figure J.1 - Projected Gas Temperature Versus Time Profiles in the Filter Vessel During a Turbine Trip Transient

Once again, after review of the actual gas temperature versus time profile that resulted in the filter vessel during this test, we concluded that the cross flow filters were again subjected to more severe turbine trip transient conditions in the HTHP facility than would be projected to occur for a PFBC plant.

A third test was performed in the HTHP test facility to simulate the filter heat-up cycle that is anticipated at a PFBC plant. The three intact cross flow filters from the second turbine trip transient test, and one new filter (WRTX-80; October fabrication lot) were subjected to 1100 lb/hr gas flow, 69 psia pressure, and temperatures of 950°F. The simulated heat-up transients consisted of ramping the combustor temperature 90 times, such that the inlet temperature rises to 1250°F in 150 sec (Appendix D). Under these conditions, the vessel temperature was expected to reach 1050°F, as expected at a PFBC plant (Figure J.2). After 191 hours of testing, including 90 heat-up cycles, a dust leak of approximately 14 ppm was detected. Inspection of the filters after cool-down indicated that again, the original three filters (WRTX-76, WRTX-77, and WRTX-78) which survived the second turbine trip transient series remained intact during the course of heat-up testing, and only one filter (WRTX-80), which was most recently installed, developed a partial delamination crack. A description of the location of the partial delamination within the filter, as well as the position of the filter within the HTHP vessel are provided in Section 3.

Table J.1 provides an abbreviated summary of these three system transient tests, and the status of each cross flow filter as described above.

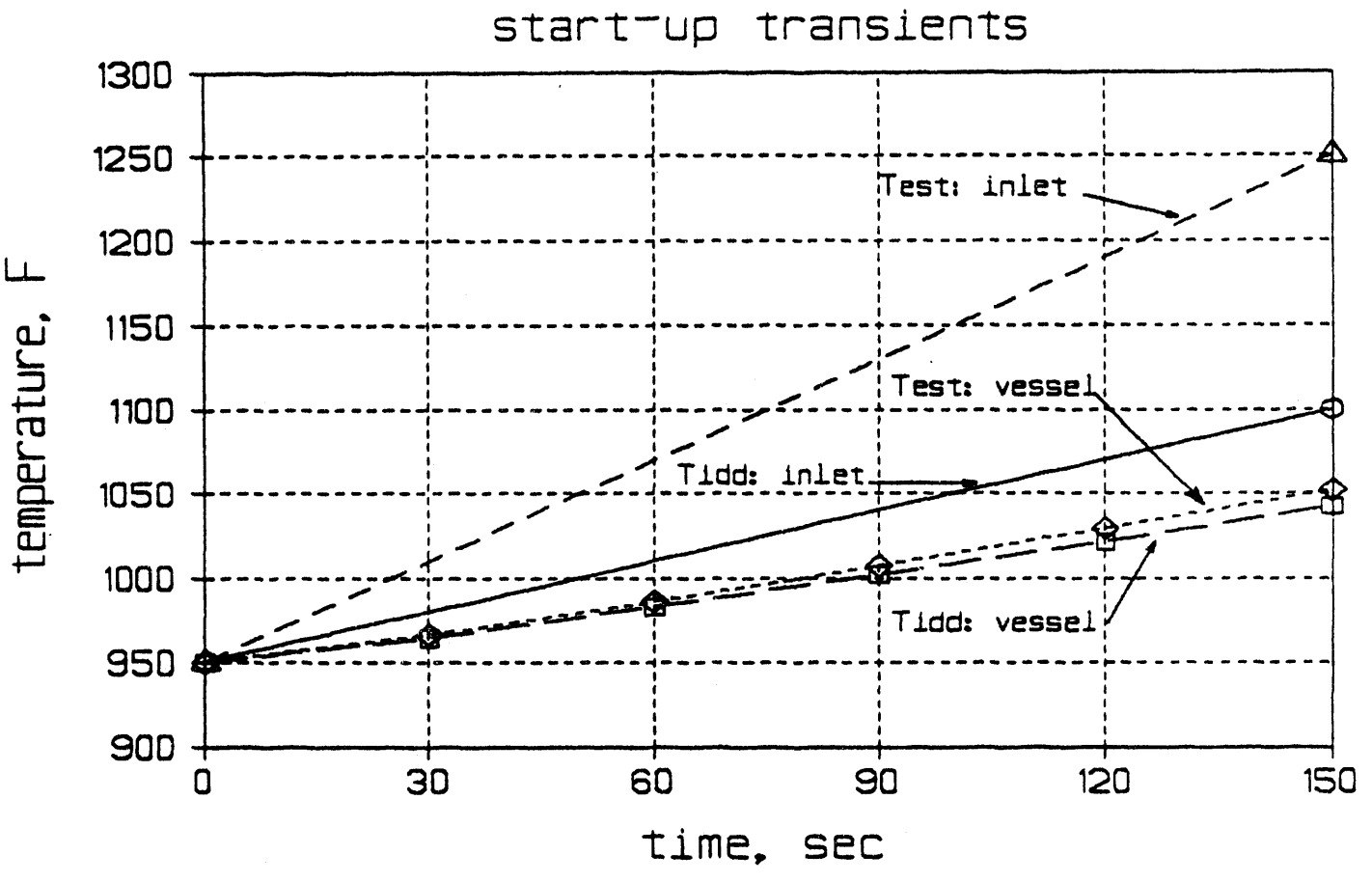

Figure J.2 - Projected Gas Temperature Versus Time Profile in the Filter Vessel During a Startup Transient

TABLE J.1

SUMMARY OF THERMAL TRANSIENT TESTING

Test	Simulation Conditions	Filter Designation Location	Fabrication Lot Date	Comment
1	Turbine Trip: 2 Mild; 1 Severe Transient; 335 Hrs For WRTX-48 & WRTX-53; 38 Hrs For WRTX-70 & WRTX-66	WRTX-48 P1T	April 90	Partial Delam
		WRTX-53 P1B	April 90	Partial Delam Complete Delam
		WRTX-70 P2T	Sept 90	Hairline Crack Side Wall Crack
		WRTX-66 P2B	Sept 90	Horizontal Crack
2	Turbine Trip: 320 Hrs; 10 Transients	WRTX-77 P1T	Oct 90	Intact
		WRTX-78 P1B	Oct 90	Intact
		WRTX-81 P2T	Oct 90	2 Complete Delam
		WRTX-76 P2B	Oct 90	Intact
3	Heat-Up Cycles: 191 Hrs; 90 Heat-Up Transients	WRTX-77 P1T	Oct 90	Intact
		WRTX-78 P1B	Oct 90	Intact
		WRTX-80 P2T	Oct 90	Partial Crack
		WRTX-76 P2B	Oct 90	Intact

1. SEVERE TURBINE TRIP TRANSIENT TEST

Cross Flow Filter WRTX-48, Figures J.3 and J.4

The cross flow filter designated as WRTX-48 was located in the top holder of plenum #1 during the initial simulated turbine trip transient test. After 335 hours of testing at 1550°F with 472 pulse cycles, 2 mild transients, and 1 severe transient, a dirty gas channel delamination crack occurred in WRTX-48. The delamination crack was located at the 12th dirty gas channel (Figure J.3), farthest from the plenum. The twelfth and thirteenth channels were not identically matched along the mid-rib bond, particularly at the top closed section of the filter element. The fourteenth through eighteenth dirty channels had "near perfect" alignment between mid-rib bonds.

The delamination crack which may have started at the top closed section of the filter appeared to have traveled along the mid-rib bond section of the dirty channels until it reached the thicker central bond section. At that point, the crack cut through the dirty channel wall (not through the thicker central bond section), and ran along the clean-to-clean channel seam for approximately two inches. The delamination crack appeared to have stopped at approximately three dirty channels above the flange area, initially keeping the entire filter body intact. These comments describe the delamination crack that ran along the filter face that was opposite from the baffle plate which separated the two filter plenums (Side A). Due to the thick AREMCO paint along the face of the filter which was closest to the baffle plate, several areas of the crack path could not be followed (Side B).

The delamination crack along Side A was identified to have occurred in the portion of the filter element which contained wider dirty channels. Wider dirty gas channels are considered to represent the top section of the filter plate stack, adjacent to where weights are applied during filter element production. Alternately, the delamination crack along Side B appeared to have occurred in the tighter dirty

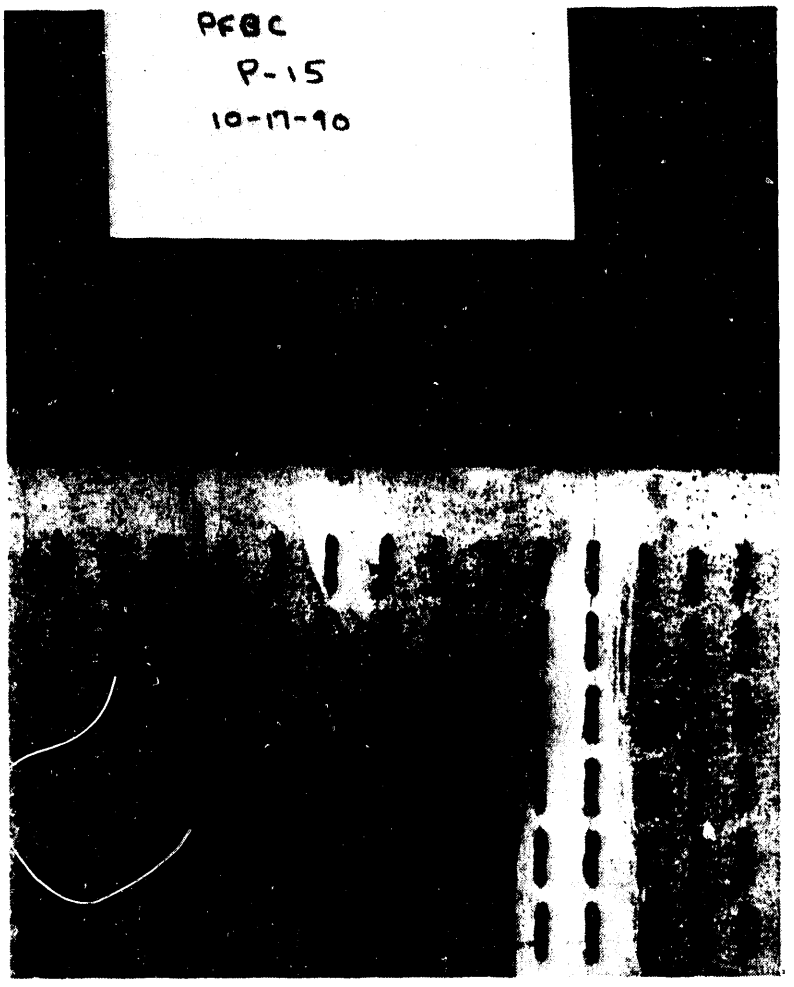

Dirty Channel Column Number

ROW	1	2	3	4	5	6	7	8	9	10	11	12	13	14	15	16	17	18
1	0	0	0	0	0	0	0	0	0	0	0	0	0	0	0	0	0	0
2	0	0	0	0	0	0	0	0	0	0	0	0	0	0	0	0	0	0
3	0	0	0	0	0	0	0	0	0	0	0	0	0	0	0	0	0	0
4	0	0	0	0	0	0	0	0	0	0	0	0	0	0	0	0	0	0
5	0	0	0	0	0	0	0	0	0	0	0	0	0	0	0	0	0	0
6	0	0	0	0	0	0	0	0	0	0	0	0	0	0	0	0	0	0
7	0	0	0	0	0	0	0	0	0	0	0	0	0	0	0	0	0	0
8	0	0	0	0	0	0	0	0	0	0	0	0	0	0	0	0	0	0
9	0	0	0	0	0	0	0	0	0	0	0	0	0	0	0	0	0	0
10	0	0	0	0	0	0	0	0	0	0	0	0	0	0	0	0	0	0
11	0	0	0	0	0	0	0	0	0	0	0	0	0	0	0	0	0	0
12	0	0	0	0	0	0	0	0	0	0	0	0	0	0	0	0	0	0

PLENUM

WEIGHTED * END * *

Bolt No. 1 2 3 4 5 6 7

Figure J.3 - Dirty Gas Channel Delamination Crack in Cross Flow Filter WRTX-48

channels. Tighter dirty gas channels are considered to represent the section of the filter which had been at the bottom of the stack of filter plates during firing. This apparent discrepancy between which end of the filter was at the bottom or top during firing, may be the result of an uneven distribution of weight applied during filter element firing.

The location of the delamination crack along the closed top section of the filter, was noticed to be along a slight arc or "bowed" section of the filter faces. Both faces were parallel, but not perfectly flat. In relation to the bolt pattern on the filter clamp, the delamination crack appeared to be located between the mid bolt (No. 4) and the first bolt (No. 5) in the subsequent series of three bolts.

A "rusty-colored" haze was evident along the bottom (underside) of the filter where the clean gas channels were located. The haze appeared to extend along the entire four inch width of the filter (from flange edge-to-flange edge as shown in Figure J.4). The section of the filter that was closer to the plenum appeared to have a "darker" and wider hazy band in comparison to the section of the filter that was located farthest from the plenum. A clean gap was evident between these two bands. A similar hazy band coloration is evidenced on the top filter surface. All of the clean channels appeared to be free of fines.

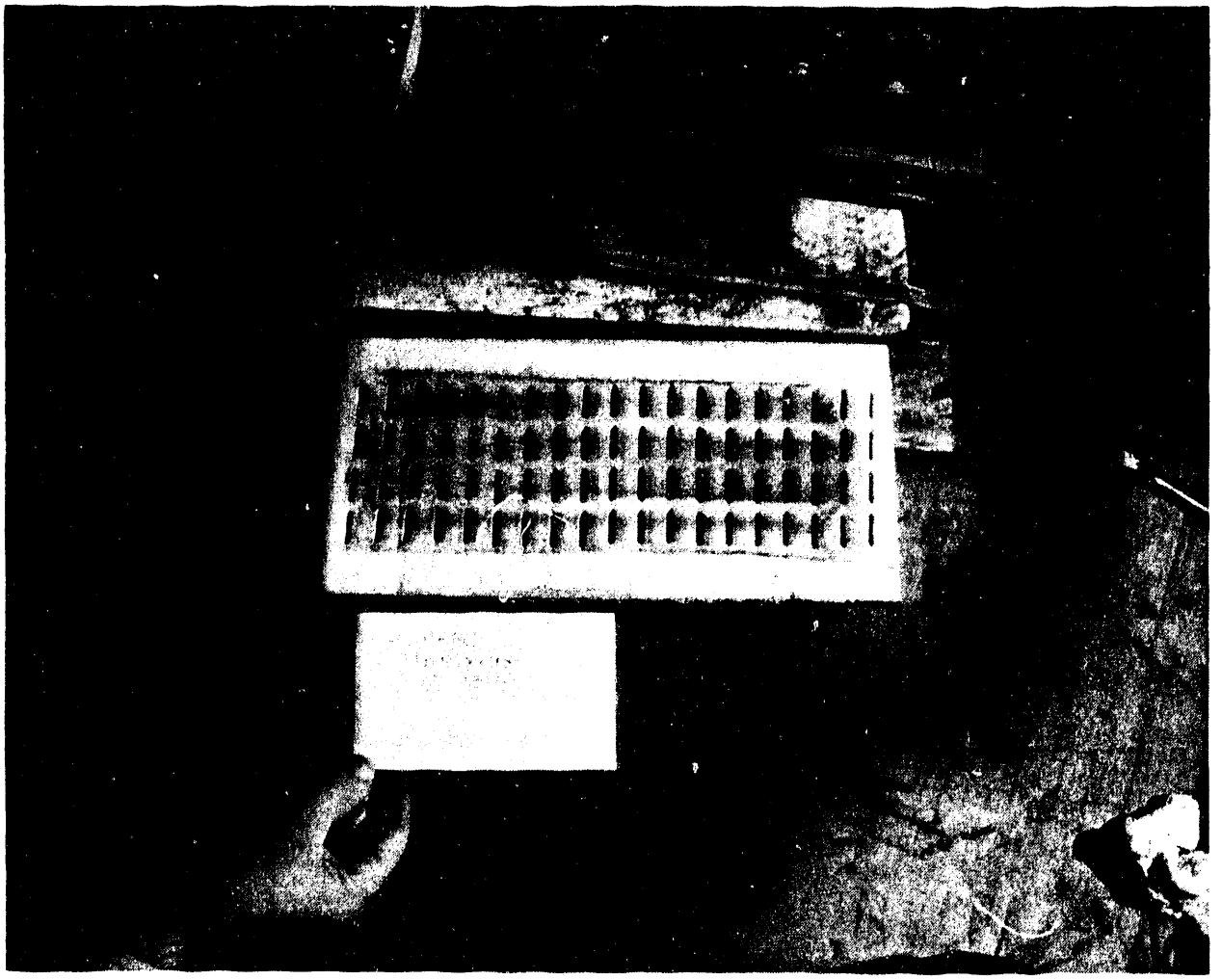

Figure J.4 - Dust Track Pattern Along the Clean Gas Channels in Cross Flow Filter WRTX-48

Cross Flow Filter WRTX-53, Figures J.5 through J.9

The cross flow filter designated as WRTX-53 was located in the bottom holder of plenum #1. After 335 hours of testing at 1550°F with 482 pulse cycles, 2 mild transients, and 1 severe transient, a dirty gas channel delamination crack which ran completely through the filter, and a partial dirty gas channel delamination crack resulted (Figure J.5).

Initially an open seam had been identified in the top closed section of the filter prior to use, and was patched with Nextel cloth and AREMCO paint. After testing, sections of the cloth were no longer attached to the filter, and debonding along the dirty gas channel mid-ribs occurred, resulting in the formation of a partial delamination (Figure J.6). The partial delamination or crack appeared to have started along the top closed section of the filter in dirty gas channel No. 14. The crack extended through the dirty channel mid-rib bonds in the upper section of the filter. The last dirty channel above the thicker central rib was the location where the crack cut through the plate, and then ran down the clean-to-clean channel seam. The crack did not appear to travel completely through the flange section. The crack path was evident along the opposite face of the filter which had been adjacent to the baffle plate. The location of this crack appeared to be at bolt No. 5. of the clamp. The patched crack appeared to be located in the tighter dirty gas channel portion of the filter. This section was considered to have been at the bottom of the stacked plates during firing and manufacturing of the filter body. Neither the partial delamination crack nor fines were evident along the bottom (underside) of the filter flange (Figure J.7).

A complete delamination crack was evident along the 9th dirty channel (Figure J.8). Initially the mid-rib bonds in this channel were well matched and bonded. The delamination was slightly to the left of the central bolt (No. 4). Caked fines were readily evident along the delaminated dirty gas channel. The mid-ribs along this section were also covered with a "greyish" perhaps "wet" mat of fines.

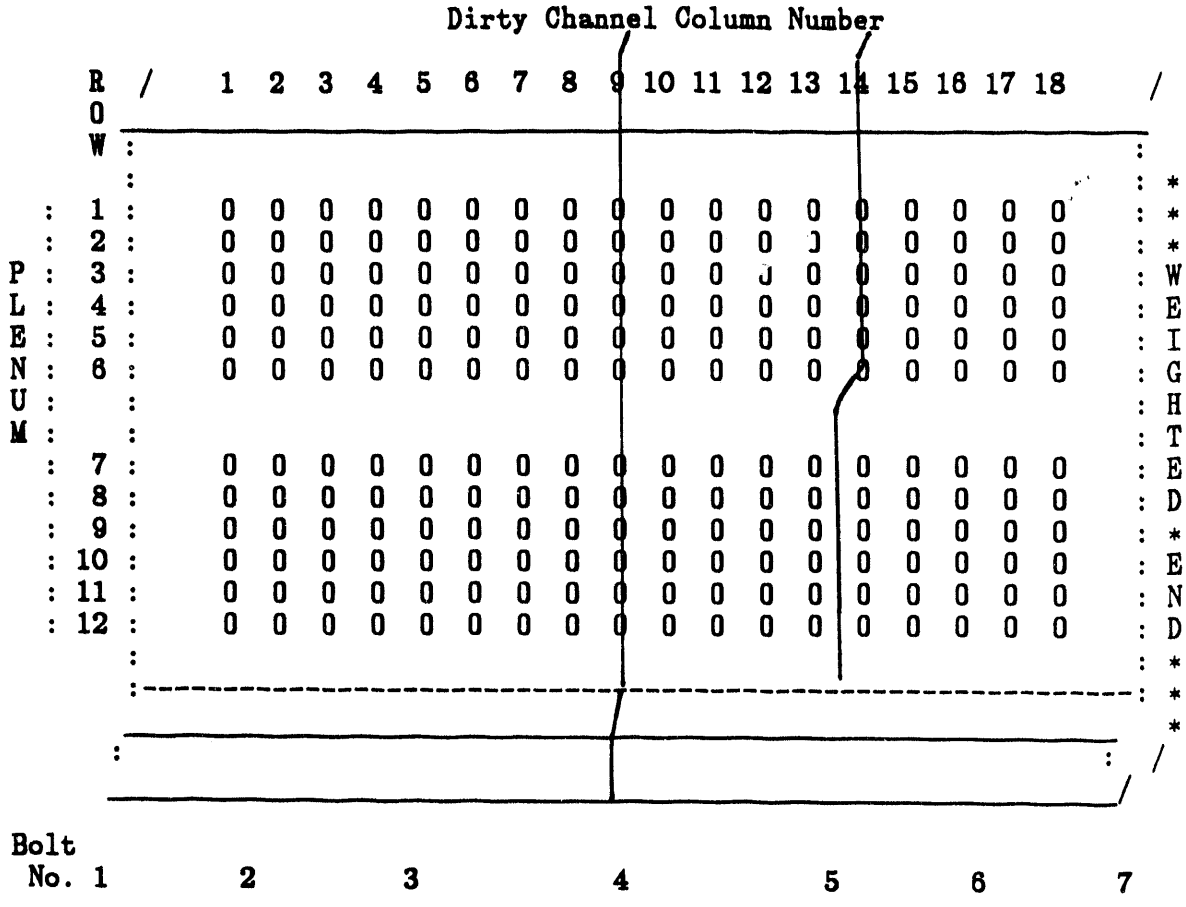

Figure J.5 - Location Of Delamination Cracks In Filter WRTX-53

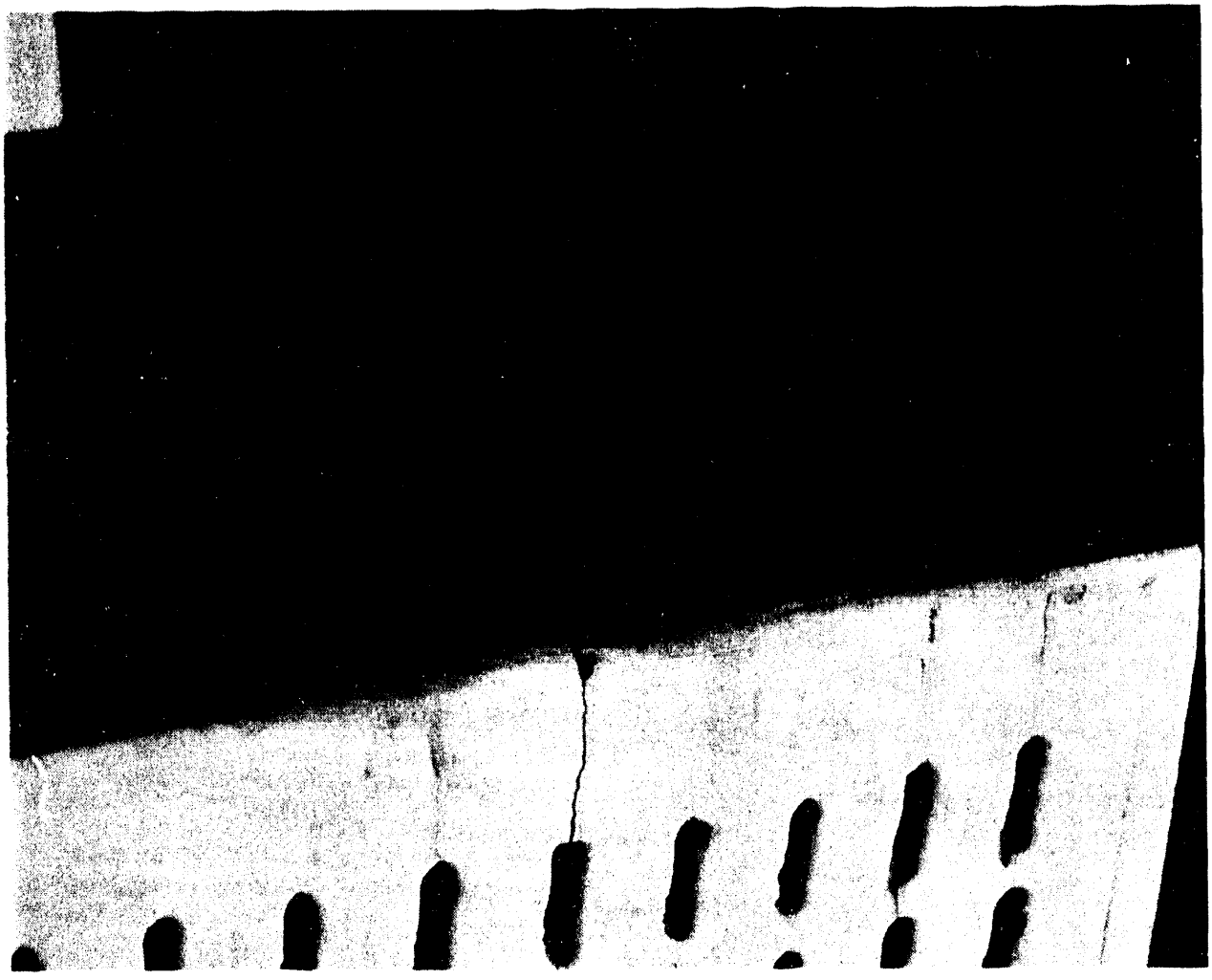

Figure J.6 - Patched Cracked Area of Cross Flow Filter WRTX-53
After Durability and Transient Testing

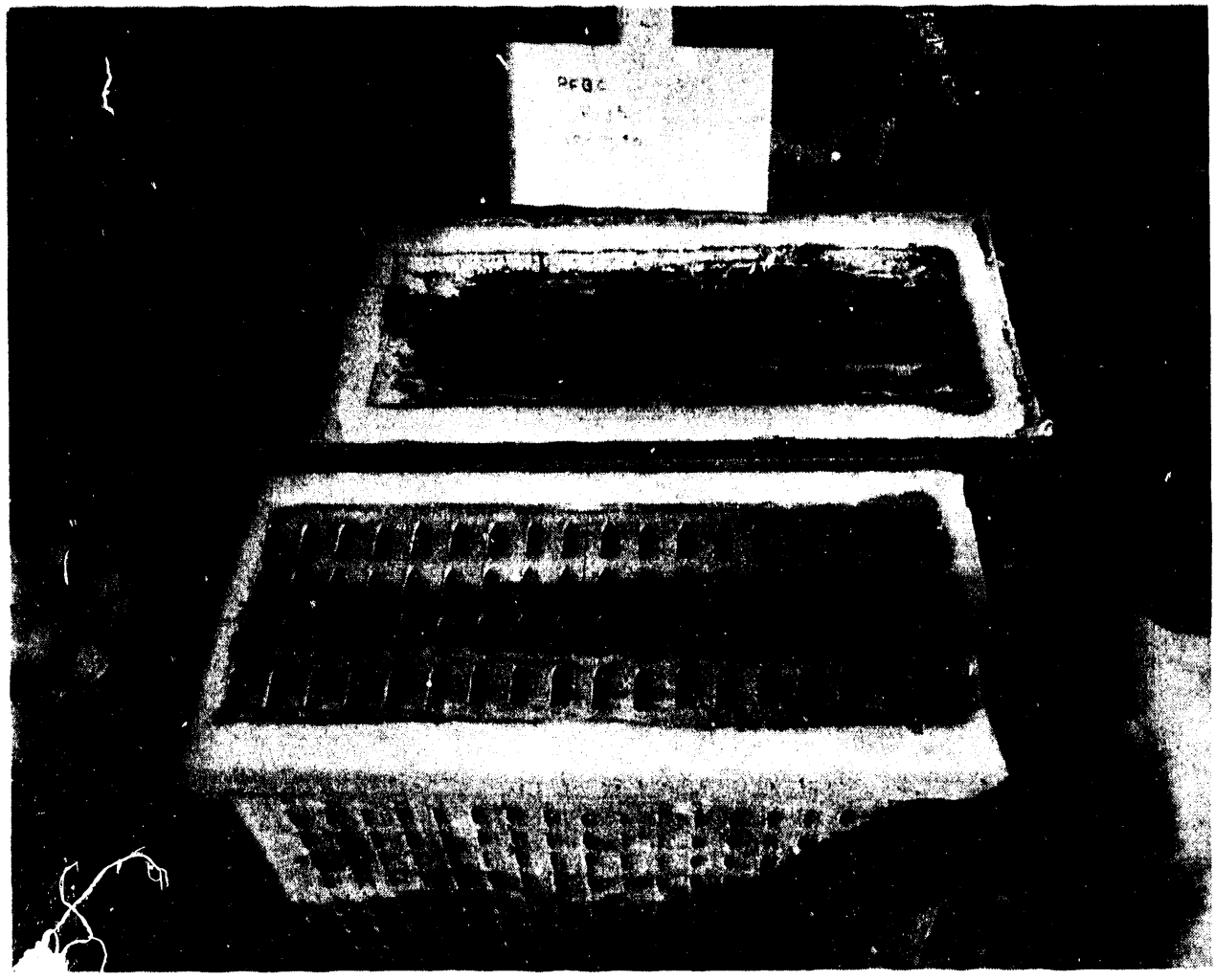

Figure J.7 - Absence of Dust Along the Clean Gas Channel Surface of Cross Flow Filter WRTX-53

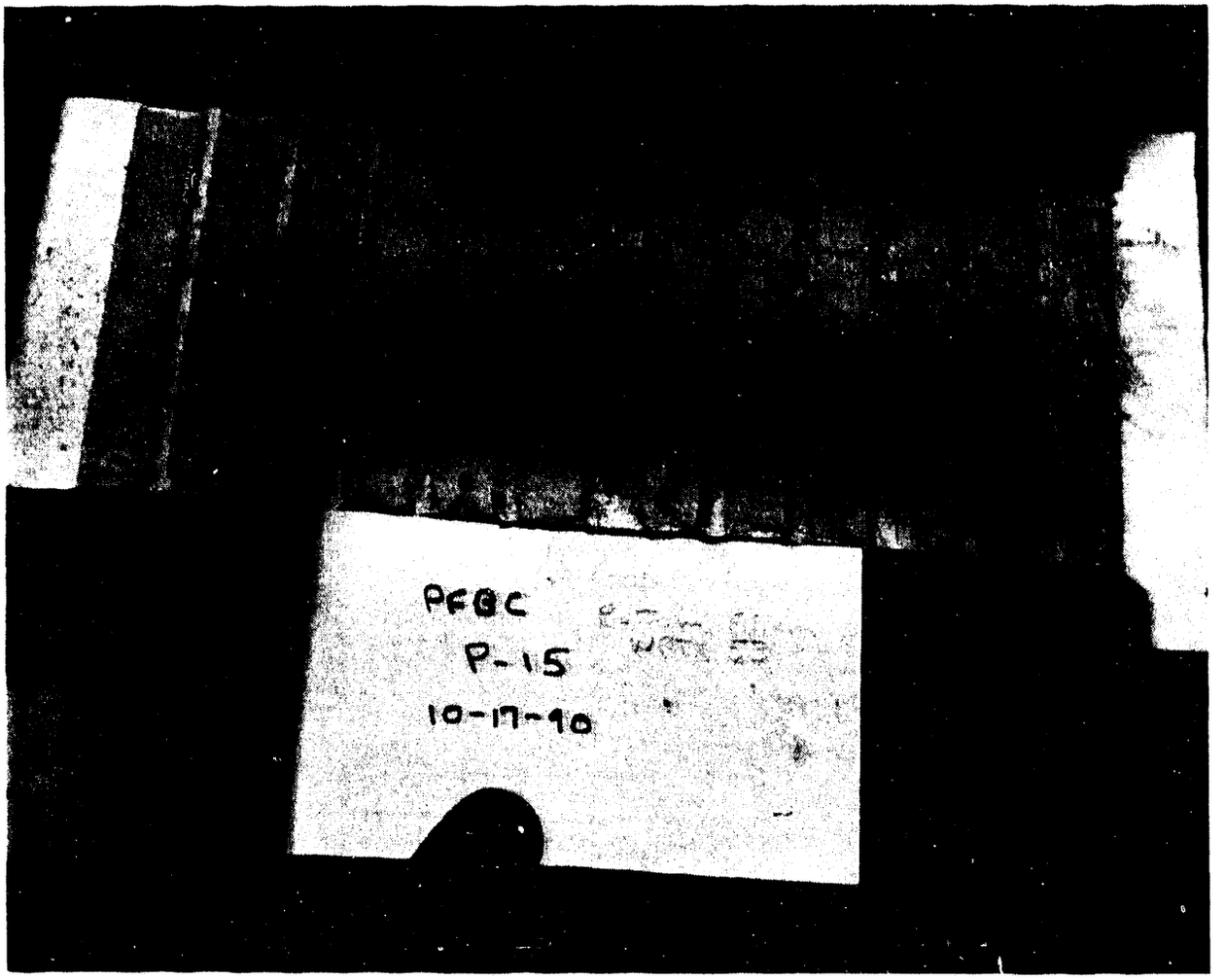

Figure J.8 - Debonding of the Mid-Rib Bonds in Cross Flow Filter WRTX-53

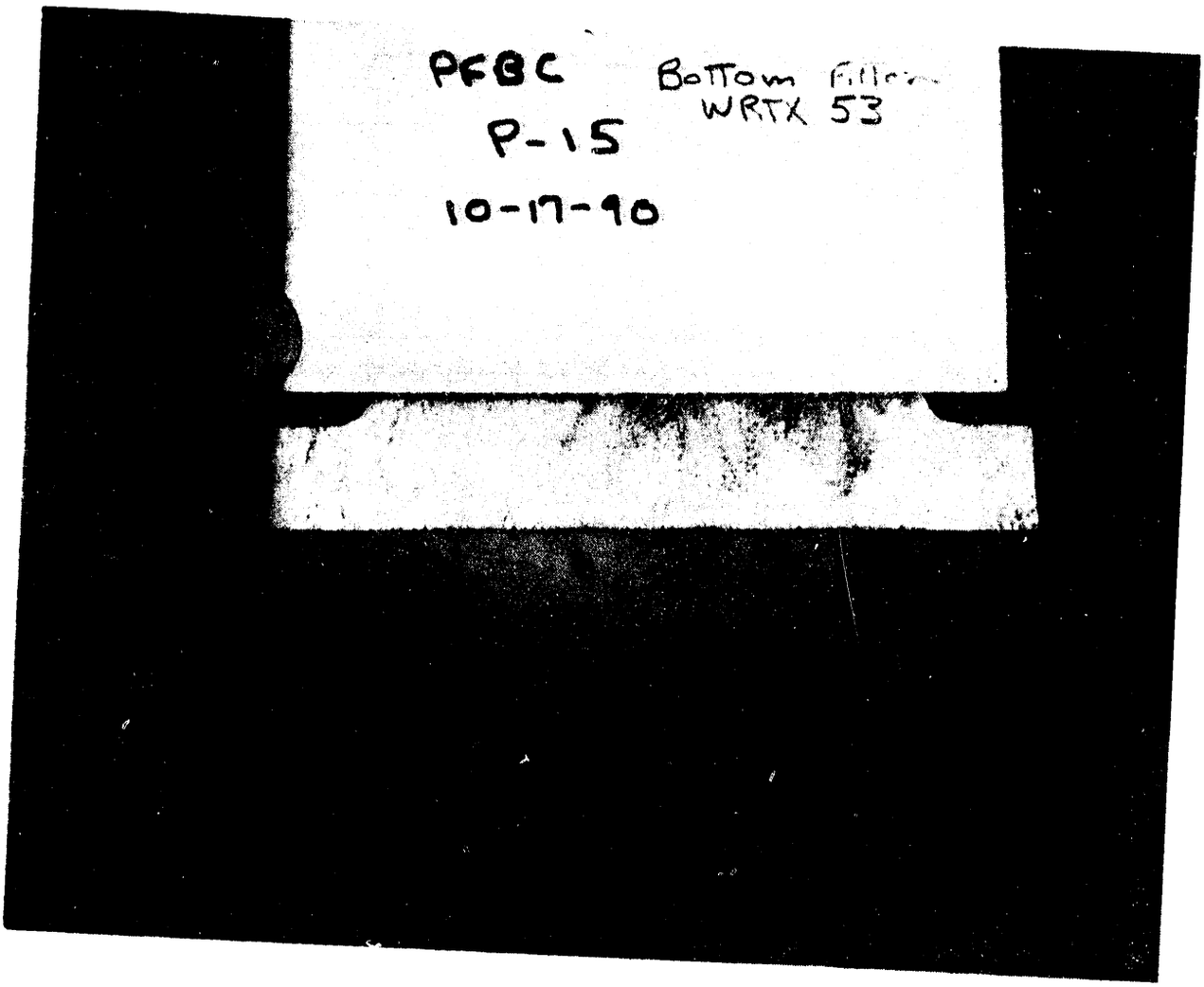

Figure J.9 - Dust Track Patterns Along the Poorly Bonded Section Of the Filter Flange Below the Last Dirty Gas Channel

Cross Flow Filter WRTX-66, Figures J.10 through J.13

The cross flow filter designated as WRTX-66 was located in the bottom holder of plenum #2. After 38 hours of testing at 1550°F with 3 pulse cycles, 2 mild transients, and 1 severe transient, a complete horizontal crack was observed through the upper section of the filter body (Figure J.10). The crack appeared to have originated along the side of the filter that was directly opposite from the plenum. Again this section of the filter contained the tighter dirty gas channels, indicating the side of the filter which had been at the bottom of the stack of plates during firing and production of the filter element body.

The horizontal crack ran from the bottom of the 5th dirty gas channel located at the side of the filter that was opposite of the plenum, to the top of the 5th dirty gas channel located at the side of the filter that was closest to the plenum.

Fines were not generally observed in the clean gas channels along the horizontal crack, except possibly in the last two clean channels (No. 17 and No. 18) farthest from the plenum (Figure J.11). Along the mid section of the horizontal crack, the clean channels appear to be free of fines. There was no apparent evidence of fines traveling to the bottom of the clean gas channels at the base of the flange (Figure J.12).

No reference is made to the position of the bolt holes, since the crack occurred horizontally. However, it should be noted that this filter was mounted with the redesigned clamping arrangement (Figure J.13).

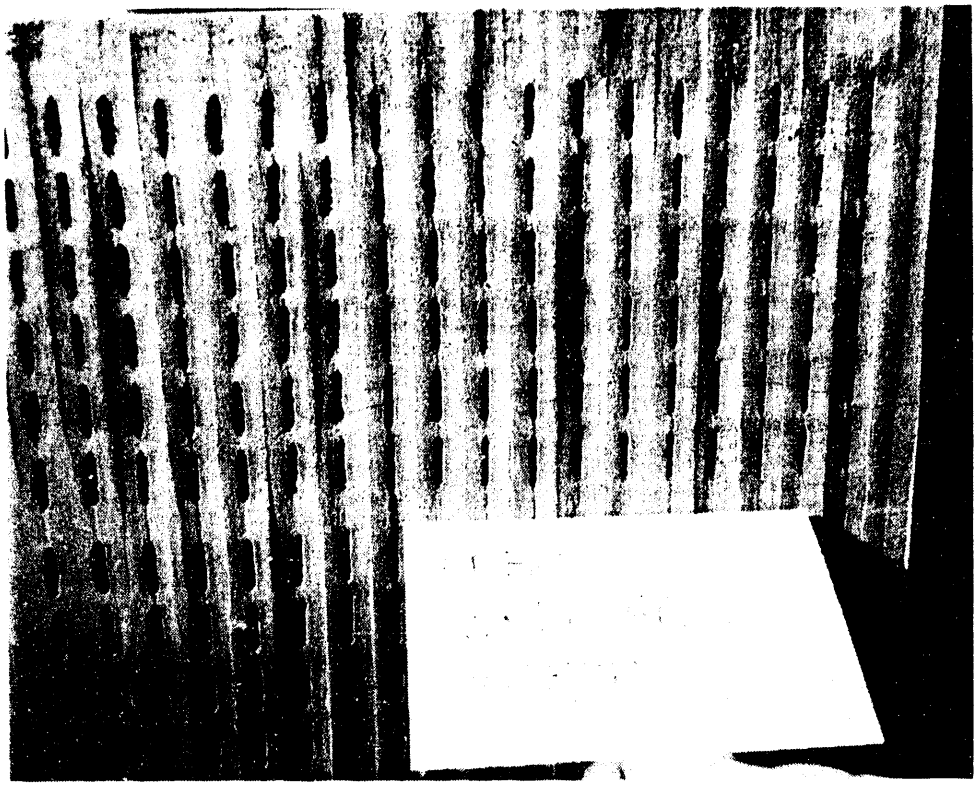

Dirty Channel Column Number

ROW	1	2	3	4	5	6	7	8	9	10	11	12	13	14	15	16	17	18
1	0	0	0	0	0	0	0	0	0	0	0	0	0	0	0	0	0	0
2	0	0	0	0	0	0	0	0	0	0	0	0	0	0	0	0	0	0
3	0	0	0	0	0	0	0	0	0	0	0	0	0	0	0	0	0	0
4	0	0	0	0	0	0	0	0	0	0	0	0	0	0	0	0	0	0
5	0	0	0	0	0	0	0	0	0	0	0	0	0	0	0	0	0	0
6	0	0	0	0	0	0	0	0	0	0	0	0	0	0	0	0	0	0
7	0	0	0	0	0	0	0	0	0	0	0	0	0	0	0	0	0	0
8	0	0	0	0	0	0	0	0	0	0	0	0	0	0	0	0	0	0
9	0	0	0	0	0	0	0	0	0	0	0	0	0	0	0	0	0	0
10	0	0	0	0	0	0	0	0	0	0	0	0	0	0	0	0	0	0
11	0	0	0	0	0	0	0	0	0	0	0	0	0	0	0	0	0	0
12	0	0	0	0	0	0	0	0	0	0	0	0	0	0	0	0	0	0

PLENUM

WEIGHTED END

Bolt No. 1 2 3 4 5 6 7

Figure J.10 - Horizontal Crack Formation Through Cross Flow Filter WRTX-60 Resulting During Thermal Transient Testing

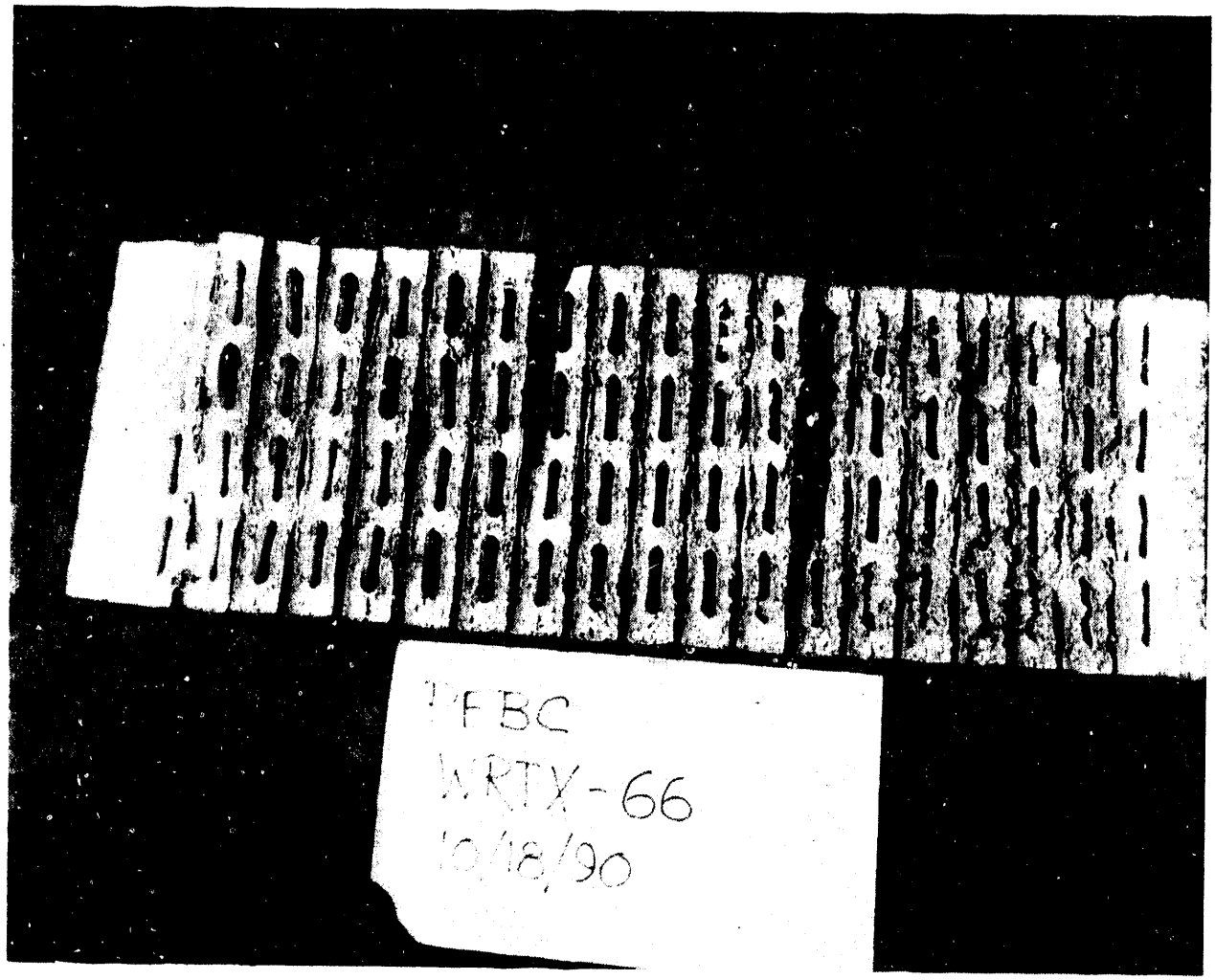

Figure J.11 - Cracked Surface Of Cross Flow Filter WRTX-66

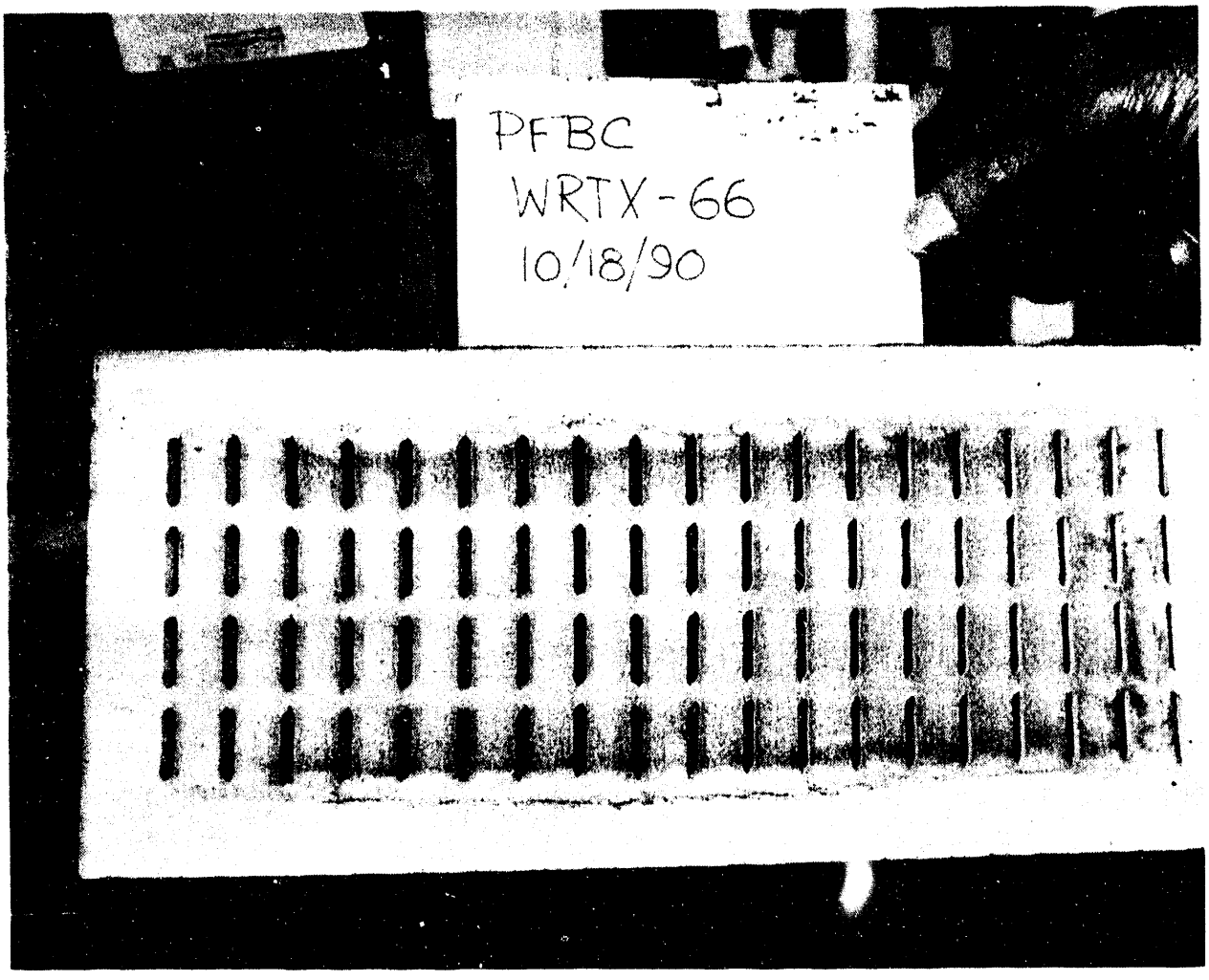

Figure J.12 - Absence Of Dust Along the Clean Gas Channel Surface Of Cross Flow Filter WRTX-66

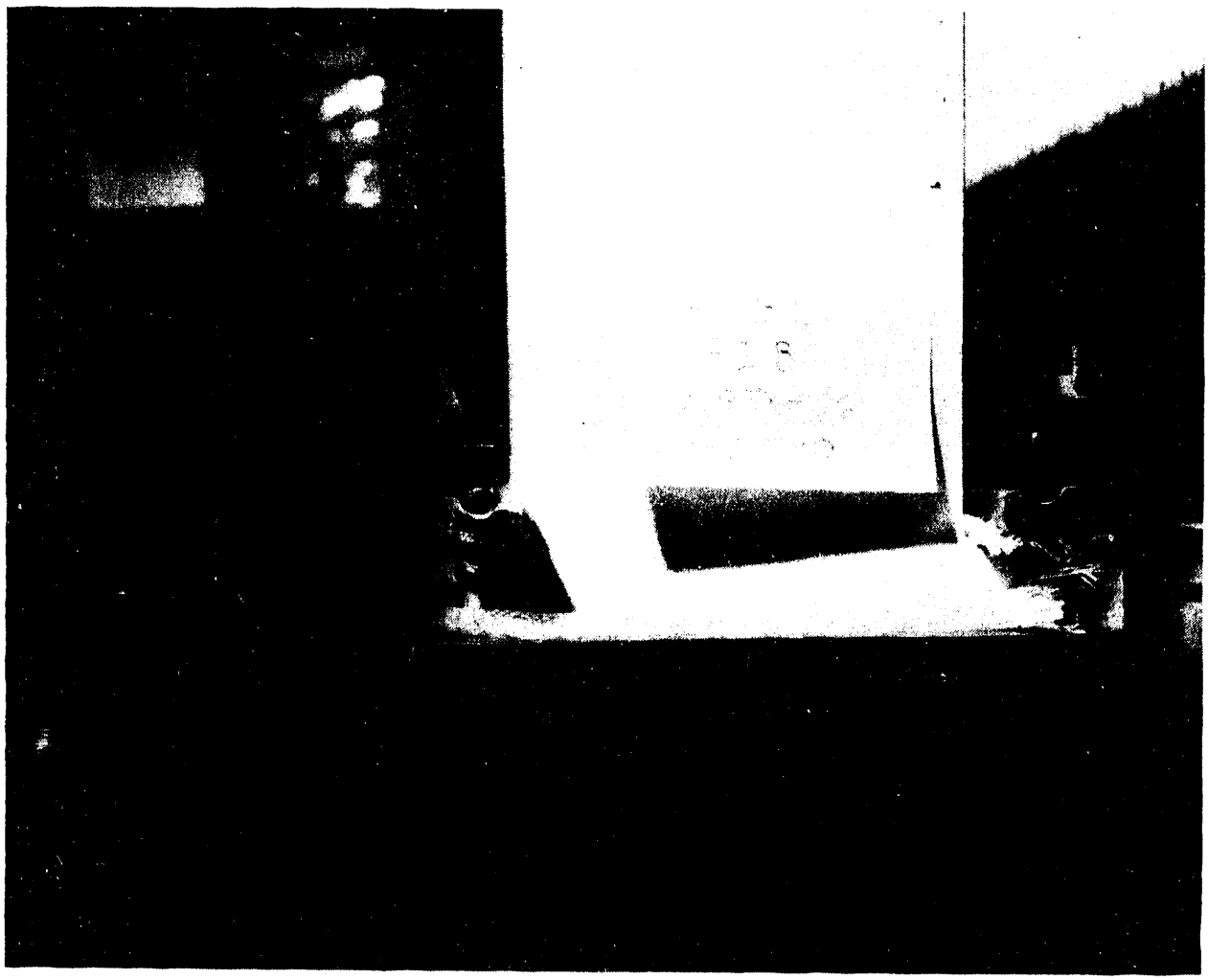

Figure J.13 - Redesigned Clamping Arrangement

Cross Flow Filter WRTX-70, Figure J.14

The cross flow filter designated as WRTX-70 was located in the top holder of plenum.[b] After 38 hours of testing at 1550°F with 3 pulse cycles, 2 mild transients, and 1 severe transient, a hairline crack was evident along the bottom (underside) of the flange, as well as along the closed side wall plate of the filter (Figure 14). The crack appeared to have originated in the 6th clean channel from the plenum side. The crack cut through the plate, and ran through the clean-to-clean mid-rib bond seam. The crack extended through the flange section and then crossed through the last plate of the dirty gas channel which was adjacent to the flange, and then into the center of the dirty gas channel. The crack path appeared to have stopped at this location. After 38 hours of testing, the clean gas channels appeared to be free of fines.

In relation to the bolt pattern, the crack appeared to have occurred at approximately the same location as bolt No. 3 of the filter clamp. As with cross flow filter WRTX-66, WRTX-70 was also mounted with the redesigned clamping arrangement (as Figure J.13).

A second minor crack formation was also evident along the closed side wall plate of this filter. The location of this crack is again at the 5th row of dirty gas channels, similar to the position of the horizontal crack which formed in cross flow filter WRTX-66. Unlike WRTX-66, the crack in WRTX-70 did not "cut" completely through the filter matrix.

Similar to the other three filter in this test series (WRTX-48, WRTX-53, and WRTX-66), the tighter dirty gas channels of filter WRTX-70 were located farthest from the plenum.

b. WRTX-70 was subsequently used at Westinghouse for optical sensor testing by VPI personnel. Sensors and bonding media are shown in the top portion of Figure J.14.

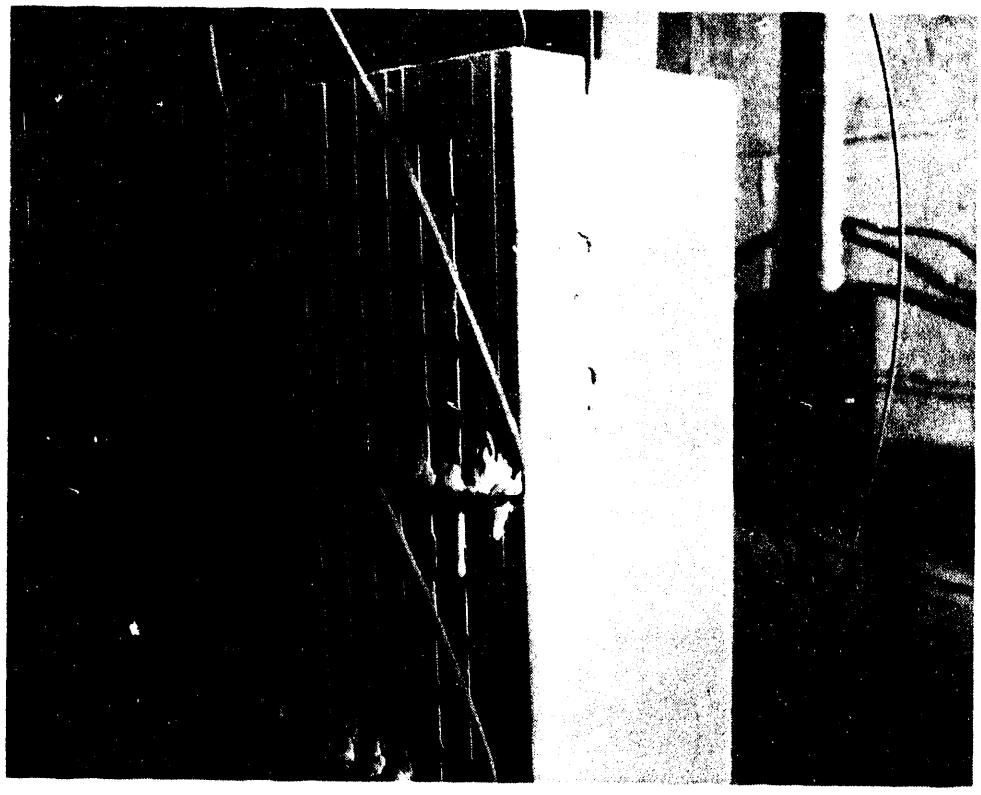

Dirty Channel Column Number

ROW	1	2	3	4	5	6	7	8	9	10	11	12	13	14	15	16	17	18
1	0	0	0	0	0	0	0	0	0	0	0	0	0	0	0	0	0	0
2	0	0	0	0	0	0	0	0	0	0	0	0	0	0	0	0	0	0
3	0	0	0	0	0	0	0	0	0	0	0	0	0	0	0	0	0	0
4	0	0	0	0	0	0	0	0	0	0	0	0	0	0	0	0	0	0
5	0	0	0	0	0	0	0	0	0	0	0	0	0	0	0	0	0	0
6	0	0	0	0	0	0	0	0	0	0	0	0	0	0	0	0	0	0
7	0	0	0	0	0	0	0	0	0	0	0	0	0	0	0	0	0	0
8	0	0	0	0	0	0	0	0	0	0	0	0	0	0	0	0	0	0
9	0	0	0	0	0	0	0	0	0	0	0	0	0	0	0	0	0	0
10	0	0	0	0	0	0	0	0	0	0	0	0	0	0	0	0	0	0
11	0	0	0	0	0	0	0	0	0	0	0	0	0	0	0	0	0	0
12	0	0	0	0	0	0	0	0	0	0	0	0	0	0	0	0	0	0

PLENUM

WEIGHTED * END * * *

Bolt No. 1 2 3 4 5 6 7

Figure J.14 - Crack Formations In Cross Flow Filter WRTX-70 After Turbine Trip Transient Testing

2. MODERATE TURBINE TRIP TRANSIENT TEST

Cross Flow Filter WRTX-81, Figures J.15 through J.17

The cross flow filter designated as WRTX-81 was located in the top holder of plenum #2. In contrast with the two previous cross flow filter fabrication lots which had 18 columns of dirty gas channels, WRTX-81 had only 17 columns of dirty gas channels. After 320 hours of transient testing, a complete delamination resulted along the mid-rib bond of dirty gas channel No. 5, as well as a partial delamination crack along dirty gas channel No. 15 (Figures J.15-J.17). After testing, the delamination crack located at dirty gas channel No. 15 was seen to be partially held together at the flange. The delamination crack was observed to diverge at the top closed section of the filter, leaving an approximate 1/8 inch gap between filter plates. Debonding occurred primarily along the mid-rib bonds. Along the top closed section, as well as along the flange area, a segment of the filter plate material was also removed (i.e., as opposed to merely debonding along the seam). A "better" bond is speculated to have been formed in these sections (i.e., top closed section and flange area) in comparison to the mid-ribbed bonds. Fines were observed along the delaminated mid-ribbed bonds after testing.

No visible identification could be made relative to which side of the filter had been weighted during filter fabrication. What was evident, however, was that the position of delamination along dirty gas channel No. 15 corresponded to the position of bolt No. 3. The delamination crack which formed along dirty gas channel No. 15 was located between bolt No. 5 and No. 6.

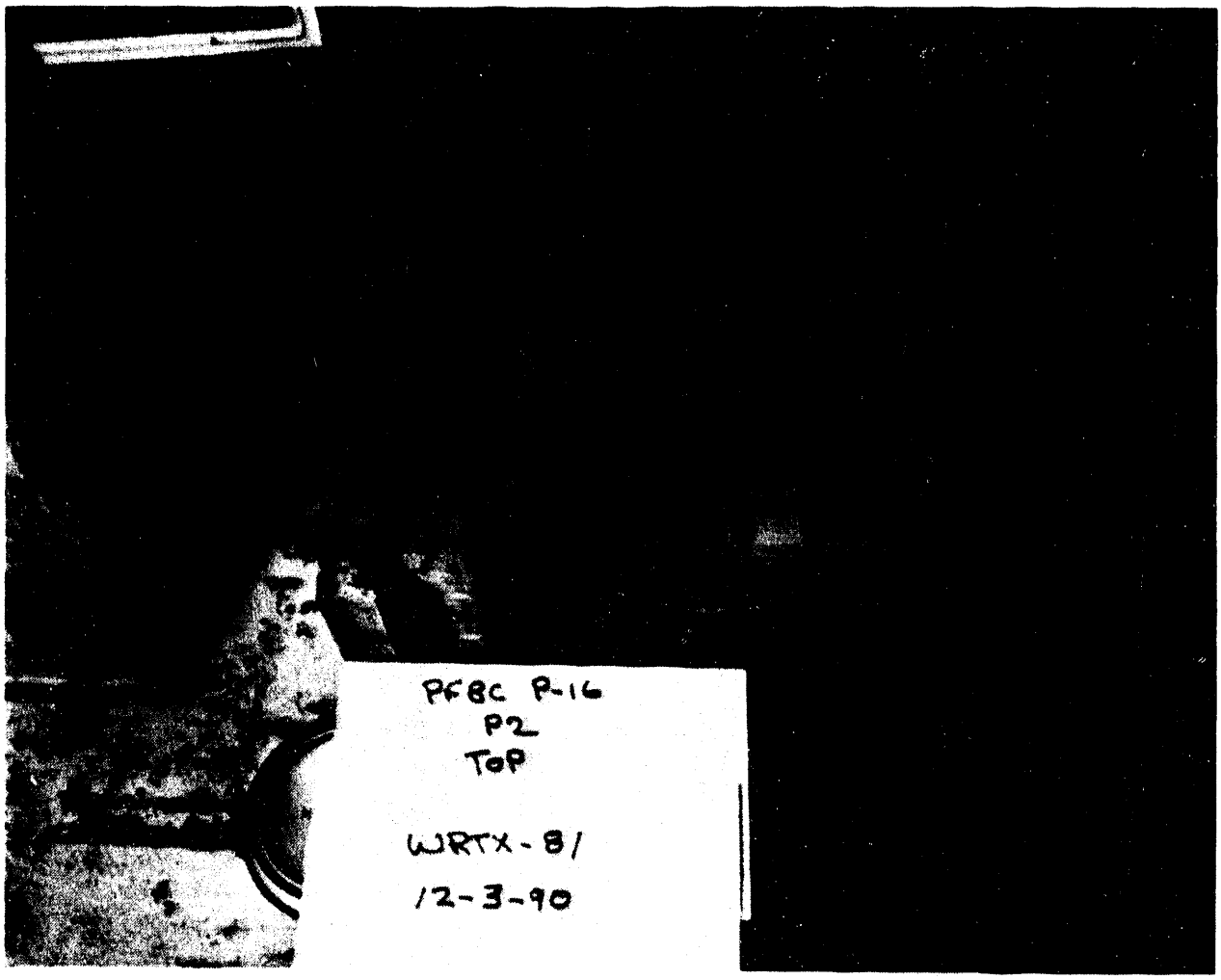

Figure J.15 - Delamination Along Dirty Gas Channel Column No. 5 Which Resulted in Cross Flow Filter WRTX-81 after Turbine Trip Transient Testing

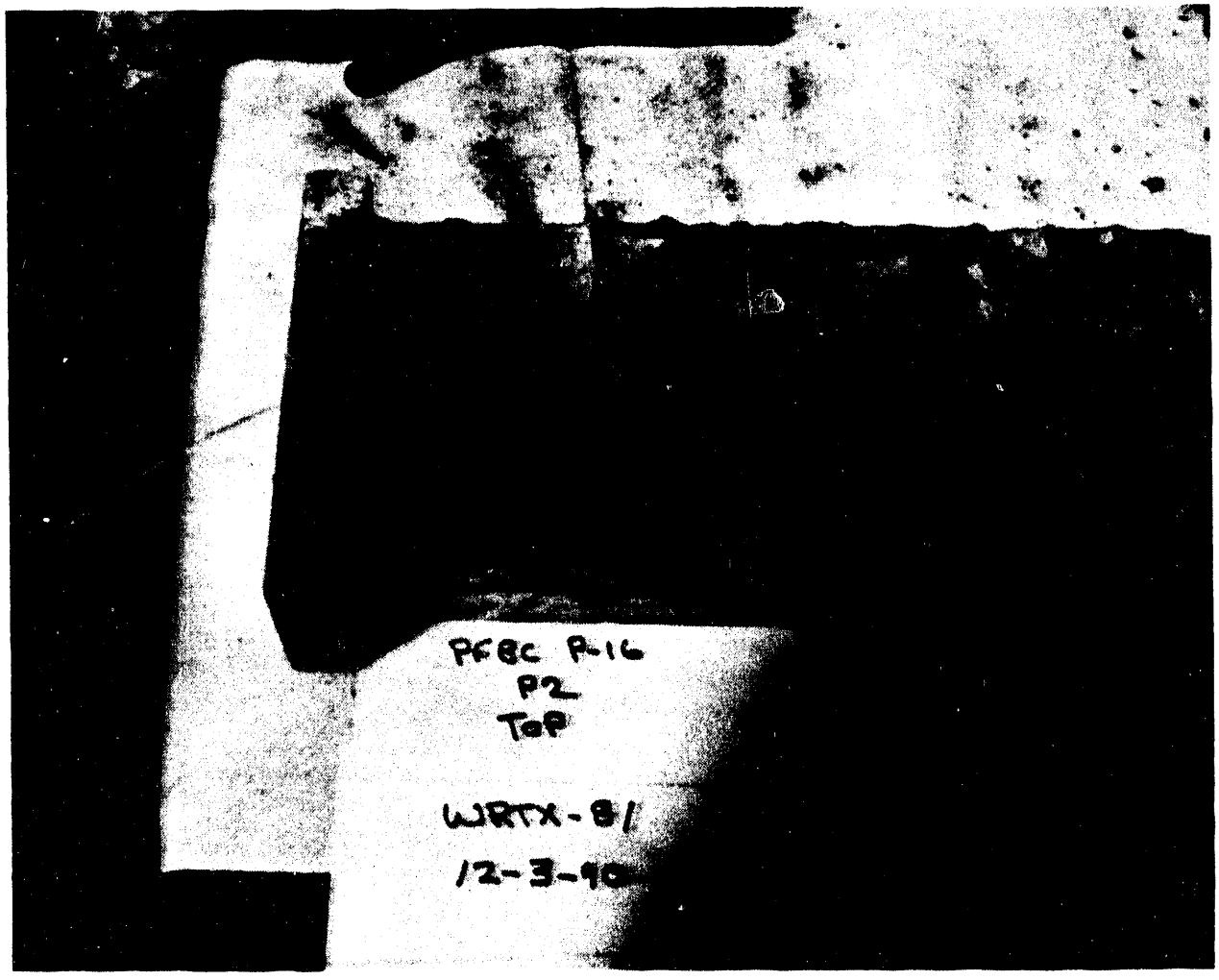

Figure J.16 - Delamination Along Dirty Gas Channel Column No. 15 Which Resulted in Cross Flow Filter WRTX-81 After Turbine Trip Transient Testing

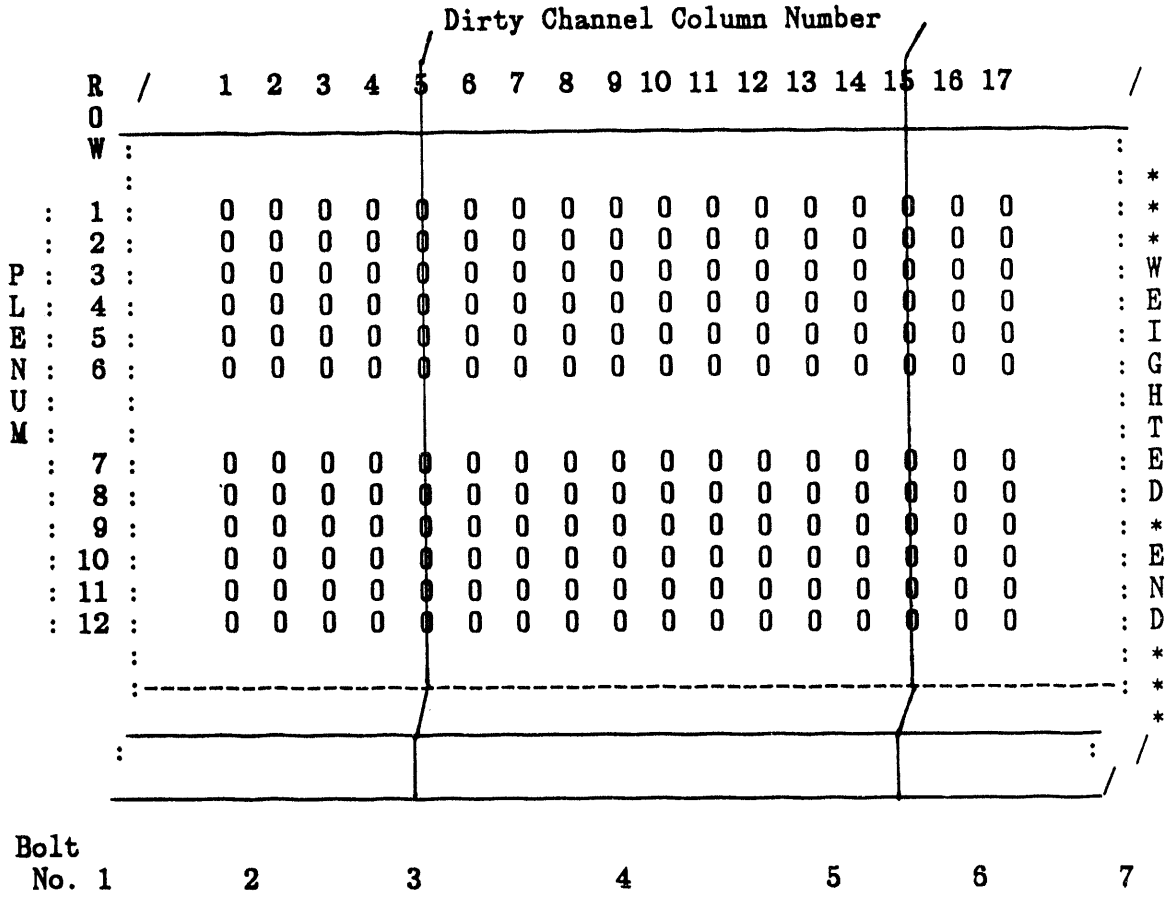

Figure J.17 - Location of Delamination Cracks in Filter WRTX-81

3. HEAT-UP CYCLE TRANSIENT TEST

Cross Flow Filter WRTX-80, Figure J.18

The cross flow filter designated as WRTX-80 was located in top holder of plenum #2 during the heat-up transient tests. After 191 hours of testing, including 90 heat-up cycles, a dust leak of approximately 14 ppm was detected. An initial inspection of the filter as it remained mounted in the filter vessel indicated that an obvious "dust seam' formed along the filter face. The "dust seam" appeared to run along the clean channel seam, between dirty gas channel No. 3 and No. 4. Further inspection of WRTX-80 after removal from the vessel and subsequent cleaning, indicated that a crack had formed in the filter flange, in approximately the same area as the clean plate "dust seam" (Figure J.18). The crack appeared to form within a filter plate (not on a clean or dirty gas channel seam), which then crossed over into the clean gas channel seam, near the last row of dirty gas channels. The distance that the crack traveled from the flange towards the top closed section of the filter could not be discerned due to the relatively wide "smile" formations along the plate edges of the clean gas channel seam.

The crack had initiated in the area of the filter that was mounted closest to the plenum, and was located between bolt No. 2 and No. 3. An attempt was made to try and identify which end of the filter was located at the top or bottom of the stack of filter plates during firing. We believe that the tighter gas channels, indicative of the bottom set of plates in the stack, were positioned opposite of the plenum.

When viewing the filter along the open clean gas channel surface, the crack was observed to run through the plate (not between clean or dirty gas channel seams), and then into the "outer-most" clean gas channel. The crack did not appear to travel completely across the

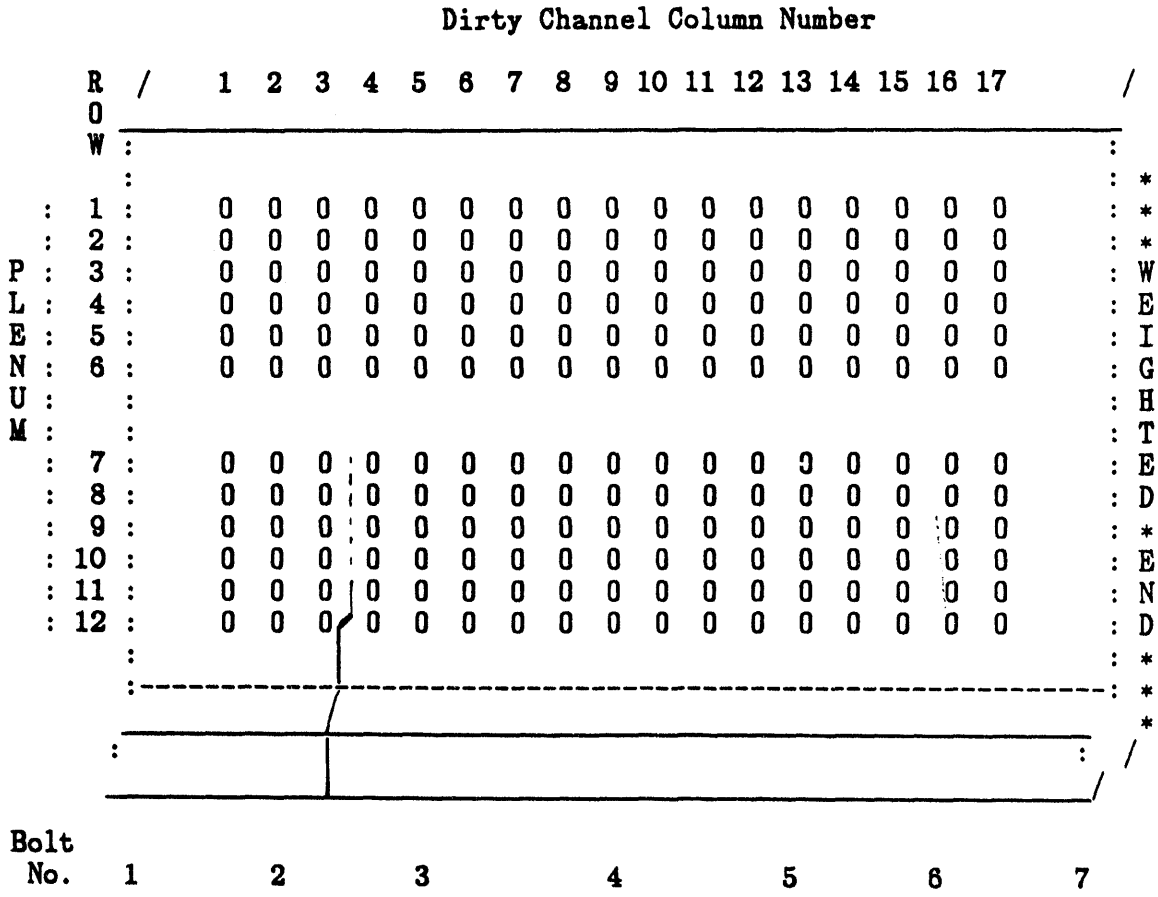

Figure J.18 - Location Of Delamination Crack In Filter WRTX-80

clean gas channel seam that runs along the underside of the filter. The crack was, however, apparent between the opposite "outer-most" clean gas channel and the edge of the flange. Dust fines were evident along the two "outer-most" clean gas channels that contained the crack formations.

COMMENT

In the thermal transient test series, Westinghouse has attempted to subject cross flow filters to conditions that may represent turbine trip and heat-up cycles similar to what may be expected in a PFBC plant. The thermal transient conditions are generally considered to be more severe than the "steady state" conditions achieved in our durability test program, where our major accomplishment was the successful demonstration of approximately 1300 hours of operational life for two cross flow filter elements (WRTX-9 and WRTX-10).

All filters that were used in the thermal transient tests were fabricated with the same type of pore former, and were considered to have experienced the same filter plate stacking assembly and firing temperature profile. WRTX-48 and WRTX-53 were produced in April 1990, while WRTX-66 and WRTX-70 were produced in September 1990. Both WRTX-80 and WRTX-81 were produced in October 1990. The April 1990 batch lot was identified to have a strength of 3.204 ksi (4-pt bend), while the September and October 1990 batch lots were identified to have strengths ranging from 2.99-3.07 ksi (4-pt bend).

In contrast with these filters are the durability test filters, WRTX-9 and WRTX-10. These filters which were fabricated in February 1989, were manufactured using a different pore former,[c] as well as filter plate stacking sequence during production. The February 1989 fabrication lot had an apparently higher initial material strength, as reflected by the vendor's 3-pt bend strength data of 4.06 ksi[d] (ANL reported a 4-pt bend strength of 3.11 ksi for a filter element from this production batch).[(1)]

---

c. The different pore formers used in fabricating the cross flow filters may have somewhat changed the porosity and pore size distribution within the ceramic matrices. This is considered as a result of possibly different initial pore former particle size distributions, and possibly the different "burn-out" patterns of the pore formers, which could lead to changes in the interconnecting pore channel geometry.

d. Caution should be exercised when attempting to compare 3-pt and 4-pt bend strength data. These values are not expected to be directly related.

The fact that the durability cross flow filters may have had an initially higher material strength, and were subjected to less severe "steady state" conditions, are perhaps criteria which directly relate to their 1300 hours of operating life in comparison to the 38 to 335 hours of filter life achieved under thermal transient test conditions. Further efforts should be directed to verifying the extent of possible variation in material strength by testing at least one as-fabricated, untested filter from each filter lot, using the same bend bar test geometry (i.e., 4-pt bend, 1/4 flexure). Similarly, data are also needed which reflect mid-rib and plate seam bond strength for both filter lots, as well as fracture toughness, porosity, pore size distribution, density, and phase composition. This information may provide insight into some of the currently considered reliability aspects of the cross flow filter from a production point of view.

The possibility also exists that the HTHP test facility may artificially induce localized stresses as a result of either system operation or design modifications. Minor modifications that were made either to the HTHP system (i.e., clamping design, blowback system, dust type) or to the individual cross flow filter elements (i.e., AREMCO painting of the seams) during the last long-term durability test and the thermal transient test series are summarized in Table J.2.

With respect to the Westinghouse HTHP filter vessel, several observations have been identified in an attempt to determine why cross flow filters delaminate or form cracks at what seems to be reoccurring locations. These include:

- The most severe failures in the initial turbine transient test (four filters) occurred in the filters located in the bottom holders (WRTX-53: complete delamination and delamination crack; WRTX-66: complete horizontal delamination). This may be related to a thermal effect (i.e., either the pulse gas is colder at this location, and

TABLE J.2

SUMMARY OF W HTHP SYSTEM MODIFICATIONS

	Filter No.	Maximum Life,Hrs	No. Plenums/ No. Filters	Type of Ash Feed	Plate Seams	Flange Clamping	Blowback	Filter Plenum Positions
Durability Testing	WRTX-9	~1300	1/2	d	e	Original	Original	P2B
	WRTX-10	~1300						P2T
Severe Thermal Transient Test No. 1	WRTX-48	335	2/4	b	e	Original	Segmented	P1T
	WRTX-53	335		b	e	Original	Segmented	P1B
	WRTX-70	38		b,c	As-Fabricated	Rocker	Original	P2T
	WRTX-66	38		b,c	As-Fabricated	Rocker	Original	P2B
Thermal Transient Test No. 2	WRTX-77	a(320)*	2/4	d	As-Fabricated	Rocker	Original	P1T
	WRTX-78	a(320)*		d	As-Fabricated	Rocker	Original	P1B
	WRTX-81	320		d	As-Fabricated	Rocker	Original	P2T
	WRTX-76	a(320)*		d	As-Fabricated	Rocker	Original	P2B
Thermal Transient Test No. 3	WRTX-77	a(191)*	2/4	d	As-Fabricated	Rocker	Original	P1T
	WRTX-78	a(191)*		d	As-Fabricated	Rocker	Original	P1B
	WRTX-80	191		d	As-Fabricated	Rocker	Original	P2T
	WRTX-76	a(191)*		d	As-Fabricated	Rocker	Original	P2B

a - Intact
* - Hours during specific test
b - Mixture of both high and low iron content Grimethorpe dust
c - Majority of operational hours with high iron content Grimethorpe dust
d - Low iron content Grimethorpe dust
e - AREMCO paint along gas channel seams

is directed to the clean gas channels farthest from the plenum, or is a combination of cold pulse gases within perhaps a hotter section of the filter vessel).

- Crack formation in the initial series of thermal transient tests appeared to result in the area of the cross flow filter farthest from the plenum. The question which arises is whether this has any relationship to either the HTHP system design (i.e., gas flow pattern, etc.), or to its operation. Perhaps the plenum provides "protection" which is not afforded to the side of the filter that is directly in the gas passage.

- In the initial thermal transient test series, the tighter channels of each filter appeared to be positioned at the location farthest from the plenum. The tighter channels represent the bottom set of plates during weighting and high firing of each filter element. This area may have experienced a higher stress under load, and therefore may be more vulnerable to failure.

- Bolt patterns may still induce crack formation, particularly in bolt positions No. 3 and No. 5, and possibly No. 4. Perhaps this region may have experienced the "coldest" portion of the pulse gas during blowback.

Although in the first turbine trip transient test, the relative strengths of the Plenum #2 (top: WRTX-70; bottom: WRTX-66) filters in the initial thermal transient test series were somewhat lower than the Plenum #1 (top: WRTX-48; bottom: WRTX-53) filters, these filters had not experienced the extensive number of hours of testing as the filters located in Plenum #1. Perhaps, during initial testing, the filters in Plenum #1 had experienced a reduction in strength, leaving them with a

resulting strength comparable to the filters in Plenum #2. If this were so, then due to the severity of the transient, both sets of filters would be expected to perform in a similar manner, forming cracking and delaminating. Alternately the "severity" of the initial turbine trip test may have been such that even the "strongest, most reliable" ceramic cross flow filter would delaminate or form cracks.

The more moderate turbine trip transient test conducted in this series certainly demonstrated the long-term "survivability" of the cross flow filters to "non-steady state" conditions, since only one filter failed under the more representative transient test conditions, as opposed to all four filters suffering a partial or complete delamination crack under the "less realistic" severe set of transient conditions. Questions which arise are:

- If the October 1990 filter lot had an initially higher material strength, would filter life for WRTX-81 have increased?

- Was WRTX-81 "perfectly" fabricated?

Since, however, three out of the four filters survived the moderate turbine trip test, and were subsequently subjected to heat-up cycle transients and survived an additional 191 hours of testing, the question which then arises is whether there is an issue with the HTHP system which induces failure in a filter that is placed in the top holder of the second plenum. Alternate systems issues which may provide insight into cross flow reliability include:

- Identifying whether similar blowback pulse durations were used in the durability and thermal transient test series, as well as tracking the time interval between pulsing.

- Identifying the change in temperature throughout an entire filter during blow back pulse delivery. Identifying whether each filter element experiences the same temperature profile per pulse.

These and other fabrication and systems issues will continued to be reviewed during the next quarter. A Taguchi approach is planned to assess the relevance of all possible fabrication and HTHP system contributing parameters.

REFERENCES

1. Singh, J. P., Majumdar, S., Wagh, A. S., Wenzel, T., and Peoppel, R. B., "Materials Qualification Technology For Ceramic Cross Flow Filters," Argonne National Laboratory, to be issued.

APPENDIX K

PROPERTY CHARACTERIZATION - ROOM TEMPERATURE

FILTER MATERIAL PROPERTY CHARACTERIZATION

Strength data are presented for an as-fabricated, untested alumina/mullite cross flow filter, and for the filter which experienced 1300 hours of operation in the Westinghouse high temperature, high pressure (HTHP) test facility. Under simulated pressurized fluidized-bed combustion (PFBC) conditions, the 1300 hour cross flow filter experienced temperatures of 1600°F, pressures of 150 psig, and 2068 pulse cleaning cycles. During filter operation, inlet mass loadings were 1000 ppm, while outlet mass loadings of 1 ppm were achieved. Testing was terminated when the filter experienced longitudinal cracks in the flange used to attach the filter to the clean gas plenum. Both filters were produced from the same fabrication lot in February 1989. Bend bar samples were prepared from the top (closed) and web (core) of both filters. Bend bars were also prepared from the flange section of the 1300 hour filter. Since the flange section of the as-fabricated, untested filter had been removed prior to shipment by the manufacturer, it was not available for strength analysis.

1. MATERIAL PROPERTY CHARACTERIZATION TECHNIQUES

Room temperature strength testing was performed on the alumina/mullite filter that had been exposed for approximately 1300 hours in the Westinghouse HTHP test facility in an attempt to determine whether changes had occurred in the physical properties of the filter during long-term operation. Four point bend strength testing was conducted at room temperature using 1/4-point flexure, with upper and lower spans of 20 and 40 mm, respectively. The crosshead speed was 0.02 cm/min.

Initially the 1300 hour cross flow filter was divided into four sections (Figure K.1). From each 6x6x4 inch web (core) section, twelve bend bars (48 in total that were 0.08 in. thick) were prepared for room temperature strength testing (4-point bend, 1/4-flexure). From the flange section of the filter, twenty-two 0.08 inch thick, and fifteen 0.12 inch thick bend bars were prepared. From the top (closed) section of the filter, twenty-six 0.08 inch thick, and twenty-three 0.12 inch thick bend bars were prepared.

In an attempt to identify whether a change in material strength has resulted after 1300 hours of filter operation, an as-received, untested filter from the same fabrication lot was sectioned for room temperature strength characterization. Thirty-three 0.08 inch thick bend bars were prepared from the top (closed) section of the filter, while thirty 0.08 inch thick bend bars were prepared from the web (core) section. Since the flange section of the as-received, untested filter had previously been removed by the manufacturer, it was not available for strength analysis. Figure K.2 identifies the location where bend bars were removed from the filters at Westinghouse.

In addition, an attempt was made to determine whether bend bar thickness had an effect on the resulting strength data. This issue was raised by ANL in a similar effort which characterized an as-fabricated alumina/mullite filter, and a filter which had operated for 77 hours in the Texaco entrained-bed gasification facility.[1] In the ANL effort, the flange material was actually a combination of samples which had been removed from the flange, as well as from the top (closed) section of the filter. ANL detected an apparent difference in strength between bend bars removed from the flange areas and the web (core) section. Even though the flange samples were thicker than the web (core) samples, the flange samples were identified to have a higher strength in comparison to the web (core) samples. The thicker the test sample is, the larger the volume of material under stress. Normally, the larger the volume of

Dwg. 9418A81

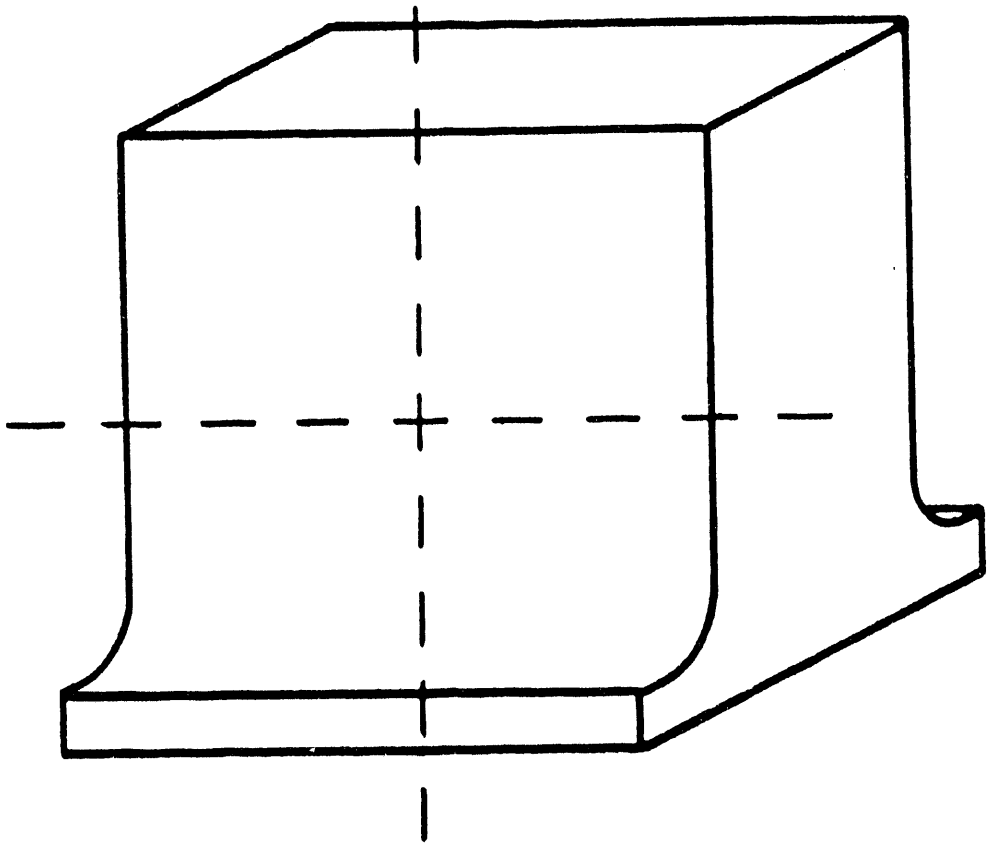

Figure K.1 - Quadrant Sections Used at Westinghouse for Determining Material Strength of the 1300 Hour Filter

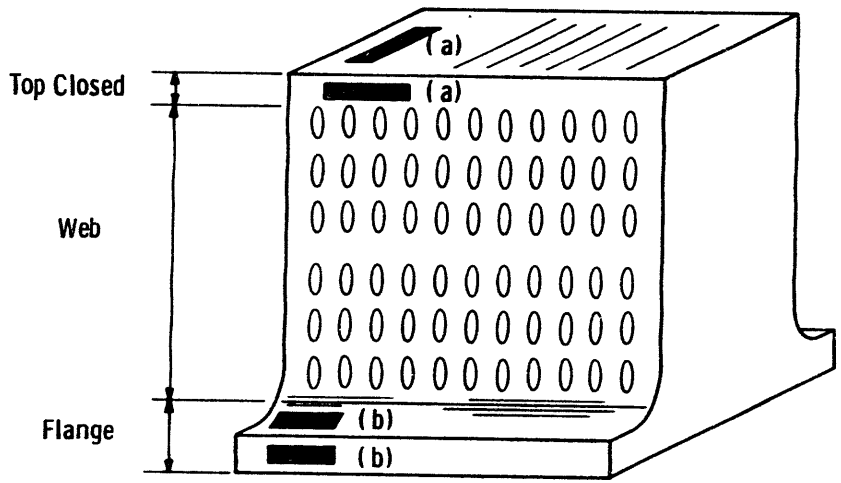

(a) Top Section Bend Bars Were Removed Both Transversely and Longitudinally to Stack Plates

(b) Flange Section Bend Bars Were Removed Transverse to Stacked Plates

Dwg. 5646B46

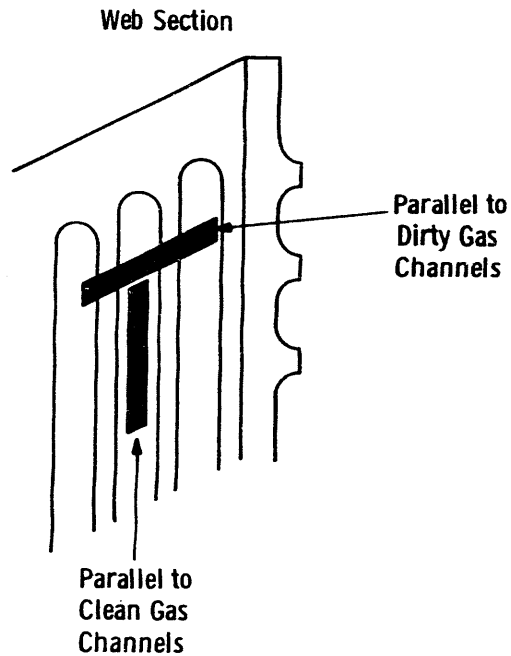

Figure K.2 - Bend Bar Locations for Material Strength Characterization at Westinghouse

sample under test, the lower the resulting strength, since the flaw population is also considered to increase, and therefore the probability of larger flaws is increased. Figure K.3 identifies the location where bend bars were removed from the filters at ANL.

2. STATISTICAL ANALYSES

Analysis of variance (ANOVA) techniques were used to determine if the strength differences observed between bend bar samples taken from different filter locations, or the differences that were observed between the 1300 hour tested filter and the as-fabricated, untested filter material were larger than what would be expected from chance or random variation. If the differences do not result from random variation, then there is an effect of the tested variable (i.e., either filter location or filter condition) on the filter material strength. The strength distribution for the given variable (i.e., filter location or filter condition) then is representative of the strength of the material for that variable.

The Weibull statistical fracture theory is widely used in ceramic material applications. This theory predicts that the strength of a ceramic material decreases with increasing sample size (i.e.,area). The most used parameter of this theory is the Weibull modulus (m), which is an index of ceramic material strength reproducibility. The higher the m value, the more reliable (i.e., predictable) the material is, since there is a lower scatter in fracture strength.

An important consideration in determining the Weibull modulus is the sample size (i.e., number). The uncertainty in the m value decreases, as sample size increases. This uncertainty, or error, is shown in Figure K.4[(2)] as a function of sample size for a 90 percent confidence interval. For example, a sample size of 40 gives an approximate error of ±22% for the calculated Weibull modulus.

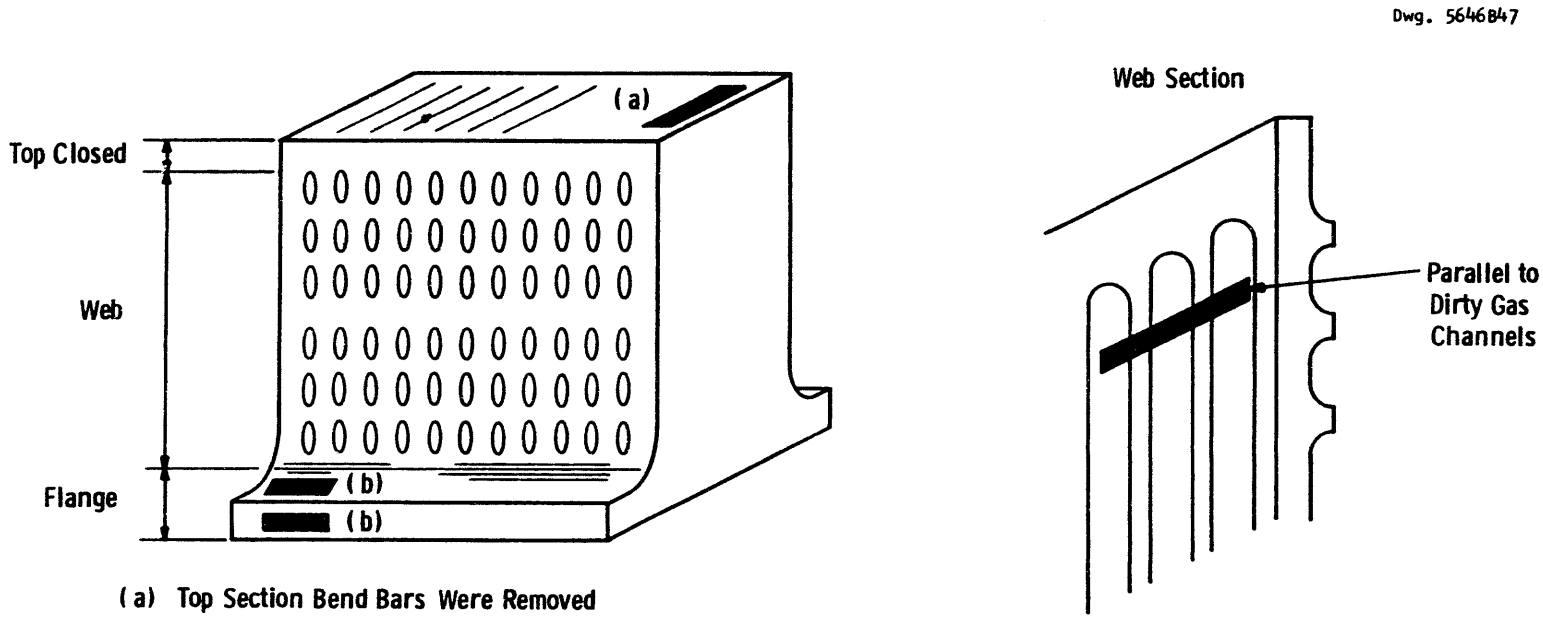

(a) Top Section Bend Bars Were Removed Parallel to Seam Plates

(b) Flange Section Bend Bars Were Removed Transverse to Stacked Plates.

Note: No Differentiation is Made Between Bend Bars Removed from the Top Closed Section and the Bottom Flange Area

Figure K.3 - Bend Bar Locations for Material Strength Characterization at ANL

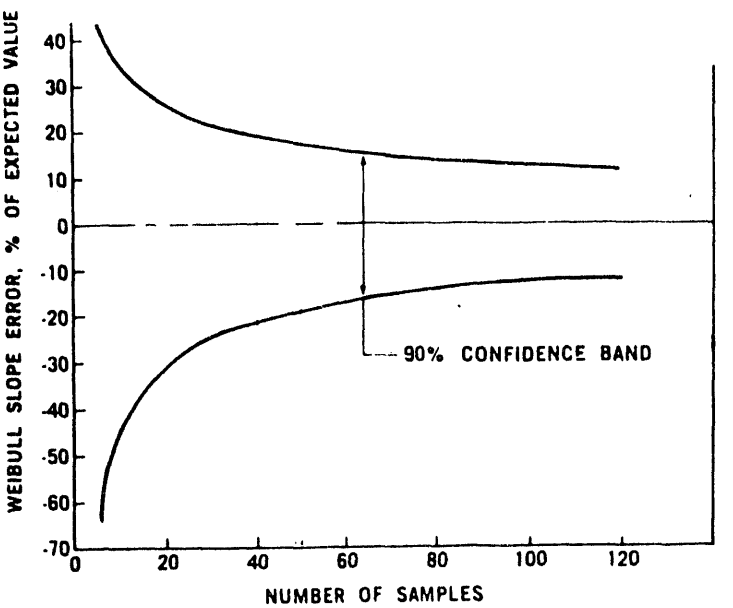

Figure K.4 - Weibull Slope Error Versus Sample Size

3. RESULTS AND DISCUSSION

Table K.1 summarizes the Westinghouse room temperature 4-point bend strength and Weibull modulus results for the as-fabricated filter material and the 1300 hour HTHP PFBC exposed filter. The strength data for all 198 bend bars are presented at the back of this appendix beginning with Table K.8. The average bend bar height and width are also shown in Table K.1. The length of the bend bar under test is the same as the lower span length (1.57 inches) of the test fixture, while the actual bend bar length used in this effort was 1.8 inches. The sample size was kept as consistent as possible to minimize the effect of sample volume variation on material strength. The height of the bend bars was limited to the thickness of the web (core) section material. For consistency, the top (closed) and flange section samples were machined to approximately the same thickness as in the web (core). Two sets of bend bars were prepared from the 1300 hour filter with a larger thickness, but a smaller width. The material strength results that are shown in Table K.1, as well as conclusions generated in the ANOVA analyses are discussed in the following sections.

3.1 As-Fabricated Filter Material

Table K.1 indicates that there is a difference in material strength between the top (closed) and web (core) sections of the as-fabricated, untested filter. The ANOVA results presented in Table K.2 indicate that the strength difference is based on where the bend bars are taken from (i.e., either the top (closed) or web (core) section), and that this difference is not a result of random variation. The strength distributions from the top (closed) and web (core) sections are therefore considered to be significantly different, and are not from the same parent distribution. This is shown more clearly by the 95 percent confidence intervals for the top (closed) and web (core) section group means in the "Group Summaries" portion of Table K.2.

TABLE K.1

MATERIAL STRENGTH AND WEIBULL VALUES FOR THE AS-FABRICATED UNTESTED ALUMINA/MULLITE FILTER AND THE 1300 HOUR HTHP PFBC TESTED FILTER

	As-Fabricated	1300 Hour Filter	
	Top*	Top	Top**
Number of Samples	33	26	23
4-Point Strength, psi	3529±222	2666±168	2653±220
Weibull Modulus, m	19.2	19.1	14.3
Height, inch	0.082±0.005	0.083±0.003	0.120±0.001
Width, inch	0.190±0.005	0.200±0.002	0.160±0.005
	Web*	Web	
Number of Samples	30	48	
4-Point Strength, psi	3148±368	2377±354	
Weibull Modulus, m	8.2	7.0	
Height, inch	0.073±0.008	0.070±0.003	
Width, inch	0.196±0.004	0.198±0.005	
		Flange	Flange**
Number of Samples		22	15
4-Point Strength, psi		2354±169	2495±258
Weibull Modulus, m		16.2	11.4
Height, inch		0.078±0.003	0.115±0.006
Width, inch		0.197±0.001	0.160±0.001

* Top (Closed Section); Web (Core).
** Thicker Bend Bars.

TABLE K.2

ANOVA AND GROUP SUMMARIES COMPARISON OF MATERIAL STRENGTH FOR THE TOP AND WEB SECTIONS OF THE AS-FABRICATED UNTESTED FILTER

ANALYSIS OF VARIANCE TABLE

	DF	SS	MS=SS/DF	F VALUE	SIG LEVEL
FACTOR	1	2273053.111688	2273053.111688	25.21	0
ERROR	61	5499273.745455	90152.028614		
TOTAL	62	7772326.857143			

The null hypothesis that the samples come from populations with equal means can be rejected (p = 0).

Group Summaries

Group Name	N	Mean	Stdev
artop	33	3528.727273	222.112341
arweb	30	3148.400000	367.685642

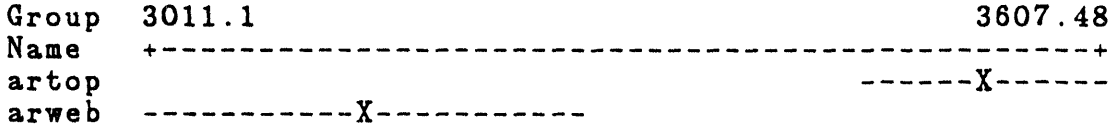

Error bars represent non-simultaneous 95 percent confidence intervals for the group means.

The resulting difference in material strength is considered to be related to the critical flaw size in the porous ceramic matrix. Critical flaws are most likely considered to result from large pores or interconnected porosity in the alumina/mullite matrix. Consequently, the strength differences between the as-fabricated untested filter top (closed) and web (core) sections are probably related to differences in the average pore size, and the pore size distribution of each section.

As shown in Table K.1, the Weibull modulus for the top (closed) section is more than twice that of the web (core) section. This indicates that there is a larger degree of scatter in the web (core) section strength data, and therefore less predictability (i.e., lower reliability) in the results. Weibull values greater than 10 are considered to be very good for ceramic materials. Weibull plots for all materials analyzed are presented in Appendix C.

3.2 Long-Term Durability Filter

Material strength and Weibull modulus comparisons were made for the HTHP PFBC 1300 hour filter based on sample location and thickness. These data are also presented in Table K.1. Similar to the as-fabricated untested cross flow filter, the top (closed) section of the HTHP PFBC 1300 hour filter appears to be stronger than its web (core) section. The flange section of the 1300 hour filter, however, appears to have a resulting strength that is similar to that of its web (core) section. Note that the apparent lower material strength in the 1300 hour filter flange area, tends to coincide with the location of filter failure.

The ANOVA results shown in Table K.3 for top (closed), web (core), and flange sections indicates that a difference in strength results depending on where the bend bar is taken from, and that this difference is not a result of random variation. The "Group Summaries" portion of Table 3 indicates that the web (core) and flange sections have similar means and 95 percent confidence intervals, whereas, the top

TABLE K.3

ANOVA AND GROUP SUMMARIES COMPARISON OF MATERIAL STRENGTH FOR THE TOP, WEB, AND FLANGE SECTIONS OF THE HTHP PFBC 1300 HOUR FILTER

ANALYSIS OF VARIANCE TABLE

	DF	SS	MS=SS/DF	F VALUE	SIG LEVEL
FACTOR	2	1677111.042249	838555.521125	10.83	0
ERROR	93	7203546.916084	77457.493721		
TOTAL	95	8880657.958333			

The null hypothesis that the samples come from populations with equal means can be rejected (p = 0).

Group Summaries

Group Name	N	Mean	Stdev
Flange	22	2354.545455	169.317602
Top	26	2666.538462	167.816622
Web	48	2376.750000	354.228229

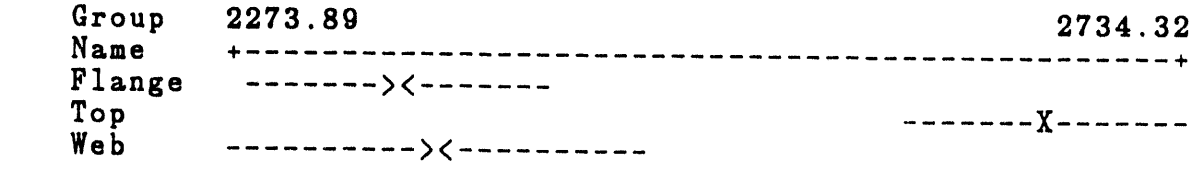

Error bars represent non-simultaneous 95 percent confidence intervals for the group means.

(closed) section mean and confidence interval differs significantly from the web (core) and flange sections. Figure K.5 graphically illustrates a comparison of the three filter sections.

From the web (core) section, an equal number of bend bars were prepared with tensile surfaces from the dirty and clean gas channels. This was done in an attempt to determine if the strength of the dirty channel surfaces was affected by direct contact with ash fines during the 1300 hours of filter operation. Most of the strength test bend bar failures were seen to be initiated at or near the outer surface, which is in tension. Table K.4 shows the ANOVA results and the "Group Summaries" data for the dirty and clean surfaces in the web (core) section. Since there are no apparent differences between the dirty (2381 ± 320 psi) and clean (2373 ± 392 psi) channel surfaces, these data are grouped together simply as web (core) section data.

The Weibull moduli for the top (closed), web (core), and flange sections are shown in Table K.1. The top (closed) and flange sections have high m values (19.1 and 16.2, respectively). The web (core) section has an m value of 7.0, which indicates considerably more scatter in the web (core) fracture strength values in comparison to the top (closed) and flange sections.

As previously discussed, the ANL data indicated that the thicker bend bar samples from the flange and top (closed) sections were as a group, stronger than the thinner samples from the web (core) section. ANL proposed that due to the high porosity of the alumina/mullite material, the large flaws, if present in the thin web (core) section, may lower the resulting material strength. This would not be expected if the web (core) bend bars were prepared with a thickness that was comparable to that of the thicker flange and top (closed) sections. A similar effort was undertaken at Westinghouse using the 1300 hour alumina/mullite filter.

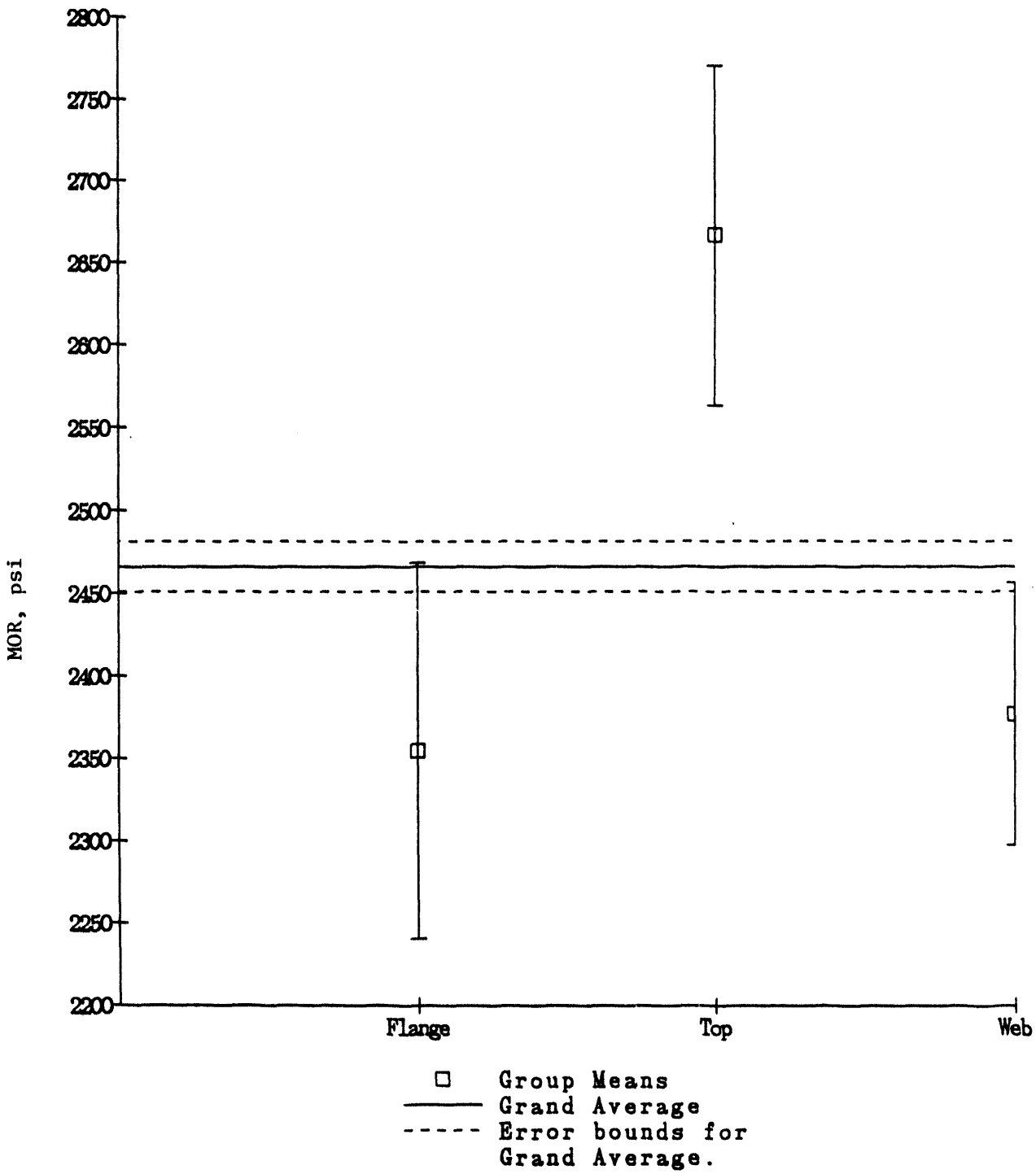

Figure K.5 - Simultaneous Comparisons Between Groups

TABLE K.4

ANOVA AND GROUP SUMMARIES COMPARISON OF MATERIAL STRENGTH FOR DIRTY AND CLEAN SIDE SURFACES IN THE WEB SECTION OF THE 1300 HOUR HTHP PFBC FILTER

ANALYSIS OF VARIANCE TABLE

	DF	SS	MS=SS/DF	F VALUE	SIG LEVEL
FACTOR	1	736.333333	736.333333	0.01	0.94
ERROR	46	5896712.666667	128189.405797		
TOTAL	47	5897449.000000			

There is insufficient evidence to reject the null hypothesis that samples come from populations with equal means (p = 0.94).

Group Summaries

Group Name	N	Mean	Stdev
clean	24	2372.833333	392.052755
dirty	24	2380.666667	320.426980

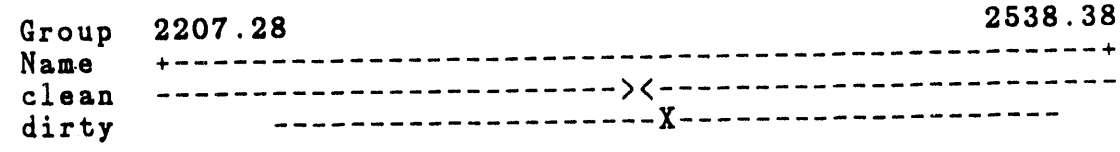

Error bars represent non-simultaneous 95 percent confidence intervals for the group means.

The intent of preparing the additional 4-point bend samples from the flange and top (closed) sections of the 1300 hour filter was that these samples would be 50 percent thicker than the web (core) bend bar thickness, but they would maintain the same width. These samples would therefore have a 50 percent larger volume than the original bend bar samples, and they would be expected to show a lower average 4-point bend strength as a result of the increased volume of material under test. However, the thicker bend bar samples were inadvertently prepared with a smaller width which resulted in only a slight increase in sample volume under test. As such, no difference in strength would be expected from the thicker samples when compared to the normal height samples. This conclusion was verified by the results in Table K.1. The flange and top (closed) section 4-point bend strength results were therefore not affected by test sample thickness for similar volume samples.

The Weibull m values do, however, indicate differences between the "thinner" and "thicker" flange and top (closed) section bend bars. The Weibull m value for the thicker bend bar samples are generally less than those of the thinner bend bars. These differences may be attributed to the large errors (Figure K.4) that could result when using relatively small sample sizes.

3.3 Comparison of the As-Fabricated and Long-Term Durability Filter Materials

Since flange data are not available for the as-fabricated, untested alumina/mullite filter material, a comparison will be made only between the top (closed) and web (core) sections of the as-fabricated and 1300 hour filter materials. This comparison will not include the thicker bend bar sample data.

There is an apparent 24 percent decrease in strength between the as-fabricated, untested alumina/mullite filter matrix and the matrix material after 1300 hours of operation in the Westinghouse HTHP PFBC

test facility. This decrease is consistent for both the top (closed) and web (core) sections of the filters. Because the strength differences between the as-fabricated, untested and 1300 hour filter are large, an ANOVA is not required to confirm that the decrease in strength is related to 1300 hours of filter operation. However, an ANOVA was performed using the as-fabricated, untested and 1300 hour filter web (core) section data. These results along with the "Group Summaries" are shown in Table K.5.

There is no apparent change in the Weibull m values for the as-fabricated, untested and 1300 hour filter top (closed) and web (core) sections. The m values for the top (closed) sections of the as-fabricated, untested and 1300 hour filters are 19.2 and 19.1, respectively, and for the web (core) sections, 8.2 and 7.0, respectively. The web (core) section continues to have a much higher degree of scatter in the material strength values.

In contrast with the Westinghouse as-fabricated, untested and the 1300 hour filter web (core) Weibull modulus data are the ANL data. The ANL data shown a definite change in the flaw population of the 77 hour Texaco tested web (core) material in comparison with the original material (14 versus 9, respectively). Further efforts are needed to generate a substantially larger material's properties data base, prior to concluding whether the variation between the Westinghouse and ANL Weibull modulus data reflect filter material variation within a given fabrication lot, or simply procedural and evaluation techniques.

If we assume that initially the strength of the 1300 hour filter flange was equivalent to that of its top (closed) section (i.e., 3529 psi) as in the ANL effort, then an apparent 33 percent decrease (i.e., 3529 to 2354 psi) in the flange material strength is expected to have occurred during the 1300 hours of filter operation. In the current filter failure mechanism, a reduction in material strength (maximum

TABLE K.5

ANOVA AND GROUP SUMMARIES COMPARISON OF MATERIAL STRENGTH FOR THE AS-FABRICATED UNTESTED AND 1300 HOUR FILTER WEB SECTIONS

ANALYSIS OF VARIANCE TABLE

	DF	SS	MS=SS/DF	F VALUE
FACTOR	1	10992807.184615	10992807.184615	85.09
ERROR	76	9818038.200000	129184.713158	
TOTAL	77	20810845.384615		

	SIG LEVEL
FACTOR	0
ERROR	
TOTAL	

The null hypothesis that the samples come from populations with equal means can be rejected (p = 0).

Group Summaries

Group Name	N	Mean	Stdev
Web	48	2376.75	354.228229
arweb	30	3148.40	367.685642

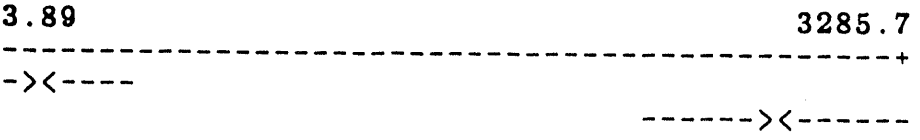

Error bars represent non-simultaneous 95 percent confidence intervals for the group means.

limit to be determined) coincides with failure in the ceramic component. Therefore over time, the entire filter body may lose strength, and when the maximum change in material strength results or a lower tolerance limit is achieved, failure occurs.

3.4 Summary

Table K.6 summarizes the room temperature strength data generated at Westinghouse for the as-fabricated, untested and 1300 hour filter materials. These data indicate that:

- As expected, for a constant volume of material, bend bar thickness does not influence the resulting room temperature strength.

- The top (closed) section from both the as-fabricated, untested and 1300 hour filters appears to be stronger than the web (core) section.

- Material strength in the web (core) and flange sections of the 1300 hour filter appears to be nearly equivalent.

- An apparent 24 percent loss in material strength results after 1300 hours of exposure to PFBC ash at 1600°F (870°C), 150 psig, and 2068 pulse cleaning cycles.

The loss of material strength data reflects only an apparent change in the properties of the filter plates, or within the thicker top or flange sections. These data do not reflect any change in bond strength which may have resulted along the mid-ribbed bond.

The apparent loss of material strength after 1300 hours of exposure in the HTHP PFBC test rig is considered to have resulted from the thermal cycling (and/or vibration) which the filter experienced

TABLE K.6

ROOM TEMPERATURE STRENGTH DATA
FOR THE 1300 HOUR WESTINGHOUSE PFBC HTHP FILTER MATERIALS

-Alumina/Mullite -

Material	Location in Filter	MOR, psi	Bend Bar Thickness, in.	Weibull
As-Received	Top[a]	3529±222(33)*	0.082±0.005	19.2
1300 Hr. Filter	Top	2666±168(26)	0.083±0.003	19.1
1300 Hr. Filter	Top	2653±220(23)	0.120±0.001	14.3
As-Received	Web[b]	3148±368(30)	0.073±0.008	8.2
1300 Hr. Filter	Web	2377±354(48)	0.070±0.003	7.0
1300 Hr. Filter	Flange	2354±169(22)	0.078±0.003	16.2
1300 Hr. Filter	Flange	2495±258(15)	0.115±0.006	11.4

* () Indicate The Number Of Bend Bars Used In Determining Bend Strength.
(a) Top (Closed) Section Of The Filter.
(b) Web Or Core Section Of The Filter Body.

during testing. In the HTHP simulator test rig, the gas phase (73% N_2, 14% H_2O, 7% CO_2, and 6% O_2; no gas phase sulfur or alkali species) and the Grimethorpe or Exxon fly ash particulates are not considered to react with the alumina/mullite matrix. What is considered at this time to have occurred, is a phase change which results in the surfacing of the mullite rods.[3] Additional efforts are needed to identify whether the extended time at filter operating temperature and/or thermal cycling induces further mullitization within the alumina/mullite filter matrix.

Comparison of the Westinghouse data presented in Table K.6 can be made with the ANL data shown in Table K.7. Note that both the as-fabricated, untested filter materials that were tested at Westinghouse and ANL, as well as the 1300 hour and Texaco exposed filters were fabricated from the same lot in February 1989.

Generally the flange and/or top closed sections have a higher Weibull value (m) in comparison with the web (core) section. This suggests that the material strength in the flange and/or top (closed) sections is relatively homogeneous, and not as widely scattered or variable as in the web (core) section.

Secondly, for the ANL data, the Weibull value for the web (core) section changes from 14 to 9 indicating a change in the flaw population when the filter material is exposed to the Texaco gasifier environment. For the Westinghouse 1300 hour simulated PFBC filter, no apparent change in the Weibull value is evident. This may imply that the Westinghouse simulated PFBC HTHP test facility which contains ash and no gas phase sulfur or alkali, is not as chemically reactive with the filter matrix, as possibly an actual process gas environment. Alternately, the Weibull variation may be attributed to variation between filters within a given fabrication lot.

TABLE K.7

ROOM TEMPERATURE STRENGTH DATA
FOR THE TEXACO EXPOSED FILTER MATERIALS

-Alumina/Mullite -

Material*	Location in Filter	MOR,** psi	Weibull
As-Received	Web(a)	3234±334	14
Texaco Exposed	Web	3089±334	9
As-Received	Flange(b)	3930±290	16
Texaco Exposed	Flange	4099±276	18

* Bend Bars: 5 cm x 0.6 cm x 0.3 cm; 60 Samples/Area.
** 4-Point Bend Mode: Outer Span = 4.45 cm; Inner Span = 0,925 cm; Cross Head Speed = 0.05 cm/min.
(a) Web or Core Section of the Filter Body.
(b) Flange Consists Of Both Top (Closed) Section Of The Filter And Actual Flange Area.

In contrast with the Westinghouse data, ANL indicates that for the Texaco gasifier filter, the flexural strength of the flange is consistently higher than in the web (core) section. Note that the flange data reported by ANL is a combination of both the flange and top (closed) sections of the filter. Perhaps the flange and top (closed) sections are initially stronger than the web (core) section due to better sintering between flat plates during manufacturing, and that with time (i.e., 167 hours at Texaco versus 1300 hours in the Westinghouse HTHP rig), the flange area is weakened due to vibration and/or thermal cycling during pulse cleaning, such that the strength in the flange section approaches (i.e., is equivalent or possibly even less than) the strength of the web (core) section. Further effort is obviously needed to more fully understand the effect that operating time, gas phase chemistry, and temperature have on changes which may be occurring in the alumina/mullite material properties during actual filter operation.

REFERENCES

1. Singh, J. P., S. Majumdar, A. S. Wagh, T. Wenzel, and R. B. Poeppel, Materials Qualification Technology For Ceramic Cross Flow Filters, Argonne National Laboratory, to be issued.

2. Baratta, F. I., Requirements For Flexure Testing of Brittle Materials, Final Report, AMMRC TR 82-20, April 1982.

3. Alvin, M. A., D. M. Bachovchin, J. E. Lane, and T. E. Lippert, Thermal/Chemical Degradation of Ceramic Cross Flow Filter Materials, Westinghouse Electric Corporation, DOE Contract No. DE-AC21-88MC25034, June 1990 Monthly Report.

FOUR-POINT BEND STRENGTH DATA

TABLE K.8
TOP AND WEB SECTIONS OF THE AS-FABRICATED UNTESTED ALUMINA/MULLITE FILTER MATERIAL

Specimen ID	RT Stress (psi)	Height (in)	Width (in)	Filter Location
T-1	3119	0.076	0.195	top
T-2	3512	0.077	0.194	top
T-3	3417	0.086	0.187	top
T-4	3403	0.085	0.182	top
T-5	3820	0.076	0.195	top
T-6	3822	0.084	0.185	top
T-7	3388	0.086	0.188	top
T-8	3558	0.078	0.195	top
T-9	3559	0.076	0.196	top
T-10	3728	0.078	0.195	top
T-11	3477	0.087	0.181	top
T-12	3347	0.087	0.185	top
T-13	3468	0.086	0.187	top
T-14	3873	0.076	0.195	top
T-15	3575	0.086	0.189	top
T-16	3707	0.077	0.196	top
T-17	3503	0.078	0.196	top
T-18	3072	0.077	0.196	top
T-19	3471	0.077	0.196	top
T-20	3631	0.088	0.189	top
T-21	3872	0.076	0.195	top
T-22	3799	0.076	0.195	top
T-23	3314	0.085	0.187	top
T-24	3112	0.091	0.183	top
T-25	3451	0.086	0.187	top
T-26	3499	0.086	0.188	top
T-27	3622	0.087	0.187	top
T-28	3840	0.077	0.196	top
T-29	3553	0.077	0.196	top
T-30	3175	0.085	0.186	top
T-31	3811	0.087	0.183	top
T-32	3454	0.076	0.196	top
T-33	3496	0.085	0.181	top
W-1	2713	0.082	0.201	web
W-2	3332	0.072	0.193	web
W-3	3010	0.073	0.192	web
W-4	3217	0.082	0.197	web
W-5	3366	0.073	0.193	web
W-6	2998	0.081	0.198	web
W-7	3438	0.072	0.193	web

TABLE K.8 (continued)

W-8	3132	0.072	0.193	web
W-9	3019	0.071	0.194	web
W-10	3456	0.071	0.192	web
W-11	3454	0.083	0.195	web
W-12	3003	0.084	0.198	web
W-13	3195	0.08	0.201	web
W-14	2994	0.074	0.192	web
W-15	3040	0.083	0.201	web
W-16	3251	0.073	0.193	web
W-17	3503	0.079	0.194	web
W-18	3014	0.073	0.188	web
W-19	3286	0.075	0.196	web
W-20	3053	0.063	0.197	web
W-21	3636	0.08	0.196	web
W-23	3438	0.081	0.192	web
W-24	1708	0.078	0.196	web
W-25	2501	0.06	0.201	web
W-26	3364	0.059	0.202	web
W-27	3297	0.06	0.202	web
W-28	3216	0.06	0.203	web
W-29	3246	0.059	0.2	web
W-30	3024	0.063	0.197	web
W-31	3548	0.078	0.195	web

TABLE K.9

WEB SECTION OF THE 1300 HOUR HTHP PFBC TESTED FILTER

Specimen ID	RT Stress (psi)	Height (in)	Width (in)	Filter Location
C1A1	2378	0.071	0.202	clean
C1A2	2536	0.07	0.201	clean
C1B1	1510	0.07	0.198	clean
C1B2	1522	0.07	0.201	clean
C1C1	2608	0.071	0.201	clean
C1C2	2780	0.071	0.201	clean
C2A1	2687	0.066	0.194	clean
C2A2	2164	0.069	0.194	clean
C2B1	2466	0.066	0.193	clean
C2B2	2783	0.066	0.192	clean
C2C1	2705	0.07	0.197	clean
C2C2	2778	0.071	0.196	clean
C3A1	2668	0.07	0.192	clean
C3A2	2768	0.07	0.192	clean
C3B1	2187	0.072	0.203	clean
C3B2	2411	0.072	0.203	clean
C3C1	2394	0.068	0.195	clean
C3C2	2113	0.067	0.196	clean
C4A1	2410	0.073	0.202	clean
C4A2	2349	0.072	0.201	clean
C4B1	2444	0.068	0.201	clean
C4B2	2572	0.07	0.2	clean
C4C1	2245	0.073	0.203	clean
C4C2	1470	0.071	0.203	clean
D1A1	2423	0.077	0.192	dirty
D1A2	2693	0.076	0.193	dirty
D1B1	2700	0.072	0.2	dirty
D1B2	2642	0.072	0.199	dirty
D1C1	2465	0.075	0.19	dirty
D1C2	2668	0.075	0.194	dirty
D2A1	2640	0.066	0.192	dirty
D2A2	2493	0.072	0.199	dirty
D2B1	2332	0.072	0.198	dirty
D2B2	1327	0.075	0.197	dirty
D2C1	2452	0.071	0.195	dirty
D2C2	2458	0.065	0.191	dirty
D3A1	2377	0.073	0.203	dirty
D3A2	2467	0.072	0.202	dirty
D3B1	1964	0.071	0.204	dirty
D3B2	2523	0.072	0.203	dirty
D3C1	2112	0.066	0.189	dirty
D3C2	2246	0.067	0.181	dirty

TABLE K.9 (continued)

D4A1	2591	0.069	0.2	dirty
D4A2	2420	0.067	0.2	dirty
D4B1	2255	0.066	0.204	dirty
D4B2	1766	0.067	0.201	dirty
D4C1	2597	0.066	0.203	dirty
D4C2	2525	0.067	0.199	dirty

TABLE K.10

FLANGE SECTION OF THE 1300 HOUR HTHP PFBC TESTED FILTER

Specimen ID	RT Stress (psi)	Height (in)	Width (in)	Filter Location
1FL-1	2355	0.081	0.198	Flange
1FL-2	2515	0.082	0.198	Flange
1FL-3	2273	0.081	0.198	Flange
1FL-4	2301	0.081	0.197	Flange
1FL-5	2273	0.081	0.198	Flange
1FL-6	2515	0.08	0.197	Flange
1FL-7	2549	0.08	0.198	Flange
1FL-8	2444	0.082	0.198	Flange
2FL-1	2215	0.076	0.197	Flange
2FL-2	2596	0.074	0.198	Flange
2FL-3	2222	0.077	0.196	Flange
2FL-4	2509	0.077	0.195	Flange
2FL-5	1862	0.074	0.197	Flange
2FL-6	2291	0.075	0.195	Flange
2FL-7	2445	0.077	0.197	Flange
2FL-8	2406	0.076	0.198	Flange
2FL-9	2301	0.075	0.196	Flange
2FL-10	2355	0.076	0.196	Flange
2FL-11	2453	0.078	0.198	Flange
2FL-12	2523	0.074	0.194	Flange
2FL-13	2304	0.076	0.198	Flange
2FL-14	2093	0.076	0.196	Flange

TABLE K.11

TOP SECTION OF THE 1300 HOUR HTHP PFBC TESTED FILTER

Specimen ID	RT Stress (psi)	Height (in)	Width (in)	Filter Location
3T-1	2693	0.086	0.202	Top
3T-2	2826	0.086	0.202	Top
3T-3	2810	0.085	0.203	Top
3T-4	2634	0.086	0.201	Top
3T-5	2865	0.086	0.203	Top
3T-6	2610	0.087	0.202	Top
3T-7	2865	0.086	0.202	Top
3T-8	2960	0.086	0.204	Top
3T-9	2810	0.086	0.203	Top
3T-10	2826	0.085	0.201	Top
3T-11	2647	0.085	0.201	Top
3T-12	2952	0.086	0.203	Top
4T-1	2480	0.079	0.198	Top
4T-2	2401	0.08	0.198	Top
4T-3	2591	0.082	0.201	Top
4T-4	2646	0.083	0.2	Top
4T-5	2791	0.082	0.2	Top
4T-6	2503	0.082	0.2	Top
4T-7	2705	0.083	0.198	Top
4T-8	2518	0.081	0.199	Top
4T-9	2728	0.082	0.198	Top
4T-10	2611	0.076	0.198	Top
4T-11	2494	0.08	0.198	Top
4T-12	2527	0.081	0.198	Top
4T-13	2463	0.083	0.198	Top
4T-14	2374	0.079	0.198	Top

TABLE K.12

FLANGE SECTION OF THE 1300 HOUR HTHP PFBC TESTED FILTER
- THICKER BEND BAR DATA -

Specimen ID	RT Stress (psi)	Height (in)	Width (in)	Filter Location
T1FL-1	2154	0.122	0.161	ThFlange
T1FL-2	1919	0.121	0.16	ThFlange
T1FL-3	2712	0.124	0.161	ThFlange
T1FL-4	2742	0.122	0.16	ThFlange
T1FL-5	2426	0.124	0.161	ThFlange
T1FL-6	2464	0.124	0.161	ThFlange
T2FL-1	2728	0.11	0.159	ThFlange
T2FL-2	2941	0.11	0.161	ThFlange
T2FL-3	2306	0.11	0.159	ThFlange
T2FL-4	2343	0.111	0.16	ThFlange
T2FL-5	2575	0.109	0.158	ThFlange
T2FL-6	2435	0.11	0.159	ThFlange
T2FL-7	2420	0.109	0.159	ThFlange
T2FL-8	2675	0.111	0.159	ThFlange
T2FL-9	2591	0.111	0.158	ThFlange

TABLE K.13

TOP SECTION OF THE 1300 HOUR HTHP PFBC TESTED FILTER
- THICKER BEND BAR DATA -

Specimen ID	RT Stress (psi)	Height (in)	Width (in)	Filter Location
T3T-1	2381	0.121	0.156	ThTop
T3T-2	3035	0.12	0.157	ThTop
T3T-3	2695	0.121	0.154	ThTop
T3T-4	2944	0.121	0.153	ThTop
T3T-5	3012	0.121	0.153	ThTop
T3T-6	2976	0.121	0.156	ThTop
T3T-7	2917	0.12	0.153	ThTop
T3T-8	2878	0.12	0.157	ThTop
T3T-9	2402	0.121	0.153	ThTop
T3T-10	2764	0.121	0.157	ThTop
T4T-1	2649	0.121	0.164	ThTop
T4T-2	2605	0.12	0.163	ThTop
T4T-3	2526	0.121	0.165	ThTop
T4T-4	2381	0.119	0.162	ThTop
T4T-5	2709	0.12	0.166	ThTop
T4T-6	2666	0.12	0.164	ThTop
T4T-7	2479	0.121	0.162	ThTop
T4T-8	2550	0.12	0.163	ThTop
T4T-9	2507	0.118	0.167	ThTop
T4T-10	2565	0.12	0.164	ThTop
T4T-11	2414	0.12	0.166	ThTop
T4T-12	2628	0.12	0.165	ThTop
T4T-13	2331	0.12	0.168	ThTop

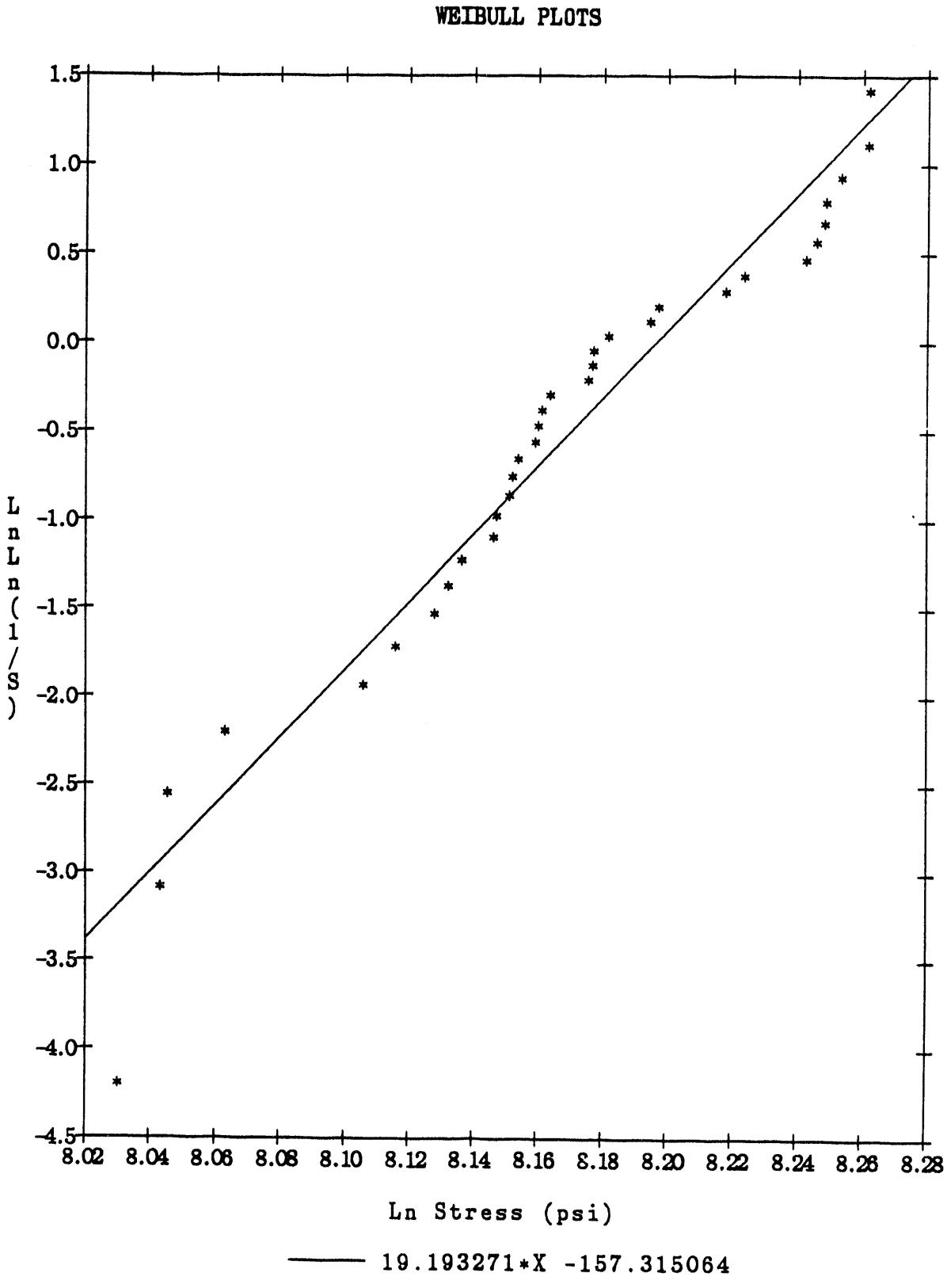

Figure K.6 - Weibull Probability of Failure For the Top (Closed) Section of the As-Fabricated Untested Alumina/Mullite Filter Material

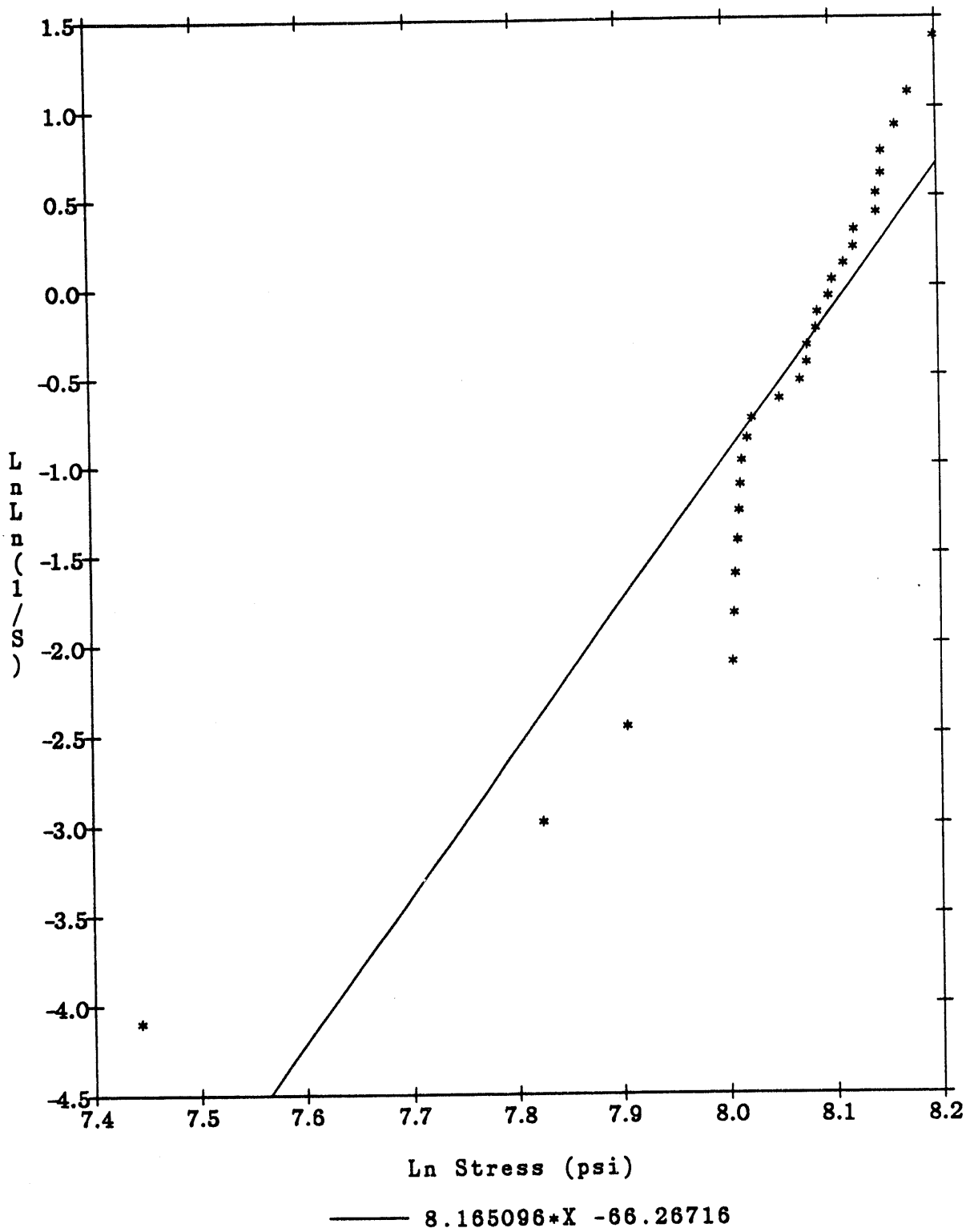

Figure K.7 - Weibull Probability of Failure For the Web Section of the As-Fabricated, Untested Alumina/Mullite Filter Material

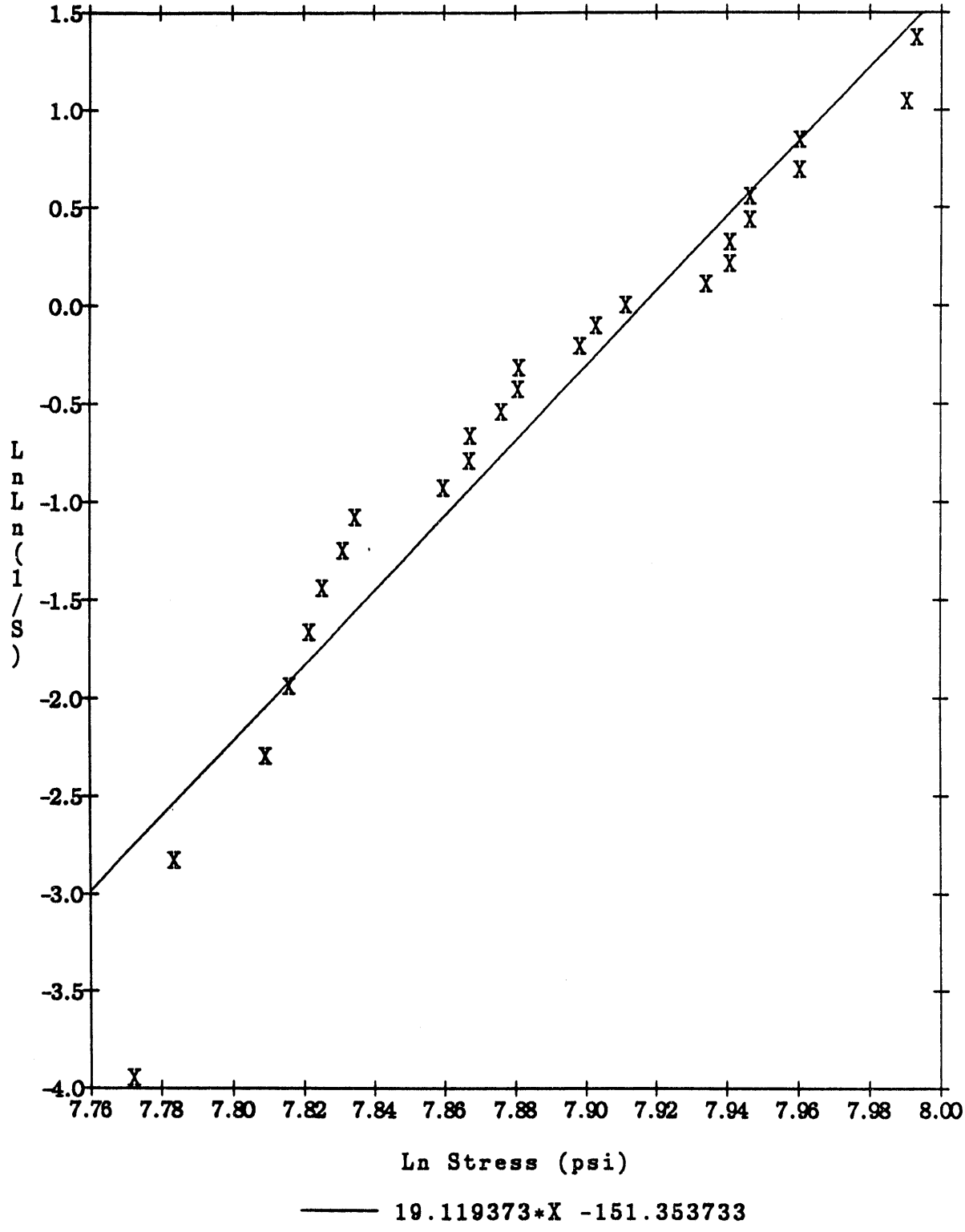

Figure K.8 - Weibull Probability of Failure For the Top Section of the 1300 Hour HTHP PFBC Filter

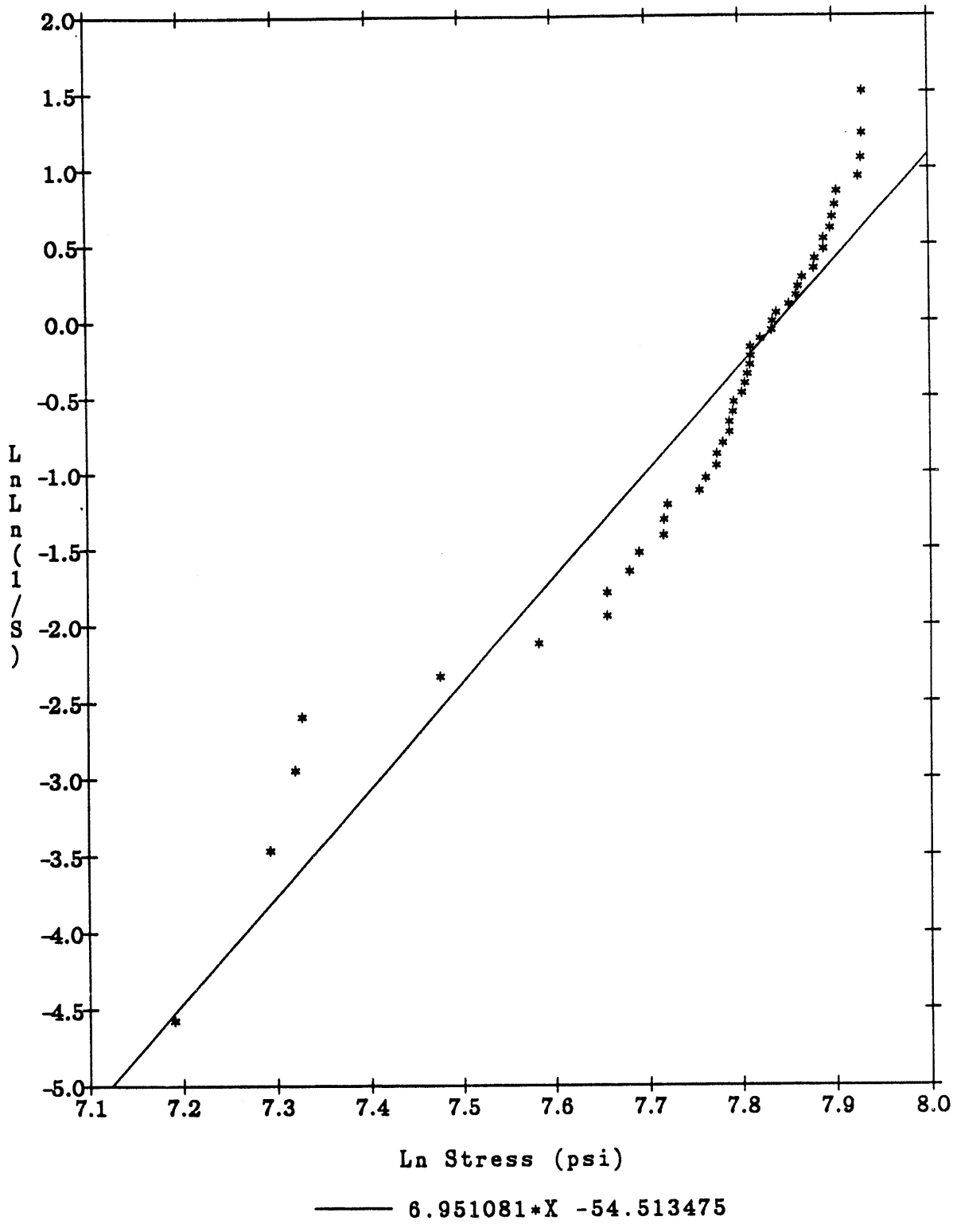

Figure K.9 - Weibull Probability of Failure For the Web Section of the 1300 Hour HTHP PFBC Filter

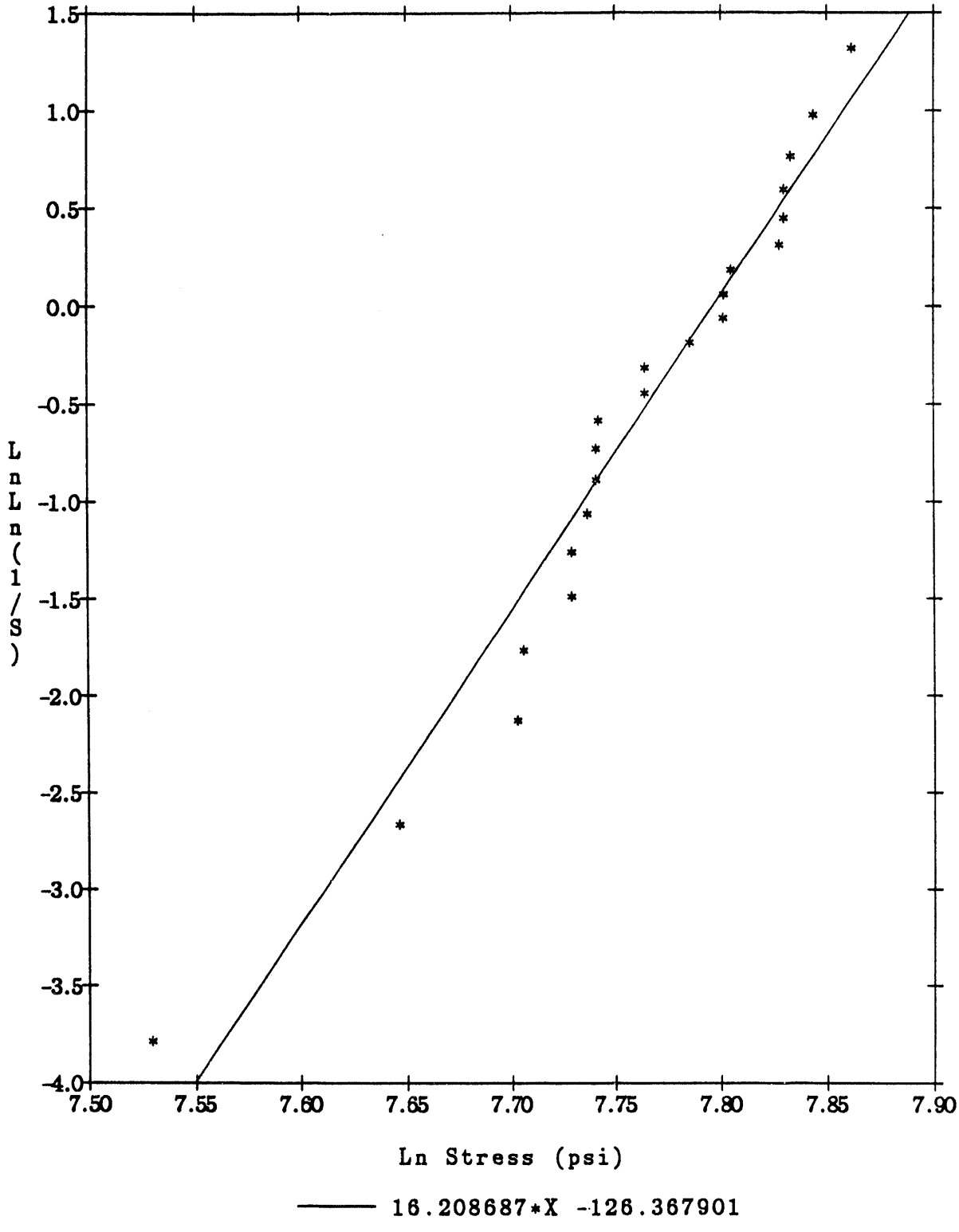

Figure K.10 - Weibull Probability of Failure For the Flange Section of the 1300 Hour HTHP PFBC Filter

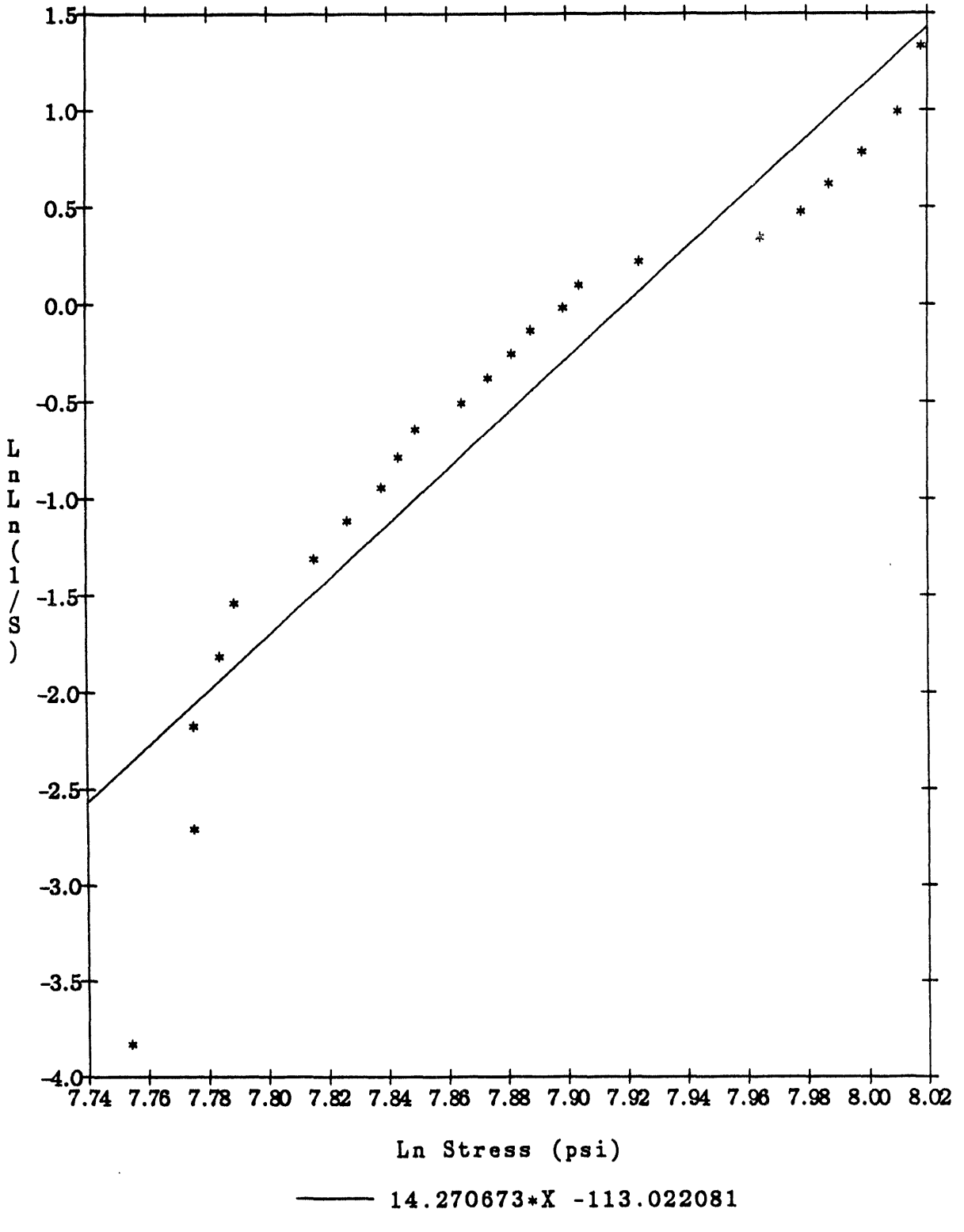

Figure K.11 - Weibull Probability of Failure For Thicker Bend Bar Samples Prepared From the Top Section of the 1300 Hour HTHP PFBC Filter

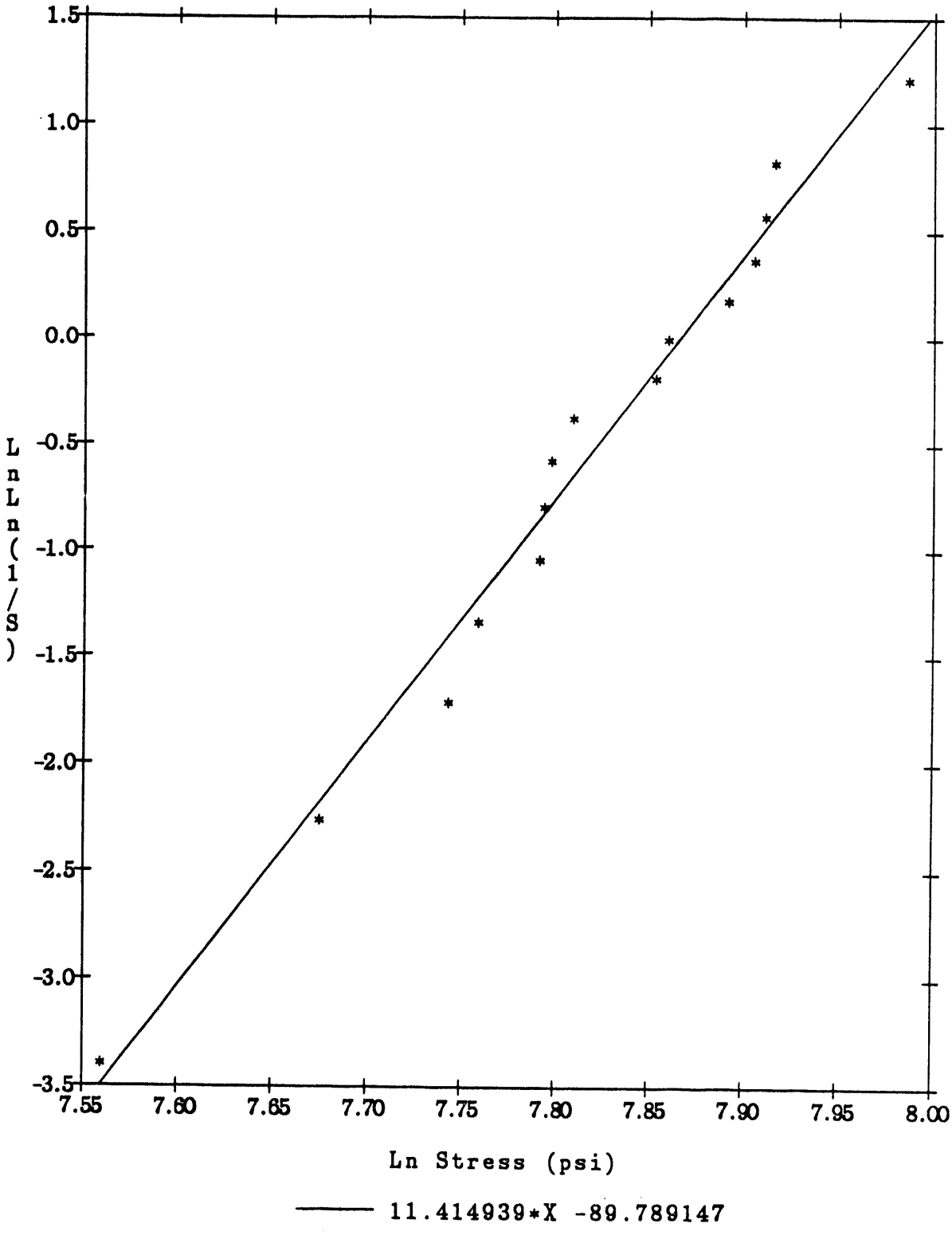

Figure K.12 - Weibull Probability of Failure For Thicker Bend Bar Samples Prepared From the Flange Section of the 1300 Hour HTHP PFBC Filter

APPENDIX L

HOT STRENGTH CHARACTERIZATION OF THE 1300 HOUR, HTHP TESTED CERAMIC CROSS FLOW FILTER

HOT STRENGTH CHARACTERIZATION OF THE 1,300 HOURS HIGH TEMPERATURE, HIGH PRESSURE TESTED CERAMIC CROSS FLOW FILTER

In order to develop the alkali kinetics and material life model for the alumina/mullite filter material in advanced coal fired processes, data have been generated at 870°C for material that has been exposed to:

- Gas phase alkali at 870°C for 100-1560 hours
- Gas phase alkali at 870°C for 100-1560 hours with pulse cycling
- 870°C for 1500 hours without gas phase alkali or pulse cycling.

As a result of this effort, we have demonstrated that the P-100A alumina/mullite matrix undergoes a conversion of the amorphous phase that is present in the material to anorthite at temperatures of 870°C in the presence of gas phase alkali. An increase in the hot strength of the material occurs as a result of anorthite formation (Figure L.1). As the period of exposure time to gas phase alkali increases, anorthite is converted into tridymite, leading to a reduction in the hot strength of the material.

When the alkali exposed alumina/mullite matrix is subjected to thermal cycling, simulating pulse cleaning, a somewhat reduced hot strength of the matrix results. We currently suspect that this results primarily from microcrack formations within the structure. Although we have not attempted to differentiate between the various phases or phase concentration through the thickness of the alkali exposed disc, the

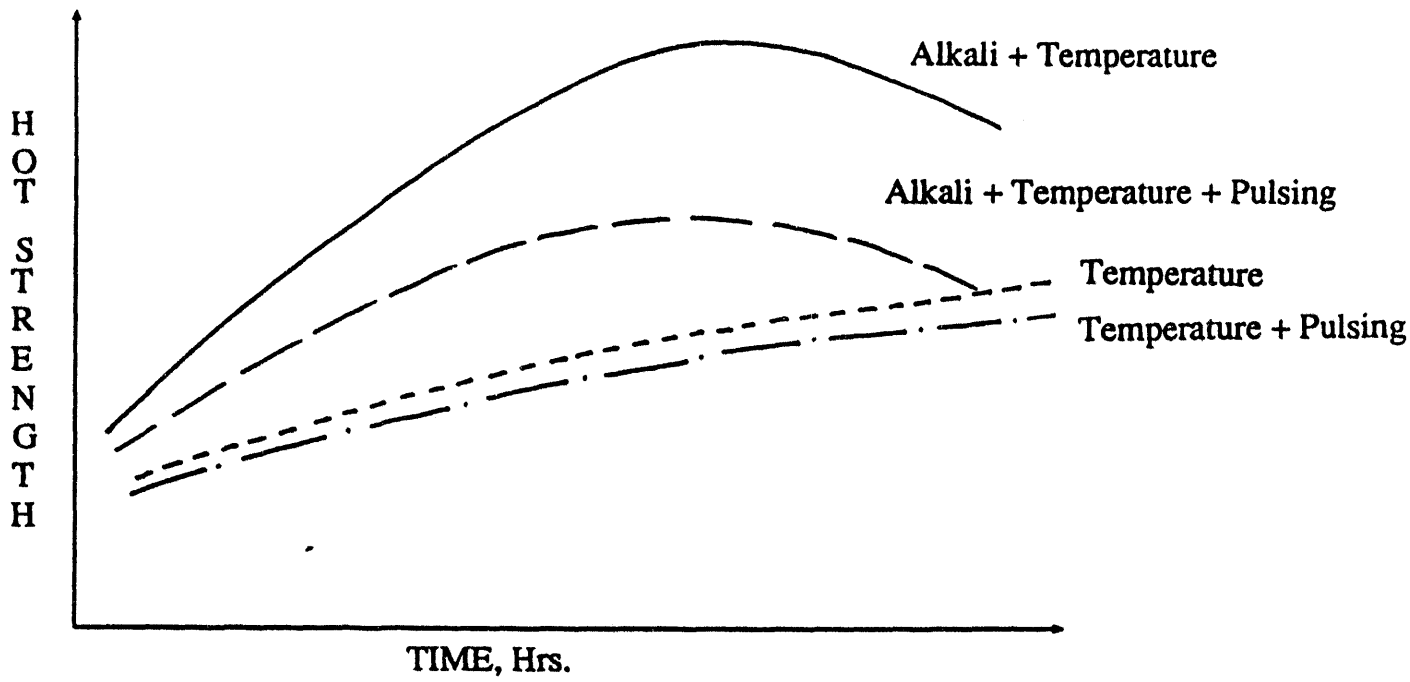

Figure L.1 - Influence of In-Service Parameters on the Hot Strength of the Alumina/Mullite Filter Matrix as a Function of Time

possibility exists that an additional or alternate phase may have formed along the pulsed surface, or that the concentration of tridymite is higher along the pulsed surface versus the alkali exposed surface.

A shown in Figure L.1, the alkali/steam/air environment tends to accelerate the increase in hot strength of the alumina/mullite matrix over that of the matrix that was simply subjected to long-term, high temperature exposure. Again we suspect that the amorphous phase is being converted into anorthite, however, as a slower rate.

In addition data have been generated for material removed from an alumina/mullite cross flow filter that operated for 1,300 hours at 850°C, filtering pressurized fluidized-bed combustion (PFBC) ash fines in one of Westinghouse's high temperature, high pressure (HTHP) test facilities. If alkali were present in the HTHP system, it was generated via the coal processed fines that were filtered during HTHP testing. No attempt was made to further introduce alkali into the system which would represent possible gas phase concentrations at actual process conditions.

Characterization of the 1,300 hour tested filter material consisted of room temperature strength analysis of the flange, web, and top closed sections of the filter, as well as x-ray diffraction analyses. As shown in Table L.1, post-test analysis room temperature flexural strength analysis of the matrix indicates that a 25% loss of strength had occurred uniformly throughout the entire cross flow filter element body. X-ray diffraction analyses of the ~1300 hour HTHP filter matrix identified the conversion of ~50% of the amorphous phase contained within the matrix to that of the crystallized anorthite phase.

As shown in Table L.2 hot strength data generated for the 1,300 hour HTHP tested filter indicate nearly comparable strengths along the clean and dirty gas channels (i.e., 3278$\pm$359 and 3362$\pm$521 psi, respectively). Note that the resulting hot strength of the filter

TABLE L.1

ROOM TEMPERATURE STRENGTH DATA FOR THE
1,300 HOUR WESTINGHOUSE PFBC HTHP TESTED FILTER MATERIAL

-Alumina/Mullite -

Material	Location in Filter	MOR, psi	Bend Bar Thickness, in.	Weibull
As-Received	Top*	3529±222(33)**	0.082±0.005	19.2
1300 Hr. Filter	Top	2666±168(26)	0.083±0.003	19.1
1300 Hr. Filter	Top	2653±220(23)	0.120±0.001	14.3
As-Received	Web	3148±368(30)	0.073±0.008	8.2
1300 Hr. Filter	Web	2377±354(48)	0.070±0.003	7.0
1300 Hr. Filter	Flange	2354±169(22)	0.078±0.003	16.2
1300 Hr. Filter	Flange	2495±258(15)	0.115±0.006	11.4

* Closed Section At The Top Of the Filter
** () Indicate The Number Of Bend Bars Used In Determining Bend Strength

Chart Speed: 5 cm/min.
Upper Span: 20 mm
Lower Span: 40 mm
4 Pt; 1/4 Flexure

TABLE L.2

HOT STRENGTH DATA FOR THE
1,300 HOUR WESTINGHOUSE PFBC HTHP TESTED FILTER MATERIAL

-Alumina/Mullite -

Test Sample No.	Temp., °C	Cross Head Speed, cm/min	Width, in.	Height, in.	Loads, lbs.	Strength, psi
Clean Gas Channels						
1	870	0.02	0.249	0.064	2.97	3429
2	870	0.02	0.248	0.063	2.68	3206
3	870	0.02	0.255	0.066	3.54	3753
4	870	0.02	0.248	0.067	3.53	3734
5	870	0.02	0.250	0.069	2.93	2899
6	870	0.02	0.249	0.069	3.30	3278
7	870	0.02	0.250	0.070	3.47	3335
8	870	0.02	0.249	0.066	3.35	3637
9	870	0.02	0.249	0.062	2.80	3445
10	870	0.02	0.256	0.067	2.84	2910
11	870	0.02	0.249	0.070	3.25	3137
12	870	0.02	0.249	0.066	2.37	2573
Dirty Gas Channels						
1	870	0.02	0.249	0.071	3.38	3171
2	870	0.02	0.249	0.071	2.83	2655
3	870	0.02	0.249	0.068	3.11	3181
4	870	0.02	0.249	0.074	3.46	2988
5	870	0.02	0.250	0.077	5.02	3988
6	870	0.02	0.249	0.073	4.20	3727
7	870	0.02	0.250	0.074	5.20	4473
8	870	0.02	0.250	0.074	4.65	4000
9	870	0.02	0.248	0.061	2.50	3190
10	870	0.02	0.249	0.062	2.64	3248
11	870	0.02	0.250	0.067	2.88	3022
12	870	0.02	0.250	0.066	2.85	3082
13	870	0.02	0.249	0.060	2.27	2982

As-Fabricated Average Hot Strength:

Clean Gas Channel Average Hot Strength: 3278±359 (12)
Dirty Gas Channel Average Hot Strength: 3362±521 (13)

Average Hot Strength (All Channels): 3321±443 (25)

Chart Speed: 5 cm/min.
Upper Span: 20 mm
Lower Span: 40 mm
4 Pt; 1/4 Flexure

material appears to be greater than than of its corresponding room temperature strength. To date we have not generated the hot strength characteristics of the as-fabricated matrix. During May we tentatively plan to recharacterize the room temperature and hot strength of a ceramic cross flow filter that was produced in the same fabrication lot as the 1,300 hour HTHP tested filter. Since we have demonstrated conversion of the amorphous to anorthite phase occurred during HTHP testing, we believe that the initial as-fabricated untested matrix will have a lower initial hot strength in comparison to the 1,300 hour HTHP filter hot strength, as well as a lower as-fabricated hot strength in comparison to its as-fabricated room temperature strength.

The as-fabricated amorphous content in the P-100A structure was apparently sufficient for the filter to survive the stresses induced by the filter mount and pulse gas cleaning cycles during the 1,300 hours of HTHP testing. As a result of these data, a reevaluation needs to be performed to determine the validity of the concept that is currently accepted which indicates that "all" porous ceramic filter materials experience a loss of strength during hot gas filtration. We are recommending that post-test evaluation of filters include hot strength testing at process temperatures, as well as a comparison of these data with the hot strength data generated for an as-fabricated filter from the same fabrication lot. In addition we need to determine whether the maximum stress levels at the critical stress areas in the filter (i.e., flange, channels, etc.) are the same at process operating temperature as at room temperature.

*U.S. GOVERNMENT PRINTING OFFICE: 1994-550-168-00016

DATE
FILMED
5/16/94
END